Sustainable alternatives for carbonyl reduction

A thesis submitted to McGill University

In partial fulfilment of the requirements of the degree of Doctor of Philosophy

by Alain Li

December 2018

Centre for Green Chemistry and Catalysis, Department of Chemistry

McGill University, Montreal, Quebec, Canada

Your dreams are sweet and obsessed and you're overworked
You're over taken by visions of being overlooked
How disappointed would D.I.D.I.P.P. be
To see such our power in our hands all wasted on greed?

Casablancas, J.; Hammond, A.; Valensi, N.; Moretti, F.; Fraiture N. Ize of the World, *First Impressions of Earth*, **2005**, 12, 41:52-46:22.

Abstract

Carbonyl reduction is a key process in chemistry, both in academic and industrial research. In the context of biomass valorization, C=O reduction shines as an essential upgrading pathway. Indeed, most biomass-derived molecules are naturally oxygen-rich in contrast to petroleum-based chemicals. H_2 gas is the most ideal reductant in terms of atom-economy. Hydrogenation catalysts have been widely studied, such as Noyori-type catalysts for enantioselective reduction of prochiral ketones. Due to pressure and flammability constraints though, alternative reducing agents may be preferred. On big scale processes, hydride salts such as $NaBH_4$ and $LiAlH_4$ are commonly used, due to their high reactivity. However, stoichiometric amounts of waste are concomitantly formed during the process. Therefore, sustainable solutions need to be developed to decrease the environmental impact of chemical processes. Key factors are energy consumption, waste generation and safety. In this thesis, we have explored alternative energy sources and novel catalysts to solve the issues mentioned above.

In the first part, we covered the catalytic applications of silver nanoparticles. Then, we applied microwave heating to the synthesis of magnetically recyclable silver nanoparticles, using a biomass-derived polymer (carboxymethyl cellulose) as a reductant and stabilizer. It was applied for the selective hydrogenation of C=O bonds in water. Then, we explored the metal-free and mechanochemical reduction of carbonyls, using polymethylhydrosiloxane as a reductant, that is a waste from the silicon industry. Due to the solvent-free conditions, we successfully reduced substrates having solubility issues (5-hydroxymethyl furfural and polyketone). Our mechanistic investigations showed the *in situ* formation of a highly reactive gas $[H_3SiFMe]^-$ during the reaction, that was responsible for the reaction. Lastly, we explored the synthesis of magnetically recyclable $(Ni_{0.5}Cu_{0.5})Fe_2O_4$ NPs by plasma induction. We have successfully applied them for the amination of alcohols under microwave irradiation, through a borrowing hydrogen pathway. Under our optimized conditions, the catalyst proved to be active at the 10-gram scale at metal loadings comparable to those of homogeneous complexes (<2 mol%).

Following the guiding principles of green chemistry, we have successfully applied various alternative sources to both nanoparticle synthesis and organic reactions. In every case they were exploited to solve issues linked to the use of solvents or due to conventional heating.

Résumé

La reduction de carbonyles est un procédé crucial en chimie, autant en recherche académique qu'en industrie. Dans le contexte de la conversion de la biomasse, ce procédé est particulièrement important car les molécules biosourcées sont riches en oxygène, contrairement à ceux issus de l'industrie pétrolière. En termes d'économie d'atomes, l'hydrogène est le réducteur idéal. Les catalyseurs d'hydrogénation ont été l'objet de recherches poussées, tels que les catalyseurs de type Noyori pour la réduction énantiosélective de cétones prochirales. Mais des réducteurs alternatifs, ne posant pas de problèmes d'inflammabilité ou de pression, peuvent être utilisés. Des sels d'hydrure très réactifs tels que $NaBH_4$ ou $LiAlH_4$ sont communément utilisés à grande échelle. Mais ces sels génèrent aussi des quantités stœchiométriques de déchets. Il est donc nécessaire de développer des solutions plus durables, pour réduire l'impact de ces procédés chimiques sur l'environnement, en considérant la consommation d'énergie, les déchets générés, et la sécurité. Pour résoudre ces problèmes, nous avons exploré des sources d'énergie alternatives et des nouveaux catalyseurs.

Tout d'abord, nous avons passé en revue les applications en catalyse des nanoparticules d'Argent. Puis, nous avons exploré la fabrication de nanoparticules d'Argent sur un support magnétique par micro-ondes, à l'aide d'un biopolymère (carboxyméthylcellulose) en tant que réducteur et stabilisateur. Ces nanoparticules se sont révélées sélective pour l'hydrogénation de liaisons C=O dans l'eau. Ensuite, nous avons exploré la réduction sans metal de carbonyles en mécanochimie, en utilisant le polymethylhydrosiloxane, un déchet de l'industrie du silicone, en tant que réducteur. Sans utiliser de solvant, nous avons résolu des problèmes de solubilité avec des substrats difficiles tels que la polycétone ou l'hydroxyméthylfurfural. Nous avons mis en évidence par des études mécanistiques la formation d'un réducteur gazeux pendant la réaction. Finalement, nous avons exploré la synthèse de nanoparticules magnétiques de $(NiCu)Fe_2O_4$ par induction plasma. Nous les avons utilisés pour catalyser l'amination d'alcools sous micro-ondes, par un mécanisme d'emprunt d'hydrogène. Nous montrons que le catalyseur fonctionne à l'échelle des 10 grammes, à des taux métalliques comparable à ceux des catalyseurs homogènes (<2 mol%).

En se basant sur les principes fondamentaux de la chimie verte, nous avons exploité des sources alternatives d'énergie sur la synthèse de nanoparticules et des réaction organiques pour résoudre des problèmes liés à l'utilisation de solvant ou du chauffage convectif.

Acknowledgments

First things first, I would like to thank Dr. Audrey Moores and Dr. Chao-Jun Li for being my mentors for all these years. I guess it really made sense to have a French-Chinese co-supervision, looking at my family background. Both of you taught me perseverance and an inextinguishable passion for green chemistry. 谢谢/merci pour tout.

Maman, Papa et Julien, merci encore pour tout votre support durant le doctorat. Vous avez fait ce que je suis en arrivant ici, et je reviendrai meilleur que ce que je fus. À Yuxi mon chaton, avec qui j'ai traversé tant d'épreuves. On s'est rencontrés à une période particulière de notre vie, et tu m'as transformé. À notre futur ensemble.

To Andréanne, my sorcerer's apprentice throughout the best part of my PhD. I would have never made it that far without you, as I've told you one thousand times already. I hope you've thoroughly enjoyed our endless discussions and rantings in the lab.

À Aurélie, Sosthène et Guillaume. Je vous adresse respectivement un kikou, koukou et un coucoucoloc. Ensemble nous avons traversé l'océan et échangé la chaleur du Sud pour le froid d'icitte. Choix audacieux. À toi Florent, mon guitariste surfeur caribéen préféré, et à nos litres de Damoiseau ingurgités immodérément sur nos mélodies approximatives. À Maxence, le Marty des forêts d'épinettes noires du Sag-Lac, et à nos escapades musico-cinématographiques dans les salles les plus obscures. Ça vous dit on se retrouve une fois de plus quelque part dans le monde?

À Naëla, qui a su représenter le meilleur des libano-colombiennes d'ascendance indo-bulgare. Au mythologique Donatien, tout simplement. À Quierre et Marco, les bienheureux et habiles potos. À Nat, Alex et Grish, que le destin réuni sous le même toit. Au spinozien Antho, meilleur colocataire s'il en est (et nous savons qu'il en est). A Sarah l'éditrice et Sarah la docteure, les plus fortes de toutes. À Soizic, qui nous a fait également le plaisir d'endurer le froid pour un temps. A la fratrie Cormier, à Camille et Robin, Arielle, Magda, Yannick, Mathias et toute la gang de l'île.

À ceux restés sur le vieux continent: ce bon vieux Francky, l'incroyable Tutu, l'inénarrable Fufu et/ou Tom je ne sais plus, l'invraisemblable Cécile, et la fantastique Céline. À Sami, que le hasard nous réunit une fois de plus. À Clémentine et nos pérégrinations méridionales.

When I had joined the Moores lab, I found four fairy godmothers: that one is about the four M of my early PhD years. A round of hugs for Monika, Madhu, Mary and Mitra! If research life can seem jolly rotten, there's people not to be forgotten. Never a dull moment, always with a grin. L'chaim to Michael (JTBA), and all the former team: Huizhi, Yuting, Paul, Shingo, Thomas, Luca, Pierre-Olivier, Hava, Olivia and Nahla.

Fear not though, for the current crew has everything under control. Let's raise our over-caffeinated beverages to every single of them. To the grumpiestest of the grumpiest, Luis. To the fire and the rain, the fiery and the placid, Alex and Blaine. To Thomas, the maker and mender of all things. To my fellow colleague impersonator and music lover Julio. To the *awesome!* backpacker Aude. Allô à Nico, à qui je souhaite un bon courage pour son doc icitte! To our ever-innocent and cheerful Tony. Hatem *habibi*, you're family too. Now send more spices!

To my other hemisphere, the members of the Li lab. To Inna, the gatekeeper -sneaky fox- of the lab. To Zoë and Allie, the heart and caring souls of the group. And a round of applause now for Harry, Yiram, Durbis, Zihang, Wenbo, ChenChen, Jianbin, Chia-Yu, Nick, Xijie, Simon, Feng and Soumen.

To the Sleimanites, and although we moved to the basement, you guys will remain our true neighbours under the sunlight. Lab 400 forever! To bloody Michael, my 河南 comrade Xin, the (real) товарищ Nicole, la increïble Empar, and มังกร Pongphak.

To the ukulele club attenders, or as I like to call it my fortnightly excuse for music and drinks. Let's play Space Oddity once more with Kamila, Catherine, Sebastian, and Max. To the brightest people of the department: the MOFia Igor and Patrick, the dendritic Enzo, Yu-Chen and Graeme, the RNA fanatics Dan and Elise, the enzymatic Fabien, Dustin and Julie, to these nerds called Elisa, Stéphane and Sylvain, and to the palladium apostles Garrison, Pierre-Louis and Giancarlo.

To Chantal, the pillar of this department, Dr. Tomislav Friščić, Dr. Bruce Arndtsen, Dr. Jean-Philip-Lumb and Dr. Scott Bohle for our fruitful discussions during my reviews. To Dr. David Liu and Dr. Robin Stein for your invaluable help.

Thesis Overview and Contribution of Authors

Chapter 1

Alain Li, Chao-Jun Li, Audrey Moores, *Sustainable alternatives for C=O reduction*, review to be submitted to *ACS Sustainable Chem. Eng*.

The author wrote the manuscript. Audrey Moores and Chao-Jun Li edited the manuscript.

Chapter 2

Alain Li, Alexandra Gellé, Andréanne Segalla, Audrey Moores, *Silver NPs in Organic Transformations*, book chapter for "Silver Catalysis in Organic Synthesis" by Xihe Bi and Chao-Jun Li, Wiley editions (accepted).

The author wrote the manuscript. Andréanne Segalla helped in the writing of a few sections (nitrile and alkyne reduction), and Alexandra Gellé wrote the photocatalysis section (not shown in the thesis). Audrey Moores designed and edited the manuscript.

Chapter 3

Alain Li, Madhu Kaushik, Chao-Jun Li, Audrey Moores, 'Microwave-Assisted Synthesis of Magnetic Carboxymethyl Cellulose-Embedded Ag–Fe_3O_4 Nanocatalysts for Selective Carbonyl Hydrogenation', *ACS Sustainable Chem. Eng.*, **2016**, 4, 965–973.

The author collected all data and wrote the manuscript. Madhu Kaushik provided training on every instrument used throughout the chapter. Chao-Jun Li gave insights on experiments and reviewed the manuscript. Audrey Moores coordinated between the collaborators, designed experiments and edited the manuscript.

Chapter 4

Alain Li, Andréanne Segalla, Chao-Jun Li, Audrey Moores, 'Mechanochemical Metal-Free Transfer Hydrogenation of Carbonyls Using Polymethylhydrosiloxane as the Hydrogen Source', *ACS Sustainable Chem. Eng.*, **2017**, 5, 11752–11760.

The author designed the experiments, collected all data and wrote the manuscript. Andréanne Segalla assisted in data collection and the author trained her for all laboratory techniques

involved in the paper. Chao-Jun Li gave insights on experiments and reviewed the manuscript. Audrey Moores coordinated between the collaborators and edited the manuscript.

Chapter 5

Alain Li and Nicolas Dumaresq, Andréanne Segalla, Nadi Braidy, Audrey Moores, 'Plasma-made (NiCu)Fe_2O_4 for alcohol amination' (manuscript in preparation)

The author designed the organic experiments, collected all the related data, and performed characterization of the catalyst (XPS, TEM of the catalyst before and after reaction) and wrote the corresponding parts in the manuscript. Andréanne Segalla assisted in data collection and the author trained her for all laboratory techniques involved in the paper. Nicolas Dumaresq performed the synthesis and characterization of the NPs (XRD, XRF, TEM of the NPs from the auxiliary reactor, EELS) and wrote the corresponding parts in the manuscript. Nadi Braidy and Audrey Moores designed and edited the manuscript.

Table of contents

List of figures

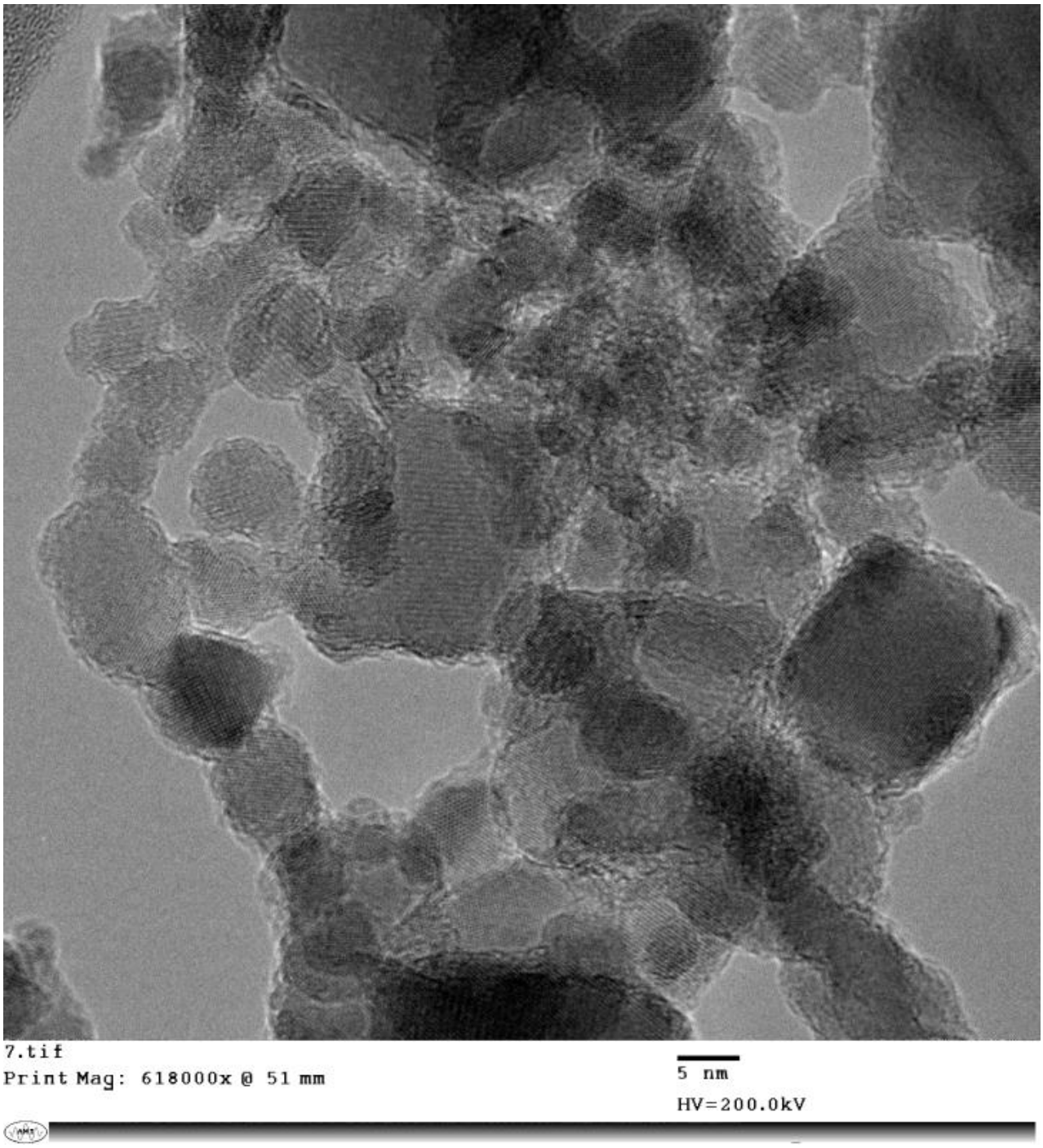

List of schemes

List of tables

List of abbreviations

5-HMF	5-(hydroxymethyl)furfural
A^3	Aldehyde-Alkyne-Amine
BINAP	2,2'-bis(diphenylphosphino)-1,1'-binaphthyl
Bu	Butyl
CDC	Cross dehydrogenative coupling
CSNPs	Core-shell NPs
DMF	Dimethylformamide
DES	Deep eutectic solvent
DFT	Density functional theory
Et	Ethyl
EtOH	Ethanol
EtOAc	Ethyl acetate
eV	Electron volt
FeCSmP	mesh 326 Fe(0) microparticles
FG	Functional group
GC	Gas chromatography
GVL	γ-valerolactone
ICP	Inductively coupled plasma
IL	Ionic liquid
*i*Pr	*iso*-propyl
JCPDS	Joint Committee on Powder Diffraction Standards
LA	Levulinic acid
M	Molar mass

Me	Methyl
MeOH	Methanol
NHC	*N*-heterocyclic carbene
mL	Milliliter
MOF	Metal-organic framework
mp	melting point
MPV	Meerwein-Ponndorf-Verley
MS	Mass spectrometry
NMR	Nuclear Magnetic Resonance
NP	Nanoparticle
PEG	Polyethylene glycol
PGM	Platinum-group metal
Ph	Phenyl
PMHS	Polymethylhydrosiloxane
ppb	parts per billion
ppm	parts per million
Pr	Propyl
PS	Polysytrene
rt	Room temperature
SEM	Scanning electron spectroscopy
T	Temperature
TAA	*tert*-Amyl alcohol
TBAF	Tetrabutylammonium fluoride
TBHP	Tert-butyl hydroperoxide

*t*Bu	*tert*-butyl
TEM	Transmission electron spectroscopy
THF	Tetrahydrofuran
TOF	Turnover frequency
TON	Turnover number
UV	Ultraviolet
XPS	X-ray photoelectron spectroscopy
XRD	X-ray diffraction

Well the night was spent, and my money was young
Then I had to get home before my neck was wrung
Everybody danced in the same old way
And if I'm feeling old and desperate, I'll be back some day

Lawler, J.; Wallace, B.; McRory, G. My friend John, *Here we stand*, **2007**, *1*, 0:00-3:02.

1 Introduction

1.1 C=O reduction in chemistry

Catalytic reductions and oxidations represent the most important chemical transformations and are routinely employed at all scales of chemical production.[1] However, reductions are preferred to oxidations on large scale, due to safety and/or waste disposal issues associated with most oxidants.[2] Hydrogen gas is the most ideal reducing agent both in terms of cost and atom economy. Indeed, hydrogenation has been largely explored in academia, with the first catalytic example reported in 1874 for olefin hydrogenation.[3] It has become a powerful tool for key processes in the industry, such as the Haber-Bosch process, the Fischer-Tropsch synthesis, or oil refining.[4]

Despite its advantages, the use of hydrogen gas may be problematic in some settings because of its flammability and the need for pressurization, and other reducing agents may be preferred. In industry, the most commonly used ones for carbonyl reductions are $LiAlH_4$ and $NaBH_4$ (Scheme 1). These inorganic salts are highly reactive toward carbonyls, and have been successfully implemented in big-scale processes (>100 mol scale).[5]

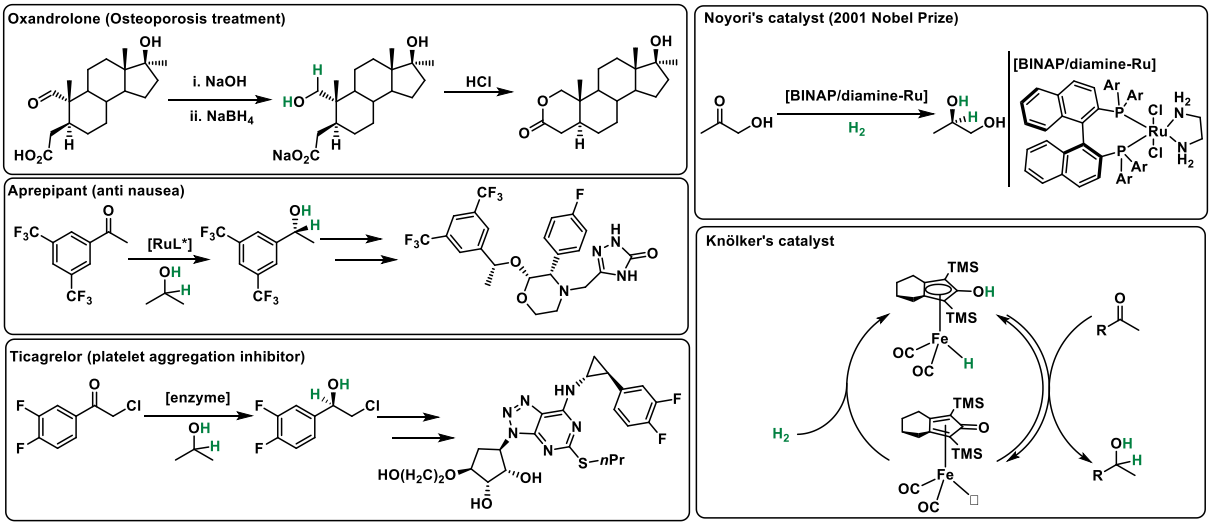

Scheme 1. Carbonyl reduction in chemistry.

In fact, hydride salts are the most commonly used reductants to convert C=O bonds to C-O bonds in the industry,[6] along with Noyori-type catalysts for asymmetric prochiral ketone reduction.[7] This observation comes in sharp contrast to the diversity of carbonyl reducing systems reported in the academic literature, showing the overall robustness and economic viability of these two methods. From the sustainability perspective though, these methods come with drawbacks. For the former, stoichiometric amounts of waste are generated that are problematic at the industrial scale. Concerning the latter, Platinum-group metal (PGMs) such

as Pd, Ru homogeneous complexes are the most commonly reported catalysts. These come with their own drawbacks: low abundance,[8] high toxicity,[9] and recycling issues.[10]

What alternatives green chemistry can offer to improve carbonyl reduction?

For any given reaction, today's chemists are facing new challenges to decrease the environmental impact of their processes while still pursuing better catalytic performance. In this thesis, carbonyl reduction is used as a benchmark reaction to introduce and explore the feasibility of a few key green chemistry concepts. Despite its simplicity, this transformation features challenging aspects such as chemoselectivity[11] and mechanistic considerations. Furthermore, in the context of biomass conversion, C=O reduction shines as an essential upgrade pathway.[12] Indeed, most biomass-derived molecules are naturally oxygen-rich (including carbonyl functionalities), in contrast to petroleum-based chemicals.

Four factors will be mainly considered in the introduction. As arbitrary as they are, they allow a classification of the numerous examples reported in the literature and give a framework for discussing the 'green aspects' of a reaction. With such categorization, other factors have been omitted for the sake of simplicity. Typically, metrics such as atom economy, turnover numbers or E-factor are not typically given in papers, which makes an actual ranking difficult.

-Energy source

-Solvent

-Catalyst

-Reductant

Naturally, these categories are complementary rather than mutually exclusive, and fortunately a substantial number of reports fit into more than one category. Some examples listed below are 'sustainable' upgrades of the two main processes mentioned before, while some other reports represent more comprehensive improvements. This underlines the complexity of defining a green reaction. The current thesis is an attempt to formalize the concepts in green chemistry outlined by Paul Anastas and John Warner 20 years ago, towards carbonyl reduction.[13]

1.2 C=O hydrogenation substrates

Benzylic carbonyls (namely benzaldehyde and acetophenone) are commonly reported as model substrates, due to their high reactivity and ease of handling. In this section, we will present some C=O hydrogenation targets that are industrially important. Their reduction products are useful building blocks available for further functionalization, showing the key role of C=O hydrogenation in chemical industry. Typically, selectivity is an important aspect, with carbonyl hydrogenation being disfavored compared to nitroarene, alkyne and alkene hydrogenation (Scheme 2).[14]

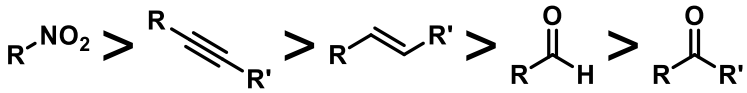

Scheme 2. Usual reactivity trends in hydrogenation.

A plethora of methods have been devised to tune the selectivity of a catalyst in the specific case of C=O/C=C selectivity. For instance the Medlin group has explored Pt surface modification with thiol (R-SH), to prevent C=C coordination on α,β-unsaturated aldehydes (Scheme 3).[15] C=O selectivity can also be tuned by encapsulating Pt/Pd into MOF, tweaking the steric environment of the active sites.[16]

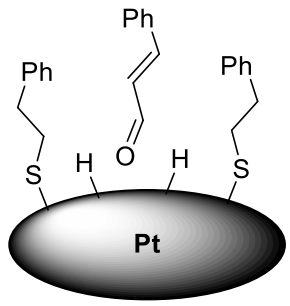

Scheme 3. Thiol poisoning for C=O hydrogenation selectivity.

Interestingly, Zhang et *al.* made a Cu(I)-based catalyst that has a switchable C=O/C=C selectivity.[17] Starting from a Cu(I) N-heterocycle thiolate complex, the catalyst had different selectivities depending on the base/hydrogen donor used during the reduction of α,β-unsaturated aldehydes. By using K_2CO_3/*n*BuOH, the catalyst adopted mostly a monohydride configuration, showing a strong C=C selectivity. By switching to NaOH/*i*PrOH, a protonated hydride Cu(I) complex forms, that is C=O selective (Scheme 4).

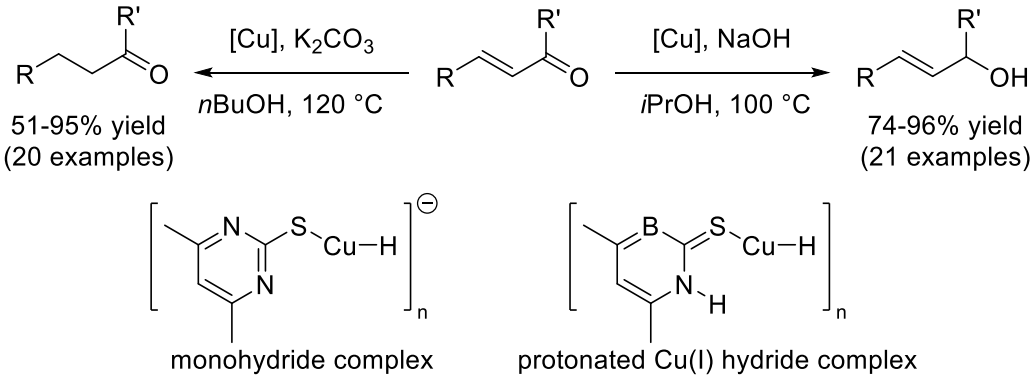

Scheme 4. Cu(I)-based switchable catalyst.

C=O is a common functionality encountered in biomass. Unsurprisingly reduction of biomass-derived platform molecules, in particular levulinic acid (LA) or 5-hydroxymethylfurfural (5-HMF), are intensely explored.[18] They can be made from acidic treatment of glucose or cellulose, and for both, pilot plants dedicated to their production from biomass have been built.[19-20] Two other industrially relevant targets are acrolein and citral. Acrolein is probably the most challenging substrate for selective C=O hydrogenation, due its C=C bond being the least sterically hindered compared to any other α,β-unsaturated aldehyde. Citral has two unsaturated C=C bonds, making for challenging selectivity issues as well.

1.2.1 Levulinic acid

LA can form γ-valerolactone (GVL) upon hydrogenation and subsequent cyclization (Scheme 5).[21] GVL is useful in itself as a fuel additive or solvent, and can be further reduced to 2-MeTHF for similar purposes. It can be further converted to α-methylene-γ-valerolactone (MeMBL) using formaldehyde, and serves as a methyl methacrylate upgrade in its polymerisation.[22] Indeed, it increases the glass transition temperature of the resulting copolymer by 100 °C compared to pure poly-methyl methacrylate. GVL can also reversibly convert to pentenoic acid (PEA),[23] which can be further hydrogenated to pentanoic acid (PA). All these intermediates can be decarboxylated or used as chemical building blocks or fuel additives.[24] Another closely related pathway to carbonyl hydrogenation is reductive amination, from which LA can form 2-pyrrolidinone derivatives.[25]

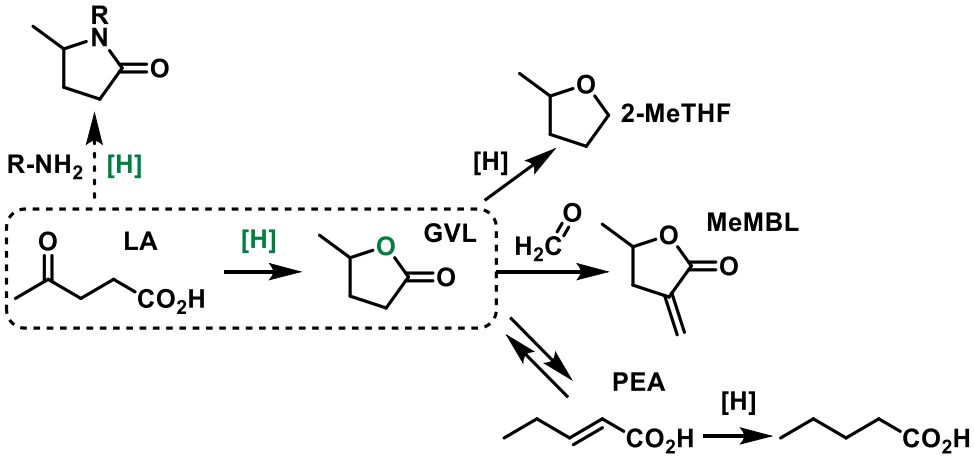

Scheme 5. LA hydrogenation and further upgrade pathways.

1.2.2 5-hydroxymethylfurfural

As for 5-HMF, its reduction to 2,5-dihydroxymethylfuran (DHMF) has been covered by Hu et *al.* (Scheme 6).[26] This symmetrical diol can be directly used as a co-monomer, for example with succinic acid to form poly(2,5-furandimethylene succinates) (PFS).[27] It can also be etherified using various short chain alcohols to form 2,5-bis(alkoxymethyl)furan (BAMF) that can be used as fuel additives.[28-29] Lastly, it can be re-arranged into 6-hydroxy-6-methyl-4-enyl-2H-pyran-3-one (HMEPO), an intermediate for the synthesis of sugar analogues and compounds with excellent biological activities.[30-31]

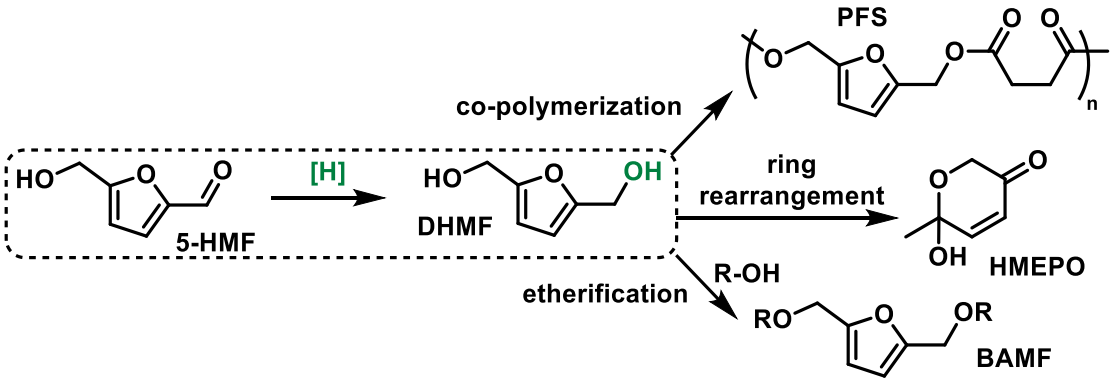

Scheme 6. 5-HMF hydrogenation and further upgrade pathways.

1.2.3 Citral

Citral, a monoterpenoid containing three unsaturations (1 C=O bond and 2 C=C bonds), is distilled from essential oils such as lemongrass oil. It is responsible for the 'citrus effect' in perfumes and other flavored consumer goods, and widely used as such. It can be cyclized into other flavours such as menthol.[32] From a purely scientific standpoint, Stolle et *al.* have identified citral hydrogenation as a challenging process, considering the selectivity issue

stemming from the presence of three double bonds (making up to 8 potential products, see Scheme 7).[33] Some metals such as Ag, Ru and Os, have intrinsic properties towards improved selectivity to C=O reduction, and once combined with acidic promoters such as In_2O_3, CeO_2 or MgO can improve the reactivity of the carbonyl.[11]

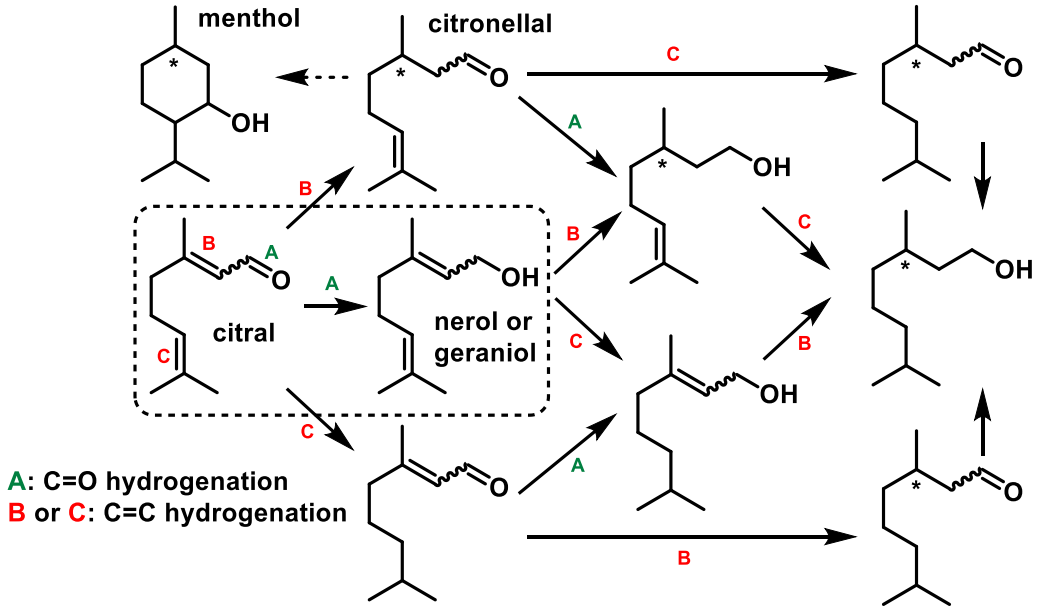

Scheme 7. Citral hydrogenation selectivity issues (each hydrogenation pathway is indicated above the arrows).

1.2.4 Acrolein

Acrolein is the simplest unsaturated aldehyde, produced from the oxidation of propylene on $Mo_xFe_yBi_z$ oxides heterogeneous catalysts.[34] Allylic alcohol, acrolein's C=O hydrogenation product, is an important intermediate in both the pharmaceutical and fragrance industries (Scheme 8).[35] Most of allyl alcohol is used for the production of glycerol through epoxidation/ring opening, and it is an intermediate in the production of polymerizable allyl ethers and esters, especially diallyl phthalate. It can be also directly co-polymerized with styrene to form poly(styrene-co-allyl alcohol), which can be used as a solid support for combinatorial chemistry.[36]

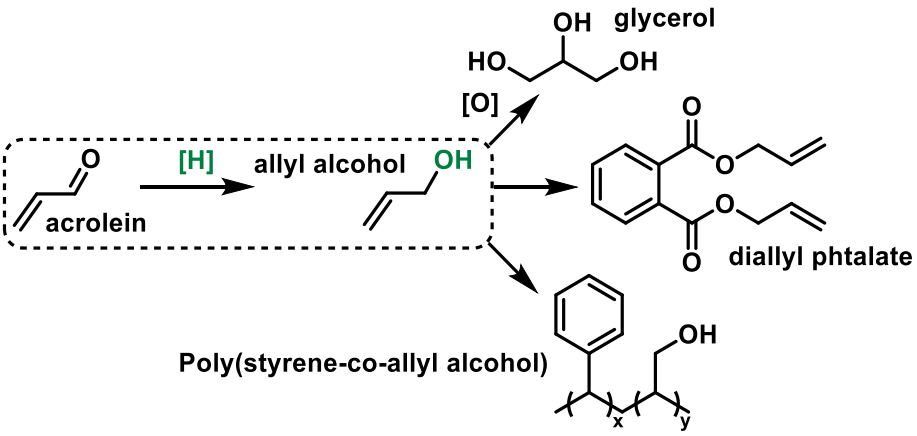

Scheme 8. Acrolein hydrogenation and further upgrade pathways.

1.3 Alternative energy sources

As outlined by Varma et *al.*, a number of alternative energy inputs have been successfully applied to both organic chemistry and material synthesis (Scheme 9).[37] These all constitute an effort towards improving the efficiency of a reaction from an energetic perspective. Indeed, most organic reactions are conducted using convective heating. This can be seen as a fairly inefficient process where most of the energy is wasted through thermal loss. Components in a chemical set-up are heated successively: heating plate, reaction flask, solvent (if present), then finally reactants. Furthermore, convection can be too slow to ensure a homogeneous heating, depending on the stirring and the heterogeneity of the reaction medium. This is particularly problematic in nano-material synthesis to obtain monodisperse NPs, and in large-scale processes where heat accumulation can be a threat.

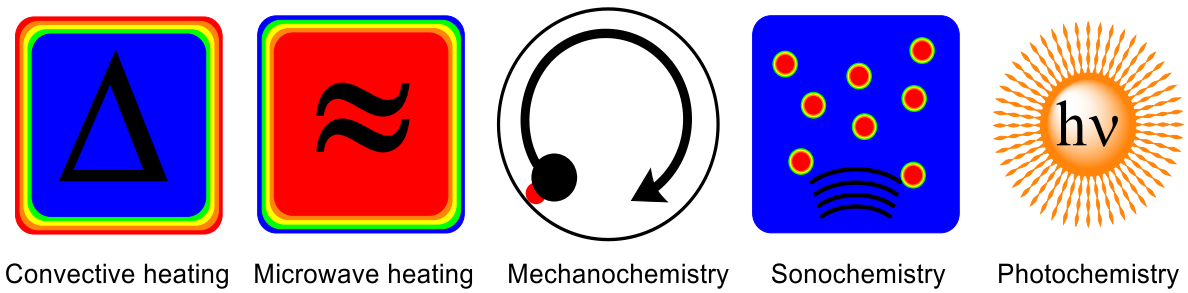

Scheme 9. Energy inputs used in chemistry.

1.3.1 Microwave heating

Microwave irradiations occur in the 0.3-300 GHz range. In domestic and chemical applications, a frequency of 2.45 GHz is applied to avoid telecommunication interference. This frequency corresponds to a wavelength of 12.24 cm, and photon energy of 0.0016 eV.[38] This is lower than Brownian motion, therefore microwave irradiations cannot directly induce chemical reactions. Instead, 'microwave dielectric heating' relies on the capacity of the reaction medium to absorb

microwave energy and dissipate it into heat. This phenomenon works as follows: upon irradiation, the dipoles and ions of the solution align with the applied electromagnetic field. As the field oscillates, dipole/ions re-align with it and generate heat through molecular friction and dielectric loss. This results in a faster and more homogeneous heating of the reaction medium and a far superior reaction reproducibility to classical heating. Thus, it has been successfully applied to both organic chemistry and nano-material synthesis.[37]

Early examples (1997-2002) of the use of microwave heating in carbonyl reduction consisted in the straightforward transposition of transfer hydrogenation reactions, namely $NaBH_4$ reduction and the Meerwein-Ponndorf-Verley reaction (see section 1.6). Then, household microwaves were mostly used, although in most cases they were fitted with a reflux condenser on the top (Scheme 10). The difficulty to stir efficiently in such set-ups led to the absence of accurate temperature control, and safety issues (some authors[39] explicitly recommend not to perform their reaction on a big scale).

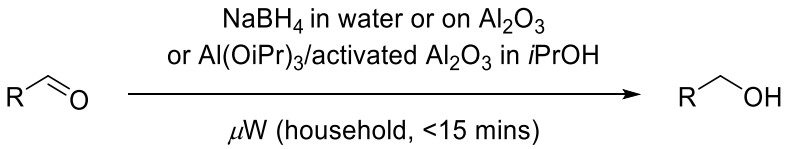

Scheme 10. Early examples of microwave heating in carbonyl transfer hydrogenation.

For instance, Torchy et *al.* transposed the MPV transfer hydrogenation to microwave heating.[40] The reaction consisted in heating stoichiometric amounts of Al(O*i*Pr)$_3$ in the presence of ketones in *i*PrOH, with a typical reaction time of 2 minutes, compared to the 3-8 hours required usually in conventional heating. Therefore, they could not exclude the possibility of solvent superheating occurring, especially in the absence of stirring. Kazemi et *al.* used microwave irradiation to activate Al_2O_3 with KOH, then used it for ketone MPV reduction in a similar set-up.[41] Meanwhile, Varma and co-workers reported the use of $NaBH_4$ impregnated on neutral alumina as a reductant.[39] Upon exposing a slurry of this solid reactant with acetophenone to microwave irradiations, the corresponding alcohol can be obtained in less than 120 seconds. Zeynizadeh et *al.* reported a similar system in an aqueous solution.[42]

Eventually, the advent of microwave reactors adapted to organic reactions led to safer and better chemical processes. Companies such as Anton Paar, CEM or Biotage now commercialize dedicated lab microwaves with pressure and temperature control which triggered wide-spread interest in microwave chemistry. In 2008, Varma and co-workers reported Ni supported on a magnetite support, using dopamine as a linker (Ni@Fe_3O_4).[43] Later

on, they published a similar reported using Ru supported on a magnetite core with a silica shell ($Ru@Fe_3O_4$).[44] Yoshida et *al.* also reported the preparation of Cu supported on hexagonal mesoporous silica (Cu@HMS) under microwave.[45] These three catalysts share similar performances for the transfer hydrogenation of ketones using *i*PrOH in microwave, requiring a base (NaOH or KOH), and showing high recyclability with no metal leaching (Scheme 11).

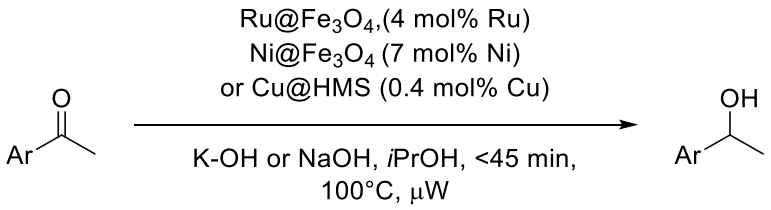

Scheme 11. Microwave heating for catalytic carbonyl transfer hydrogenation.

Gowda et *al.* reported the use of non-noble metal carbonyls (Fe, Mo, Co, W) as *in situ* precursors to nanocatalysts for LA hydrogenation to GVL (Scheme 12).[46] While under conventional heating HCO_2H/NEt_3 reductant was used, EtOH under microwave served as both solvent and reductant in the reaction. Most notably, reaction time was decreased from 48 h to 20 min. Rather than being made *in situ*, the NPs can be prepared in presence of organic polymers (PVP or Poly(methyl methacrylate)) as stabilizers. The catalyst could then be re-used 5 times with no yield drop.

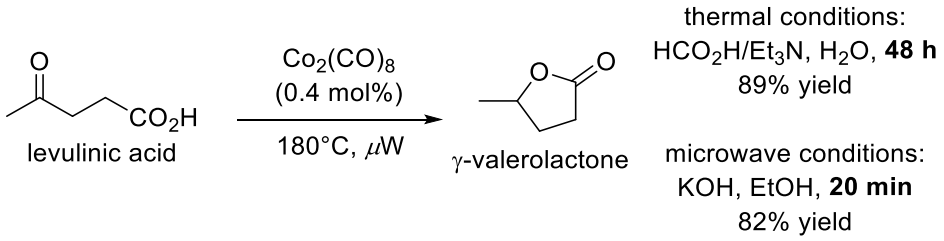

Scheme 12. Metal carbonyls as catalyst precursors for LA transfer hydrogenation under microwave.

1.3.2 Mechanochemistry

20 million tons of organic solvents are produced every year, and make up to 85% in mass of waste emission for the synthesis of active pharmaceutical ingredients.[47] These large quantities are required not only to ensure the homogenization of a chemical mixture, but also to perform extraction, purification and cleaning purposes.[48] A mechanochemical reactions is defined by the IUPAC as ‘a chemical reaction that is induced by the direct absorption of mechanical energy”. Indeed, mechanochemical impact and/or shearing can enable chemical reactions in absence or with drastically reduced use of a solvent.[49] Furthermore, the absence of

solvent can favor an acceleration of reaction rate through high concentration, and offers an opportunity to solve substrate solubility issues.

In fact, mechanochemical reactions are the oldest and simplest techniques used in history.[50] In most ancient civilizations mechanical treatments with pestle and mortar for food and medicine preparation have been well documented. Unlike in liquid-phase chemistry, organic and inorganic oxidations are prevalent compared to reductions. This is explained by the wider availability of solid oxidants, along with the natural presence of oxygen in air.

In the context of carbonyl hydrogenation, the sole reductive systems reported involve $NaBH_4$ and related salts. Early on, Toda et *al.* reported the manual grinding of a ketone with a tenfold excess of $NaBH_4$.[51] Their process was slow, requiring a 3-5 days aging in a dry box with a daily grinding. In the case of Wieland–Miescher ketones, they succeed in the fully enantioselective reduction into the chiral secondary alcohol. Cho et *al.* tested a few acidic activators in conjunction with $NaBH_4$ in a mortar, such as benzoic acid or *p*-toluene sulfonic acid.[52] In the case of sterically hindered ketones such as 1-indanone, the presence of H_3BO_3 powder could increase the yield by up to 50-fold.

An interesting development was brought up by Zeynizadeh et *al.*, using wet SiO_2 powder as a reaction medium for $NaBH_4$.[42] Although the reaction is not mechanochemical *per se* (the mixture is heated in an oil bath at 80 °C), it was conducted in solvent-free conditions with minimal amounts of liquid. Using dry SiO_2, benzaldehyde gets reduced with a 5% yield after 3h of mixing at room temperature, whereas by using wet SiO_2 (30%w/w H_2O loading) they reached full conversion at 1 h of mixing.

A decade later, Mack et *al.* reported the mechanochemical reduction of carbonyls using $NaBH_4$, using a ball-mill mixer.[53] Notably, the addition of LiCl salt could induce the *in situ* formation of $LiBH_4$ that is reactive enough to reduce esters. An additional study on the reaction intermediates and chemoselectivity of their system was published later on by Naimi-Jamal et *al.*[54] Lastly, Solà et *al.* reported a sustainable route for the synthesis of Fluoxetine (Prozac), using microwave heating and ball-milling.[55] In their second step, ball-milling with $NaBH_4$ was successfully applied for the reduction of an aminoketone (Scheme 13).

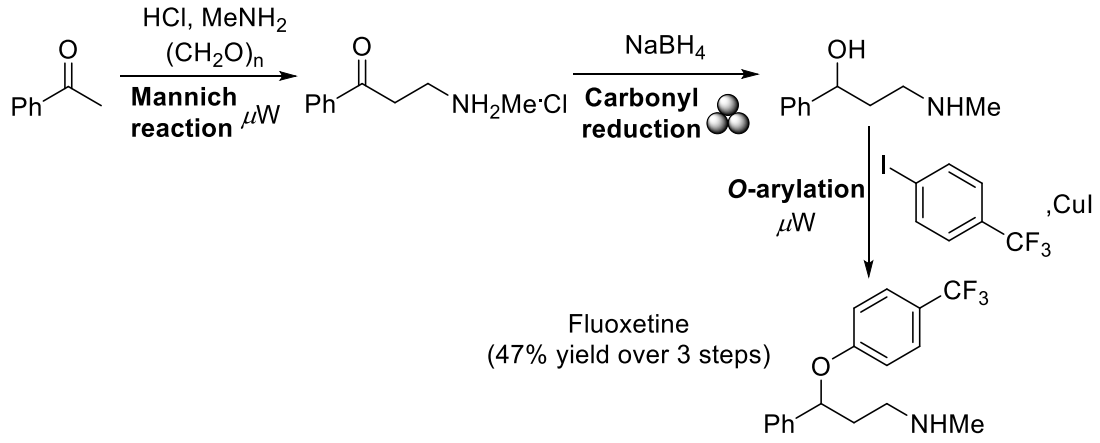

Scheme 13. Sustainable synthesis of Fluoxetine.

1.3.3 Photochemistry

Photocatalysis is characterized by the increase in the rate of a light-induced reaction. A typical example of photocatalyzed reduction consists of the separation of e^- and h^+ charges under light irradiation to reduce carbonyls section (line 1 in Scheme 14). The h^+ recombines either with a sacrificial electron donor (Et_3N, line 2) or with an alcohol to generate H· radicals (line 3). The generated electron e^- recombines with the substrate to generate a negatively charged radical intermediate (line 4). This intermediate can either dimerize into a pinacol, or trap H+/ H· to form the desired alcohol. Thiols can be added to inhibit dimerization into pinacol, as shown in some examples below.

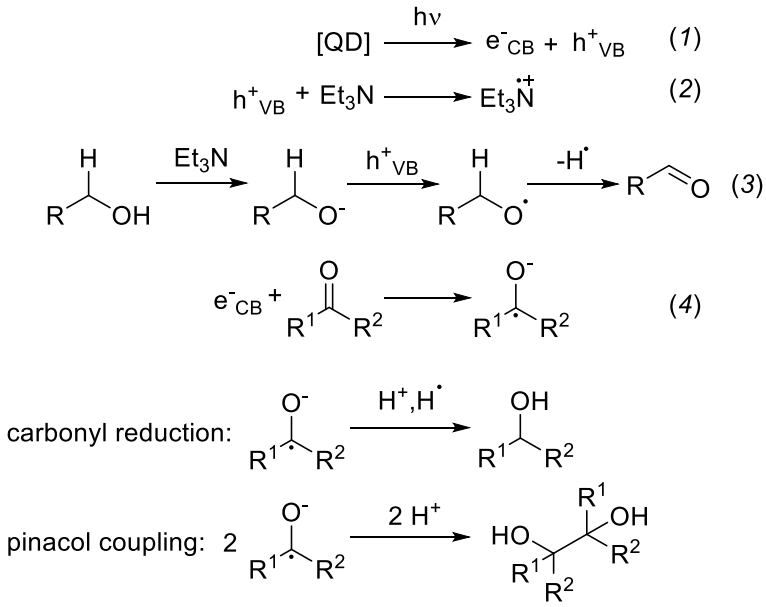

Scheme 14. General mechanism for photocatalytic carbonyl reduction.

Heterogeneous systems. Shiragami et *al*. reported semi-conductors, such as CdS and TiO_2 NPs, as catalyst being able to harvest visible light (>400 nm) and enable transfer

hydrogenations. CdS colloids (2-5 nm) were shown to reduce ketones to alcohols using MeOH as reductant and Et_3N as an electron donor (Scheme 15).[56]

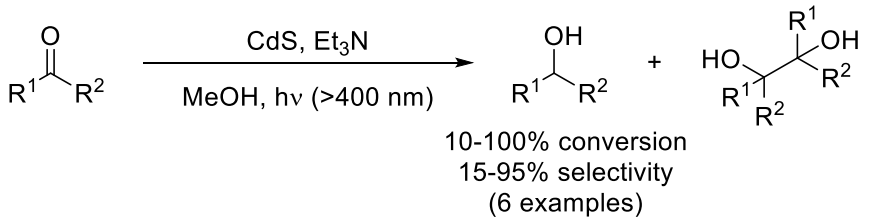

Scheme 15. CdS-catalyzed photocatalytic transfer hydrogenation of ketones.

Li et *al*. showed that CdS can also be used in conjunction with an Ir-based complex, using lactic acid as a sacrificial electron donor this time.[57] Rather than transferring its electron directly to the carbonyl, CdS can transfer it to the Ir complex, allowing the production of H_2 from H^+ of lactic acid and then hydrogenation of the carbonyl substrate (Scheme 16). Eventually, Liu et *al*. showed that the Ir complex could be replaced with $[Ru(bpy)_2(CO)_2](PF_6)_2$.[58]

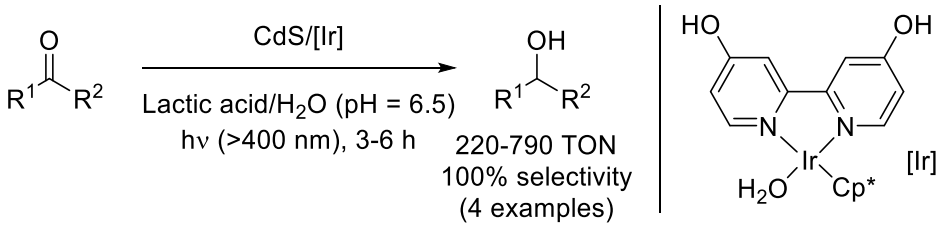

Scheme 16. CdS/Ir-catalyzed photocatalytic transfer hydrogenation of carbonyls.

Joyce-Pruden et *al*. reported TiO_2 NPs (anatase) to reduce benzaldehyde, using EtOH/*i*Pr_2NH and UV light (>340 nm) this time.[59] Later on, Kohtani et *al*. expanded the substrate scope (64-99% yield, 11 examples), without *i*Pr_2NH (Scheme 17).[60] In their case though, polycrystalline TiO_2 was used (90% anatase, 10% rutile).

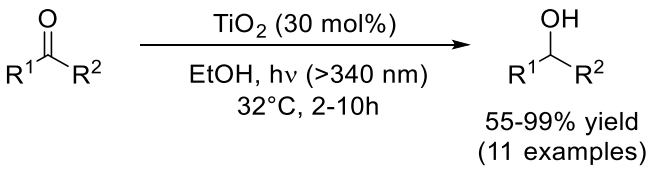

Scheme 17. TiO_2-catalyzed photocatalytic transfer hydrogenation of ketones.

Zhang et *al*. opted for poly(*p*-phenylene) (PPP) as an organic photosensitizer, due to its stronger reductive potential compared to TiO_2 (its conduction band is at -2.0 V vs NHE, as opposed to -0.5 V vs NHE for TiO_2) (Scheme 18).[61] The authors used Et_3N and β-mercaptoethanol (BME)

as sacrificial electron donors, with the thiol fully inhibiting pinacol formation (0-76% of pinacol was formed in absence of BME).

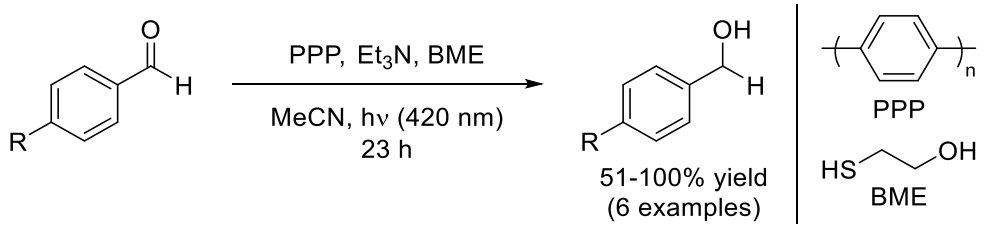

Scheme 18. PPP-catalyzed photocatalytic transfer hydrogenation of aldehydes.

Sharma et *al*. reported a base-free system, using Ru supported on graphitic carbon nitride (Ru@g-C_3N_4) and short chain alcohols as reductants (EtOH, *n*PrOH, *i*PrOH).[62] C_3N_4 is a semi-conducting material that serves the same role than TiO_2 and CdS mentioned above. Due to its heterogeneous nature, the catalyst could be recycled up to 6 times, although with a 20% yield drop overall (Scheme 19).

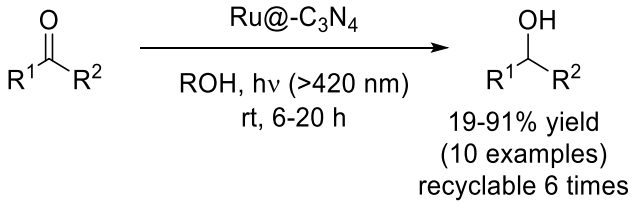

Scheme 19. Ru@g-C_3N_4-catalyzed photocatalytic transfer hydrogenation of carbonyls.

Homogeneous systems. König et *al.* reported the synergistic activity of proflavine (PF) and a [Cp*Rh(III)(bpy)H]Cl complex for aldehyde reduction (Scheme 20).[63] PF is able to harvest blue light (455 nm) and regenerate the Rh(III)-H active species using TEOA as a sacrificial electron donor. The system proved to be selective towards aldehydes (<3% yield on ketones), and flow conditions proved beneficial to the reactivity due to the more efficient light exposure (resulting in a 5-fold increase of reaction rate).

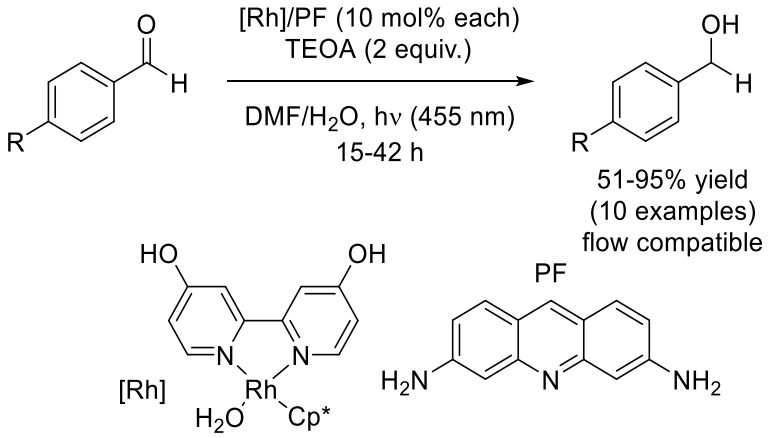

Scheme 20. [Rh]/PF-catalyzed photocatalytic transfer hydrogenation of aldehydes.

Call et *al*. improved the system with an earth abundant, oxygen- and water-stable tandem: a Cu-based photosensitizer (PSCu) coupled with Co-based reduction catalyst (Scheme 21).[64] Their system was able to reduce a wide range of aldehydes, including aliphatic ones, using H_2O as a hydrogen source. Furthermore, their process had a similar or higher ketone versus aliphatic aldehyde selectivity to/than the Luche process (selectivity >11:1 in all cases).

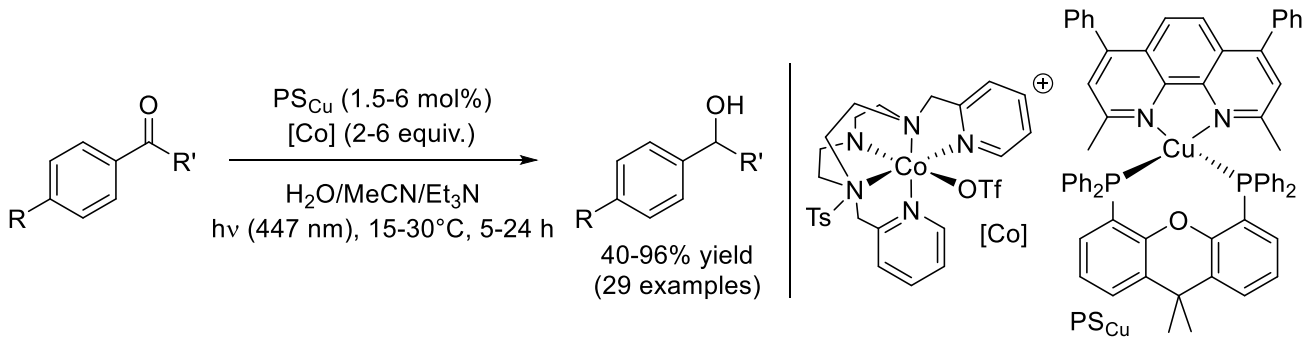

Scheme 21. Cu/Co-catalyzed photocatalytic transfer hydrogenation of aldehydes.

Plasmonic catalysis. Plasmonic photocatalysis is based on visible-light absorption of metal NPs resulting from their localized surface plasmon resonances (LSPR).[65] Indeed, visible light can enable the collective oscillation of the valence electrons of coinage metal NPs (Au, Ag, Cu) and Al NPs, allowing them to act as catalyst through the generation of high-energy electrons.

Hao et *al*. used Au NPs supported on SiC (Au@SiC) as plasmonic catalysts for the C=O-selective transfer hydrogenation of α,β-unsaturated carbonyls under visible light (Scheme 22).[66] In their model, the LSPR allows the transition of electrons from Au NPs to the conduction band of the support, leading to slightly positively charged Au NPs and charge accumulation at the Au/SiC interface. This phenomenon allows the catalyst to dehydrogenate *i*PrOH at room temperature, with a high C=O reduction selectivity (72-100%) due to the higher polarization of C=O bonds from $Au^{\delta+}$.

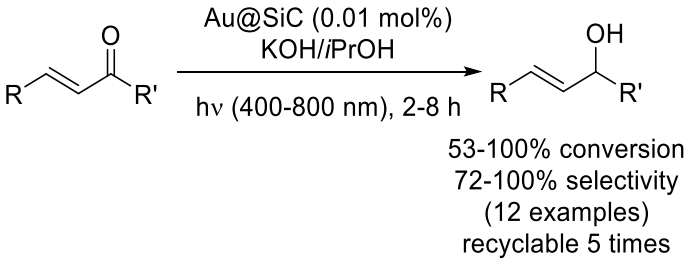

Scheme 22. Plasmon-driven selective reduction of carbonyls using Au@SiC.

Similarly, Landry et *al*. exploited the same phenomenon with Ag nanocubes (Ag NC, Scheme 23).[67] Under mild H_2 pressure (1 bar), especially for Ag NPs (see section 2.4.1), the authors successfully reduced a range of 12 carbonyls including aliphatic ketones and cinnamaldehyde at the C=O position.

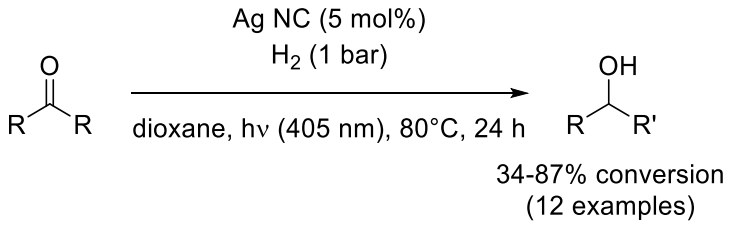

Scheme 23. Plasmon-driven selective reduction of carbonyls using Ag NC.

1.3.4 Sonochemistry

Ultrasound is a sound field with frequency between 20 kHz-10 MHz.[68] Once applied to a liquid, cavities nucleate from pre-existing bubbles in solution, and solid impurities.[69] This phenomenon of cavitation generate bubbles that will go through cycles and collapsing. It has been hypothesized (through the hot spot mechanism) that extreme conditions (around 5000 K, 2000 atm) are reached during the collapsing of the bubbles, giving sufficient energy to the surroundings to induce chemical reaction.[70-71]

An early example of sonochemistry for C=O reduction was reported by Salvador et *al*., using Zn powder in a AcOH solvent.[72] Within 1 h, they succeeded in reducing a 16-en-20-one pregnenolone derivative to its enantiomerically pure 16-en-20(R)-ol counterpart. Firdaus et *al.* transposed $NaBH_4$ to sonication-induced reduction of aldehydes in neat conditions.[73] Xu et *al.* showed that ultrasonication could induce the asymmetric transfer hydrogenation of ketones, using a chiral Rh cationic complex supported on mesoporous silica ([Rh*]@SBA-16).[74] Using HCO_2Na as a reductant, they obtained chiral alcohols in extremely high yield and enantioselectivity from a range of acetophenones (Scheme 24). Compared to identical conditions without ultrasound irradiation, the reaction was around four times faster with a 10-20% gain in ee.

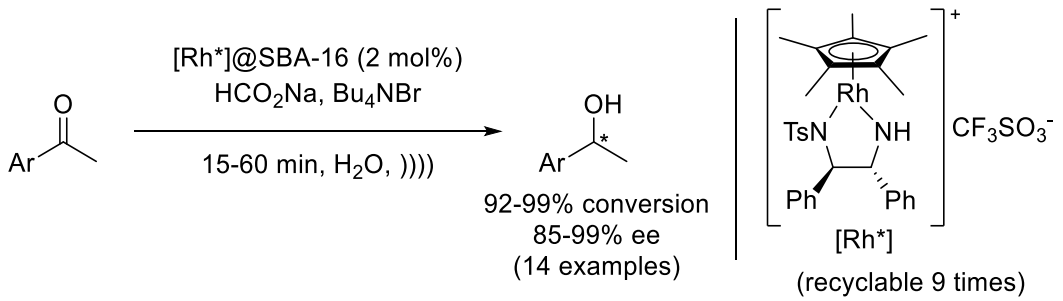

Scheme 24. Asymmetric Rh complex for acetophenone reduction using ultrasound.

1.4 Solvents

A lot of organic solvents are harmful, toxic and environmentally damaging. However, they are crucial in most organic reactions to dissolve chemical compounds, enable heat dispersion and ensure proper mass transfer. Substituting them or alleviating their use is no simple task, as many factors (such as safety, separation cost, viscosity, solvation properties, chemical stability) must be taken in account to evaluate their impact.[75] As stated earlier switching to solvent-free processes is a viable option, whether it is in liquid or solid phase (see section 1.3.2 for the latter case) depending on the substrate. Not using solvents allows higher reaction rates due to higher concentration (for bimolecular reactions and beyond), as well as lower costs. However, low diffusion rates and heat dispersion issues due to higher mixture viscosity can be encountered in solvent-free conditions. Ultimately, the impact of a solvent on the performance of a reaction or on the economics of a process are the governing parameters, respectively in academia and industry.

In 2010, Prof. Jessop conducted a survey with the following question: "*If the adoption of greener solvents over the next 20–30 years will reduce environmental damage from human activities, then the adoption of what class of solvents will be responsible for the greatest reduction in environmental damage*?". A relative consensus pointed at supercritical CO_2, water and carefully chosen traditional organic solvents (these 3 categories added up to 75%, with the rest of the answers comprising bio-derived solvents and solventless systems).[76] This came in stark contrast to the overwhelming proportion of papers published in the journal Green Chemistry describing solvents being focused on ILs (around 50% of the papers). He listed a few scientific challenges in green solvent development, such as developing more diverse solvents in terms of polarity and hydrogen bond donor capacity (cf. Kamlet-Taft diagram), while taking in account the synthetic route and safety parameters. For instance, developing a bio-derived low boiling-point polar aprotic solvent is still highly desirable.

1.4.1 Ionic liquids and deep eutectic solvents

ILs are salts with melting point below 100 °C. Due to their low vapour pressure and high polarity, they have been used to replace more 'conventional' organic solvents.[77] Although their toxicity and flammability drastically vary among each IL type, they have attracted organic chemists' attention for a variety of reasons.[78] First, some ILs can dissolve usually insoluble

substrates such as cellulose or lignin, allowing for an easy extraction and functionalization.[79] By a careful design of IL-miscible catalysts, ILs can be used as a convenient separation and recycling medium.[80] Hydrogenations in an IL medium have been reviewed elsewhere, with most examples on C=C hydrogenation.[81] From a C=O/C=C selectivity standpoint, ILs actually favour C=C reduction in the case of Pd/C-mediated hydrogenation of citral in ILs.[82] At 10 atm and room temperature, H_2 solubility in ILs is about the same as in H_2O (around $0.8.10^{-3}$M) whereas H_2 is more soluble in MeOH, EtOH and toluene ($3.75.10^{-3}$, $2.98.10^{-3}$ and $3.50.10^{-3}$M respectively).[83]

These factors make ILs suboptimal for carbonyl hydrogenation. Furthermore, one must take into account the synthetic cost and potential toxicity of these highly-functionalized solvents, although efforts have been made for synthesizing them from biomass to lower their environmental impact.[84] For all these reasons, ILs cannot be used universally as a 'green' solvent, and their use must be justified by a specific need in the process design (such as substrate solubility, catalyst recyclability, solvent effect).

Another closely related class of compounds are DES. They are defined as a mixture of two compounds that has a lower melting point than their isolated components. For ILs, the lowered melting point of the ionic pair came from the large size and conformational flexibility of the ions.[85] This leads to small lattice enthalpies and large entropy changes that favor the liquid state. As for DES, the increased hydrogen bonding interaction is the reason for the formation of the eutectic mixture. Upon mixing the right combination of hydrogen bond donor and acceptor (HBD and HBA), a eutectic mixture is formed, resulting from the increased hydrogen bonding. This comes with a great practical advantage, as the simple mixing of the HBD and HBA is usually enough to make a DES.[86] Furthermore, most HBDs can be naturally-occurring alcohols or polyols, while most HBAs are amino acids or ammonium derivatives. Yet again, to the best of our knowledge and according to the most recent reviews on organic reaction conducted in DES, carbonyl hydrogenation has not been explored in this context.[87-88]

1.4.2 H_2O

H_2O as a solvent. For a long time, H_2O as a solvent has been deemed as unsuitable for organic chemistry, due to the low solubility of most organic compounds in aqueous solutions. Yet, most reactions in nature take place as aqueous enzymatic processes. Breslow et *al.* made a first breakthrough in 1980 by showing that Diels-Alder reactions proceeded *faster* in H_2O than in

less polar organic solvents.[89] Indeed, they observed up to 700-fold increase in the reaction rate by switching the solvent from iso-octane to H_2O for the cyclization of cyclopentadiene with butanone.

Later on, the same group exploited the hydrophobic effect to tune the selectivity of $RLiBH_3$-mediated reduction of ketones in water (R = H, Ph, C_6F_5).[90] The authors mixed aromatic and aliphatic ketones, showing the "salting out" effect in water by adding NaCl or LiCl salts, and using a bulkier aromatic ring, or using a hydrophobic reducing agent such as C_6F_5-$LiBH_3$ would all contribute to increasing the selectivity towards the more hydrophobic aromatic ketone (Scheme 25). In the best case, using a naphthyl-substituted ketone and C_6F_5-$LiBH_3$ in LiCl/D_2O gave a 95:5 selectivity against the corresponding methyl-substituted ketone. The reaction was also greatly accelerated, with a 40-fold rate increase compared to a classical $LiBH_4$/MeOH setup. Conversely, adding salts such as $NaClO_4$ or guanidium chloride, or using MeOH as a solvent decreased hydrophobic interactions and chemoselectivity alike. The same trend was observed in intramolecular competition with a substrate bearing both functionalities.

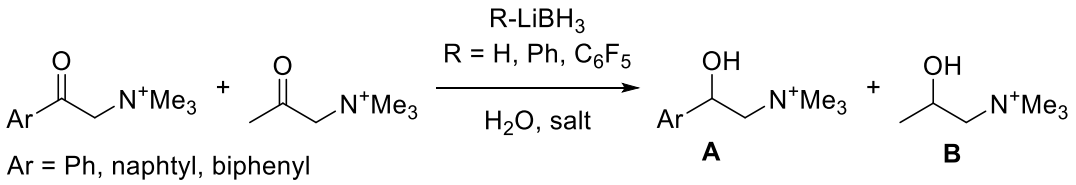

A/B ratio **increases**:
-with LiCl, NaCl salts
-with hydrophobicity of R-$LiBH_3$

A/B ratio **decreases**:
-with $NaClO_4$, guanidium chloride salts
-with MeOH as a solvent

Scheme 25. Hydrophobic effect on selectivity.

In 2005, Sharpless et *al.* noted an almost 300-fold rate acceleration of quadricyclane cycloaddition to dimethyl azodicarboxylate (DMAD) by switching from neat conditions to aqueous solutions (Scheme 26). Such observation shows that reaction rate acceleration does not just stem from a higher substrate concentration (in neat conditions), but also from the presence of H_2O itself.[91]

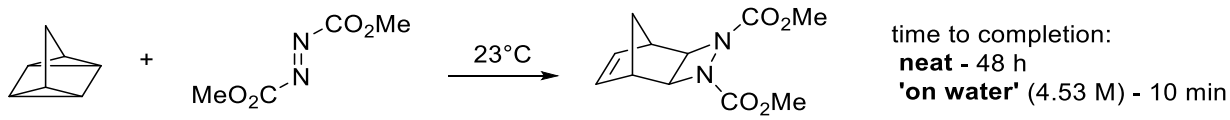

Scheme 26. 'On water' effect.

The authors coined the term 'on water' to describe the reaction conditions, a vigorously stirred aqueous suspension possessing an oil–water interface. Still, the explanation for this accelerated

reaction rate remained unclear. Shen et *al.* analyzed by surface vibrational spectroscopy H_2O-hexane and H_2O-air interfaces, showing that in all cases, about 25% of surface water molecules at the hydrophobic interface have one dangling -OH group.[92] These bonds are not H-bonded to other H_2O molecules, protruding into the hydrophobic phase unlike the other -OH group of the same molecule. Thus, Marcus et *al.* suggested that these dangling bonds could decrease activation barriers in Sharpless' report, effectively showing experimentally and theoretically that H_2O acted as a catalyst.[93] More generally, the authors suggested that the 'on water' effect will benefit any transition state that is more H-bonded to the surface H_2O than the reactants are. Interestingly, Sharpless' reaction exhibited a strong isotopic effect, with a 4.5-fold decrease of the reaction rate when D_2O was used instead of H_2O.

Using surfactants in H_2O. The water-organic layer interface can be further mediated using surfactants. Above a certain critical micelle concentration (cmc), small supramolecular structures (<100 surfactant molecules) form by aggregation around hydrophobic droplets. These assemblies are in thermodynamic equilibrium through monomer exchange, with a typical lifetime on the order of 10^{-5}-10^{-6} s.[94] Akin to solvent-free conditions, surfactants allow a higher local concentration of substrate, but with the presence of surrounding H_2O for heat dispersion. In general less catalyst is required, and down to ppm levels of metals can be employed.[95] By tuning the charge number on the monomer (cationic, anionic or neutral), this allows water-insoluble products and metal complexes to be compatible with aqueous solutions.[96] After the reaction, minimal amounts of organic solvents are sufficient for product extraction, and the surfactants remain in aqueous phase ready for re-use. Overall, switching to micellar catalysis drastically reduces the E-factor of a reaction initially conducted in organic media, up to a tenth of its original value.[97] Conveniently, surfactants can be made from natural precursors such as vitamin E, sebacic acid, succinic acid, which means surfactant leaching or decomposition in H_2O poses no major environmental concern.

Denis et *al.* showed that aqueous solutions of glycosidic amphiphiles such as sucrose were able to increase regioselectivity of $NaBH_4$-mediated reduction of ketones (Scheme 27).[98] On α,β-enones, chemoselectivity to 1,2-addition typically ranged between 50:50 and 80:20 in MeOH solutions, while the addition of sucrose boosted selectivity up to 99:1.

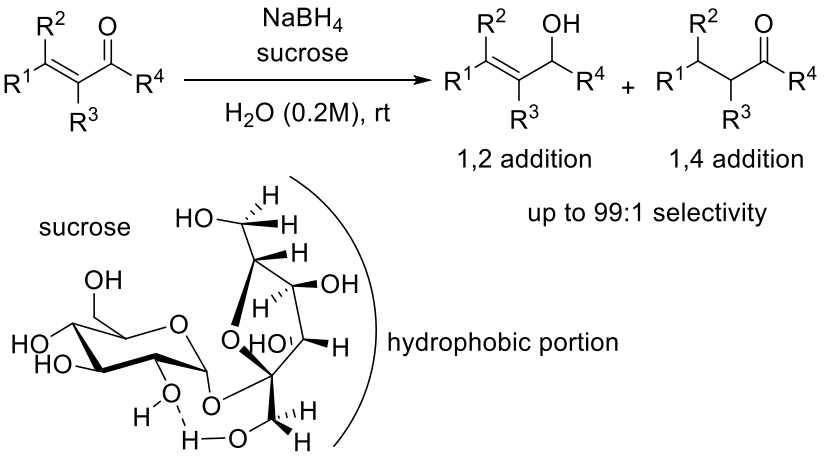

Scheme 27. Sucrose as amphiphilic species for $NaBH_4$ selective reduction of α,β-enones.

Akin to H_2O-based examples, surfactants have been applied for great effect on metal-catalyzed asymmetric ketone transfer hydrogenation. The Deng group functionalized TsDPEN ligand with -SO_3Na hydrophobic groups, showing that with $[RuCl_2(p\text{-cymene})]_2$ and sodium dodecyl sulfate (SDS) surfactant, aromatic ketones could be reduced in 80-94% ee in H_2O.[99] Ahlford et *al.* showed that the TsDPEN could be directly functionalized with an hydrophobic dodecylbenzenesulfonylated tail (Scheme 28).[100] In conjunction with $[Cp^*RhCl_2]_2$ the system proved successful for aromatic ketones (76-86% ee) and aliphatic ketones although less efficiently (40% ee in average). Upon functionalization of the diphenyl ligand with an hydrophilic group (-NMe^{3+}), the Deng group improved the ee's (72-94%, aliphatic included) compared to the previous system.[101] Lower temperature (-5 °C instead of room temperature) and longer reaction times (36-48h instead of 17h) were required to achieve full conversion.

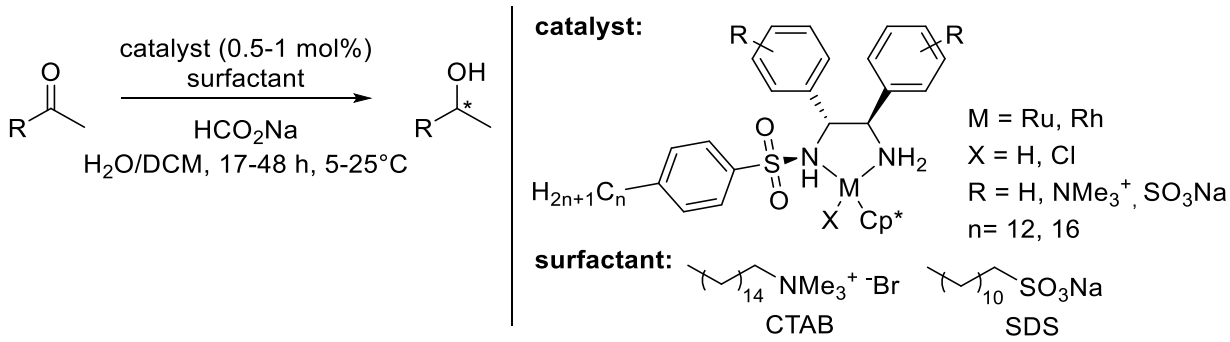

Scheme 28. Asymmetric transfer hydrogenation of carbonyls in water, using SDS-functionalized ligands.

By adding cetrimonium bromide (CTAB) as a surfactant and functionalizing the TsDPEN ligand with -SO_3Na hydrophilic groups, the same authors reduced the reaction time to 1 h while maintaining 85-97% ee's. Furthermore, the catalyst proved to be recyclable for at least 21 times.[102]

Water-soluble catalysts. Water-soluble homogeneous metal complexes are accessed by tuning of their ligands functionality. Indeed, hydrophilic groups such as $-SO_3^-$, $-CO_2^-$, $-NR_3^+$ can be easily grafted on aromatic rings present on most phosphine ligands.[103] These ionic functionalities can remain in their ionic form over a broad range of pH, and they do not bind to transition metals, thus avoiding the interferences with the catalytic activity. Thus, such catalysts allow an easy product separation while still keeping a high activity and tunability.[104] A typical example is the sulfonation of triphenylphosphine ligand, using oleum, yielding a water-soluble ligand (TPPTS) after treatment with NaOH (Scheme 29).

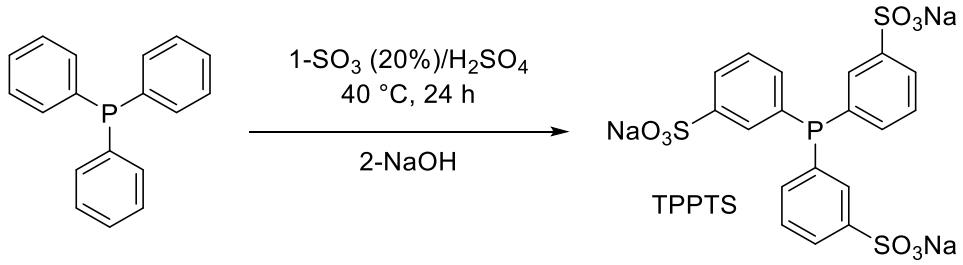

Scheme 29. A typical sulfonation of triphenyl phosphine.

The Ruhrchemie/Rhône-Poulenc process for propene hydroformylation constitutes the first successful commercial application of a water-soluble catalyst.[105] Using a 50-fold excess of TPPTS ligand, a water-soluble and recyclable Rh-based catalyst was developed for propene hydroformylation into butanal (Scheme 30). A plant was built in 1984 at Hoechst AG in Oberhausen (Germany) using this process, reaching an annual production of up to 500 000 tons of butyraldehyde.

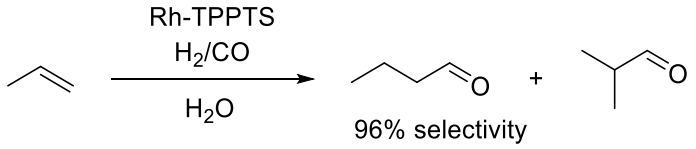

Scheme 30. Ruhrchemie/Rhône-Poulenc process for propene hydroformylation.

With the support of Rhône-Poulenc, Fache et *al.* performed early studies on the Ru-TPPTS system for aldehyde hydrogenation in water (Scheme 31).[106] Starting from $RuXY(TPPTS)_3$ complexes (X,Y = Cl, H, OAc), the addition of 10 mol% NaI under 50 bar H_2 leads to the generation of $RuHI(TPPTS)_3$, that was active for propionaldehyde reduction (with a 5-fold increase of the turnover frequency).

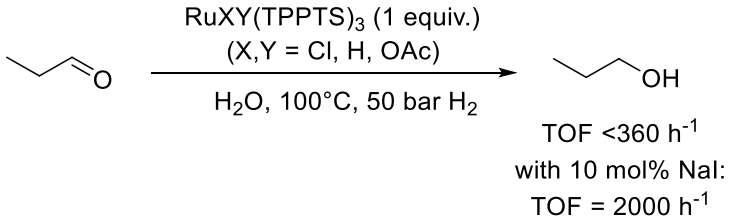

Scheme 31. Ru-TPPTS system for propionaldehyde hydrogenation in H_2O.

At the same time, Bényei et *al.* used $RuCl_2(TPPMS)_2$ (m-sulfophenyl diphenylphosphine) for aldehyde transfer hydrogenation in H_2O (Scheme 32).[107] The catalyst was stable to air conditions, and active for benzaldehyde derivative reduction, with the exception of ortho-substituted substrates.

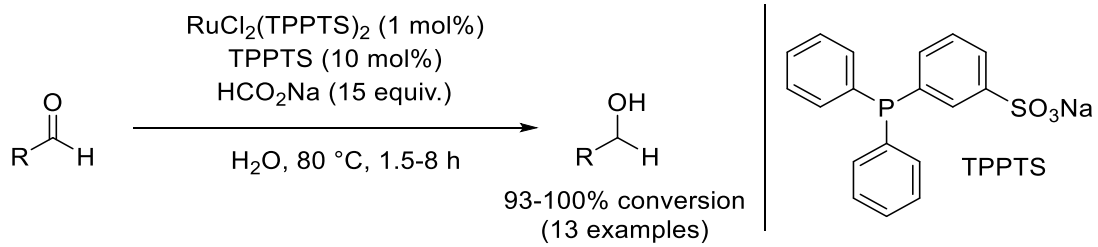

Scheme 32. Ru-TPPMS system for aldehyde transfer hydrogenation in H_2O using sodium formate.

Later on, the same authors showed that the Ru-TPPMS system was pH-sensitive, provided that an excess of ligand was present.[108] At lower pH (<5), $[HRuCl(TPPMS)_3]$ was predominant, while at higher pH (>9) $[H_2Ru(TPPMS)_4]$ was found to prevail. Interestingly, the catalyst had opposite selectivity on cinnamaldehyde hydrogenation, as the former was selective to C=C hydrogenation and the latter selective to C=O hydrogenation (Scheme 33). Adding a $NaHCO_3$ basic promoter (20-50 mol% to Ru) could even double the cinnamaldehyde conversion to cinnamyl alcohol.[109] The authors tested the system on alkynes as well, showing that the catalyst performed semi-hydrogenation at pH<3, and full hydrogenation at pH>9.[110] A similar pH-controlled complex was designed by Makihara, this time based on a $[Cp^*Ir^{III}(H_2O)_3]^{2+}$ complex.[111]

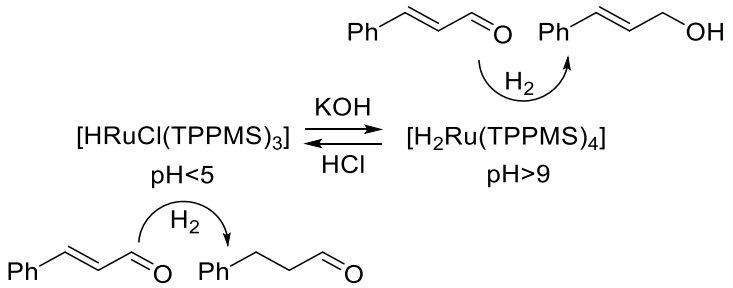

Scheme 33. pH-controlled selective hydrogenation using Ru-TPPTMS.

With these early examples, no recyclability study was performed despite being the greatest asset of hydrophilic complexes. In the second report though, sodium formate allowed milder reduction conditions due to its higher water solubility (14 M) compared to that of H_2 gas ($0.8.10^{-3}$M). Darensbourg et *al.* showed that Rh-1,3,5-triaza-7-phosphaadamantane (TPA) was a suitable hydrosoluble complex as well for the same reaction, with the added benefit of being recyclable without requiring an excess of ligand.[112-113] The authors could not exclude an heterogeneous mechanism for the reaction, as adding surface poisons such as Hg(0) and cyclo-octatetraene showed only partial poisoning.[114]

Grosselin et *al.* from Rhône-Poulenc company furthered the field by exploring Ru and Rh-catalyzed selective hydrogenation of α,β-unsaturated aldehydes in H_2O (Scheme 34).[115] The metals respectively enhanced selective C=O and C=C hydrogenation, with both catalysts easily separable from the product and re-used three times. The authors used a 5-fold excess of TPPTS ligand to enable a proper metal recyclability.

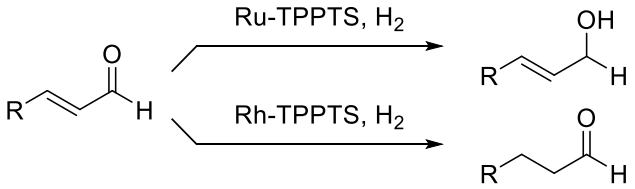

Scheme 34. Tunable hydrogenation selectivity using M-TPPTS systems.

Since 2014, H_2O has seen many applications in metal-catalyzed ketone asymmetric transfer hydrogenation (ATH) as reviewed by Wu et *al.*[116] Through the use of HCO_2Na as a traceless, hydrosoluble and cheap reductant, H_2O allowed the asymmetric reduction of a variety of prochiral ketones (Scheme 35). Up to 97% ee at 97% conversion could be afforded with $[Cp^*RhCl_2]_2$ and *N*-tosylated diphenylethylenediamine ligand (TsDPEN) for acetophenone reduction at room temperature.[117] For recyclability purposes, the ligand could be switched to a bpy-containing covalent triazine framework (CTF) support, at the cost of loss of chirality.[118]

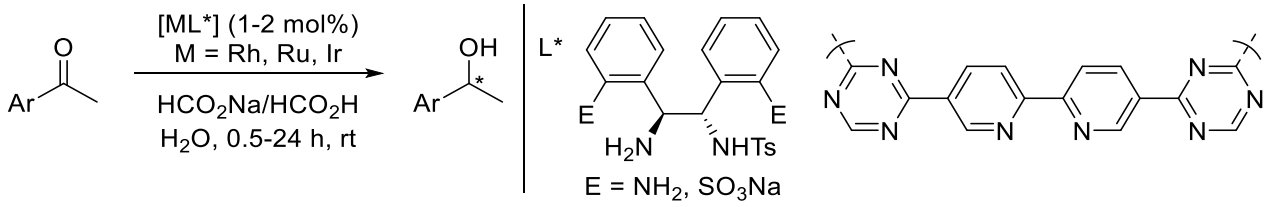

Scheme 35. Asymmetric transfer hydrogenation of carbonyls in water.

More recent developments were applied to LA hydrogenation, as shown by Delhomme et *al.* and Moustani et *al.*[119-120]

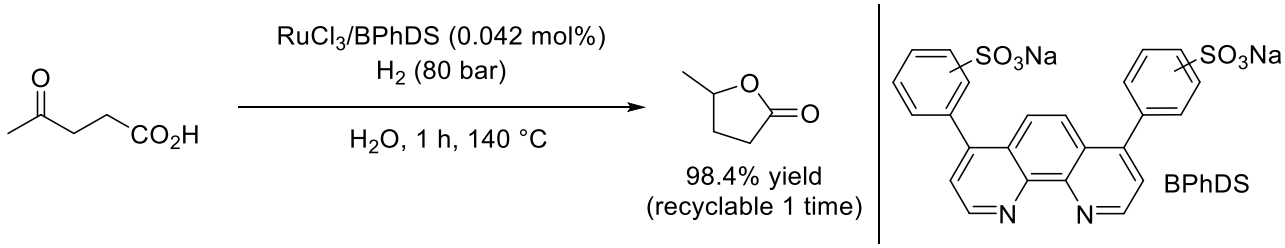

Scheme 36. LA hydrogenation by hydrosoluble Ru complexes.

1.4.3 Supercritical carbon dioxide

Supercritical fluids are substances at temperature and pressure above their critical point, where distinct liquid and gas phases no longer exist. The critical point of CO_2 is fairly mild (304K, 73.8 atm), and because of this, supercritical CO_2 (sCO_2) has been successfully used as a solvent substitute in organic reactions.[121] It has seen great applications in carbonyl reduction due to the innocuous nature and non-flammability of CO_2, the ease of post-synthesis removal, and notably the high miscibility of H_2 in sCO_2. Indeed at ambient temperature and atmospheric pressure, the molar solubility of H_2 in various solvents is as following: $0.8.10^{-3}$ M in H_2O, $1.95x10^{-4}$ M in EtOH, 2.64 $x10^{-4}$ M in acetone,[122] whereas H_2 is completely miscible with sCO_2, greatly limiting mass transfer issues compared to liquid phase.[123] For instance, the concentration of H_2 in a supercritical mixture of H_2 (85 bar) and CO_2 (120 bar) at 50 °C is 3.2 M, while the concentration of H_2 in THF under the same pressure is 0.4 M.[124]

The first examples of sCO_2 being used as a reaction medium were transpositions of the asymmetric hydrogenation of alkenes, using homogeneous chiral metal complexes by Burk et *al.* (Scheme 37).[125] At full conversion, enantiomeric excesses were similar or superior to the hexane or MeOH-based processes (up to 20% ee gain). In the case of heterogeneous Pt@Al_2O_3-catalyzed ethyl pyruvate hydrogenation though, Minder et *al.* showed that sCO_2 deactivated the catalyst.[126] Deactivation stemmed from the reduction of the CO_2 onto the catalyst surface into CO which is a known poison for metallic surfaces.

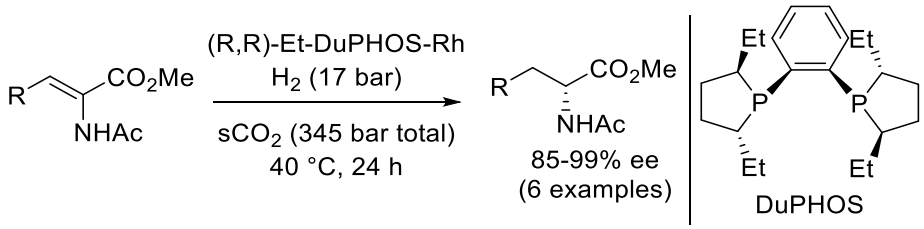

Scheme 37. Early examples of asymmetric hydrogenations in sCO_2.

In the case of α,β-unsaturated carbonyls hydrogenation, the Arai group successfully exploited sCO_2 as a medium for selective C=O/C=C using catalyst (Scheme 38).

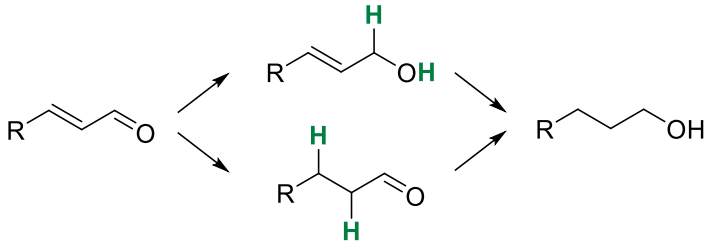

Scheme 38. α,β-unsaturated carbonyl hydrogenation pathways.

They first reported the unpromoted Pt@Al_2O_3 for selective C=O hydrogenation (Scheme 39).[124] Although conversions reported were lower than 80%, selectivity to the unsaturated alcohol was higher (71-92%) than in EtOH-based conditions (45-79%). The dielectric constant of CO_2 increases with pressure, making sCO_2 a polar solvent, which is the reason proposed by the authors for the selectivity increase.[127] The same group reported Pt@SiO_2 for the same process, although with inferior selectivity and activity.[128] As for Pd/C as a catalyst, they noticed reverse selectivity towards C=C bond hydrogenation.[129]

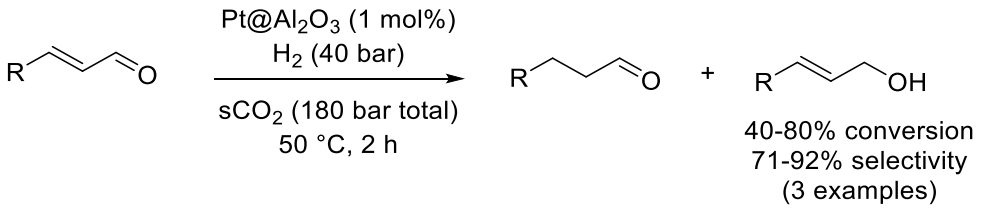

Scheme 39. Selective α,β-unsaturated carbonyls hydrogenations in sCO_2.

The Arai group explored homogeneous metal complexes as well for cinnamaldehyde hydrogenation in sCO_2. Typically, fluorinated ligands are known to provide a better solubility in sCO_2 than classical phosphines.[130] Using a fluorinated 1,2-bis(diphenylphosphino)ethane (F-dppe) ligand, selectivity was low towards C=O hydrogenation (31%), although with a significantly higher turnover in sCO_2 (690) than in classical solvents (320 in *i*PrOH).[131] By switching to bis(pentafluorophenyl)phenylphosphine, an almost full selectivity towards cinnamyl alcohol (98%) was observed (Scheme 40).[132] Under these conditions (160 bar CO_2/40 bar H_2, 50 °C) an important amount of H_2/CO_2-expanded cinnamaldehyde liquid layer was observed rather than having a purely supercritical CO_2 phase. This helped concentrating the cinnamaldehyde, which has been shown to be beneficial in maintaining high selectivity for C=O reduction.[14, 133]

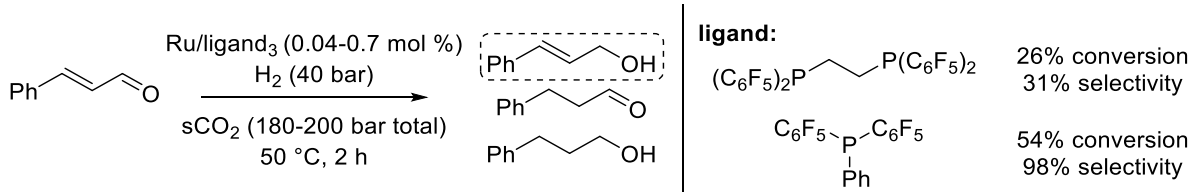

Scheme 40. Selective cinnamaldehyde hydrogenation in sCO_2 using homogeneous complexes.

Finally, the authors explored citral as a model substrate, using M/PPh_3 catalysts (M = Ru, Pd, Rh, Ni) (Scheme 41).[134] Using Ru, the major product was the C=O reduction product (65% selectivity), while with Pd they obtained the selective reduction of the neighbouring C=C bond (75% selectivity).

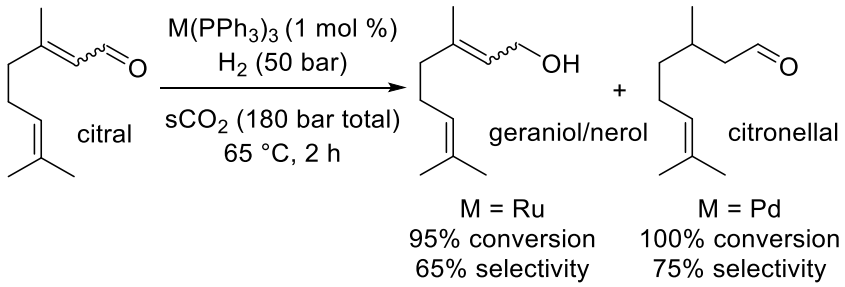

Scheme 41. Selective citral hydrogenation in sCO_2 using homogeneous complexes.

Chatterjee et *al.* explored the heterogeneous route for citral hydrogenation in sCO_2, employing bimetallic Pt-Ru NPs supported on a mesoporous silica support (Pt-Ru@MCM-48). In similar conditions than previously, monometallic Pt@MCM-48 was highly selective to C=O reduction (89% selectivity), while the bimetallic catalyst afforded a higher selectivity to C=C bond (67%).[135]

Li et *al.* exploited sCO_2 as a medium for Zn/H_2O-mediated reduction of aldehydes.[136] While former reports of the Zn/H_2O reducing system involved either Pd[137] or toxic $SbCl_3$ salts,[138] the simple decrease of pH (<5) of H_2O in presence of sCO_2 was sufficient to induce H_2O splitting and carbonyl reduction (Scheme 42).

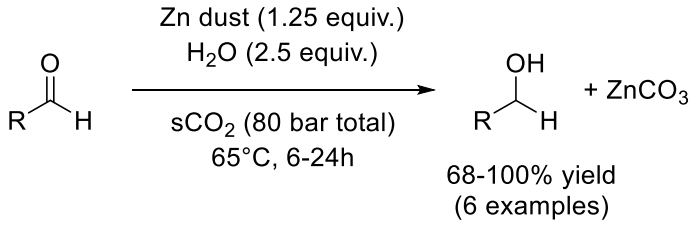

Scheme 42. H_2O/Zn as a reducing agent for carbonyls in sCO_2.

To conclude this section, the choice of a solvent is a key choice in the waste emission of a reaction. As much as the best solvent is 'no solvent', sometimes their use is unavoidable due to heat dispersion or mixing issue. Solvents must be chosen carefully, to positively affect not only the reaction rate but also selectivity, a major factor in C=O reduction. Alcohols, typically glycerol and *i*PrOH, have not been tackled in this section due to their reducing ability, and will be reviewed in section 1.6.1.

1.5 Catalysts

The principle of catalysis implies that catalysts do not get consumed at the end of a reaction, but rather remain active to engage into further reactive cycles. Practically though, they may by 'lost' in the sense that their separation from the product and reuse may be difficult and not cost effective. Not only it is problematic from an economical perspective, it causes toxicity issues in the final product, especially for most PGMs. Methods to allow low loadings of PGM have been described earlier in this chapter (see section 1.4.2). In industrial production of fine and bulk chemicals, heterogeneous catalysts are preferred due to their easy recyclability, although it comes with a lower activity and selectivity compared to homogeneous complexes. In high-added value synthesis such as pharmaceutical compounds, the use of homogeneous catalysts remains essential. Nonetheless, efforts towards diminishing metal loading or shifting to base metals are on the rise.[139] From these constraints, the following challenges should be addressed from *both* sides of catalysis:

-Improve post-reaction separation and recyclability. This is also possible on homogeneous catalysts, for example by using hydrosoluble complexes,[104] or IL-soluble complexes.[140]

-Further investigate base metal catalysis. Indeed, base metals such as Co, Cu, Fe, Ni and Mn are more abundant than most PGMs but have remained comparatively underdeveloped.[141-142]

-Maintain a high level of activity and selectivity. In the context of carbonyl reduction, this means that investigation on C=O/C=C selectivity, low H_2 pressure and/or mild reductants should be further pursued.[143]

1.5.1 Base-metal catalysts

Iron. The Knölker complex is the direct analogue of the famed Shvo complex, by replacing the Ru center with Fe (Scheme 43). In both cases, the hydroxycyclopentadienyl ligand plays a key role, as it assists the metal center for heterolytic splitting of H_2.[144] Indeed, the ligand is in equilibrium with the η^4-cyclopentadienone form (right hand side of Scheme 43) that has a basic

character, thus binding H^+. The Fe center can then bind a H^- species, enabling the hydrogenation of polar C=X bonds (X = O, N).

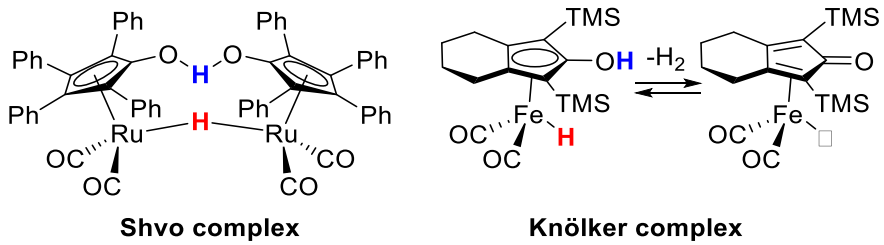

Scheme 43. Shvo and Knölker complexes.

The metal complex synthesis proceeds through a convenient [2+2+1] cyclization between $Fe(CO)_5$ and the corresponding diyne or alkynes (Scheme 44).[145] Then, by sequential treatment with NaOH then H_3PO_4 the complex is transformed in its reducing form.[146] For alcohol oxidation purposes, Me_3NO can be used to simply remove a CO substituent, making an hydrogen-accepting complex.[147]

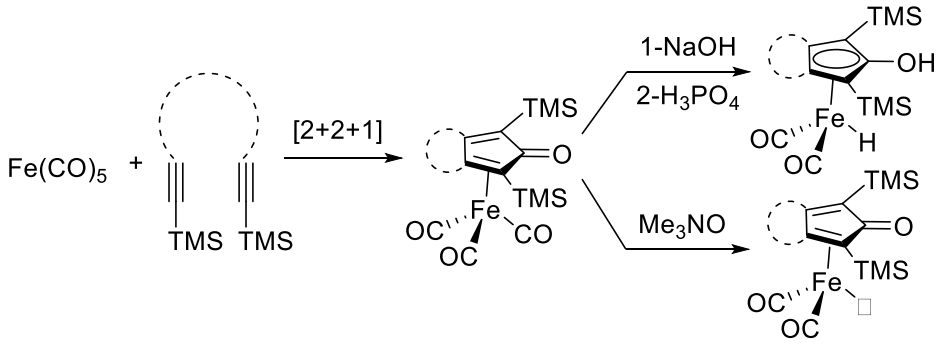

Scheme 44. Knölker complex preparation.

Naturally, this polar complex was found to be particularly effective for carbonyl hydrogenation, as shown first by Casey and Guan.[148] In this seminal report, the authors managed to reduce a whole range of 16 carbonyls at room temperature and 3 bar H_2 (Scheme 45). It was active as well for transfer hydrogenation using *i*PrOH, and for both cases it was chemoselective against epoxides, esters, and alkynes. However in the case of α,β-unsaturated carbonyls 50% of C=C hydrogenation was observed as well.

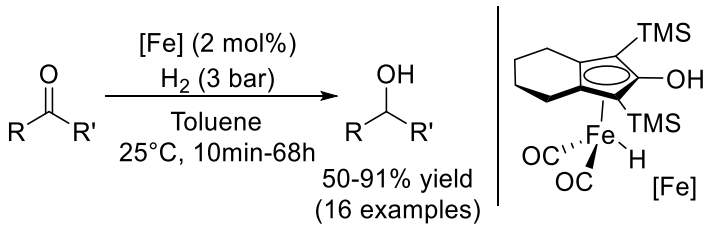

Scheme 45. Knölker complex for carbonyl hydrogenation.

Fleischer et *al.* solved the chemoselectivity problem by using the non-activated form of the complex, which proved to be simpler to handle since it is stable to air and H_2O (Scheme 46).[149] In order to activate it, minute amounts of K_2CO_3 were able to induce the selective C=O reduction of α,β-unsaturated aldehydes in low metal loadings (<1 mol%). Although harsher conditions were required (30 bar H_2, 100 °C), even sterically hindered aliphatic ketones such as 4-heptanone gave high yields (76-98% yield).

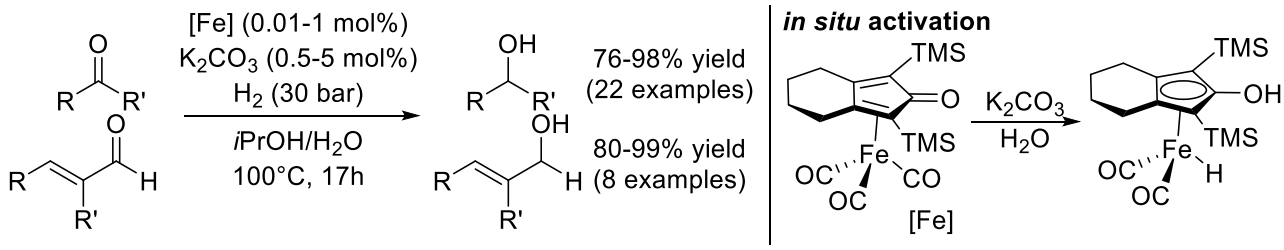

Scheme 46. *In situ* activation of Knölker complex for chemoselective hydrogenation of carbonyls.

In parallel to the Knölker complex, PNNP pincer ligands have seen a synchronous development, fostered by the Morris group.[150] Exploring a tetradentate diiminodiphosphine scaffold, they released the first example of Fe-catalyzed transfer hydrogenation of prochiral ketones,[151] quickly followed by an improved complex with a less constrained PNNP ligand scaffold (Scheme 47).[152] Their complexes were both inactive for H_2 activation, although showing high activity for transfer hydrogenation over a large range of ketones (up to 4900 h^{-1} TOF for 2-aceto-naphthone).

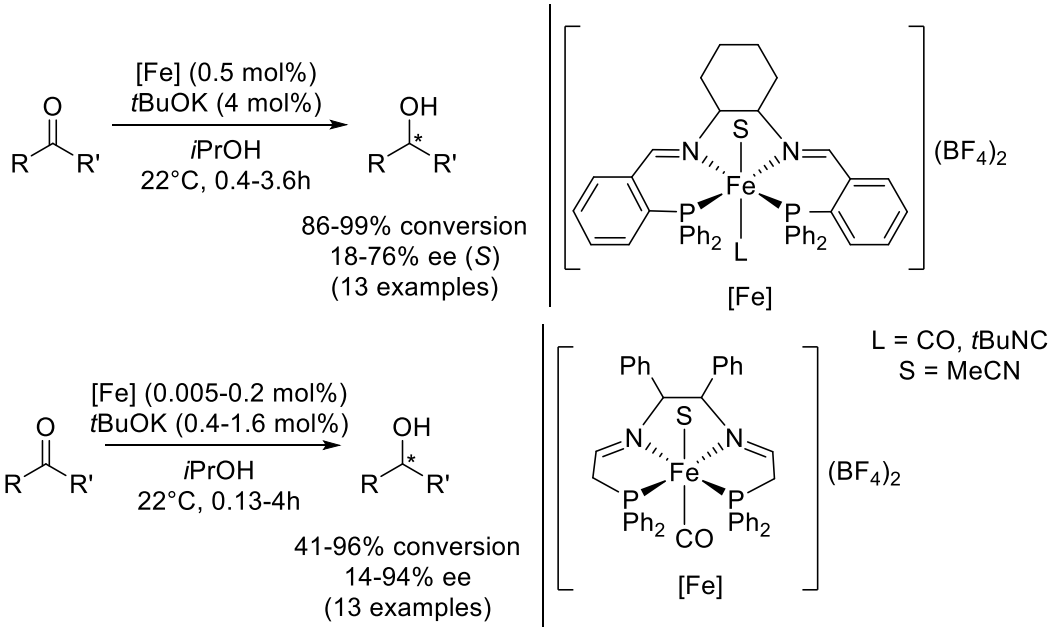

Scheme 47. PNNP-Fe-catalyzed asymmetric transfer hydrogenation of prochiral ketones.

The mechanism of the reaction remained unclear for the first report, as the authors were not able to isolate an amine intermediate. It was hypothesized that such an intermediate would be generated from the heterolytic splitting of H_2 over a Fe-N bond, resulting in the reduction of the imine C=N bond, similar to what could be expected from the Ru analogues.[153]

Four years later they identified the formation of Fe(0) NPs during the reaction, surface-functionalized with the PNNP pincer ligands.[154] This mechanism offers an explanation for the induction period observed experimentally. Using 10% of PMe_3 as a surface poison was enough to shut down the reaction, proving both a heterogeneous mechanism and suggesting that 10% of the total Fe amount was present on the surface of the NPs. By scanning transmission electron microscopy (STEM) analysis of the dried solution after reaction, they observed clusters of Fe NPs (4.5 ± 1.2 nm), further confirmed by energy dispersive X-ray spectroscopy (EDX). Finally, they made a polymer-bound substrate, by covalently grafting benzaldehyde on a Wang resin. They carefully tuned the pore size so that the Fe NPs could not pass through, showing indeed a shutting down of the reaction (Scheme 48).

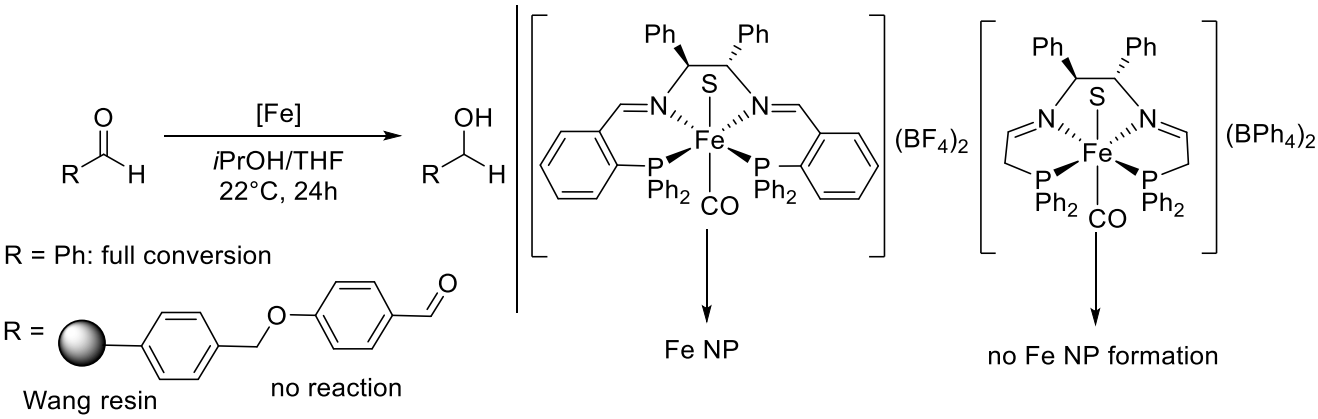

Scheme 48. Mechanistic investigation on Fe-PNNP-catalyzed carbonyl transfer hydrogenation.

Based on these characterization techniques, the Morris group eventually showed that the less constrained scaffold used in their second report did not form Fe NPs.[155] In contrast, Kelsen et *al.* showed the decomposition of $(Fe(N[Si(CH_3)_3]_2)_2)_2$ could yield small Fe NPs as well, but gave negligible activity towards C=O hydrogenation compared to C=C reduction.[156]

Weber et *al.* used a hydrophobic polar IL/*n*-heptane system as a reaction medium for their N,N,N tri-coordinating pincer Fe catalyst.[157] In their design, the catalyst is dissolved in the IL phase, while the products remain in heptane, allowing easy separation (Scheme 49). Their

catalyst proved to be recyclable twice, with a severe yield drop (50% of its original value) upon the third cycle.

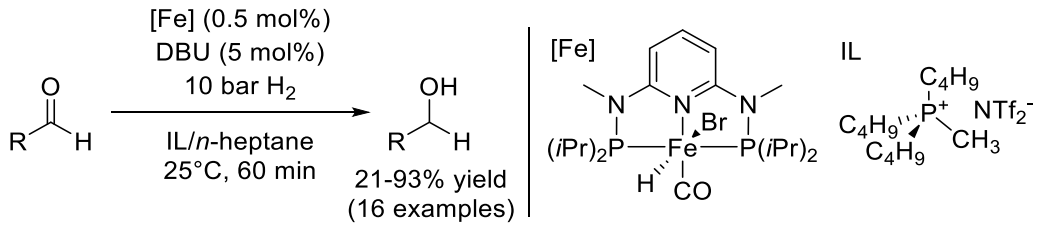

Scheme 49. IL/*n*-heptane biphasic solution for Fe-catalyzed aldehyde hydrogenation.

Copper. Adkins and Connor reported in 1931 a copper chromite hydrogenation catalyst, that later on will be named after Adkins (Scheme 50).[158] By heating $Cu(OH)NH_4CrO_4$ using a Bunsen burner, they obtained $Cu_2Cr_2O_5$, a catalyst active for hydrogenation of various unsaturated compounds ($-NO_2$, C=O (esters and carbonyls), C=N, C=C). In most cases, they observed the quantitative conversion of the substrate (0.11-2.2 equiv. of Cu, >100 bar H_2, >150 °C) into the corresponding alcohols with some substrates reacting instantly and exhibiting an exothermic profile (with up to a 15 °C over heating). A few different synthesis methods have been reported around the same time by other authors, all based on the decomposition of $Cu(OH)NH_4CrO_4$. Adkins identified that heating of the precursor must be kept under 400 °C to ensure high catalytic activity. The material acted as a 'hydrogen sponge', adsorbing up to 150 mL of H_2 per gram of catalyst after exposure to 250 bar H_2 at 100 °C, making it pyrophoric.[159]

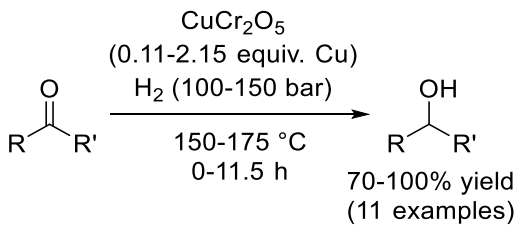

Scheme 50. Former report of Adkins catalyst.

$Cu_2Cr_2O_5$ has a poor selectivity towards C=O hydrogenation α,β-unsaturated carbonyls, as shown by Hubaut et *al*.[160-161] The C=C hydrogenation product is first formed, followed by isomerization into the allylic alcohols, resulting in a formal 1,4-addition overall (Scheme 51). In contrast, its selectivity towards monohydrogenation of dienes was excellent, as only the least sterically hindered alkene gets reduced. Jenck et *al*. showed that when the C=O and the C=C are not conjugated though, C=O hydrogenation was predominant.[162]

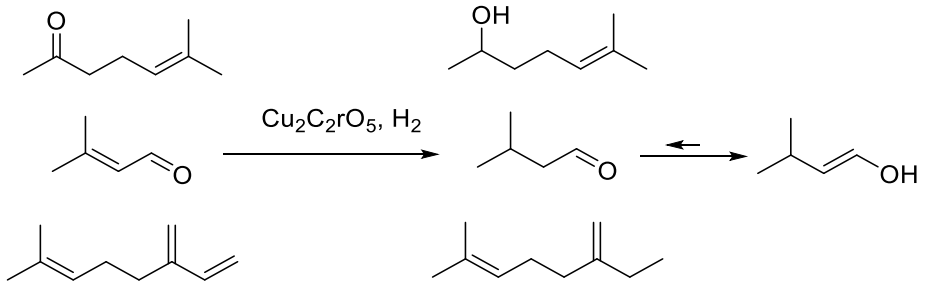

Scheme 51. Hydrogenation selectivity trends with $Cu_2Cr_2O_5$.

Huang et *al.* supported Adkins catalyst on TiO_2, *via* sonication of $K_2Cr_2O_7$ and $CuAc_2$ in the presence of Ti(*i*PrO)$_4$.[163] Upon calcination at 500 °C for 3h, they obtained an active catalyst for furfural hydrogenation at 140 °C. Comparatively, unsupported Adkins catalysts were inactive at the same temperature (Scheme 52).

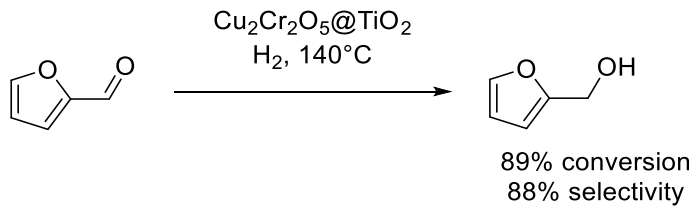

Scheme 52. Adkins catalyst supported on TiO_2 for furfural hydrogenation.

Gutiérrez et *al.* prepared Cu NPs by reducing $CuCl_2$ with Li salt and 4,4-di-tert butylbiphenyl in THF.[164] The naked Cu NPs had a high selectivity towards C=O hydrogenation on cinnamaldehyde (87% at 90% conversion). Upon supporting the Cu NPs on CeO_2, they attained a 72% selectivity (at 30% conversion) on crotonaldehyde C=O hydrogenation.

A few homogeneous Cu complexes have been developed as well. Stryker and co-workers reported a phenyldimethylphosphine-stabilized copper(I) hydride complex, that could be either pre-synthesized or made *in situ* for carbonyl hydrogenation. Interestingly in the case of α,β-unsaturated carbonyls, the selectivity could be tuned through the ligand (Scheme 53).[165] With no ligand, C=C reduction got predominant (91% selectivity) while $PhPMe_2$ enhanced C=O reduction (92% selectivity). When Ph_3P was used, both bonds were reduced (92% selectivity).

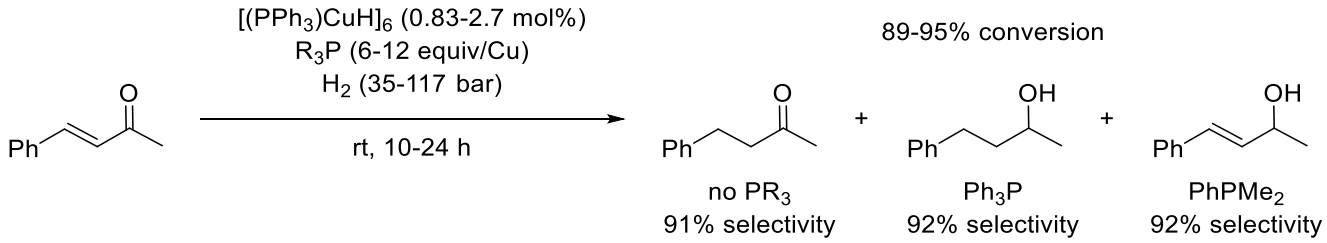

Scheme 53. Tunable hydrogenation selectivity of $[(Ph_3P)CuH]_6$.

The authors further proved the high selectivity of their catalytic system against C=C bonds, as well as its stereospecificity on decalin and steroidal derivatives (Scheme 54).[166]

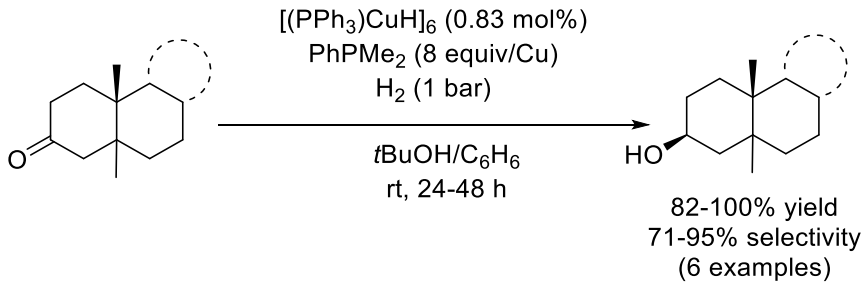

Scheme 54. Stereospecificity of $[(Ph_3P)CuH]_6$.

Cu can be functionalized using chiral ligands for prochiral ketone selective reduction using silanes or H_2, as shown respectively by Sirol and Shimizu.[167-168]In the former example, the catalyst was made *in situ* from CuF_2 and (*S*)-BINAP, and the presence of air proved to beneficial to its activity as it allowed using 1 mol% instead of 4 mol% catalyst for full conversion. Notably, their most active silane was $PhSiH_3$, but PMHS or $Me(OEt)_2SiH$ were also suitable reductants, although much slower, with up to 6 times longer reactions.

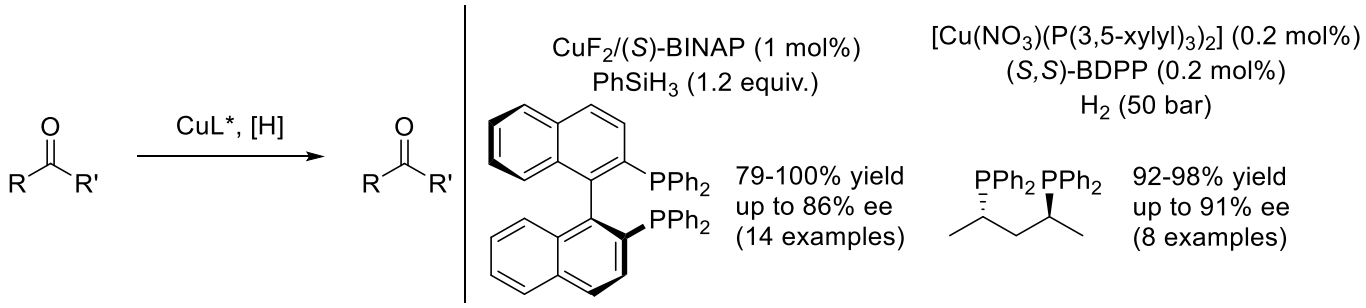

Scheme 55. Chiral reduction of carbonyls catalyzed by Cu complexes.

Cobalt. The earliest example of carbonyl hydrogenation involving Co was reported by Kazuhiko et *al.* in 1969.[169] By impregnating Fe as a promoter on a Raney Co (up to 0.5 mmol/g Co), the authors observed up to 90% hydrogenation selectivity towards the C=O reduction of 2-methyl-pentanal (Scheme 56). Upon absorbing on a metal surface, a promoter acts as a surface poison and thus affects a catalyst's selectivity. In C=O hydrogenation, generally the promoter is an electron-poor metal that can enhance C=O adsorption through a metal-oxygen interaction. Later on the authors tested other metal chlorides (Co, Mn, Ni and Pd) as promoters, showing that $NiCl_2$ was able to both slow down C=C reduction and accelerate C=O reduction rate.[170]

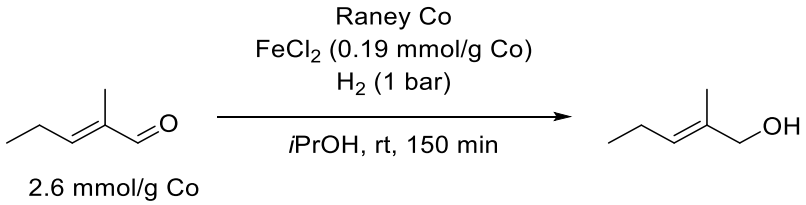

Scheme 56. Raney Co-catalyzed hydrogenation of 2-methyl-pentanal.

In contrast, Goetz et *al.* noted that $HCo(CO)_4$ complexes had a higher selectivity towards C=C reduction.[171] Nitta et *al.* explored more chlorides promoters (Cr, Cu and Ru) as well as acetates (Cd, Zn, Co) deposited on cobalt boride catalysts (Co-B), this time showing that $CrCl_3$ enabled a 90% selectivity for cinnamaldehyde C=O hydrogenation.[172] Chen *al.* furthered studied Co-B and Ni-B as hydrogenation catalysts, prepared by the reduction of $Co(OAc)_2$ or $Ni(OAc)_2$ with $NaBH_4$ in H_2O (Scheme 57).[173] Co-B and Ni-B had a complementary selectivity towards cinnamaldehyde reduction, with the former reducing C=O bonds (97% selectivity) and the latter selectively reducing C=C bonds (75% selectivity). The authors explored the addition of various atomic promoters adsorbed on the catalyst surface, showing that Th was able to increase both selectivity to C=O hydrogenation and activity (up to 90% selectivity at 90% conversion).[174]

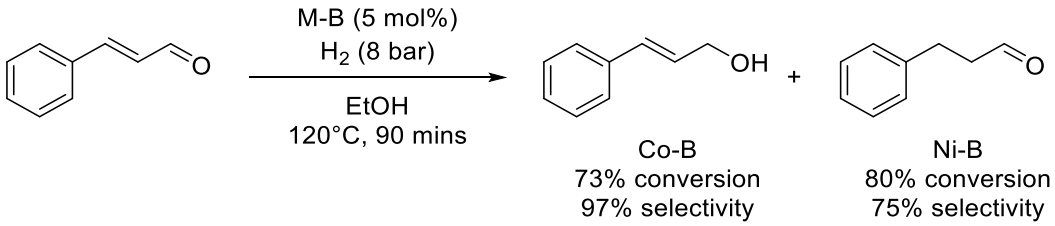

Scheme 57. Complementary selectivity for cinnamaldehyde hydrogenation.

In the 2010s the Hanson group explored homogeneous Co complexes for olefin and carbonyl hydrogenation in a series of three reports. They first showed that Co(II)-bis[2-(dicyclohexylphosphino)ethyl]amine ($PNHP^{Cy}$) were able to reduce olefins and carbonyls in mild conditions (<4 atm H_2, <60 °C, Scheme 58).[175] Although the catalyst could not discriminate against C=C bonds, the system was tolerant to caroboxylates and minute amounts of H_2O (10 mol%). Finally, they showed that their catalyst was competent for transfer hydrogenation in *i*PrOH as well.[176]

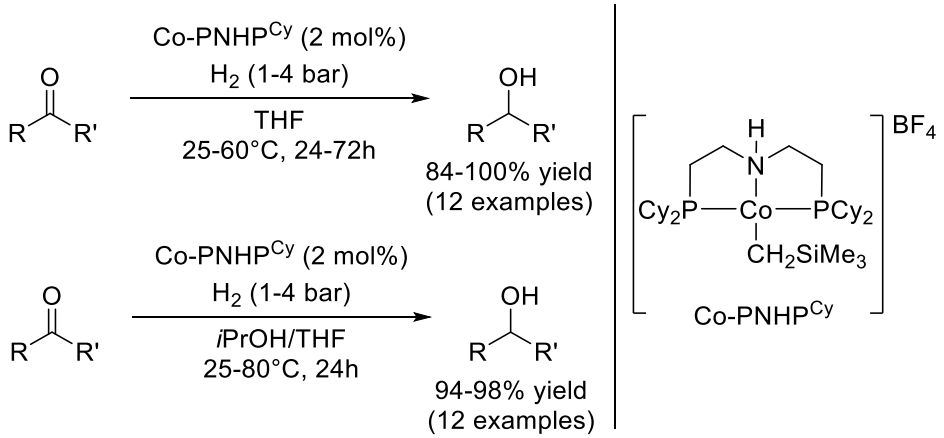

Scheme 58. Co-PNHP^{Cy} ligand pincer – former reports by Hanson group.

The authors conducted further scrutiny of the reaction mechanism, showing a ligand-metal cooperation for H_2 activation. Indeed, by substituting the N-H bond with a N-Me bond (Co-PNMeP^{Cy}), acetophenone hydrogenation was totally suppressed (Scheme 59).[177]

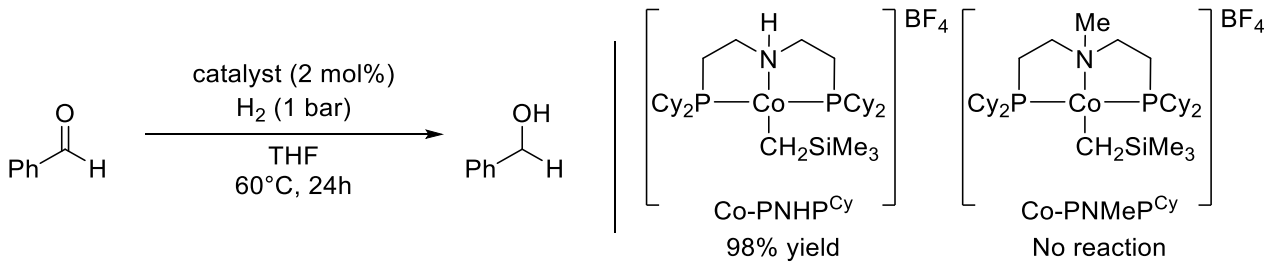

Scheme 59. Co-PNHP^{Cy} and Co-PNMeP^{Cy} – mechanistic studies.

Manganese. Homogeneous Mn has seen tremendous developments in the last two years, since a breakthrough by Beller and co-workers in 2016.[178] Using an air-stable PNP pincer ligand complex (Scheme 60), they managed to reduce a range of nitriles and carbonyls in high yields (92-99% yield for carbonyls). Interestingly, citral was reduced selectively at the carbonyl position (69% isolated yield). The authors tested 5-HMF hydrogenation was well, though the reduction product decomposed during isolation (26% loss, 64% isolated yield).

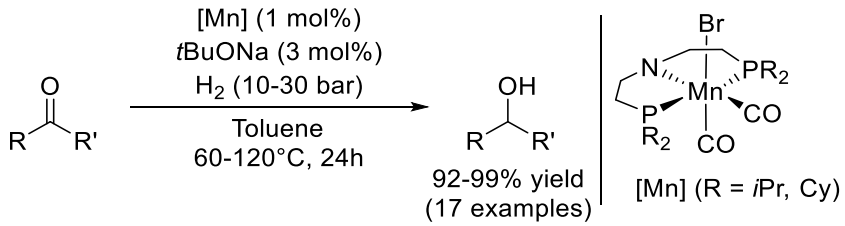

Scheme 60. Mn-PNP ligand pincer – former report by Beller group.

Due to the abundance of Mn (the third most abundant transition metal in the Earth's crust after Fe and Ti), their report triggered a tremendous development of Mn-catalyzed hydrogenation

soon after.[179] Furthermore, Mn contamination limit in pharmaceutical compounds is 250 ppm compared to 10 ppm for Ru. Within the next two years (2016-2018), ten reports were published on that subject. The Kempe group used a triazine-based PNP pincer ligand, affording milder conditions than in Beller's report (20 bar H_2, 80 °C).[180] Kirchner and co-workers opted for an aminopyridine-based pincer, alleviating the need of a base and allowing room temperature conditions at low loadings (0.05-0.1 mol%), although at 50 bar H_2.[181] Lastly, Sortais used a bidentate PN ligand, with KHMDS as an activator (Scheme 61).[182]

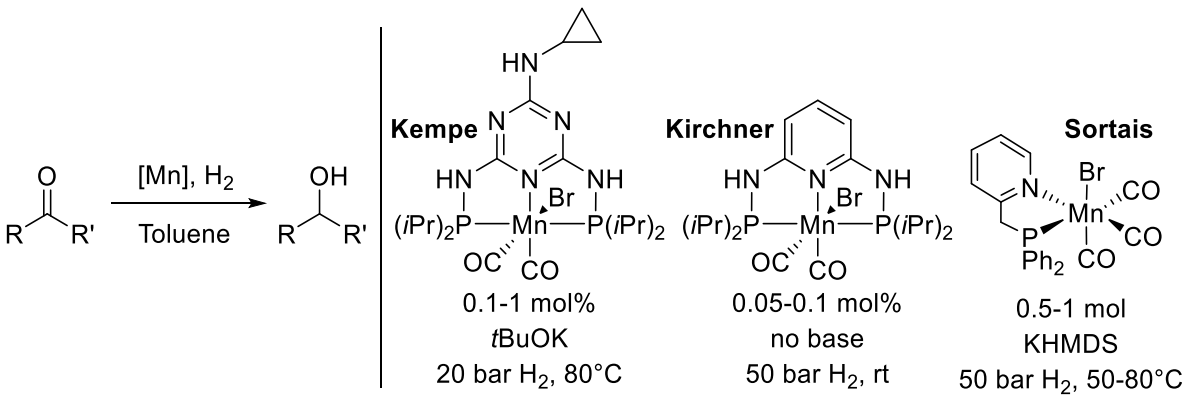

Scheme 61. Variants of the Mn-PNP system for carbonyl hydrogenation.

It appeared that no phosphine was required in Mn-catalyzed transfer hydrogenation of ketones using *i*PrOH examples were reported (Scheme 62). Yet, the introduction of phosphine moieties within a ligand design greatly increases its price, superseding the price tag of the metal itself. This calls for the design of simpler, phosphine-free ligands. Beller and co-workers transposed their system to a N,N,N pincer ligand, using *t*BuOK as an activator.[183] The Sortais group reported an aminopyridine bidentate ligand, exhibiting an extremely high activity (2000 TON, 3600 h^{-1} TOF).[184] Then, the Leitner group reported an aminotriazole ligand for Mn, that was made by click cyclization.[185]

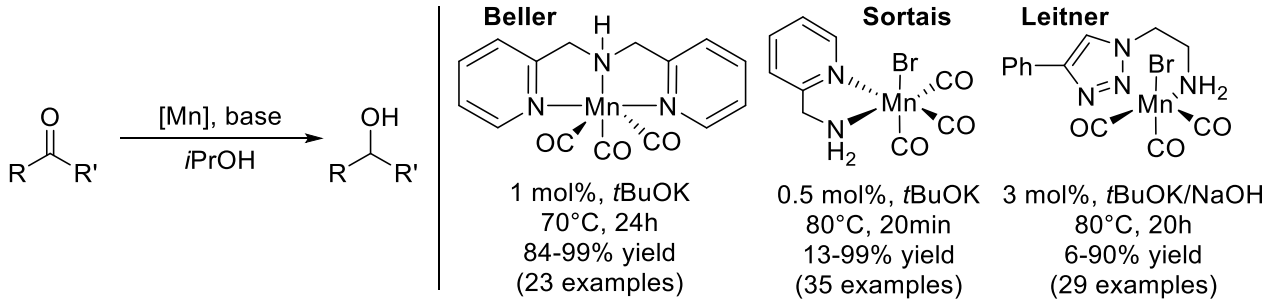

Scheme 62. Phosphine-free, Mn-catalyzed transfer hydrogenation.

Chiral variants were also developed by diverse research groups (Scheme 63). The Clarke group reported a ferrocene-containing chiral PNN ligand, applied with great success to prochiral

ketones in EtOH.[186] Their catalyst was further explored for ester hydrogenation to primary alcohols. Beller et *al.* modified their previous complex (see Scheme 60) by functionalizing the phosphines groups with (2R,5R)-2,5-dimethylphospholane cycles.[187] Notably, their catalyst proved to be more enantioselective on aliphatic ketones (30-84% ee) than on aromatic ones (1-80%).

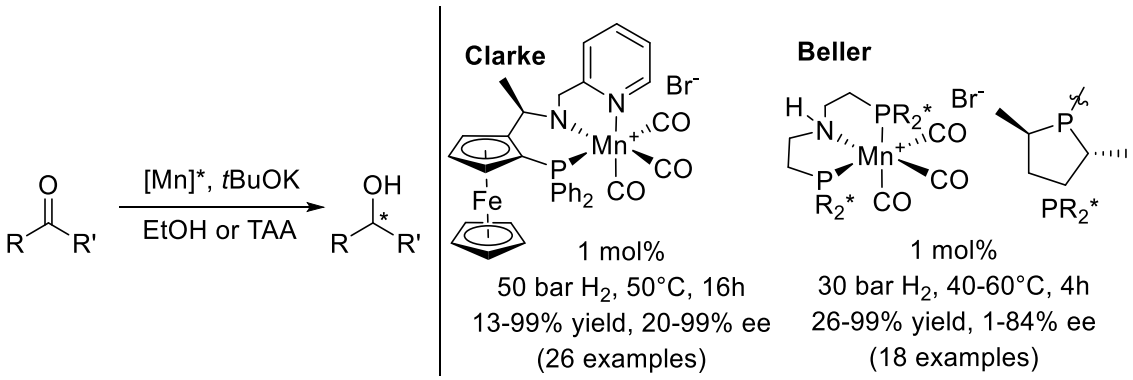

Scheme 63. Chiral Mn-catalyzed hydrogenation of prochiral ketones.

Kirchner and co-workers reported a PNP neutral complex for asymmetric transfer hydrogenation, although with lower enantioselectivity than previous examples (85% ee at most).[188] Finally, the Sortais group explored chiral diamine ligands, also suitable for the same process (Scheme 64).[189]

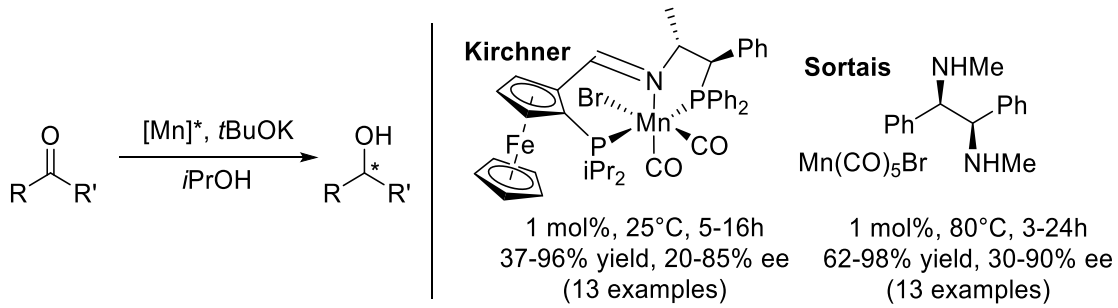

Scheme 64. Chiral Mn-catalyzed transfer hydrogenation of prochiral ketones.

These few examples published in only 2 years reveal the scientific excitement around Mn-based complexes. With common features such as low metal loading (<1 mol%) and relatively mild conditions (25-80 °C usually), Mn coupled with pincer ligands show a great potential in ketone reduction. Additional developments such as phosphine removal, chirality and transfer hydrogenation reports reinforce the relevance of this concept.

Nickel. Early mentions of Ni(II) salts for carbonyl transfer hydrogenation were reported with *i*PrOH by Le Page, Phukan, and Iyer et *al*. In the first study, the authors used simple $NiBr_2$ salts in NaOH/*i*PrOH and reduced a small scope of ketones in high yields (73-100% conversion), as

well as oct-1-ene (quantitative reduction in 30 min).[190] Phukan et *al.* used a macrocyclic ligand to chelate Ni(II), showing that HCO_2H/HCO_2NH_4 were suitable reducing agents as well for the process.[191] Finally, Iyer et *al.* used 2 equivalents of PPh_3 as ligands, showing additionally that the catalyst was fully selective for cinnamaldehyde C=O reduction.[192]

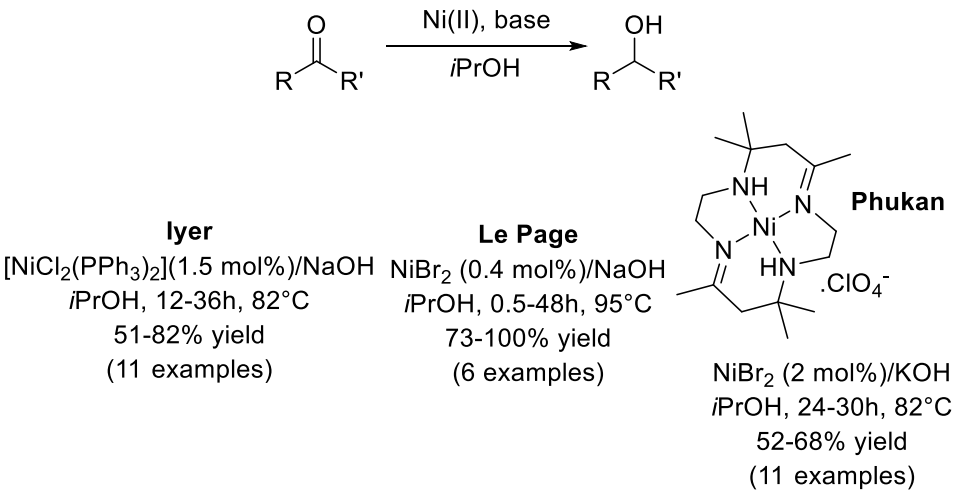

Scheme 65. Early examples of Ni(II)-catalyzed carbonyl transfer hydrogenation.

Contrary to Fe and Mn, Ni for carbonyl hydrogenation has then been massively investigated in the form of nanocatalysts rather than homogeneous complexes (Scheme 66).[193] Upadhya et *al.* made a Ni-doped zirconia ($Zr_{0.8}Ni_{0.2}O_2$), showing its potency on nitroarene reduction as well.[194] Mebane et *al.* showed that commercially available Raney Ni was competent for aliphatic aldehyde reduction, with the addition of a drop of HCl to accelerate 3-fold the reaction.[195] Alonso et *al.* prepared Ni(0) NPs by reduction of Ni(II) salts using Li in THF, with catalytic amounts of 4,4′-di-*tert*-butylbiphenyl. They were successfully applied to carbonyl reduction, with selectivity issues on benzylic substrates due to partial deoxygenation. Unlike the other examples, the catalyst did not require a base and despite not being magnetic, was shown to be recyclable 4 times without a yield drop.[193, 196] Shimura et *al.* supported Ni on ceria ($Ni@CeO_2$), again under base-free conditions due to the basic sites on CeO_2.[197] Upon 5 successful reuse cycles by centrifugation, the cumulated TON was 464, a value that is even superior to that of previous Ni NPs (<10). Finally, Escande et *al.* prepared EcoNi(0) from the thermal decomposition of a Ni hyperaccumulating plant, *Psychotria gabriellae*, found in New Caledonia.[198] The authors switched the typically used NaOH with Al_2O_3 and although the catalyst was not recyclable, it could be regenerated using an additional thermal treatment.

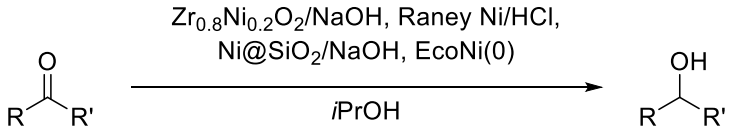

Scheme 66. Ni NPs-catalyzed carbonyl transfer hydrogenation.

1.5.2 Magnetic catalysts

A convenient method to simplify catalyst separation is to use magnetically recoverable NPs (MNPs).[199] A few different strategies exist around this concept: the MNPs can be used directly as catalysts for carbonyl reduction, or they can serve as support for other catalysts. This section is intertwined with the following section (see section 1.5.1) as the most commonly used magnetic supports/catalysts are Fe, Ni, and Co (both metals and oxides).

Kantam et *al.* showed that $CuFe_2O_4$ MNPs can be functionalized with a chiral ligand such as BINAP to serve for asymmetric reduction of carbonyls using PMHS.[200] After magnetic decantation, the catalyst could be re-cycled up to 4 times with no activity or enantioselectivity drop (Scheme 67).

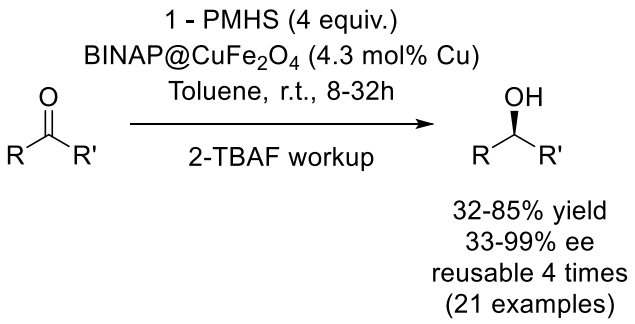

Scheme 67. BINAP-$CuFe_2O_4$ for chiral reduction of ketones.

Baig et *al.* worked on Ru grafting on a magnetic support. In the former case, the authors coated silica on a magnetite core, and grafted Ru NPs on the silica (Ru@SiO_2@Fe_3O_4).[44] The catalyst was active for carbonyl transfer hydrogenation in microwave, and easily recyclable up to 3 times (Scheme 68, top section).

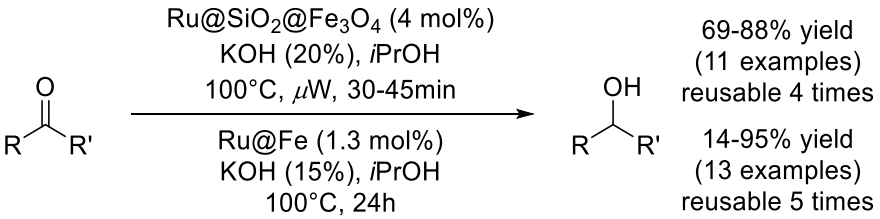

Scheme 68. Ru@SiO_2@Fe_3O_4 and Ru@Fe for carbonyl transfer hydrogenation.

Hudson et *al.* adopted a similar approach, though by directly grafting Ru NPs on Fe(0) NPs by galvanic reduction (Ru@Fe, Scheme 68, bottom section).[201] In convective heating conditions, reaction times were significantly longer (24h instead of 45 min) although a lower loading was required (1.3 mol% instead of 4 mol%).

Poly(ionic liquids) can be supported on Ni NPs, that were used as catalyst by Vijayakrishna et *al.* for base-free and transfer reduction of carbonyls in *i*PrOH (Scheme 69).[202] The PIL was tuned to carry a basic hydroxide group, while still allowing recyclability of the catalyst (up to 4 times with a 20% drop). Presence of H_2O in the reaction helped maintaining high activity due to the regeneration of the PIL. Furthermore, the catalyst proved to be 100% selective for C=O reduction of cinnamaldehyde.

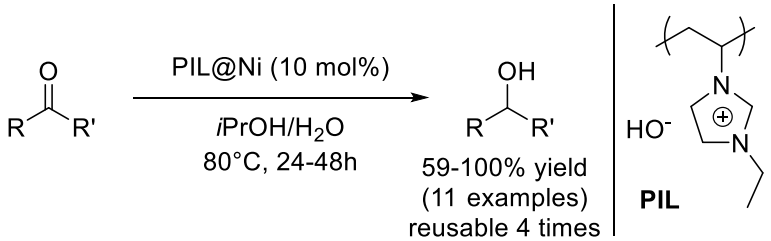

Scheme 69. PIL@Ni for carbonyl transfer hydrogenation.

Finally, Dasgupta et *al.* supported Ni(0) species on a Fe_3O_4 support, using 3-amino-4-hydroxybenzoicacid as a linker (Ni@AHBA@ Fe_3O_4).[203] Their catalyst proved to be active for carbonyl hydrogenation using glycerol as a solvent and reductant, and recyclable up to 7 times (Scheme 70).

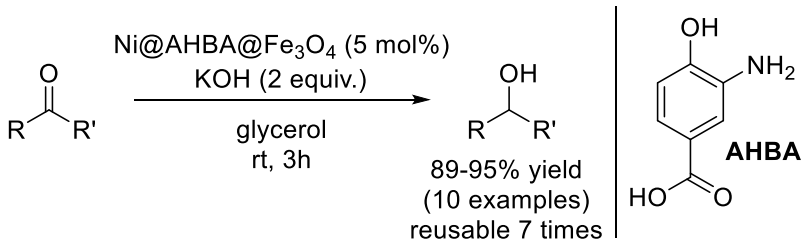

Scheme 70. Ni@AHBA@ Fe_3O_4 for carbonyl transfer hydrogenation in glycerol.

1.5.3 Frustrated Lewis Pairs

Frustrated Lewis Pairs (FLPs) are a combination of Lewis acids and bases, in which sterics are designed to hinder dative bond formation (Scheme 71).[204-205] They are expected to play a key role in metal-free hydrogenation processes in the future, since the first report by Stephan and co-workers where a FLP was shown to be able to split H_2.[206] Furthermore, the

heterolytic nature of the splitting should enhance their reactivity toward polar unsaturations such as carbonyl functions.

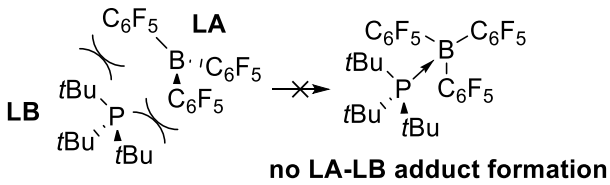

Scheme 71. Frustrated Lewis Pairs.

A major breakthrough in this field was made simultaneously by both the Stephan[207] and the Ashley[208] group, showing that $B(C_6F_5)_3$ (strong Lewis acid) could catalytically reduce carbonyls, in conjunction with an ether solvent as a weak Lewis base. In the former report, Et_2O was used with $B(C_6F_5)_3$ at 60 bar H_2, 70 °C, while in the latter case 1,4-dioxane was used at 5 bar H_2, 100 °C (Scheme 72). In both cases, aliphatic and benzylic ketones were successfully reduced, up to 99% yield.

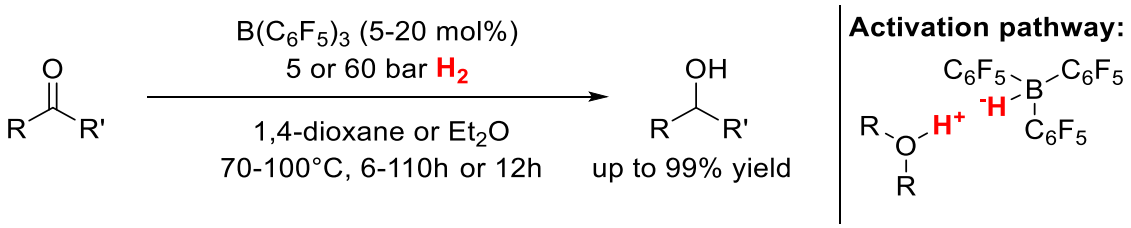

Scheme 72. FLP-catalyzed hydrogenation of ketones.

Later on, Stephan *et. al.* showed that the ether could be substituted with α-cyclodextrin or molecular sieves (4Å MS) as Lewis bases.[209] In the case of benzylic ketones with molecular sieves, the resulting alcohol was further dehydrated into the corresponding styrene. On their side, the Ashley group showed that their 1,4-dioxane/ $B(C_6F_5)_3$ was H_2O-tolerant, which is a crucial feature for large scale applications.[210] At the same time, Gyömöre et *al.* developed a similar FLP moisture-stable complex, $B(C_6F_5)_2(C_6Cl_{2+n}F_{3-n})_2$ (n = 0,1) in conjunction with THF as a solvent.[211] Das et *al.* complemented previous authors' mechanistic studies by DFT calculations, confirming that the [B]/R_2O adduct was indeed the FLP responsible for H_2 splitting.[212] The other possible pathway, a carbonyl-[B]-mediated H_2 splitting was found to be kinetically unfavourable.

Eventually, different approaches to FLP-mediated carbonyl hydrogenation were developed. Ashley and co-workers reported iPr_3Sn^+/2,4,6-collidine as a boron-free FLP system for carbonyl and imine hydrogenation.[213] Despite the high temperature employed (180 °C), this constituted the first example of homogeneous Sn for carbonyl hydrogenation (Scheme 73).

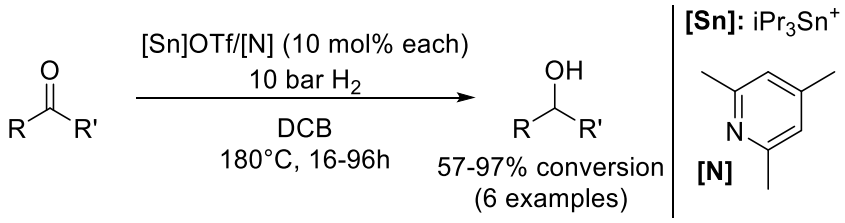

Scheme 73. Sn-based FLP for carbonyl hydrogenation.

Mummadi et *al.* adopted the opposite approach from Ashley and Stephan. Instead of using $B(C_6F_5)_3$ as a strong Lewis acid, they used instead an aryl-substituted 9-BBN borane as a *weak* Lewis acid, in conjunction with a *strong* Lewis base (Scheme 74).[214] In the case of carbonyl reduction to alcohols, the presence of strong Lewis acids can induce further etherification of the alcohol product, as well as dehydration as mentioned before. Using their configuration, no olefin formation was observed. Furthermore, they applied their system to the gram-scale conversion of ethyl levulinate to GVL (74% yield).

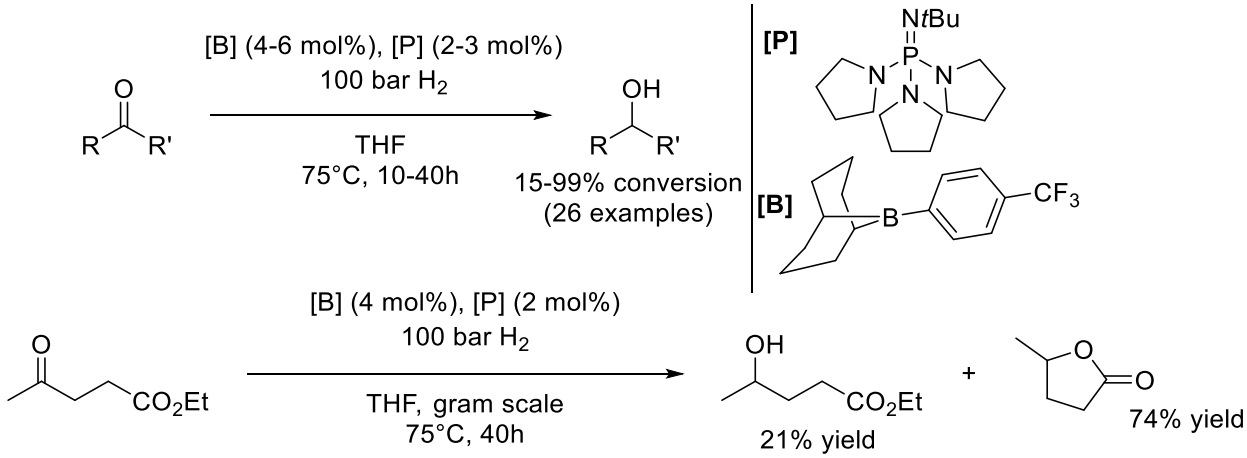

Scheme 74. 'Inverse' FLP for carbonyl hydrogenation.

Due to the novelty of FLPs in hydrogenations (the first example catalytic example having been reported in 2014), no formally heterogenized version has been reported so far. A few closely related systems are worth mentioning though, as they could give hints on the future of heterogeneous FLPs. Primo et *al.* reported in 2014 exfoliated graphene as a C=C hydrogenation catalyst.[215] While the nature of the active sites remains unclear, the authors did mention the co-existence of basic and acidic sites on their material, effectively exerting a FLP-induced H_2 activation. Later on, they applied graphene made from alginate pyrolysis for nitroarene hydrogenation.[216] Their results suggested that basic sites could be the carboxylate groups stemming from the alginate precursor, while the nature of the acidic group remained unclear (carbon vacancies or carboxylic groups). Not all the LA/LB pairs on the graphene were active, since they were required to be less than 4Å from each other without mutual neutralization.

Lastly, Ding et *al.* doped graphene with B/N by pyrolysis of a 1-butyl-3-methylimidazoliumtetrafluoroborate IL, and used it as a catalyst for cyclooctene hydrogenation.[217]

1.6 Hydrogen sources

We displayed below the atom economy of each reductant discussed here (Table 1). Unsurprisingly, H_2 gas exhibits a full efficiency in terms of atoms employed to reduce a carbonyl, while the atom efficiency of any other reductant falls below 11%. But other parameters must be taken in account in the choice of a reductant, including safety (both in terms of pressure and flammability), reactivity, solubility/miscibility and availability.[218-219] Under this array of parameters, transfer hydrogenation shines as a viable alternative to direct hydrogenation.[220]

Reductant	**% Active H**
H_2	100%
$NaBH_4$	11%
PMHS	7%
HCO_2H	4%
*i*PrOH	3%
glycerol	2%
NaH_2PO_2	2%
glucose	1%
Hantzsch ester	0.7%

Table 1. Common reductants in carbonyl reduction-atom economy.

The most popular hydrogen sources, shown by their prevalence in big scale processes, are hydride salts ($NaBH_4$, $LiAlH_4$). These are respectively obtained from the treating of $B(OMe)_3$ with NaH (discovered in 1953[221]) and $AlCl_3$ with LiH (discovered in 1947[222]). Hydride salts must be used in stoichiometric amounts, despite efforts made to use them in catalytic amounts,[223] and they mostly suffer from flammability and cumbersome waste generation. Alcoholic hydrogen sources are available from the biomass (EtOH, MeOH) and their byproduct can be potentially recycled (Scheme 75).[218] Moreover, some waste chemicals from the biodiesel and silicon industry can be re-used as reductants (respectively glycerol and PMHS), opening up new avenues in sustainable transfer hydrogenation.

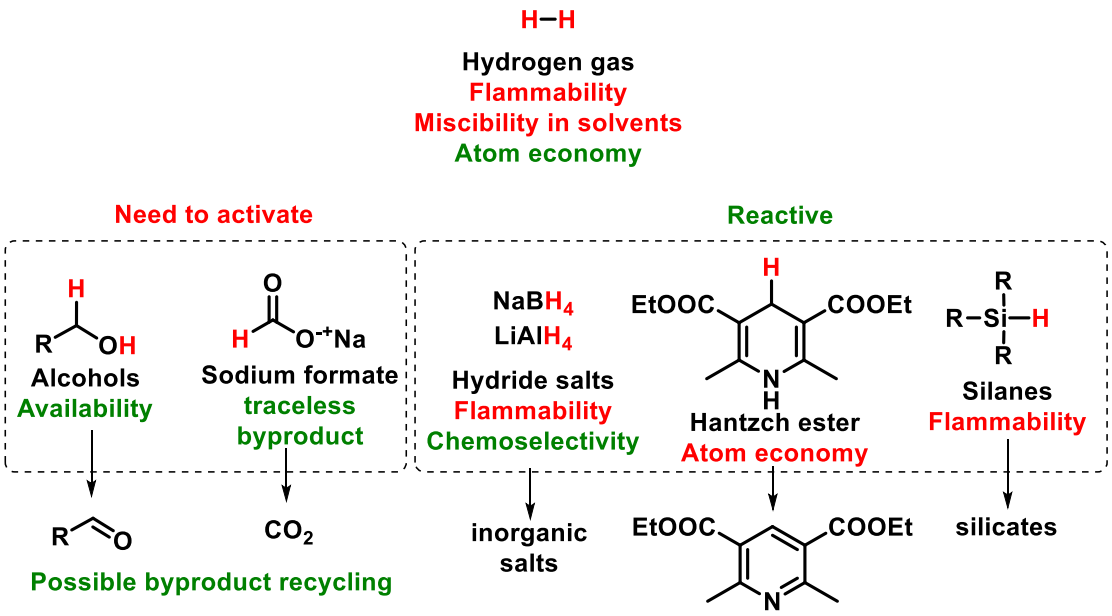

Scheme 75. An overview of hydrogenation sources.

Manna et *al.* successfully used glucose as hydrogen source using $[Cp^*RhCl_2]_2$ as a catalyst (Scheme 76).[224] The complex is able to extract the hydride from the aldehyde form of glucose, resulting in the formation of gluconic acid as a by-product. The authors were able to perform alkyne reduction to alkenes, with a tunable selectivity by switching the solvent.

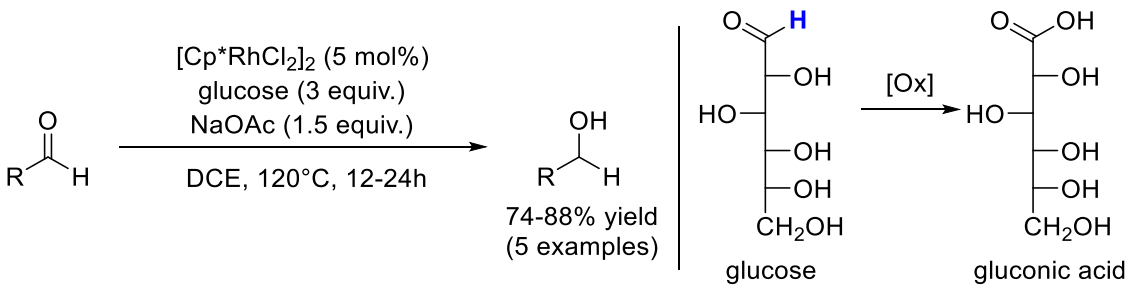

Scheme 76. Glucose as a reductant.

Sodium hypophosphite (NaH_2PO_2) has been reported by Guyon et *al.* as an air/moisture-stable, inexpensive reducing agent, using a $[RuCl_2(p\text{-cymene})]_2$ and 2,2'-bipyridine complex (Scheme 77).[225] NaH_2PO_2 is a reductant used in industrial nickel plating, being available in bulk quantity and having no obvious toxicity per its REACH safety sheet.[226] The authors extensively explored their reducing system, using glycerol as a solvent for achiral reduction of ketones. They checked that glycerol was not the reducing agent in their reaction. Then, they explored asymmetric reduction, using [(*R*,*R*)-TsDPEN] as a ligand, and switching to a biphasic glycerol/2Me-THF solvent to attain up to 96% ee.

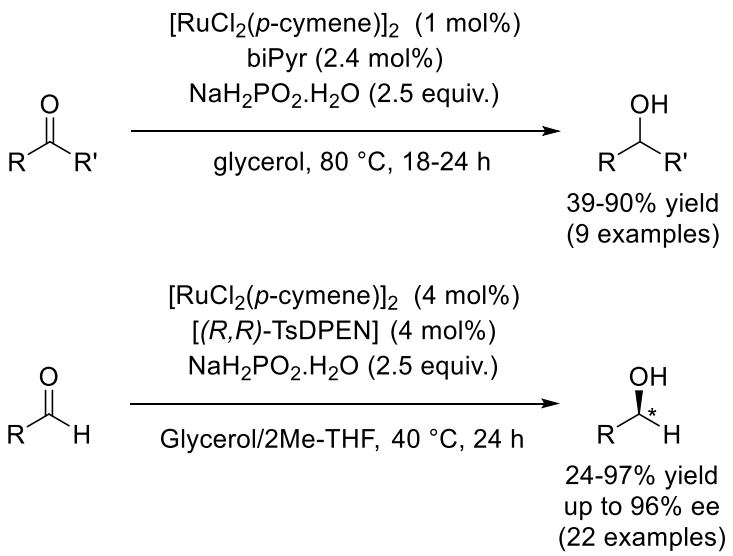

Scheme 77. Sodium hypophosphite as a reductant.

1.6.1 Short chain alcohols

The discovery of hydride salts as reductants allowed in their time supplanting the 'classical' reduction methods such as the MPV reduction.[227] MPV reduction remains however an inspiring system, evoked even in recent discovery. It was discovered independently by Verley[228] and Meerwein et *al.* in 1925,[229] using $Al(OEt)_3$ in EtOH and further developed in 1926 by Ponndorf using $Al(O\textit{i}Pr)_3$ and *i*PrOH.[230] In essence, the carbonyl is introduced with an excess of reducing alcohol, with an Al or B-based transfer agent. Upon coordination of an alkoxide to Al^{3+} or B^{3+}, its α-hydride can be readily transferred to a ketone through a 6-member transition state (Scheme 78).

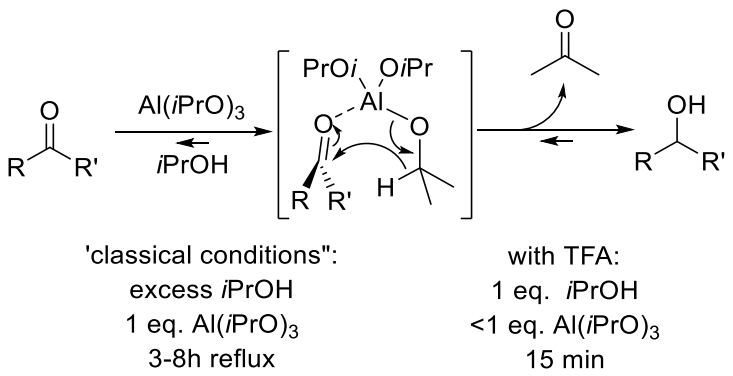

Scheme 78. MPV reduction.

Since the process is reversible, an excess of *i*PrOH is required to drive the reaction to completion. Although the acetone byproduct can be distilled off, the reaction still proceeds sluggishly (3-8 h under reflux) and side reactions such as aldolization and Tischenko condensation are prone to occur due to the presence of alkoxides. In practice, a stoichiometric

amount of Al(O*i*Pr)$_3$ is required due to the slow ligand exchange around Al.[231] This, along with low chemoselectivity and the elevated amount of reductant hamper the efficiency of the MPV process. However, the prospect of using alcohols as safe reducing agents sparked interest into improving over the original MPV reaction. Akamanchi et *al.* showed that stoichiometric[232] or catalytic amounts[231] of trifluoroacetic acid greatly enhanced the reaction rate, cutting the reaction time down to 15 minutes at room temperature and allowing the use of catalytic amounts of Al(O*i*Pr)$_3$. Another improvement was to accelerate ligand exchange by coordinating Al or B to sterically hindered ligands, such as bidentate biphenylenes,[233] porphyrins,[234] or siloxides.[235]

The MPV reaction has seen in the last 5 years much development on biomass conversion, based on Al[236-237] and Zr[238-242] oxides as catalysts. Dumesic et *al.* calculated the thermodynamic profile for the MPV hydrogenation of ethyl levulinate (EL) using Al(III), Sn(IV), and Zr(IV) isopropoxides in *i*PrOH.[243] Both EL and LA can be easily converted to GVL through this reductive method.[244] However, the carboxylate function in LA has a catalytic poisoning ability, which explains the high occurrence of EL or butyl levulinate (BL) as model substrates.

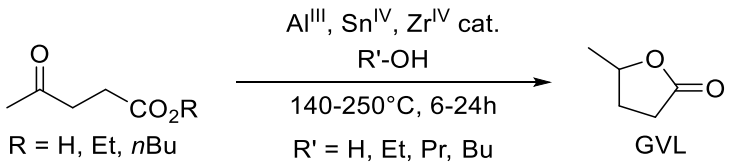

Scheme 79. Heterogeneous Al, Sn or Zr for biomass conversion.

Finally, Castellanos-Blanco et *al.* reported a (dippe)Ni(cod) complex that was able to exploit EtOH as a reducing agent (Scheme 80).[245] Although not formally being a MPV process, it is interesting that EtOH is a drastically more active reductant compared to other short chain alcohols (MeOH, *i*PrOH, *n*BuOH) (95% yield for acetophenone reduction, versus 13%, 4% and 53% for the others respectively).

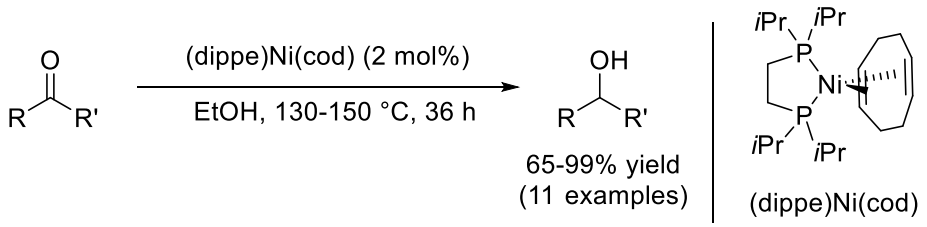

Scheme 80. EtOH as a reducing agent catalyzed by Ni(0).

A more recent variant of MPV reactions was co-discovered by the Taillefer[246] and the Varma[247] groups, by using cheap and widely available metal alkali M-B (M = Li, Na, K, Cs and B = OH,

O*t*Bu, PO_4, CO_3). The former group was screening basic additives for Fe-catalyzed transfer hydrogenation of carbonyl when they discovered that metal alkali could catalyze the reaction on its own. Among all the M-B combinations tested, NaOH conveniently gave the highest reactivity (full conversion of benzaldehyde at 18h with 10% NaOH). In order to disprove the presence of trace contaminants such as metals, the authors performed ICP-MS on the base. The main metal contaminant detected was Fe (1.8 ppm) along with Rh, Ir, and Ru in much smaller amounts (<55 ppb): the observed TOF of their reaction could not be correlated to any of these metal levels. Therefore, the authors conclude that M^+ cations were able to mediate the direct hydride transfer through a 6-member intermediate (Scheme 81). Wang et *al.* further showed that EtOH was a suitable H-donor as well in the process.[248]

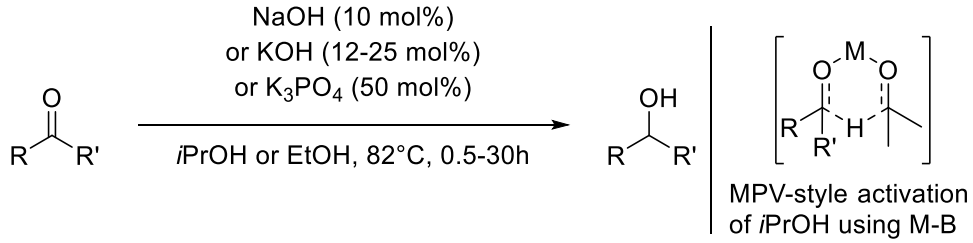

Scheme 81. Bases as transfer hydrogenation catalysts.

The Varma group attained a way higher catalytic activity for aldehyde reduction by switching to KOH in a sealed vial (3 h for full conversion for benzaldehyde with 12% KOH, as opposed to 18 h in Taillefer's example). However, the reaction still proved to be much slower for ketone reduction as it required a higher base loading (25 mol% KOH) and reaction time (18-24 h). Ikhile et *al.* eventually showed that the addition of 0.5 mol% 1,3-diarylimidazolium salt doubled the activity of KOH for cyclohexanone reduction.[249] Finally, Radhakrishan et *al.* showed that calcinated K_3PO_4 was a suitable heterogeneous base substitute.[250] Although pre-treatment at 600 °C, 5 h and higher loadings were required (50 mol%, 10 h for benzaldehyde full conversion), K_3PO_4 is a re-usable and inexpensive catalyst.

1.6.2 Formate

Formic acid (HCO_2H, FA) is the simplest of carboxylic acids, made from the carbonylation of MeOH into HCO_2Me, and subsequent hydrolysis.[251] In conjunction with a base (such as Et_3N) or as sodium formate, it has been widely used as a reducing agent, decomposing into CO_2 and H_2 under catalytic conditions. It has been particularly useful in prochiral ketone reduction into secondary alcohol, using Ir[252], Ru[253-255], Rh[256] complexes, or enzymes[257] (Scheme 82, see Scheme 35 and Scheme 28 for examples in water).

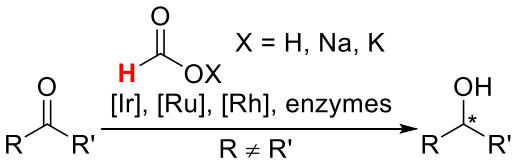

Scheme 82. Formic acid/akali metal formate in prochiral reduction.

Gao et *al.* supported Ru on an aluminum oxyhydroxide support (Ru@AlO(OH)) for benzylic aldehyde transfer reduction using HCO_2K.[258] In parallel, FA has also been widely applied to biomass upgrading using heterogeneous catalysts, in particular for LA reduction to GVL.[12] Indeed, LA is co-generated with LA from carbohydrate acidolysis, going through a 5-HMF intermediate.[20] Therefore, both products can be reacted together to drive the formation of GVL (Scheme 83). One notable feature is the requirement of H_2O as a solvent, stemming from the acidolysis step that is performed in aqueous solution. A seminal example was reported by Du et *al.*, using small Au NPs supported on ZrO_2 (Au@ZrO_2).[259] The catalyst was tested on freshly prepared solutions of LA/FA mixture made from the treatment of carbohydrates with H_2SO_4, establishing the robustness of their method. The Fu group also showed the viability of homogeneous Fe/Tris[(2-diphenylphosphino)ethyl]phosphine complexes for LA reduction.[260] Finally, Varkolu et *al.* used Ni supported on SiO_2 (Ni@ SiO_2) and applied in continuous flow for GVL synthesis.[261]

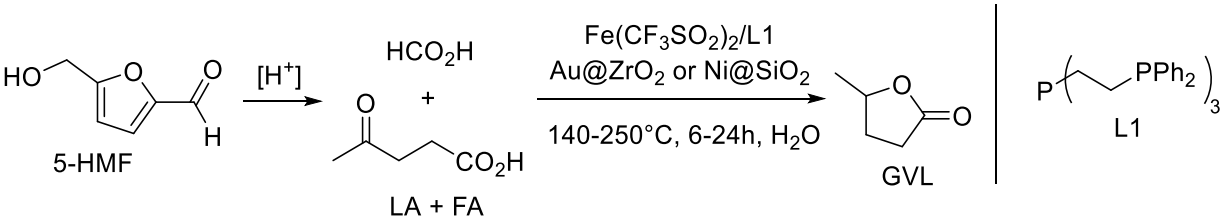

Scheme 83. Co-generation of LA and FA from 5-HMF and subsequent reduction to GVL.

LA has also been successfully applied as a reductant on vanillin, to yield 2-methoxy-4-methylphenol. To this purpose, Wang et *al.* reported the use of Pd supported on TiO_2 dispersed on a N-doped carbon support (Pd@TiO_2@N-C).[262]

1.6.3 Glycerol

Glycerol is a non-toxic, non-hazardous, and non-volatile liquid, the 1,3-dihydroxylated analogue of *i*PrOH.[263] Contrary to *i*PrOH, glycerol is a biomass waste, generated as a by-product in the manufacture of biodiesel fuel from vegetable oils (Scheme 84). For every ton of biodiesel produced, 100 kg of glycerol is generated.[264] With its low price, there has been a strong economic incentive to use it as a solvent and a reducing agent. Its own oxidation by-product, dihydroxyacetone, is an ingredient in the formulation of sunless tanning cosmetics.

Finally, it can be used in the polyol process, as a reductant to form metal NPs such as Ag, Pd, Pt, Ru, Au.[265]

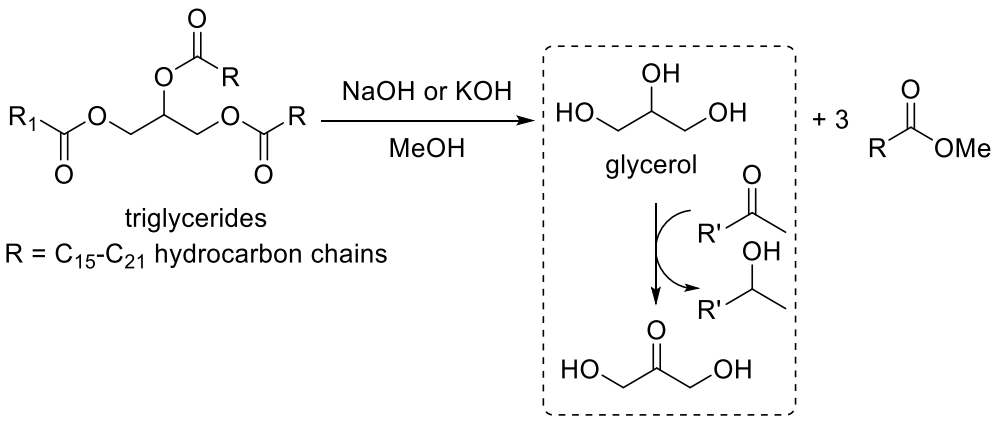

Scheme 84. Glycerol production.

In catalytic carbonyl reduction, homogeneous Ru and Ir complexes have been mostly used, in conjunction with KOH. Early results were reported by Tavor et *al.* using $[RuCl_2(p\text{-cymene})]_2$ as a catalyst.[266] Due to the low amounts of KOH used (14 mol%), they obtained low catalytic activities with a 90% yield on benzaldehyde after 90 h of reaction at 70 °C (Scheme 85).

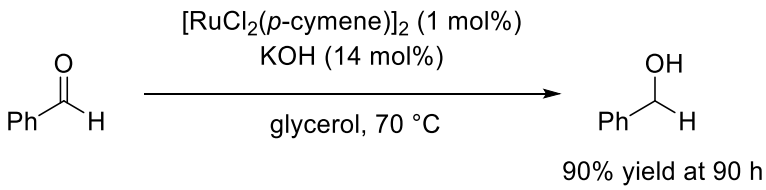

Scheme 85. Early works on Ru-catalyzed reduction of carbonyls using glycerol.

Their discovery was later expanded by other authors, by increasing the base amount (to 1-2 equiv.). Azua et *al.* introduced a sulfonated NHC-Ir complex that proved more active for benzaldehyde reduction (99% yield after 1.5 h), and diphenyl ketone (91% yield after 20 h) (Scheme 86).[267] However, on other more sterically hindered ketones, yields were below 55%, and the catalyst was C=C selective on α,β-unsaturated aldehydes.

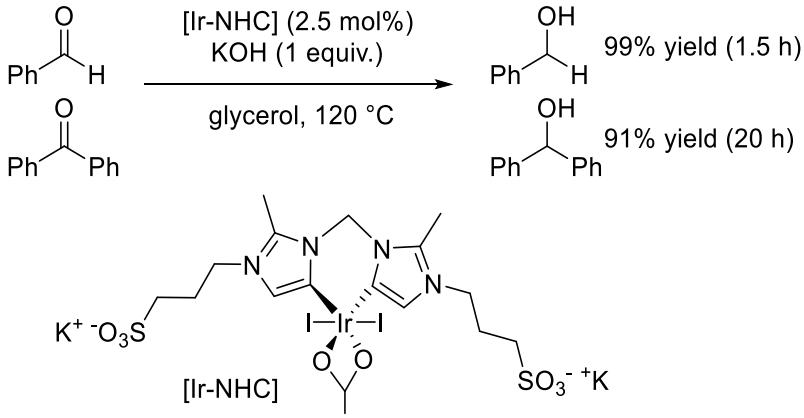

Scheme 86. Sulfonated-NHC-Ir for carbonyl reduction in glycerol.

Eventually the same authors explored related Ir-NHC complexes in ultrasound setups, showing its superiority in the case of benzaldehyde reduction (11% yield in oil bath vs 73% in ultrasound) (selected example shown in Scheme 87).[268]

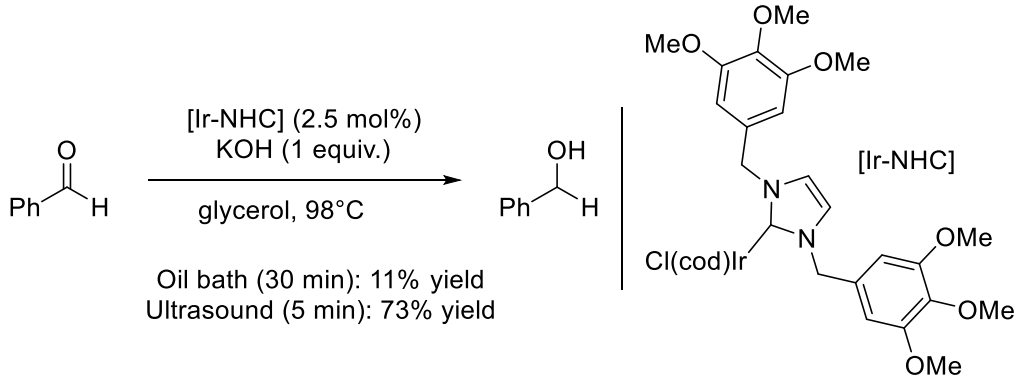

Scheme 87. NHC-Ir for carbonyl reduction in glycerol: comparison of oil bath heating vs ultrasound (selected example).

Sharma et *al.* further explored Ru-based complexes, this time with asymmetric bidentate chalcogen ligands (Se,S-containing NHCs).[269] In a side-to-side comparison with *i*PrOH, glycerol proved to be a less active reducing agent with an average of 5-10% yield loss (Scheme 88). Nonetheless, using sub-stoichiometric amounts of KOH (40 mol%), the authors obtained from good to excellent yields on 7 ketones.

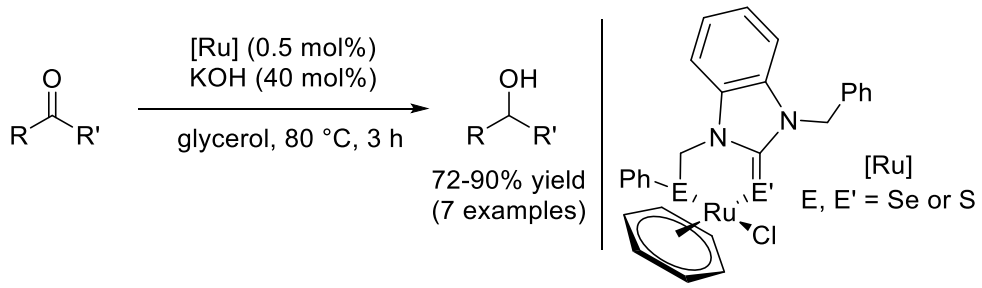

Scheme 88. Bidentate chalcogen ligands with Ru for glycerol as a reductant.

An exception to these examples was reported by Gawande et *al.* who supported Ni NPs on Fe_3O_4 NPs (Ni@Fe_3O_4), primarily for nitroarene reduction in glycerol (Scheme 89).[270] Although the scope was very limited, they successfully applied their catalyst for carbonyl hydrogenation as well. Due to the magneticity of both components of their catalyst, they managed to recycle it 8 times with no yield drop.

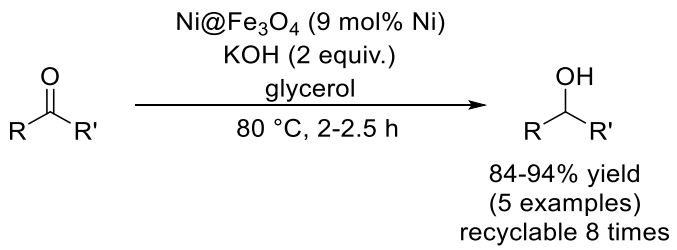

Scheme 89. Ni@Fe_3O_4 for carbonyl reduction in glycerol.

So far, glycerol has been used mostly in Ru/Ir homogeneous complexes, and even in base metal-based systems, high amounts of KOH are required (typically 1 equivalent or above). Carbonyl reduction processes using glycerol can be seen from a different perspective though, the oxidation of glycerol (and subsequent trapping of the hydrogens by the carbonyl). In this framework, base-free systems have been widely for aerobic oxidation of glycerol, typically with bimetallic systems based on combinations of Au with Pd/Pt.[271-273] Based on our section concerning other alcohols (EtOH, *i*PrOH) as reductants though, there should be opportunities for noble metal-free and/or base-free catalytic systems to tackle this challenge.

1.6.4 PMHS

In contrast to most silanes, PMHS is an inexpensive and non-toxic reducing agent. In the absence of an activator, it is an inert and easy to handle liquid. It was first prepared by Sauer and co-workers,[274] and has been since reported in a substantial number of reduction processes.[275] Upon treatment with BF_3OEt_2, the resulting PDMS byproduct can be recycled into $MeSiH_{3-x}F_x$ synthons that are useful building blocks in the silicon industry.[276] Early reports consisted in using tin salts as activators,[277-279] and since then a wider variety of activators has been reported. Nucleophilic activators such as fluorides,[280] phosphines[281] or bases[282] have been successfully applied to PMHS-mediated ketone hydrosilylation (Scheme 90). Eventually, non-noble metals such as Fe[283-285] and Zn were shown to activate PMHS as well, with Zn being able to enantioselective prochiral ketones into chiral secondary alcohols.[286-289]

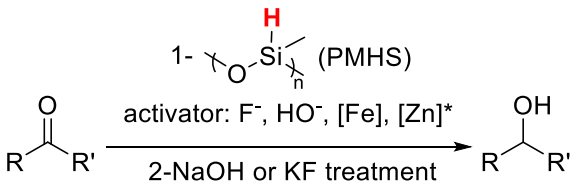

Scheme 90. Overview of PMHS for carbonyl reduction.

1.7 Concluding remarks for the introduction

As seen throughout the plethora of examples of carbonyl hydrogenation exposed here, a broad and diverse toolbox of chemical methods is available to chemists to design a performant

reduction process. Yet, the introductory question “What alternatives green chemistry offers to improve carbonyl reduction?” remains rhetorical at this stage, with a plethora of developments on the subject with no definitive answer so far. A wide range of green chemistry metrics is available to assess each alternative. Yet, none of them is systematically used throughout the many reports covered here. Furthermore, there is no universal green metric, reflecting the complexity to design an universally green reaction. As many alternatives as possible should be developed to tailor every process to every need.

For this to happen, green metrics should be more widely used, to discriminate deceptively ‘green’ reports from holistically designed processes with a clear goal in mind. For instance, the use of ILs should remain a niche application in organic chemistry, to circumvent solubility issues or enable catalyst recycling. The use of every technology covered here should be justified in terms of economy (energy, atom, waste generation) or because it enables pathways that were not formerly possible.

In this thesis, we will exploit to our best the specificities and limitations of alternative energy inputs in chemistry (see section 1.3 of this chapter), applied either to the synthesis of nanoparticle, or for the reaction itself.

1.8 References

1. Vries, J. G. d.; Elsevier, C. J., *The Handbook of Homogeneous Hydrogenation*. 2008.
2. Caron, S.; Dugger, R. W.; Ruggeri, S. G.; Ragan, J. A.; Ripin, D. H. B., Large-Scale Oxidations in the Pharmaceutical Industry. *Chem. Rev.* **2006,** *106* (7), 2943-2989.
3. Wilde, M. v., Vermischte Mittheilungen. *Chem. Ber.* **1874,** *7* (1), 352-357.
4. Sanfilippo, D.; Rylander, P. N., Hydrogenation and Dehydrogenation. In *Ullmann's Encyclopedia of Industrial Chemistry*, Wiley-WCH, Ed. 2009.
5. Burkhardt, E. R.; Matos, K., Boron Reagents in Process Chemistry: Excellent Tools for Selective Reductions. *Chem. Rev.* **2006,** *106* (7), 2617-2650.
6. Magano, J.; Dunetz, J. R., Large-Scale Carbonyl Reductions in the Pharmaceutical Industry. *Org. Proc. Res. Dev.* **2012,** *16* (6), 1156-1184.
7. Hedberg, C., Carbonyl Hydrogenation. In *Modern Reduction Methods*, Wiley-WCH, Ed. 2008.
8. Bernardis, F. L.; Grant, R. A.; Sherrington, D. C., A review of methods of separation of the platinum-group metals through their chloro-complexes. *React. Funct. Polym.* **2005,** *65* (3), 205-217.
9. Ravindra, K.; Bencs, L.; Van Grieken, R., Platinum group elements in the environment and their health risk. *Sci. Total Environ.* **2004,** *318* (1), 1-43.
10. Jantan, K. A.; Kwok, C. Y.; Chan, K. W.; Marchiò, L.; White, A. J. P.; Deplano, P.; Serpe, A.; Wilton-Ely, J. D. E. T., From recovered metal waste to high-performance palladium catalysts. *Green Chem.* **2017,** *19* (24), 5846-5853.
11. Mäki-Arvela, P.; Hájek, J.; Salmi, T.; Murzin, D. Y., Chemoselective hydrogenation of carbonyl compounds over heterogeneous catalysts. *Appl. Catal., A* **2005,** *292*, 1-49.

12. Gilkey, M. J.; Xu, B., Heterogeneous Catalytic Transfer Hydrogenation as an Effective Pathway in Biomass Upgrading. *ACS Catal.* **2016,** *6* (3), 1420-1436.
13. Anastas, P. T.; Warner, J. C., *Green chemistry : theory and practice*. Oxford University Press: Oxford ;, 2000.
14. Gallezot, P.; Richard, D., Selective Hydrogenation of α,β-Unsaturated Aldehydes. *Catal. Rev.* **1998,** *40* (1-2), 81-126.
15. Kahsar, K. R.; Schwartz, D. K.; Medlin, J. W., Control of Metal Catalyst Selectivity through Specific Noncovalent Molecular Interactions. *J. Am. Chem. Soc.* **2014,** *136* (1), 520-526.
16. **!!! INVALID CITATION !!! 16-17**.
17. Zhang, M.-J.; Tan, D.-W.; Li, H.-X.; Young, D. J.; Wang, H.-F.; Li, H.-Y.; Lang, J.-P., Switchable Chemoselective Transfer Hydrogenations of Unsaturated Carbonyls Using Copper(I) N-Donor Thiolate Clusters. *J. Org. Chem.* **2018,** *83* (3), 1204-1215.
18. Alonso, D. M.; Bond, J. Q.; Dumesic, J. A., Catalytic conversion of biomass to biofuels. *Green Chem.* **2010,** *12* (9), 1493-1513.
19. Kamm, B., Production of Platform Chemicals and Synthesis Gas from Biomass. *Angew. Chem. Int. Ed.* **2007,** *46* (27), 5056-5058.
20. Pileidis, F.; Titirici, M.-M., Levulinic Acid Biorefineries: New Challenges for Efficient Utilization of Biomass. *ChemSusChem* **2016,** *9* (6), 562-582.
21. Bozell, J. J.; Moens, L.; Elliott, D. C.; Wang, Y.; Neuenscwander, G. G.; Fitzpatrick, S. W.; Bilski, R. J.; Jarnefeld, J. L., Production of levulinic acid and use as a platform chemical for derived products. *Resour. Conserv. Recycl.* **2000,** *28* (3), 227-239.
22. Manzer, L. E., Catalytic synthesis of α-methylene-γ-valerolactone: a biomass-derived acrylic monomer. *Appl. Catal., A* **2004,** *272* (1), 249-256.
23. Bond, J. Q.; Wang, D.; Alonso, D. M.; Dumesic, J. A., Interconversion between γ-valerolactone and pentenoic acid combined with decarboxylation to form butene over silica/alumina. *J. Catal.* **2011,** *281* (2), 290-299.
24. Serrano-Ruiz, J. C.; Wang, D.; Dumesic, J. A., Catalytic upgrading of levulinic acid to 5-nonanone. *Green Chem.* **2010,** *12* (4), 574-577.
25. Touchy, A. S.; Hakim Siddiki, S. M. A.; Kon, K.; Shimizu, K.-i., Heterogeneous Pt Catalysts for Reductive Amination of Levulinic Acid to Pyrrolidones. *ACS Catal.* **2014,** *4* (9), 3045-3050.
26. Hu, L.; Xu, J.; Zhou, S.; He, A.; Tang, X.; Lin, L.; Xu, J.; Zhao, Y., Catalytic Advances in the Production and Application of Biomass-Derived 2,5-Dihydroxymethylfuran. *ACS Catal.* **2018,** *8* (4), 2959-2980.
27. **!!! INVALID CITATION !!! 27-28**.
28. Sacia, E. R.; Balakrishnan, M.; Bell, A. T., Biomass conversion to diesel via the etherification of furanyl alcohols catalyzed by Amberlyst-15. *J. Catal.* **2014,** *313*, 70-79.
29. Han, J.; Kim, Y.-H.; Jung, B. Y.; Hwang, S. H.; Jegal, J.; Kim, J. W.; Lee, Y.-S., Highly Selective Catalytic Hydrogenation and Etherification of 5-Hydroxymethyl-2-furaldehyde to 2,5-Bis(alkoxymethyl)furans for Potential Biodiesel Production. *Synlett* **2017,** *28* (17), 2299-2302.
30. Harris, J. M.; Keranen, M. D.; O'Doherty, G. A., Syntheses of d- and l-Mannose, Gulose, and Talose via Diastereoselective and Enantioselective Dihydroxylation Reactions. *J. Org. Chem.* **1999,** *64* (9), 2982-2983.
31. Martin, S. F.; Chen, H. J.; Yang, C. P., Facile asymmetric syntheses of 1-deoxycastanospermine and 1-deoxy-8a-epi-castanospermine. *J. Org. Chem.* **1993,** *58* (10), 2867-2873.
32. Trasarti, A. F.; Marchi, A. J.; Apesteguía, C. R., Highly selective synthesis of menthols from citral in a one-step process. *J. Catal.* **2004,** *224* (2), 484-488.

33. Stolle, A.; Gallert, T.; Schmoger, C.; Ondruschka, B., Hydrogenation of citral: a widespread model reaction for selective reduction of α,β-unsaturated aldehydes. *RSC Adv.* **2013,** *3* (7), 2112-2153.
34. Arntz, D.; Fischer, A.; Hopp, M.; Jacobi, S.; Sauer, J.; Ohara, T.; Sato, T.; Shimizu, N.; Schwind, H., Acrolein and Methacrolein. In *Ullmann's Encyclopedia of Industrial Chemistry*, Wiley-VCH, Ed. 2007.
35. Kliewer, C. J.; Bieri, M.; Somorjai, G. A., Hydrogenation of the α,β-Unsaturated Aldehydes Acrolein, Crotonaldehyde, and Prenal over Pt Single Crystals: A Kinetic and Sum-Frequency Generation Vibrational Spectroscopy Study. *J. Am. Chem. Soc.* **2009,** *131* (29), 9958-9966.
36. Vanden Eynde, J. J.; Rutot, D., Microwave-mediated derivatization of poly(styrene-co-allyl alcohol), a key step for the soluble polymer-assisted synthesis of heterocycles. *Tetrahedron* **1999,** *55* (9), 2687-2694.
37. Gawande, M. B.; Shelke, S. N.; Zboril, R.; Varma, R. S., Microwave-Assisted Chemistry: Synthetic Applications for Rapid Assembly of Nanomaterials and Organics. *Acc. Chem. Res.* **2014,** *47* (4), 1338-1348.
38. Kappe, C. O., Controlled Microwave Heating in Modern Organic Synthesis. *Angew. Chem. Int. Ed.* **2004,** *43* (46), 6250-6284.
39. Varma, R. S.; Saini, R. K., Microwave-assisted reduction of carbonyl compounds in solid state using sodium borohydride supported on alumina. *Tetrahedron Lett.* **1997,** *38* (25), 4337-4338.
40. Barbry, D.; Torchy, S., Accelerated Reduction of Carbonyl Compounds under Microwave Irradiation. *Tetrahedron Lett.* **1997,** *38* (17), 2959-2960.
41. Kazemi, F.; Kiasat, A. R., Reduction of carbonyl compounds to the corresponding alcohols with isopropanol on dehydrated alumina under microwave irradiation. *Synth. Comm.* **2002,** *32* (14), 2255-2260.
42. Behzad, Z.; Davood, S., Water as a Green Solvent for Fast and Efficient Reduction of Carbonyl Compounds with NaBH4 under Microwave Irradiation. *J. Chin. Chem. Soc.* **2005,** *52* (6), 1179-1184.
43. Polshettiwar, V.; Baruwati, B.; Varma, R. S., Nanoparticle-supported and magnetically recoverable nickel catalyst: a robust and economic hydrogenation and transfer hydrogenation protocol. *Green Chem.* **2009,** *11* (1), 127-131.
44. Nasir Baig, R. B.; Varma, R. S., Magnetic Silica-Supported Ruthenium Nanoparticles: An Efficient Catalyst for Transfer Hydrogenation of Carbonyl Compounds. *ACS Sustainable Chem. Eng.* **2013,** *1* (7), 805-809.
45. Yoshida, K.; Gonzalez-Arellano, C.; Luque, R.; Gai, P. L., Efficient hydrogenation of carbonyl compounds using low-loaded supported copper nanoparticles under microwave irradiation. *Appl. Catal., A* **2010,** *379* (1), 38-44.
46. Gowda, R.; Chen, E., Recyclable Earth-Abundant Metal Nanoparticle Catalysts for Selective Transfer Hydrogenation of Levulinic Acid to Produce γ-Valerolactone. *ChemSusChem* **2016,** *9* (2), 181-185.
47. Clark, J.; Farmer, T.; Hunt, A.; Sherwood, J., Opportunities for Bio-Based Solvents Created as Petrochemical and Fuel Products Transition towards Renewable Resources. *Int. J. Mol. Sci.* **2015,** *16* (8), 17101.
48. Clarke, C. J.; Tu, W.-C.; Levers, O.; Bröhl, A.; Hallett, J. P., Green and Sustainable Solvents in Chemical Processes. *Chem. Rev.* **2018,** *118* (2), 747-800.
49. Do, J.-L.; Friščić, T., Mechanochemistry: A Force of Synthesis. *ACS Cent. Sci.* **2017,** *3* (1), 13-19.

50. Cravotto, G.; Gaudino, E. C., CHAPTER 3 Oxidation and Reduction by Solid Oxidants and Reducing Agents using Ball-Milling. In *Ball Milling Towards Green Synthesis: Applications, Projects, Challenges*, The Royal Society of Chemistry: 2015; pp 58-80.
51. Fumio, T.; Koji, K.; Minoru, Y., NaBH4 Reduction of Ketones in the Solid State. *Angew. Chem. Int. Ed.* **1989,** *28* (3), 320-321.
52. Cho, B. T.; Kang, S. K.; Kim, M. S.; Ryu, S. R.; An, D. K., Solvent-free reduction of aldehydes and ketones using solid acid-activated sodium borohydride. *Tetrahedron* **2006,** *62* (34), 8164-8168.
53. Mack, J.; Fulmer, D.; Stofel, S.; Santos, N., The first solvent-free method for the reduction of esters. *Green Chem.* **2007,** *9* (10), 1041-1043.
54. Reza, N.-J. M.; Javad, M.; G., D. M.; Gerd, K., Sodium Tetraalkoxyborates: Intermediates for the Quantitative Reduction of Aldehydes and Ketones to Alcohols through Ball Milling with NaBH4. *Eur. J. Org. Chem.* **2009,** *2009* (21), 3567-3572.
55. Solà, R.; Sutcliffe, O. B.; Banks, C. E.; Maciá, B., Ball mill and microwave assisted synthetic routes to Fluoxetine. *Sust. Chem. Pharma.* **2017,** *5*, 14-21.
56. Shiragami, T.; Ankyu, H.; Fukami, S.; Pac, C.; Yanaglda, S.; Mori, H.; Fujita, H., Semiconductor photocatalysis: visible light induced photoreduction of aromatic ketones and electron-deficient alkenes catalysed by quantised cadmium sulfide. *J. Chem. Soc. Faraday Trans.* **1992,** *88* (7), 1055-1061.
57. Li, J.; Yang, J.; Wen, F.; Li, C., A visible-light-driven transfer hydrogenation on CdS nanoparticles combined with iridium complexes. *Chem. Commun.* **2011,** *47* (25), 7080-7082.
58. Liu, X.; Sun, D.; Yuan, R.; Fu, X.; Li, Z., Efficient visible-light-induced hydrogenation over composites of CdS and ruthenium carbonyl complexes. *J. Catal.* **2013,** *304*, 1-6.
59. Joyce-Pruden, C.; Pross, J. K.; Li, Y., Photoinduced reduction of aldehydes on titanium dioxide. *J. Org. Chem.* **1992,** *57* (19), 5087-5091.
60. Kohtani, S.; Yoshioka, E.; Saito, K.; Kudo, A.; Miyabe, H., Photocatalytic hydrogenation of acetophenone derivatives and diaryl ketones on polycrystalline titanium dioxide. *Catal. Commun.* **2010,** *11* (13), 1049-1053.
61. Zhang, M.; Rouch, W. D.; McCulla, R. D., Conjugated Polymers as Photoredox Catalysts: Visible-Light-Driven Reduction of Aryl Aldehydes by Poly(p-phenylene). *Eur. J. Org. Chem.* **2012,** *2012* (31), 6187-6196.
62. Sharma, P.; Sasson, Y., A photoactive catalyst Ru–g-C3N4 for hydrogen transfer reaction of aldehydes and ketones. *Green Chem.* **2017,** *19* (3), 844-852.
63. Ghosh, T.; Slanina, T.; König, B., Visible light photocatalytic reduction of aldehydes by Rh(iii)–H: a detailed mechanistic study. *Chem. Sci.* **2015,** *6* (3), 2027-2034.
64. Call, A.; Casadevall, C.; Acuña-Parés, F.; Casitas, A.; Lloret-Fillol, J., Dual cobalt–copper light-driven catalytic reduction of aldehydes and aromatic ketones in aqueous media. *Chem. Sci.* **2017,** *8* (7), 4739-4749.
65. Halas, N. J.; Lal, S.; Chang, W.-S.; Link, S.; Nordlander, P., Plasmons in Strongly Coupled Metallic Nanostructures. *Chem. Rev.* **2011,** *111* (6), 3913-3961.
66. Hao, C.-H.; Guo, X.-N.; Pan, Y.-T.; Chen, S.; Jiao, Z.-F.; Yang, H.; Guo, X.-Y., Visible-Light-Driven Selective Photocatalytic Hydrogenation of Cinnamaldehyde over Au/SiC Catalysts. *J. Am. Chem. Soc.* **2016,** *138* (30), 9361-9364.
67. Landry, M. J.; Gellé, A.; Meng, B. Y.; Barrett, C. J.; Moores, A., Surface-Plasmon-Mediated Hydrogenation of Carbonyls Catalyzed by Silver Nanocubes under Visible Light. *ACS Catal.* **2017,** *7* (9), 6128-6133.
68. Wood, R. J.; Lee, J.; Bussemaker, M. J., A parametric review of sonochemistry: Control and augmentation of sonochemical activity in aqueous solutions. *Ultrason. Sonochem.* **2017,** *38*, 351-370.

69. Gedanken, A., Using sonochemistry for the fabrication of nanomaterials. *Ultrason. Sonochem.* **2004,** *11* (2), 47-55.
70. Suslick, K. S.; Choe, S.-B.; Cichowlas, A. A.; Grinstaff, M. W., Sonochemical synthesis of amorphous iron. *Nature* **1991,** *353*, 414.
71. Mason, T. J., Ultrasound in synthetic organic chemistry. *Chem. Soc. Rev.* **1997,** *26* (6), 443-451.
72. Salvador, J. A. R.; e Melo, M. L. S.; Neves, A. S. C., Ultrasound assisted zinc reactions in synthesis 1. Efficient reduction of enones. *Tetrahedron Lett.* **1993,** *34* (2), 357-360.
73. Firdaus, M.; Handayani, N.; Marfu'ah, L. T., Reduction of Aldehydes Using Sodium Borohydride under Ultrasonic Irradiation. *Indones. J. Chem.* **2016,** *16* (2), 229-332.
74. Yulong, X.; Tanyu, C.; Jie, L.; Ketang, L.; Qingqian, Q.; Fei, G.; Guohua, L.; Hexing, L., An Ion-Pair Immobilization Strategy in Rhodium-Catalyzed Asymmetric Transfer Hydrogenation of Aromatic Ketones. *Adv. Synth. Catal.* **2012,** *354* (17), 3250-3258.
75. Gu, Y.; Jérôme, F., Bio-based solvents: an emerging generation of fluids for the design of eco-efficient processes in catalysis and organic chemistry. *Chem. Soc. Rev.* **2013,** *42* (24), 9550-9570.
76. Jessop, P. G., Searching for green solvents. *Green Chem.* **2011,** *13* (6), 1391-1398.
77. Marsh, K. N.; Deev, A.; Wu, A. C.-T.; Tran, E.; Klamt, A., Room temperature ionic liquids as replacements for conventional solvents – A review. *Kor. J. Chem. Eng.* **2002,** *19* (3), 357-362.
78. Seddon, K. R., Ionic Liquids for Clean Technology. *J. Chem. Technol. Biotechnol.* **1997,** *68* (4), 351-356.
79. Zhu, S.; Wu, Y.; Chen, Q.; Yu, Z.; Wang, C.; Jin, S.; Ding, Y.; Wu, G., Dissolution of cellulose with ionic liquids and its application: a mini-review. *Green Chem.* **2006,** *8* (4), 325-327.
80. Álvarez de Cienfuegos, L.; Robles, R.; Miguel, D.; Justicia, J.; Cuerva, J. M., Reduction Reactions in Green Solvents: Water, Supercritical Carbon Dioxide, and Ionic Liquids. *ChemSusChem* **2011,** *4* (8), 1035-1048.
81. Olivier-Bourbigou, H.; Magna, L., Ionic liquids: perspectives for organic and catalytic reactions. *J. Mol. Catal. A: Chem.* **2002,** *182-183*, 419-437.
82. Anderson, K.; Goodrich, P.; Hardacre, C.; Rooney, D. W., Heterogeneously catalysed selective hydrogenation reactions in ionic liquids. *Green Chem.* **2003,** *5* (4), 448-453.
83. Dyson, P. J.; Laurenczy, G.; André Ohlin, C.; Vallance, J.; Welton, T., Determination of hydrogen concentration in ionic liquids and the effect (or lack of) on rates of hydrogenation. *Chem. Commun.* **2003,** (19), 2418-2419.
84. Hulsbosch, J.; De Vos, D. E.; Binnemans, K.; Ameloot, R., Biobased Ionic Liquids: Solvents for a Green Processing Industry? *ACS Sustainable Chem. Eng.* **2016,** *4* (6), 2917-2931.
85. Krossing, I.; Slattery, J. M.; Daguenet, C.; Dyson, P. J.; Oleinikova, A.; Weingärtner, H., Why Are Ionic Liquids Liquid? A Simple Explanation Based on Lattice and Solvation Energies. *J. Am. Chem. Soc.* **2006,** *128* (41), 13427-13434.
86. Vanda, H.; Dai, Y.; Wilson, E. G.; Verpoorte, R.; Choi, Y. H., Green solvents from ionic liquids and deep eutectic solvents to natural deep eutectic solvents. *C. R. Chim.* **2018,** *21* (6), 628-638.
87. García-Álvarez, J., Deep Eutectic Mixtures: Promising Sustainable Solvents for Metal-Catalysed and Metal-Mediated Organic Reactions. *Eur. J. Inorg. Chem.* **2015,** *2015* (31), 5147-5157.
88. Alonso, D. A.; Baeza, A.; Chinchilla, R.; Guillena, G.; Pastor, I. M.; Ramón, D. J., Deep Eutectic Solvents: The Organic Reaction Medium of the Century. *Eur. J. Org. Chem.* **2016,** *2016* (4), 612-632.

89. Rideout, D. C.; Breslow, R., Hydrophobic acceleration of Diels-Alder reactions. *J. Am. Chem. Soc.* **1980,** *102* (26), 7816-7817.
90. Biscoe, M. R.; Breslow, R., Hydrophobically Directed Selective Reduction of Ketones. *J. Am. Chem. Soc.* **2003,** *125* (42), 12718-12719.
91. Narayan, S.; Muldoon, J.; Finn, M. G.; Fokin, V. V.; Kolb, H. C.; Sharpless, K. B., "On Water": Unique Reactivity of Organic Compounds in Aqueous Suspension. *Angew. Chem. Int. Ed.* **2005,** *44* (21), 3275-3279.
92. Du, Q.; Freysz, E.; Shen, Y. R., Surface Vibrational Spectroscopic Studies of Hydrogen Bonding and Hydrophobicity. *Science* **1994,** *264* (5160), 826-828.
93. Jung, Y.; Marcus, R. A., On the Theory of Organic Catalysis "on Water". *J. Am. Chem. Soc.* **2007,** *129* (17), 5492-5502.
94. Aniansson, E. A. G.; Wall, S. N.; Almgren, M.; Hoffmann, H.; Kielmann, I.; Ulbricht, W.; Zana, R.; Lang, J.; Tondre, C., Theory of the kinetics of micellar equilibria and quantitative interpretation of chemical relaxation studies of micellar solutions of ionic surfactants. *J. Phys. Chem.* **1976,** *80* (9), 905-922.
95. Lipshutz, B. H.; Ghorai, S.; Cortes-Clerget, M., The Hydrophobic Effect Applied to Organic Synthesis: Recent Synthetic Chemistry "in Water". *Chem. Eur. J.* **2018,** *24* (26), 6672-6695.
96. La Sorella, G.; Strukul, G.; Scarso, A., Recent advances in catalysis in micellar media. *Green Chem.* **2015,** *17* (2), 644-683.
97. Lipshutz, B. H.; Isley, N. A.; Fennewald, J. C.; Slack, E. D., On the Way Towards Greener Transition-Metal-Catalyzed Processes as Quantified by E Factors. *Angew. Chem. Int. Ed.* **2013,** *52* (42), 10952-10958.
98. Denis, C.; Laignel, B.; Plusquellec, D.; Marouille, J.-Y. L.; Botrel, A., Highly Regio- and Stereoselective Reductions of Carbonyl Compounds in Aqueous Glycosidic Media. *Tetrahedron Lett.* **1996,** *37* (1), 53-56.
99. Ma, Y.; Liu, H.; Chen, L.; Cui, X.; Zhu, J.; Deng, J., Asymmetric Transfer Hydrogenation of Prochiral Ketones in Aqueous Media with New Water-Soluble Chiral Vicinal Diamine as Ligand. *Org. Lett.* **2003,** *5* (12), 2103-2106.
100. Ahlford, K.; Lind, J.; Mäler, L.; Adolfsson, H., Rhodium-catalyzed asymmetric transfer hydrogenation of alkyl and aryl ketones in aqueous media. *Green Chem.* **2008,** *10* (8), 832-835.
101. Li, J.; Tang, Y.; Wang, Q.; Li, X.; Cun, L.; Zhang, X.; Zhu, J.; Li, L.; Deng, J., Chiral Surfactant-Type Catalyst for Asymmetric Reduction of Aliphatic Ketones in Water. *J. Am. Chem. Soc.* **2012,** *134* (45), 18522-18525.
102. Li, J.; Li, X.; Ma, Y.; Wu, J.; Wang, F.; Xiang, J.; Zhu, J.; Wang, Q.; Deng, J., Surfactant-accelerated asymmetric transfer hydrogenation with recyclable water-soluble catalyst in aqueous media. *RSC Adv.* **2013,** *3* (6), 1825-1834.
103. Shaughnessy, K. H., Hydrophilic Ligands and Their Application in Aqueous-Phase Metal-Catalyzed Reactions. *Chem. Rev.* **2009,** *109* (2), 643-710.
104. Herrmann, W. A.; Kohlpaintner, C. W., Water-Soluble Ligands, Metal Complexes, and Catalysts: Synergism of Homogeneous and Heterogeneous Catalysis. *Angew. Chem. Int. Ed.* **1993,** *32* (11), 1524-1544.
105. Wiebus, E.; Cornils, B., Die großtechnische Oxosynthese mit immobilisiertem Katalysator. *Chem. Ing. Tech.* **1994,** *66* (7), 916-923.
106. Fache, E.; Senocq, F.; Santini, C.; Basset, J.-M., Homogeneous catalysis in water: a remarkable salt effect in the hydrogenation of propionaldehyde with RuCl2(tppts)3 and related complexes [tppts =(m-NaSO3C6H4)3P]. *J. Chem. Soc., Chem. Commun* **1990,** (24), 1776-1778.

107. Bényei, A.; Joó, F., Organometallic catalysis in aqueous solutions: the biphasic transfer hydrogenation of aldehydes catalyzed by water-soluble phosphine complexes of ruthenium, rhodium and iridium. *J. Mol. Catal.* **1990,** *58* (2), 151-163.
108. Joó, F.; Kovács, J.; Bényei, A. C.; Kathó, Á., Solution pH: A Selectivity Switch in Aqueous Organometallic Catalysis—Hydrogenation of Unsaturated Aldehydes Catalyzed by Sulfonatophenylphosphane–Ru Complexes. *Angew. Chem. Int. Ed.* **1998,** *37* (7), 969-970.
109. Szatmári, I.; Papp, G.; Joó, F.; Kathó, Á., Promoter effect of bicarbonate in hydrogenation of cinnamaldehyde catalyzed by a water-soluble Ru(II)-phosphine complex. *Inorg. Chim. Acta* **2018,** *472*, 302-306.
110. Horváth, H. H.; Joó, F., Stereoselective homogeneous catalytic hydrogenation of disubstituted alkynes in aqueous-organic biphasic media. *React. Kin. Catal. Lett.* **2005,** *85* (2), 355-360.
111. Makihara, N.; Ogo, S.; Watanabe, Y., pH-Selective Hydrogenation of Water-Soluble Carbonyl Compounds and Alkenes with [Cp*IrIII(H2O)3]2+ (Cp* = η5-C5Me5) as a Catalyst Precursor in Very Acidic Media. *Organometallics* **2001,** *20* (3), 497-500.
112. Darensbourg, D. J.; Joo, F.; Kannisto, M.; Katho, A.; Reibenspies, J. H.; Daigle, D. J., Water-soluble organometallic compounds. 4. Catalytic hydrogenation of aldehydes in an aqueous two-phase solvent system using a 1,3,5-triaza-7-phosphaadamantane complex of ruthenium. *Inorg. Chem.* **1994,** *33* (2), 200-208.
113. Darensbourg, D. J.; Joo, F.; Kannisto, M.; Katho, A.; Reibenspies, J. H., Water-soluble organometallic compounds. 2. Catalytic hydrogenation of aldehydes and olefins by new water-soluble 1,3,5-triaza-7-phosphaadamantane complexes of ruthenium and rhodium. *Organometallics* **1992,** *11* (6), 1990-1993.
114. Darensbourg, D. J.; Stafford, N. W.; Joó, F.; Reibenspies, J. H., Water-soluble organometallic compounds. 5. The regio-selective catalytic hydrogenation of unsaturated aldehydes to saturated aldehydes in an aqueous two-phase solvent system using 1,3,5-triaza-7-phosphaadamantane complexes of rhodium. *J. Organomet. Chem.* **1995,** *488* (1), 99-108.
115. Grosselin, J. M.; Mercier, C.; Allmang, G.; Grass, F., Selective hydrogenation of .alpha.,.beta.-unsaturated aldehydes in aqueous organic two-phase solvent systems using ruthenium or rhodium complexes of sulfonated phosphines. *Organometallics* **1991,** *10* (7), 2126-2133.
116. Wu, X.; Xiao, J., Aqueous-phase asymmetric transfer hydrogenation of ketones – a greener approach to chiral alcohols. *Chem. Commun.* **2007,** (24), 2449-2466.
117. Li, L.; Wu, J.; Wang, F.; Liao, J.; Zhang, H.; Lian, C.; Zhu, J.; Deng, J., Asymmetric transfer hydrogenation of ketones and imines with novel water-soluble chiral diamine as ligand in neat water. *Green Chem.* **2007,** *9* (1), 23-25.
118. Sudakar, P.; Gunasekar, G. H.; Baek, I. H.; Yoon, S., Recyclable and efficient heterogenized Rh and Ir catalysts for the transfer hydrogenation of carbonyl compounds in aqueous medium. *Green Chem.* **2016,** *18* (24), 6456-6461.
119. Delhomme, C.; Schaper, L.-A.; Zhang-Preße, M.; Raudaschl-Sieber, G.; Weuster-Botz, D.; Kühn, F. E., Catalytic hydrogenation of levulinic acid in aqueous phase. *J. Organomet. Chem.* **2013,** *724*, 297-299.
120. Moustani, C.; Anagnostopoulou, E.; Krommyda, K.; Panopoulou, C.; Koukoulakis, K. G.; Bakeas, E. B.; Papadogianakis, G., Novel aqueous-phase hydrogenation reaction of the key biorefinery platform chemical levulinic acid into γ-valerolactone employing highly active, selective and stable water-soluble ruthenium catalysts modified with nitrogen-containing ligands. *Appl. Catal., B* **2018,** *238*, 82-92.
121. Jessop, P. G.; Ikariya, T.; Noyori, R., Homogeneous Catalysis in Supercritical Fluids. *Chem. Rev.* **1999,** *99* (2), 475-494.

122. Purwanto; Deshpande, R. M.; Chaudhari, R. V.; Delmas, H., Solubility of Hydrogen, Carbon Monoxide, and 1-Octene in Various Solvents and Solvent Mixtures. *J. Chem. Eng. Data* **1996,** *41* (6), 1414-1417.
123. Budisa, N.; Schulze-Makuch, D., Supercritical Carbon Dioxide and Its Potential as a Life-Sustaining Solvent in a Planetary Environment. *Life* **2014,** *4* (3), 331.
124. Bhanage, B. M.; Ikushima, Y.; Shirai, M.; Arai, M., The selective formation of unsaturated alcohols by hydrogenation of α,β-unsaturated aldehydes in supercritical carbon dioxide using unpromoted Pt/Al2O3 catalyst. *Catal. Lett.* **1999,** *62* (2), 175-177.
125. Burk, M. J.; Feng, S.; Gross, M. F.; Tumas, W., Asymmetric catalytic hydrogenation reactions in supercritical carbon dioxide. *J. Am. Chem. Soc.* **1995,** *117* (31), 8277-8278.
126. Minder, B.; Mallat, T.; Pickel, K. H.; Steiner, K.; Baiker, A., Enantioselective hydrogenation of ethyl pyruvate in supercritical fluids. *Catal. Lett.* **1995,** *34* (1), 1-9.
127. Moriyoshi, T.; Kita, T.; Uosaki, Y., Static Relative Permittivity of Carbon Dioxide and Nitrous Oxide up to 30 MPa. *Ber. Bunsenges. Phys. Chem.* **1993,** *97* (4), 589-596.
128. Zhao, F.; Ikushima, Y.; Shirai, M.; Ebina, T.; Arai, M., Influence of electronic state and dispersion of platinum particles on the conversion and selectivity of hydrogenation of an α,β-unsaturated aldehyde in supercritical carbon dioxide. *J. Mol. Catal. A: Chem.* **2002,** *180* (1), 259-265.
129. Zhao, F.; Ikushima, Y.; Chatterjee, M.; Shirai, M.; Arai, M., An effective and recyclable catalyst for hydrogenation of α,β-unsaturated aldehydes into saturated aldehydes in supercritical carbon dioxide. *Green Chem.* **2003,** *5* (1), 76-79.
130. Fujita, S.; Yuzawa, K.; Bhanage, B. M.; Ikushima, Y.; Arai, M., Palladium-catalyzed Heck coupling reactions using different fluorinated phosphine ligands in compressed carbon dioxide and conventional organic solvents. *J. Mol. Catal. A: Chem.* **2002,** *180* (1), 35-42.
131. Zhao, F.; Ikushima, Y.; Chatterjee, M.; Sato, O.; Arai, M., Hydrogenation of an α,β-unsaturated aldehyde catalyzed with ruthenium complexes with different fluorinated phosphine compounds in supercritical carbon dioxide and conventional organic solvents. *J. of Supercritical Fluids* **2003,** *27* (1), 65-72.
132. Zhao, F.; Fujita, S.-i.; Sun, J.; Ikushima, Y.; Arai, M., Carbon dioxide-expanded liquid substrate phase: an effective medium for selective hydrogenation of cinnamaldehyde to cinnamyl alcohol. *Chem. Commun.* **2004,** (20), 2326-2327.
133. Shirai, M.; Tanaka, T.; Arai, M., Selective hydrogenation of α-, β-unsaturated aldehyde to unsaturated alcohol with supported platinum catalysts at high pressures of hydrogen. *J. Mol. Catal. A: Chem.* **2001,** *168* (1), 99-103.
134. Liu, R.; Zhao, F.; Fujita, S.-i.; Arai, M., Selective hydrogenation of citral with transition metal complexes in supercritical carbon dioxide. *Appl. Catal., A* **2007,** *316* (2), 127-133.
135. Chatterjee, M.; Zhao, F. Y.; Ikushima, Y., Hydrogenation of Citral using Monometallic Pt and Bimetallic Pt-Ru Catalysts on a Mesoporous Support in Supercritical Carbon Dioxide Medium. *Adv. Synth. Catal.* **2004,** *346* (4), 459-466.
136. Li, G.; Jiang, H.; Li, J., Use of water as a direct hydrogen donor in supercritical carbon dioxide: a novel and efficient Zn–HO–CO system for selective reduction of aldehydes to alcohols. *Green Chem.* **2001,** *3* (5), 250-251.
137. Mukhopadhyay, S.; Rothenberg, G.; Wiener, H.; Sasson, Y., Solid–solid palladium-catalysed water reduction with zinc: mechanisms of hydrogen generation and direct hydrogen transfer reactions. *New J. Chem.* **2000,** *24* (5), 305-308.
138. Wei-Bo, W.; Li-Lan, S.; Yao-Zeng, H., A novel reduction system — SbCl3-Al/ or SbCl3-Zn/DMF-H2O for conversion of aldehydes to alcohols. *Tetrahedron Lett.* **1990,** *31* (8), 1185-1186.
139. Hayler, J. D.; Leahy, D. K.; Simmons, E. M., A Pharmaceutical Industry Perspective on Sustainable Metal Catalysis. *Organometallics* **2018**.

140. Mehnert, C. P., Supported Ionic Liquid Catalysis. *Chem. Eur. J.* **2005,** *11* (1), 50-56.
141. Li, Y.-Y.; Yu, S.-L.; Shen, W.-Y.; Gao, J.-X., Iron-, Cobalt-, and Nickel-Catalyzed Asymmetric Transfer Hydrogenation and Asymmetric Hydrogenation of Ketones. *Acc. Chem. Res.* **2015,** *48* (9), 2587-2598.
142. Wang, D.; Astruc, D., The recent development of efficient Earth-abundant transition-metal nanocatalysts. *Chem. Soc. Rev.* **2017,** *46* (3), 816-854.
143. Štefane, B.; Požgan, F., Metal-Catalysed Transfer Hydrogenation of Ketones. *Top. Curr. Chem.* **2016,** *374* (2), 18.
144. Bullock, R. M., An Iron Catalyst for Ketone Hydrogenations under Mild Conditions. *Angew. Chem. Int. Ed.* **2007,** *46* (39), 7360-7363.
145. Knölker, H.-J.; Heber, J.; Mahler, C. H., Transition Metal-Diene Complexes in Organic Synthesis, Part 14.1 Regioselective Iron-Mediated [2+2+1] Cycloadditions of Alkynes and Carbon Monoxide: Synthesis of Substituted Cyclopentadienones. *Synlett* **1992,** *1992* (12), 1002-1004.
146. Knölker, H.-J.; Baum, E.; Goesmann, H.; Klauss, R., Demetalation of Tricarbonyl(cyclopentadienone)iron Complexes Initiated by a Ligand Exchange Reaction with NaOH—X-Ray Analysis of a Complex with Nearly Square-Planar Coordinated Sodium. *Angew. Chem. Int. Ed.* **1999,** *38* (13-14), 2064-2066.
147. Johnson, T. C.; Clarkson, G. J.; Wills, M., (Cyclopentadienone)iron Shvo Complexes: Synthesis and Applications to Hydrogen Transfer Reactions. *Organometallics* **2011,** *30* (7), 1859-1868.
148. Casey, C. P.; Guan, H., An Efficient and Chemoselective Iron Catalyst for the Hydrogenation of Ketones. *J. Am. Chem. Soc.* **2007,** *129* (18), 5816-5817.
149. Fleischer, S.; Zhou, S.; Junge, K.; Beller, M., General and Highly Efficient Iron-Catalyzed Hydrogenation of Aldehydes, Ketones, and α,β-Unsaturated Aldehydes. *Angew. Chem. Int. Ed.* **2013,** *52* (19), 5120-5124.
150. Morris, R. H., Asymmetric hydrogenation, transfer hydrogenation and hydrosilylation of ketones catalyzed by iron complexes. *Chem. Soc. Rev.* **2009,** *38* (8), 2282-2291.
151. Sui-Seng, C.; Freutel, F.; Lough, A. J.; Morris, R. H., Highly Efficient Catalyst Systems Using Iron Complexes with a Tetradentate PNNP Ligand for the Asymmetric Hydrogenation of Polar Bonds. *Angew. Chem. Int. Ed.* **2008,** *47* (5), 940-943.
152. Mikhailine, A.; Lough, A. J.; Morris, R. H., Efficient Asymmetric Transfer Hydrogenation of Ketones Catalyzed by an Iron Complex Containing a P−N−N−P Tetradentate Ligand Formed by Template Synthesis. *J. Am. Chem. Soc.* **2009,** *131* (4), 1394-1395.
153. Rautenstrauch, V.; Hoang-Cong, X.; Churlaud, R.; Abdur-Rashid, K.; Morris, R. H., Hydrogenation versus Transfer Hydrogenation of Ketones: Two Established Ruthenium Systems Catalyze Both. *Chem. Eur. J.* **2003,** *9* (20), 4954-4967.
154. Sonnenberg, J. F.; Coombs, N.; Dube, P. A.; Morris, R. H., Iron Nanoparticles Catalyzing the Asymmetric Transfer Hydrogenation of Ketones. *J. Am. Chem. Soc.* **2012,** *134* (13), 5893-5899.
155. Sonnenberg, J. F.; Morris, R. H., Distinguishing homogeneous from nanoparticle asymmetric iron catalysis. *Catal. Sci. Technol.* **2014,** *4* (10), 3426-3438.
156. Kelsen, V.; Wendt, B.; Werkmeister, S.; Junge, K.; Beller, M.; Chaudret, B., The use of ultrasmall iron(0) nanoparticles as catalysts for the selective hydrogenation of unsaturated C–C bonds. *Chem. Commun.* **2013,** *49* (33), 3416-3418.
157. Weber, S.; Brünig, J.; Zeindlhofer, V.; Schröder, C.; Stöger, B.; Limbeck, A.; Kirchner, K.; Bica, K., Selective Hydrogenation of Aldehydes Using a Well-Defined Fe(II) PNP Pincer Complex in Biphasic Medium. *ChemCatChem* **2018,** *10* (9), 4386-4394.
158. Adkins, H.; Connor, R., The catalytic hydrogenation of organic compounds over copper chromite. *J. Am. Chem. Soc.* **1931,** *53* (3), 1091-1095.

159. Adkins, H.; Burgoyne, E. E.; Schneider, H. J., The Copper—Chromium Oxide Catalyst for Hydrogenation. *J. Am. Chem. Soc.* **1950,** *72* (6), 2626-2629.
160. Hubaut, R.; Bonnelle, J. P.; Daage, M., Selective hydrogenation of heavy polyunsaturated molecules on copper-chromium catalysts. *J. Mol. Catal.* **1989,** *55* (1), 170-183.
161. Hubaut, R.; Daage, M.; Bonnelle, J. P., Selective hydrogenation on copper chromite catalysts. *Appl. Catal.* **1986,** *22* (2), 243-255.
162. Jenck, J.; Germain, J.-E., High-pressure competitive hydrogenation of aldehydes, ketones, and olefins on copper chromite catalyst. *J. Catal.* **1980,** *65* (1), 141-149.
163. Huang, W.; Li, H.; Zhu, B.; Feng, Y.; Wang, S.; Zhang, S., Selective hydrogenation of furfural to furfuryl alcohol over catalysts prepared via sonochemistry. *Ultrason. Sonochem.* **2007,** *14* (1), 67-74.
164. Gutiérrez, V.; Nador, F.; Radivoy, G.; Volpe, M. A., Highly selective copper nanoparticles for the hydrogenation of α,β-unsaturated aldehydes in liquid phase. *Appl. Catal., A* **2013,** *464-465*, 109-115.
165. Chen, J.-X.; Daeuble, J. F.; Brestensky, D. M.; Stryker, J. M., Highly Chemoselective Catalytic Hydrogenation of Unsaturated Ketones and Aldehydes to Unsaturated Alcohols Using Phosphine-Stabilized Copper(I) Hydride Complexes. *Tetrahedron* **2000,** *56* (15), 2153-2166.
166. Chen, J.-X.; Daeuble, J. F.; Stryker, J. M., Phosphine Effects in the Copper(I) Hydride-Catalyzed Hydrogenation of Ketones and Regioselective 1,2-Reduction of α,β-Unsaturated Ketones and Aldehydes. Hydrogenation of Decalin and Steroidal Ketones and Enones. *Tetrahedron* **2000,** *56* (18), 2789-2798.
167. Sirol, S.; Courmarcel, J.; Mostefai, N.; Riant, O., Efficient Enantioselective Hydrosilylation of Ketones Catalyzed by Air Stable Copper Fluoride−Phosphine Complexes. *Org. Lett.* **2001,** *3* (25), 4111-4113.
168. Shimizu, H.; Igarashi, D.; Kuriyama, W.; Yusa, Y.; Sayo, N.; Saito, T., Asymmetric Hydrogenation of Aryl Ketones Mediated by a Copper Catalyst. *Org. Lett.* **2007,** *9* (9), 1655-1657.
169. Kazuhiko, H.; Teruo, K., Liquid-phase Selective Hydrogenation of an Aliphatic α,β-Unsaturated Aldehyde over Raney Cobalt Catalyst Modified with Ferrous Chloride. *Bull. Chem. Soc. Jap.* **1969,** *42* (5), 1447-1449.
170. Kazuhiko, H.; Teruo, K., Kinetics of Liquid-phase Hydrogenation of Aliphatic α,β-Unsaturated Aldehyde over Raney Cobalt Catalyst Modified with Co-, Mn-, Ni-, and PdCl2. *Bull. Chem. Soc. Jap.* **1972,** *45* (10), 3118-3121.
171. Goetz, R. W.; Orchin, M., The reaction of cobalt hydrocarbonyl with α,β-unsaturated aldehydes and ketones. *J. Am. Chem. Soc.* **1963,** *85* (18), 2782-2784.
172. Nitta, Y.; Imanaka, T.; Teranishi, S., Hydrogenation activity and selectivity of cobalt boride and cobalt nickel binary boride catalysts. *Bull. Chem. Soc. Jap.* **1980,** *53* (11), 3154-3158.
173. Chen, Y. Z.; Wu, K. J., Hydrogenation activity and selectivity of cobalt borides. *Appl. Catal.* **1991,** *78* (2), 185-197.
174. Chen, Y. Z.; Wei, S. W.; Wu, K. J., Effect of promoter on selective hydrogenation of α,β-unsaturated aldehydes over cobalt borides. *Appl. Catal., A* **1993,** *99* (2), 85-96.
175. Zhang, G.; Scott, B. L.; Hanson, S. K., Mild and Homogeneous Cobalt-Catalyzed Hydrogenation of C=C, C=O, and C=N Bonds. *Angew. Chem. Int. Ed.* **2012,** *51* (48), 12102-12106.
176. Zhang, G.; Hanson, S. K., Cobalt-catalyzed transfer hydrogenation of C=O and C=N bonds. *Chem. Commun.* **2013,** *49* (86), 10151-10153.

177. Zhang, G.; Vasudevan, K. V.; Scott, B. L.; Hanson, S. K., Understanding the Mechanisms of Cobalt-Catalyzed Hydrogenation and Dehydrogenation Reactions. *J. Am. Chem. Soc.* **2013,** *135* (23), 8668-8681.
178. Elangovan, S.; Topf, C.; Fischer, S.; Jiao, H.; Spannenberg, A.; Baumann, W.; Ludwig, R.; Junge, K.; Beller, M., Selective Catalytic Hydrogenations of Nitriles, Ketones, and Aldehydes by Well-Defined Manganese Pincer Complexes. *J. Am. Chem. Soc.* **2016,** *138* (28), 8809-8814.
179. Garbe, M.; Junge, K.; Beller, M., Homogeneous Catalysis by Manganese-Based Pincer Complexes. *Eur. J. Org. Chem.* **2017,** *2017* (30), 4344-4362.
180. Kallmeier, F.; Irrgang, T.; Dietel, T.; Kempe, R., Highly Active and Selective Manganese C=O Bond Hydrogenation Catalysts: The Importance of the Multidentate Ligand, the Ancillary Ligands, and the Oxidation State. *Angew. Chem. Int. Ed.* **2016,** *55* (39), 11806-11809.
181. Glatz, M.; Stöger, B.; Himmelbauer, D.; Veiros, L. F.; Kirchner, K., Chemoselective Hydrogenation of Aldehydes under Mild, Base-Free Conditions: Manganese Outperforms Rhenium. *ACS Catal.* **2018,** *8* (5), 4009-4016.
182. Wei, D.; Bruneau-Voisine, A.; Chauvin, T.; Dorcet, V.; Roisnel, T.; Valyaev, D. A.; Lugan, N.; Sortais, J.-B., Hydrogenation of Carbonyl Derivatives Catalysed by Manganese Complexes Bearing Bidentate Pyridinyl-Phosphine Ligands. *Adv. Synth. Catal.* **2018,** *360* (4), 676-681.
183. Perez, M.; Elangovan, S.; Spannenberg, A.; Junge, K.; Beller, M., Molecularly Defined Manganese Pincer Complexes for Selective Transfer Hydrogenation of Ketones. *ChemSusChem* **2017,** *10* (1), 83-86.
184. Bruneau-Voisine, A.; Wang, D.; Dorcet, V.; Roisnel, T.; Darcel, C.; Sortais, J.-B., Transfer Hydrogenation of Carbonyl Derivatives Catalyzed by an Inexpensive Phosphine-Free Manganese Precatalyst. *Org. Lett.* **2017,** *19* (13), 3656-3659.
185. Martínez-Ferraté, O.; Werlé, C.; Franciò, G.; Leitner, W., Aminotriazole Mn(I) Complexes as Effective Catalysts for Transfer Hydrogenation of Ketones. *ChemCatChem* **2018,** *10* (20), 4514-4518.
186. Widegren, M. B.; Harkness, G. J.; Slawin, A. M. Z.; Cordes, D. B.; Clarke, M. L., A Highly Active Manganese Catalyst for Enantioselective Ketone and Ester Hydrogenation. *Angew. Chem. Int. Ed.* **2017,** *56* (21), 5825-5828.
187. Garbe, M.; Junge, K.; Walker, S.; Wei, Z.; Jiao, H.; Spannenberg, A.; Bachmann, S.; Scalone, M.; Beller, M., Manganese(I)-Catalyzed Enantioselective Hydrogenation of Ketones Using a Defined Chiral PNP Pincer Ligand. *Angew. Chem. Int. Ed.* **2017,** *56* (37), 11237-11241.
188. Zirakzadeh, A.; de Aguiar, S. R. M. M.; Stöger, B.; Widhalm, M.; Kirchner, K., Enantioselective Transfer Hydrogenation of Ketones Catalyzed by a Manganese Complex Containing an Unsymmetrical Chiral PNP′ Tridentate Ligand. *ChemCatChem* **2017,** *9* (10), 1744-1748.
189. Wang, D.; Bruneau-Voisine, A.; Sortais, J.-B., Practical (asymmetric) transfer hydrogenation of ketones catalyzed by manganese with (chiral) diamines ligands. *Catal. Commun.* **2018,** *105*, 31-36.
190. Le Page, M. D.; James, B. R., Nickel bromide as a hydrogen transfer catalyst. *Chem. Commun.* **2000,** (17), 1647-1648.
191. Phukan, P.; Sudalai, A., Chemoselective Transfer Hydrogenation of Carbonyl Compounds Catalyzed by Macrocyclic Nickel (II) Complex. *Synth. Comm.* **2000,** *30* (13), 2401-2405.
192. Iyer, S.; Varghese, J. P., [NiCl2(PPh3)2] catalysed transfer hydrogenation of ketones and aldehydes by propan-2-ol. *J. Chem. Soc., Chem. Commun* **1995,** (4), 465-466.

193. Alonso, F.; Riente, P.; Yus, M., Hydrogen-transfer reduction of carbonyl compounds promoted by nickel nanoparticles. *Tetrahedron* **2008,** *64* (8), 1847-1852.
194. T. Upadhya, T.; P. Katdare, S.; P. Sabde, D.; Ramaswamy, V.; Sudalai, A., Chemoselective transfer hydrogenation of nitroarenes, aldehydes and ketones with propan-2-ol catalysed by Ni-stabilized zirconia. *Chem. Commun.* **1997,** (12), 1119-1120.
195. Mebane, R. C.; Holte, K. L.; Gross, B. H., Transfer Hydrogenation of Ketones with 2-Propanol and Raney® Nickel. *Synth. Comm.* **2007,** *37* (16), 2787-2791.
196. Alonso, F.; Riente, P.; Yus, M., Hydrogen-transfer reduction of carbonyl compounds catalysed by nickel nanoparticles. *Tetrahedron Lett.* **2008,** *49* (12), 1939-1942.
197. Shimura, K.; Shimizu, K.-i., Transfer hydrogenation of ketones by ceria-supported Ni catalysts. *Green Chem.* **2012,** *14* (11), 2983-2985.
198. Escande, V.; Poullain, C.; Clavé, G.; Petit, E.; Masquelez, N.; Hesemann, P.; Grison, C., Bio-based and environmental input for transfer hydrogenation using EcoNi(0) catalyst in isopropanol. *Appl. Catal., B* **2017,** *210*, 495-503.
199. Hudson, R.; Feng, Y.; Varma, R. S.; Moores, A., Bare magnetic nanoparticles: sustainable synthesis and applications in catalytic organic transformations. *Green Chem.* **2014,** *16* (10), 4493-4505.
200. Kantam, M. L.; Yadav, J.; Laha, S.; Srinivas, P.; Sreedhar, B.; Figueras, F., Asymmetric Hydrosilylation of Ketones Catalyzed by Magnetically Recoverable and Reusable Copper Ferrite Nanoparticles. *J. Org. Chem.* **2009,** *74* (12), 4608-4611.
201. Hudson, R.; Chazelle, V.; Bateman, M.; Roy, R.; Li, C.-J.; Moores, A., Sustainable Synthesis of Magnetic Ruthenium-Coated Iron Nanoparticles and Application in the Catalytic Transfer Hydrogenation of Ketones. *ACS Sustainable Chem. Eng.* **2015,** *3* (5), 814-820.
202. Vijayakrishna, K.; Charan, K. T. P.; Manojkumar, K.; Venkatesh, S.; Pothanagandhi, N.; Sivaramakrishna, A.; Mayuri, P.; Kumar, A. S.; Sreedhar, B., Ni Nanoparticles Stabilized by Poly(Ionic Liquids) as Chemoselective and Magnetically Recoverable Catalysts for Transfer Hydrogenation Reactions of Carbonyl Compounds. *ChemCatChem* **2016,** *8* (6), 1139-1145.
203. Dasgupta, S.; Chakraborty, A.; Chatterjee, S.; Chattopadhyay, T., Synthesis and characterization of magnetically separable Fe3O4@AHBA@Ni(0) [AHBA = 3-amino-4-hydroxybenzoicacid] nanocatalyst: Applications for carbonyl hydrogenation and alcohol oxidation. *Inorg. Chim. Acta* **2018,** *474*, 1-10.
204. Stephan, D. W., The broadening reach of frustrated Lewis pair chemistry. *Science* **2016,** *354* (6317).
205. Scott, D. J.; Fuchter, M. J.; Ashley, A. E., Designing effective 'frustrated Lewis pair' hydrogenation catalysts. *Chem. Soc. Rev.* **2017,** *46* (19), 5689-5700.
206. Welch, G. C.; Juan, R. R. S.; Masuda, J. D.; Stephan, D. W., Reversible, Metal-Free Hydrogen Activation. *Science* **2006,** *314* (5802), 1124-1126.
207. Mahdi, T.; Stephan, D. W., Enabling Catalytic Ketone Hydrogenation by Frustrated Lewis Pairs. *J. Am. Chem. Soc.* **2014,** *136* (45), 15809-15812.
208. Scott, D. J.; Fuchter, M. J.; Ashley, A. E., Nonmetal Catalyzed Hydrogenation of Carbonyl Compounds. *J. Am. Chem. Soc.* **2014,** *136* (45), 15813-15816.
209. Mahdi, T.; Stephan, D. W., Facile Protocol for Catalytic Frustrated Lewis Pair Hydrogenation and Reductive Deoxygenation of Ketones and Aldehydes. *Angew. Chem. Int. Ed.* **2015,** *54* (29), 8511-8514.
210. Scott, D. J.; Simmons, T. R.; Lawrence, E. J.; Wildgoose, G. G.; Fuchter, M. J.; Ashley, A. E., Facile Protocol for Water-Tolerant "Frustrated Lewis Pair"-Catalyzed Hydrogenation. *ACS Catal.* **2015,** *5* (9), 5540-5544.

211. Gyömöre, Á.; Bakos, M.; Földes, T.; Pápai, I.; Domján, A.; Soós, T., Moisture-Tolerant Frustrated Lewis Pair Catalyst for Hydrogenation of Aldehydes and Ketones. *ACS Catal.* **2015,** *5* (9), 5366-5372.
212. Das, S.; Pati, S. K., On the Mechanism of Frustrated Lewis Pair Catalysed Hydrogenation of Carbonyl Compounds. *Chem. Eur. J.* **2017,** *23* (5), 1078-1085.
213. Scott, D. J.; Phillips, N. A.; Sapsford, J. S.; Deacy, A. C.; Fuchter, M. J.; Ashley, A. E., Versatile Catalytic Hydrogenation Using A Simple Tin(IV) Lewis Acid. *Angew. Chem.* **2016,** *128* (47), 14958-14962.
214. Krempner, C.; Mummadi, S.; Brar, A.; Wang, G.; Kenefake, D.; Diaz, R.; Unruh, D.; Li, S., 'Inverse' Frustrated Lewis Pairs - An Inverse FLP Approach to the Catalytic Metal Free Hydrogenation of Ketones. *Chem. Eur. J.* **2018,** *24* (62), 16526-16531.
215. Primo, A.; Neatu, F.; Florea, M.; Parvulescu, V.; Garcia, H., Graphenes in the absence of metals as carbocatalysts for selective acetylene hydrogenation and alkene hydrogenation. *Nat. Commun.* **2014,** *5*, 5291.
216. Trandafir, M.-M.; Florea, M.; Neaţu, F.; Primo, A.; Parvulescu, V. I.; García, H., Graphene from Alginate Pyrolysis as a Metal-Free Catalyst for Hydrogenation of Nitro Compounds. *ChemSusChem* **2016,** *9* (13), 1565-1569.
217. Ding, Y.; Huang, X.; Yi, X.; Qiao, Y.; Sun, X.; Zheng, A.; Su, D. S., A Heterogeneous Metal-Free Catalyst for Hydrogenation: Lewis Acid–Base Pairs Integrated into a Carbon Lattice. *Angew. Chem. Int. Ed.* **2018,** *57* (0).
218. Wang, D.; Astruc, D., The Golden Age of Transfer Hydrogenation. *Chem. Rev.* **2015,** *115* (13), 6621-6686.
219. G. Hitzler, M.; Poliakoff, M., Continuous hydrogenation of organic compounds in supercritical fluids. *Chem. Commun.* **1997,** (17), 1667-1668.
220. Brieger, G.; Nestrick, T. J., Catalytic transfer hydrogenation. *Chem. Rev.* **1974,** *74* (5), 567-580.
221. Schlesinger, H. I.; Brown, H. C.; Finholt, A. E., The Preparation of Sodium Borohydride by the High Temperature Reaction of Sodium Hydride with Borate Esters. *J. Am. Chem. Soc.* **1953,** *75* (1), 205-209.
222. Finholt, A. E.; Bond, A. C.; Schlesinger, H. I., Lithium Aluminum Hydride, Aluminum Hydride and Lithium Gallium Hydride, and Some of their Applications in Organic and Inorganic Chemistry. *J. Am. Chem. Soc.* **1947,** *69* (5), 1199-1203.
223. Holger, E.; Christian, F.; Gerd, B.; Sjoerd, H., LiAlH4: From Stoichiometric Reduction to Imine Hydrogenation Catalysis. *Angew. Chem. Int. Ed.* **2018,** *57* (24), 7156-7160.
224. Manna, S.; Antonchick, A. P., Catalytic Transfer Hydrogenation Using Biomass as Hydrogen Source. *ChemSusChem 0* (ja).
225. Guyon, C.; Métay, E.; Duguet, N.; Lemaire, M., Biphasic Glycerol/2-MeTHF, Ruthenium-Catalysed Enantioselective Transfer Hydrogenation of Ketones Using Sodium Hypophosphite as Hydrogen Donor. *Eur. J. Org. Chem.* **2013,** *2013* (24), 5439-5444.
226. Agency, E. C. Phosphinic acid - substance information. https://echa.europa.eu/substance-information/-/substanceinfo/100.118.170 (accessed 30/09/2018).
227. Cha, J. S., Recent Developments In Meerwein−Ponndorf−Verley and Related Reactions for the Reduction of Organic Functional Groups Using Aluminum, Boron, and Other Metal Reagents: A Review. *Org. Proc. Res. Dev.* **2006,** *10* (5), 1032-1053.
228. Verley, A., Exchange of functional groups between two molecules. Exchange of alcohol and aldehyde groups. *Bull. Soc. Chim. Fr.* **1925,** *37*, 871.
229. Hans, M.; Rudolf, S., Ein neues Verfahren zur Reduktion von Aldehyden und Ketonen. *Liebigs Ann.* **1925,** *444* (1), 221-238.

230. Wolfgang, P., Der reversible Austausch der Oxydationsstufen zwischen Aldehyden oder Ketonen einerseits und primären oder sekundären Alkoholen anderseits. *Angew. Chem.* **1926,** *39* (5), 138-143.
231. Akamanchi, K. G.; Noorani, V. R., Truly catalytic Meerwein-Ponndorf-Verley (MPV) reduction. *Tetrahedron Lett.* **1995,** *36* (28), 5085-5088.
232. Akamanchi, K. G.; Varalakshmy, N. R., Aluminium isopropoxide - TFA, a modified catalyst for highly accelerated meerwein - ponndorf - verley (MPV) reduction. *Tetrahedron Lett.* **1995,** *36* (20), 3571-3572.
233. Ooi, T.; Miura, T.; Itagaki, Y.; Ichikawa, H.; Maruoka, K., Catalytic Meerwein-Ponndorf-Verley (MPV) and Oppenauer (OPP) Reactions: Remarkable Acceleration of the Hydride Transfer by Powerful Bidentate Aluminum Alkoxides. *Synthesis* **2002,** *2002* (02), 0279-0291.
234. Konishi, K.; Makita, K.; Aida, T.; Inoue, S., Highly stereoselective hydrogen transfer from alcohols to carbonyl compounds catalysed by aluminium porphyrins. *J. Chem. Soc., Chem. Commun* **1988,** (10), 643-645.
235. McNerney, B.; Whittlesey, B.; Cordes, D. B.; Krempner, C., A Well-Defined Monomeric Aluminum Complex as an Efficient and General Catalyst in the Meerwein–Ponndorf–Verley Reduction. *Chem. Eur. J.* **2014,** *20* (46), 14959-14964.
236. López-Asensio, R.; Cecilia, J. A.; Jiménez-Gómez, C. P.; García-Sancho, C.; Moreno-Tost, R.; Maireles-Torres, P., Selective production of furfuryl alcohol from furfural by catalytic transfer hydrogenation over commercial aluminas. *Appl. Catal., A* **2018,** *556*, 1-9.
237. He, J.; Li, H.; Lu, Y.-M.; Liu, Y.-X.; Wu, Z.-B.; Hu, D.-Y.; Yang, S., Cascade catalytic transfer hydrogenation–cyclization of ethyl levulinate to γ-valerolactone with Al–Zr mixed oxides. *Appl. Catal., A* **2016,** *510*, 11-19.
238. Chia, M.; Dumesic, J. A., Liquid-phase catalytic transfer hydrogenation and cyclization of levulinic acid and its esters to γ-valerolactone over metal oxide catalysts. *Chem. Commun.* **2011,** *47* (44), 12233-12235.
239. Wang, J.; Jaenicke, S.; Chuah, G.-K., Zirconium–Beta zeolite as a robust catalyst for the transformation of levulinic acid to γ-valerolactone via Meerwein–Ponndorf–Verley reduction. *RSC Adv.* **2014,** *4* (26), 13481-13489.
240. Li, F.; France, L. J.; Cai, Z.; Li, Y.; Liu, S.; Lou, H.; Long, J.; Li, X., Catalytic transfer hydrogenation of butyl levulinate to γ-valerolactone over zirconium phosphates with adjustable Lewis and Brønsted acid sites. *Appl. Catal., B* **2017,** *214*, 67-77.
241. Valekar, A. H.; Cho, K.-H.; Chitale, S. K.; Hong, D.-Y.; Cha, G.-Y.; Lee, U. H.; Hwang, D. W.; Serre, C.; Chang, J.-S.; Hwang, Y. K., Catalytic transfer hydrogenation of ethyl levulinate to γ-valerolactone over zirconium-based metal–organic frameworks. *Green Chem.* **2016,** *18* (16), 4542-4552.
242. Song, J.; Wu, L.; Zhou, B.; Zhou, H.; Fan, H.; Yang, Y.; Meng, Q.; Han, B., A new porous Zr-containing catalyst with a phenate group: an efficient catalyst for the catalytic transfer hydrogenation of ethyl levulinate to γ-valerolactone. *Green Chem.* **2015,** *17* (3), 1626-1632.
243. Assary, R. S.; Curtiss, L. A.; Dumesic, J. A., Exploring Meerwein–Ponndorf–Verley Reduction Chemistry for Biomass Catalysis Using a First-Principles Approach. *ACS Catal.* **2013,** *3* (12), 2694-2704.
244. Cai, B.; Zhou, X.-C.; Miao, Y.-C.; Luo, J.-Y.; Pan, H.; Huang, Y.-B., Enhanced Catalytic Transfer Hydrogenation of Ethyl Levulinate to γ-Valerolactone over a Robust Cu–Ni Bimetallic Catalyst. *ACS Sustainable Chem. Eng.* **2017,** *5* (2), 1322-1331.
245. Castellanos-Blanco, N.; Arévalo, A.; García, J. J., Nickel-catalyzed transfer hydrogenation of ketones using ethanol as a solvent and a hydrogen donor. *Dalton Trans.* **2016,** *45* (34), 13604-13614.

246. Ouali, A.; Majoral, J.-P.; Caminade, A.-M.; Taillefer, M., NaOH-Promoted Hydrogen Transfer: Does NaOH or Traces of Transition Metals Catalyze the Reaction? *ChemCatChem* **2009,** *1* (4), 504-509.
247. Polshettiwar, V.; Varma, R. S., Revisiting the Meerwein–Ponndorf–Verley reduction: a sustainable protocol for transfer hydrogenation of aldehydes and ketones. *Green Chem.* **2009,** *11* (9), 1313-1316.
248. Wang, D.; Deraedt, C.; Ruiz, J.; Astruc, D., Sodium hydroxide-catalyzed transfer hydrogenation of carbonyl compounds and nitroarenes using ethanol or isopropanol as both solvent and hydrogen donor. *J. Mol. Catal. A: Chem.* **2015,** *400*, 14-21.
249. Ikhile, M. I.; Nyamori, V. O.; Bala, M. D., Transition metal free transfer hydrogenation of ketones promoted by 1,3-diarylimidazolium salts and KOH. *Tetrahedron Lett.* **2012,** *53* (37), 4925-4928.
250. Radhakrishan, R.; Do, D. M.; Jaenicke, S.; Sasson, Y.; Chuah, G.-K., Potassium Phosphate as a Solid Base Catalyst for the Catalytic Transfer Hydrogenation of Aldehydes and Ketones. *ACS Catal.* **2011,** *1* (11), 1631-1636.
251. Hietala, J.; Vuori, A.; Johnsson, P.; Pollari, I.; Reutemann, W.; Kieczka, H., Formic Acid. In *Ullmann's Encyclopedia of Industrial Chemistry*, Wiley-VCH, Ed. 2016.
252. Ariger, M. A.; Carreira, E. M., pH-Independent Transfer Hydrogenation in Water: Catalytic, Enantioselective Reduction of β-Keto Esters. *Org. Lett.* **2012,** *14* (17), 4522-4524.
253. Wu, X.; Li, X.; Hems, W.; King, F.; Xiao, J., Accelerated asymmetric transfer hydrogenation of aromatic ketones in water. *Org. Biomol. Chem.* **2004,** *2* (13), 1818-1821.
254. Soltani, O.; Ariger, M. A.; Vázquez-Villa, H.; Carreira, E. M., Transfer Hydrogenation in Water: Enantioselective, Catalytic Reduction of α-Cyano and α-Nitro Substituted Acetophenones. *Org. Lett.* **2010,** *12* (13), 2893-2895.
255. Seashore-Ludlow, B.; Saint-Dizier, F.; Somfai, P., Asymmetric Transfer Hydrogenation Coupled with Dynamic Kinetic Resolution in Water: Synthesis of anti-β-Hydroxy-α-amino Acid Derivatives. *Org. Lett.* **2012,** *14* (24), 6334-6337.
256. Zheng, L.-S.; Llopis, Q.; Echeverria, P.-G.; Férard, C.; Guillamot, G.; Phansavath, P.; Ratovelomanana-Vidal, V., Asymmetric Transfer Hydrogenation of (Hetero)arylketones with Tethered Rh(III)–N-(p-Tolylsulfonyl)-1,2-diphenylethylene-1,2-diamine Complexes: Scope and Limitations. *J. Org. Chem.* **2017,** *82* (11), 5607-5615.
257. Gröger, H.; Hummel, W.; Buchholz, S.; Drauz, K.; Nguyen, T. V.; Rollmann, C.; Hüsken, H.; Abokitse, K., Practical Asymmetric Enzymatic Reduction through Discovery of a Dehydrogenase-Compatible Biphasic Reaction Media. *Org. Lett.* **2003,** *5* (2), 173-176.
258. Gao, Y.; Jaenicke, S.; Chuah, G.-K., Highly efficient transfer hydrogenation of aldehydes and ketones using potassium formate over AlO(OH)-entrapped ruthenium catalysts. *Appl. Catal., A* **2014,** *484*, 51-58.
259. Xian-Long, D.; Lin, H.; She, Z.; Yong-Mei, L.; Yong, C.; He-Yong, H.; Kang-Nian, F., Hydrogen-independent reductive transformation of carbohydrate biomass into γ-valerolactone and pyrrolidone derivatives with supported gold catalysts. *Angew. Chem. Int. Ed.* **2011,** *50* (34), 7815-7819.
260. Fu, M.-C.; Shang, R.; Huang, Z.; Fu, Y., Conversion of Levulinate Ester and Formic Acid into γ-Valerolactone Using a Homogeneous Iron Catalyst. *Synlett* **2014,** *25* (19), 2748-2752.
261. Mohan, V.; David, R. B.; Rama, R. K. S.; B., J. S.; E., v. Z. W., Hydrogenation of Levulinic Acid Using Formic Acid as a Hydrogen Source over Ni/SiO2 Catalysts. *Chem. Eng. Tech.* **2017,** *40* (4), 719-726.
262. Liang, W.; Bingsen, Z.; Xiangju, M.; Sheng, S. D.; Feng-Shou, X., Hydrogenation of Biofuels with Formic Acid over a Palladium-Based Ternary Catalyst with Two Types of Active Sites. *ChemSusChem* **2014,** *7* (6), 1537-1541.

263. García, J. I.; García-Marín, H.; Pires, E., Glycerol based solvents: synthesis, properties and applications. *Green Chem.* **2014,** *16* (3), 1007-1033.
264. Díaz-Álvarez, A.; Cadierno, V., Glycerol: A promising Green Solvent and Reducing Agent for Metal-Catalyzed Transfer Hydrogenation Reactions and Nanoparticles Formation. *Appl. Sci.* **2013,** *3* (1), 55.
265. Carroll, K. J.; Reveles, J. U.; Shultz, M. D.; Khanna, S. N.; Carpenter, E. E., Preparation of Elemental Cu and Ni Nanoparticles by the Polyol Method: An Experimental and Theoretical Approach. *J Phys. Chem. C* **2011,** *115* (6), 2656-2664.
266. Tavor, D.; Sheviev, O.; Dlugy, C.; Wolfson, A., Transfer hydrogenations of benzaldehyde using glycerol as solvent and hydrogen source. *Can. J. Chem.* **2010,** *88* (4), 305-308.
267. Azua, A.; Mata, J. A.; Peris, E., Iridium NHC Based Catalysts for Transfer Hydrogenation Processes Using Glycerol as Solvent and Hydrogen Donor. *Organometallics* **2011,** *30* (20), 5532-5536.
268. Azua, A.; Mata, J. A.; Peris, E.; Lamaty, F.; Martinez, J.; Colacino, E., Alternative Energy Input for Transfer Hydrogenation using Iridium NHC Based Catalysts in Glycerol as Hydrogen Donor and Solvent. *Organometallics* **2012,** *31* (10), 3911-3919.
269. Sharma, A. K.; Joshi, H.; Sharma, K. N.; Gupta, P. L.; Singh, A. K., 2-Propanol vs Glycerol as Hydrogen Source in Catalytic Activation of Transfer Hydrogenation with (η6-Benzene)ruthenium(II) Complexes of Unsymmetrical Bidentate Chalcogen Ligands. *Organometallics* **2014,** *33* (13), 3629-3639.
270. Gawande, M. B.; Rathi, A. K.; Branco, P. S.; Nogueira, I. D.; Velhinho, A.; Shrikhande, J. J.; Indulkar, U. U.; Jayaram, R. V.; Ghumman, C. A. A.; Bundaleski, N.; Teodoro, O. M. N. D., Regio- and Chemoselective Reduction of Nitroarenes and Carbonyl Compounds over Recyclable Magnetic Ferrite-Nickel Nanoparticles (Fe3O4-Ni) by Using Glycerol as a Hydrogen Source. *Chem. Eur. J.* **2012,** *18* (40), 12628-12632.
271. Brett, G. L.; He, Q.; Hammond, C.; Miedziak, P. J.; Dimitratos, N.; Sankar, M.; Herzing, A. A.; Conte, M.; Lopez-Sanchez, J. A.; Kiely, C. J.; Knight, D. W.; Taylor, S. H.; Hutchings, G. J., Selective Oxidation of Glycerol by Highly Active Bimetallic Catalysts at Ambient Temperature under Base-Free Conditions. *Angew. Chem. Int. Ed.* **2011,** *50* (43), 10136-10139.
272. Sánchez, B. S.; Gross, M. S.; Querini, C. A., Pt catalysts supported on ion exchange resins for selective glycerol oxidation. Effect of Au incorporation. *Catal. Today* **2017,** *296*, 35-42.
273. Villa, A.; Jouve, A.; Sanchez Trujillo, F.; Motta, D.; Prati, L.; Dimitratos, N., Exploring the Effect of Au/Pt Ratio on Glycerol Oxidation in Presence and Absence of a Base. *Catalysts* **2018,** *8* (2), 54.
274. Sauer, R. O.; Scheiber, W. J.; Brewer, S. D., Derivatives of the Methylchlorosilanes. V. Polysiloxanes from Methyldichlorosilane. *J. Am. Chem. Soc.* **1946,** *68* (6), 962-963.
275. J. Lawrence, N.; D. Drew, M.; M. Bushell, S., Polymethylhydrosiloxane: a versatile reducing agent for organic synthesis. *J. Chem. Soc., Perkin Trans. 1,* **1999,** (23), 3381-3391.
276. Döhlert, P.; Enthaler, S., Conversion of Poly(methylhydrosiloxane) Waste to Useful Commodities. *Catal. Lett.* **2016,** *146* (2), 345-352.
277. Lipowitz, J.; Bowman, S. A., Use of polymethylhydrosiloxane as a selective, neutral reducing agent for aldehydes, ketones, olefins, and aromatic nitro compounds. *J. Org. Chem.* **1973,** *38* (1), 162-165.
278. Grady, G. L.; Kuivila, H. G., Simple technique for performing reactions with organotin hydrides. *J. Org. Chem.* **1969,** *34* (6), 2014-2016.
279. Lawrence, N. J.; Bushell, S. M., An efficient protocol for the reduction of ketones with tin(II) complexes and PMHS. *Tetrahedron Lett.* **2000,** *41* (22), 4507-4512.

280. Kobayashi, Y.; Takahisa, E.; Nakano, M.; Watatani, K., Reduction of carbonyl compounds by using polymethylhydro-siloxane: reactivity and selectivity. *Tetrahedron* **1997,** *53* (5), 1627-1634.
281. Wang, Z.; Wroblewski, A. E.; Verkade, J. G., P(MeNCH2CH2)3N: An Efficient Promoter for the Reduction of Aldehydes and Ketones with Poly(methylhydrosiloxane). *J. Org. Chem.* **1999,** *64* (21), 8021-8023.
282. Kseniya, R.; I., N. G., Base-Catalyzed Hydrosilylation of Ketones and Esters and Insight into the Mechanism. *Chem. Eur. J.* **2014,** *20* (3), 839-845.
283. Misal, C. L. C.; David, B.; Jean-Baptiste, S.; Christophe, D., Iron dihydride complex as the pre-catalyst for efficient hydrosilylation of aldehydes and ketones under visible light activation. *Adv. Synth. Catal.* **2011,** *353* (8), 1279-1284.
284. Elina, B.; Lorenzo, Z.; Hans, A., Selective hydrosilylation of ketones catalyzed by in situ-generated iron NHC complexes. *Appl. Organomet. Chem.* **2011,** *25* (10), 748-752.
285. Daniele, A.; Nadim, S.; Shaolin, Z.; Shoubhik, D.; Kathrin, J.; Matthias, B., Chemo- and Stereoselective Iron-Catalyzed Hydrosilylation of Ketones. *Chem. Asian J.* **2010,** *5* (7), 1687-1691.
286. Marcin, S.; Agata, B.; Jacek, M., Zinc-Catalyzed Enantioselective Hydrosilylation of Ketones and Imines under Solvent-Free Conditions. *ChemCatChem* **2016,** *8* (23), 3575-3579.
287. Mimoun, H., Selective Reduction of Carbonyl Compounds by Polymethylhydrosiloxane in the Presence of Metal Hydride Catalysts. *J. Org. Chem.* **1999,** *64* (7), 2582-2589.
288. Bette, V.; Mortreux, A.; Savoia, D.; Carpentier, J.-F., New developments in zinc-catalyzed asymmetric hydrosilylation of ketones with PMHS. *Tetrahedron* **2004,** *60* (12), 2837-2842.
289. Mimoun, H.; de Saint Laumer, J. Y.; Giannini, L.; Scopelliti, R.; Floriani, C., Enantioselective Reduction of Ketones by Polymethylhydrosiloxane in the Presence of Chiral Zinc Catalysts. *J. Am. Chem. Soc.* **1999,** *121* (26), 6158-6166.

Singsong 'round the money tree
This stunning documentary that no one else unfortunately saw
Such beautiful photography, it's worth it for the opening scene
I've been driving 'round listening to the score
Or maybe, I just imagined it all

Turner, A.; Helders, M.; Cook, J.; O'Malley, N. One Point Perspective, *Tranquility Base Hotel & Casino*, **2018**, *2*, 5:55-9:22.

Owing to the challenges in C=O reduction mentioned previously, Ag NPs shine as highly selective catalysts. Their applications in C=O hydrogenation, and many other organic reactions, are covered below.

2 Silver NPs in organic transformations

This chapter is adapted from a published article, whose citation appear below, which is reprinted with permission from Wiley editions and all co-authors.

Alain Y. Li, Alexandra Gellé, Andreanne Segalla, and Audrey Moores, Silver NPs in Organic Transformations, book chapter for "Silver Catalysis in Organic Synthesis" by Xihe Bi and Chao-Jun Li, Wiley editions (accepted).

2.1 Abstract

Silver is a versatile element, differing from gold in that only half of its supplies is used toward jewelry, the rest being geared toward industrial applications, including alloys, batteries, dentistry, glass coatings, LED chips, medicine, nuclear reactors, photography, photovoltaic energy, tracking chips, semiconductors, touch screens, water purification, wood preservatives, and many other uses. Beyond their main use in the chemical industry as an industrial epoxidation catalyst, Ag NPs have been successfully applied to various chemical reactions. This chapter covers the catalytic processes catalyzed Ag NPs, with a special interest in the scope and mechanism of these reactions. Most notably, they are active for both carbonyl reduction and alcohol oxidation, making them competent for versatile oxidative couplings. Furthermore, they have been widely explored as selective hydrogenation catalysts, for nitriles, alkynes and carbonyls against olefins. We have also surveyed their applications in alkynylation, nitrile hydrolysis, silanol chemistry, and Lewis acid catalysis.

2.2 Introduction

The past decades have seen a tremendous development in nanoscience, resulting in successful applications in fields, such as medicine, energy, sensing, environmental remediation, and agriculture.[1-3] Owing to their unique properties – such as high surface-to-volume ratio, extensive size and shape, compositional tunability, and amenability to recovery – they are particularly interesting in the context of sustainable science and in particular for catalysis.[4] The use of silver nanomaterials for catalysis has a long history, with alcohol oxidation being investigated in the 1880s[5-6] and ethylene epoxidation patented in the 1930s.[7] The research on Ag NPs for catalysis is yet very dynamic to date, developing both known processes for improved activity, selectivity or scope, and novel ones, and has been the topic of recent reviews.[8-11]

Silver is a versatile element, differing from gold in that only half of its supplies is used towards jewelry, the rest being geared towards industrial applications, including alloys, batteries, dentistry, glass coatings, LED chips, medicine, nuclear reactors, photography, photovoltaic (or solar) energy, tracking chips, semiconductors, touch screens, water purification, wood preservatives and many other uses.[12] Silver is key in some chemical processes, as will be discussed below.

In this review, we are covering the catalytic processes catalyzed by Ag NPs, with a special interest in the scope and mechanism of these reactions. Because of the specific position of the Ag^+/Ag^0 couple redox potential (E° = +0.7996 V), Ag has the ability to oxidize then reduce back to metal zero under mild conditions, making Ag-based NPs good catalysts in both reductive and oxidative processes. As developed in more details below, the role of Ag(I) species is not innocent and has been investigated for a number of reactions, both experimentally and *in silico*. Hence they are covered below under epoxidation of alkenes, oxidation of alcohols, and reduction reactions. Ag NPs also have interesting an optical property, the localized surface plasmon resonance, which was at the center of recent development in catalysis for both oxidation and reduction. Finally, we complete our survey with alkynylation, oxidation couplings and miscellaneous processes, towards nitrile hydrolysis, silanol chemistry, and Lewis-acid catalysis.

2.3 Epoxidation

2.3.1 Epoxidation of alkenes

Alkene epoxidation is a critical process in the chemical industry. Since Lefort's patent on 1931 on direct epoxidation of ethylene into ethylene oxide (EO) using O_2 catalyzed by Ag,[7] four different major and industrially used variations have been discovered by Union carbide, Scientific Design Co.,[13] Japan Catalytic Chemical Co., and Shell International Chemicals BV.[14] 11% of ethylene is used for EO production, and constitutes the 14th most produced organic chemical (20 million tonnes in 2009).[15] Although air is convenient as a reactant, pure oxygen is preferred in newer processes as it allows achieving higher reaction rates.[16]

Ethylene oxide is primarily used to access ethylene glycols (monomer, oligomers and polymers). Ethylene glycol itself is used as antifreeze and also as monomers for the production of poylesters, including polyethylene terephtalate. Propylene oxide is also produced industrially by epoxidation, for about half of its production, but it relies on organic oxidants, such as cumene hydroperoxide (Sumitomo process).[17] Epoxidation of propylene by silver is still lacking in selectivity to be applicable in the large scale. Hence, because of the importance of alkene oxide for major industrial streams, the epoxidation reaction is crucial. As we will

present below, Ag-based nanomaterials occupies a central place in this chemistry and research is very active in this area, to oxidize ethylene, propylene, but also styrene and several others. Importantly, for this process, the role of surface oxides, chlorides, or other additives is often non-innocent in triggering both activity and selectivity.

2.3.2 Epoxidation of ethylene

Ethylene oxide (EO) is an essential gateway chemical. The reference industrial catalyst for this reaction consists of large Ag NPs (100–200 nm) supported (circa 15% wt.) on low-surface-area Al_2O_3, with alkaline species as promoters.[18] Ethylene epoxidation is competing with isomerization of the product towards acetaldehyde (AA) through re-adsorption on the catalyst, and combustion by C-H activation (Scheme 91). Indeed, EO formation is reported to be moderately exothermic when the complete oxidation of ethylene and EO to CO_2 is strongly exothermic.[19]

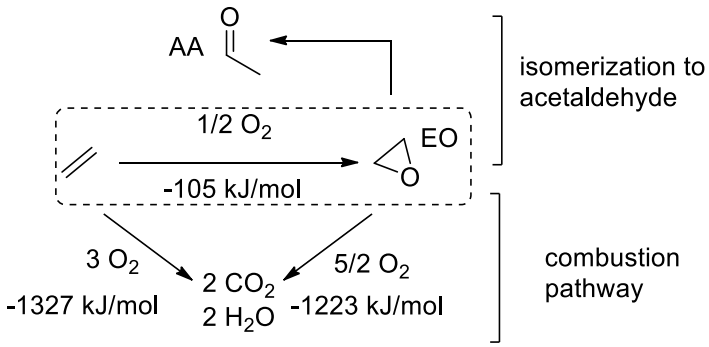

Scheme 91. Ethylene epoxidation and competing processes.

Since 1931 when metallic Ag was first shown to be an active catalyst for ethylene epoxidation with a selectivity of around 40-50%,[20] several additives have been studied to improve its selectivity. Adding ppm levels of chlorine-containing molecules in the reaction stream, such as vinyl chloride, [21] or oxides, including cesium oxides[22] and rhenium oxides[23] help increasing the selectivity of the reaction, with typical values found in modern literature around 80%. Increasing the selectivity, and avoiding combustion are crucial to reduce CO_2 emission, considering the scale of EO production (more than 27 million tons are projected in 2017[24]). Furthermore, an 1% improvement in selectivity would result in tens of millions of dollars per year of financial gain, underlining this other important aspect of the process.[25] Finally, using more sustainable synthetic methods and supports is also crucial, as pointed by Li *et al.*[26] using biomass to prepare the catalyst.

The ethylene epoxidation mechanism with Ag has been extensively studied, as attested by Bukhtiyarov *et al.* and around 1000 papers have been published on that subject.[27] Therefore, the whole literature will not be covered in this chapter and we invite the reader to refer to

specialized reviews such as the one mentioned previously, along with others.[20, 28]

It is generally accepted that chemisorbed atomic electrophilic oxygen adds to ethylene in the rate determining step to form EO.[28] Indeed, XPS showed two different types of oxygens during reaction conditions: nucleophilic oxygen has an O_{1s} binding energy (BE) of ≈528.5 eV and participates in total combustion whereas electrophilic oxygen has an O_{1s} BE of ≈530 eV and participates in epoxidation.[29] Although nucleophilic atomic oxygens have been well characterized,[30] the nature of electrophilic atomic oxygens has remained elusive until a very recent report by Jones *et al.*[31] They showed that sulfur impurities in Ag or ethylene resulted in the generation of SO_4 species adsorbed on the surface that are the source of electrophilic atomic oxygen, as shown by *in situ* XPS technique.

Medlin first showed theoretically and experimentally for butadiene that an oxametallacycle (OMC) intermediate formed on the surface of metallic silver, that can then go through 1,2-ring closure to form the epoxide product.[32] Eventually, Linic then proved that a similar pathway for ethylene occurred.[33-34] Depending on the silver surface the OMC intermediate forms, it favors either EO for (100) and (110) faces or acetaldehyde for (111) faces. Therefore, engineered silver structures such as nanowires or nanocubes, featuring predominantly (100) faces, greatly enhance selectivity.[35] Cheng *et al.* further explored this structure/activity relationship and established the following order for EO-selectivity: (110) > (100) > (111) > (211), as a consequence of the difference in adsorption strength and geometry of the OMC intermediate on the different surface (Scheme 92).[36]

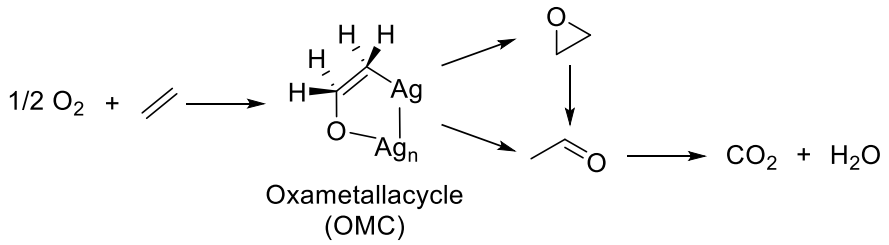

Scheme 92. Mechanism of ethylene epoxidation mediated by silver through an oxometallacycle intermediate (adsorption steps omitted).

The amount of low valence sites also correlates with low selectivity.[37] To minimize their presence, larger NPs can be used, or low coordination sites can be poisoned using chlorides. Furthermore, both surface and subsurface chlorine weakens Ag-O interactions, making oxygen more reactive for epoxidation. Chemisorbed chlorine also helps selectivity by assisting EO desorption, as long standing EO adsorption is associated with its combust or isomerization to AA.[38] Interestingly, Basset and co-workers showed that AgCl nanocubes were not active for ethylene epoxidation, thus linking the structural difference between AgCl and Cl-exposed Ag

to distinct activities.[39] Upon a mild NH_4OH washing, surface chloride could be removed and the cubes became active for catalysis. Cs acts as a binder between Ag and its support enhancing the catalyst coverage, as shown by Minahan *et al*. for Ag and Al_2O_3. This will minimize the surface area of basic sites on Al_2O_3, lowering the combustion pathway.[40] Furthermore, Linic *et al.* showed that Cs and Cl both favorably affected the epoxidation transition state by an electric field/dipole interaction. Used in conjunction with Cl, these two additives can cooperatively boost the catalyst by electronic effects.[41]

Though other transition metals can perform epoxidation through an OMC intermediate, they are either too stable and favor AA formation as the thermodynamic product, either too unstable and do not allow epoxidation at all. Mavrikakis *et al.* showed that Ag happens to be in the sweet spot where the OMC intermediate and EO are equally stable on the metal surface, therefore favoring the epoxidation.[42]

Van Santen compared the energetic barriers for ethylene oxidation for the three coinage metal oxides (Au, Ag, Cu) using DFT calculations.[43] Among the (100) oxide surfaces, Ag_2O was shown to be the only one suitable for the catalytic epoxidation of ethylene. Ag_2O allows a barrier-free direct epoxidation of ethylene using surface atomic oxygen and does not react again with EO to decompose it. While Cu_2O is suitable for catalytic epoxidation, it can isomerize ethylene oxide to acetaldehyde (AA). Since Au_2O is an unstable species, it cannot be regenerated which disqualifies it as catalyst for epoxidation.

As for Ag_2O (001) surfaces, the selectivity decreases with the presence of oxygen-vacant sites, where the formation of acetaldehyde is favored. These oxygen-vacant sites are less likely to form in presence of chlorine and cesium.[44] However cesium alone will decrease the selectivity by the formation CsO_x surface complexes that consume surface oxygen.

2.3.3 Epoxidation of propylene

Propylene oxide (PO) is an important bulk chemical to manufacture polyurethane, unsaturated resins, surfactants and other products (2.28×10^6 ton/year, with a 4%/year increase). Industrially, it is produced by either the chlorohydrin process, or stoichiometric epoxidation, such as the Halcon process.[45] In the chlorohydrin process, it produces a large amount of chlorinated by-products which are toxic and can also erode equipments. As for the Halcon process, tert-butyl hydroperoxide is used as an oxidant and PO is produced together with an equimolar amount of *tert*-butanol byproduct.[46] Degussa-Uhde built in 2009 a new plant involving a more efficient process: hydrogen peroxide to propylene oxide (HPPO). Here, only water is generated as a byproduct, using titanium silicalite as a catalyst. However, its commercialization has been hindered largely by the supply and demand of H_2O_2.[47] Contrary to

ethylene oxide, propylene oxide industrial production does not rely on silver catalyst.

The epoxidation of propylene with H_2 and O_2 over Au catalysts supported on Ti-containing materials was first reported by the Haruta group in 1998 (Scheme 93).[48] Although hydrogen does not contribute to the end product, it helps generate a peroxo species at the interface of Au^0 and Ti^{4+}, that is the active species. This said, hydrogen is not required in the case of silver.

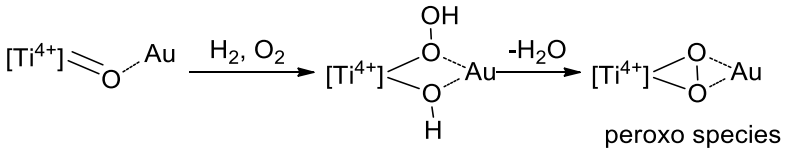

Scheme 93. Haruta's proposed mechanism for Au@TiO_2-catalyzed propylene epoxidation through a peroxo intermediate.

Contrary to ethylene epoxidation, the additional presence of an alpha-proton on propylene leads into additional selectivity issues since it can be attacked by a nucleophilic oxygen atom adsorbed on the Ag surface.[49] Therefore authors such as Lambert[50-51] and Lu[52] proposed using Cu as a catalyst, though so far the selectivity has been limited to 70%.

Dai *et al.* recently provided DFT calculations for rationalizing the intermediates involved in Ag-catalyzed propylene epoxidation.[53] They revised the OMC intermediate, arguing that adsorbed atomic oxygen on Ag surfaces favored both direct epoxidation and α-H abstraction, that leads to combustion (Scheme 94).[54] Indeed, both pathways are exothermic (-0.14 and -0.16 eV respectively, for Ag(100)) and the combustion pathway is actually kinetically favored (the energy barrier is at 0.29 eV, against 0.44 eV for epoxidation on Ag(100)). This stems from the strong nucleophilic character of the adsorbed atomic oxygen that will readily attack the α-H rather than forming the epoxide. However, by considering a new intermediate involving molecular dioxygen (OOMC), they showed that both oxygen atoms were less likely to exert α-H abstraction. It can electrophilically attack the C=C bond, giving a higher epoxidation selectivity. Once cannot exclude the co-existence of these pathways during the reaction, but this constitutes a good rationale in catalyst design for tuning the selectivity.

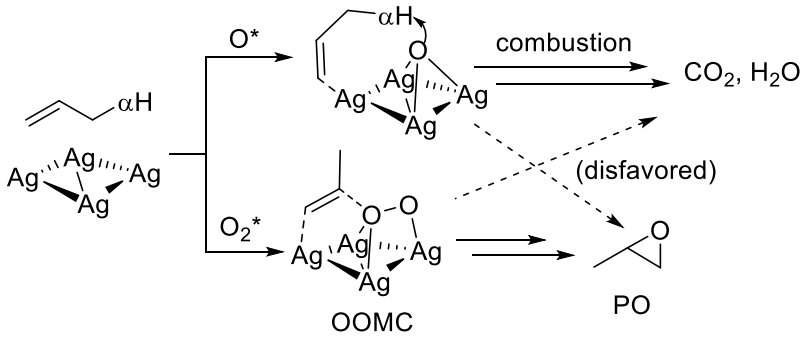

Scheme 94. Molecular oxygen vs atomic oxygen absorption's influence on propylene epoxidation selectivity.

A breakthrough in the field of Ag catalysis was made by the Vajda group when they reported the successful use of Ag_3 nanoclusters supported on amorphous alumina for this reaction.[55] These clusters are known to sinter (aggregate into bigger NPs) upon heating above 110 °C, and stabilize at 3.5 nm around 200 °C. These small NPs proved to be extremely reactive for propylene epoxidation and showed an increased activity as a function of temperature, while selectivity drops past 140 °C (Scheme 95). At 100 °C, the highest selectivity was obtained (c.a. 90% selectivity to PO, with 10% acrolein formed). For both Ag_3 and Ag NPs, the rate of propylene oxide molecules formed per surface silver atom was ~1 s^{-1} at 110 °C, which is much greater than that reported for any Ag catalyst.

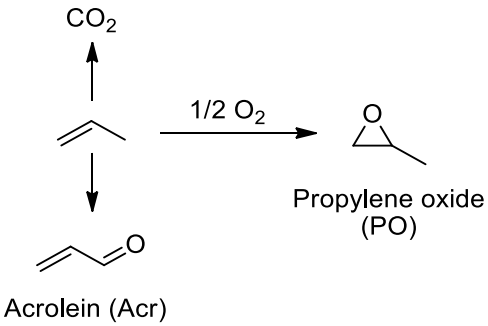

Scheme 95. Epoxidation reaction of propylene and competing side reaction.

The Vajda group showed that O_2 dissociation proceeded most favorable at the Ag/Al_2O_3 interface.[56] Ag-borne O atoms were found to be responsible for PO formation while Al_2O_3-borne ones were responsible for acrolein formation. In addition, the barrier to O_2 dissociation on these $Ag@Al_2O_3$ was small compared to that on crystalline Ag surfaces, which accounts for a higher activity overall.

Ag_{20} nanoclusters have been studied in the context of propylene epoxidation through DFT calculations by Kuz'menko *et al.*[57] Molecular oxygen coordinates preferentially on edge or apex positions of Ag NPs, leading into an electron density transfer from silver to oxygen and

generating cationic $Ag^{\delta+}$ sites. These sites also favorably bind propylene and go through a four-member OMC intermediate that has a low activation barrier towards PO formation. Similarly to ethylene epoxidation, (100) Ag facets were more selective than (111) facets [58] and chlorides boosted the selectivity to propylene oxide.[59]

Lu *et al.* reported the use of bimetallic Ag-Cu catalysts supported on $BaCO_3$ for propylene epoxidation.[52] The highest PO selectivity of 55.1% and the propylene conversion of 3.6% were achieved over Ag_{95}–Cu_5@$BaCO_3$ bimetallic catalyst. The doping of 5% Cu in Ag helped increasing the electropositivity of Ag, as shown by XPS and boosted oxygen adsorption to restrain Ag NP agglomeration. A selectivity of 71.2% was achieved by the same group by impregnating ppm levels of $CuCl_2$ on the catalyst, where Cl^- effect has been shown to exalt Ag's electropositivity.[60] Other Ag supports have been successfully reported since for this reaction, such as molybdenum oxide-impregnated silver supported on zirconium oxide (Ag–MoO_3@ZrO_2),[61], as well as Ag–Y_2O_3–K_2O@Al_2O_3,[62] ball-milled treated Ag@$CaCO_3$,[63-64] and Ag@NaCl.[65]

2.3.4 Epoxidation of styrene and other alkenes

Styrene epoxidation has been reported in a wider variety of methods, including enzymatic systems for enantioselective epoxidations such as P450[66], styrene monooxygenase[67], or microbial systems.[68] Industrially, oxidation of styrene is carried out by using stoichiometric amounts of organic peracids as oxidant. Tert-butyl hydrogen peroxide (TBHP),[69-70] H_2O_2,[71] molecular oxygen,[72-74] or mixtures[75] are more common oxidants on the lab scale. Ag catalysts are also active for this reaction and, again, (100) facets provided the best activity, as shown by Li *et al.*[76] As a result, the rate for this reaction over Ag nanocubes was more than fourteen times higher than that on nanoplates and four times higher than that on near spherical NPs.

Luck *et al.* reported the use of mesoporous MCM-41 silica, as a support for Ag NPs.[77] Using TBHP as a radical initiator (the actual oxidant being air), they managed to oxidize 4 alkenes with varying selectivities (Scheme 96). Cyclohexene gave 2-cyclohexen-1-one as a major product whereas cyclooctene gave the corresponding epoxide as a major product. Benzaldehyde was formed in majority when styrene was oxidized. Using 1,2-dichlorethane (DCE) as a solvent, the Ag surfaces passivated completely *via* formation of an AgCl layer. The same effect can be observed by using NaCl in a H_2O/*t*BuOH. H_2O_2 could not be used as a radical initiator with the fresh catalyst as it decomposed immediately upon exposure to the catalyst. On subsequent recycling cycles however, due to the surface passivation of the catalyst with chlorides, H_2O_2 was compatible and used instead of TBHP.

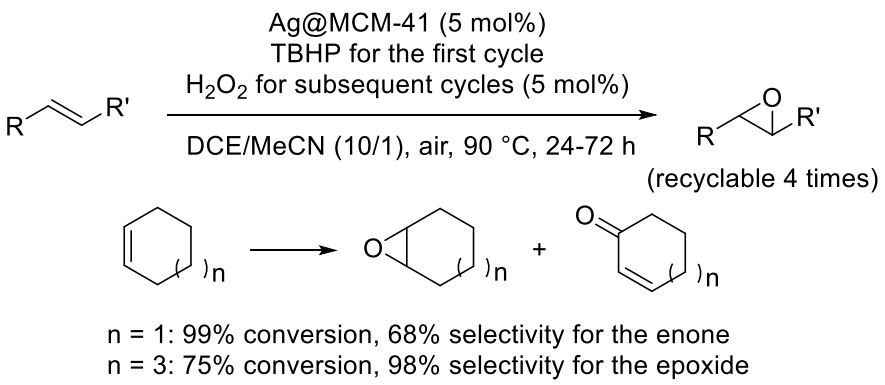

Scheme 96. Ag@MCM-41-catalyzed oxidations of olefins.

Chen *et al*. reported the synthesis of magnetically recyclable Ag@Fe_3O_4 performed under hydrothermal conditions.[78] It was active for styrene epoxidation using TBHP, affording a turnover frequency (TOF) of 1473 $mmol.mol^{-1}.h^{-1}$ with the added benefit of being recyclable 5 times with no deactivation. The presence of Fe_3O_4 was claimed to assist the epoxidation by providing additional reactive oxygen sites. The authors eventually developed a series of magnetically supported mixed metal-Ag NPs $AgM_{1-x}@Fe_{2+x}O_4$ (M = Co, Ni, Mn, Zn).[79]

Li *et al.* used carbon nanofibers (CNFs) as supports for various forms of Ag nanocatalysts.[80-81] By electrospinning deposition, they decorated CNF with Ag NPs, before they were calcinated to obtain the active catalyst (Scheme 97). Whether an oxide was added as a promoter or not (MgO, Al_2O_3), their optimized conditions all gave similar results for the epoxidation of styrene (43% conversion, 39% selectivity to styrene oxide).

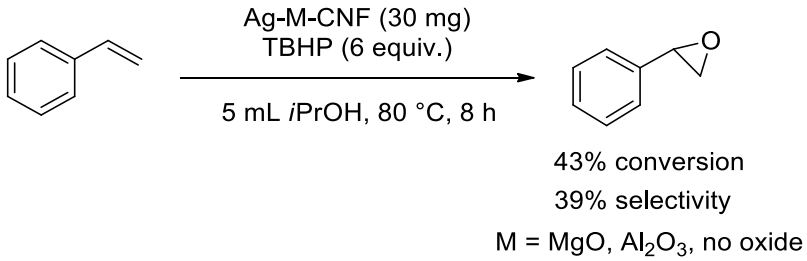

Scheme 97. CNF-supported Ag for styrene epoxidation.

Magnesium and aluminum oxides as double-layered oxides (LDH) have been exploited by Xu *et al*. as well, showing improved catalytic performances (Scheme 98). [82]

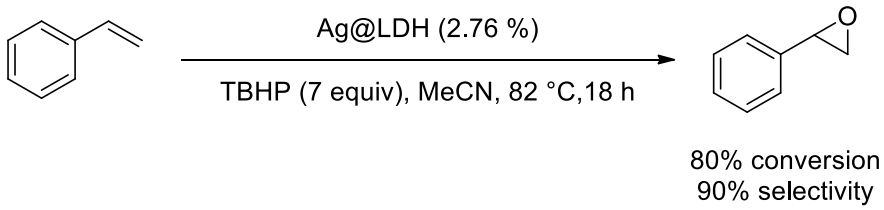

Scheme 98. Epoxidation of styrene catalyzed by Ag@LDH.

The Li group eventually opted for a different strategy by loading silver in zeolite using supercritical carbon dioxide and hydrogen as a reductant.[83-84] These small and monodisperse NPs (3-6 nm) showed an improved performance for styrene epoxidation, using different oxides to tune the selectivity to styrene oxide or benzaldehyde (Scheme 99).

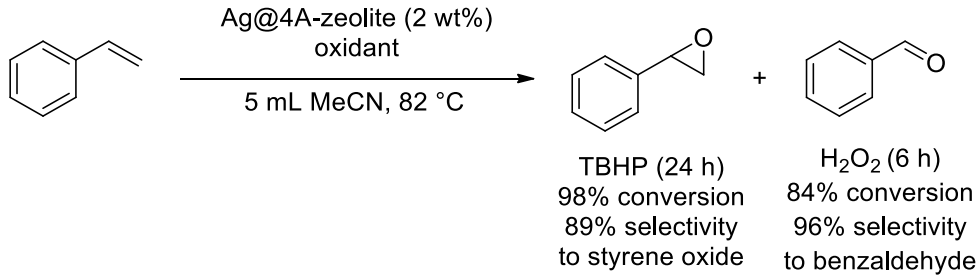

Scheme 99. Zeolite-supported Ag for styrene epoxidation.

Activated layered manganese oxides are inexpensive supports that can be used for styrene epoxidation in conjunction with sodium carbonate, hydrogen peroxide and either gold or silver, as shown by Bagherzadeh *et al.* (Scheme 100).[85] A mechanism was proposed by the authors, where silver and manganese act in conjunction to activate the alkene (Scheme 101). Sodium carbonate helps activating hydrogen peroxide into HCO_4^-,[86] which ultimately provides the oxygen atom for the epoxidation.

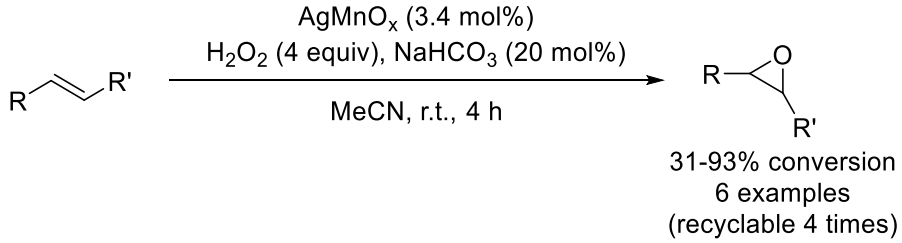

Scheme 100. Ag supported on manganese oxide for alkene epoxidation using hydrogen peroxide.

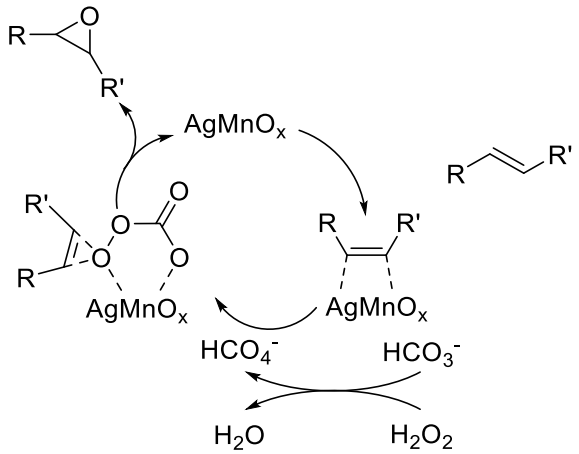

Scheme 101. Proposed mechanism for carbonate-assisted epoxidation of alkenes.

Raichur *et al.* reported the synthesis of hollow silver nanocages built using silica as a sacrificial template.[87] Because of the increased surface area, the nanocages showed high reactivity and selectivity towards TBHP-induced alkene epoxidation, and recyclable up to 4 times (Scheme 102).

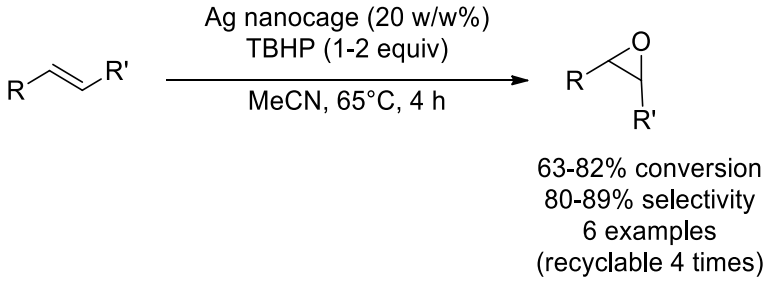

Scheme 102. Ag nanocage as recyclable catalysts for alkene epoxidation.

Methyltrimethoxysilane/3-mercaptopropyltrimethoxysilane hybrid films (Ag@MeTMS/MPTPS) have been showed by Macquarrie *et al.* to be suitable supports for silver in catalyzing styrene epoxidation under microwave.[88] The thiols allowed the stabilization of Ag NPs, making the catalyst recyclable up to 4 times. However, it was shown that Ag slowly leached into solution, thus explaining the high selectivity and activity, similar to the one of $AgNO_3$ on its own (Scheme 103).

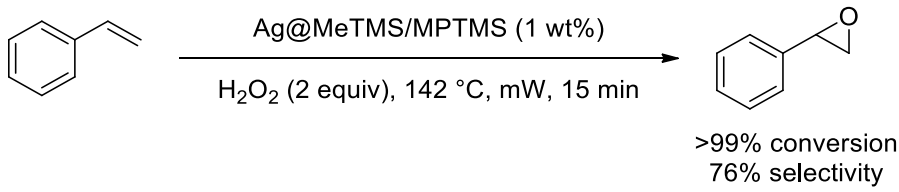

Scheme 103. Epoxidation of styrene catalyzed by Ag@MeTMS/MPTPS under microwave.

Bal *et al.* used Ag/Mn_3O_4 nanowhiskers for styrene epoxidation, using cetyl alcohol as a soft template to obtain the nanowhiskers after calcination.[89] Their system is remarkable in that they used oxygen (10 bar) as an oxidant, affording a full selectivity to styrene oxide (Scheme 104). The catalyst did not leach and was recyclable up to 5 times.

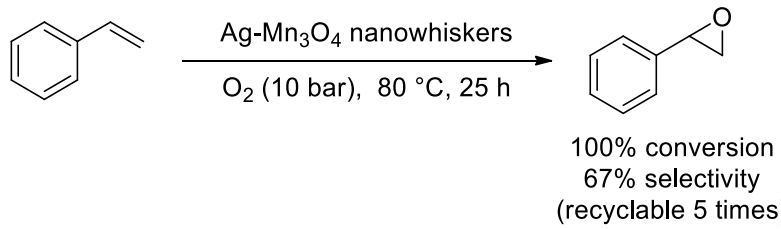

Scheme 104. Styrene epoxidation under oxygen with Ag/Mn_3O_4 nanowhiskers.

Polyoxometalates (POM) such as $H_5PV_2Mo_{10}O_{40}$ are also suitable supports for catalysis,

as shown by Neumann *et al.*[90] This particular species was shown to inhibit free radical autoxidation reactions by the same group,[91-92] and possess a high anionic charge for nanoparticle stabilization.[93] Both properties supported their use in the silver-catalyzed epoxidation of alkenes in air. Among the metals tested, Ru and Ag proved to give the best catalytic results, though they observed some product loss due to the formation of oxygenated polymeric products (Scheme 105).

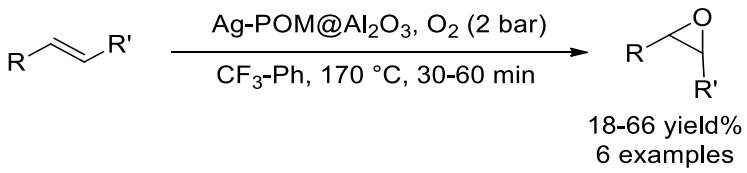

Scheme 105. Aerobic epoxidation of alkenes using Ag-POM supported on alumina.

Kobe *et al.* finally pointed in their survey on industrial epoxidation the emergence of 3,4-epoxybut-1-ene production (EpB), developed by Eastman Chemical Company.[15] EpB has four non-equivalent carbons along with two functional groups (epoxy and vinyl), hence its considerable potential as a chemical intermediate. For example Eastman Chemical Company proposed the manufacturing of 1,4-butanediol from EpB,[94] which is itelf a precursor of THF and biodegradable plastics such as poly(butylene succinate).[95]

In conclusion, the silver-catalyzed epoxidation of simple alkenes such as ethylene and propylene, using oxygen as an oxidant, has been widely studied. In contrast, a wider variety of oxidants has been reported for bigger alkenes, reflecting the better availability of peroxides on the lab scale with oxygen remaining the most atom-economical choice. For all cases, the trend for facet selectivity is consistent, with the (100) facet favoring the formation of the epoxide.

2.4 Alcohol oxidation

The oxidation of methanol to formaldehyde over Ag is considered to be the first successful example of heterogeneous catalysis.[96] Along with Cu and Au-catalyzed oxidation of MeOH, these represent one of the oldest industrial catalytic technologies dating back to the 1880s and the first non-Pt based catalytic industrial processes. Since then, Ag has gradually been replaced by Fe/Mo catalysts in the industry for MeOH oxidation, now accounting for 45% of world's production of formaldehyde.[5-6] On the lab scale, the reactivity of Ag NPs has been extended to the oxidation of a variety of benzylic and aliphatic alcohols using oxygen as an oxidant and will be covered in this part.

The mechanism of alcohol oxidation over metal NPs was described in an excellent review by Davis and co-workers,[97] and is illustrated in Scheme 106. First, the hydroxy group is deprotonated, while the resulting alkoxide bounds to the metal surface. For coinage metals, this

step typically requires the presence of a base since they feature poor ability for alcohol proton abstraction, unlike platinum-group metals.[98] Indeed, M-H bonds are poorly stable when M is a coinage metal.[99] With metal oxide support such as Al_2O_3 or SiO_2, the lattice oxygen can act as the base. Alternatively, Ag_2O can also act as a base. Then, a β-hydride elimination occurs, leading to the formation of the carbonyl. The metal hydride then gets oxidized. If dioxygen is present, the overall reaction is called aerobic oxidation and the hydride is quenched to form water. In cases where aldehydes are formed from primary alcohols, selectivity can be an issue as the aldehyde may react further with water to form germinal diols, and ultimately carboxylic acids by β-hydride elimination. Conversely, if anaerobic conditions are used, the hydride can recombine with the proton from the first step to form H_2 gas. Here, the poor binding affinity of Ag for hydrides helps drive the dehydrogenation forward (See 3.1-Carbonyl reduction). In this case, the overall reaction is called alcohol dehydrogenation. Since no oxygen is present, there is no over-oxidation issue. Interestingly, the presence of water may lead to catalyst deactivation.[100]

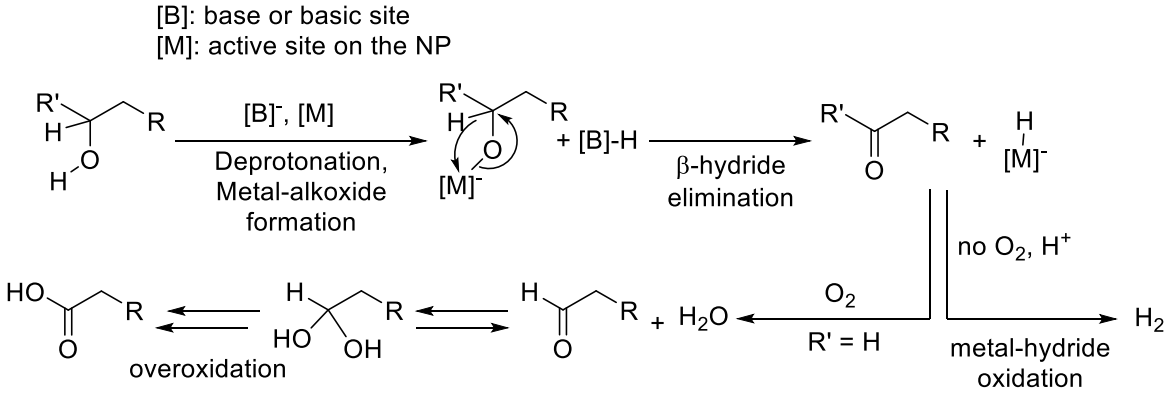

Scheme 106. Mechanism of the metal nanoparticle-catalyzed alcohol oxidation.

Liu *et al.* questioned the distinction between alcohol aerobic oxidation and dehydrogenation in a recent study.[101] From a thermodynamics standpoint, alcohol dehydrogenation is energetically uphill, with a positive enthalpy of reaction. Entropy being the sole driving force, only temperatures above 200 °C may favor the equilibrium towards the carbonyl and H_2 products. For example, the Gibbs free energy of the dehydrogenation of benzyl alcohol to benzaldehyde and H_2 is +33.4 kJ/mol at 25 °C but this decreases to +20.6 kJ/mol at 120 °C and +9.7 kJ/mol at 200 °C. Water formation having a highly negative Gibbs free energy of –230.8 kJ mol^{-1} under standard conditions, its formation seems the only way to rationalize alcohol oxidation at low temperatures. This suggests trace amounts of oxygen in the reaction are necessary to drive the reaction under such conditions. This also explains why reported

alcohol dehydrogenation-based oxidation processes are typically taking place under hasher conditions than their aerobic counterparts.

The nature and speciation of the Ag NP surface is central to the catalytic alcohol oxidation, as highlighted by Yang *et al.*[102] The absorption of O_2 on the silver surface, and the formation of Ag-O pairs plays a key role in its reactivity. According to Sanderson's classification of transition metal oxides, the oxygen in the Ag-O pair bears the strongest negative effective charge (-0.46e), along with Cu_2O (-0.44e).[103] This provides the basic site on the surface for deprotonating the hydroxy function. On the other side, an acidic site must be provided to abstract the α-hydrogen of the alcohol. Ag^+ is a soft acid according to Misono's classification, with a parameter of 3.99, compared to harder acids such as Cu^+ and Cu^{2+}.[104] This will minimize the interaction with the hydroxy group and avoid alcohol dehydration into alkenes, which is another unwanted outcome in alcohol oxidation (Scheme 107). Therefore, the Ag-O pair acts as a strong Lewis base/soft Lewis acid pair, whereby the good basicity of the O site favors alcohol dehydrogenation, while the low acidity of the Ag site limits dehydration side reactions. Cu oxide, on the contrary, features weaker Lewis base/stronger Lewis acid pair and is less efficient for the selection oxidation of alcohols.

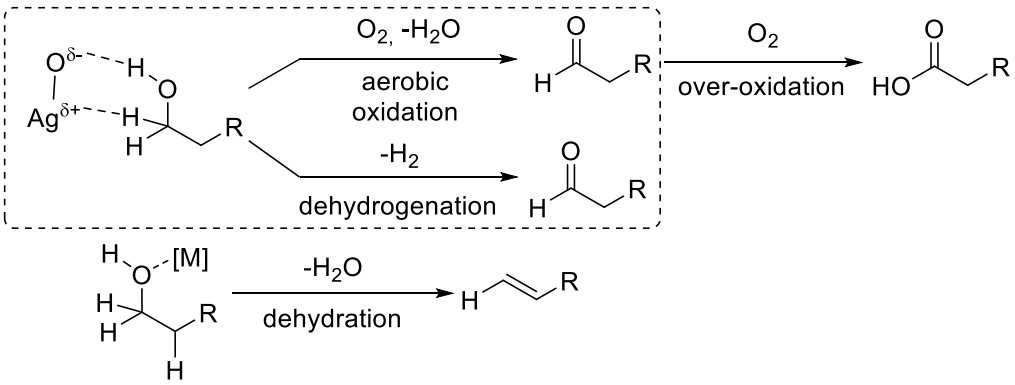

Scheme 107. Alcohol oxidation: pathways and side reactions.

In the following, we describe selected examples of both proposed pathways for this reaction: the aerobic oxidation and the dehydrogenation.

2.4.1 Aerobic alcohol oxidation

One of the most efficient systems, in terms of silver loading, was proposed by Hosseini-Monfared *et al.* where they supported Ag on different graphene-based supports for the aerobic oxidation of benzyl alcohol (Scheme 108).[105] *N*-Hydroxyphthalimide (NHPI) was used to increase both the oxidation conversion (from 7% without NHPI to 61%) and selectivity to benzaldehyde (from 19% to 58%). Indeed NHPI has been shown previously to react with Co to generate *N*-oxyl radicals by electron transfer, initiating a radical chain mechanism with

alkene and oxygen to generate epoxides.[106] By functionalizing graphene with thiols (Ag@GOSH), they enabled a better adhesion and dispersion of Ag on the support, making it recyclable 5 times with no Ag leaching.

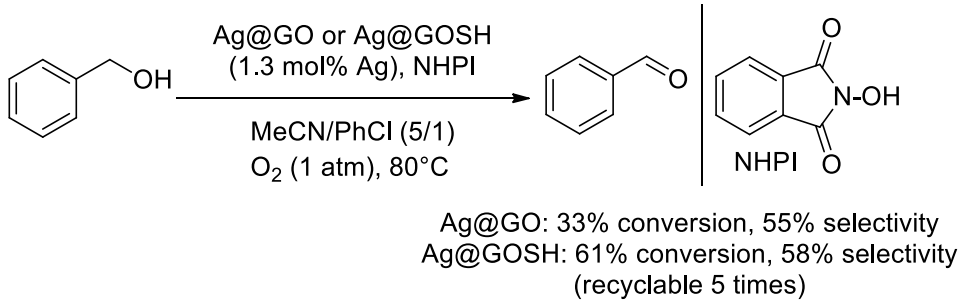

Scheme 108. Graphite-supported Ag NPs for aerobic oxidation of benzyl alcohol.

CeO_2 is able to reversibly bind O_2, and can serve as an oxygen storage material. In the context of catalytic oxidation it helps providing active oxygen sites. For instance, Kundakovic *et al.* boosted Ag and Cu oxide catalytic activity in methane oxidation by supporting them onto CeO_2.[107] Beier *et al.* exploited this material for the oxidation of alcohols using a mixture of CeO_2 NPs and Ag supported on SiO_2 (Scheme 109).[100] They compared the catalytic activity of Ag@SiO_2 with Pd supported on Al_2O_3, showing that the Ag benefitted more from CeO_2 addition (6 to 98% conversion increase) than Pd (81 to 94% conversion) with a high selectivity (>95% for Ag in both cases, and <70% for Pd in both cases).

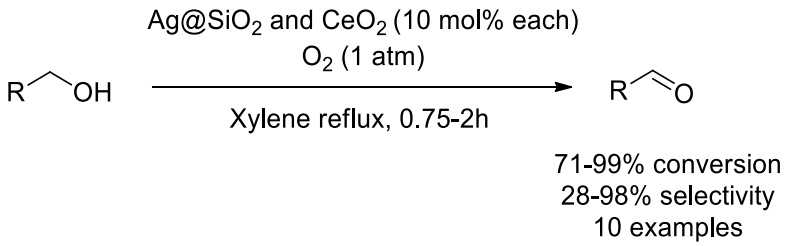

Scheme 109. Oxidation of alcohols by Ag@SiO_2 assisted by CeO_2.

Rana,[108] Kang,[109] and Ma[110] further extended the discussion on the CeO_2 interaction with supported Ag. According to them, Ag NPs act as a crystal defect in CeO_2, which results in the activation of the lattice oxygen. Oxygen can indeed move from CeO_2 to Ag NPs, and be available for a bioethanol selective oxidation to acetaldehyde in Rana's case. Overall, the oxygen storage capacity of Ag@CeO_2 increases by around 10-fold after Ag is added to CeO_2.

Erasmus *et al.* studied the impregnation a flat silica wafer with silver nitrate by spin-coating, followed by reduction under hydrogen at 350 °C to afford a thin layer of homogeneously dispersed metallic Ag NPs (3-5 nm).[111] Using this they could oxidize octadecanol at 105 °C under aerobic conditions (Scheme 110).

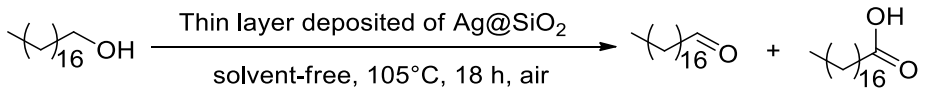

Scheme 110. Octadecanol oxidation on Ag supported on SiO_2 wafer.

Ag nanomaterials as catalysts and air as oxidant are readily transposable into flow setups. In this fashion, Ding *et al.* reported the use of nanoporous Ag to oxidize short-chain linear alcohols into the corresponding carbonyl with high selectivities in continuous gas phase flow (Scheme 111).[112] The nanoporous catalyst was synthesized by treating $Ag_{77}Mg_{23}$ alloys with tartaric acid, etching Mg and affording nanoporous Ag.

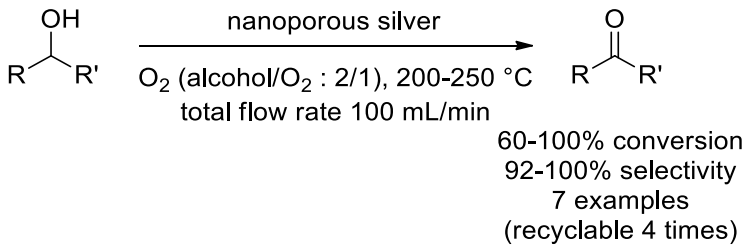

Scheme 111. Nanoropous Ag-catalyzed alcohol oxidation in continuous gas phase.

By substituting K with Ag on cryptomelane octahedral molecular sieves (Ag@OMS-2), Yadav *et al.* produced an active catalyst for the selective oxidation of 1-octanol to 1-octanal in gas flow at 325 °C (Weight hourly space velocity (WHSV = Mass Flow/Catalyst Mass was 16.74 h^{-1}) (Scheme 112).[113] Toluene added to the reactive medium served to avoid 1-octanal over-oxidation, giving comparable results in terms of selectivity and conversion to Ru-based catalysts. The yield decreased slightly upon re-use, but the catalytic activity could be restored after a treatment under air. The same design was developed for ethanol oxidation by Dutov *et al.*[114]

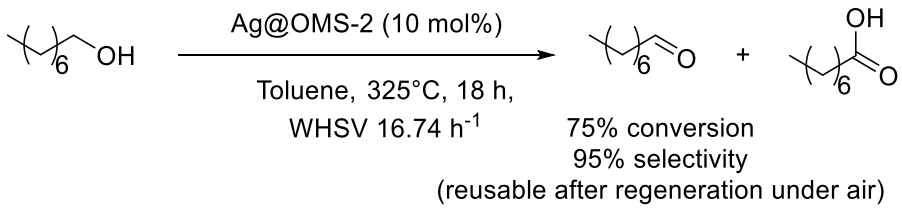

Scheme 112. Ag-OMS-2 for 1-octanol oxidation in gas flow.

2.4.2 Alcohol dehydrogenation

Alumina, as an amphoteric support, can assist Ag in both steps of the reaction, as shown by the Satsuma group (Scheme 113).[115] In this scheme, the basic sites on alumina (Al-OH) are responsible for the alcohol deprotonation (Scheme 114). The formed alkoxide replaces the resulting water molecule on alumina, and undergo a hydride abstraction by Ag. The latter is the rate-determining step (Scheme 114). The authors probed this hypothesis with different oxide

supports (CeO_2, MgO, ZrO_2, SiO_2), correlating a high activity with an optimum of electronegativity of the support cation around 1.6. Either more acidic supports with more electronegative cations (Si^{4+}) or basic supports with less electronegative cations (Ce^{4+}, Mg^{2+}, Zr^{4+}) gave lower yields.

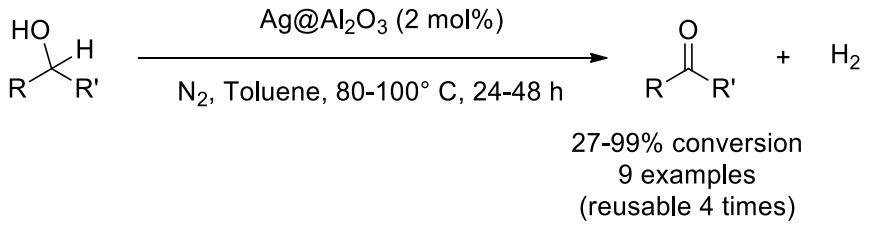

Scheme 113. Ag@Al_2O_3-assisted dehydrogenation of alcohols.

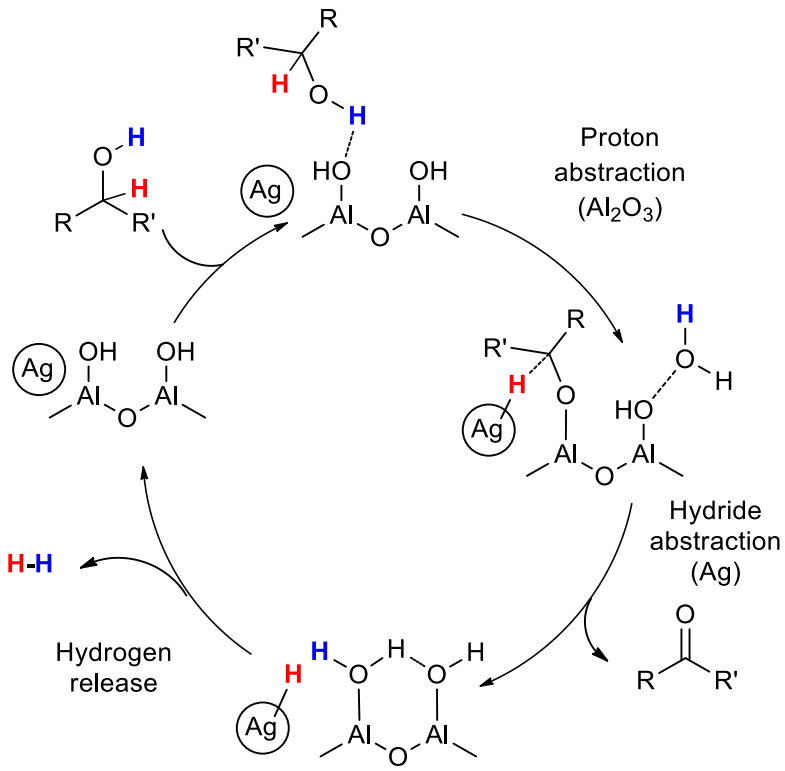

Scheme 114. Assistance of Al_2O_3 for Ag-catalyzed alcohol dehydrogenation. Active protons and hydrides are displayed in blue and red respectively.

Recently, Golshadi *et al.* reported the *in situ* formation of PVP-stabilized Ag NPs (c.a. 15nm) for primary alcohol dehydrogenation to the corresponding carboxylic acid (Scheme 115).[116] Here the addition of K-OH drives the complete oxidation through the nucleophilic attack of HO^- on the carbonyl center, resulting in an acetal and the corresponding carboxylic acid by β-hydride elimination. The excess of K-OH generates carboxylate, favoring the precipitation of the product. This also prevents that free acids deactivate the catalyst surface.[117] The role of $MnBr_2$ is not clear, though Mn catalysts alone have been reported for alcohol dehydrogenation reports. When benzaldehyde was subjected to the reaction conditions,

formation of benzyl alcohol was observed, showing that a parallel Cannizzaro reaction takes place under these basic conditions.

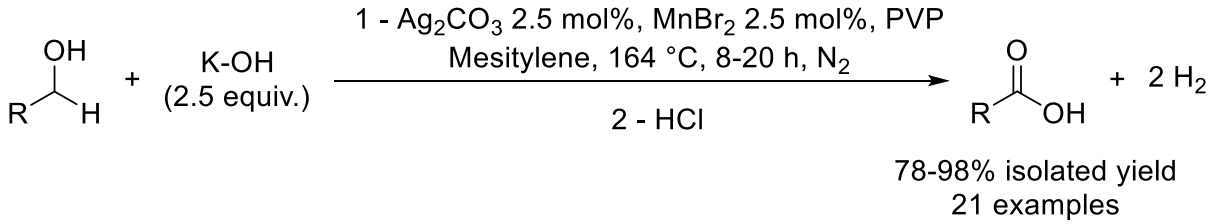

Scheme 115. *In situ* generation of Ag NPs for alcohol oxidation to carboxylic acids.

Mitsudome reported one of the highest turn-over-number (20.000) for alcohol oxidation with hydrotalcite-supported Ag (Scheme 116).[118] Hydrotalcite is a layered double hydroxide of general formula $Mg_6Al_2CO_3(OH)_{16}\cdot 4H_2O$. Both the catalyst and the support proved to be superior than their classical counter parts (Pd, Ru and SiO_2, TiO_2 respectively). This system proved selective as well for unsaturated alcohols, with absence of reduction of C=C bonds by H_2 byproduct, unlike typical PGM-based catalysts.

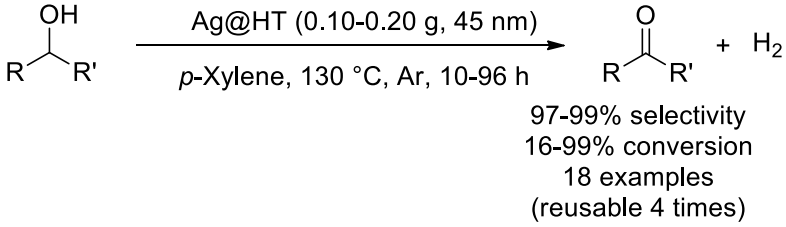

Scheme 116. Ag@HT-catalyzed dehydrogenation of alcohol.

Bayat *et al.* used silica coated on magnetite as a support for Ag NPs ($Ag@SiO_2@Fe_3O_4$), making them easily recyclable and active for the dehydrogenation of a wide range of alcohols, except for aliphatics (Scheme 117).[119] Similarly to Satsuma's example, SiO_2 assists the catalysis by proton abstraction from the alcohol.

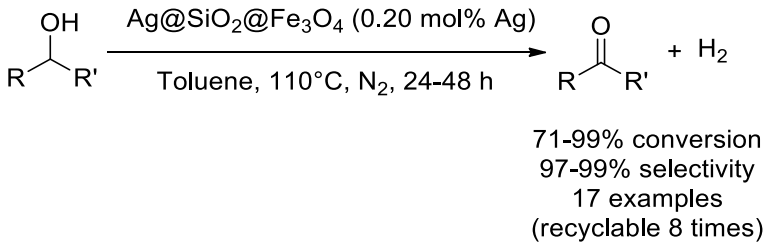

Scheme 117. Magnetically recyclable, silica-supported Ag for alcohol dehydrogenation.

Kurhe *et al.* entrapped Ag NPs into nanoporous chitosan/polyacrylamide interpenetrating polymer networks (Ag@IPN). Such a support helps reducing metal leaching by 60% compared to chitosan alone, allowing the catalyst to be re-used up to 7 cycles.[120] Here chitosan is suspected to help the dehydrogenation mechanism through hydrogen bonding (Scheme 118).

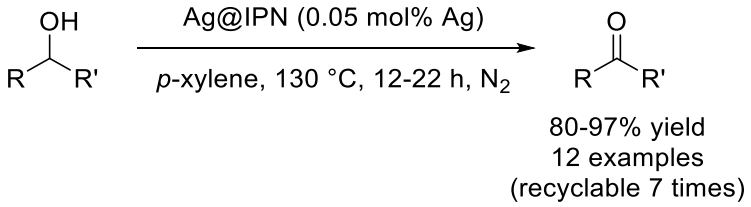

Scheme 118. Ag@IPN-catalyzed alcohol dehydrogenation.

2.4.3 Silver alloys in alcohol oxidation

Silver can also be combined to other metals to increase conversion and/or selectivity for alcohol oxidation. For instance, Feng *et al.* (Scheme 119) showed that PdAg supported on hydroxyapatite (PdAg@HAP) exhibited a higher selectivity for the oxidation of 1,2-propanediol to lactic acid compared to Pd_2/HAP.[121]

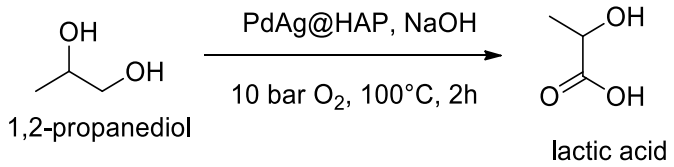

Scheme 119. Selectivity of 1,2-propanediol oxidation to lactic acid with PdAg@HAP.

Hirasawa probed a similar alloy for the selective oxidation of glycerol to dihydroxyacetone, combining Pd high activity and Ag selectivity.[122] Their proposed mechanism showed that Ag helps coordinating one primary -OH group on glycerol, allowing the selective oxidation of the secondary hydroxy group by Pd (Scheme 120). This prevents the oxidation of the primary hydroxy groups, that can further oxidize to carboxylic acids. By preventing the formation of glyceric acid, the deactivation of Pd-Ag by surface poisoning was avoided.

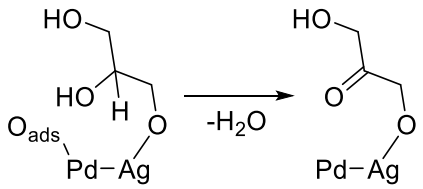

Scheme 120. Pd-Ag synergy for the selective oxidation of glycerol.

With Pd and Pd/Ag films[123], Yamamura studied the selective oxidation of allyl alcohol to acrolein, leaving the C=C double bond unreacted (Scheme 121). This reaction is particularly difficult since one has to circumvent the ability of Ag to epoxidize C=C double bonds in the presence of O_2 (see section 2.3), and the one of Pd to reduce it with any transient adsorbed hydrogen. A Pd/Ag ratio of 7 mol% was shown to be optimal compared to pure Pd, affording an improved selectivity to acrolein of 96% (compared to 84% for pure Pd), at the cost of an

activity loss ($2.6*10^{-9}$ mol.cm^{-2}s^{-1}, compared to $34.2*10^{-9}$ mol.cm^{-2}s^{-1}); a higher temperature of 300 °C could help improve the activity ($40.1*10^{-9}$ mol.cm^{-2}s^{-1}).

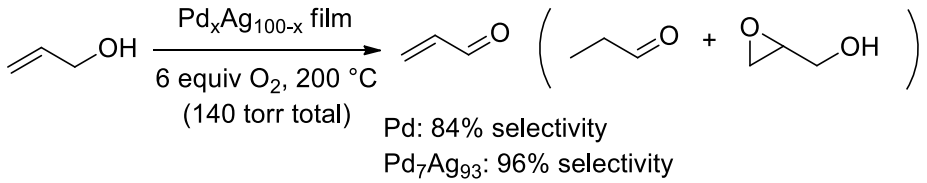

Scheme 121. P and Pd_7Ag_{93} films-catalyzed selective oxidation of allyl alcohol to acrolein

Au/Ag bimetallic alloy clusters have also been explored where Ag serves to boost the otherwise sluggish activity of Au. Tsukuda *et al.* were among the first to explore this avenue, with polyvinylpyrrolidone (PVP) as stabilizer (Scheme 122).[124] As Ag/Au ratio was increased, up to 10%, the catalyst activity improved for the oxidation of 4-hydroxybenzyl alcohol. The hypothesis is that the more electropositive Au atoms can transfer electron density to Ag ones, reinforcing the cationic character of Au.

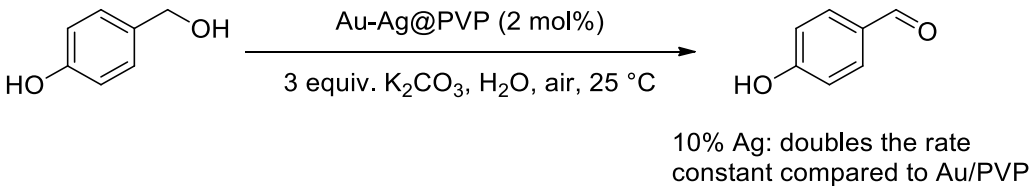

Scheme 122. Ag doping into Au@PVP for 4-hydroxybenzyl alcohol oxidation.

Huang made a similar observation,[125] confirming by XPS the charge transfer from Au to Ag atoms, resulting in different reaction mechanisms and different kinetics for the aerobic oxidation of benzyl alcohol from those for pure Au. The oxidation of benzyl alcohol follows a 1.5-order kinetic with respect to benzyl alcohol for the whole reaction with pure Au, with alcohol deprotonation and oxygen adsorption being the limiting steps. Upon the addition of Ag, the more cationic character of Au enhances alcohol deprotonation, while Ag helps dissociating oxygen.[126] The kinetic shifts to a 0.5-order with respect to benzyl alcohol. Finally, Guan *et al.* showed that Ag can form a layer of Ag oxide around TiO_2 supported-Au, and hypothesize this provides extra stabilization of the ensemble in the benzyl alcohol aerobic oxidation.[69]

Costa *et al.* studied the selectivity of Au-Ag nanotubes (Au-Ag NT) made by galvanic replacement on Ag nanowires for cinnamyl alcohol oxidation.[127] In their case, Au boosted Ag's activity but decreased its selectivity against radical side reactions. Pure Ag nanowires afforded the oxidative cleavage of cinnamaldehyde to benzaldehyde through a radical-chain reaction

(60% selectivity), at the expense of the desired cinnamyl alcohol oxidation (2%). Replacing of half of the Ag atoms with Au atoms increased the catalyst activity to almost full conversion, but with a decreased selectivity to cinnamaldehyde (20% selectivity). Surface-enhanced Raman spectroscopy (SERS) studies showed that cinnamyl alcohol was first oxidized on the catalyst surface, while the C=C cleavage step occurred in solution. Upon adding 2,6-di-tert-butyl-4-methylphenol (BHT), the C=C cleavage was inhibited and cinnamaldehyde became the major product (70% conversion, 97% selectivity) (Scheme 123).

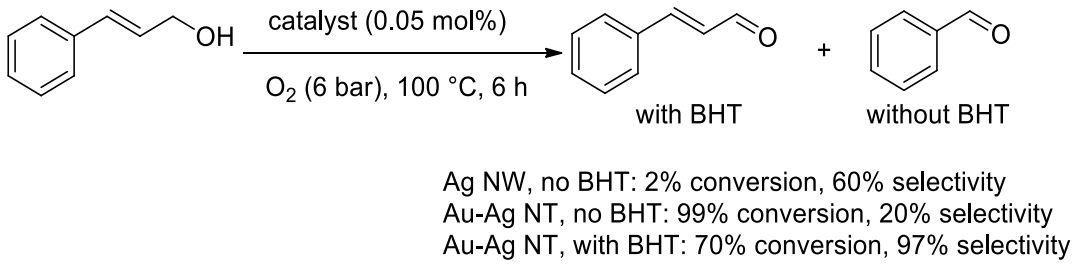

Scheme 123. Oxidation selectivity of Au-Ag NT.

Coinage metals have been used in different combinations to control alcohol oxidation selectivity. Dai[128] used Au/Ag@TiO_2 (Au/Ag atomic ratio: 3) for the complete oxidation of benzyl alcohol to benzoic acid, while Rossi[129] showed the Au/Cu could stop the oxidation at the benzaldehyde.

In conclusion, Ag NPs exhibit specific traits for alcohol oxidation that are neither encountered with homogeneous Ag or other metals. The Ag-O pair has been extensively shown to perform hydride abstraction from alcohols, with or without the assistance of a support. The presence of hydride acceptor such as dioxygen increases the reaction rate, at the cost of selectivity through overoxidation. The last part showed that Ag could be used in conjunction with other metals to fine tune activity and selectivity.

2.4.4 Alcohol-amine coupling

Amines are key intermediates in the chemical industry, especially in agrochemicals, pharmaceuticals, detergents, and the food industry.[130] NH_3, the simplest amine, is the main source of nitrogen in most organic amines[131] and calls for functionalization through C-N bond formation. Various reactions have been devised to do so, such as the Pd-catalysed Buchwald–Hartwig amination[132] or alkyl halide substitution. These processes come at expense of halide salts generation, thus negatively impacting atom economy. Alcohols are 'ideal' electrophile coupling partners in the sense they are readily available, in particular from biomass,[131] and only generate water as a byproduct during their condensation with amine derivatives.[133] They are

however less reactive than, for instance halide compounds, due the high energy of the C-O bonds (c.a. 90 kcal/mol), and the poor leaving group character of the hydroxide group.[134]
To overcome this major hurdle, the alcohol may be transformed *in situ* into a more reactive group. The borrowing hydrogen mechanism (BHM), or hydrogen autotransfer, is a catalytic concept where a H_2 molecule, or a hydride/proton pair, is abstracted from a starting material to render it more reactive and then transferred to another molecule to obtain the end product (Scheme 124).[135] In alcohol-amine couplings, the alcohol is first oxidized into the corresponding carbonyl, then the amine-carbonyl condensation takes place, before the 'borrowed' H_2 is used to hydrogenate the resulting imine. This concept is not only useful to perform N-alkylation of amines using alcohols, it can also be used to activate alcohols for C-C couplings through aldol-type or Wittig-type condensations.[136] As shown in the alcohol oxidation section, Ag is competent for abstracting the α-hydride of the alcohol, but less so for the abstraction of the protic hydrogen, which is usually accomplished by the support or a co-catalyst.

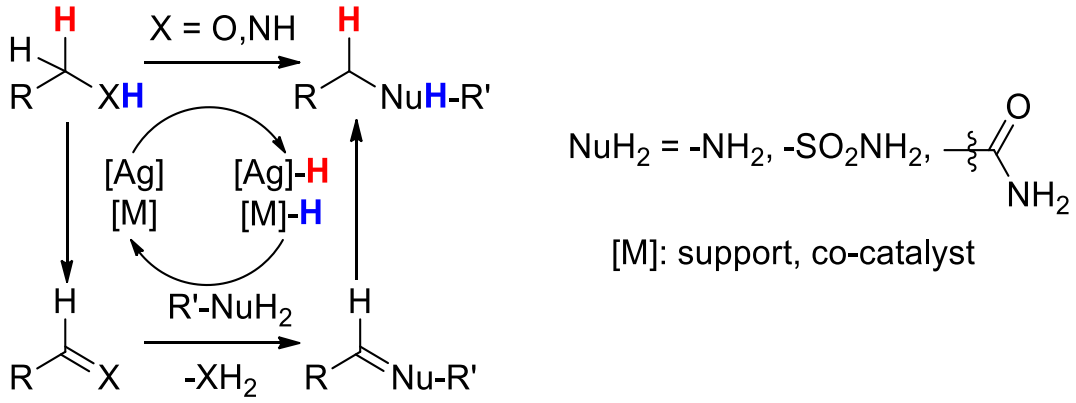

Scheme 124. General figure for borrowing hydrogen mechanism. The 'borrowed' hydrogens were put in bold.

One testament of the versatility of this approach is Deng and co-workers' report, where a Ag/Mo hybrid material was used to couple various nucleophiles (such as amines, amides, sulfonamides and ketones) with alcohols, in a diverse and extensive scope (Scheme 125).[137] Their rationale was to use silver as a potent alcohol dehydrogenation catalyst and molybdenum that showed some potential for C=N reduction.[138] The catalyst synthesis was fine tuned to afford $Ag_6Mo_{10}O_{33}$ crystals, which proved to be active without the addition of any organic ligand.

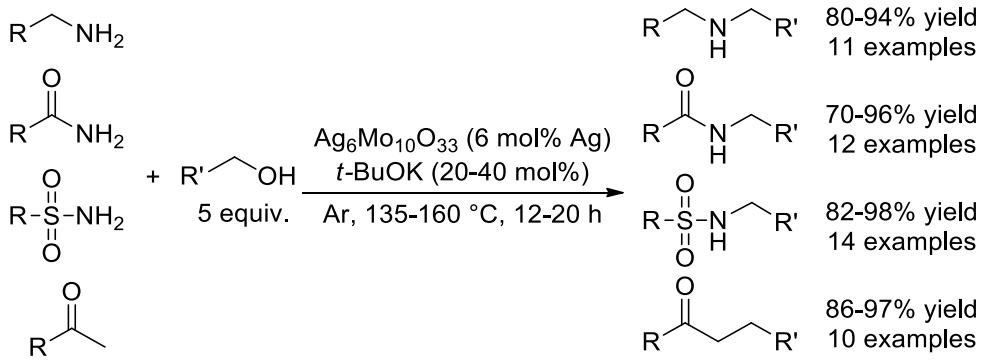

Scheme 125. Ag/Mo-catalyzed alcohol coupling with amines, amides, sulfonamides and ketones.

Satsuma and co-workers, having already reported silver supported on γ-alumina ($Ag@Al_2O_3$) for alcohol dehydrogenation,[115] naturally followed up with hydrogen borrowing on alcohols. As stated in their previous study, alumina as an amphoteric support not only stabilizes the catalyst, but also provides basic sites that can reversibly abstract proton from the alcohol. The acidic sites of alumina help the coordination of the various intermediates such as the ketone and the imine. A typical procedure for the catalyst preparation consisted in the impregnation of γ-alumina with a silver nitrate solution. The solid was dried and calcinated at 600 °C for 1 h then reduced under hydrogen 100 °C, 10 min.

These reports constitute the earliest examples of Ag NP-catalyzed BHM. Typically $Ag@Al_2O_3$ catalyzed the amination of a series of alcohols in the presence of two equivalents of aniline derivatives, in good to high yields (70-94%, Scheme 126).[139] They eventually showed that silver could also be introduced as small nanoclusters into copper NPs supported on alumina ($Ag\text{-}Cu@Al_2O_3$), allowing a lower catalyst loading (1 mol% of metal) and avoiding the use of $FeCl_3$ as a co-catalyst.[140]

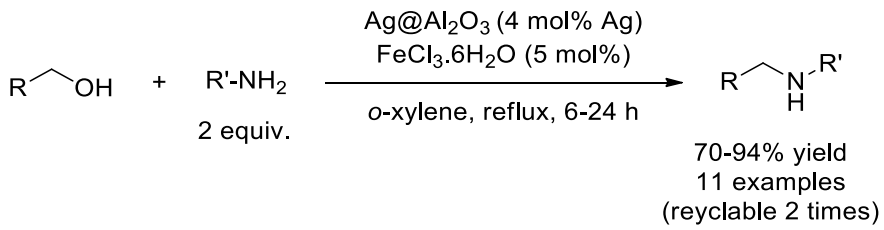

Scheme 126. $Ag@Al_2O_3$-catalyzed aniline *N*-alkylation using alcohols, with $FeCl_3$ as an additive.

The oxidation of alcohols into carbonyl intermediate proceeds similarly to alcohol dehydrogenation.[115] In short, a basic site from alumina (Al-O) borrows the proton from the alcohol, and the silver borrows the α-hydride from the alkoxylate (Scheme 127). Upon condensation of the amine with the carbonyl, a hemiaminal intermediate is formed. $FeCl_3$

accelerates water elimination step to form the imine, that subsequently gets protonated back from the borrowed proton. The resulting immonium cation is then activated again with $FeCl_3$ towards the attack of the borrowed hydride, yielding the amine. Overall, the amine yield was increased from 16 to 96% due to the addition of iron chloride.

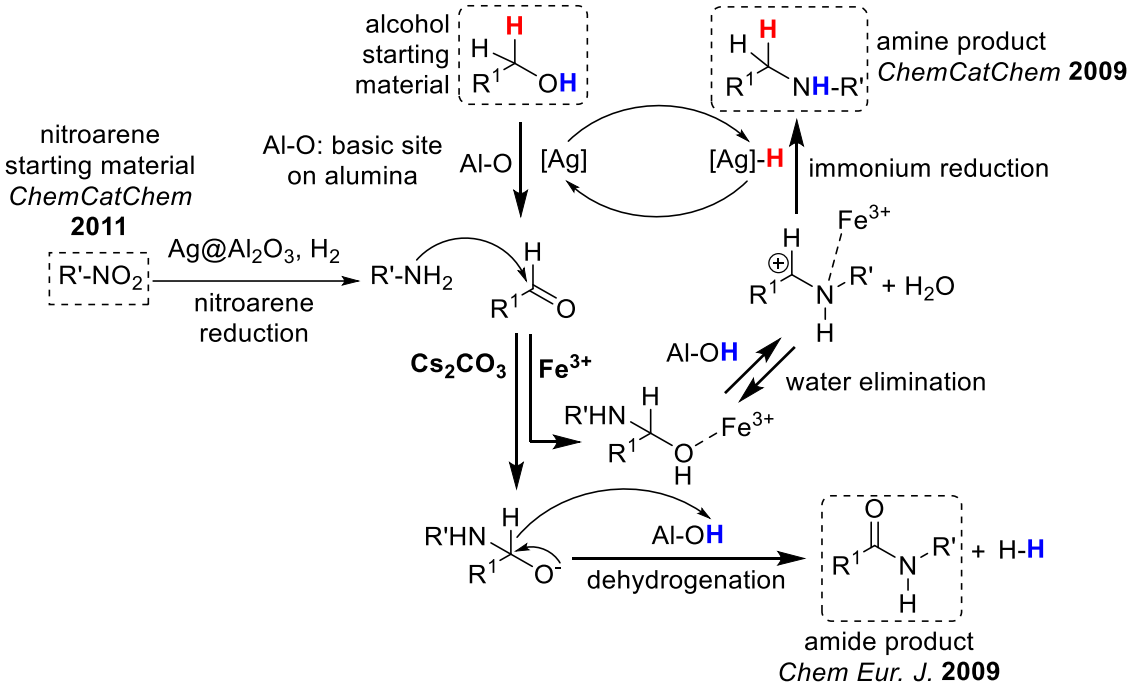

Scheme 127. Satsuma's proposed pathways for alcohol amination versus alcohol amidation using $Ag@Al_2O_3$ (adsorption steps omitted for clarity).

Upon adding a base rather than a Lewis acid, the hemiaminal intermediate can go through a dehydrogenation pathway, yielding the amide rather than the amine if a primary alcohol is used as a starting material. This was shown by the same group, under fairly similar conditions but using Cs_2CO_3 rather than $FeCl_3$ as additive (Scheme 128).[141]

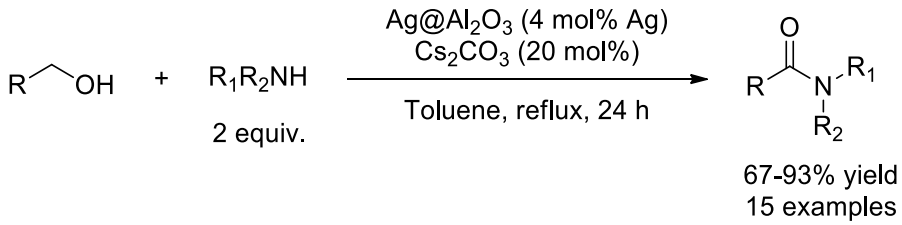

Scheme 128. $Ag@Al_2O_3$-catalyzed amidation of alcohols, using Cs_2CO_3 as an additive.

The Satsuma group also brought an yet another variation by replacing the amine with a nitroarene, which gets reduced *in situ* to aniline derivatives under 2 bar of H_2.[142] In terms of price, nitroarenes and alcohols are cheaper than anilines and carbonyls respectively, which motivated them to explore this pathway. This time, KF was used as a co-catalyst, although no clear indication of its role was given. The catalytic system was tested on a small range of

molecules, showing high yields (80-93%, Scheme 129). A similar system was reported by Mandi *et al.*, using polyacrylic acid as a support.[143]

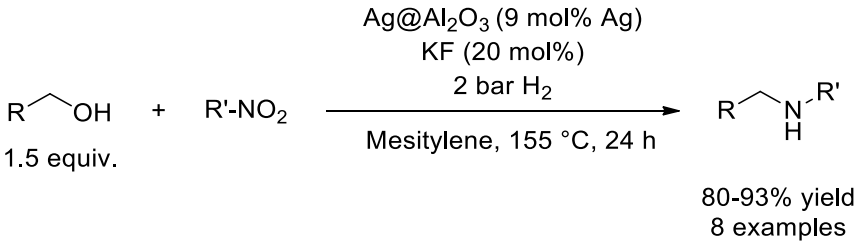

Scheme 129. Ag@Al_2O_3-catalyzed nitroarene *N*-alkylation using alcohols under reductive conditions.

Liu *et al.* also used Ag@Al_2O_3 in conjunction with Cs_2CO_3, but inverted the alcohol:amine ratio (2:1, Satsuma used 1:2).[144] The coupling of aniline and benzyl alcohol gave a high yield towards the amination product, but whenever aniline was replaced by a secondary amine or aliphatic alcohols were used, the conversion dropped below 70% with low selectivities to the amine product (Scheme 130). Typically, the coupling of pyrrolidine or piperidine to benzyl alcohol gave predominantly the amide product (76 and 78% selectivity respectively) in low conversions (51 and 18%). In other cases, such as the coupling of benzyl alcohols with cyclohexylamines or 1-phenylethylamine, the reaction stopped at the imine formation step.

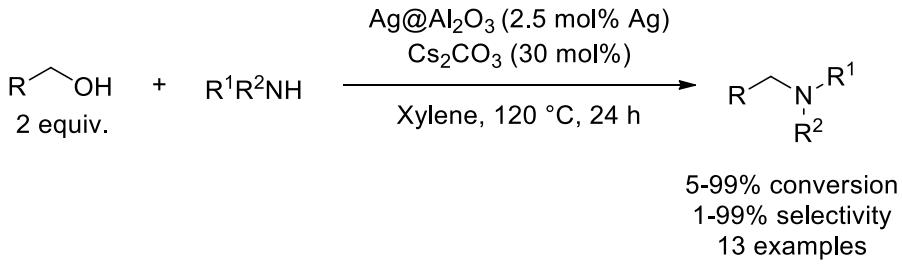

Scheme 130. Ag@Al_2O_3-catalyzed amination of alcohols, using Cs_2CO_3 as an additive.

One last example on Ag@Al_2O_3 for alcohol amination was provided by Paul *et al.*,[145] where lower amounts of Ag were used (0.3 mol% as opposed 2.5-4 mol% in other examples) at the expense of using an excess of Cs_2CO_3 (2 equivalents). Their substrate scope was quite extensive (Scheme 131), including aminopyridines, aminopyrimidines and 2-aminobenzothiazoles as amine coupling partners. An effort has been made to explore the recyclability of their catalyst on four different substrates, showing that all of them allowed the catalyst to be re-used at least 5 times with no significant yield drop.

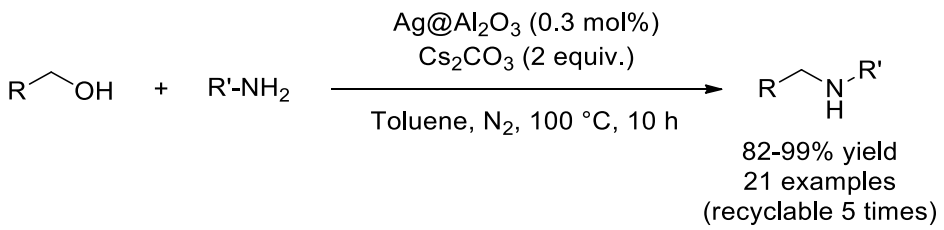

Scheme 131. Ag@Al_2O_3-catalyzed amination of alcohols.

Ortho-anilines (-NH_2, -SH, -OH) were shown to condense with benzyl alcohol derivatives into benzimidazoles with the same catalyst, demonstrating the versatility of the catalyst (Scheme 132). The same group also established that polypyrroles were suitable supports for Ag NPs, with a similar set-up and substrate scope.[146]

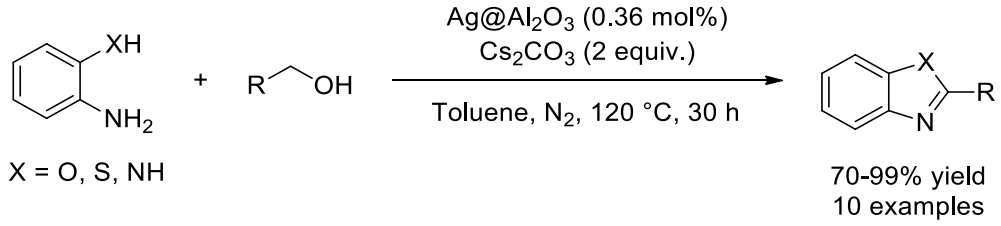

Scheme 132. Ag@Al_2O_3-catalyzed one-pot condensation of benzimidazoles.

Geukens *et al.* discovered that Ag NPs, generated *in situ* by reaction of $AgNO_3$ with NaH, were active for benzyl alcohol condensation with 4-ethynylaniline mild conditions (110 °C, 20 h, 38% conversion).[147] NaH was shown to both reduce $AgNO_3$ and also help deprotonating the alcohol, which is consistent with the examples shown so far in alcohol amination. Rather than using Al_2O_3 to stabilize their Ag NPs, the authors employed a Al_2O_3-Ga_2O_3 composite, featuring stronger Lewis acid sites and alleviating the need for $FeCl_3$ additives (Scheme 133).

Scheme 133. Ag@Al_2O_3-Ga_2O_3-catalyzed amination of alcohols.

The Kegnaes group studied the individual steps of the Ag@Al_2O_3-catalyzed alcohol amination over two reports, providing useful insight into the reaction mechanism. In a first report, they focused on Ag@Al_2O_3-catalyzed oxidation of alcohols, as well as their *in situ* condensation into an imine.[148] There, the over-oxidation of the benzaldehyde to benzoic acid was a concern for the overall reaction yield. Furthermore, benzoic acid can condense with the alcohol starting material, affecting even more the selectivity. Under air, the selectivity to benzaldehyde was

surprisingly higher at 100 °C (97%) than at lower temperatures (less than 75% at 60 °C and 80 °C) while one would have expected a higher over-oxidation rate at higher temperatures (Scheme 134). Conveniently, the oxidation works better under air (95% yield at 100 °C, 50 h) than under argon or pure oxygen (55% and 80% yield at 100 °C, 50 h respectively) showing that only small amounts of oxygen are needed to remove the hydrogen forming on the silver surface (cf. Alcohol Oxidation).

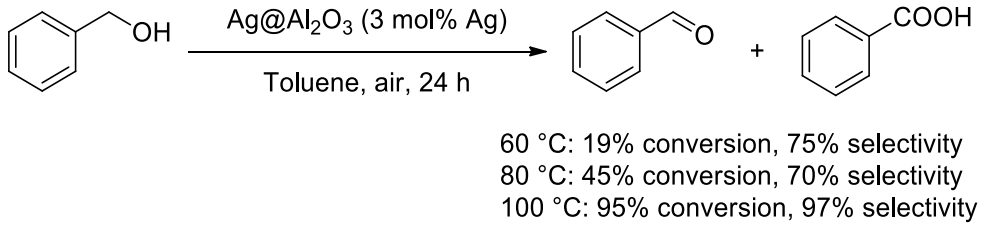

Scheme 134. Study on Ag@Al_2O_3-catalyzed oxidation of benzyl alcohol.

As expected, if an amine is present, less carboxylic acid is observed since the aldehyde is quickly consumed into the imine (Scheme 135).

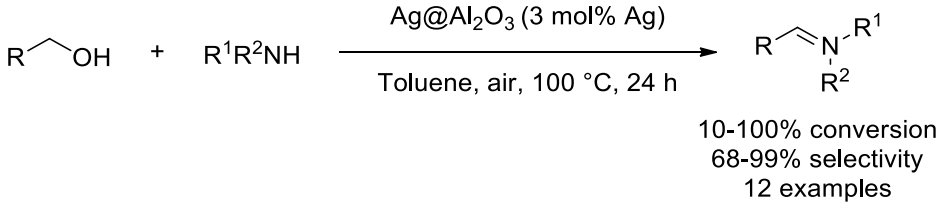

Scheme 135. Ag@Al_2O_3-catalyzed conversion of alcohols into imines.

In a second report, the Kegnaes group studied with the same catalyst the hydrogenation of imines into amines, attaining high yields (90-97%) for the 8 imines they tested (Scheme 136).[149] A small drop in selectivity (<5%) was observed due to the retro-imine condensation, with subsequent hydrogenation of the aldehyde.

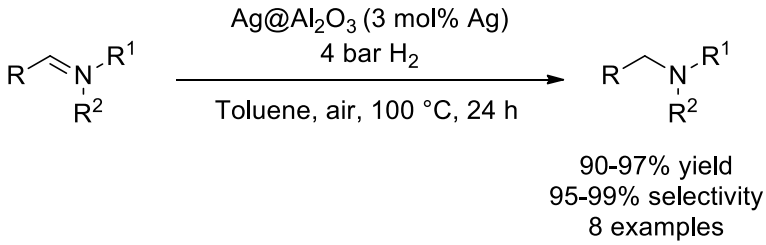

Scheme 136. Ag@Al_2O_3-catalyzed hydrogenation of imines.

With the two separate steps in hand, they attempted the overall alcohol amination reaction in one-pot (Scheme 137). The yield in amine product was 60% for the two steps, with alcohol oxidation/imine condensation step being quantitative, and the imine hydrogenation being responsible for the drop (60% yield). Compared to Satsuma's system, where the reaction was conducted in one step, no additive such as $FeCl_3$ was added.[139]

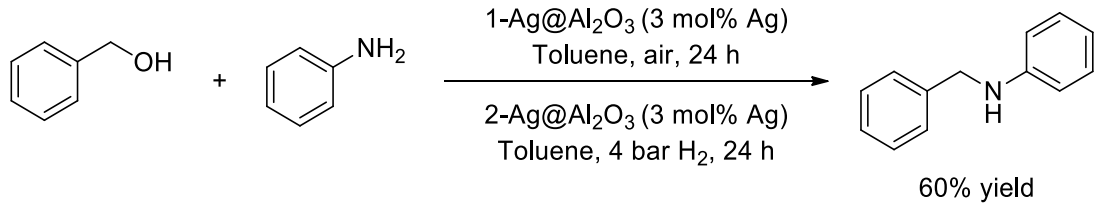

Scheme 137. Study on Ag@Al_2O_3-catalyzed oxidation of benzyl alcohol.

Xu *et al.* prepared bimetallic Ag@Fe_2O_3 nanocacatalysts, that were active for the condensation of alcohols and electron-poor amines (Scheme 138, 53 to 93% yield).[150] They demonstrated the power of their method on an intramolecular system to access 1,2-dihydroquinilines derivatives in high yields (77-98%). The catalyst was easily recyclable up to 5 times, using an external magnet.

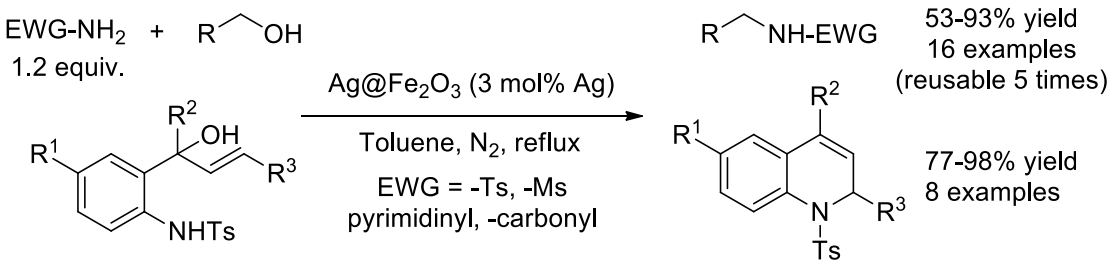

Scheme 138. Ag@Fe_2O_3-catalyzed one-pot condensation of benzimidazoles.

As a conclusion, alcohol amination is a powerful method to easily and cleanly obtain *N*-alkylated amines. Ag@Al_2O_3 has shown great potential for this reaction, thanks to, notably, the work of the Satsuma group. It demonstrated versatility to prepare *in situ* carbonyls from their corresponding alcohols and condense them with amines or other nucleophiles. Commonly observed features were good recyclability, and chemoselectivity to the secondary amine. The latter property is noteworthy, because secondary amines are better nucleophiles than primary ones.[151] In contrast with Ru or Ir-based homogeneous complexes,[152] no report of primary alcohol conversion to primary amine with NH_3 or an ammonia surrogate has been reported so far according to our literature survey, which is an interesting development to seek.

2.4.5 Alcohol-alcohol coupling

The Satsuma group exploited their catalyst, Ag@Al_2O_3, as well for the C-C coupling of primary alcohols with secondary alcohols to form ketones (Scheme 139).[153] The catalyst was able to perform the *in situ* oxidation of the starting materials into the corresponding carbonyls, followed by an aldol condensation mediated by C_2CO_3 (Scheme 140), before the catalyst reduces the resulting aldol, using the hydrogen extracted from the starting material. The scope of this reaction covered aliphatic and heterocycles-containing primary alcohols but was restricted to benzylic substrates for the secondary alcohol coupling partner. Indeed, the

cleavage of the α-carbon of the secondary alcohols was determined to be the rate-determining step. However, no explanation was given to explain the chemoselectivity of the reduction of the C=C bond of the aldol over its C=O bond.

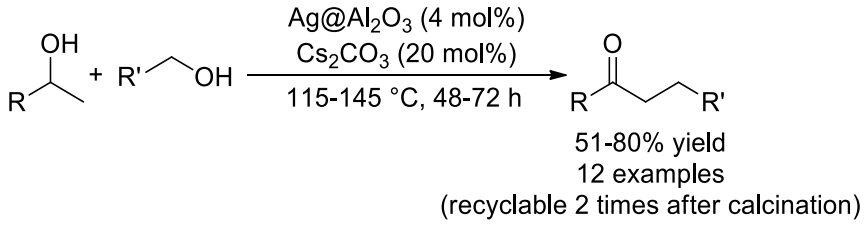

Scheme 139. Ag@Al_2O_3-catalyzed alcohol C-C coupling.

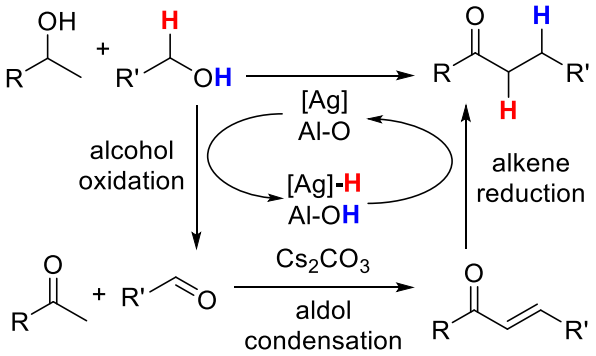

Scheme 140. Ag@Al_2O_3-catalyzed alcohol C-C coupling-mechanistic pathway.

By using dimethylsulfoxide (DMSO) as a solvent, the reaction was interrupted, after the oxidation of the starting alcohol. The solvent can condense with an equivalent of aldehyde with the assistance of KOH, forming a styryl sulfoxide intermediate. It can then condense with another equivalent of alcohol to form styryl ethers (Scheme 141). This modification from the previous example was exploited by Zhang *et al.*, using Ag supported on carbon as a catalyst (Ag@C, Scheme 142).[154] The presence of air was shown to be crucial for both the oxidation steps as well as the elimination of the sulfone fragment. In order to prove their mechanism, the authors showed that the reaction could be also conducted with one equivalent of styryl sulfoxide and alcohol, leading to the same product.

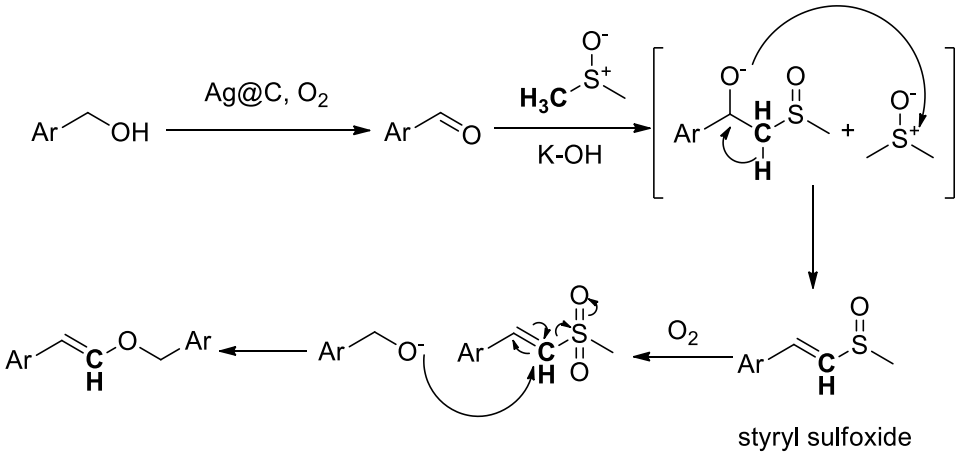

Scheme 141. Proposed mechanism for the formation of the styryl sulfoxide intermediate, and subsequent formation of styryl ether.

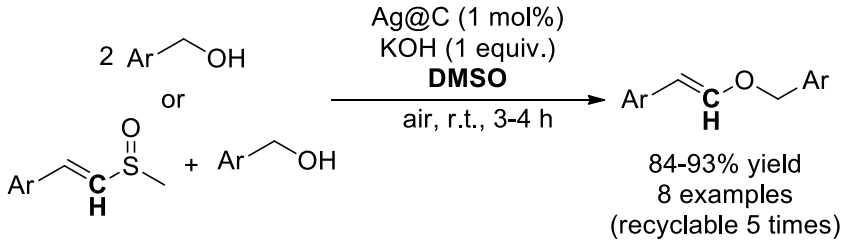

Scheme 142. Ag@C-catalyzed alcohol homocoupling to styryl ethers, through a styryl sulfoxide intermediate.

2.5 Reduction

2.5.1 Carbonyl reduction

The synthesis of many fine chemicals, particularly in the field of flavor, fragrance and pharmaceutical chemistry involves the selective hydrogenation of unsaturated carbonyl intermediates as a critical step.[155] The development of reduction systems able to selectively hydrogenate unsaturated carbonyls at the C=O bond solely are thus particularly important (Scheme 143). The challenge here lies in the fact that the C=C reduction is more thermodynamically favored than the C=O one.[156-157]

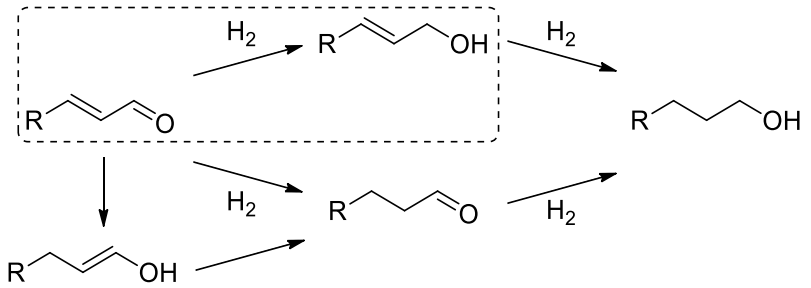

Scheme 143. C=O selective hydrogenation.

Selective hydrogenation is well established under stoichiometric conditions using metal hydride salts, such as $NaBH_4$ or $LiAlH_4$ as reducers. Despite their efficiency, catalytic alternatives are more desirable to reduce waste generation and improve safety.[158] Transition metal NPs are particularly active for catalytic hydrogenations, and feature a wide variety of selectivities and activities. While Ir and Os possess a high selectivity to C=O bonds at the expense of their activity, Pd, Rh and Ni have the opposite attributes. Pt, Ru and Co have moderate activity and selectivity.[159] In order to improve the C=O selectivity of transition metal NPs, another more electropositive metal or metal oxide can be added.[160] These components will introduce Lewis acid sites able to interact with the lone pair on the oxygen atom of the C=O bond, polarizing it and favoring its reduction. Adding a basic species can also help polarize the C=O bond, although it is a little less explored.[161] Polar solvents have been reported in the past to increase the selectivity as well.[162] Other means of increasing the selectivity have been reported, such as NP size,[163] electronic and steric[164] effects from the ligand/support, metal precursor,[165] oxygen pretreatment, defect sites,[166] or catalyst poisoning for PGM.[167-168]

In this landscape, Ag appears as a cheap alternative to Ir and Os. Like its pricey counterparts, Ag is very selective, but features a poor activity. Indeed, it is well established that Ag is a poor activator of the H_2 molecule. H_2 dissociation on its surface is endothermic (40 kJ/mol) with an high activation energy (125 kJ/mol).[169] Hammer and Norskov compared by DFT calculation the dissociation of H_2 over (111) surfaces of Ni, Cu, Pt and Au.[99] Although they did not specifically consider Ag, their conclusions on Cu and Au are easily extendible to all coinage metals. The bonding between the H_2 molecule and a transition metal surface proceeds *via* two main interactions, which are allowed by symmetry. On one hand, the σ_g orbital of H_2 can engage into interacting with the ns orbital of the metal. On the other hand, the filled d orbitals of the metal can back donate into the empty σ_u* of H_2. Both interactions are important in securing the weakening and ultimately the breakage of the H_2 bond. However, for coinage metals such as Ag, the Fermi level is higher than for other metals. In particular, the d/σ_u* interaction, resulting in a bonding and an antibonding state, becomes populated with 4 electrons, thus leading to a repelling interaction. This explains why coinage metal are less reactive than other transition metals towards the activation of H_2.[170-171]

Interestingly, in the presence of surface oxygen, the process becomes highly exothermic (-200 kJ/mol) with a more favorable activation barrier (70 kJ/mol).[172] These results were shown by DFT calculations by Rösch *et al.*, who eventually demonstrated that subsurface oxygen also have the same effect.[173] Consequently, oxygen pre-treatment of the catalyst has a strong positive influence on C=O/C=C selectivity, as shown both theoretically and experimentally.[174]

The pretreatment effect is durable as shown by Claus *et al.*, [175-176] since re-treating the catalyst with hydrogen afterwards did not lead to loss of selectivity. This stems from the slight dissolution of subsurface oxygen in Ag (especially on defect sites), creating more electropositive $Ag^{\delta+}$ sites that are more polar and favor C=O adsorption. Finally, the authors show by XPS and catalytic tests that the surface is not equivalent to a silver oxide Ag_2O surface.

Various groups correlated a greater proportion of (111) Ag facets to a higher yield towards the unsaturated alcohol. Wei *et al.* also noticed that at higher pressures, selectivity to C=O bond increases for acrolein hydrogenation, though the product tends to isomerize to propanal. Indeed, as the pressure increases (from 1 to 5 atm) the silver surface gets saturated in substrate, that preferably coordinates through the C=O bond. At lower pressures, acrolein can coordinate in a parallel way to the surface; making the C=C bond available for reduction.

In contrast with other reports, Lambert *et al.* found that high gas pressure reduced chemoselectivity, by looking at the adsorption geometry of crotonaldehyde on a silver (111) surface in gas phase.[177] Under low substrate coverage on the surface conditions, they showed that the C=O bond will be parallel to the metal surface, whereas the C=C is tilted so it cannot interact. This tilting decreases at higher surface coverage, making the C=C bond almost parallel to the surface, and making it available for hydrogenation.

Typical model substrates for C=O selectivity tests are α,β-unsaturated aldehydes, due to their industrial relevance. Besides the C=C/C=O selectivity issue, they can also go through double bond isomerization, or C-O hydrogenolysis. Because it has the least sterically hindered C=C bond, acrolein is the probably the most challenging substrate. Another typically studied substrate is citral, that possesses two different C=C bond, and yields industrially relevant bulk products, such as citronellol. It is prone as well to acetalization, and cyclization to terpenes, making it even more challenging.[178]

De Vos *et al.* reported one of the first examples of Ag NPs in liquid phase for selective hydrogenation.[179] They used Ag^0 and Co^0 nanocolloids (4 and 20 nm respectively) for the selective hydrogenation of α,β-unsaturated aldehydes to allylic alcohols, with moderate to high yields and selectivity (Scheme 144). The selectivity was boosted using Lewis acid promoters (Fe^{2+}, Sn^{2+}), and amide solvents such as dimethylformamide (DMF) or dimethylacetamide (DMA), as they helped stabilize the colloid suspension. However, alcohols and water led to acetalization and catalyst deactivation. In the case of citral, the catalyst proved to be recyclable up to 3 times with good selectivity retention despite a slight conversion drop due to loss by filtration.

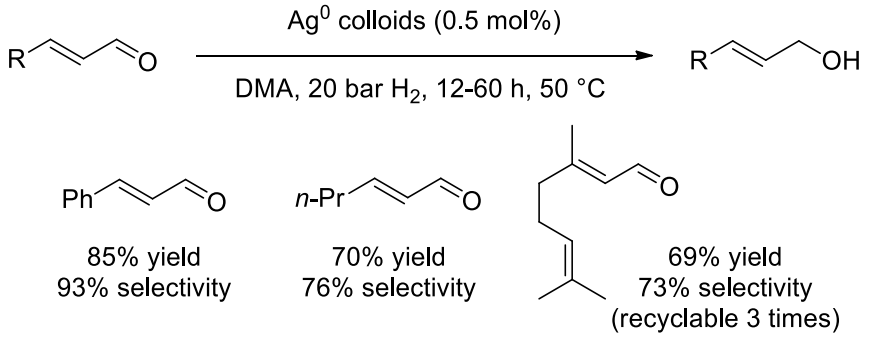

Scheme 144. Ag^0 colloid-catalyzed selective hydrogenation of α,β-unsaturated aldehydes to allylic alcohols.

Bron *et al.* exploited the oxygen pre-treatment of Ag@SiO_2 in acrolein hydrogenation.[180] They demonstrated that an oxygen treatment increased the hydrogenation activity from two- to three-fold, as well as the selectivity, and the best overall results were obtained under subatmospheric pressure. The catalyst was made from SiO_2 impregnation with $AgNO_3$ followed by calcination, and shortly after Steffan *et al.* showed that Ag carboxylate as a organic-soluble precursor could also be used.[181]

Doping Ag with In_2O_3 provides additional Lewis acid sites, and proved to increase the selectivity for crotonaldehyde reduction by Tian *et al.*[182] Indeed, by adding In_2O_3 (1.9 wt% In) into SBA-15 supported silver (6.1 wt% Ag), the selectivity of crotonaldehyde hydrogenation into crotyl alcohol can be boosted from 54% to 87%, at the cost of a longer reaction time (Scheme 145). NP size strongly affected the selectivity, which is consistent with previous reports.[183-184] Smaller size increased the amount of uncoordinated silver, making them more electropositively charged and coordinate selectively C=O bonds over C=C bonds.

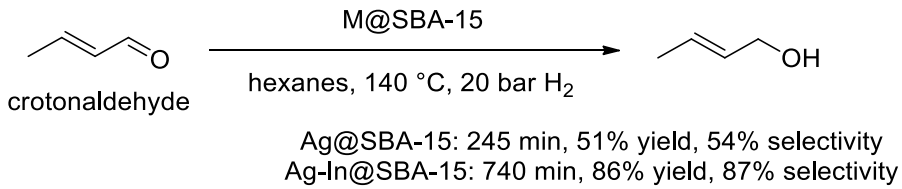

Scheme 145. Effect of In_2O_3 on Ag@SBA-15 catalyzed crotonaldehyde hydrogenation.

Kaneda *et al.* studied a different setup, where a core-shell structure was design with an Ag NP as core and a shell of CeO_2. The resulting nano-composites were dispersed onto CeO_2 (CeO_2@Ag@CeO_2). This system allowed both high activity and selectivity for the hydrogenation of a whole range of unsaturated aldehydes (Scheme 146).[185] The role of CeO_2 was rationalized as following: its strong interaction with Ag as a 'macroligand' and its basicity assisted in the heterolytic cleavage of H_2 to Ag-hydride and proton. This hydridic character is the most likely explanation for the high chemoselectivity towards carbonyls of their catalyst.

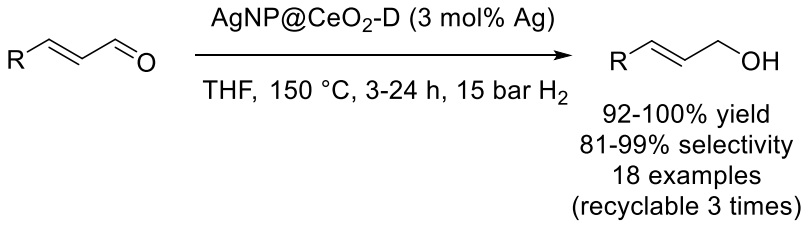

Scheme 146. CeO_2@Ag@CeO_2-catalyzed hydrogenation of unsaturated aldehydes.

Extremely small Ag NPs (1.3 nm ± 0.3 nm) were produced from the slow Ag^+ leaching of a bulk piece of silver, and there reduction onto cellulose nanocrystals (CNC) in water, with no external reducing agent, as shown by our group.[186] These NPs can catalyze the hydrogenation of aldehydes and nitrophenol in water (Scheme 147) while being easily re-used up to 4 times. However, the catalyst was also active for C=C bond hydrogenation.

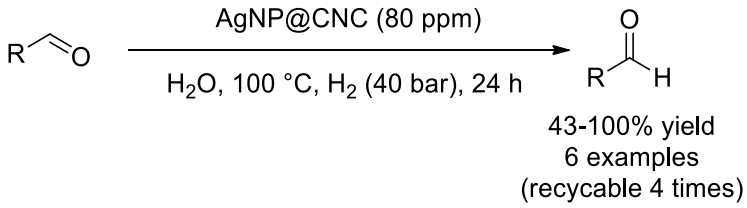

Scheme 147. AgNP@CNC-catalyzed hydrogenation of aldehydes and nitroarenes in water (not shown).

A similar system was designed, also by our group, where Ag was supported under microwave irradiation on a magnetic support made of magnetite and carboxymethyl cellulose (Ag-Fe_3O_4@CMC).[187] The system was easily recyclable using an external magnet, and was shown to be fully selective to C=O bonds in citral and α-methyl-trans-cinnamaldehyde (Scheme 148).

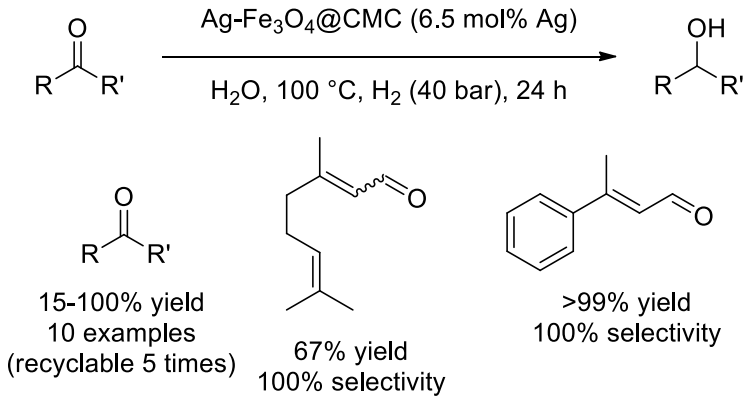

Scheme 148. Ag-Fe_3O_4@CMC-catalyzed hydrogenation of aldehydes in water.

Ag can be alloyed with other metals such as Pd, for example by partial galvanic exchange.[188] Zamborini *et al.* showed that adding up to 9% of Ag into Pd increased its chemoselectivity to C=O bonds, but also the NP stability towards the exposition to hydrogen

gas and hydrogenation substrates.[189]

In conclusion, Ag has been shown both theoretically and experimentally to possess an exceptional potential for C=O chemoselective hydrogenation. Compared to homogeneous complexes, the heterogeneity of Ag NPs gives further options for catalyst tuning, such as NP size and oxygen pre-treatment. These parameters permit the superior selectivity of Ag against Pt-group metals, whether it was tested on challenging substrates (acrolein) or industrially important molecules (citral).

2.5.2 Reduction of Alkynes

The reduction of alkynes to alkenes (semihydrogenation) is a key reaction in the chemical industry. Typically, this reaction is of crucial importance to the purification of olefin streams.[190] The Lindlar catalyst is one of the most widely used for this reaction: it consists of Pd/CaO_3 poisoned with Pb salts to trigger alkene selectivity. Despite its ubiquity, Pd has a number of disadvantages for alkyne semihydrogenation. Most notably, it is toxic, and it lacks selectivity towards alkenes. Alternatives to Pd catalysts are being actively sought out. However, metals like Ag, despite being highly selective towards alkenes tend to lack in activity.

A creative solution to this issue, based on a core-shell nanostructure, has been offered by Kaneda *et al.*[191] With a core of Pd and the shell of Ag, the selectivity of Ag could be combined with the activity of Pd. It was hypothesized that the Pd core could enhance the activity of the shell by acting as a hydrogen source. The shell permits better selectivity by forbidding any contact between the alkyne and Pd atoms. This model afforded quantitative yields across 16 alkynes (Scheme 149). Additionally, the catalysis was re-usable without activity loss up to 5 times.

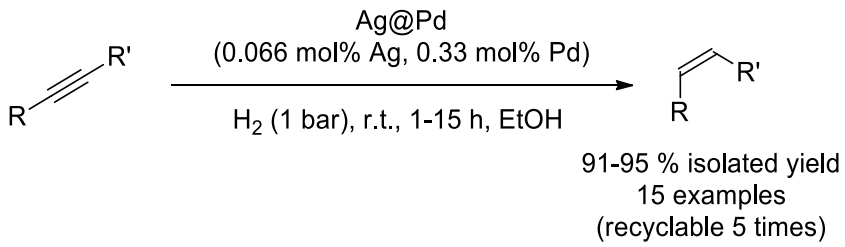

Scheme 149. Core-shell Ag@Pd for alkyne semihydrogenation.

Pérez-Ramírez and coworkers offered another approach using non-modified Au and Ag NPs.[192] The limited hydrogen activation of these NPs is of particular interest to cause high alkene selectivity. The use of supported Ag NPs of different sizes was investigated and compared with traditional Pd based catalysts under flow chemistry conditions for the three-phase hydrogenation of alkynes. NPs synthesized had spherical shapes with mono-dispersed size distribution (around 4.5 nm), which maximizes the number of active sites. In the case of

Ag, the best support material was found to be SiO_2, apparently because this support allowed to maximize Ag content, resulting in excellent stereo (-Z) and chemoselectivity in the hydrogenation of functionalized alkynes. This result is of particular interest because of the low cost of Ag compared to Pd.

The same authors further studied the semihydrogenation of propyne to propene using supported Ag NPs, with alkene selectivities up to 93%.[192] But most notably, they were able to provide new insights into the mechanism of the selective hydrogenation of alkynes on Ag surface. They demonstrated that the partial hydrogenation of propyne follows an associative scheme where adsorbed H_2 directly reacts with the alkyne, as opposed to the dissociative Horiuti-Polanyi mechanism. This adsorption occurs preferentially at B5 step sites, the surface density of which is optimized when the NPs have a 4.5 nm diameter. The heterolytic splitting of H_2 was shown by DFT calculations to be the rate limiting step, and over-hydrogenation of propyne is hindered by a large energy barrier (1.01 eV). These findings have been recently consolidated by Hughes *et al.* [193] who confirmed that the hydrogenation reaction of acetylene to ethylene over Ag NPs followed a non-Horuiti-Polyani mechanism.

Copéret and coworkers investigated the effect of surface passivation on the activity and selectivity of SiO_2-supported Ag NPs in the semi-hydrogenation of alkynes.[194] Research into SiO_2 surface passivation is of interest because it has previously been shown that it could have a key role in the formation of undesirable by-products [195]. In this case the hydroxy groups on silica are known to be responsible for these by-products. Their system offered up to 90% selectivity in the hydrogenation of propyne, they showed that propene selectivity was independent of surface passivation. Unsurprisingly, surface passivation also was responsible for a decreased reaction rate.

2.5.3 Reduction of Epoxides

Deoxygenation of epoxides into the corresponding alkenes is a vital reaction in biological systems for the production of vitamin K.[196] It is also a very important reaction in total synthesis for the deprotection of the oxirane ring, a protecting group for C=C bonds.[197-199] The reaction is usually carried out using a stoichiometric or excess amount of reducing agents, such as phosphines,[200] silanes,[201] iodides,[202-203] sodium,[204] hydride salts[205-206], and tungsten salts,[207] with a concomitant formation of copious amounts of waste. More recent developments involve the use of catalytic amounts of rhenium salts and hydrogen,[208] polyphosphoric acids,[209] or titanium dioxide with *i*PrOH as a photocatalytic reducing system.[210]

Ag NPs for epoxide deoxygenation has been mostly explored by Kaneda and co-workers.[211] Using hydrotalcite (HT) as a support, they made Au and Ag NPs-based catalyst for

epoxide deoxygenation (Scheme 150). Using *i*PrOH as a reducing agent, they managed to reduce a wide scope of epoxides with this catalyst. Notably, Au proved to be superior to Ag as more substrates could be reduced, including aliphatic epoxides while Ag mostly worked for benzylic epoxides. The catalyst proved to be recyclable by simple filtration.

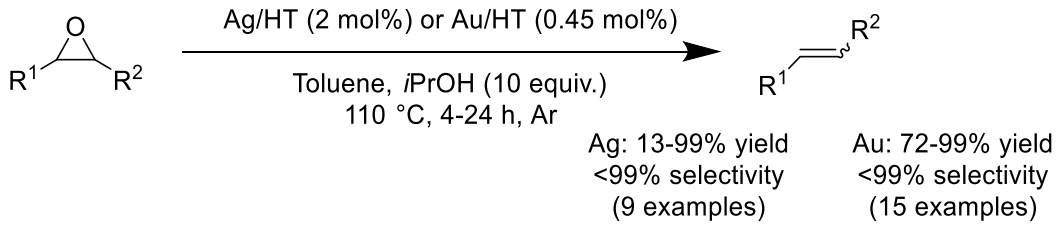

Scheme 150. M NPs@HT (M=Au or Ag) for epoxide transfer hydrogenation.

A tentative mechanism was shown, based on control experiments. HT bears basic sites [B] that can deprotonate the alcohol, while Ag operates hydride abstraction by β-elimination from the alkoxide. It is worth noting that this pathway is very similar to AgNPs@HT-catalyzed alcohol oxidation, also reported by Kaneda as well (see section 2.4.1).[118] The generated intermediate, Ag-H$^-$/[B]-H$^+$ is then able to open the epoxide cycle, which then gets dehydrated into the alkene product (Scheme 151).

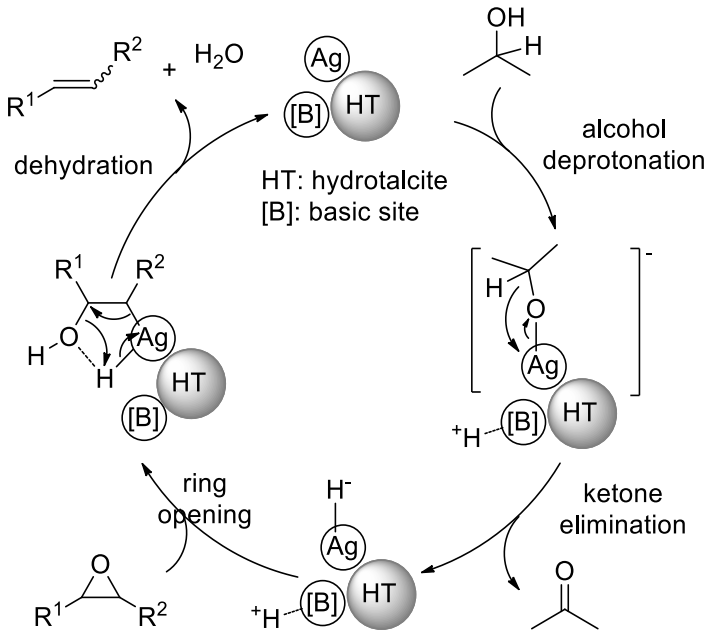

Scheme 151. Mechanism for Ag NPs/HT-catalyzed epoxide deoxygenation.

The same group also showed that the reducing agent could be also switched to H_2O/CO, showing superior performances at the cost of a higher catalyst loading (Scheme 152).[212]

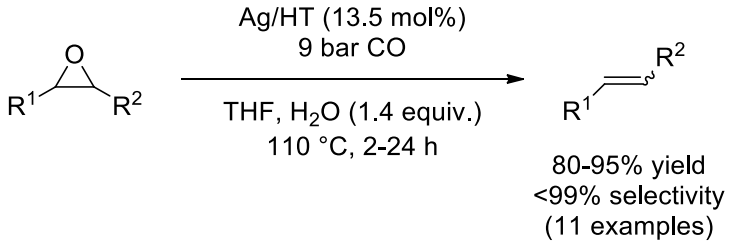

Scheme 152. Hydrotalcite-supported Ag for epoxide transfer hydrogenation under CO atmosphere.

Kaneda *et al.* reused another Ag-based catalyst, Ag@CeO_2, to perform epoxide deoxygenation.[213] Using H_2 gas this time as a reductant, they managed to deoxygenate a broader scope of epoxides with notably higher yields (Scheme 153). Here again the basic sites on CeO_2 helped cleaving hydrogen into the active species, working in synergy with Ag.

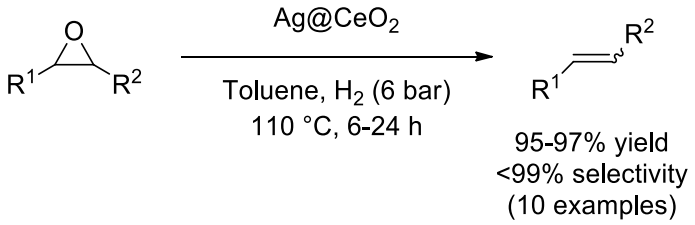

Scheme 153. Ag@CeO_2-catalyzed epoxide deoxygenation.

In conclusion, the Kaneda group is, to the best of our knowledge, the only group that successfully reported Ag NPs for epoxide deoxygenation. Using various supports containing basic sites, and a variety of reducing agents, they showed the viability of Ag NPs as recyclable catalysts.

2.5.4 Nitro compound reduction

In the industry, the hydrogenation of nitrobenzene is a crucial step in the production of aniline,[214-217] using typically Raney Ni or Pt/Pd on carbon as hydrogenation catalysts, with H_2 as a reductant at temperature of 200-300 °C. The use of reductants such as $NaBH_4$ is not realistic on a big scale, because of their price and generation of stoichiometric amounts of waste. Despite these limitations, the catalytic reduction of 4-nitrophenol using $NaBH_4$ is heavily studied by many research groups. This interest is mainly driven by the fact this reaction is extremely fast and easy to set up, as it can be followed by visible spectrophotometry, with the decrease of the sharp peak at 400 nm from the starting material.[215] Typically, under mild conditions with Au NP or Ag NPs, this 6-electron reduction process readily reaches completion within 5 minutes in water.[216] For these reasons, 4-nitrophenol reduction has become a benchmark for metal NP catalytic activity and is probably the most studied NP-catalyzed reaction. For instance, the first example on Ag NP application to catalysis, reported in 2002 by

Pradhan.[217] Because of this importance, it has been already reviewed extensively. For instance the reader is referred to a feature article of Pal and coworkers for general considerations on this reaction, including mechanism,[216] and a review by Blaser *et al.* for a review of this reaction.[218] In this chapter's framework, the reduction of nitroarenes using hydrogen gas will be solely covered, due to their higher relevance for industry. The first example was reported by Chen *et al*. in 2005, using Ag@SiO_2 (Scheme 154).[219] The authors used *o*-chloronitrobenzene as a model substrate, showing a full conversion and selectivity, satisfyingly with no hydrodechlorination side reaction.

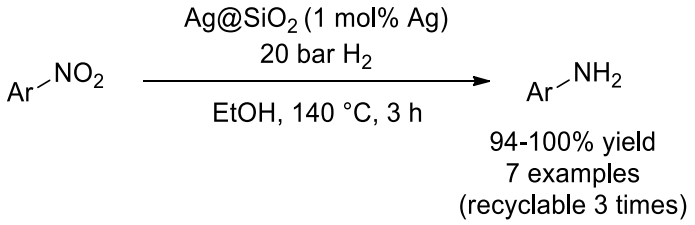

Scheme 154. Ag@SiO_2-catalyzed selective hydrogenation of nitroarenes.

The Satsuma group used Ag@Al_2O_3 for nitroarene hydrogenation instead, showing that their catalyst was compatible as well with olefinic groups using 4-vinylnitroarene as a model substrate (Scheme 155).[220] By decreasing the catalytic loading (from 2 to 0.2-0.8 mol%) and increasing the reaction from 1 h to 20 h, they also performed the reaction in presence of carbonyl, nitrile and amide functions with full selectivity. Later on, our group showed that the nitrophenol reduction could also take place in water, using Ag supported on crystalline nanocellulose (Ag@CNC).[186]

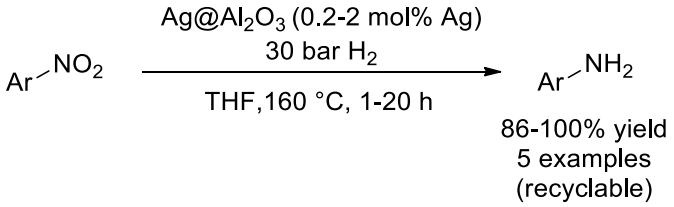

Scheme 155. Ag@Al_2O_3-catalyzed selective hydrogenation of nitroarenes.

Paun *et al.* showed that Ag@Al_2O_3 was applicable in a flow system (50 bar H_2, 80 °C, 0.2 mL/min, 70 s residency time for full conversion).[221] Artiukha *et al.* further developed nitroarene hydrogenation in flow systems by adding aldehydes to the mixture, to perform reductive amination (Scheme 156).[222] Notably, the scope was limited to nitroarenes as surrogate nucleophiles though it was tolerant to aliphatic aldehydes. The accumulation of a carbonaceous deposit on the catalyst led to catalyst deactivation after the third cycle, but an oxidative treatment in air helped regenerating the catalyst.

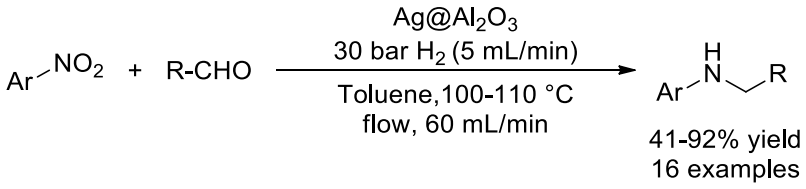

Scheme 156. Ag@Al_2O_3-catalyzed reductive amination in flow.

Cárdenas-Lizana *et al.* showed that Au NP and Ag NP supported on TiO_2 was suitable for gas flow reduction of nitroarene, though with no chemoselectivity test.[223]

2.6 Alkynylations

Alkynes are very valuable chemical synthons, able to react by CH activation, or by direct reaction *via* their triple C≡C bond to build up molecular complexity rapidly and in a controlled fashion. Ag is a metal of choice for this chemistry, because of its known ability to coordinate to triple C≡C bonds. Ag complexes have been exploited to this end, below we will focus on the heterogeneous Ag reactivity.[224]

2.6.1 Cyclizations

Van der Eycken *et al.* successfully used AgNPs supported on SBA-15 mesoporous SiO_2 to cyclize 3-substituted indoles into 3-spiroindolenines, with a loss of aromaticity on the heterocycle (Scheme 157).[225] The starting materials were easily made using the Ugi condensation. The catalyst was recyclable up to 10 times with no activity drop and worked for many types of 3-substituted indoles, with the exception of internal alkynes. Hot filtration experiments showed the heterogeneous nature of the catalyst, and transmission electron microscopy (TEM) studies showed that the catalyst started aggregating by crystal ripening somewhere between 40 and 60 °C.

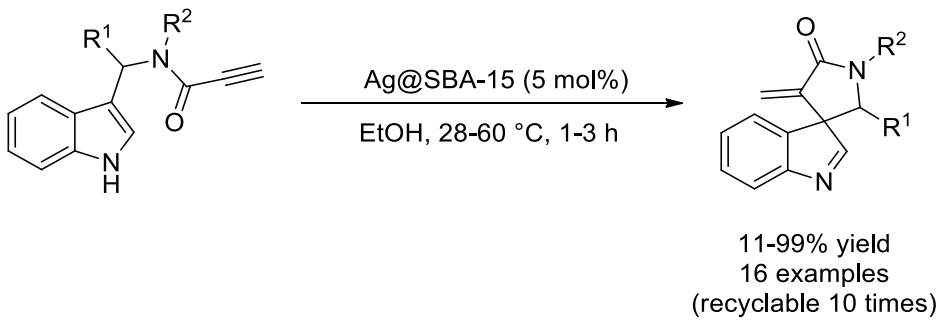

Scheme 157. Ag-Al@SBA-15-catalyzed 5-exo-dig spirocyclization of indoles to 3-Spiroindolenines.

Here, a 5-exo-dig cyclization was mostly observed, in contrast with other reports where a 5-endo-dig process occurred. Indeed, Unsworth *et al*. reported silver nitrate supported on silica ($AgNO_3$@SiO_2) as a Ag NPs surrogate for alkyne-tethered alkynes with a reverse selectivity

(Scheme 158).[226-227] $AgNO_3@SiO_2$ was formerly used in the 1960s as a support for column separation of *Z*- and *E*- alkenes and can be bought as a commercial product.[228] The author showed that Ag NPs were formed *in situ*, as evidenced by TEM imaging, which explains the induction period time for the reaction (2 h). Finally, they exploited the heterogeneous catalyst to perform a flow reactor experiment to prepare 20 g of spirocycle.

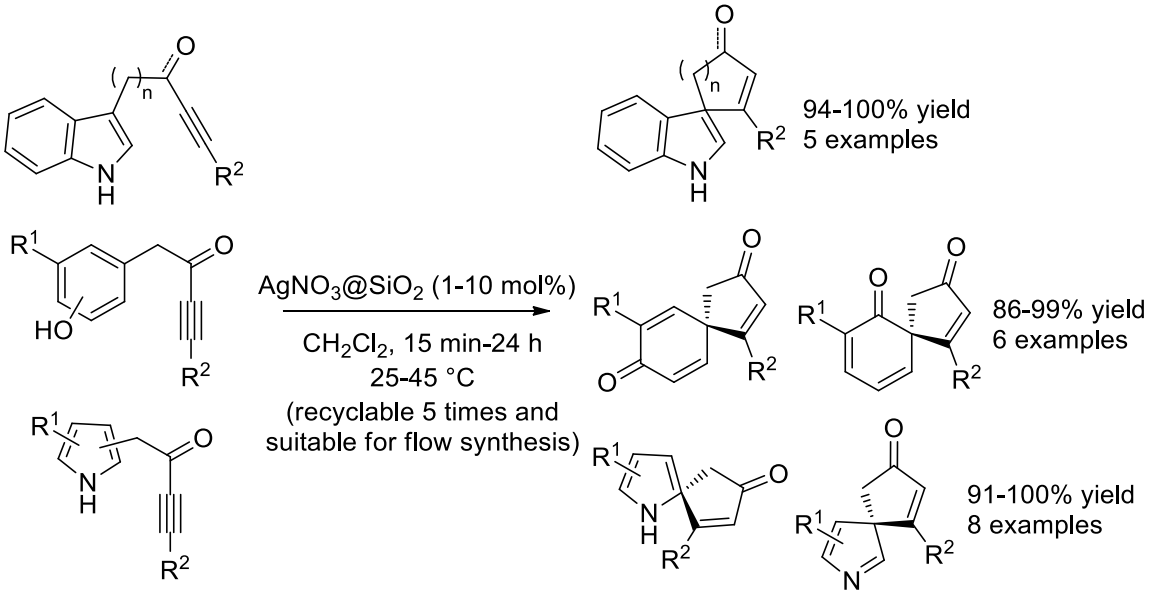

Scheme 158. $AgNO_3@SiO_2$ catalyzed 5-endo-dig spirocyclization of heterocycle-tethered alkynes to spirocycles.

Aurones are structural isomers of flavones, and such heterocycles could be potential antifungal agents and antioxidants.[229] They can be obtained by oxidation of 2,3-dihydrobenzofuran-3-ol precursors. Yu et *al*. showed that these precursors can be obtained from 2-(1-hydroxy-3-arylprop-2-ynyl) phenol cyclization, using Ag NPs supported on carbon black (AgNPs@C).[230] Along with triphenylphosphine and *N,N*-diisopropylethylamine, the catalyst was able to generate 2,3-dihydrobenzofuran-3-ol derivatives in high yields, at room temperature in a mixture of toluene and water (Scheme 159).

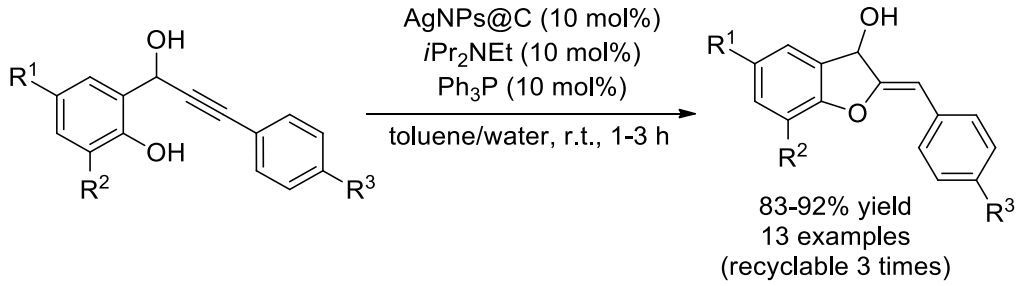

Scheme 159. AgNPs@C for 2-(1-hydroxy-3-arylprop-2-ynyl)phenols cyclization.

Finally, Madhavan *et al.* used Ag supported on silica ($Ag@SiO_2$) for the one-pot 1,3-dipolar

cyclization of azomethine ylides with 2'-hydroxychalcones to make highly functionalized pyrrolizidines and indolizidines.[231] The recyclability was excellent, with a good selectivity towards the exo- cyclization product (Scheme 160).

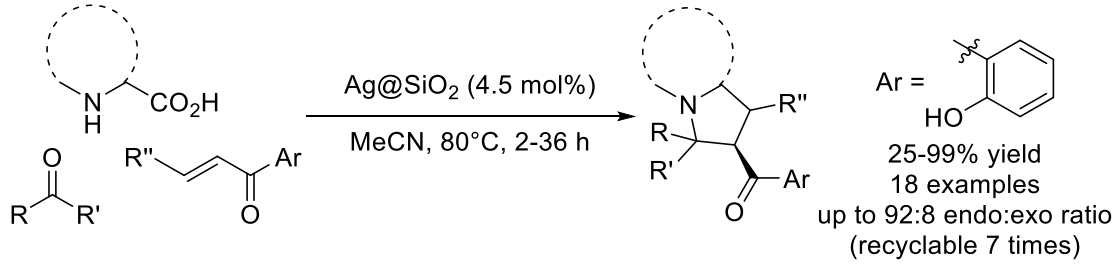

Scheme 160. Ag@SiO_2 for pyrrolizidine and indolizidine synthesis.

2.6.2 A^3 coupling

The first example of A^3 coupling catalyzed using a Ag complex in water was reported by Li *et al.*[232] and was expanded eventually to work in ionic liquids.[233] As opposed to earlier systems with Au [234] or Ru-In in water,[235] AgI works better on aliphatic aldehydes and slower on benzylic aldehydes.

An early example of heterogeneous Ag for A^3 coupling was reported by Lingaiah *et al.* where they used 12-tungstophosphoric acid as a support for Ag (Scheme 161, $Ag_3PW_{12}O_{40}$),[236] prepared according to a previous report.[237]

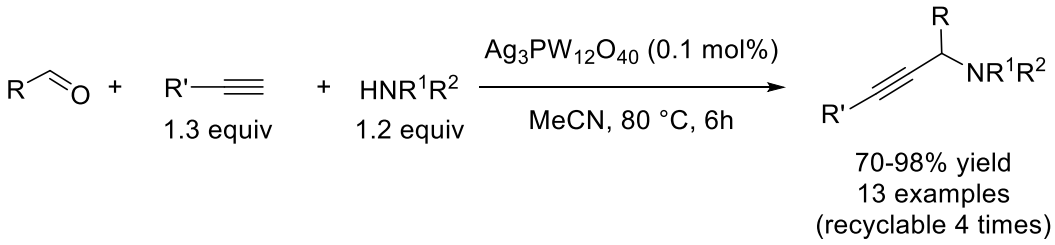

Scheme 161. $Ag_3PW_{12}O_{40}$-catalyzed A^3 coupling.

By simply bubbling H_2 gas into PEG in the presence of $AgNO_3$, Zhou *et al.* obtained Ag NPs (8-10 nm) suspended in solution that were used for A^3 coupling (Scheme 162).[238] The catalyst could be re-used up to 3 times though at the cost of increasing reaction time at each recycling.

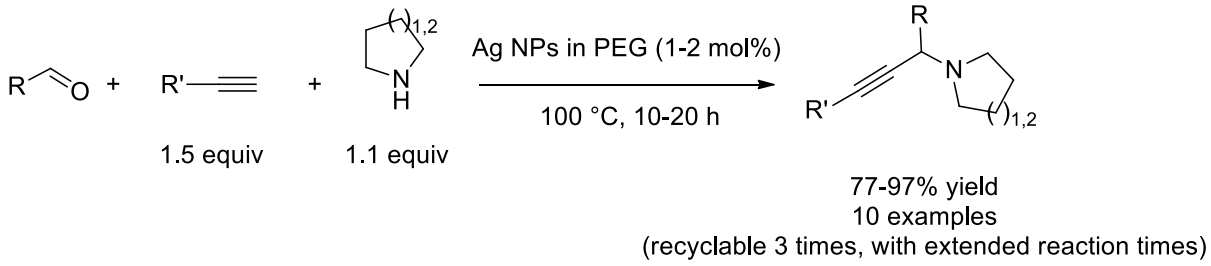

Scheme 162. Ag in PEG for A^3 coupling.

Heravi *et al.* made a magnetic hollow Fe_2O_3 shell as a support for Ag NPs, with SiO_2 and cyclodextrin as a support (Ag@CD@SiO_2@h-Fe_2O_3).[239] Upon short sonication times, the catalyst was able to condense carbonyls (both aldehydes and ketones), alkynes and secondary amines in high yields (Scheme 163).

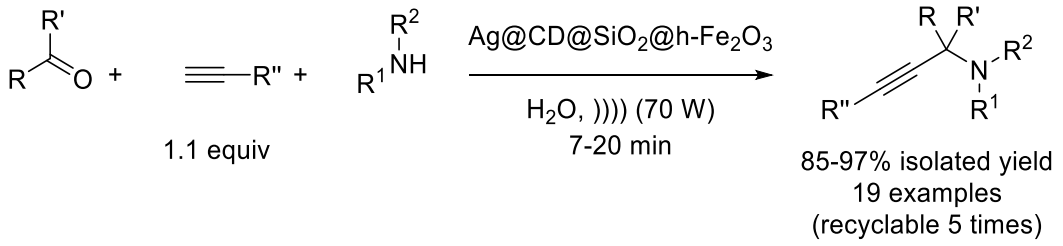

Scheme 163. Magnetically recyclable silver for A^3 coupling.

Movahedi *et al.* immobilized Ag NPs on ionic liquids supported on ZnO (AgNPs@IL@ZnO, Scheme 164).[240] The ILs grafted on the ZnO surface enables the stabilization of small and crystalline Ag NPs (6-10 nm), which in conjunction with water favors the contacts of the substrates with the catalyst surface.

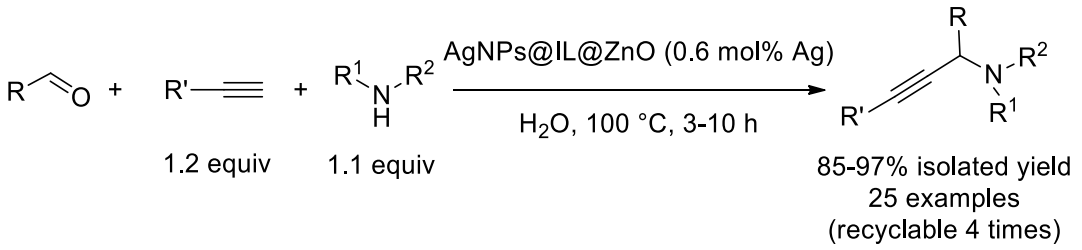

Scheme 164. A^3 coupling catalyzed by AgNPs@IL@ZnO.

Ag_2O nanocubes can be used for A^3 coupling at room temperature in chloroform, as reported by Sun *et al.* (Scheme 165),[241] while Ag_2O commercial powder does not work due to a smaller surface area.[242]

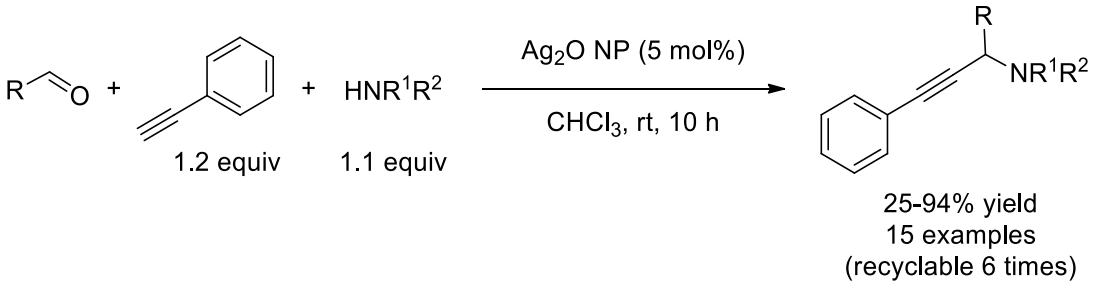

Scheme 165. Ag_2O nanocube-catalyzed A^3 coupling at room temperature.

Wang *et al.* supported silver oxide on alumina (Ag_2O@Al_2O_3) and multi-wall carbon nanotubes (Ag_2O@MWCNT) for A^3 coupling in water (Scheme 166).[243] Unfortunately, they showed that their catalyst was reduced to Ag(0) during the reaction, making it unrecyclable (showing around a 20% yield drop per cycle).

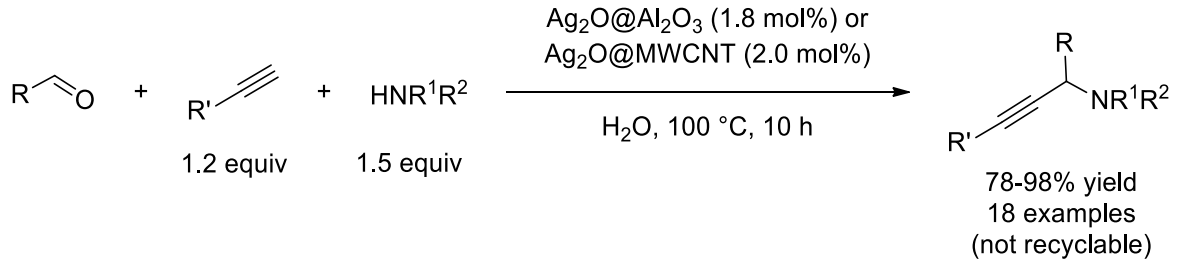

Scheme 166. $Ag_2O@Al_2O_3$ or Ag_2O@MWCNT-catalyzed A^3 coupling in water.

Islam *et al.* prepared Ag NPs supported on graphene (AgNPs@Gr), that exhibit high activity for A^3 coupling and the Huisgen condensation (Scheme 167).[244] The catalyst proved to be recyclable up to 5 times with neither NP aggregation nor leaching into the solution.

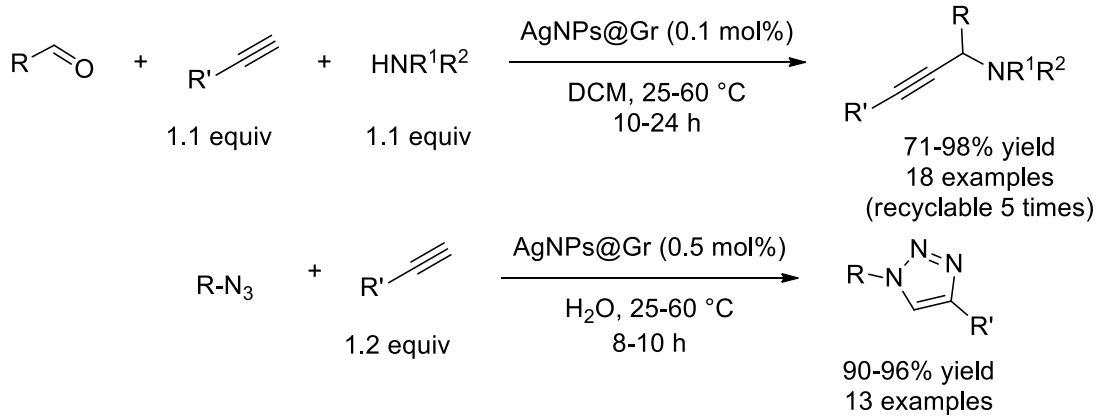

Scheme 167. AgNPs@Gr for A^3 coupling and click reaction.

Liu *et al.* supported Ag NPs on mesoporous silica (AgNPs@SBA-15) for A^3 coupling in ethylene glycol.[245] The catalyst was recyclable up to 4 times, after which the yield drops drastically to a third of its former value (Scheme 168).

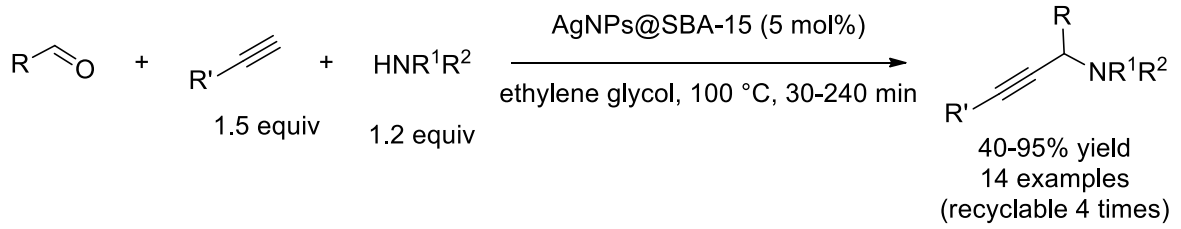

Scheme 168. A^3 coupling catalyzed by Ag@SBA-15-6 in ethylene glycol.

Ghasemzadeh *et al.* reported the AgI NPs catalyzed one-pot synthesis of benzofurans, made by the A^3-coupling of salicaldehydes, phenylacetylene and secondary amines followed by the cyclization into the desired product (Scheme 169).[246]

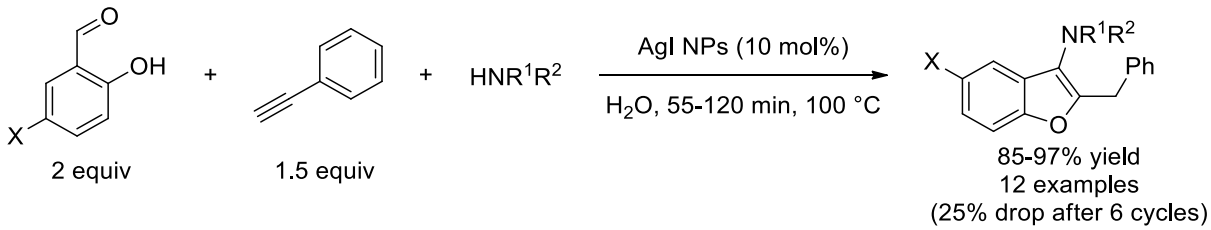

Scheme 169. AgI NP-catalyzed one-pot synthesis of benzofurans.

Supramolecular structures can be used to finely tune the properties of a heterogeneous catalyst, such as pore size with a maximal surface area.[247] In the two following examples, exceptionally mild conditions can be attained with Ag supported on MOF.

$AgNO_3$ can self-assemble with a 1,4-bis(4,5-dihydro-2-oxazolyl)benzene ligand (L) to form a three-dimensional supramolecular structure [Ag(L)(NO_3)], as proved by Yu *et al.* to catalyze the A^3 coupling reaction at room temperature in air (Scheme 170).[248] It is worth noting that the Ag acetylide formed during the reaction usually needs to be protected from air to attack iminium cations, whereas in this case the supramolecular structure gave a better stabilization, therefore allowing aerobic conditions.

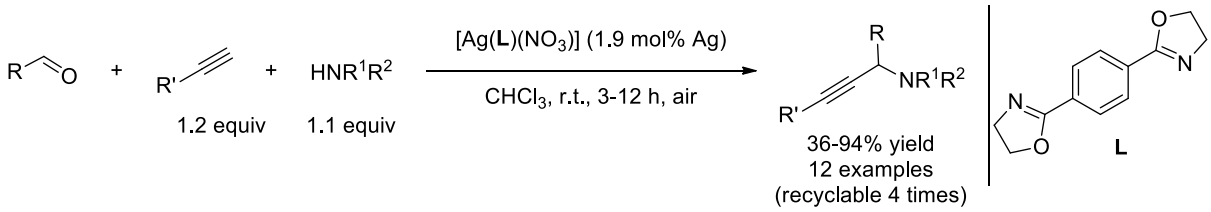

Scheme 170. A^3 coupling catalyzed by a silver supramolecular structure.

Wang *et al.* used a Ni-based MOF as a template for Ag NPs.[249] The use of a MOF enabled steric selectivity, allowing the reaction to go fast for small aliphatic aldehydes such as formaldehyde, and considerably slower for aromatic or branched aliphatic aldehydes (Scheme 171).

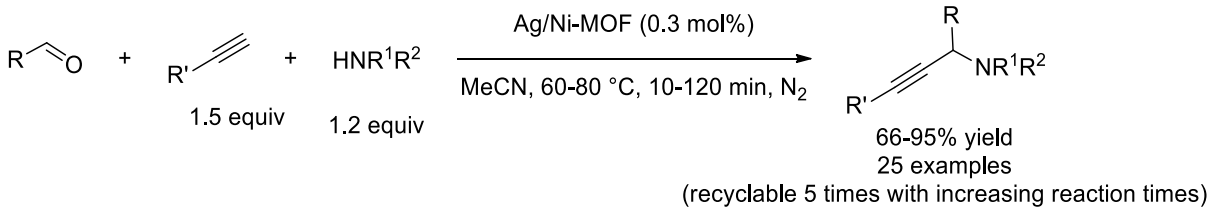

Scheme 171. MOF-supported Ag for A^3 coupling.

Aldehydes can also be used rather than imines to make propargyl alcohols as shown by Yu *et al.*[250] Different supports for Ag NPs in presence of triphenylphosphine were tested (SiO_2, Al_2O_3, TiO_2 and CeO_2), and AgNPs@TiO_2 proved to be the most suitable catalyst (Scheme 172).

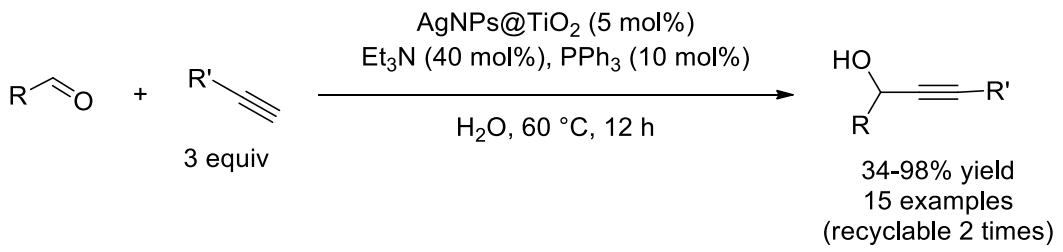

Scheme 172. Ag@TiO_2-catalyzed addition of alkynes to aldehydes.

AgNPs@TiO_2 was further studied by Wang *et al.*, by supporting them on a PMHS-based semi-interpenetrating networks (Ag@TiO_2@PMHSIPN).[251] PMHS is a polymer bearing Si-H moieties, that can be co-polymerized with ethyl acrylate to form an interpenetrating network. TiO_2 was easily dispersed on this network, and the overall serves as a composite support for Ag NPs. Two different NP size distributions were obtained by varying the reaction time of the synthesis: 10-30 nm (**B**), and 80-120 nm (**A**). The catalyst **A** was sufficiently active for alkyne addition to trifluoromethylketones in water, affording high yields (88-98% yield) after 2 hours at 60 °C (Scheme 173). Then, the authors further expanded the scope by exploring α,β-unsaturated trifluoromethyl ketones, though they used catalyst **B** to retain the high activity (83-95% yield). Lastly, the addition to aldehydes proved to be more sluggish, requiring 24 h of reaction time, as well as the addition of 10 mol% of 2,2,2-trifluoro-1-phenylethanone ($PhCOCF_3$) (67-99% yield, with a 20-40% yield due to the additive). The role of $PhCOCF_3$ is still unclear, though the authors propose that it activates the silver phenylacetylide intermediate towards the aldehyde.

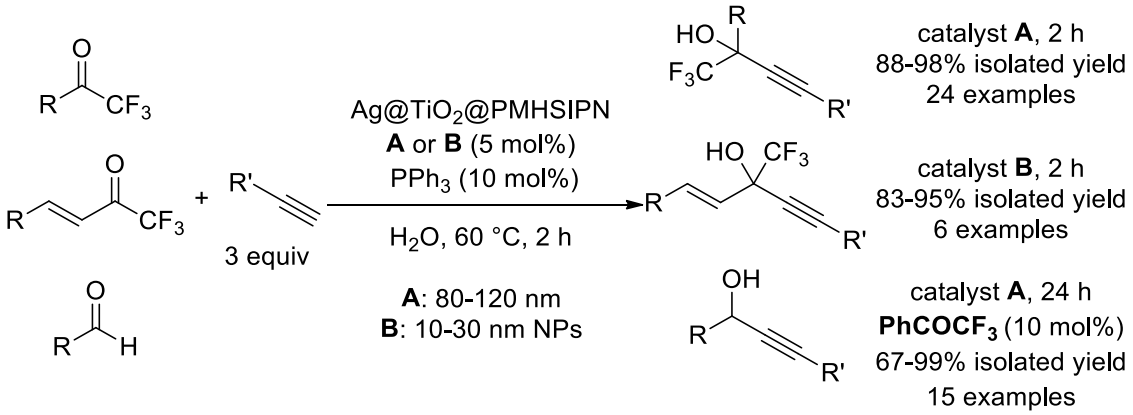

Scheme 173. Ag@TiO_2@PMHSIPN-catalyzed addition of alkynes to carbonyls.

2.6.3 Alkyne coupling to carbon dioxide

Zhang *et al.* grafted Ag NPs on a polymer containing N-heterocyclic carbenes (Ag@P-NHC) and use it for the synergistic coupling of alkynes to CO_2 and form alkynyl carboxylic acids.[252] According to their proposed mechanism, the poly N-heterocyclic carbene acts as an organocatalyst that can do a nucleophilic attack on CO_2, forming an NHC-carboxylate (Scheme

174). Concomitantly, Ag in presence of a base and the alkyne can form silver acetylide, that can attack the carboxylate and release the product.

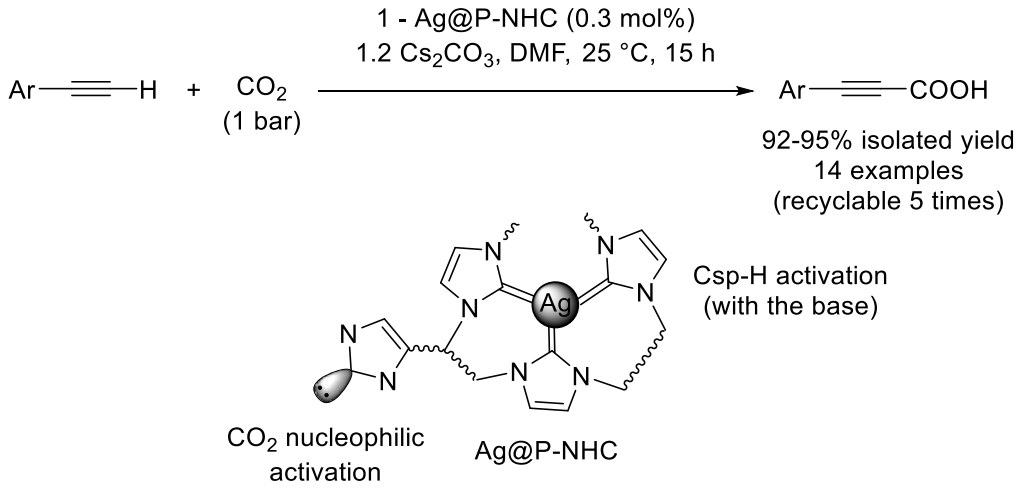

Scheme 174. Ag@P-NHC-catalyzed carbon dioxide addition to alkynes, schematic representation of Ag@P-NHC (polymer linkers were omitted for clarity).

Interestingly, Yang *et al.* used a MOF (MIL-100(Fe)) as a support for small Ag NPs (1.5 nm in average) to capture carbon dioxide and couple it to terminal alkynes to afford the carboxylic acid (Scheme 175).[253]

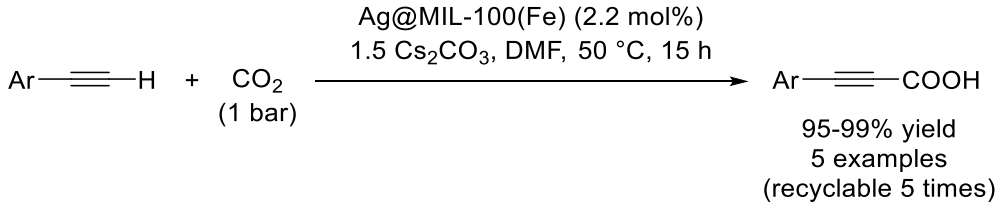

Scheme 175. Ag@MIL-100(Fe) for carbon dioxide capture and coupling to terminal alkynes.

Lastly, Huang *et al.* reported a framework of mesoporous knitting aryl network polymers as a support for Ag NPs (Ag@KAPs-P, Scheme 176).[193] The support provided a CO_2 sorption capacity of 17 cm^3/g, as opposed to 25 cm^3/g for the MIL-100(Fe) MOF in the previous example. However, a much lower loading was used (0.01 mol% Ag instead of 0.3-2.2 mol% Ag for the previous reports), affording a high TON of 9936 which is the highest reported so far for the conversion of CO_2 into alkynyl carboxylic acids.

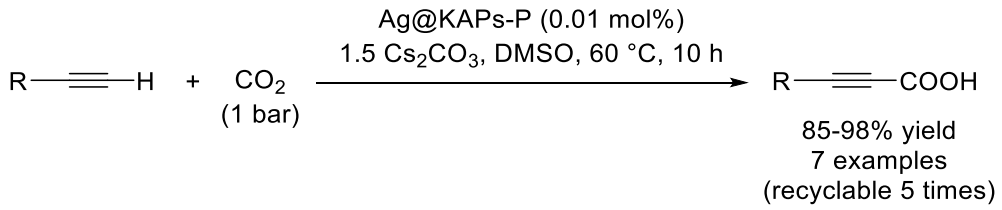

Scheme 176. Ag-supported on aryl network polymers for carbon dioxide coupling to terminal alkynes.

2.6.4 Alkyne cross-coupling

The coupling of alkynes to an aryl halide is the famed Sonogashira coupling. It is classically conducted using Pd homogeneous catalysts with Cu as a transmetallation agent, although Cu alone emerged as a suitable catalyst (both homogeneous complexes and NPs).[254] Au also was proven to catalyze the Sonogashira coupling in homogeneous catalysis,[255] and it was unambiguously proven that it was also able to act as an heterogeneous catalyst.[256]

Pd/Au/Ag trimetallic NPs have been reported by Santhanalakshmi *et al.* as stable and reusable nanocatalysts for the Sonogashira cross-coupling (Scheme 177).[257] The trimetallic nanoparticle had a slightly higher activity than pure Pd NPs (99% and 94% yield respectively) while using comparatively less Pd.

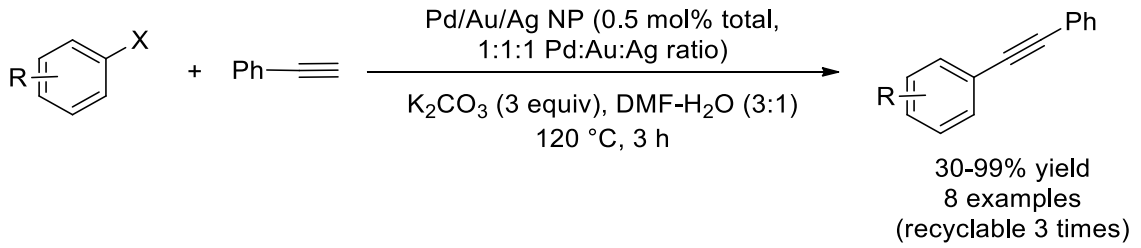

Scheme 177. Pd/Au/Ag trimetallic NPs for Sonogashira coupling.

However Ag alone has not been reported for such reactions yet, with the exception of an early study by Lambert group.[258] In this work, preliminary theoretical and experimental results for chlorobenzene-phenylacetylene coupling over a metallic (100) Ag surface were provided. In a vacuum environment, the molecules underwent cross-coupling on the catalyst surface, adopting a flat-lying conformation during the process. In the condensed phase however, due to the two starting materials forming mutually exclusive, pure 'islands' on the metal surface, homo-coupling was favored. In their conditions at 105 K, desorption of the unreacted starting materials was predominant, accounting for the low coupling product formation rates observed.

The Lambert group followed up their findings by exploring further phenylacetylene homo-coupling on Ag (100) under vacuum.[259] They underlined the importance of oxygen, that enables the generation of a phenylacetylide radical, crucial for the coupling. In absence of oxygen, the coupling does not happen since acetylenic hydrogen abstraction is an endothermic process for Ag. These findings were found to be valid as well when transposed to solution phase experiments, though excessive amounts of oxygen decrease the reaction selectivity and forms benzaldehyde.

Similarly, the Barth group showed the capacity of multifunctional molecule (1,4-bis(3,5-diethynylphenyl)butadiyne-1,3) to self-couple, as well as self-assemble when deposited on a Ag (111) surface at 305 K. [260] It self-couples following two different modes: terminal alkyne

coupling like in Lambert's work, and diyne-terminal alkyne coupling (Scheme 178).

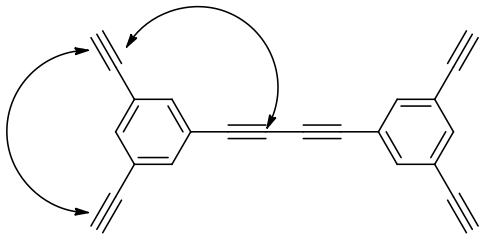

1,4-bis(3,5-diethynylphenyl)butadiyne-1,3

Scheme 178. 1,4-bis(3,5-diethynylphenyl)butadiyne-1,3 self-coupling modes on Ag(111) at 305 K.

In conclusion, Ag NPs have been widely explored for A^3 coupling reactions, with high standards in terms of activity and recyclability. The Ag-acetylide complex can also be added to CO_2, as shown by the few reports covered here, using porous materials to trap and activate the gas. Early studies towards Sonogashira coupling show difficulties in activating coupling agent to alkynes, favoring homocoupling.

2.7 Oxidative coupling

2.7.1 C-H oxidation

An early example of Ag-catalyzed C-H oxidation was provided in 1972 by Van Ham *et al.*, exploring different alloys of coinage metals.[261] Cu@Al_2O_3, Ag@Al_2O_3, and Au@Al_2O_3 catalysts were prepared and tested for cumene oxidation using oxygen. Pure Au and Cu proved to be inactive as catalysts, in opposition with Ag that increased the steady-state rate of oxidation compared to the reaction in absence of catalyst. An alloy containing 95% Ag and 5% of Au allowed a 1.2-fold increase of the oxidation rate. Crites *et al.* made in 2014 an in-depth study of the mechanism of cumene oxidation over Ag and Au NPs supported on hydrotalcite supports (Ag@HT and Au@HT).[262] While Ag stops at the cumene hydroperoxide, Au decomposes it further into cumyl alcohol at 80 °C.

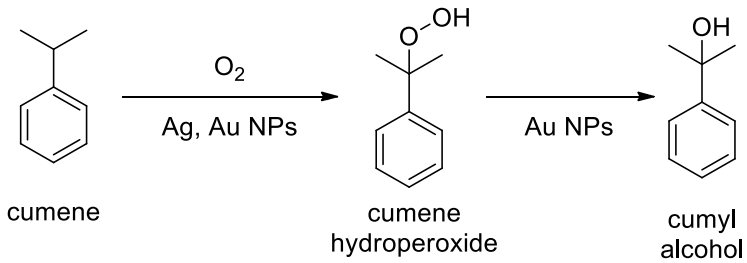

Scheme 179. Cumene oxidation.

From Van Ham's report though, Ag-catalyzed C-H oxidation remained dormant until 2006 when Zhao *et al.* reported Ag supported on a mesoporous SiO_2 support (Ag@MCM-41) for

cyclohexane oxidation.[263] After a careful optimization of the reaction conditions (142 °C, 3 h) and using oxygen as an oxidant, they managed to obtain a 45% selectivity to cyclohexanone and 38% cyclohexanol at 11% conversion (Scheme 180). This particular set of results is interesting considering that KA-oil, a mixture of cyclohexanone and cyclohexanol, is an important precursor in the nylon industry for adipic acid and caprolactam.[264] C-H selectivity is difficult to maintain at high conversion considering the higher reactivity of the oxidation products (both the ketone and the alcohol) compared to the starting material. Mesoporous supports have been reported to increase the selectivity of cyclohexane oxidation over cyclohexanol oxidation.[265] Finally, the undesired formation of cyclohexyl hydroperoxide in non-optimized conditions along with the reaction being quenched upon the addition of 2,6-di-tertbutyl-4-methylphenol hint at a free-radical mechanism.

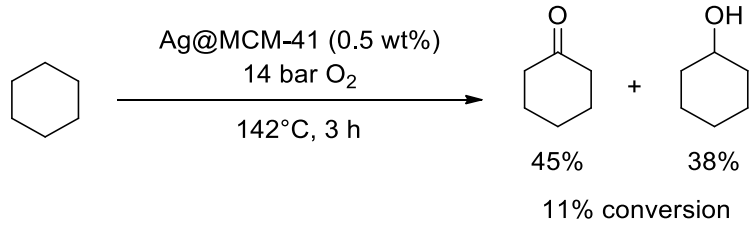

Scheme 180. Ag@MCM-41 for cyclohexane oxidation under air.

Since then, cyclohexane oxidation has been covered by additional reports, for example Acharyya *et al.* used Mn_3O_4 nanorods (Ag@Mn_3O_4) with H_2O_2 (Scheme 181).[266] Cyclohexane was converted to cyclohexanone with high yields (66%, with 75% selectivity at 88% conversion) and the catalyst could be easily recycled 8 times with only a 10% yield drop after the 8th cycle. The same system was used for 3-picoline to niacin (vitamin B3) oxidation.[267]

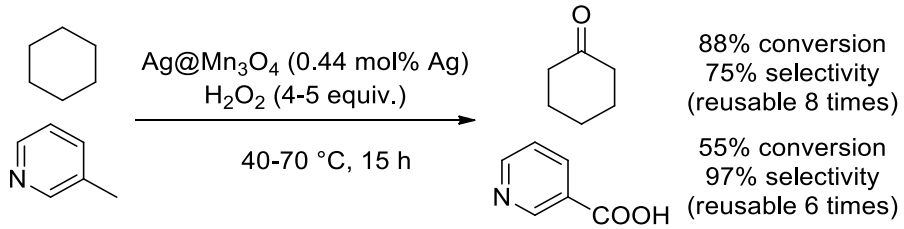

Scheme 181. Ag@Mn_3O_4 nanorods for cyclohexane and 3-picoline oxidation using hydrogen peroxide.

The same research group also explored cyclohexene as an oxidation substrate, which constitutes an alternative route towards adipic acid production in the nylon industry.[268] They used a similar support, tungsten oxide nanorods (Ag@WO_3), that exhibited high selectivity (94%) with an excellent conversion (99%). Later on, they showed that it was active as well for Baeyer-Villiger oxidation of cyclic ketones,[269], tertiary amine oxidation to N-oxides,[270] as well as toluene oxidation to benzaldehyde (Scheme 182).[271] The latter case is remarkable in that the

product does not over-oxidize into benzoic acid. The solvent choice is not trivial since acetonitrile activates hydrogen peroxide by forming peroxyacetimidic acid, that could be the active oxidant.[272]

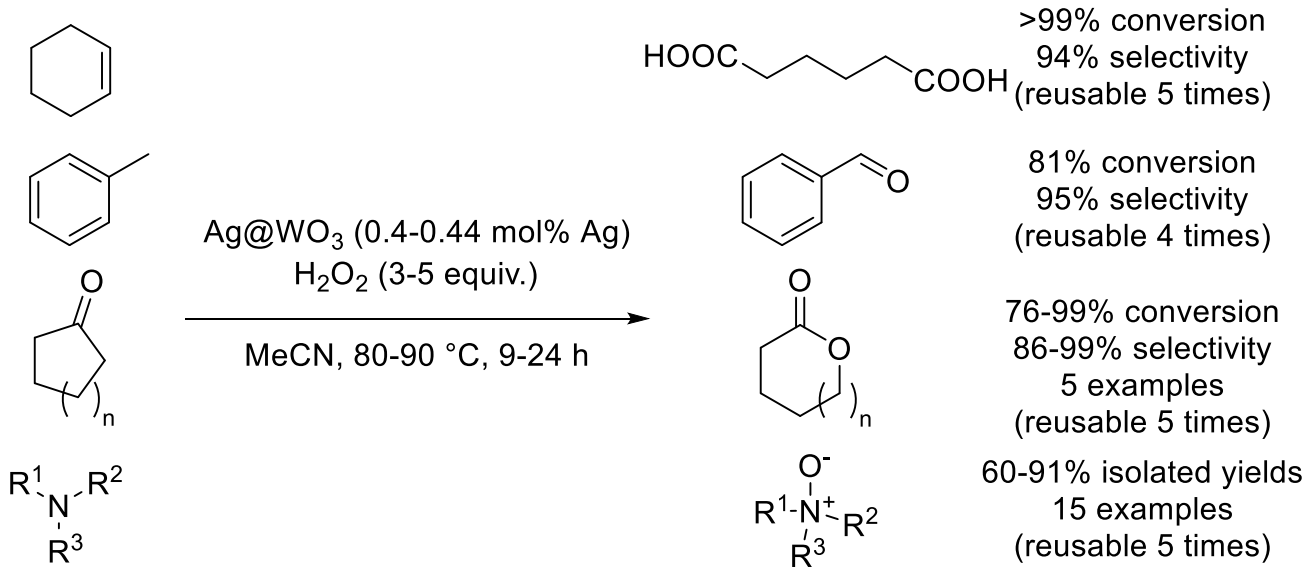

Scheme 182. Ag@WO_3 nanorods-catalyzed oxidations.

Benzylic C-H bonds have been further explored by Raji *et al.*, converting ethylbenzene into acetophenone using Ag NPs supported on ZnO (Ag@ZnO).[273] At 120 °C, using TBHP as an oxidant, they obtained a 88% selectivity at 38% conversion towards acetophenone with α-methylbenzyl alcohol as a byproduct (Scheme 183).

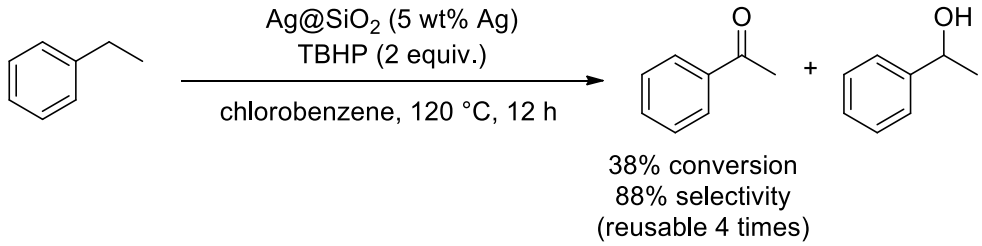

Scheme 183. Ag@SiO_2-catalyzed oxidation of ethylbenze into acetophenone.

Beier *et al.* showed that CeO_2, in conjunction with the addition of catalytic amounts of benzoic acid (3 mol%), could enhance Ag@SiO_2-catalyzed oxidation of four alkylarenes (toluene, *p*-xylene, ethylbenzene and cumene).[274] Typically in the case of *p*-xylene, the yield in oxygenated products (i.e. the corresponding alcohol, aldehyde and carboxylic acid) was more than doubled with the addition of CeO_2 and benzoic acid (from 3% to 7%). The second methyl group in *p*-xylene was left untouched due to the strong deactivating effect of the first oxygenated methyl group. CeO_2 is believed to both assist the initiation and the termination steps of the radical process, while benzoic acid decomposes the peroxo- intermediates, increasing the conversion into the carbonyls and alcohols (Scheme 184).

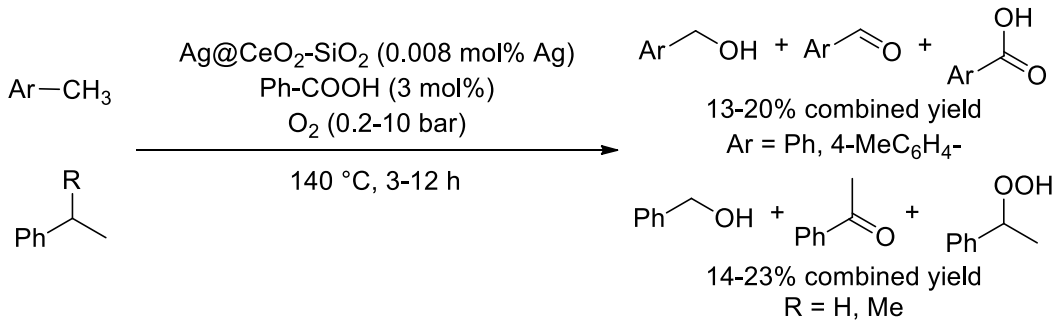

Scheme 184. Ag@CeO_2-SiO_2-catalyzed oxidation of alkylarenes using oxygen, with benzoic acid as an additive.

Finally, Hosseini-Sarvari *et al.* used ZnO as a support for Ag NPs (Ag@ZnO) and H_2O_2.[275] The scope was extended to 5 benzylic C-H-containing arenes, showing good to excellent yields (66-90%). The reaction proved to show promising results at the gram-scale (5.3 g), with 46% yield for ethylbenzene oxidation as opposed to 90% yield on the milligram scale (100 mg) but with the same amount of Ag@ZnO (Scheme 185).

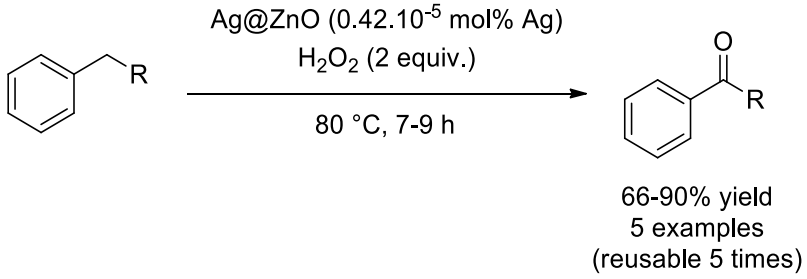

Scheme 185. Ag@ZnO-assisted oxidation of benzylic C-H bonds using hydrogen peroxide.

2.7.2 Azo coupling

Azo compounds are typically used in the dye industry, exhibiting vivid colors as a consequence of extended π-delocalization. On the big scale, they are produced by diazotization, requiring stoichiometric amounts of $NaNO_2$ and a strong acid at low temperature, with subsequent coupling.[276] Therefore, metal-catalyzed methods, using milder oxidants are desirable. The oxidative coupling of amines is interesting in that regard, although it comes at the cost of selectivity issues in the case of the coupling of two different amines.

Cai *et al.* studied a whole range of different metal NPs supported on carbon (M@C, M = Ag, Pt, Co, Cu, Ni, Pd, and Au) with Ag@C being the most active for aniline oxidative coupling under mild aerobic conditions (Scheme 186).[277] Aniline hetero-coupling was made possible by adding an excess (1.8 equivalents) of the most electron-poor aniline.

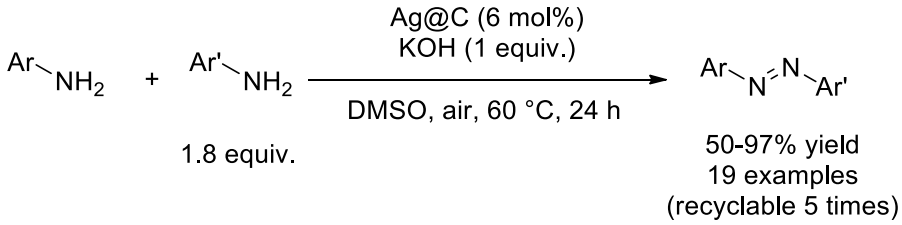

Scheme 186. Ag@C-catalyzed azo coupling.

Kumar *et al.* used an Ag-Ni alloy ($Ag_{0.6}Ni_{0.4}$) in relatively similar conditions (Scheme 187).[278]

Scheme 187. $Ag_{0.6}Ni_{0.4}$-catalyzed azoarene synthesis.

By using $Ag@WO_3$ in conjunction with H_2O_2 instead of air, as reported in examples mentioned earlier for C-H oxidation,[267-268] Ghosh *et al.* showed that anilines can be coupled into azoxybenzene, the oxygenated version of azobenzenes (Scheme 188).[279]

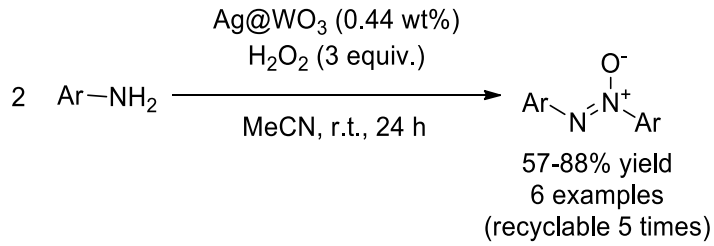

Scheme 188. $Ag@WO_3$-catalyzed azoxyarene synthesis.

2.8 Miscellaneous applications

2.8.1 Nitrile hydrolysis

The industrial production of amides is of interest given their important role in the synthesis of various acrylic monomers such as acrylamide or nicotineamide.[280] They can be obtained by nitrile hydrolysis, under acidic or basic conditions. These approaches have a few drawbacks, namely the generation of salt waste from neutralization of the reaction medium, or the over-hydrolysis to the corresponding carboxylic acid.[281] Activating the nitrile using a metal-based catalyst can increase the hydrolysis rate up to 10^{10}-fold while stopping at the amide stage (Scheme 189). A few Ag nanocatalysts have been reported in this area, using PVP[282], Fe_3O_4[283], or organic ligands[284] as supports/capping agents.

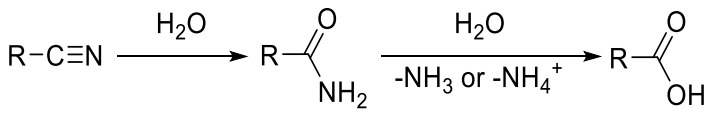

Scheme 189. Nitrile hydrolysis pathways.

Mitsudome *et al.* were the first to successfully hydrolyze nitriles to amides using hydroxyapatite-supported Ag NPs (AgHAP).[285] This catalyst was effective in hydrating benzonitrile derivatives and heteroatomic nitriles, but aliphatic nitriles proved to be unreactive (Scheme 190).

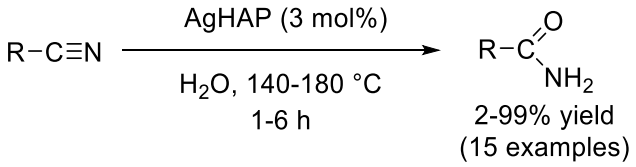

Scheme 190. Hydroxyapatite-supported Ag NPs for nitrile hydrolysis.

Shimizu *et al.* also reported nitrile hydration with Ag NP supported on SiO_2.[286] Their system was notable for its capacity to hydrate aliphatic nitriles, as well as heterocyclic nitriles. High TOFs were correlated to high oxygen coverage on the Ag surface, which is consistent with the exceptional electronegativity of adsorbed oxygen on Ag surfaces. Akin to other Ag NP-catalyzed reactions, Ag acts then as weak soft Lewis acid, with O_{ads} acting as a strong Lewis base, that is effective in water dissociation (Scheme 191).

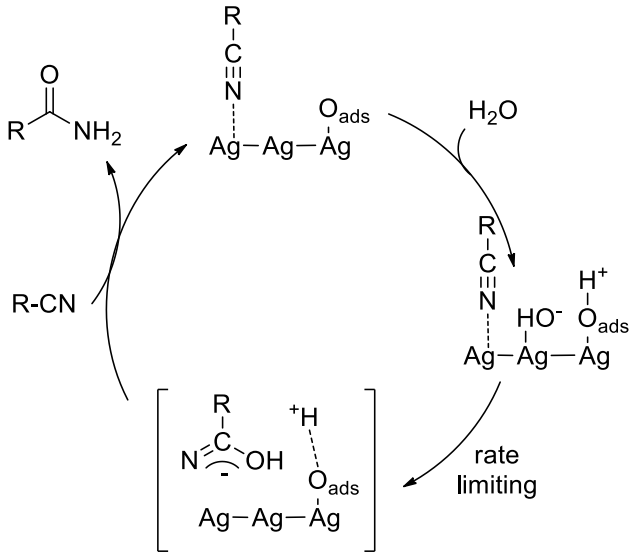

Scheme 191. Proposed mechanism for Ag-catalyzed hydration of nitriles.

Sherbow *et al.* proposed a 1,3,5-Triaza-7-phosphaadamantane-stabilized Ag water-soluble catalyst (Ag-PTA).[287] It remarkably proved to be effective for cyanohydrin derivatives (Scheme 192).

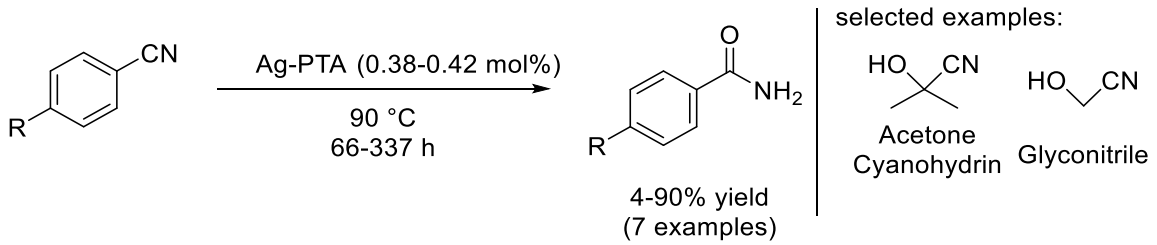

Scheme 192. Ag-PTA-catalyzed nitrile hydration.

This is remarkable in that cyanide generally poisons the catalyst. Indeed, cyanohydrins tend to form an equilibrium with hydrogen cyanide, which is known to poison homogeneous Ag complexes. The authors were able to overcome this problem using nanocatalysis. They showed that $Ag(CN)_2^-$ was a likely active species, that does not get further poisoned by cyanides, most likely due to the lability of Ag(I).

Finally, Li *et al.* proposed an Ag catalyst stabilized by polyamic acid salt (Ag-PAAS).[288] This quasi-homogeneous catalysis was notable for its recyclability. Indeed, PAAS is pH responsive making it exceptionally simple to recover and reuse (Scheme 193). A simple addition of acetic acid bringing the pH of the solution below 3 will cause the Ag-PAAS to precipitate out of the solution. The process is fully reversible by adding NEt_3, bringing the pH back up to 10 which allows redispersing of the catalyst, making it reusable up to 8 times without significant loss of activity or leaching.

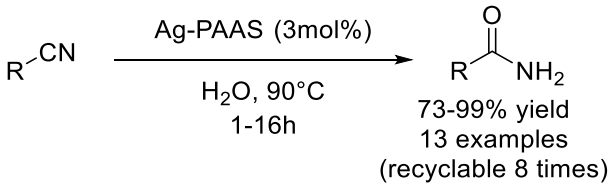

Scheme 193. Polyamic acid salt-supported Ag for nitrile hydrolysis.

The use of Ag NPs for the hydration of nitriles was first reported in 2009. Since, promising research has been conducted showing the stable NPs bound to a variety of different ligands and supports. A number of these reports show promise with regards to recyclability, allowing hope for more sustainable industrial nitrile synthesis in the future. Typically, after initial success at hydrating benzonitriles more challenging substrates such as aliphatic nitriles and cyanohydrins were successfully hydrated.

2.8.2 Silanol chemistry

Silanols are compounds bearing a Si-OH group, that are useful intermediates for the synthesis of silicon-based polymers[289-291] as well as nucleophilic coupling partners in cross-coupling.[292-293] While chlorosilanes are commonly used as precursors to silanols, they are prone

to condensation into siloxanes, thus requiring stabilization.[294] Alternatively, silanes are readily oxidizable using water, generating H_2 gas as the sole byproduct. Heterogeneous catalyst with TOF and TON as high as 20,000 h^{-1} and 99,000 have been reported for Pd@Al_2O_3 at room temperature.[295]

Hydroxyapatite is a phosphate mineral species found in teeth and bones and was proved to be a suitable support for Ag NPs (Ag@HAp) by Kaneda *et al.*[296] They were active for phenylsilane oxidation using water both as an oxidant and a solvent (Scheme 194). The support provides an hydrophilic environment for the Ag NP, and allows water to act as a nucleophile and effectively suppresses disiloxane formation. In comparison, water-soluble Ag salts such as $AgNO_3$ or AgOTf gave lower yields, showing the synergistic interaction between Ag and its support.

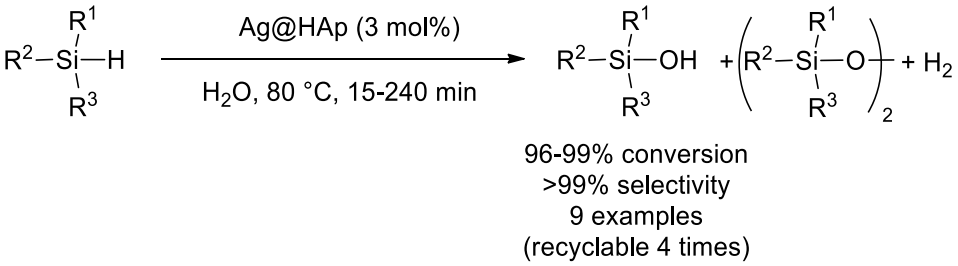

Scheme 194. Ag@Hap-mediated silane oxidation to silanol in water.

Mizuno *et al.* managed to stabilize Ag nanoclusters on silicotungstates (Ag_4@SIW10), which can be prepared beforehand or made in situ by mixing SIW10 with AgOAc.[297] In both cases, the resulting entrapped active species $[Ag_4]^{4+}$ was extremely active for silane oxidation with small amounts of water (5.6 equivalents) in acetonitrile (Scheme 195). Lower loadings (0.5 mol% to 0.0008 mol%) affording an optimal TON of 15625, though no recycling test was reported.

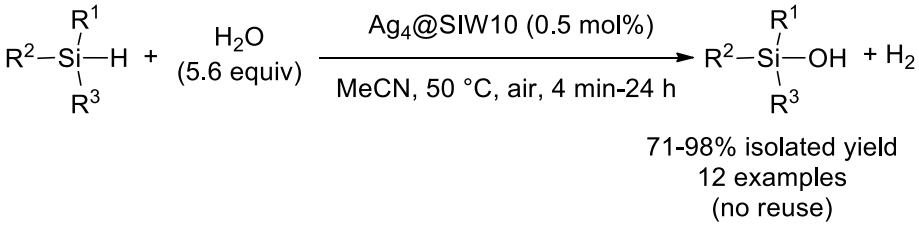

Scheme 195. Silicotungstate-supported Ag nanoclusters for silane oxidation.

Ding and co-workers made a nanoporous Ag catalyst by selective leaching of Mg from $Ag_{23}Mg_{77}$ wires (np-Ag).[298] They exploited not only its capacity to oxidize silanols using water (Scheme 196), but its capacity to couple silanols to alcohols (Scheme 197). Moderate to high yields were obtained at room temperature, and the catalyst was recyclable 4 times.

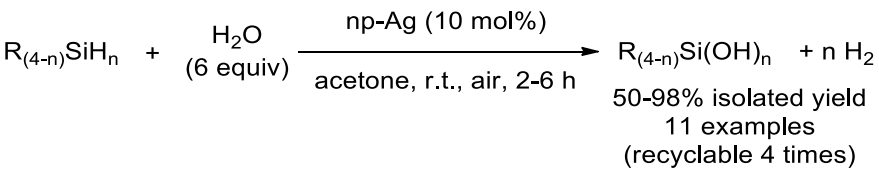

Scheme 196. Nanoporous Ag for silane oxidation with water.

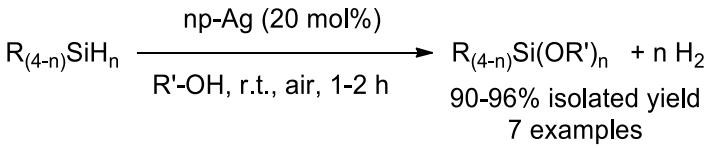

Scheme 197. Nanoporous Ag for silane coupling with alcohols.

Defect-rich Ag nanowires (Ag NW) have been reported for silanol coupling with alcohols by Jin *et al*. as well, made by templated reduction of Ag in SBA-15 channels and subsequent template removal using NaOH (Scheme 198).[299]

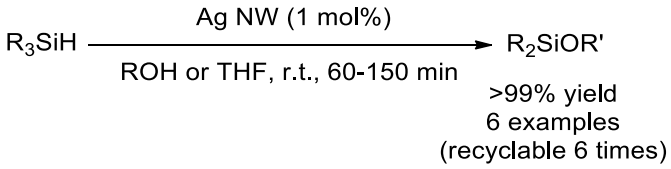

Scheme 198. Ag nanowire-catalyzed alcohol coupling to silanols.

Kobayashi *et al.* used commercial Ag_2O as a catalyst for coupling allylsilanes with aldehydes.[300] In the case of α-methylallylsilanes, up to 10/90 syn/anti ratios were observed, using catalytic amounts of DMAP to enhance the coupling and the selectivity (Scheme 199). Notably, by adding a chiral diphosphine ligand, the authors showed that moderate enantioselectivities could be obtained (63% ee, Scheme 200). Finally, the catalyst loading could be reduced to 0.005 mol% while still maintaining a high productivity, exhibiting a TON of 7680.

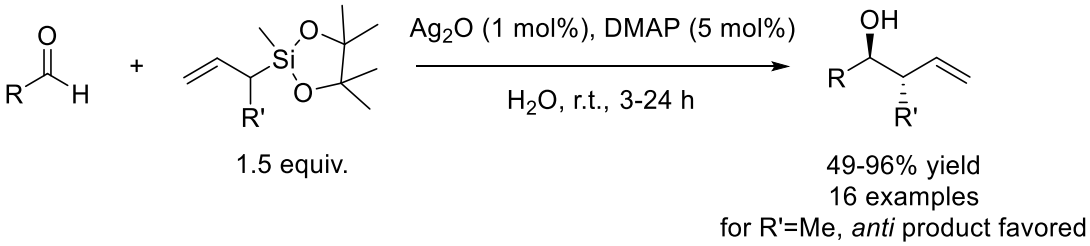

Scheme 199. Ag_2O-catalyzed allylsilanes coupling to aldehydes.

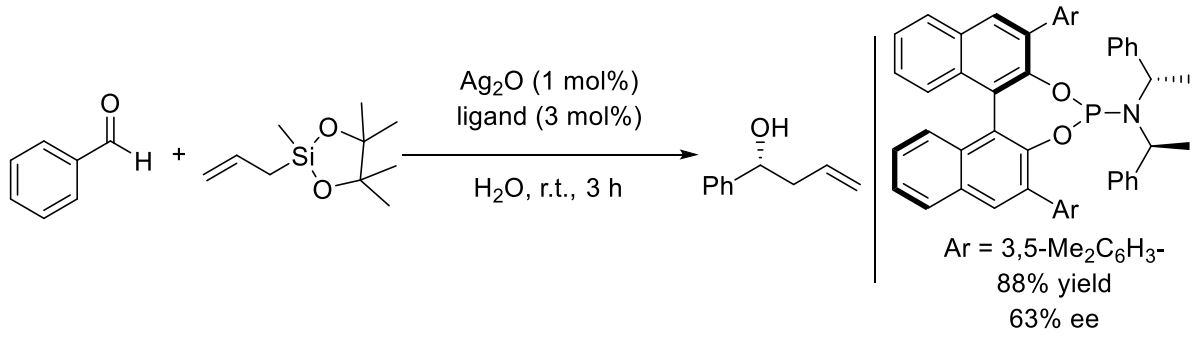

Scheme 200. Asymmetric coupling of allylsilanes coupling to benzaldehyde.

2.8.3 Silver as a Lewis acid

Safari *et al.* used Ag supported on multi-walled nanotubes (Ag@CNT) as a catalyst to condense anthranilamides and aldehydes into 2-aryl-2,3-dihydroquinazolin-4(1H)-ones, under sonication (Scheme 201).[301]

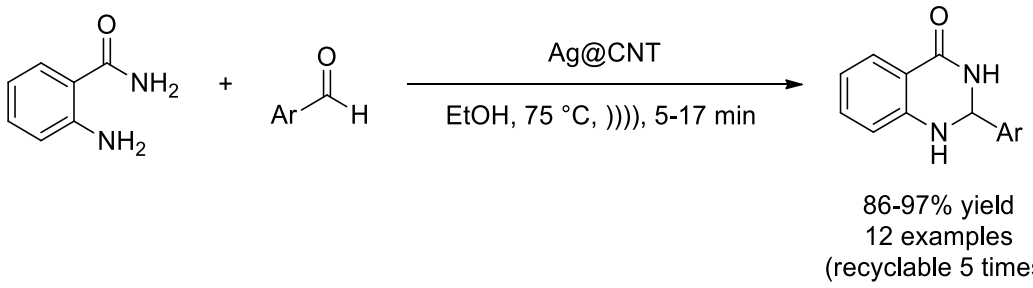

Scheme 201. Ag@CNT-catalyzed condensation of anthranilamides and benzaldehydes under sonication.

Mandi *et al.* showed that Ag supported on mesoporous polyaniline (Ag@mPANI) could catalyze the acylation of a range of anilines and benzyl alcohols (Scheme 202).[302]

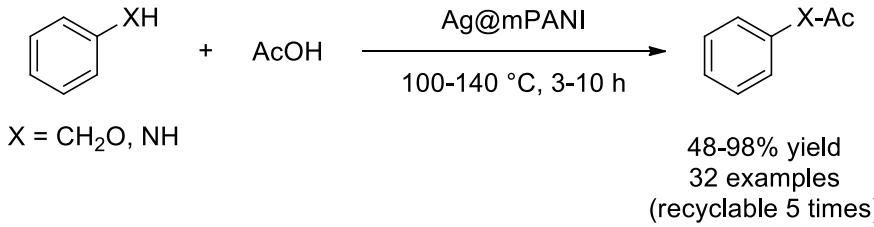

Scheme 202. Ag@mPANI-catalyzed acylation of anilines and benzyl alcohols.

2.9 Conclusion

As shown throughout this chapter, Ag NPs possess appealing features such as applicability to large variety of reactions, with a high level of chemoselectivity. A number of systems are also featured as recyclable which is an important attribute in nanocatalysis. Above we tried to indicate for each example, when possible, how many times could the catalyst be recycled, as well as emphasizing the growing importance of translations to flow-systems. As for selectivity, Ag NPs have been shown to selectively reduce C=O bonds over C=C bonds,

epoxidize ethylene without combusting it, oxidize primary alcohols into aldehydes without forming an acid, or semihydrogenate alkynes into alkenes. In the vast majority of the examples covered, these feats were made possible without the use of expensive ligands or wasteful additives, but rather by using cheap metal oxide supports (SiO_2, Al_2O_3, CeO_2…), or by exploiting the Ag-O interaction.

Some key challenges should be addressed in the future, especially related to silver criticality. Silver is not among the scarcest metals, but its versatile use, including towards electronics, medical, jewelry and processes, is imposing a serious burden on supplies.[12, 303] Depending on the sources, silver is quoted as "not critical",[304] "insecure"[305] and "medium risk",[306] illustrating the difficulty to determine precise criticality in an absolute fashion.[303] This uncertainty calls for Ag NP recyclability in catalytic applications. Nanocatalyst enantioselectivity is another major issue to tackle, in the context where silver shows promising selectivity for perfume/pharma relevant molecules. More research is definitely needed, considering the paucity of reports involving Ag NPs with high enantiomeric excesses.[307]

2.10 References

1. White, R. J.; Luque, R.; Budarin, V. L.; Clark, J. H.; Macquarrie, D. J., Supported metal nanoparticles on porous materials. Methods and applications. *Chem. Soc. Rev.* **2009,** *38* (2), 481-494.
2. Xia, Y.; Xiong, Y.; Lim, B.; Skrabalak, S. E., Shape-Controlled Synthesis of Metal Nanocrystals: Simple Chemistry Meets Complex Physics? *Angew. Chem. Int. Ed.* **2009,** *48* (1), 60-103.
3. Divins, N. J.; Angurell, I.; Escudero, C.; Pérez-Dieste, V.; Llorca, J., Influence of the support on surface rearrangements of bimetallic nanoparticles in real catalysts. *Science* **2014,** *346* (6209), 620-623.
4. Astruc, D., Transition-metal Nanoparticles in Catalysis: From Historical Background to the State-of-the Art. In *Nanoparticles and Catalysis*, Wiley-VCH Verlag GmbH & Co. KGaA: 2008; pp 1-48.
5. Wachs, I. E.; Madix, R. J., The oxidation of methanol on a silver (110) catalyst. *Surf. Sci.* **1978,** *76* (2), 531-558.
6. Millar, G. J.; Collins, M., Industrial Production of Formaldehyde Using Polycrystalline Silver Catalyst. *Ind. Eng. Chem. Res.* **2017,** *56* (33), 9247-9265.
7. Lefort, E. Process for the production of ethylene oxide. April 23 1935, 1935.
8. Wen, C.; Yin, A.; Dai, W.-L., Recent advances in silver-based heterogeneous catalysts for green chemistry processes. *Appl. Catal., B* **2014,** *160-161*, 730-741.
9. Dong, X.-Y.; Gao, Z.-W.; Yang, K.-F.; Zhang, W.-Q.; Xu, L.-W., Nanosilver as a new generation of silver catalysts in organic transformations for efficient synthesis of fine chemicals. *Catal. Sci. Technol.* **2015,** *5* (5), 2554-2574.
10. Manohar, A. B.; Bhalchandra, M. B., Silver Nanoparticles: Synthesis, Characterization and their Application as a Sustainable Catalyst for Organic Transformations. *Current Organic Chemistry* **2015,** *19* (8), 708-727.

11. Shimizu, K.-i.; Satsuma, A., Silver cluster catalysts for green organic synthesis. *Journal of the Japan Petroleum Institute* **2011,** *54* (6), 347-360.
12. BullionVault What is silver used for in industry? https://www.bullionvault.com/silver-guide/silver-industrial-demand (accessed 2018).
13. Bloch, H. P.; Godse, A., *Compressors and modern process applications*. John Wiley & Sons: 2006.
14. Eley, D. D.; Pines, H.; Weisz, P. B., Catalytic oxidation of olefins. In *Advances in catalysis and related subjects*, Inc., N. Y. A. P., Ed. 1967; Vol. 17, pp 156-157.
15. Kobe, J. M.; Evans, W. E.; June, R. L.; Lemanski, M. F., Epoxidation – Industrial. In *Encyclopedia of Catalysis*, John Wiley & Sons, Inc.: 2002.
16. Chauvel, A.; Lefebvre, G., *Petrochemical Processes*. Editions OPHRYS: 1989.
17. Tsuji, J.; Yamamoto, J.; Ishino, M.; OKU, N. *Development of new propylene oxide process*; Sumitomo Chemical Co., Ltd.: 2006.
18. Ramirez, A.; Hueso, J. L.; Suarez, H.; Mallada, R.; Ibarra, A.; Irusta, S.; Santamaria, J., A Nanoarchitecture Based on Silver and Copper Oxide with an Exceptional Response in the Chlorine-Promoted Epoxidation of Ethylene. *Angew. Chem. Int. Ed.* **2016,** *55* (37), 11158-11161.
19. Kestenbaum, H.; Lange de Oliveira, A.; Schmidt, W.; Schüth, F.; Ehrfeld, W.; Gebauer, K.; Löwe, H.; Richter, T.; Lebiedz, D.; Untiedt, I.; Züchner, H., Silver-Catalyzed Oxidation of Ethylene to Ethylene Oxide in a Microreaction System. *Ind. Eng. Chem. Res.* **2002,** *41* (4), 710-719.
20. Van Santen, R.; Kuipers, H., The mechanism of ethylene epoxidation. *Adv. Catal.* **1987,** *35*, 265-321.
21. Beckham, L. J. Ethylene oxide production. November 5, 1951, 1956.
22. Nielsen, R. P.; Rochelle, J. H. L. Ethylene oxide process. 1977.
23. Jun, Y.; Jingfa, D.; Xiaohong, Y.; Shi, Z., Rhenium as a promoter for ethylene epoxidation. *Appl. Catal., A* **1992,** *92* (2), 73-80.
24. *Ethylene Oxide (EO) - A Global Strategic Business Report*; Global Industry Analysts, Inc.: 2011.
25. Takada, H., *Shokubai* **1996,** *38* (213).
26. Sun, D.; Wang, H.; Zhang, G.; Huang, J.; Li, Q., Preparation of Ag/[small alpha]-Al2O3 for ethylene epoxidation through thermal decomposition assisted by extract of Cinnamomum camphora. *RSC Adv.* **2013,** *3* (43), 20732-20737.
27. Bukhtiyarov, V. I.; Knop-Gericke, A., Chapter 9 Ethylene Epoxidation over Silver Catalysts. In *Nanostructured Catalysts: Selective Oxidations*, The Royal Society of Chemistry: 2011; pp 214-247.
28. Serafin, J. G.; Liu, A. C.; Seyedmonir, S. R., Surface science and the silver-catalyzed epoxidation of ethylene: an industrial perspective. *J. Mol. Catal. A: Chem.* **1998,** *131* (1), 157-168.
29. Jones, T. E.; Rocha, T. C. R.; Knop-Gericke, A.; Stampfl, C.; Schlögl, R.; Piccinin, S., Insights into the Electronic Structure of the Oxygen Species Active in Alkene Epoxidation on Silver. *ACS Catal.* **2015,** *5* (10), 5846-5850.
30. Bukhtiyarov, V. I.; Prosvirin, I. P.; Kvon, R. I., Study of reactivity of oxygen states adsorbed at a silver surface towards C2H4 by XPS, TPD and TPR. *Surf. Sci.* **1994,** *320* (1), L47-L50.
31. Jones, T. E.; Wyrwich, R.; Böcklein, S.; Carbonio, E. A.; Greiner, M. T.; Klyushin, A. Y.; Moritz, W.; Locatelli, A.; Menteş, T. O.; Niño, M. A.; Knop-Gericke, A.; Schlögl, R.; Günther, S.; Wintterlin, J.; Piccinin, S., The Selective Species in Ethylene Epoxidation on Silver. *ACS Catal.* **2018,** *8* (5), 3844-3852.

32. Medlin, J. W.; Barteau, M. A.; Vohs, J. M., Oxametallacycle formation via ring-opening of 1-epoxy-3-butene on Ag(110): a combined experimental/theoretical approach. *J. Mol. Catal. A: Chem.* **2000,** *163* (1), 129-145.
33. Linic, S.; Barteau, M. A., Formation of a Stable Surface Oxametallacycle that Produces Ethylene Oxide. *J. Am. Chem. Soc.* **2002,** *124* (2), 310-317.
34. Linic, S.; Barteau, M. A., Construction of a reaction coordinate and a microkinetic model for ethylene epoxidation on silver from DFT calculations and surface science experiments. *J. Catal.* **2003,** *214* (2), 200-212.
35. Christopher, P.; Linic, S., Engineering Selectivity in Heterogeneous Catalysis: Ag Nanowires as Selective Ethylene Epoxidation Catalysts. *J. Am. Chem. Soc.* **2008,** *130* (34), 11264-11265.
36. Zhu, L.; Zhang, W.; Zhu, J.; Cheng, D., Mechanistic insight into the facet-dependent selectivity of ethylene epoxidation on Ag nanocatalysts. *Appl. Catal., A* **2017,** *538* (Supplement C), 27-36.
37. Christopher, P.; Linic, S., Shape- and Size-Specific Chemistry of Ag Nanostructures in Catalytic Ethylene Epoxidation. *ChemCatChem* **2010,** *2* (1), 78-83.
38. Torres, D.; Illas, F.; Lambert, R. M., Towards an understanding of promoter action in heterogeneously catalyzed ethene epoxidation: Why chlorine is the best halogen. *J. Catal.* **2008,** *260* (2), 380-383.
39. Sangaru, S. S.; Zhu, H.; Rosenfeld, D. C.; Samal, A. K.; Anjum, D.; Basset, J.-M., Surface Composition of Silver Nanocubes and Their Influence on Morphological Stabilization and Catalytic Performance in Ethylene Epoxidation. *ACS Appl. Mater. Interfaces* **2015,** *7* (51), 28576-28584.
40. Minahan, D. M.; Hoflund, G. B.; Epling, W. S.; Schoenfeld, D. W., Study of Cs-Promoted, α-Alumina-Supported Silver, Ethylene Epoxidation Catalysts: III. Characterization of Cs-Promoted and Nonpromoted Catalysts. *J. Catal.* **1997,** *168* (2), 393-399.
41. Linic, S.; Barteau, M. A., On the Mechanism of Cs Promotion in Ethylene Epoxidation on Ag. *J. Am. Chem. Soc.* **2004,** *126* (26), 8086-8087.
42. Mavrikakis, M.; Doren, D. J.; Barteau, M. A., Density Functional Theory Calculations for Simple Oxametallacycles: Trends across the Periodic Table. *J. Phys. Chem. B* **1998,** *102* (2), 394-399.
43. Ozbek, M. O.; Onal, I.; van Santen, R. A., Why silver is the unique catalyst for ethylene epoxidation. *J. Catal.* **2011,** *284* (2), 230-235.
44. Özbek, M. O.; Önal, I.; van Santen, R. A., Chlorine and Caesium Promotion of Silver Ethylene Epoxidation Catalysts. *ChemCatChem* **2013,** *5* (2), 443-451.
45. Trent, D. L., Propylene Oxide. In *Kirk-Othmer Encyclopedia of Chemical Technology*, John Wiley & Sons, Inc.: 2000.
46. Nijhuis, T. A.; Makkee, M.; Moulijn, J. A.; Weckhuysen, B. M., The Production of Propene Oxide: Catalytic Processes and Recent Developments. *Ind. Eng. Chem. Res.* **2006,** *45* (10), 3447-3459.
47. Blanco-Brieva, G.; Capel-Sanchez, M. C.; de Frutos, M. P.; Padilla-Polo, A.; Campos-Martin, J. M.; Fierro, J. L. G., New Two-Step Process for Propene Oxide Production (HPPO) Based on the Direct Synthesis of Hydrogen Peroxide. *Ind. Eng. Chem. Res.* **2008,** *47* (21), 8011-8015.
48. Hayashi, T.; Tanaka, K.; Haruta, M., Selective Vapor-Phase Epoxidation of Propylene over Au/TiO2Catalysts in the Presence of Oxygen and Hydrogen. *J. Catal.* **1998,** *178* (2), 566-575.
49. Torres, D.; Lopez, N.; Illas, F.; Lambert, R. M., Low-Basicity Oxygen Atoms: A Key in the Search for Propylene Epoxidation Catalysts. *Angew. Chem. Int. Ed.* **2007,** *46* (12), 2055-2058.

50. Cowell, J. J.; Santra, A. K.; Lindsay, R.; Lambert, R. M.; Baraldi, A.; Goldoni, A., Bonding and reactivity of styrene on Cu(110): heterogeneous alkene epoxidation without the use of silver. *Surf. Sci.* **1999,** *437* (1), 1-8.
51. Cowell, J. J.; Santra, A. K.; Lambert, R. M., Ultraselective Epoxidation of Butadiene on Cu{111} and the Effects of Cs Promotion. *J. Am. Chem. Soc.* **2000,** *122* (10), 2381-2382.
52. Zheng, X.; Zhang, Q.; Guo, Y.; Zhan, W.; Guo, Y.; Wang, Y.; Lu, G., Epoxidation of propylene by molecular oxygen over supported Ag–Cu bimetallic catalysts with low Ag loading. *J. Mol. Catal. A: Chem.* **2012,** *357* (Supplement C), 106-111.
53. Dai, Y.; Chen, Z.; Guo, Y.; Lu, G.; Zhao, Y.; Wang, H.; Hu, P., Significant enhancement of the selectivity of propylene epoxidation for propylene oxide: a molecular oxygen mechanism. *Phys. Chem. Chem. Phys* **2017,** *19* (36), 25129-25139.
54. Roldan, A.; Torres, D.; Ricart, J. M.; Illas, F., On the effectiveness of partial oxidation of propylene by gold: A density functional theory study. *J. Mol. Catal. A: Chem.* **2009,** *306* (1), 6-10.
55. Lei, Y.; Mehmood, F.; Lee, S.; Greeley, J.; Lee, B.; Seifert, S.; Winans, R. E.; Elam, J. W.; Meyer, R. J.; Redfern, P. C.; Teschner, D.; Schlögl, R.; Pellin, M. J.; Curtiss, L. A.; Vajda, S., Increased Silver Activity for Direct Propylene Epoxidation via Subnanometer Size Effects. *Science* **2010,** *328* (5975), 224-228.
56. Cheng, L.; Yin, C.; Mehmood, F.; Liu, B.; Greeley, J.; Lee, S.; Lee, B.; Seifert, S.; Winans, R. E.; Teschner, D.; Schlögl, R.; Vajda, S.; Curtiss, L. A., Reaction Mechanism for Direct Propylene Epoxidation by Alumina-Supported Silver Aggregates: The Role of the Particle/Support Interface. *ACS Catal.* **2014,** *4* (1), 32-39.
57. Polynskaya, Y. G.; Pichugina, D. A.; Beletskaya, A. V.; Kuz'menko, N. E., Quantum chemical simulation of propylene oxidation on Ag20. *Kinet. Catal.* **2016,** *57* (2), 184-190.
58. Pulido, A.; Concepción, P.; Boronat, M.; Corma, A., Aerobic epoxidation of propene over silver (111) and (100) facet catalysts. *J. Catal.* **2012,** *292* (Supplement C), 138-147.
59. Lu, G.; Zuo, X., Epoxidation of propylene by air over modified silver catalyst. *Catal. Lett.* **1999,** *58* (1), 67-70.
60. Zhang, Q.; Chai, G.; Guo, Y.; Zhan, W.; Guo, Y.; Wang, L.; Wang, Y.; Lu, G., Gas-phase epoxidation of propylene by molecular oxygen over Ag-CuCl2/BaCO3 catalyst with low CuCl2 doping: Catalytic performance, deactivation and regeneration. *J. Mol. Catal. A: Chem.* **2016,** *424* (Supplement C), 65-76.
61. Jin, G.; Lu, G.; Guo, Y.; Guo, Y.; Wang, J.; Kong, W.; Liu, X., Effect of preparation condition on performance of Ag–MoO3/ZrO2 catalyst for direct epoxidation of propylene by molecular oxygen. *J. Mol. Catal. A: Chem.* **2005,** *232* (1), 165-172.
62. Yao, W.; Guo, Y. L.; Liu, X. H.; Guo, Y.; Wang, Y. Q.; Wang, Y. S.; Zhang, Z. G.; Lu, G. Z., Epoxidation of Propylene by Molecular Oxygen Over the Ag–Y2O3–K2O/α-Al2O3 Catalyst. *Catal. Lett.* **2007,** *119* (1), 185-190.
63. Lu, J.; Bravo-Suárez, J. J.; Haruta, M.; Oyama, S. T., Direct propylene epoxidation over modified Ag/CaCO3 catalysts. *Appl. Catal., A* **2006,** *302* (2), 283-295.
64. Lu, J.; Bravo-Suárez, J. J.; Takahashi, A.; Haruta, M.; Oyama, S. T., In situ UV–vis studies of the effect of particle size on the epoxidation of ethylene and propylene on supported silver catalysts with molecular oxygen. *J. Catal.* **2005,** *232* (1), 85-95.
65. Lu, J.; Luo, M.; Lei, H.; Li, C., Epoxidation of propylene on NaCl-modified silver catalysts with air as the oxidant. *Appl. Catal., A* **2002,** *237* (1), 11-19.
66. Farinas, E. T.; Alcalde, M.; Arnold, F., Alkene epoxidation catalyzed by cytochrome P450 BM-3 139-3. *Tetrahedron* **2004,** *60* (3), 525-528.
67. Otto, K.; Hofstetter, K.; Röthlisberger, M.; Witholt, B.; Schmid, A., Biochemical Characterization of StyAB from Pseudomonas sp. Strain VLB120 as a Two-Component Flavin-Diffusible Monooxygenase. *J. Bacteriol.* **2004,** *186* (16), 5292-5302.

68. Warhurst, A. M.; Fewson, C. A., Microbial metabolism and biotransformations of styrene. *J. Appl. Bacteriol.* **1994,** *77* (6), 597-606.
69. Guan, Y.; Zhao, N.; Tang, B.; Jia, Q.; Xu, X.; Liu, H.; Boughton, R. I., A stable bimetallic Au-Ag/TiO2 nanopaper for aerobic oxidation of benzyl alcohol. *Chem. Commun.* **2013,** *49* (98), 11524-11526.
70. Das, S.; Goswami, A.; Hesari, M.; Al-Sharab, J. F.; Mikmeková, E.; Maran, F.; Asefa, T., Reductive Deprotection of Monolayer Protected Nanoclusters: An Efficient Route to Supported Ultrasmall Au Nanocatalysts for Selective Oxidation. *Small* **2014,** *10* (8), 1473-1478.
71. Rezaeifard, A.; Haddad, R.; Jafarpour, M.; Hakimi, M., {Mo132} Nanoball as an Efficient and Cost-Effective Catalyst for Sustainable Oxidation of Sulfides and Olefins with Hydrogen Peroxide. *ACS Sustainable Chem. Eng.* **2014,** *2* (4), 942-950.
72. Rak, M. J.; Lerro, M.; Moores, A., Hollow iron oxide nanoshells are active and selective catalysts for the partial oxidation of styrene with molecular oxygen. *Chem. Commun.* **2014,** *50* (83), 12482-12485.
73. Liu, X.; Klust, A.; Madix, R. J.; Friend, C. M., Structure Sensitivity in the Partial Oxidation of Styrene, Styrene Oxide, and Phenylacetaldehyde on Silver Single Crystals. *J Phys. Chem. C* **2007,** *111* (9), 3675-3679.
74. Dhakshinamoorthy, A.; Primo, A.; Concepcion, P.; Alvaro, M.; Garcia, H., Doped Graphene as a Metal-Free Carbocatalyst for the Selective Aerobic Oxidation of Benzylic Hydrocarbons, Cyclooctane and Styrene. *Chem. Eur. J.* **2013,** *19* (23), 7547-7554.
75. Sharma, S.; Sinha, S.; Chand, S., Polymer Anchored Catalysts for Oxidation of Styrene Using TBHP and Molecular Oxygen. *Ind. Eng. Chem. Res.* **2012,** *51* (26), 8806-8814.
76. Xu, R.; Wang, D.; Zhang, J.; Li, Y., Shape-Dependent Catalytic Activity of Silver Nanoparticles for the Oxidation of Styrene. *Chem. Asian J.* **2006,** *1* (6), 888-893.
77. Chen, Z.; Luck, R. L., Oxidation of olefins using atmospheric oxygen atoms initiated by tert-butylhydroperoxide or hydrogen peroxide with silver nanoparticles deposited on MCM-41 as catalysts. *Green Chem.* **2016,** *18* (11), 3354-3359.
78. Zhang, D.-H.; Li, G.-D.; Li, J.-X.; Chen, J.-S., One-pot synthesis of Ag-Fe3O4 nanocomposite: a magnetically recyclable and efficient catalyst for epoxidation of styrene. *Chem. Commun.* **2008,** (29), 3414-3416.
79. Zhang, D.-H.; Li, H.-B.; Li, G.-D.; Chen, J.-S., Magnetically recyclable Ag-ferrite catalysts: general synthesis and support effects in the epoxidation of styrene. *Dalton Trans.* **2009,** (47), 10527-10533.
80. Liu, H.; Bai, J.; Wang, S.; Li, C.; Guo, L.; Liang, H.; Xu, T.; Sun, W.; Li, H., The preparation of silver nanoparticles/carbon nanofibers as catalyst in the styrene epoxidation. *Colloids Surf., A* **2014,** *448* (Supplement C), 154-159.
81. Liu, H.; Bai, J.; Li, C.; Xu, W.; Sun, W.; Xu, T.; Huang, Y.; Li, H., An effective approach to preparing MgO-Ag NPs-CNFs and Al2O3-Ag NPs-CNFs for styrene epoxidation action. *RSC Adv.* **2014,** *4* (7), 3195-3200.
82. Wang, X.; Liang, Z.; Zhang, F.; Yang, L.; Xu, S., Enhanced catalytic performances of Ag nanoparticles supported on layered double hydroxide for styrene epoxidation. *J. Mater. Sci.* **2013,** *48* (17), 5899-5903.
83. Hu, X.; Bai, J.; Hong, H.; Li, C., Supercritical carbon dioxide anchored highly dispersed silver nanoparticles on 4A-zeolite and selective oxidation of styrene performance. *CrystEngComm* **2016,** *18* (14), 2469-2476.
84. Hu, X.; Bai, J.; Hong, H.; Li, C., Synthesis of Ag-loaded 4A-zeolite composite catalyst via supercritical CO2 fluid for styrene epoxidation. *Microporous Mesoporous Mater.* **2016,** *228* (Supplement C), 224-230.

85. Najafpour, M. M.; Amini, M.; Sedigh, D. J.; Rahimi, F.; Bagherzadeh, M., Activated layered manganese oxides with deposited nano-sized gold or silver as an efficient catalyst for epoxidation of olefins. *RSC Adv.* **2013,** *3* (46), 24069-24074.
86. Richardson, D. E.; Yao, H.; Frank, K. M.; Bennett, D. A., Equilibria, Kinetics, and Mechanism in the Bicarbonate Activation of Hydrogen Peroxide: Oxidation of Sulfides by Peroxymonocarbonate. *J. Am. Chem. Soc.* **2000,** *122* (8), 1729-1739.
87. Anandhakumar, S.; Sasidharan, M.; Tsao, C.-W.; Raichur, A. M., Tailor-Made Hollow Silver Nanoparticle Cages Assembled with Silver Nanoparticles: An Efficient Catalyst for Epoxidation. *ACS Appl. Mater. Interfaces* **2014,** *6* (5), 3275-3281.
88. Purcar, V.; Donescu, D.; Petcu, C.; Luque, R.; Macquarrie, D. J., Efficient preparation of silver nanoparticles supported on hybrid films and their activity in the oxidation of styrene under microwave irradiation. *Appl. Catal., A* **2009,** *363* (1), 122-128.
89. Acharyya, S. S.; Ghosh, S.; Sharma, S. K.; Bal, R., Cetyl alcohol mediated fabrication of forest of Ag/Mn3O4 nanowhiskers catalyst for the selective oxidation of styrene with molecular oxygen. *RSC Adv.* **2015,** *5* (109), 89879-89887.
90. Maayan, G.; Neumann, R., Direct aerobic epoxidation of alkenes catalyzed by metal nanoparticles stabilized by the H5PV2Mo10O40 polyoxometalate. *Chem. Commun.* **2005,** (36), 4595-4597.
91. Khenkin, A. M.; Neumann, R., Redirection of Oxidation Reactions by a Polyoxomolybdate: Oxydehydrogenation Instead of Oxygenation of Alkanes with tert-Butylhydroperoxide in Acetic Acid. *J. Am. Chem. Soc.* **2001,** *123* (26), 6437-6438.
92. Khenkin, A. M.; Weiner, L.; Wang, Y.; Neumann, R., Electron and Oxygen Transfer in Polyoxometalate, H5PV2Mo10O40, Catalyzed Oxidation of Aromatic and Alkyl Aromatic Compounds: Evidence for Aerobic Mars−van Krevelen-Type Reactions in the Liquid Homogeneous Phase. *J. Am. Chem. Soc.* **2001,** *123* (35), 8531-8542.
93. Finke, R. G.; Özkar, S., Molecular insights for how preferred oxoanions bind to and stabilize transition-metal nanoclusters: a tridentate, C3 symmetry, lattice size-matching binding model. *Coord. Chem. Rev.* **2004,** *248* (1), 135-146.
94. Izawa, Y.; Yokoyama, T., 1,4-Butanediol from 1,3-Butadiene. In *Liquid Phase Aerobic Oxidation Catalysis: Industrial Applications and Academic Perspectives*, Wiley-VCH Verlag GmbH & Co. KGaA: 2016; pp 159-171.
95. Fujimaki, T., Processability and properties of aliphatic polyesters, 'BIONOLLE', synthesized by polycondensation reaction. *Polym. Degrad. Stab.* **1998,** *59* (1), 209-214.
96. Wachs, I. E., Extending surface science studies to industrial reaction conditions: mechanism and kinetics of methanol oxidation over silver surfaces. *Surf. Sci.* **2003,** *544* (1), 1-4.
97. Davis, S. E.; Ide, M. S.; Davis, R. J., Selective oxidation of alcohols and aldehydes over supported metal nanoparticles. *Green Chem.* **2013,** *15* (1), 17-45.
98. Matsumoto, T.; Ueno, M.; Wang, N.; Kobayashi, S., Recent Advances in Immobilized Metal Catalysts for Environmentally Benign Oxidation of Alcohols. *Chem. Asian J.* **2008,** *3* (2), 196-214.
99. Hammer, B.; Norskov, J. K., Why gold is the noblest of all the metals. *Nature* **1995,** *376*, 238.
100. Beier, M. J.; Hansen, T. W.; Grunwaldt, J.-D., Selective liquid-phase oxidation of alcohols catalyzed by a silver-based catalyst promoted by the presence of ceria. *J. Catal.* **2009,** *266* (2), 320-330.
101. He, J.; Li, H.; Lu, Y.-M.; Liu, Y.-X.; Wu, Z.-B.; Hu, D.-Y.; Yang, S., Cascade catalytic transfer hydrogenation–cyclization of ethyl levulinate to γ-valerolactone with Al–Zr mixed oxides. *Appl. Catal., A* **2016,** *510*, 11-19.

102. Yang, Z.; Li, J.; Yang, X.; Xie, X.; Wu, Y., Gas-phase oxidation of alcohols over silver: The extension of catalytic cycles of oxidation of alcohols in liquid-phase. *J. Mol. Catal. A: Chem.* **2005,** *241* (1), 15-22.
103. Sanderson, R. T., *Chemical periodicity*. University of Iowa: 1960.
104. Misono, M.; Ochiai, E. i.; Saito, Y.; Yoneda, Y., A new dual parameter scale for the strength of lewis acids and bases with the evaluation of their softness. *J. Inorg. Nucl. Chem.* **1967,** *29* (11), 2685-2691.
105. Zahed, B.; Hosseini-Monfared, H., A comparative study of silver-graphene oxide nanocomposites as a recyclable catalyst for the aerobic oxidation of benzyl alcohol: Support effect. *Appl. Surf. Sci.* **2015,** *328*, 536-547.
106. Iwahama, T.; Yoshino, Y.; Keitoku, T.; Sakaguchi, S.; Ishii, Y., Efficient Oxidation of Alcohols to Carbonyl Compounds with Molecular Oxygen Catalyzed by N-Hydroxyphthalimide Combined with a Co Species. *J. Org. Chem.* **2000,** *65* (20), 6502-6507.
107. Kundakovic, L.; Flytzani-Stephanopoulos, M., Cu- and Ag-Modified Cerium Oxide Catalysts for Methane Oxidation. *J. Catal.* **1998,** *179* (1), 203-221.
108. Rana, P. H.; Parikh, P. A., Bioethanol selective oxidation to acetaldehyde over Ag-CeO2: role of metal-support interactions. *New J. Chem.* **2017,** *41* (7), 2636-2641.
109. Kang, Y.; Sun, M.; Li, A., Studies of the Catalytic Oxidation of CO Over Ag/CeO2 Catalyst. *Catal. Lett.* **2012,** *142* (12), 1498-1504.
110. Ma, L.; Wang, D.; Li, J.; Bai, B.; Fu, L.; Li, Y., Ag/CeO2 nanospheres: Efficient catalysts for formaldehyde oxidation. *Appl. Catal., B* **2014,** *148*, 36-43.
111. Erasmus, E.; Thüne, P. C.; Verhoeven, M. W. G. M.; Niemantsverdriet, J. W.; Swarts, J. C., A new approach to silver-catalysed aerobic oxidation of octadecanol: Probing catalysts utilising a flat, two-dimensional silicon-based model support system. *Catal. Commun.* **2012,** *27*, 193-199.
112. Li, Z.; Xu, J.; Gu, X.; Wang, K.; Wang, W.; Zhang, X.; Zhang, Z.; Ding, Y., Selective Gas-Phase Oxidation of Alcohols over Nanoporous Silver. *ChemCatChem* **2013,** *5* (7), 1705-1708.
113. Yadav, G. D.; Mewada, R. K., Selectivity engineering in the synthesis of value added chemicals: Oxidation of 1-octanol to 1-octanal over nano-fibrous Ag–OMS-2 catalysts. *Chem. Eng. Res. Des.* **2012,** *90* (1), 86-97.
114. Dutov, V. V.; Mamontov, G. V.; Sobolev, V. I.; Vodyankina, O. V., Silica-supported silver-containing OMS-2 catalysts for ethanol oxidative dehydrogenation. *Catal. Today* **2016,** *278*, 164-173.
115. Shimizu, K.-i.; Sugino, K.; Sawabe, K.; Satsuma, A., Oxidant-Free Dehydrogenation of Alcohols Heterogeneously Catalyzed by Cooperation of Silver Clusters and Acid–Base Sites on Alumina. *Chem. Eur. J.* **2009,** *15* (10), 2341-2351.
116. Ghalehshahi, H. G.; Madsen, R., Silver-Catalyzed Dehydrogenative Synthesis of Carboxylic Acids from Primary Alcohols. *Chem. Eur. J.* **2017,** *23* (49), 11920-11926.
117. Mukherjee, A.; Nerush, A.; Leitus, G.; Shimon, L. J. W.; Ben David, Y.; Espinosa Jalapa, N. A.; Milstein, D., Manganese-Catalyzed Environmentally Benign Dehydrogenative Coupling of Alcohols and Amines to Form Aldimines and H2: A Catalytic and Mechanistic Study. *J. Am. Chem. Soc.* **2016,** *138* (13), 4298-4301.
118. Mitsudome, T.; Mikami, Y.; Funai, H.; Mizugaki, T.; Jitsukawa, K.; Kaneda, K., Oxidant-Free Alcohol Dehydrogenation Using a Reusable Hydrotalcite-Supported Silver Nanoparticle Catalyst. *Angew. Chem. Int. Ed.* **2008,** *47* (1), 138-141.
119. Bayat, A.; Shakourian-Fard, M.; Ehyaei, N.; Mahmoodi Hashemi, M., Silver nanoparticles supported on silica-coated ferrite as magnetic and reusable catalysts for oxidant-free alcohol dehydrogenation. *RSC Adv.* **2015,** *5* (29), 22503-22509.

120. Kurhe, D. K.; Fernandes, T. A.; Deore, T. S.; Jayaram, R. V., Oxidant free dehydrogenation of alcohols using chitosan/polyacrylamide entrapped Ag nanoparticles. *RSC Adv.* **2015,** *5* (58), 46443-46447.
121. Feng, Y.; Xue, W.; Yin, H.; Meng, M.; Wang, A.; Liu, S., Selective oxidation of 1,2-propanediol to lactic acid catalyzed by hydroxyapatite-supported Pd and Pd-Ag nanoparticles. *RSC Adv.* **2015,** *5* (129), 106918-106929.
122. Hirasawa, S.; Watanabe, H.; Kizuka, T.; Nakagawa, Y.; Tomishige, K., Performance, structure and mechanism of Pd–Ag alloy catalyst for selective oxidation of glycerol to dihydroxyacetone. *J. Catal.* **2013,** *300*, 205-216.
123. Yamamura, M.; Kaneda, K.; Imanaka, T., Preparation of Pd-Ag thin films by the RF-sputtering method and its catalysis for oxidative dehydrogenation of allylic alcohols. *Catal. Lett.* **1989,** *3* (3), 203-208.
124. Chaki, N. K.; Tsunoyama, H.; Negishi, Y.; Sakurai, H.; Tsukuda, T., Effect of Ag-Doping on the Catalytic Activity of Polymer-Stabilized Au Clusters in Aerobic Oxidation of Alcohol. *J Phys. Chem. C* **2007,** *111* (13), 4885-4888.
125. Huang, X.; Wang, X.; Wang, X.; Wang, X.; Tan, M.; Ding, W.; Lu, X., P123-stabilized Au–Ag alloy nanoparticles for kinetics of aerobic oxidation of benzyl alcohol in aqueous solution. *J. Catal.* **2013,** *301*, 217-226.
126. Falsig, H.; Hvolbæk, B.; Kristensen, I. S.; Jiang, T.; Bligaard, T.; Christensen, C. H.; Nørskov, J. K., Trends in the Catalytic CO Oxidation Activity of Nanoparticles. *Angew. Chem. Int. Ed.* **2008,** *47* (26), 4835-4839.
127. Costa, J. C. S.; Corio, P.; Rossi, L. M., Catalytic oxidation of cinnamyl alcohol using Au-Ag nanotubes investigated by surface-enhanced Raman spectroscopy. *Nanoscale* **2015,** *7* (18), 8536-8543.
128. Wang, Y.; Zheng, J.-M.; Fan, K.; Dai, W.-L., One-pot solvent-free synthesis of sodium benzoate from the oxidation of benzyl alcohol over novel efficient AuAg/TiO2 catalysts. *Green Chem.* **2011,** *13* (7), 1644-1647.
129. Della Pina, C.; Falletta, E.; Rossi, M., Highly selective oxidation of benzyl alcohol to benzaldehyde catalyzed by bimetallic gold–copper catalyst. *J. Catal.* **2008,** *260* (2), 384-386.
130. Lawrence, S. A., *Amines: synthesis, properties and applications*. Cambridge University Press: 2004.
131. Pera-Titus, M.; Shi, F., Catalytic Amination of Biomass-Based Alcohols. *ChemSusChem* **2014,** *7* (3), 720-722.
132. Hartwig, J. F., Evolution of a Fourth Generation Catalyst for the Amination and Thioetherification of Aryl Halides. *Acc. Chem. Res.* **2008,** *41* (11), 1534-1544.
133. Hamid, M. H. S. A.; Slatford, P. A.; Williams, J. M. J., Borrowing Hydrogen in the Activation of Alcohols. *Adv. Synth. Catal.* **2007,** *349* (10), 1555-1575.
134. Guillena, G.; Ramón, D. J.; Yus, M., Alcohols as Electrophiles in C□C Bond-Forming Reactions: The Hydrogen Autotransfer Process. *Angew. Chem. Int. Ed.* **2007,** *46* (14), 2358-2364.
135. Watson, A. J. A.; Williams, J. M. J., The Give and Take of Alcohol Activation. *Science* **2010,** *329* (5992), 635-636.
136. Nixon, T. D.; Whittlesey, M. K.; Williams, J. M. J., Transition metal catalysed reactions of alcohols using borrowing hydrogen methodology. *Dalton Trans.* **2009,** (5), 753-762.
137. Cui, X.; Zhang, Y.; Shi, F.; Deng, Y., Organic Ligand-Free Alkylation of Amines, Carboxamides, Sulfonamides, and Ketones by Using Alcohols Catalyzed by Heterogeneous Ag/Mo Oxides. *Chem. Eur. J.* **2011,** *17* (3), 1021-1028.
138. Zhu, G.; Pang, K.; Parkin, G., New Modes for Coordination of Aromatic Heterocyclic Nitrogen Compounds to Molybdenum: Catalytic Hydrogenation of Quinoline, Isoquinoline, and Quinoxaline by Mo(PMe3)4H4. *J. Am. Chem. Soc.* **2008,** *130* (5), 1564-1565.

139. Shimizu, K.; Nishimura, M.; Satsuma, A., γ-Alumina-Supported Silver Cluster for N-Benzylation of Anilines with Alcohols. *ChemCatChem* **2009,** *1* (4), 497-503.
140. Shimizu, K.-i.; Shimura, K.; Nishimura, M.; Satsuma, A., Silver cluster-promoted heterogeneous copper catalyst for N-alkylation of amines with alcohols. *RSC Adv.* **2011,** *1* (7), 1310-1317.
141. Shimizu, K.-i.; Ohshima, K.; Satsuma, A., Direct Dehydrogenative Amide Synthesis from Alcohols and Amines Catalyzed by γ-Alumina Supported Silver Cluster. *Chem. Eur. J.* **2009,** *15* (39), 9977-9980.
142. Shimizu, K.; Shimura, K.; Nishimura, M.; Satsuma, A., Direct Synthesis of N-Substituted Anilines from Nitroaromatics and Alcohols under H2 by Alumina-Supported Silver Cluster Catalysts. *ChemCatChem* **2011,** *3* (11), 1755-1758.
143. Mandi, U.; Roy, A. S.; Kundu, S. K.; Roy, S.; Bhaumik, A.; Islam, S. M., Mesoporous polyacrylic acid supported silver nanoparticles as an efficient catalyst for reductive coupling of nitrobenzenes and alcohols using glycerol as hydrogen source. *J. Colloid Interf. Sci.* **2016,** *472* (Supplement C), 202-209.
144. Liu, H.; Chuah, G.-K.; Jaenicke, S., N-alkylation of amines with alcohols over alumina-entrapped Ag catalysts using the "borrowing hydrogen" methodology. *J. Catal.* **2012,** *292* (Supplement C), 130-137.
145. Paul, P.; Bhanja, P.; Salam, N.; Mandi, U.; Bhaumik, A.; Alam, S. M.; Islam, S. M., Silver nanoparticles supported over mesoporous alumina as an efficient nanocatalyst for N-alkylation of hetero (aromatic) amines and aromatic amines using alcohols as alkylating agent. *J. Colloid Interf. Sci.* **2017,** *493* (Supplement C), 206-217.
146. Mandi, U.; Kundu, S. K.; Salam, N.; Bhaumik, A.; Islam, S. M., Ag@polypyrrole: A highly efficient nanocatalyst for the N-alkylation of amines using alcohols. *J. Colloid Interf. Sci.* **2016,** *467* (Supplement C), 291-299.
147. Geukens, I.; Vermoortele, F.; Meledina, M.; Turner, S.; Van Tendeloo, G.; De Vos, D. E., Ag nanoparticles on mixed Al2O3–Ga2O3 supports as catalysts for the N-alkylation of amines with alcohols. *Appl. Catal., A* **2014,** *469* (Supplement C), 373-379.
148. Mielby, J.; Poreddy, R.; Engelbrekt, C.; Kegnæs, S., Highly selective formation of imines catalyzed by silver nanoparticles supported on alumina. *Chin. J. Catal.* **2014,** *35* (5), 670-676.
149. Poreddy, R.; Garcia-Suarez, E. J.; Riisager, A.; Kegnaes, S., Silver nanoparticles supported on alumina-a highly efficient and selective nanocatalyst for imine reduction. *Dalton Trans.* **2014,** *43* (11), 4255-4259.
150. Xu, X.; Wu, H.; Li, Z.; Sun, X.; Wang, Z., Iron oxide-silver magnetic nanoparticles as simple heterogeneous catalysts for the direct inter/intramolecular nucleophilic substitution of π-activated alcohols with electron-deficient amines. *Tetrahedron* **2015,** *71* (33), 5254-5259.
151. Brotzel, F.; Chu, Y. C.; Mayr, H., Nucleophilicities of Primary and Secondary Amines in Water. *J. Org. Chem.* **2007,** *72* (10), 3679-3688.
152. Imm, S.; Bähn, S.; Neubert, L.; Neumann, H.; Beller, M., An Efficient and General Synthesis of Primary Amines by Ruthenium-Catalyzed Amination of Secondary Alcohols with Ammonia. *Angew. Chem. Int. Ed.* **2010,** *49* (44), 8126-8129.
153. Shimizu, K.-i.; Sato, R.; Satsuma, A., Direct C□C Cross-Coupling of Secondary and Primary Alcohols Catalyzed by a γ-Alumina-Supported Silver Subnanocluster. *Angew. Chem. Int. Ed.* **2009,** *48* (22), 3982-3986.
154. Zhang, Q.; Cai, S.; Li, L.; Chen, Y.; Rong, H.; Niu, Z.; Liu, J.; He, W.; Li, Y., Direct Syntheses of Styryl Ethers from Benzyl Alcohols via Ag Nanoparticle-Catalyzed Tandem Aerobic Oxidation. *ACS Catal.* **2013,** *3* (7), 1681-1684.

155. Mäki-Arvela, P.; Hájek, J.; Salmi, T.; Murzin, D. Y., Chemoselective hydrogenation of carbonyl compounds over heterogeneous catalysts. *Appl. Catal., A* **2005,** *292* (Supplement C), 1-49.
156. Wei, H. Selective hydrogenation of acrolein over supported silver and silver alloy catalysts. Chicago, Illinois, 2013.
157. Medlin, J. W., Understanding and controlling reactivity of unsaturated oxygenates and polyols on metal catalysts. *ACS Catal.* **2011,** *1* (10), 1284-1297.
158. Gallezot, P.; Richard, D., Selective Hydrogenation of α,β-Unsaturated Aldehydes. *Catal. Rev. - Sci Eng.* **1998,** *40* (1-2), 81-126.
159. Rylander, P., Chapter 5 - Hydrogenation of Aldehydes. In *The Catalytic Hydrogenation in Organic Syntheses*, Academic Press: 1979; pp 72-81.
160. Yadav, G. D.; Mewada, R. K., Selective hydrogenation of acetophenone to 1-phenyl ethanol over nanofibrous Ag-OMS-2 catalysts. *Catal. Today* **2012,** *198* (1), 330-337.
161. Tsutomu, M.; Katsumi, S.; Shun-ichi, M.; Atsumu, O., Rhodium complex catalyzed hydrogenation of α,β-unsaturated aldehydes to unsaturated alcohols. *Bull. Chem. Soc. Jap.* **1977,** *50* (8), 2148-2152.
162. Yamada, H.; Goto, S., The Effect of Solvents Polarity on Selective Hydrogenation of Unsaturated Aldehyde in Gas-Liquid-Solid Three Phase Reactor. *J. Chem. Eng. Jpn.* **2003,** *36* (5), 586-589.
163. Nitta, Y.; Ueno, K.; Imanaka, T., Selective hydrogenation of αβ-unsaturated aldehydes on cobalt-silica catalysts obtained from cobalt chrysotile. *Appl. Catal.* **1989,** *56* (1), 9-22.
164. Blackmond, D. G.; Oukaci, R.; Blanc, B.; Gallezot, P., Geometric and electronic effects in the selective hydrogenation of α, β-unsaturated aldehydes over zeolite-supported metals. *J. Catal.* **1991,** *131* (2), 401-411.
165. Neri, G.; Mercadante, L.; Donato, A.; Visco, A. M.; Galvagno, S., Influence of Ru precursor, support and solvent in the hydrogenation of citral over ruthenium catalysts. *Catal. Lett.* **1994,** *29* (3), 379-386.
166. Vannice, M. A.; Sen, B., Metal-support effects on the intramolecular selectivity of crotonaldehyde hydrogenation over platinum. *J. Catal.* **1989,** *115* (1), 65-78.
167. Hutchings, G. J.; King, F.; Okoye, I. P.; Rochester, C. H., Influence of sulphur poisoning of copper/alumina catalyst on the selective hydrogenation of crotonaldehyde. *Appl. Catal., A* **1992,** *83* (2), L7-L13.
168. Claus, P., Selective hydrogenation of α,β-unsaturated aldehydes and other C=O and C=C bonds containing compounds. *Top. Catal.* **1998,** *5* (1), 51-62.
169. Andoni, A.; van Santen, R. A., Propenal hydrogenation on silver surface-a theoretical approach. *Chem. Eng. Trans.* **2013,** *34* (34), 19-24.
170. Lee, G.; Plummer, E. W., Covalent interaction of H with the d electrons at the (111) surface of Ag. *Phys. Rev. B* **2000,** *62* (3), 1651-1654.
171. Healey, F.; Carter, R. N.; Worthy, G.; Hodgson, A., Endothermic dissociative chemisorption of molecular D2 on Ag(111). *Chem. Phys. Lett.* **1995,** *243* (1), 133-139.
172. Mohammad, A. B.; Hwa Lim, K.; Yudanov, I. V.; Neyman, K. M.; Rosch, N., A computational study of H2 dissociation on silver surfaces: The effect of oxygen in the added row structure of Ag(110). *Phys. Chem. Chem. Phys* **2007,** *9* (10), 1247-1254.
173. Mohammad, A. B.; Yudanov, I. V.; Lim, K. H.; Neyman, K. M.; Rösch, N., Hydrogen Activation on Silver: A Computational Study on Surface and Subsurface Oxygen Species. *J Phys. Chem. C* **2008,** *112* (5), 1628-1635.
174. Lim, K. H.; Mohammad, A. B.; Yudanov, I. V.; Neyman, K. M.; Bron, M.; Claus, P.; Rösch, N., Mechanism of Selective Hydrogenation of α,β-Unsaturated Aldehydes on Silver Catalysts: A Density Functional Study. *J Phys. Chem. C* **2009,** *113* (30), 13231-13240.

175. Bron, M.; Teschner, D.; Knop-Gericke, A.; Jentoft, F. C.; Krohnert, J.; Hohmeyer, J.; Volckmar, C.; Steinhauer, B.; Schlogl, R.; Claus, P., Silver as acrolein hydrogenation catalyst: intricate effects of catalyst nature and reactant partial pressures. *Phys. Chem. Chem. Phys* **2007,** *9* (27), 3559-3569.
176. Hohmeyer, J.; Kondratenko, E. V.; Bron, M.; Kröhnert, J.; Jentoft, F. C.; Schlögl, R.; Claus, P., Activation of dihydrogen on supported and unsupported silver catalysts. *J. Catal.* **2010,** *269* (1), 5-14.
177. Brandt, K.; Chiu, M. E.; Watson, D. J.; Tikhov, M. S.; Lambert, R. M., Adsorption Geometry Determines Catalytic Selectivity in Highly Chemoselective Hydrogenation of Crotonaldehyde on Ag(111). *J Phys. Chem. C* **2012,** *116* (7), 4605-4611.
178. Stolle, A.; Gallert, T.; Schmöger, C.; Ondruschka, B., Hydrogenation of citral: a widespread model reaction for selective reduction of α,β-unsaturated aldehydes. *RSC Adv.* **2013,** *3* (7), 2112-2153.
179. Mertens, P. G. N.; Cuypers, F.; Vandezande, P.; Ye, X.; Verpoort, F.; Vankelecom, I. F. J.; De Vos, D. E., Ag0 and Co0 nanocolloids as recyclable quasihomogeneous metal catalysts for the hydrogenation of α,β-unsaturated aldehydes to allylic alcohol fragrances. *Appl. Catal., A* **2007,** *325* (1), 130-139.
180. Bron, M.; Teschner, D.; Wild, U.; Steinhauer, B.; Knop-Gericke, A.; Volckmar, C.; Wootsch, A.; Schlögl, R.; Claus, P., Oxygen-induced activation of silica supported silver in acrolein hydrogenation. *Appl. Catal., A* **2008,** *341* (1), 127-132.
181. Steffan, M.; Jakob, A.; Claus, P.; Lang, H., Silica supported silver nanoparticles from a silver(I) carboxylate: Highly active catalyst for regioselective hydrogenation. *Catal. Commun.* **2009,** *10* (5), 437-441.
182. Tian, L.; Yang, Q.; Jiang, Z.; Zhu, Y.; Pei, Y.; Qiao, M.; Fan, K., Highly chemoselective hydrogenation of crotonaldehyde over Ag-In/SBA-15 fabricated by a modified "two solvents" strategy. *Chem. Commun.* **2011,** *47* (21), 6168-6170.
183. Yang, X.; Wang, A.; Wang, X.; Zhang, T.; Han, K.; Li, J., Combined Experimental and Theoretical Investigation on the Selectivities of Ag, Au, and Pt Catalysts for Hydrogenation of Crotonaldehyde. *J Phys. Chem. C* **2009,** *113* (49), 20918-20926.
184. Bron, M.; Teschner, D.; Knop-Gericke, A.; Steinhauer, B.; Scheybal, A.; Hävecker, M.; Wang, D.; Födisch, R.; Hönicke, D.; Wootsch, A.; Schlögl, R.; Claus, P., Bridging the pressure and materials gap: in-depth characterisation and reaction studies of silver-catalysed acrolein hydrogenation. *J. Catal.* **2005,** *234* (1), 37-47.
185. Mitsudome, T.; Matoba, M.; Mizugaki, T.; Jitsukawa, K.; Kaneda, K., Core–Shell AgNP@CeO2 Nanocomposite Catalyst for Highly Chemoselective Reductions of Unsaturated Aldehydes. *Chem. Eur. J.* **2013,** *19* (17), 5255-5258.
186. Kaushik, M.; Li, A. Y.; Hudson, R.; Masnadi, M.; Li, C.-J.; Moores, A., Reversing aggregation: direct synthesis of nanocatalysts from bulk metal. Cellulose nanocrystals as active support to access efficient hydrogenation silver nanocatalysts. *Green Chem.* **2016,** *18* (1), 129-133.
187. Li, A. Y.; Kaushik, M.; Li, C.-J.; Moores, A., Microwave-Assisted Synthesis of Magnetic Carboxymethyl Cellulose-Embedded Ag–Fe3O4 Nanocatalysts for Selective Carbonyl Hydrogenation. *ACS Sustainable Chem. Eng.* **2016,** *4* (3), 965-973.
188. Calver, C. F.; Dash, P.; Scott, R. W. J., Selective Hydrogenations with Ag-Pd Catalysts Prepared by Galvanic Exchange Reactions. *ChemCatChem* **2011,** *3* (4), 695-697.
189. Moreno, M.; Kissell, L. N.; Jasinski, J. B.; Zamborini, F. P., Selectivity and Reactivity of Alkylamine- and Alkanethiolate-Stabilized Pd and PdAg Nanoparticles for Hydrogenation and Isomerization of Allyl Alcohol. *ACS Catal.* **2012,** *2* (12), 2602-2613.

190. Derrien, M. L., Chapter 18 selective hydrogenation applied to the refining of petrochemical raw materials produced by steam cracking. In *Studies in Surface Science and Catalysis*, Cerveny, L., Ed. Elsevier: 1986; Vol. 27, pp 613-666.
191. Mitsudome, T.; Urayama, T.; Yamazaki, K.; Maehara, Y.; Yamasaki, J.; Gohara, K.; Maeno, Z.; Mizugaki, T.; Jitsukawa, K.; Kaneda, K., Design of core-Pd/shell-Ag nanocomposite catalyst for selective semihydrogenation of alkynes. *ACS Catal.* **2015,** *6* (2), 666-670.
192. Vilé, G.; Pérez-Ramírez, J., Beyond the use of modifiers in selective alkyne hydrogenation: silver and gold nanocatalysts in flow mode for sustainable alkene production. *Nanoscale* **2014,** *6* (22), 13476-13482.
193. Wu, Z.; Liu, Q.; Yang, X.; Ye, X.; Duan, H.; Zhang, J.; Zhao, B.; Huang, Y., Knitting Aryl Network Polymers-Incorporated Ag Nanoparticles: A Mild and Efficient Catalyst for the Fixation of CO2 as Carboxylic Acid. *ACS Sustainable Chem. Eng.* **2017,** *5* (11), 9634-9639.
194. Oakton, E.; Vilé, G.; Levine, D. S.; Zocher, E.; Baudouin, D.; Pérez-Ramírez, J.; Copéret, C., Silver nanoparticles supported on passivated silica: preparation and catalytic performance in alkyne semi-hydrogenation. *Dalton Trans.* **2014,** *43* (40), 15138-15142.
195. Ruta, M.; Semagina, N.; Kiwi-Minsker, L., Monodispersed Pd nanoparticles for acetylene selective hydrogenation: particle size and support effects. *J Phys. Chem. C* **2008,** *112* (35), 13635-13641.
196. Silverman, R. B., Model studies for a molecular mechanism of action of oral anticoagulants. *J. Am. Chem. Soc.* **1981,** *103* (13), 3910-3915.
197. Corey, E. J.; Su, W. G., Total synthesis of a C15 ginkgolide, (.+-.)-bilobalide. *J. Am. Chem. Soc.* **1987,** *109* (24), 7534-7536.
198. Kraus, G. A.; Thomas, P. J., Synthesis of 7,7,8-trideuteriated trichothecenes. *J. Org. Chem.* **1988,** *53* (7), 1395-1397.
199. Florio, S.; Perna, F. M.; Salomone, A.; Vitale, P., 8.29 Reduction of Epoxides A2 - Knochel, Paul. In *Comprehensive Organic Synthesis II (Second Edition)*, Elsevier: Amsterdam, 2014; pp 1086-1122.
200. Zhu, Z.; Espenson, J. H., Methylrhenium trioxide as a catalyst for oxidations with molecular oxygen and for oxygen transfer. *J. Mol. Catal. A: Chem.* **1995,** *103* (2), 87-94.
201. Tamao, K.; Nakajo, E.; Ito, Y., Silafunctional compounds in organic synthesis. 36. A novel deoxygenation from .alpha.,.beta.-epoxy silanes to vinylsilanes by the copper-catalyzed Grignard reactions: a dramatic effect by alkoxy groups on silicon. *J. Org. Chem.* **1988,** *53* (2), 414-417.
202. Jung, K. Y.; Koreeda, M., Synthesis of 1,4-, 2,4-, and 3,4-dimethylphenanthrenes: a novel deoxygenation of arene 1,4-endoxides with trimethylsilyl iodide. *J. Org. Chem.* **1989,** *54* (24), 5667-5675.
203. Firouzabadi, H.; Iranpoor, N.; Jafarpour, M., Rapid, highly efficient and stereoselective deoxygenation of epoxides by ZrCl4/NaI. *Tetrahedron Lett.* **2005,** *46* (23), 4107-4110.
204. Isobe, H.; Branchaud, B. P., Epoxide deoxygenation mediated by Salen complexes. *Tetrahedron Lett.* **1999,** *40* (50), 8747-8749.
205. McMurry, J. E.; Silvestri, M. G.; Fleming, M. P.; Hoz, T.; Grayston, M. W., Some deoxygenation reactions with low-valent titanium (titanium trichloride/lithium tetrahydroaluminate). *J. Org. Chem.* **1978,** *43* (17), 3249-3255.
206. Itoh, T.; Nagano, T.; Sato, M.; Hirobe, M., Deoxygenation of oxiran compounds to olefins by [Fe4S4(SC6H5)4]2− in the presence of NaBH4. *Tetrahedron Lett.* **1989,** *30* (46), 6387-6388.
207. Sharpless, K. B.; Umbreit, M. A.; Nieh, M. T.; Flood, T. C., Lower valent tungsten halides. New class of reagents for deoxygenation of organic molecules. *J. Am. Chem. Soc.* **1972,** *94* (18), 6538-6540.

208. Ziegler, J. E.; Zdilla, M. J.; Evans, A. J.; Abu-Omar, M. M., H2-Driven Deoxygenation of Epoxides and Diols to Alkenes Catalyzed by Methyltrioxorhenium. *Inorg. Chem.* **2009,** *48* (21), 9998-10000.
209. Pathe, G. K.; Ahmed, N., An efficient protocol for the eliminative deoxygenation of aliphatic and aromatic epoxides to olefins with polyphosphoric acid as a promoter. *Tetrahedron Lett.* **2015,** *56* (45), 6202-6206.
210. Shiraishi, Y.; Hirakawa, H.; Togawa, Y.; Hirai, T., Noble-Metal-Free Deoxygenation of Epoxides: Titanium Dioxide as a Photocatalytically Regenerable Electron-Transfer Catalyst. *ACS Catal.* **2014,** *4* (6), 1642-1649.
211. Mitsudome, T.; Noujima, A.; Mikami, Y.; Mizugaki, T.; Jitsukawa, K.; Kaneda, K., Supported Gold and Silver Nanoparticles for Catalytic Deoxygenation of Epoxides into Alkenes. *Angew. Chem. Int. Ed.* **2010,** *49* (32), 5545-5548.
212. Mikami, Y.; Noujima, A.; Mitsudome, T.; Mizugaki, T.; Jitsukawa, K.; Kaneda, K., Selective deoxygenation of styrene oxides under a CO atmosphere using silver nanoparticle catalyst. *Tetrahedron Lett.* **2010,** *51* (41), 5466-5468.
213. Mitsudome, T.; Mikami, Y.; Matoba, M.; Mizugaki, T.; Jitsukawa, K.; Kaneda, K., Design of a Silver–Cerium Dioxide Core–Shell Nanocomposite Catalyst for Chemoselective Reduction Reactions. *Angew. Chem. Int. Ed.* **2012,** *51* (1), 136-139.
214. Saha, B.; De, S.; Dutta, S., Recent Advancements of Replacing Existing Aniline Production Process With Environmentally Friendly One-Pot Process: An Overview. *Crit. Rev. Environ. Sci. Technol.* **2013,** *43* (1), 84-120.
215. Herves, P.; Perez-Lorenzo, M.; Liz-Marzan, L. M.; Dzubiella, J.; Lu, Y.; Ballauff, M., Catalysis by metallic nanoparticles in aqueous solution: model reactions. *Chem. Soc. Rev.* **2012,** *41* (17), 5577-5587.
216. Aditya, T.; Pal, A.; Pal, T., Nitroarene reduction: a trusted model reaction to test nanoparticle catalysts. *Chem. Commun.* **2015,** *51* (46), 9410-9431.
217. Pradhan, N.; Pal, A.; Pal, T., Silver nanoparticle catalyzed reduction of aromatic nitro compounds. *Colloids Surf., A* **2002,** *196* (2), 247-257.
218. Blaser, H.-U.; Steiner, H.; Studer, M., Selective Catalytic Hydrogenation of Functionalized Nitroarenes: An Update. *ChemCatChem* **2009,** *1* (2), 210-221.
219. Chen, Y.; Wang, C.; Liu, H.; Qiu, J.; Bao, X., Ag/SiO2: a novel catalyst with high activity and selectivity for hydrogenation of chloronitrobenzenes. *Chem. Commun.* **2005,** (42), 5298-5300.
220. Shimizu, K.-i.; Miyamoto, Y.; Satsuma, A., Size- and support-dependent silver cluster catalysis for chemoselective hydrogenation of nitroaromatics. *J. Catal.* **2010,** *270* (1), 86-94.
221. Paun, C.; Slowik, G.; Lewin, E.; Sa, J., Flow hydrogenation of p-nitrophenol with nano-Ag/Al2O3. *RSC Adv.* **2016,** *6* (90), 87564-87568.
222. Artiukha, E. A.; Nuzhdin, A.; Bukhtiyarova, G. A.; Bukhtiyarov, V. I., Flow synthesis of secondary amines over Ag/Al2O3 catalyst by one-pot reductive amination of aldehydes with nitroarenes. *RSC Adv.* **2017,** *7* (72), 45856-45861.
223. Cárdenas-Lizana, F.; de Pedro, Z. M.; Gómez-Quero, S.; Keane, M. A., Gas phase hydrogenation of nitroarenes: A comparison of the catalytic action of titania supported gold and silver. *J. Mol. Catal. A: Chem.* **2010,** *326* (1), 48-54.
224. Fang, G.; Bi, X., Silver-catalysed reactions of alkynes: recent advances. *Chem. Soc. Rev.* **2015,** *44* (22), 8124-8173.
225. Schröder, F.; Sharma, U. K.; Mertens, M.; Devred, F.; Debecker, D. P.; Luque, R.; Eycken, E. V. V. d., Silver-Nanoparticle-Catalyzed Dearomatization of Indoles toward 3-Spiroindolenines via a 5-exo-dig Spirocyclization. *ACS Catal.* **2016,** *6* (12), 8156-8161.
226. James, M. J.; Clubley, R. E.; Palate, K. Y.; Procter, T. J.; Wyton, A. C.; O'Brien, P.; Taylor, R. J. K.; Unsworth, W. P., Silver(I)-Catalyzed Dearomatization of Alkyne-Tethered

Indoles: Divergent Synthesis of Spirocyclic Indolenines and Carbazoles. *Org. Lett.* **2015,** *17* (17), 4372-4375.
227. Clarke, A. K.; James, M. J.; O'Brien, P.; Taylor, R. J. K.; Unsworth, W. P., Silica-Supported Silver Nitrate as a Highly Active Dearomatizing Spirocyclization Catalyst: Synergistic Alkyne Activation by Silver Nanoparticles and Silica. *Angew. Chem.* **2016,** *128* (44), 14002-14006.
228. Williams, C. M.; Mander, L. N., Chromatography with silver nitrate. *Tetrahedron* **2001,** *57* (3), 425-447.
229. Boumendjel, A., [General Articles] Aurones: A Subclass of Flavones with Promising Biological Potential. *Curr. Med. Chem.* **2003,** *10* (23), 2621-2630.
230. Yu, M.; Lin, M.; Han, C.; Zhu, L.; Li, C.-J.; Yao, X., Ligand-promoted reaction on silver nanoparticles: phosphine-promoted, silver nanoparticle-catalyzed cyclization of 2-(1-hydroxy-3-arylprop-2-ynyl)phenols. *Tetrahedron Lett.* **2010,** *51* (51), 6722-6725.
231. Suchithra, M.; Sentaro, O., Silica-Supported Silver as a Green and Sustainable Catalyst for the [3+2]-Cycloaddition Reaction of Azomethine Ylides with 2′-Hydroxychalcone Derivatives. *ChemCatChem* **2018,** *10* (9), 2014-2018.
232. Wei, C.; Li, Z.; Li, C.-J., The First Silver-Catalyzed Three-Component Coupling of Aldehyde, Alkyne, and Amine. *Org. Lett.* **2003,** *5* (23), 4473-4475.
233. Li, Z.; Wei, C.; Chen, L.; Varma, R. S.; Li, C.-J., Three-component coupling of aldehyde, alkyne, and amine catalyzed by silver in ionic liquid. *Tetrahedron Lett.* **2004,** *45* (11), 2443-2446.
234. Wei, C.; Li, C.-J., A Highly Efficient Three-Component Coupling of Aldehyde, Alkyne, and Amines via C−H Activation Catalyzed by Gold in Water. *J. Am. Chem. Soc.* **2003,** *125* (32), 9584-9585.
235. Wei, C.; Li, C.-J., Grignard type reaction via C-H bond activation in water. *Green Chem.* **2002,** *4* (1), 39-41.
236. Mohan Reddy, K.; Seshu Babu, N.; Suryanarayana, I.; Sai Prasad, P. S.; Lingaiah, N., The silver salt of 12-tungstophosphoric acid: an efficient catalyst for the three-component coupling of an aldehyde, an amine and an alkyne. *Tetrahedron Lett.* **2006,** *47* (43), 7563-7566.
237. Haber, J.; Pamin, K.; Matachowski, L.; Napruszewska, B.; Połtowicz, J., Potassium and Silver Salts of Tungstophosphoric Acid as Catalysts in Dehydration of Ethanol and Hydration of Ethylene. *J. Catal.* **2002,** *207* (2), 296-306.
238. Yan, W.; Wang, R.; Xu, Z.; Xu, J.; Lin, L.; Shen, Z.; Zhou, Y., A novel, practical and green synthesis of Ag nanoparticles catalyst and its application in three-component coupling of aldehyde, alkyne, and amine. *J. Mol. Catal. A: Chem.* **2006,** *255* (1), 81-85.
239. Sadjadi, S.; Malmir, M.; Heravi, M. M., A green approach to the synthesis of Ag doped nano magnetic [gamma]-Fe2O3@SiO2-CD core-shell hollow spheres as an efficient and heterogeneous catalyst for ultrasonic-assisted A3 and KA2 coupling reactions. *RSC Adv.* **2017,** *7* (58), 36807-36818.
240. Movahedi, F.; Masrouri, H.; Kassaee, M. Z., Immobilized silver on surface-modified ZnO nanoparticles: As an efficient catalyst for synthesis of propargylamines in water. *J. Mol. Catal. A: Chem.* **2014,** *395* (Supplement C), 52-57.
241. Zhou, X.; Lu, Y.; Zhai, L.-L.; Zhao, Y.; Liu, Q.; Sun, W.-Y., Propargylamines formed from three-component coupling reactions catalyzed by silver oxide nanoparticles. *RSC Adv.* **2013,** *3* (6), 1732-1734.
242. Lyu, L.-M.; Wang, W.-C.; Huang, M. H., Synthesis of Ag2O Nanocrystals with Systematic Shape Evolution from Cubic to Hexapod Structures and Their Surface Properties. *Chem. Eur. J.* **2010,** *16* (47), 14167-14174.

243. Yuqing Zhou, T. H., and Zhiyong Wang, Nanoparticles of silver oxide immobilized on different templates: highly efficient catalysts for three-component coupling of aldehyde-amine-alkyne. *Arkivoc* **2008,** *xiii*, 80-90.
244. Salam, N.; Sinha, A.; Roy, A. S.; Mondal, P.; Jana, N. R.; Islam, S. M., Synthesis of silver-graphene nanocomposite and its catalytic application for the one-pot three-component coupling reaction and one-pot synthesis of 1,4-disubstituted 1,2,3-triazoles in water. *RSC Adv.* **2014,** *4* (20), 10001-10012.
245. Yong, G.-P.; Tian, D.; Tong, H.-W.; Liu, S.-M., Mesoporous SBA-15 supported silver nanoparticles as environmentally friendly catalysts for three-component reaction of aldehydes, alkynes and amines with glycol as a “green” solvent. *J. Mol. Catal. A: Chem.* **2010,** *323* (1), 40-44.
246. Safaei-Ghomi, J.; Ghasemzadeh, M. A., Silver iodide nanoparticle as an efficient and reusable catalyst for the one-pot synthesis of benzofurans under aqueous conditions. *J. Chem Sci* **2013,** *125* (5), 1003-1008.
247. Liu, J.; Chen, L.; Cui, H.; Zhang, J.; Zhang, L.; Su, C.-Y., Applications of metal-organic frameworks in heterogeneous supramolecular catalysis. *Chem. Soc. Rev.* **2014,** *43* (16), 6011-6061.
248. Zhao, Y.; Zhou, X.; Okamura, T.-a.; Chen, M.; Lu, Y.; Sun, W.-Y.; Yu, J.-Q., Silver supramolecule catalyzed multicomponent reactions under mild conditions. *Dalton Trans.* **2012,** *41* (19), 5889-5896.
249. Wang, S.; He, X.; Song, L.; Wang, Z., Silver Nanoparticles Supported by Novel Nickel Metal-Organic Frameworks: An Efficient Heterogeneous Catalyst for an A^3 Coupling Reaction. *Synlett* **2009,** *2009* (03), 447-450.
250. Yu, M.; Wang, Y.; Sun, W.; Yao, X., A Mild, Highly Efficient Addition of Alkynes to Aldehydes Catalyzed by Titanium Dioxide-Supported Silver Nanoparticles. *Adv. Synth. Catal.* **2012,** *354* (1), 71-76.
251. Wang, H.; Yang, K.-F.; Li, L.; Bai, Y.; Zheng, Z.-J.; Zhang, W.-Q.; Gao, Z.-W.; Xu, L.-W., Modulation of Silver–Titania Nanoparticles on Polymethylhydrosiloxane-based Semi-Interpenetrating Networks for Catalytic Alkynylation of Trifluoromethyl Ketones and Aromatic Aldehydes in Water. *ChemCatChem* **2014,** *6* (2), 580-591.
252. Yu, D.; Tan, M. X.; Zhang, Y., Carboxylation of Terminal Alkynes with Carbon Dioxide Catalyzed by Poly(N-Heterocyclic Carbene)-Supported Silver Nanoparticles. *Adv. Synth. Catal.* **2012,** *354* (6), 969-974.
253. Zhu, N.-N.; Liu, X.-H.; Li, T.; Ma, J.-G.; Cheng, P.; Yang, G.-M., Composite System of Ag Nanoparticles and Metal–Organic Frameworks for the Capture and Conversion of Carbon Dioxide under Mild Conditions. *Inorg. Chem.* **2017,** *56* (6), 3414-3420.
254. Thomas, A. M.; Sujatha, A.; Anilkumar, G., Recent advances and perspectives in copper-catalyzed Sonogashira coupling reactions. *RSC Adv.* **2014,** *4* (42), 21688-21698.
255. Garcia, P.; Malacria, M.; Aubert, C.; Gandon, V.; Fensterbank, L., Gold-Catalyzed Cross-Couplings: New Opportunities for C-C Bond Formation. *ChemCatChem* **2010,** *2* (5), 493-497.
256. Kyriakou, G.; Beaumont, S. K.; Humphrey, S. M.; Antonetti, C.; Lambert, R. M., Sonogashira Coupling Catalyzed by Gold Nanoparticles: Does Homogeneous or Heterogeneous Catalysis Dominate? *ChemCatChem* **2010,** *2* (11), 1444-1449.
257. Venkatesan, P.; Santhanalakshmi, J., Designed Synthesis of Au/Ag/Pd Trimetallic Nanoparticle-Based Catalysts for Sonogashira Coupling Reactions. *Langmuir* **2010,** *26* (14), 12225-12229.
258. Sanchez-Sanchez, C.; Orozco, N.; Holgado, J. P.; Beaumont, S. K.; Kyriakou, G.; Watson, D. J.; Gonzalez-Elipe, A. R.; Feria, L.; Fernández Sanz, J.; Lambert, R. M.,

Sonogashira Cross-Coupling and Homocoupling on a Silver Surface: Chlorobenzene and Phenylacetylene on Ag(100). *J. Am. Chem. Soc.* **2015,** *137* (2), 940-947.
259. Orozco, N.; Kyriakou, G.; Beaumont, S. K.; Fernandez Sanz, J.; Holgado, J. P.; Taylor, M. J.; Espinós, J. P.; Márquez, A. M.; Watson, D. J.; Gonzalez-Elipe, A. R.; Lambert, R. M., Critical Role of Oxygen in Silver-Catalyzed Glaser–Hay Coupling on Ag(100) under Vacuum and in Solution on Ag Particles. *ACS Catal.* **2017,** *7* (5), 3113-3120.
260. Cirera, B.; Zhang, Y.-Q.; Klyatskaya, S.; Ruben, M.; Klappenberger, F.; Barth, J. V., 2 D Self-Assembly and Catalytic Homo-coupling of the Terminal Alkyne 1,4-Bis(3,5-diethynyl-phenyl)butadiyne-1,3 on Ag(111). *ChemCatChem* **2013,** *5* (11), 3281-3288.
261. Van Ham, N. H. A.; Nieuwenhuys, B. E.; Sachtler, W. M. H., The oxidation of cumene on silver and silver-gold alloys. *J. Catal.* **1971,** *20* (3), 408-411.
262. Crites, C.-O. L.; Hallett-Tapley, G. L.; Frenette, M.; González-Béjar, M.; Netto-Ferreira, J. C.; Scaiano, J. C., Insights into the Mechanism of Cumene Peroxidation Using Supported Gold and Silver Nanoparticles. *ACS Catal.* **2013,** *3* (9), 2062-2071.
263. Zhao, H.; Zhou, J.; Luo, H.; Zeng, C.; Li, D.; Liu, Y., Synthesis, Characterization of Ag/MCM-41 and the Catalytic Performance for Liquid-phase Oxidation of Cyclohexane. *Catal. Lett.* **2006,** *108* (1), 49-54.
264. Schuchardt, U.; Cardoso, D.; Sercheli, R.; Pereira, R.; da Cruz, R. S.; Guerreiro, M. C.; Mandelli, D.; Spinacé, E. V.; Pires, E. L., Cyclohexane oxidation continues to be a challenge. *Appl. Catal., A* **2001,** *211* (1), 1-17.
265. Li, Z.; Divakara, S. G.; Richards, R. M., Oxidation Catalysis by Nanoscale Gold, Silver, and Copper. In *Advanced Nanomaterials*, Wiley-VCH Verlag GmbH & Co. KGaA: 2010; pp 333-364.
266. Acharyya, S. S.; Ghosh, S.; Sharma, S. K.; Bal, R., Fabrication of Ag nanoparticles supported on one-dimensional (1D) Mn3O4 spinel nanorods for selective oxidation of cyclohexane at room temperature. *New J. Chem.* **2016,** *40* (4), 3812-3820.
267. Ghosh, S.; Acharyya, S. S.; Sharma, S. K.; Bal, R., Fabrication of Ag/Mn3O4 nano-architectures for the one-step selective oxidation of 3-picoline to niacin: a key to vitamin B3 production. *Catal. Sci. Technol.* **2016,** *6* (12), 4644-4654.
268. Ghosh, S.; Acharyya, S. S.; Adak, S.; Konathala, L. N. S.; Sasaki, T.; Bal, R., Selective oxidation of cyclohexene to adipic acid over silver supported tungsten oxide nanostructured catalysts. *Green Chem.* **2014,** *16* (5), 2826-2834.
269. Ghosh, S.; Acharyya, S. S.; Singh, R.; Gupta, P.; Bal, R., Fabrication of Ag/WO3 nanobars for Baeyer–Villiger oxidation using hydrogen peroxide. *Catal. Commun.* **2015,** *72* (Supplement C), 33-37.
270. Ghosh, S.; Acharyya, S. S.; Kumar, M.; Bal, R., Chloride promoted room temperature preparation of silver nanoparticles on two dimensional tungsten oxide nanoarchitectures for the catalytic oxidation of tertiary N-compounds to N-oxides. *Nanoscale* **2015,** *7* (37), 15197-15208.
271. Ghosh, S.; Acharyya, S. S.; Tripathi, D.; Bal, R., Preparation of silver-tungsten nanostructure materials for selective oxidation of toluene to benzaldehyde with hydrogen peroxide. *J. Mater. Chem. A* **2014,** *2* (38), 15726-15733.
272. Laus, G., Kinetics of acetonitrile-assisted oxidation of tertiary amines by hydrogen peroxide. *J. Chem. Soc., Perkin Trans. 2* **2001,** (6), 864-868.
273. Raji, V.; Chakraborty, M.; Parikh, P. A., Catalytic Performance of Silica-Supported Silver Nanoparticles for Liquid-Phase Oxidation of Ethylbenzene. *Ind. Eng. Chem. Res.* **2012,** *51* (16), 5691-5698.
274. Beier, M. J.; Schimmoeller, B.; Hansen, T. W.; Andersen, J. E. T.; Pratsinis, S. E.; Grunwaldt, J.-D., Selective side-chain oxidation of alkyl aromatic compounds catalyzed by cerium modified silver catalysts. *J. Mol. Catal. A: Chem.* **2010,** *331* (1), 40-49.

275. Hosseini-Sarvari, M.; Ataee-Kachouei, T.; Moeini, F., Preparation, characterization, and catalytic application of nano Ag/ZnO in the oxidation of benzylic C-H bonds in sustainable media. *RSC Adv.* **2015,** *5* (12), 9050-9056.
276. Hunger, K.; Mischke, P.; Rieper, W.; Zhang, S., Azo Dyes, 1. General. In *Ullmann's Encyclopedia of Industrial Chemistry*, Wiley-VCH Verlag GmbH & Co. KGaA: 2000.
277. Cai, S.; Rong, H.; Yu, X.; Liu, X.; Wang, D.; He, W.; Li, Y., Room Temperature Activation of Oxygen by Monodispersed Metal Nanoparticles: Oxidative Dehydrogenative Coupling of Anilines for Azobenzene Syntheses. *ACS Catal.* **2013,** *3* (4), 478-486.
278. Kumar, M.; Soni, K.; Yadav, G. D.; Singh, S.; Deka, S., Surfactant directed Ag1−xNix alloy nanoparticle catalysed synthesis of aromatic azo derivatives from aromatic amines. *Appl. Catal., A* **2016,** *525* (Supplement C), 50-58.
279. Ghosh, S.; Acharyya, S. S.; Sasaki, T.; Bal, R., Room temperature selective oxidation of aniline to azoxybenzene over a silver supported tungsten oxide nanostructured catalyst. *Green Chem.* **2015,** *17* (3), 1867-1876.
280. Ahmed, T. J.; Knapp, S. M. M.; Tyler, D. R., Frontiers in catalytic nitrile hydration: Nitrile and cyanohydrin hydration catalyzed by homogeneous organometallic complexes. *Coord. Chem. Rev.* **2011,** *255* (7), 949-974.
281. Kukushkin, V. Y.; Pombeiro, A. J. L., Metal-mediated and metal-catalyzed hydrolysis of nitriles. *Inorg. Chim. Acta* **2005,** *358* (1), 1-21.
282. Kim, A. Y.; Bae, H. S.; Park, S.; Park, S.; Park, K. H., Silver nanoparticle catalyzed selective hydration of nitriles to amides in water under neutral conditions. *Catal. Lett.* **2011,** *141* (5), 685-690.
283. Woo, H.; Lee, K.; Park, S.; Park, K., Magnetically Separable and Recyclable Fe3O4-Supported Ag Nanocatalysts for Reduction of Nitro Compounds and Selective Hydration of Nitriles to Amides in Water. *Molecules* **2014,** *19* (1), 699.
284. Kawai, K.; Kawakami, H.; Narushima, T.; Yonezawa, T., Selective and reactive hydration of nitriles to amides in water using silver nanoparticles stabilized by organic ligands. *J. Nanopart. Res.* **2015,** *17* (2), 60.
285. Mitsudome, T.; Mikami, Y.; Mori, H.; Arita, S.; Mizugaki, T.; Jitsukawa, K.; Kaneda, K., Supported silver nanoparticle catalyst for selective hydration of nitriles to amides in water. *Chem. Commun.* **2009,** (22), 3258-3260.
286. Shimizu, K.-i.; Imaiida, N.; Sawabe, K.; Satsuma, A., Hydration of nitriles to amides in water by SiO2-supported Ag catalysts promoted by adsorbed oxygen atoms. *Appl. Catal., A* **2012,** *421*, 114-120.
287. Sherbow, T. J.; Downs, E. L.; Sayler, R. I.; Razink, J. J.; Juliette, J. J.; Tyler, D. R., Investigation of 1,3,5-Triaza-7-phosphaadamantane-Stabilized Silver Nanoparticles as Catalysts for the Hydration of Benzonitriles and Acetone Cyanohydrin. *ACS Catal.* **2014,** *4* (9), 3096-3104.
288. Pileidis, F.; Titirici, M.-M., Levulinic Acid Biorefineries: New Challenges for Efficient Utilization of Biomass. *ChemSusChem* **2016,** *9* (6), 562-582.
289. Murugavel, R.; Voigt, A.; Walawalkar, M. G.; Roesky, H. W., Hetero- and Metallasiloxanes Derived from Silanediols, Disilanols, Silanetriols, and Trisilanols. *Chem. Rev.* **1996,** *96* (6), 2205-2236.
290. Brown, J. F., The Polycondensation of Phenylsilanetriol. *J. Am. Chem. Soc.* **1965,** *87* (19), 4317-4324.
291. Brown, J. F.; Vogt, L. H., The polycondensation of cyclohexylsilanetriol. *J. Am. Chem. Soc.* **1965,** *87* (19), 4313-4317.
292. Denmark, S. E., The Interplay of Invention, Discovery, Development, and Application in Organic Synthetic Methodology: A Case Study. *J. Org. Chem.* **2009,** *74* (8), 2915-2927.

293. Denmark, S. E.; Regens, C. S., Palladium-Catalyzed Cross-Coupling Reactions of Organosilanols and Their Salts: Practical Alternatives to Boron- and Tin-Based Methods. *Acc. Chem. Res.* **2008,** *41* (11), 1486-1499.
294. Jeon, M.; Han, J.; Park, J., Catalytic Synthesis of Silanols from Hydrosilanes and Applications. *ACS Catal.* **2012,** *2* (8), 1539-1549.
295. Jeon, M.; Han, J.; Park, J., Transformation of Silanes into Silanols using Water and Recyclable Metal Nanoparticle Catalysts. *ChemCatChem* **2012,** *4* (4), 521-524.
296. Mitsudome, T.; Arita, S.; Mori, H.; Mizugaki, T.; Jitsukawa, K.; Kaneda, K., Supported Silver-Nanoparticle-Catalyzed Highly Efficient Aqueous Oxidation of Phenylsilanes to Silanols. *Angew. Chem. Int. Ed.* **2008,** *47* (41), 7938-7940.
297. Kikukawa, Y.; Kuroda, Y.; Yamaguchi, K.; Mizuno, N., Diamond-Shaped [Ag4]4+ Cluster Encapsulated by Silicotungstate Ligands: Synthesis and Catalysis of Hydrolytic Oxidation of Silanes. *Angew. Chem. Int. Ed.* **2012,** *51* (10), 2434-2437.
298. Li, Z.; Zhang, C.; Tian, J.; Zhang, Z.; Zhang, X.; Ding, Y., Highly selective oxidation of organosilanes with a reusable nanoporous silver catalyst. *Catal. Commun.* **2014,** *53* (Supplement C), 53-56.
299. Wang, C.; Zhang, Z.; Yang, G.; Chen, Q.; Yin, Y.; Jin, M., Creation of Controllable High-Density Defects in Silver Nanowires for Enhanced Catalytic Property. *Nano Lett.* **2016,** *16* (9), 5669-5674.
300. Masaharu, U.; Arata, T.; Shū, K., Catalytic Organic Reactions on the Surface of Silver(I) Oxide in Water. *Chem. Lett.* **2014,** *43* (12), 1867-1869.
301. Safari, J.; Gandomi-Ravandi, S., Silver decorated multi-walled carbon nanotubes as a heterogeneous catalyst in the sonication of 2-aryl-2,3-dihydroquinazolin-4(1H)-ones. *RSC Adv.* **2014,** *4* (23), 11654-11660.
302. Mandi, U.; Roy, A. S.; Banerjee, B.; Islam, S. M., A novel silver nanoparticle embedded mesoporous polyaniline (mPANI/Ag) nanocomposite as a recyclable catalyst in the acylation of amines and alcohols under solvent free conditions. *RSC Adv.* **2014,** *4* (80), 42670-42681.
303. Nassar, N. T.; Barr, R.; Browning, M.; Diao, Z.; Friedlander, E.; Harper, E. M.; Henly, C.; Kavlak, G.; Kwatra, S.; Jun, C.; Warren, S.; Yang, M.-Y.; Graedel, T. E., Criticality of the Geological Copper Family. *Environ. Sci. Tech.* **2012,** *46* (2), 1071-1078.
304. Catinat, M. *Critical raw materials for the EU: Report of the Ad-hoc Working Group on defining critical raw materials*; European Commission, Enterprise and Industry: 2010.
305. Morley, N.; Eatherley, D. *Material Security Technology Strategy Board Ensuring resource availability for the UK economy*; Resource Efficiency Knowledge Transfer Network: 2008.
306. Pfleger, P.; Lichtblau, K.; Bardt, H.; Reller, A. *Rohstoffsituation Bayern – keine Zukunft ohne Rohstoffe*; Vereinigung der Bayerischen Wirtschaft: Munich (Germany), 2011.
307. Yasukawa, T.; Saito, Y.; Miyamura, H.; Kobayashi, S., Chiral Nanoparticles/Lewis Acids as Cooperative Catalysts for Asymmetric 1,4-Addition of Arylboronic Acids to α,β-Unsaturated Amides. *Angew. Chem. Int. Ed.* **2016,** *55* (28), 8058-8061.

Dans le dressage de la ville, peut-être faudrait-il refaire encore une fois
L'histoire du ressentiment peut-être, l'histoire de la menace.
[…]
Et puis inversons les valeurs, valorisons les martyrs.
Célébrons la souffrance, impuissants dans les soupirs.

Josset, F.-X.; Vaillant, A.; Jouneau, O.; Lefloch, F.; Domecyn, J.; Affreux, Sales et Méchants, *Accident n°7*, **2008**, *14*, 26:29-29:12.

In the previous chapter, we covered the versatility of Ag NPs as catalysts in organic reactions. Their main features for carbonyl hydrogenation have been identified: low reactivity and high C=O/C=C selectivity. The recyclability issue is not trivial in the case of Ag though, being an endangered metal. Here we discuss the simple synthesis of magnetically recoverable Ag NPs, made by microwave and using bio-derived polymers as support and reductant, and their application for the selective hydrogenation of carbonyls in water.

3. Microwave-assisted synthesis of magnetic carboxymethyl cellulose-embedded Ag-Fe_3O_4 nanocatalysts for selective carbonyl hydrogenation

This chapter is based upon one published article. The American Chemical Society granted permission to reprint the published article, as did all co-authors.

Alain Li, Madhu Kaushik, Chao Jun Li, Audrey Moores, 'Microwave-Assisted Synthesis of Magnetic Carboxymethyl Cellulose-Embedded Ag–Fe_3O_4 Nanocatalysts for Selective Carbonyl Hydrogenation', *ACS Sustainable Chem. Eng.*, **2016**, 4, 965–973.

3.1 Abstract

Magnetic nanoparticles enable an efficient catalyst recovery at the end of a chemical reaction, and therefore contribute to more sustainable and greener industrial processes. Herein we report the synthesis of magnetically retrievable Ag NPs for the catalytic hydrogenation and oxidation of aldehydes in water. Upon brief exposure to microwave irradiation, Ag and Fe_3O_4 NPs formed directly within carboxymethyl cellulose (CMC), an inexpensive, biobased polymer support. The catalyst was tested for the hydrogenation of aldehydes in water, showing a high activity and selectivity to C=O bonds against C=C bonds. Aldehydes can also be oxidized to the corresponding carboxylic acid with the same catalyst, even with substrates that do not self-oxidize under air. The organic matrix and the magnetic support allowed the catalyst to be recycled up to five times with negligible metal leaching in the reaction medium.

3.2 General Introduction.

Metal NPs are intensely researched in the field of catalysis, as they combine the recyclability of heterogeneous catalytic systems and the activity and selectivity of homogenous ones.[1] Among them, Ag NPs have proved active for the selective hydrogenation of aldehydes (Scheme 203). Despite the low affinity of silver towards H_2 it is intrinsically selective towards C=O bonds over C=C bonds (see section 2.5.1).[2] Alternatives exist for this transformation, relying on platinum group catalysts or inorganic salts ($NaBH_4$, H_3NBH_3[3]), but they either require acidic promoters or stoichiometric amounts of reductants.

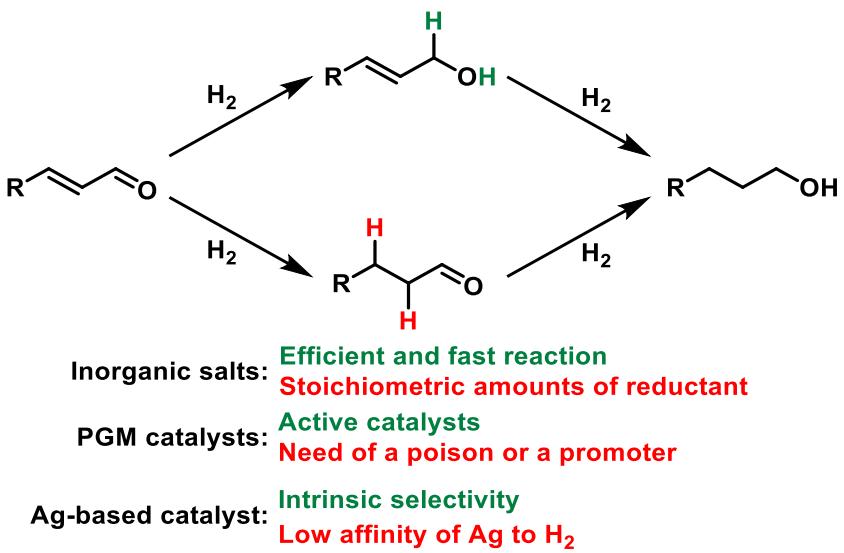

Scheme 203. Strategies for the selective hydrogenation of carbonyls.

Claus *et al.*[2, 4-8] produced an abundant literature on silica-supported Ag NPs for the selective hydrogenation of C=O bonds over C=C bonds. Similarly, Yadav *et al*. reported manganese oxide-supported AgNP for the selective hydrogenation of acetophenone to 1-phenethyl alcohol.[9] Finally Mertens *et al.* worked on recyclable PVP-stabilized Ag NPs for the selective reduction of α,β-unsaturated aldehydes, including acrolein.[10] A silver(I)-NHC complex was also reported by Jia et *al.* as an efficient homogeneous catalyst to oxidize aldehydes to the corresponding acids in water,[11] using atmospheric O_2.

The appealing reactivity and selectivity of these catalytic material is however hindered by the harsh synthetic conditions required for their synthesis, such as calcination steps or strong acidic conditions. Moreover, the recyclability and re-usability of these catalysts were not investigated: the separation and the robustness of Ag NPs still remains an important challenge.

Besides, magnetic NPs (MNPs) have been explored as a means to conveniently support catalysts, or act as one themselves.[12] When used as supports, core-shell structures, silica layer,[13]

or organic linkers may be used in solid form to anchor organocatalysts,[14] metal complexes[15] or metal NPs. They are particularly attractive as they allow an easy catalyst separation using a simple external magnetic field, circumventing the need to use filtration or centrifugation.[16-18] Recent reviews and articles have covered, in particular, their use in water[19] and for hydrogenation reactions.[20] Iron and iron oxides (Fe(0), Fe_2O_3, Fe_3O_4) are commonly used MNPs[21-23] and are accessed *via* several synthetic routes, including co-precipitation, sonolysis, hydrothermal reaction.[24] To the best of our knowledge, no example of such MNP-supported Ag NPs for hydrogenation reactions has been reported so far (Scheme 204).

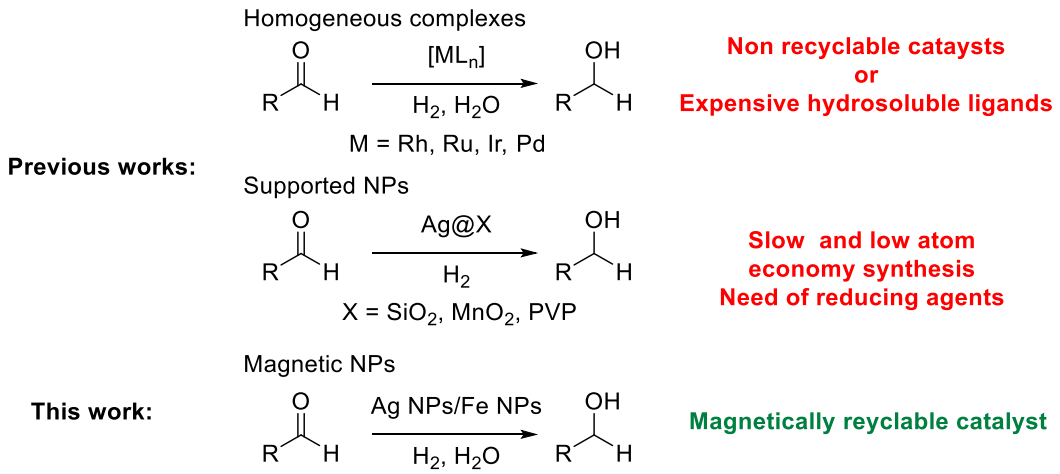

Scheme 204. Different systems for aldehyde hydrogenation.

3.3 Ag NP supported on Fe(0) NPs by galvanic deposition

3.3.1 Introduction.

Hudson et *al.* previously established in the Moores group the direct deposition of various metals over Fe(0) NPs (M@Fe, M = Cu, Ru).[25-26] A similar procedure has been developed as well by Zhou et *al.* for Pd.[27] The protocol is straightforward, as Fe(0) acts as both magnetic support and reductant. They can be made by the reduction of $FeSO_4$ using $NaBH_4$, in $MeOH/H_2O$ under inert atmosphere, yielding Fe(0) NPs. The surface gets quickly oxidized, yielding Fe(0)/Fe_3O_4 core/shell NPs (FeCSNP). The crystallinity of the iron oxide shell determines its passivation ability. An amorphous shell provides a long-term passivation capacity, whereas a crystalline shell allows both electron and metal ion diffusion from the core.[28]

Alternatively, commercial sources of Fe(0) are available, such as FeCSmP, bearing a crystalline iron oxide shell. Subsequently, metals salts are added to FeCSmP, then an electron transfer occurs from Fe(0) to the metal salt ($E°(Fe/Fe^{2+})$ = -0.44 V vs SHE at 25 °C). This galvanic exchange results in the deposition of the corresponding metal on the surface, without requiring any external linker or reductant (Scheme 205).

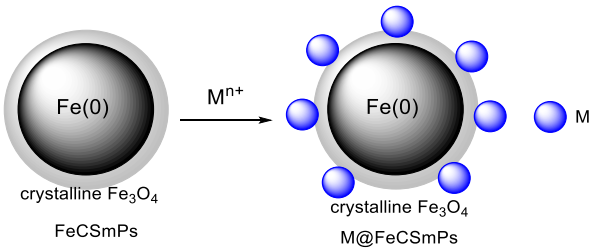

Scheme 205. Direct deposition of metals (Cu,Ru,Pd) over FeCSmPs (black = Fe(0) core, gray = crystalline Fe_3O_4 shell)

3.3.2 Results and discussion.

Ag@FeSCmP was made with a process similar to the one reported previously by Hudson et *al*. After complete drying of the resulting catalyst, Ag@FeSCmP kept its strong magneticity, initially present for commercial FeSCmP. Ag@FeSCmP was observed by SEM complemented with HAADF-EDS elemental mapping (Figure 1).

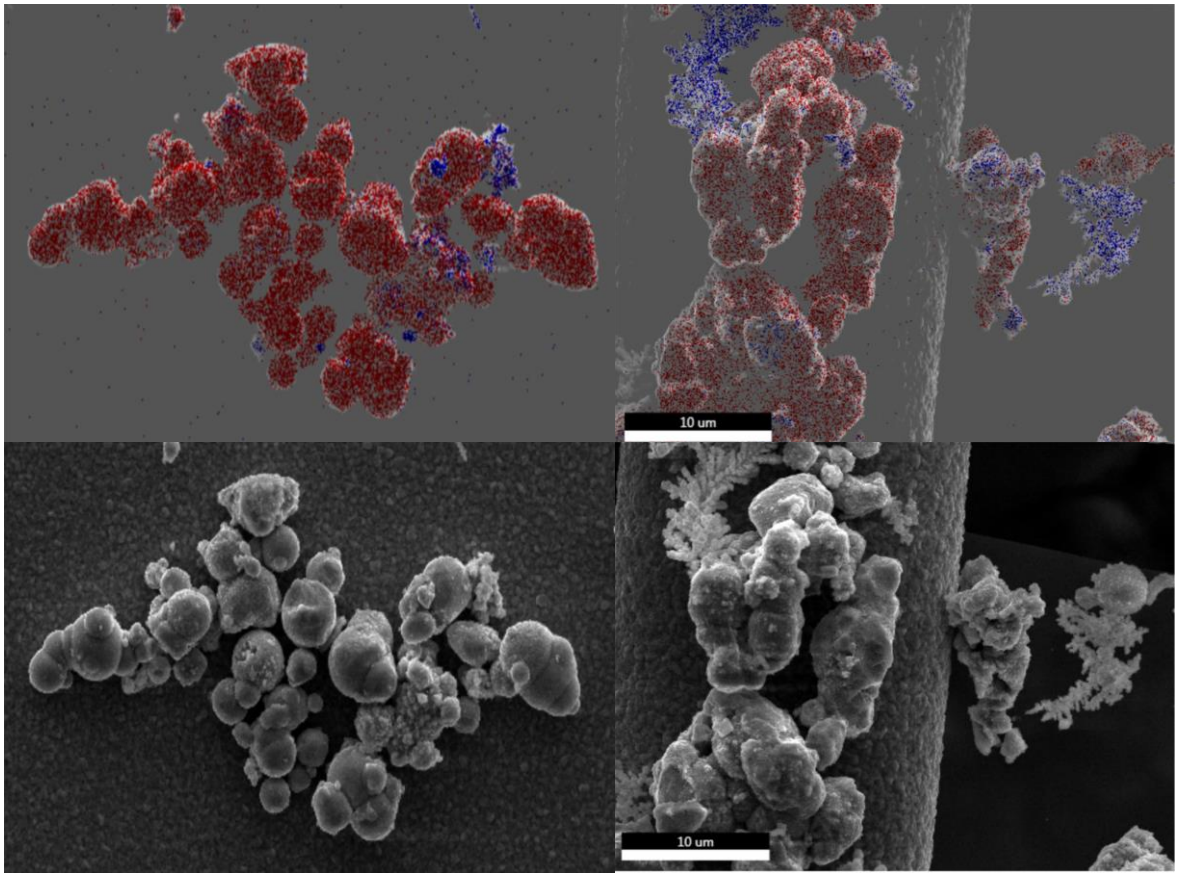

Figure 1. Ag@FeSCmPs particles made by galvanic reduction – SEM images (Fe NPs in red, Ag NPs in blue).

Akin to what was observed by previous members of the group for Cu, fern-like structures were observed.[29] In the case of Cu, these fractal structures stemmed from the extremely fast reduction of Cu^{2+} over Fe(0) ($E°(Cu/Cu^{2+})$ = + 0.34 V vs SHE at 25 °C). Indeed, at Cu/Fe ratios above 1/100, Cu grows preferentially over itself than over the Fe support. In the case of Ag, due to the even higher oxidation potential of Ag+ (($E°(Ag/Ag^{+})$ = + 0.80 V at 25 °C), and its larger conductivity ($6{,}30.10^{7}$ S/m for Ag, $5{,}98.10^{7}$ S/m for Cu), we believe a similar mechanism takes place.

Ag@FeSCmPs was then tested for benzaldehyde hydrogenation in H_2O (40 bar H_2, 100 °C, 24h), yielding 80% reduction yield (Scheme 206). Upon recycling tests though, the yield quickly dropped to 50% (cycle 2) then 20% yield (cycle 3). Although the catalyst synthesis and the hydrogenation tests were run under inert atmosphere, the catalyst got inevitably exposed to

air during the work-ups and recycling tests. This could explain the sharp yield drop upon catalyst re-use. Furthermore, the fern-like structures gave a high catalytic activity, probably due to their higher Ag surface area. However, these structures are fragile, and make Ag all the more sensitive to oxidation, along with the inherent sensitivity of FeSCMPs to air.

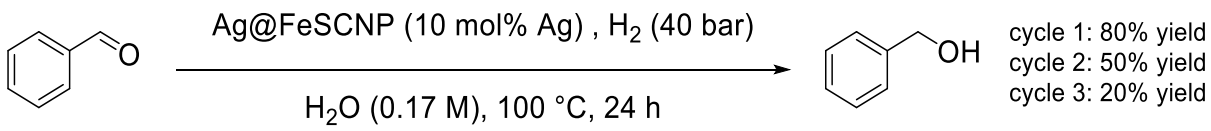

Scheme 206. Ag@ FeSCMP-catalyzed benzaldehyde hydrogenation in H_2O.

3.4 Ag NP supported on carboxymethyl cellulose

3.4.1 Introduction

We turned to alternative procedures to make magnetically supported Ag NPs, while keeping the features from the previous system: magneticity, high surface area, and good dispersity in water. In order to maintain a high colloidal stability, both against work-ups exposed to air and hydrogenation conditions, capping agents are necessary. Environmentally benign and bio-sourced molecules such as sucrose,[30] starch,[31] sodium citrate,[32] alginate,[33] or orange peel extract[34] have been successfully used as reducing and capping agents for Ag NPs synthesis.[35] Furthermore, microwave irradiation has been used in several reports as an efficient and fast route to generate Ag NPs in water.[36] It provides both a uniform and fast growth environment for the NPs and can assist the digestive ripening of these particles to afford a monodisperse size distribution.[37] In this particular context, Raveendran,[38] Kumar,[39] Nadagouda,[40] Liu,[41] and Horikoshi[42] reported the synthesis of Ag NPs stabilized by cellulose derivatives under short heating conditions (Scheme 207). In the latter system, $Ag(NH_3)_2^+$ was exposed to microwave irradiation in presence of carboxymethyl cellulose (CMC) in H_2O, yielding small and monodisperse Ag NPs dispersed in water (Ag@CMC, 1-2 nm).

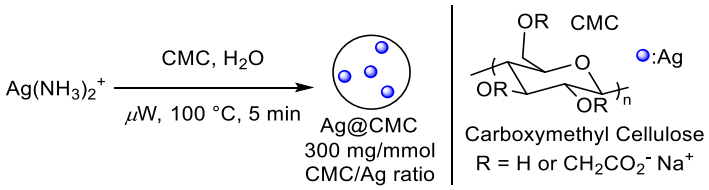

Scheme 207. Ag@CMC microwave-assisted synthesis.

$Ag(NH_3)_2^+$ (commonly named Tollens' reagent) was used in most reports and is made from the treatment of $AgNO_3$ with NaOH, then NH_3 (Scheme 208). This reagent is more stable than $AgNO_3$ to reductants. Indeed, Yin et *al.* reported that using $Ag(NH_3)_2^+$ provides a delay time of 5 mins before the Ag^+ cation gets reduced by a sorbitol/formaldehyde solution, allowing a better control of NP growth.[43]

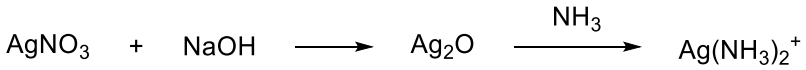

Scheme 208. $Ag(NH_3)_2^+$ synthesis.

Liu et *al.* investigated the mechanism of Ag^+ reduction using carboxymethyl chitosan (CMCh).[41] The authors monitored the evolution of CMCh by ^{13}C NMR (DEPT-135) before and after reduction of $Ag(NH_3)_2^+$ ($E°(Ag^+/Ag) = + 0.37$ V at 25 °C) under microwave. Notably, the carboxymethyl groups get decarboxylated during the reaction into methyl groups, reducing Ag^+ in the process (Scheme 209a). We believe that two other reduction pathways are likely to occur concomitantly. First, the end chains of CMC are in equilibrium with their opened form, revealing a reducing aldehyde function (Scheme 209b). Then, considering that our CMC source is still 30% hydroxylated, we cannot exclude a polyol-type reduction of Ag(I) by the remaining primary -OH groups (Scheme 209c).[44]

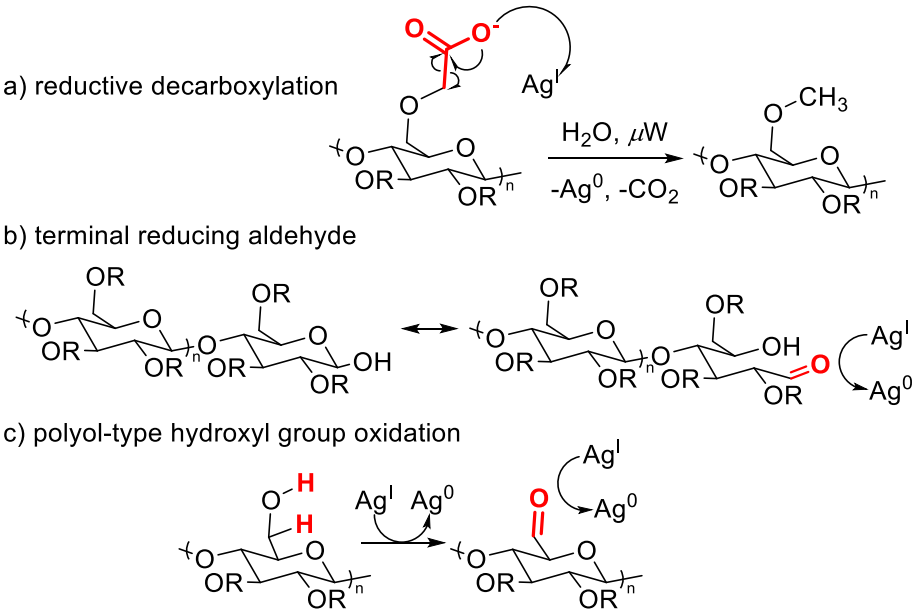

Scheme 209. Possible pathways for CMC-mediated Ag^+ reduction

3.4.2 Results and discussion

Horikoshi's synthesis was reproduced, yielding a green colloidal suspension. TEM analysis showed the reproducibility of their protocol, with a narrow distribution on the small Ag NPs obtained (Figure 2, 2.3 ± 0.3 nm).

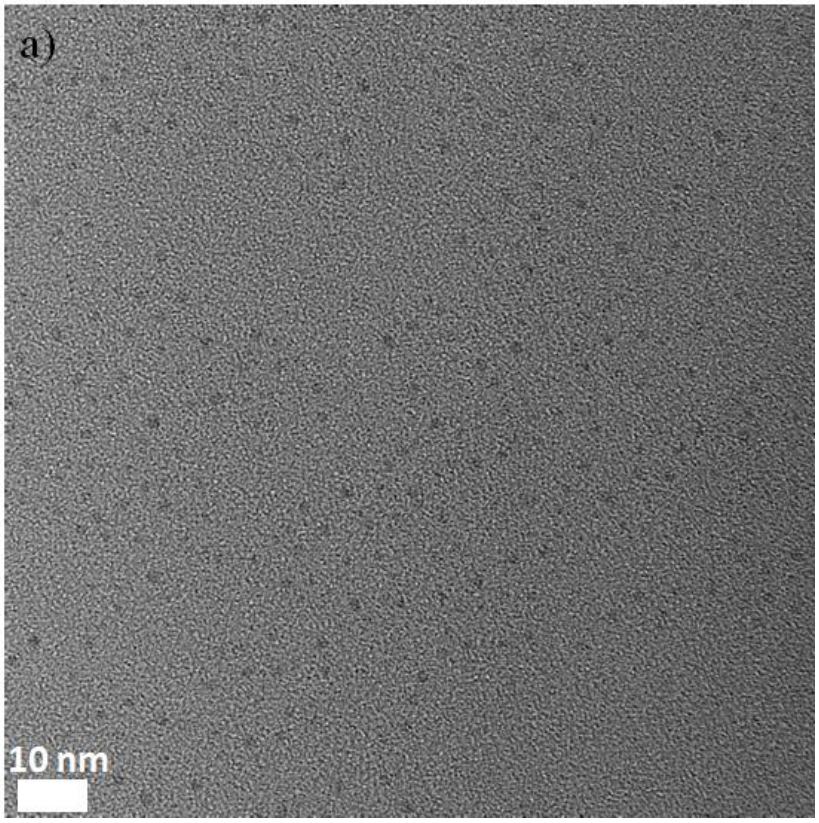

Figure 2. TEM image of Ag@CMC.

Ag@CMC was directly tested for benzaldehyde hydrogenation in water (Scheme 210, Table 2). The Ag@CMC catalyst proved to be active under conditions similar to the ones used with the homogeneous Ag complexes,[45] with the significant difference that, in the present work, neither base nor ligands were needed. Remarkably, lower temperatures and safer solvents were needed here compared to the conditions used in other Ag NP-catalyzed aldehyde hydrogenations.[8, 46] Pressure could be dropped to 30 bar without affecting the yield, while it decreased dramatically at 20 bar (95% and 33% yield respectively, Table 2, entries 2 and 3). Likewise, a loading of 5 mol % proved equally efficient but lowering the loading to 3 or 1 mol% decreased drastically the activity (97%, 60% and 33% respectively, Table 2, entries 4 to6). Combining 30 bar of hydrogen pressure with 5 mol % loading afforded 72% yield (Table 2, entry 7). The reaction temperature was identified to be crucial for catalytic activity as a decrease to 80 °C led to a sharp yield decrease (51%, Table 2, entry 8). The catalyst could be prepared by using $AgNO_3$ salts directly instead of $Ag(NH_3)_2^+$ as a precursor, although with a lower activity (80%, Table 2, entry 9). It could also be prepared under an atmosphere of air with no effect on the activity (94%, Table 2, entry 10).

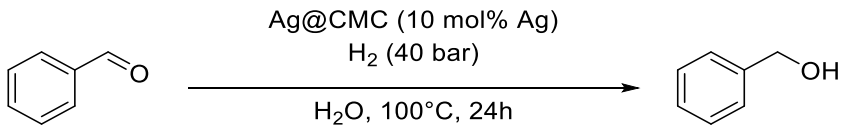

Scheme 210. Ag@CMC-catalyzed benzaldehyde hydrogenation in water.

Entry	Modification	Crude NMR yield (%)
1	-	94%
2	30 bar H_2	95%
3	20 bar H_2	33%
4	5 mol% Ag	97%
5	3 mol% Ag	60%
6	1 mol% Ag	50%

7	5 mol% Ag, 30 bar H_2	72%
8	80 °C	51%
9[b]	-	80%
10[c]	-	94%

[a]Standard reaction conditions: 0.33 mmol benzaldehyde, 9 mL H_2O, 24 h, 100 °C, 10 mol% Ag, 40 bar H_2. Cyclohexanol was used as an internal standard for ^{1}H NMR quantification.

[b]$AgNO_3$ was used as a precursor instead of $Ag(NH_3)_2^+$

[c] The Ag@CMC catalyst was prepared in air

Table 2. Ag@CMC-catalyzed hydrogenation of benzaldehyde in water.

Following these encouraging results with Ag@CMC, we turned to their magnetically retrievable version, Ag-Fe_3O_4@CMC.

3.5 Ag NP bound on Fe_3O_4 NPs using carboxymethyl cellulose

3.5.1 Introduction

In the case of magnetically-supported Ag NPs, L-arginine,[47] chitin[48] and chitosan[49] supports have been reported as well. In these protocols, magnetite (Fe_3O_4) NPs were used instead of Fe(0) NPs. Although the oxide's saturation magnetization is lower than that of the zero-valent metal (Ms = 220 emu/g for Fe(0), 92 emu/g for Fe_3O_4),[17] its higher stability to O_2 and H_2O makes it more practical for catalytic applications. Fe_3O_4 can be directly co-precipitated under alkaline conditions following the Massart process, under inert conditions:[50]

$$Fe^{2+} + 2\ Fe^{3+} + 8\ HO^- \rightarrow Fe_3O_4 + 4\ H_2O$$

Notably, CMC has been reported previously to bind and stabilize Fe(0)[51] or Fe_3O_4 NPs.[52] We thus turned to the idea to synthesize both Ag NPs and Fe_3O_4 NPs in presence of CMC as a supporting matrix, using microwave irradiation.

3.5.2 Results and discussion

We initially attempted performing first Fe_3O_4 co-precipitation in presence of CMC under microwave, then adding $Ag(NH_3)_2^+$ at different Ag/CMC/Fe_3O_4 ratios (Scheme 211). The first step consisted in the co-precipitation of CMC-coated Fe_3O_4, using soluble iron salts

($FeSO_4$ and $FeCl_3$) and base (NaOH) to ensure a better homogeneity of the mixture. Subsequently, a solution of freshly prepared $Ag(NH_3)_2^+$ was added for Ag NP formation. The sample was named Fe_3O_4-Ag@CMC.

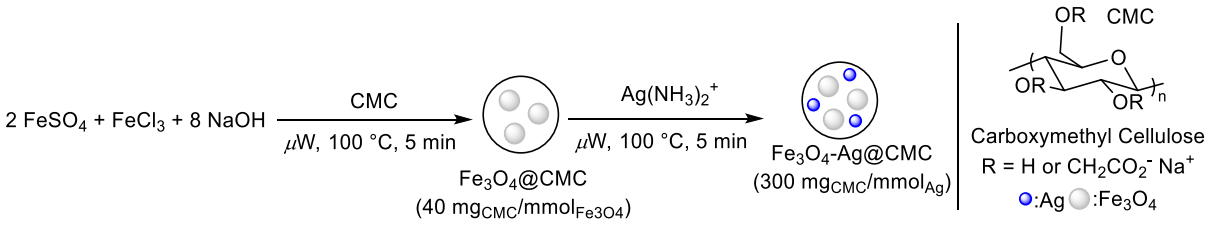

Scheme 211. Initial Fe_3O_4-Ag@CMC synthesis strategy.

Fe_3O_4-Ag@CMC was analyzed by TEM, showing the absence of the small Ag NPs seen in Ag@CMC (Figure 3).. Overall, Ag was only present as big aggregates (>10 nm), showing that the presence of Fe_3O_4 or leftover NaOH somehow affected the growth or agglomeration of Ag under microwave.

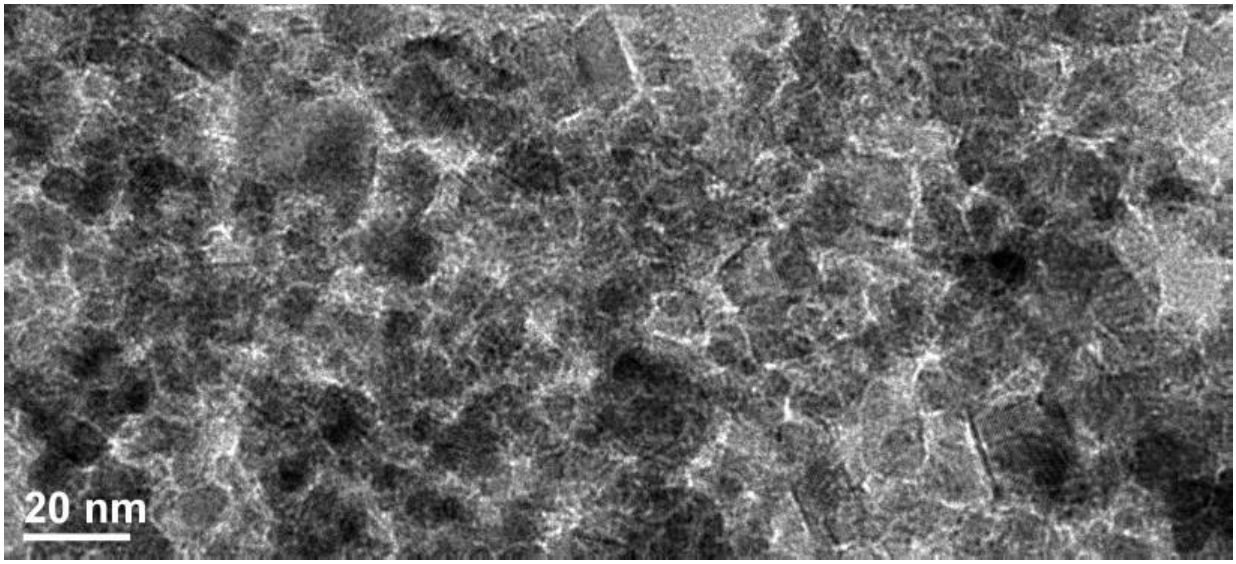

Figure 3. TEM image of Fe_3O_4-Ag@CMC.

It is worth noting that when an oil bath was used instead of microwave heating (for the rigorously identical reaction times/temperatures), a different result was noticed for each step. For Fe_3O_4 co-precipitation, a non-magnetic dark red powder was formed. This correlated with the results of Komamerni et *al.* who compared classical heating and microwave heating for the co-precipitation of Fe_3O_4.[53] In their study, they showed by XRD that microwave heating allows

reaching the same crystallinity for Fe_3O_4 than classical heating, within 8 to 16 min of heating for the former and 8–16 h for the latter. As for $Ag(NH_3)_2^+$ reduction with CMC under convective heating, a silver mirror was formed on the vial, similarly to what the Horikoshi et *al.* had observed.[42] This further shows the advantage of using microwave heating, in terms of heating efficiency and homogeneity. With the conditions described in Scheme 211, black NPs with low magneticity were obtained. Nonetheless, they were tested for the catalytic hydrogenation of benzaldehyde in water, under the same standard conditions described in Table 2 (Scheme 212). The yield reached 88%, which is slightly lower than the one observed with Ag@CMC (94% yield), which could account for a slight loss during the rinsing of the NP during synthesis.

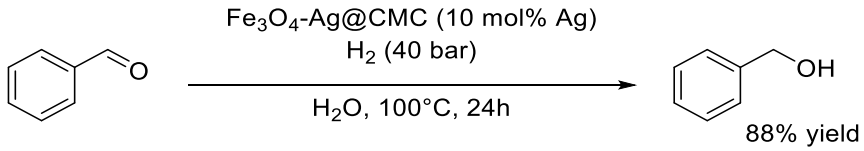

Scheme 212. Fe_3O_4-Ag@CMC-catalyzed benzaldehyde hydrogenation in water.

In parallel, we explored the opposite approach as well, by first making Ag@CMC then co-precipitating Fe_3O_4 under microwave (Scheme 213). This material, with the same Ag/Fe/CMC ratios than in Scheme 211, was called Ag-Fe_3O_4@CMC.

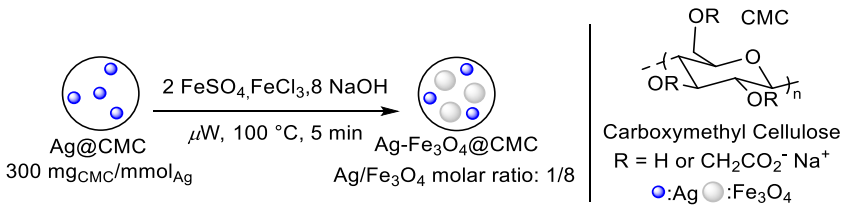

Scheme 213. Ag-Fe_3O_4@CMC microwave-assisted synthesis.

The material could be retrieved using an external magnet within one minute, whereas the previous material took more than 10 minutes to aggregate. In both routes, CMC made the catalyst easy to disperse in polar solvents, such as water and ethanol, while it adhered to the vial glass wall in less polar solvents, such as ethyl acetate and toluene.

TEM images of Ag-Fe_3O_4@CMC revealed two kinds of inorganic NPs with distinct electronic densities, and thus different shades on the tomograph (Figure 4). Fe_3O_4 NPs appeared as moderately polydisperse, light gray NPs of diameter 15.3 ± 3.5 nm and aggregated in large clusters. Ag NPs were found in two different forms: dark, large, and polydisperse NPs (37.7 ± 9.5 nm), as seen in Figure 4b and 4c, and small aggregated NPs (2.3 ± 0.3 nm), observed in Figure 4c on the top left.

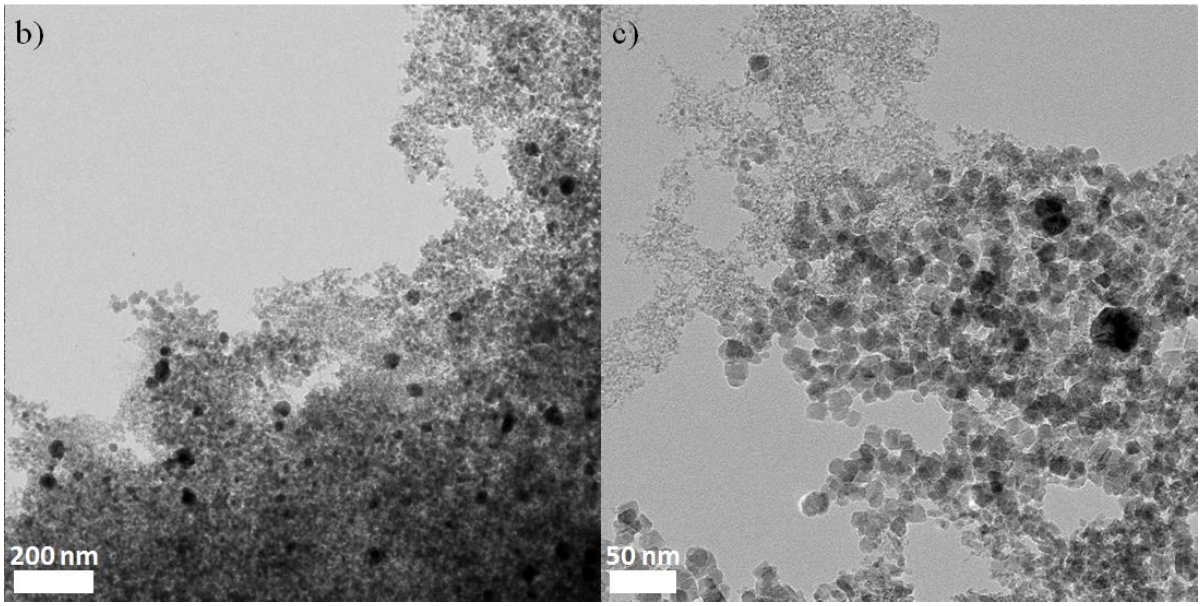

Figure 4. TEM images of Ag-Fe_3O_4@CMC.

The TEM image size distribution averages were calculated on >300 particles for each metal (Chart 1 and Chart 2), except for the Ag aggregates (around 100 particles) due to the low number of particles observed.

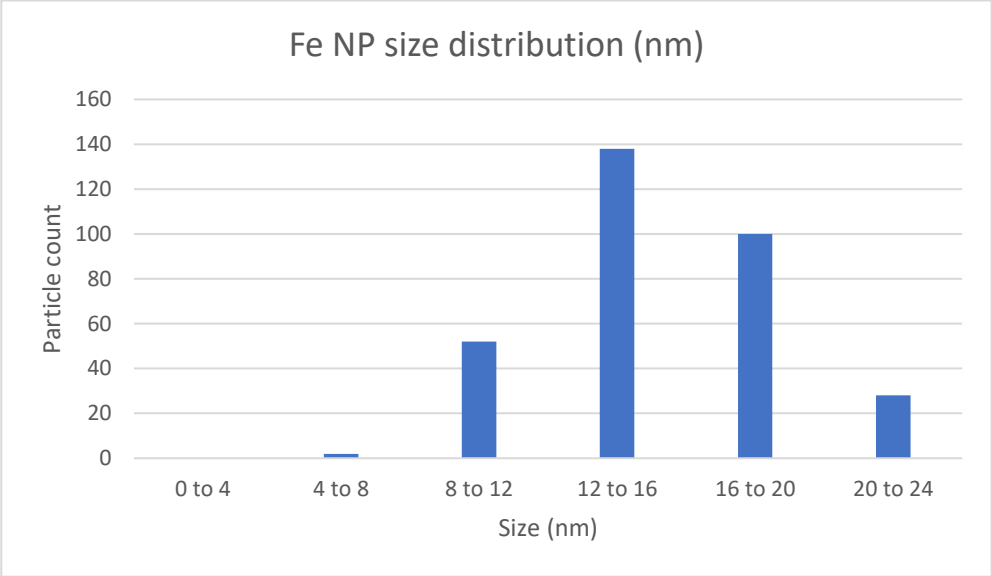

Chart 1. Fe NP size distribution in Ag@Fe_3O_4.

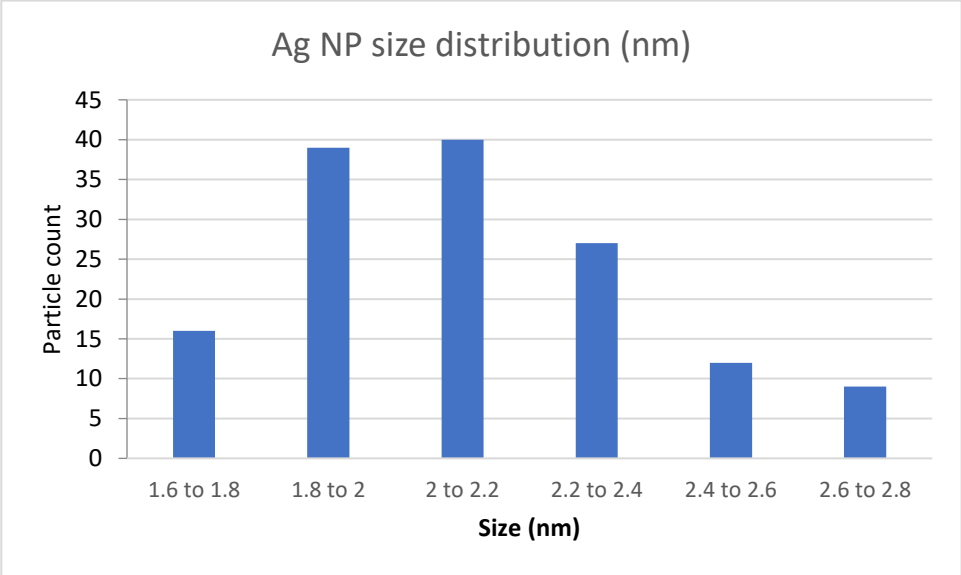

Chart 2. Ag NP size distribution in Ag@Fe_3O_4.

A typical Ag aggregate is shown in Figure 5.

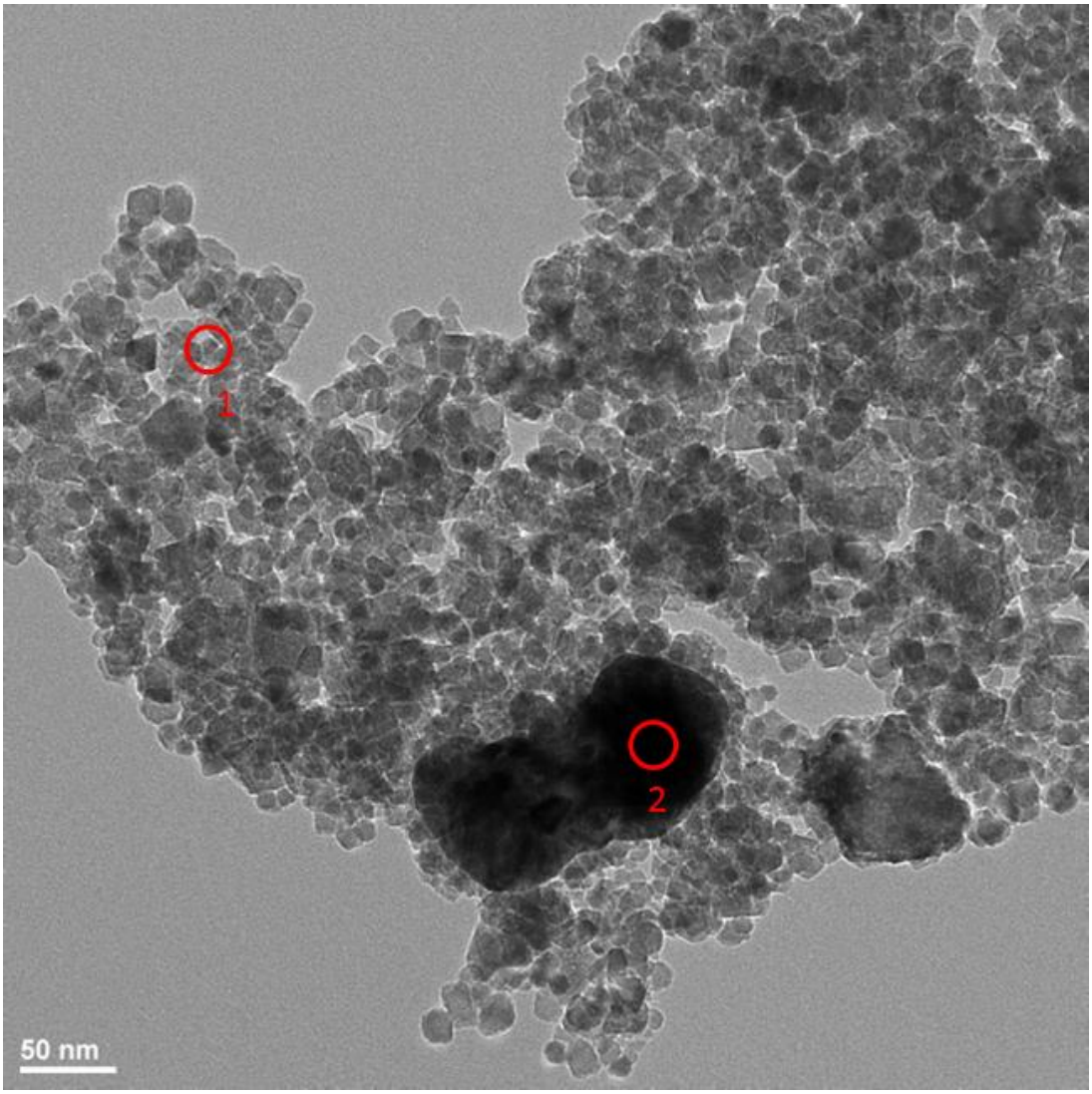

Figure 5. TEM image of Ag-Fe_3O_4@CMC. Ag aggregate (2).

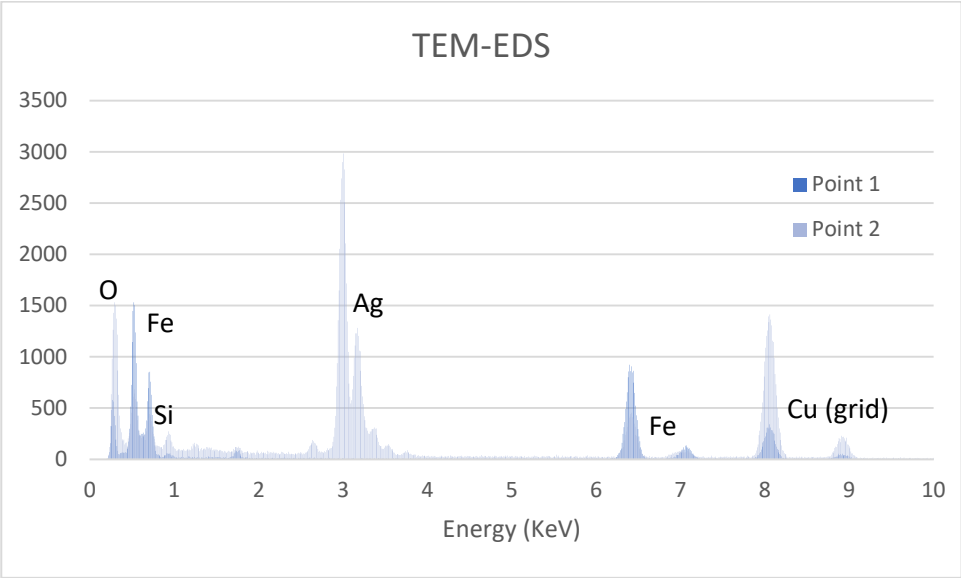

Chart 3. EDS analysis of Figure 5.

HAADF was used as a means to further establish the presence of the two metals since Ag appears as a much brighter spot than iron oxide (Figure 6).

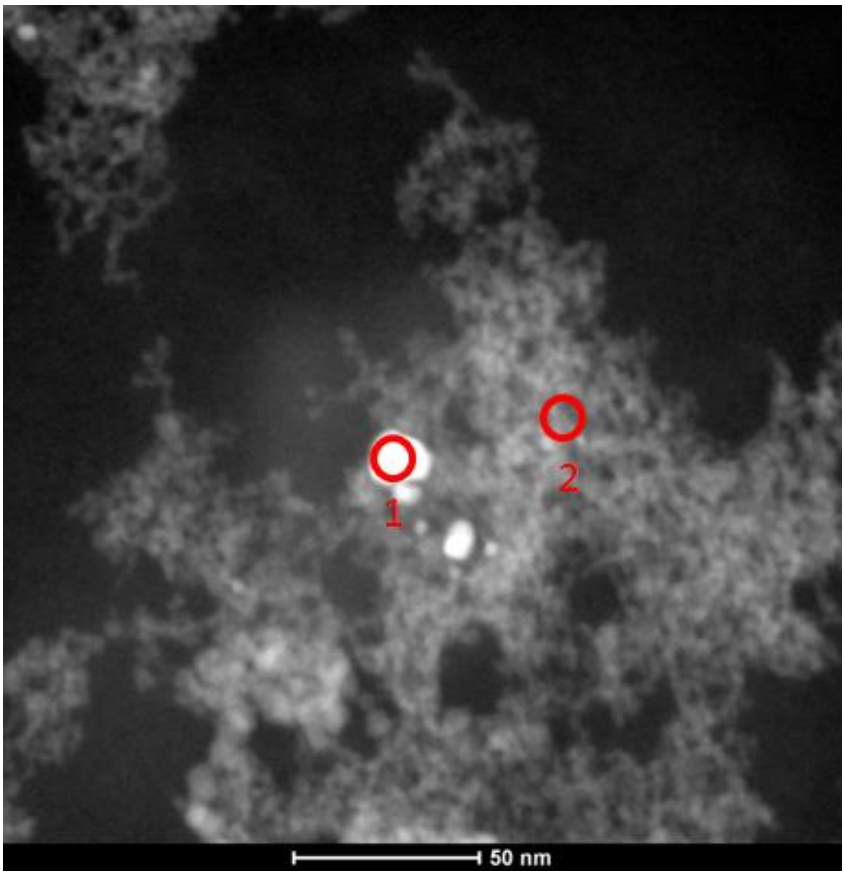

Figure 6. TEM-HAADF characterization of Ag-Fe_3O_4@CMC.

EDS further confirmed the identity of the metal NPs (Chart 4).

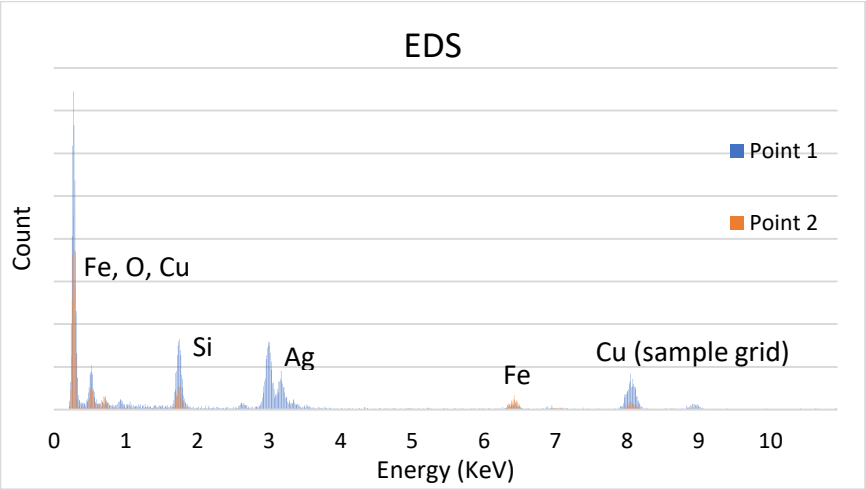

Chart 4. EDS characterization of Ag-Fe_3O_4@CMC. (point 1 and 2 refer to the HAADF micrograph on Figure 6)

Interestingly, the regions of the Ag-Fe_3O_4@CMC material where the larger Ag NPs were featured on the TEM images corresponded to the ones where the Fe_3O_4 NPs were seen (Figure 7, Figure 8). Where the Fe_3O_4 NPs were absent, the smaller Ag NPs were observed and shared the same size and shape with the NPs seen in Ag@CMC, suggesting that there were unaffected by the co-precipitation. Thus, the observed Ag NPs size growth can be directly linked to the formation of the Fe_3O_4 NPs in their vicinity. Two mechanisms are proposed: the Fe_3O_4 NPs growth provided a surface onto which Ag NPs could diffuse and coalesce. Alternatively, Cl^- and HO^- anions introduced during the Fe_3O_4 co-precipitation step, helped generate silver chlorides and oxides from the Ag NPs, thereby allowing an Ostwald ripening mechanism.

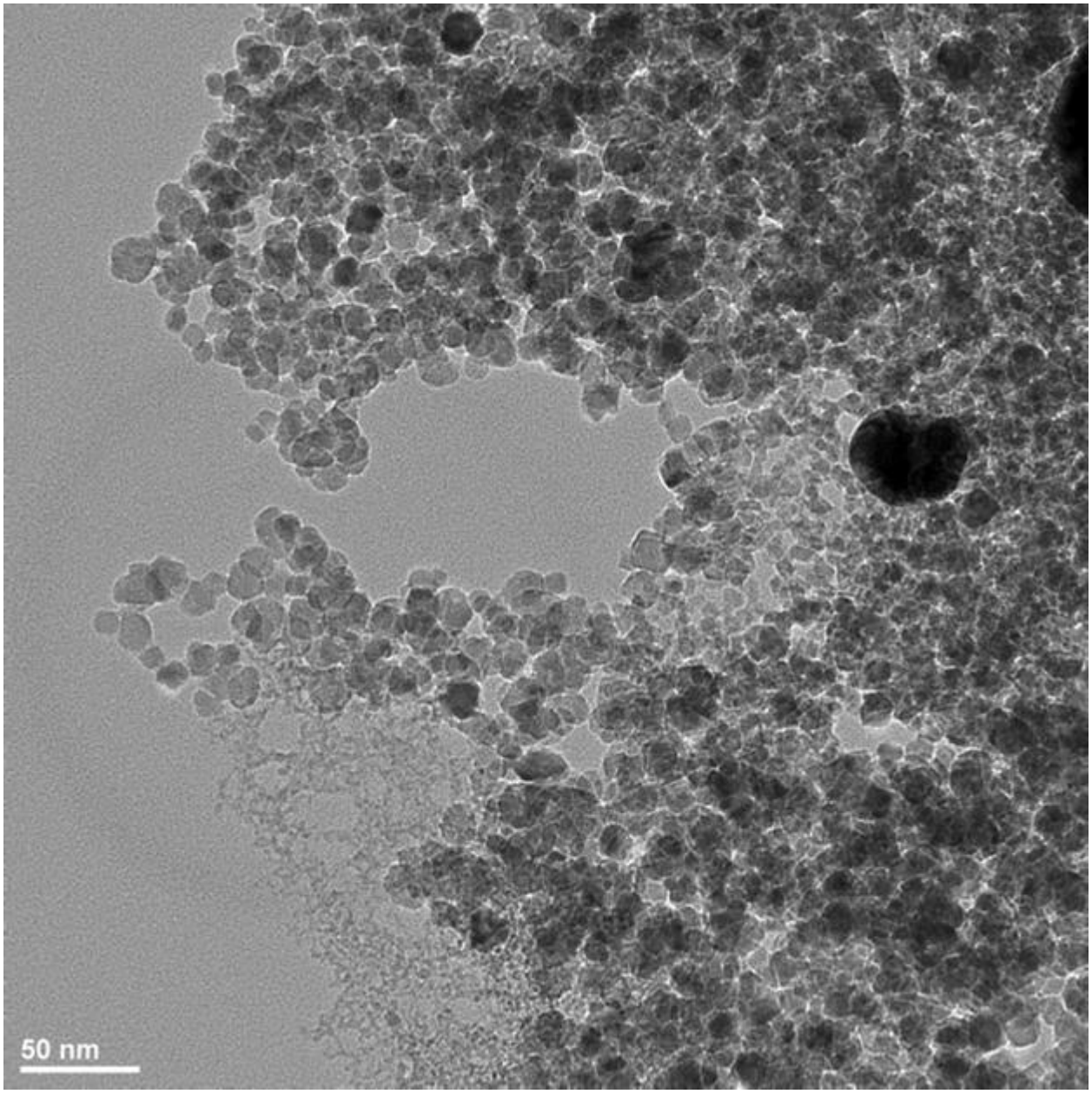

Figure 7. TEM image of Ag-Fe_3O_4@CMC.

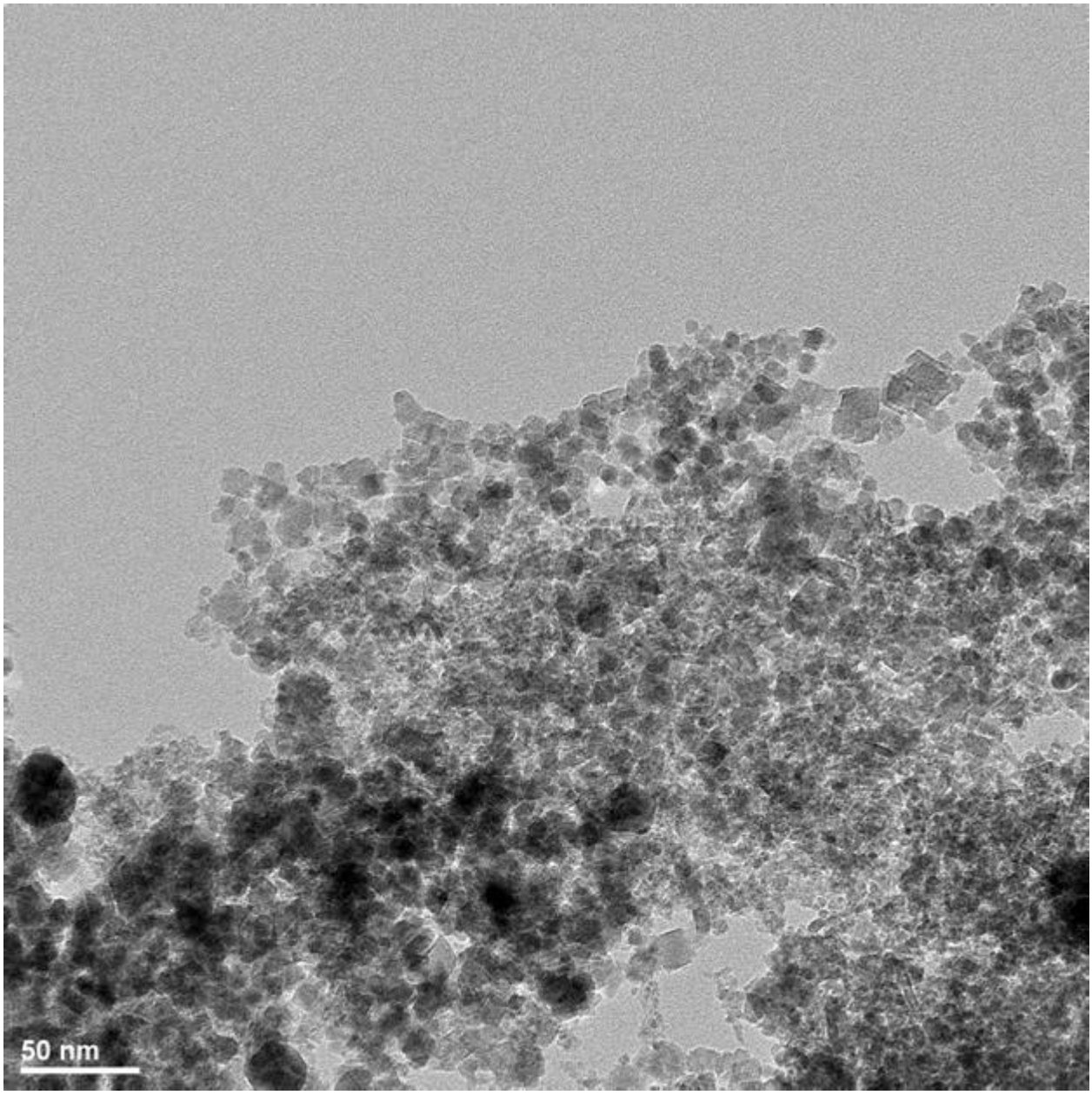

Figure 8. TEM image of Ag-Fe_3O_4@CMC.

The CMC matrix was not directly visible under the TEM conditions used, however, the arrangement of particles in clusters is consistent with the idea that all particles are embedded within the same matrix. In a TGA analysis, 8 % of the total weight was lost between 150 °C and 400 °C, which was attributed to the CMC. This is in full agreement with the amount introduced (7 mg) for the catalyst synthesis (Chart 5).

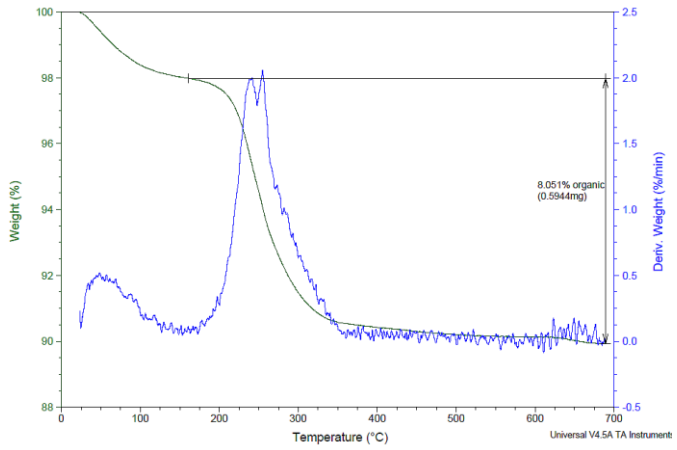

Chart 5. TGA analysis of Ag-Fe_3O_4@CMC.

XPS analysis was performed next on Ag-Fe_3O_4@CMC. In the Ag region, the $3d_{5/2}$ peak at 367.3eV is too low in energy to account for pure Ag(0) (Chart 6).[54] It was hypothesized before that this can be caused by the interaction of the Ag surface with CMC. Ag_2O is also likely to form at the surface and account for a similar binding energy. Under the hydrogenation conditions, an oxygen atom on the surface of silver can activate 2 equivalents of H_2, leading to the elimination of H_2O and leaving adsorbed hydrogens on the surface.[55] Furthermore, DFT calculations made by Lim *et al.*[56] showed that the oxygen under the silver surface promotes the selectivity of the catalyst towards C=O bonds.

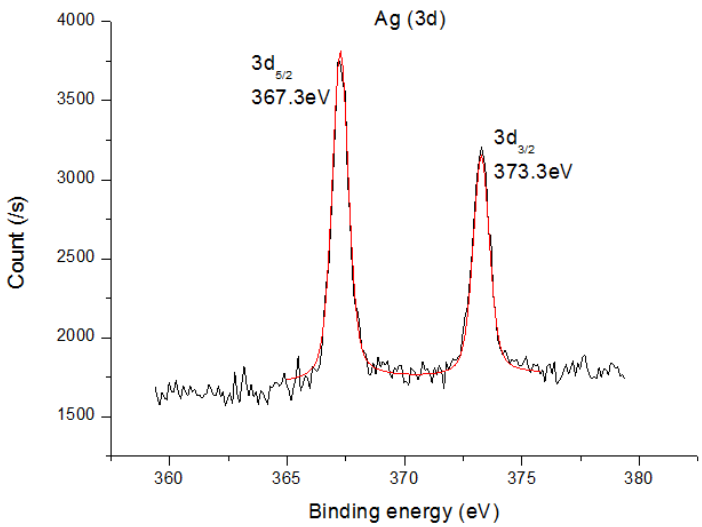

Chart 6. XPS of Ag-Fe_3O_4@CMC, Ag $3d_{5/2}$ region.

Concerning Fe (Chart 7), the fitting of the Fe $2p_{3/2}$ envelope could not help us determine unequivocally which iron oxide was formed.[57] Furthermore, the Fe $2p_{3/2}$ region overlapped with Ag's Auger peaks.

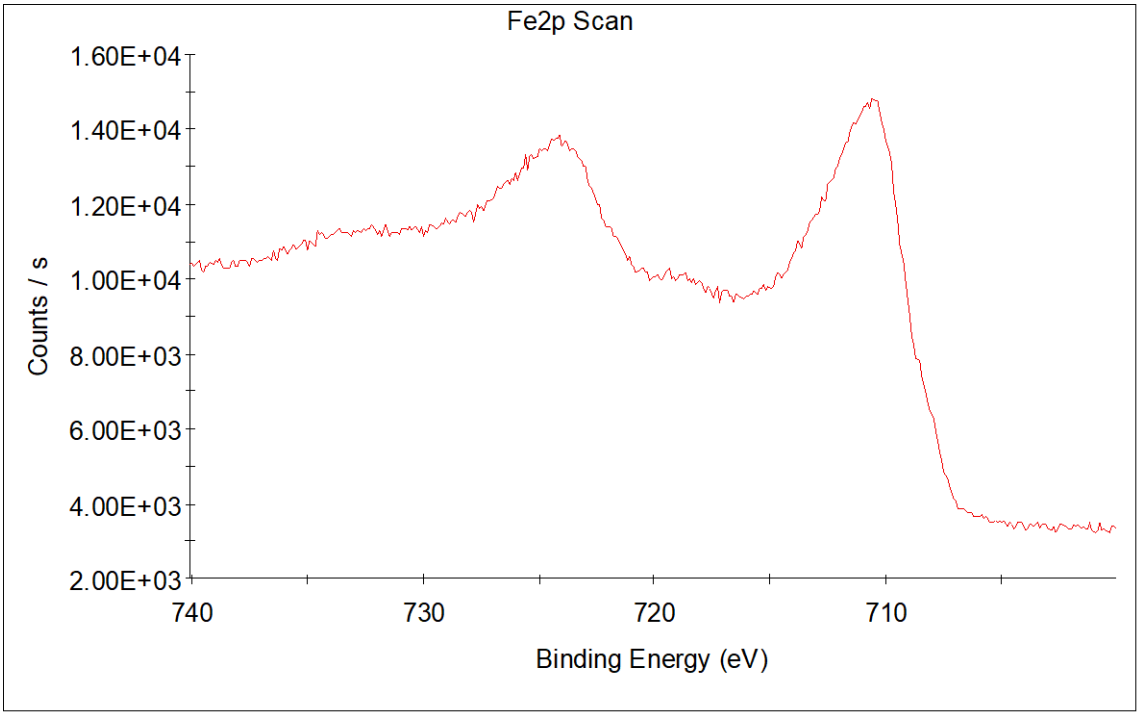

Chart 7. XPS of Ag-Fe3O4@CMC, Fe 2p3/2 region.

Therefore a XRD pattern of Fe_3O_4@CMC was taken (Chart 8), showing a good fit with Fe_3O_4 (JCPDS no. 65-3107).[58] Ag was omitted from the synthesis of the XRD sample to a clearer pattern. The sample was heated for 1 h instead of 5 min to obtain a better XRD signal.

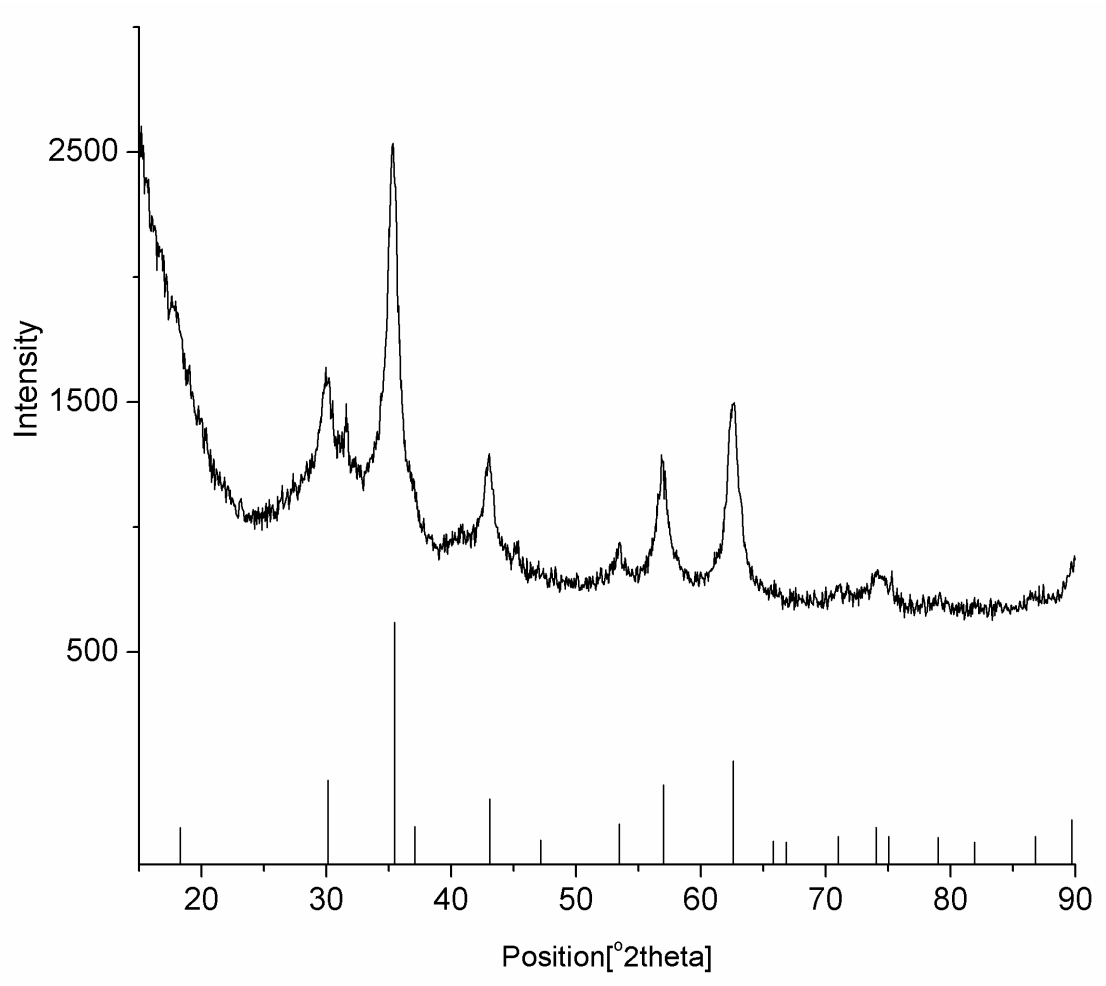

Chart 8. XRD pattern of Fe_3O_4@CMC (top) and face-centered Fe_3O_4 XRD pattern (JCPDS no. 65-3107, bottom).

Once fully characterized, Ag-Fe_3O_4@CMC was tested towards the selective hydrogenation of aldehydes in water (Scheme 214). The catalyst was directly usable as a water suspension after its preparation (Table 3).

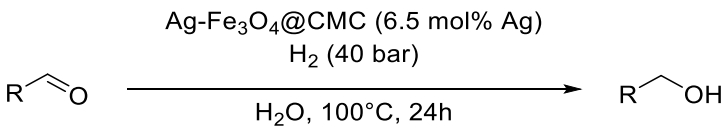

Scheme 214. Ag-Fe_3O_4@CMC-catalyzed aldehyde hydrogenation in water.

Entry	Reagent	Product	Crude NMR yield (%)

1	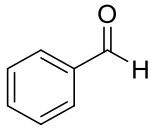	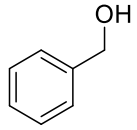	95%
2	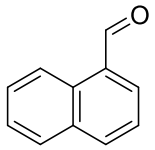	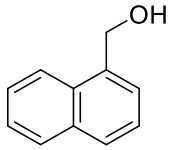	>99%
3	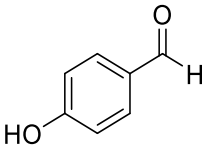	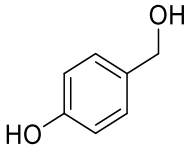	>99%
4	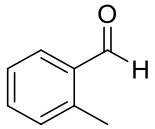	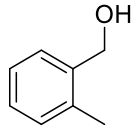	>99%
5	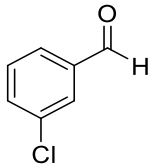	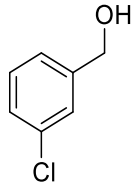	>99%
6	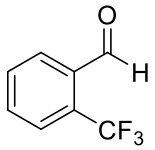	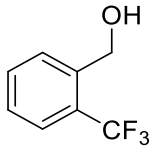	0%
7	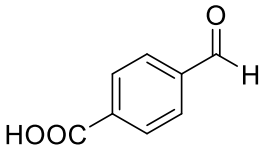	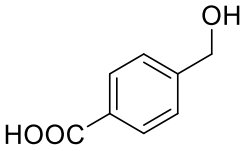	15%
8	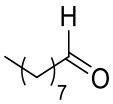	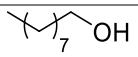	95%

9	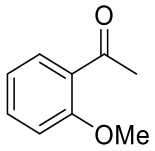	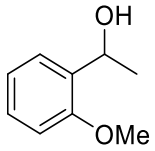	90%
10	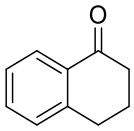	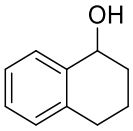	35%
11	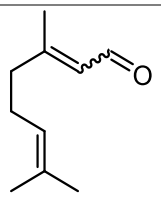	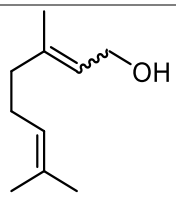	63%[a]
12	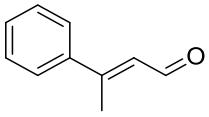	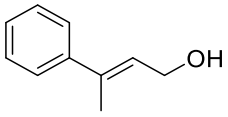	>99%

Reaction conditions: 0.33 mmol benzaldehyde, 6.5 mol % Ag-Fe_3O_4@CMC catalyst, 9 mL H_2O, 40 bars H_2, 100 °C, 24 h. Cyclohexanol was used as an external NMR standard

[a]No C=C reduction product was observed (result confirmed by GC-MS)

Table 3. Substrate scope for the Ag-Fe_3O_4@CMC-catalyzed hydrogenation of carbonyls in water.

Benzaldehyde hydrogenation (Table 3, entry 1) proceeded smoothly with Ag-Fe_3O_4@CMC, although with a slightly higher catalytic loading of 6.5 mol% compared to Ag@CMC (Table 3, entry 4). This is psrobably due to some Ag NP aggregation during the Fe_3O_4 grafting step, as Cl^-, SO_4^{2-}, and HO^- anions were added during that step. Benzaldehyde derivatives with electron-donating groups performed well (Table 3, entries 2-5). However, 2-trifluoromethylbenzaldehyde and 4-carboxybenzaldehyde had almost no conversion (Table 3, entries 6 and 7), presumably because of the electron-withdrawing groups and the hydrophobicity of the former one. It is worth noting that none of the auxiliary functionalities

(-CF_3 and -COOH respectively) were affected by our method, as we fully recovered the starting material. Aliphatic aldehydes and methyl ketones such as nonanaldehyde and 2-methoxyacetophenone (Table 3, entries 8 and 9) worked as well, though α-tetralone (Table 3, entry 10) gave a lower performance, pointing towards the importance of steric hindrance for ketones. The selectivity of the catalyst was investigated with citral, an important substrate in the fine chemical industry.[59] Under the standard conditions, citral and α-methyl-trans-cinnamaldehyde were reduced to the corresponding alcohol with no trace of the C=C reduction products (Table 3, entry 11 and 12). Remarkably, no Lewis acid additive was needed to achieve the selectivity (see section 1.2.3).[46] The combination of water and CMC as a polar environment for the catalyst could also explain the selectivity, as it would promote the coordination of the C=O bond on the surface.

After the reaction, the catalysts could be retrieved magnetically, washed with water and ethyl acetate, and then recycled in a new reaction. For 5 cycles the catalyst demonstrated high activity (Chart 9, Table 4). At the 6th cycle, the catalytic activity dropped, presumably due to NPs growth, as it will be further explained below. To test catalyst storage capacity, Ag-Fe_3O_4@CMC was freeze-dried, re-suspended in water and tested again. A yield of 94 % was then measured showing the robustness of this catalytic system.

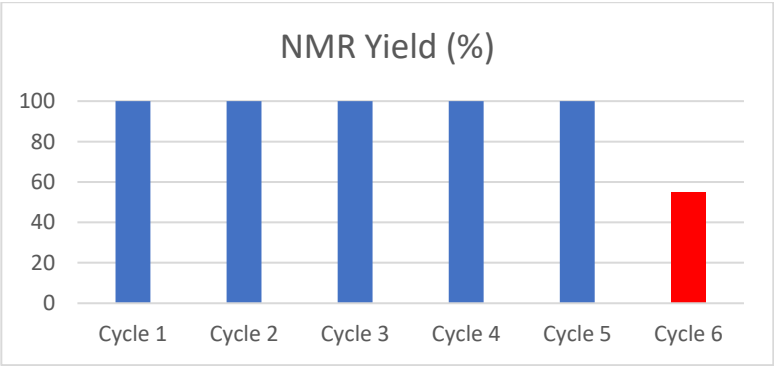

Chart 9. Recyclability tests for Ag-Fe_3O_4@CMC-catalyzed benzaldehyde hydrogenation.

Cycle	Crude NMR Yield (%)[a]

1	95% yield
2	95% yield
3	95% yield
4	95% yield
5	95% yield
6	56% yield

Reaction conditions: 0.33 mmol benzaldehyde, 6.5 mol % catalyst, 9 mL H_2O, 40 bars H_2, 100 °C, 24 h

[a]NMR Yield was calculated as an average of three measurements from separate batches.

Table 4. Ag@Fe_3O_4 recyclability results for benzaldehyde hydrogenation in water.

After the 6th catalytic cycle, the catalyst was analyzed by TEM to see its new morphology (Figure 9, Figure 10).

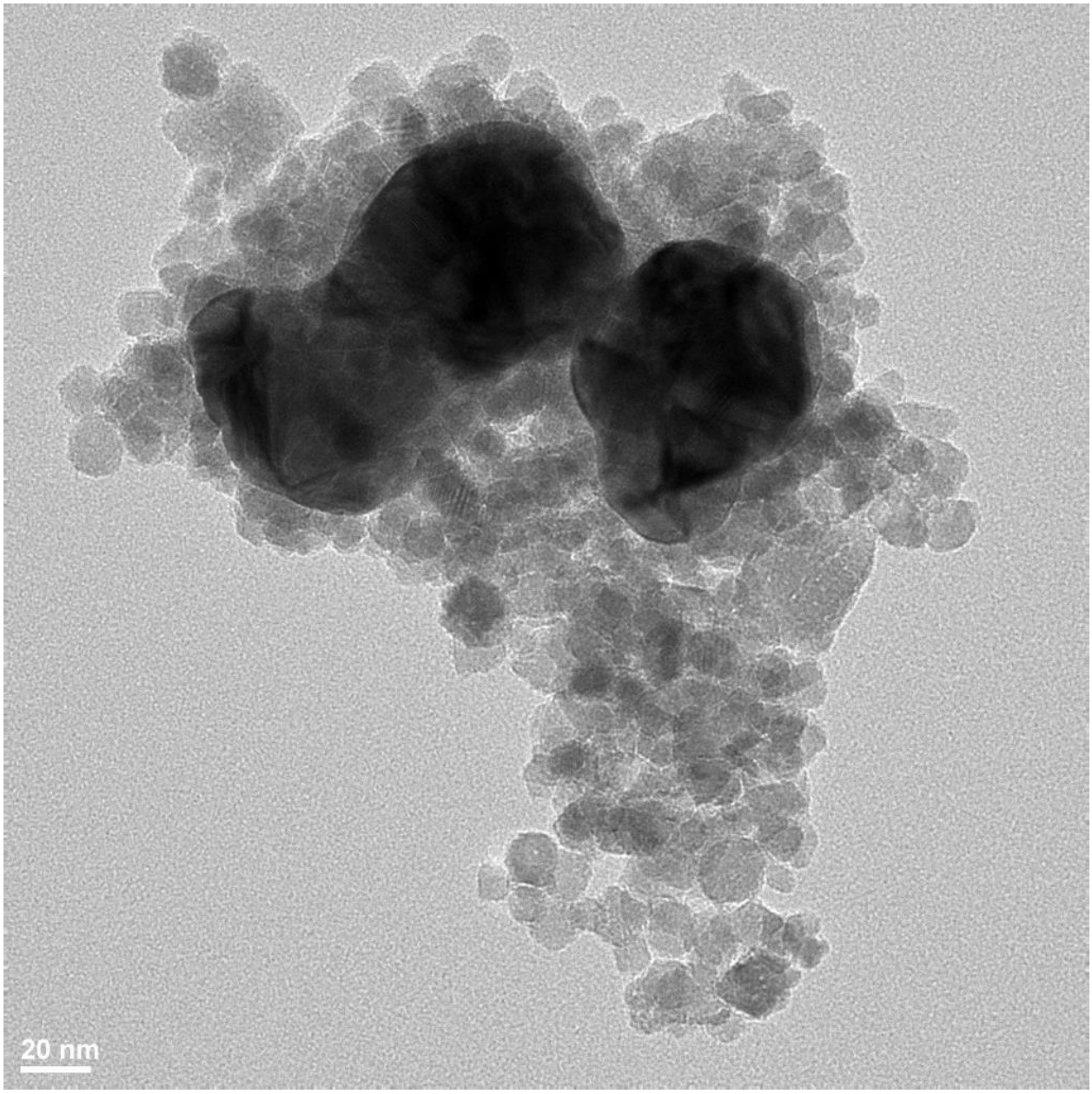

Figure 9. TEM image of Ag-Fe_3O_4@CMC after 6 catalytic cycles.

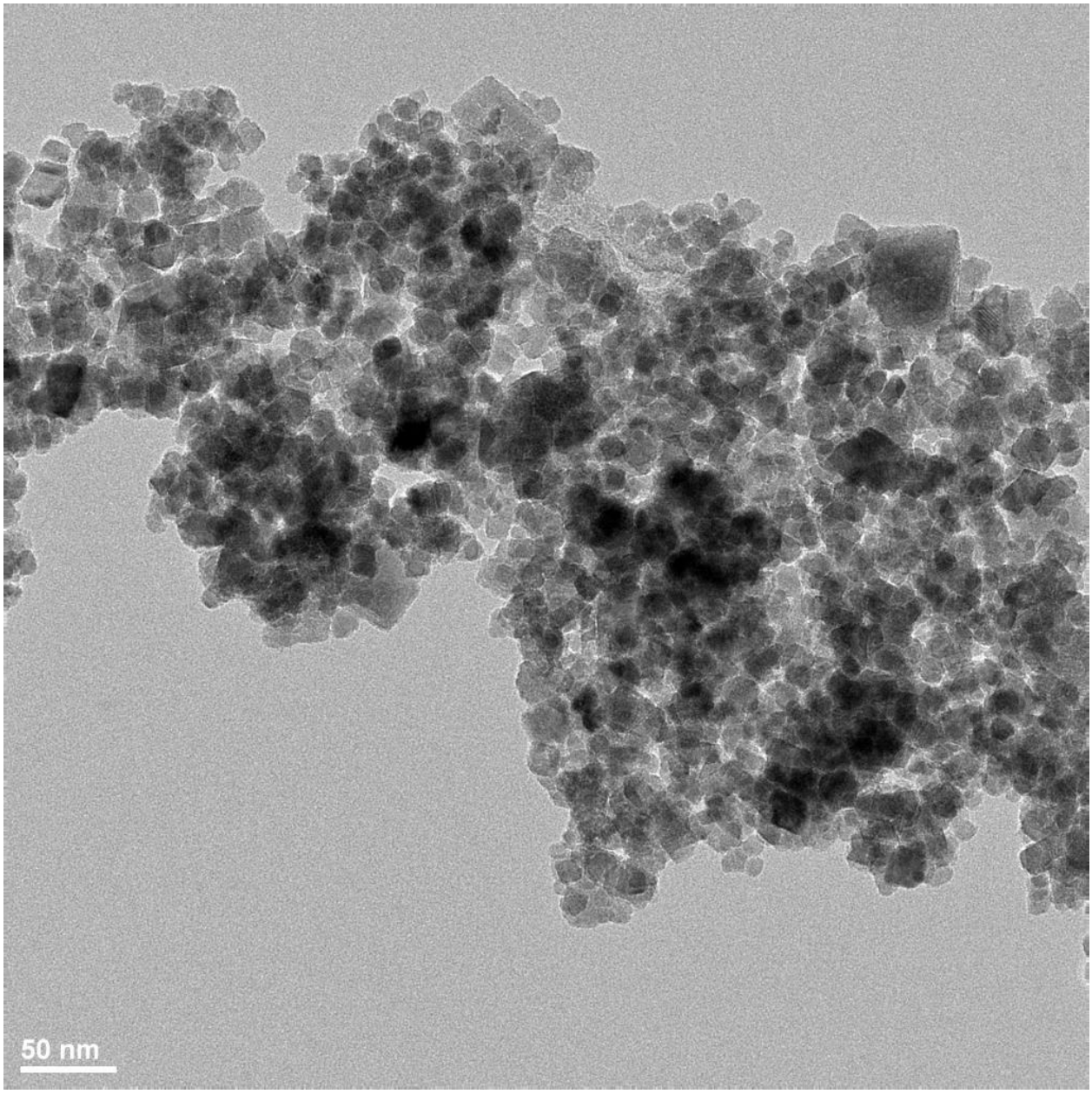

Figure 10. TEM image of Ag-Fe_3O_4@CMC after 6 catalytic cycles.

TEM images of the catalyst after 6 catalytic cycles showed the disappearing of small Ag NPs, though silver is still present in the sample in the form of big aggregates (>60 nm). Due to the small amount of these aggregates and their high discrepancy in shape and size, a meaningful size distribution histogram could not be obtained. The size distribution of the Fe_3O_4 NPs was obtained (Chart 10), showing a growth from 15.3 ± 3.5 nm to 21.8 ± 8.3 nm. The loss of the very small Ag NPs may explain the activity drop observed after the 6th cycle.

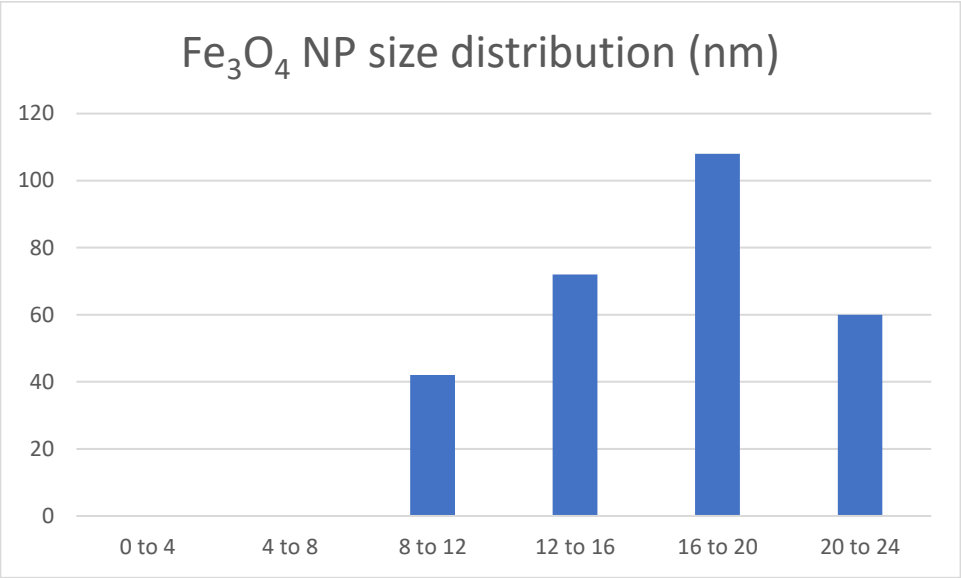

Chart 10. Fe_3O_4 NP size distribution in the catalyst after 6 cycles.

ICP measurements were done on the fresh catalyst, as well on the washing solutions and the organic product after the reaction (Scheme 215). The catalyst before use contained 4.3 wt% Ag and 86 wt% Fe. This revealed that 20% of the silver introduced was lost during the synthesis, possibly due to an incomplete grafting of Ag NPs within Ag@CMC, or to the absence of Fe_3O_4 NPs in some regions of the Ag-Fe_3O_4@CMC. Ag could not be detected in the organic product solution, while Fe was present in negligible quantity (0.1 ppm). Similar quantities were observed after each cycle for the aqueous phase for the 5 cycles. Therefore, we can conclude that activity loss stems from Ag NP aggregation rather than leaching Ag in solution.

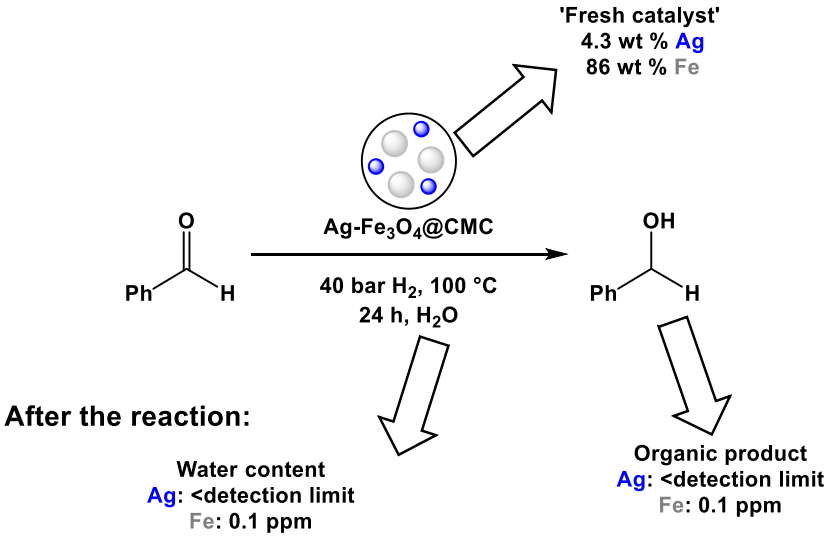

Scheme 215. ICP measurement on Ag-Fe_3O_4@CMC, washing solutions and the organic product after reaction.

Control experiments helped identifying the active species for the reaction (Table 5).

Entry	Conditions	Crude NMR yield (%)
1	No catalyst	0% yield
2	Fe_3O_4@CMC (30 mol% Fe)	0% yield
3	$AgNO_3$ (15 mol% Ag)	0% yield
4	$AgNO_3$ and CMC (15 mol% Ag, 8 mg CMC)	>99% yield
5	CMC only	0% yield

Reaction: 0.33 mmol benzaldehyde, 9 mL H_2O, 40 bar H_2, 100 °C, 24 h.

Table 5. Control experiments.

No activity was detected in the absence of any catalyst (Table 5, entry 1) or if Ag was absent (Table 5, entry 2). However $AgNO_3$ salts alone were not effective, proving that activity in the homogeneous form requires the use of specific ligands, as we previously established.[45] Interestingly, an active hydrogenation catalyst could be generated *in situ* by adding $AgNO_3$ to CMC in the reaction solution (Table 5, entries 3 and 4). Indeed, under reducing condition, it is expected that Ag NPs can form directly into CMC and behave in a similar fashion to the ones made under microwave irradiation. TEM images of the NPs generated form this reaction are

given below (Figure 11, Figure 12, Chart 11), showing highly polydisperse and aggregated Ag NPs. At last, the organic matrix alone (CMC) could not reduce aldehyde on its own (Table 5, entry 5). Overall, this information strongly suggests that Ag NPs are the active species in the reaction.

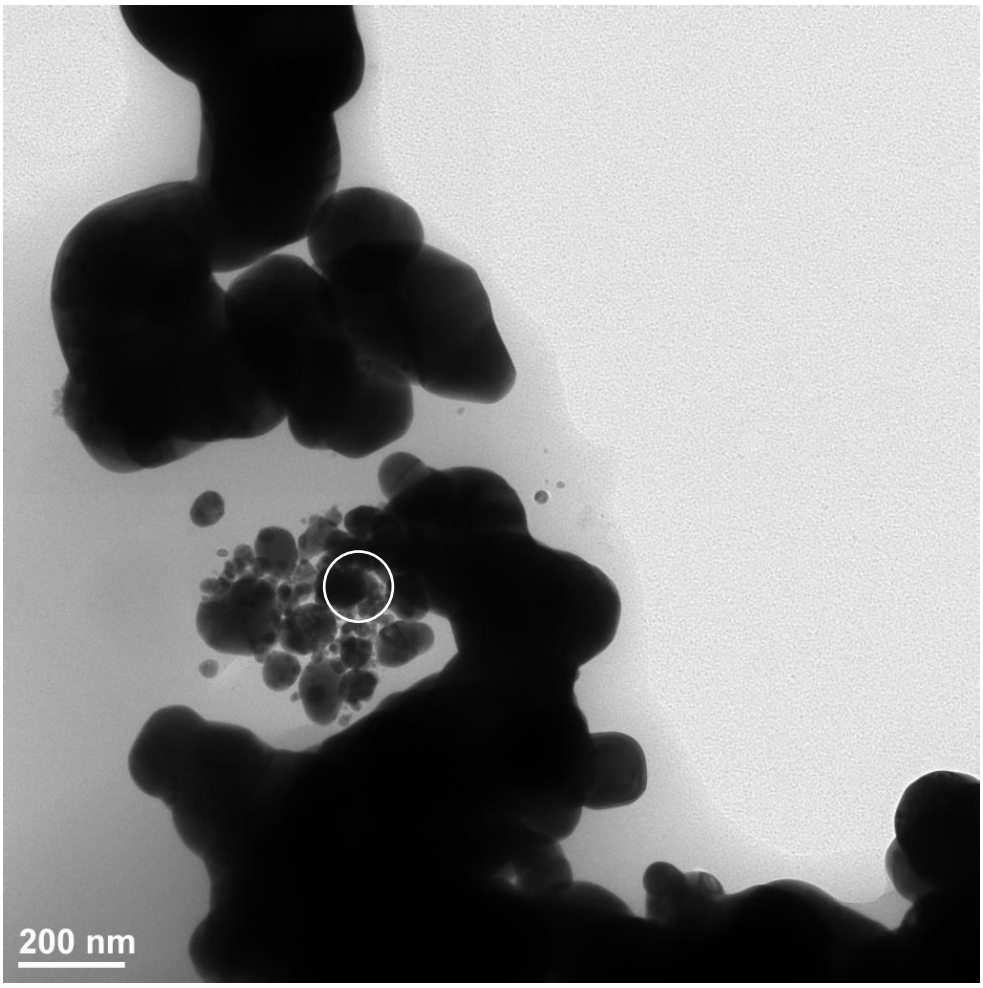

Figure 11. TEM image of $AgNO_3$ and CMC after a hydrogenation reaction. The circle shows the position measured by EDS

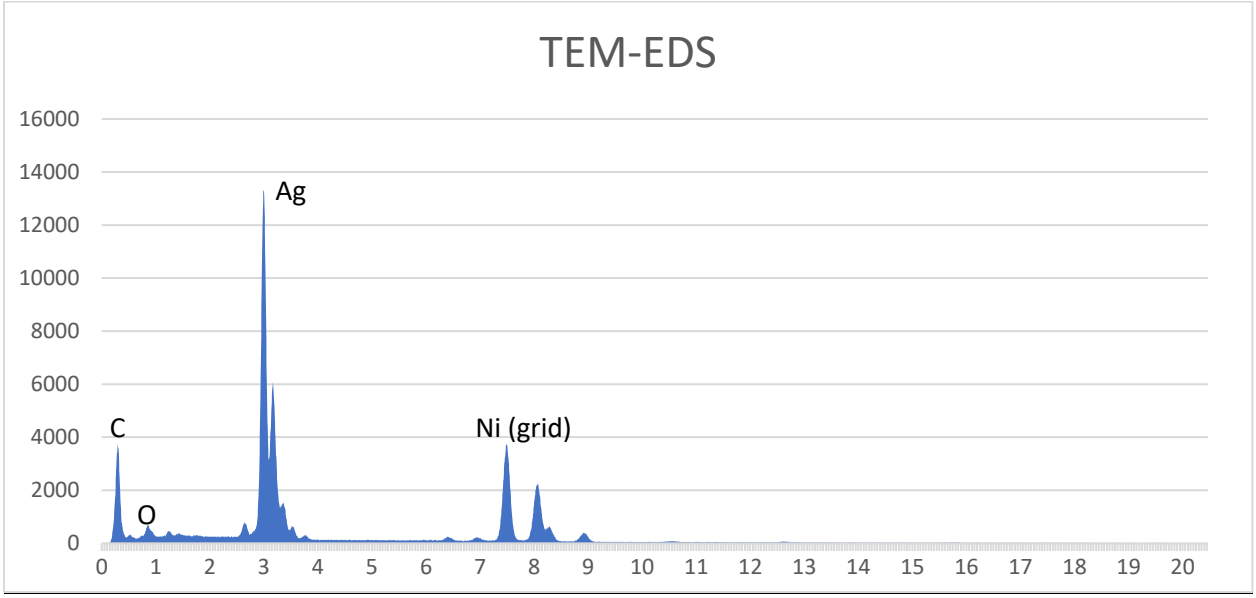

Chart 11. EDS of Figure 11

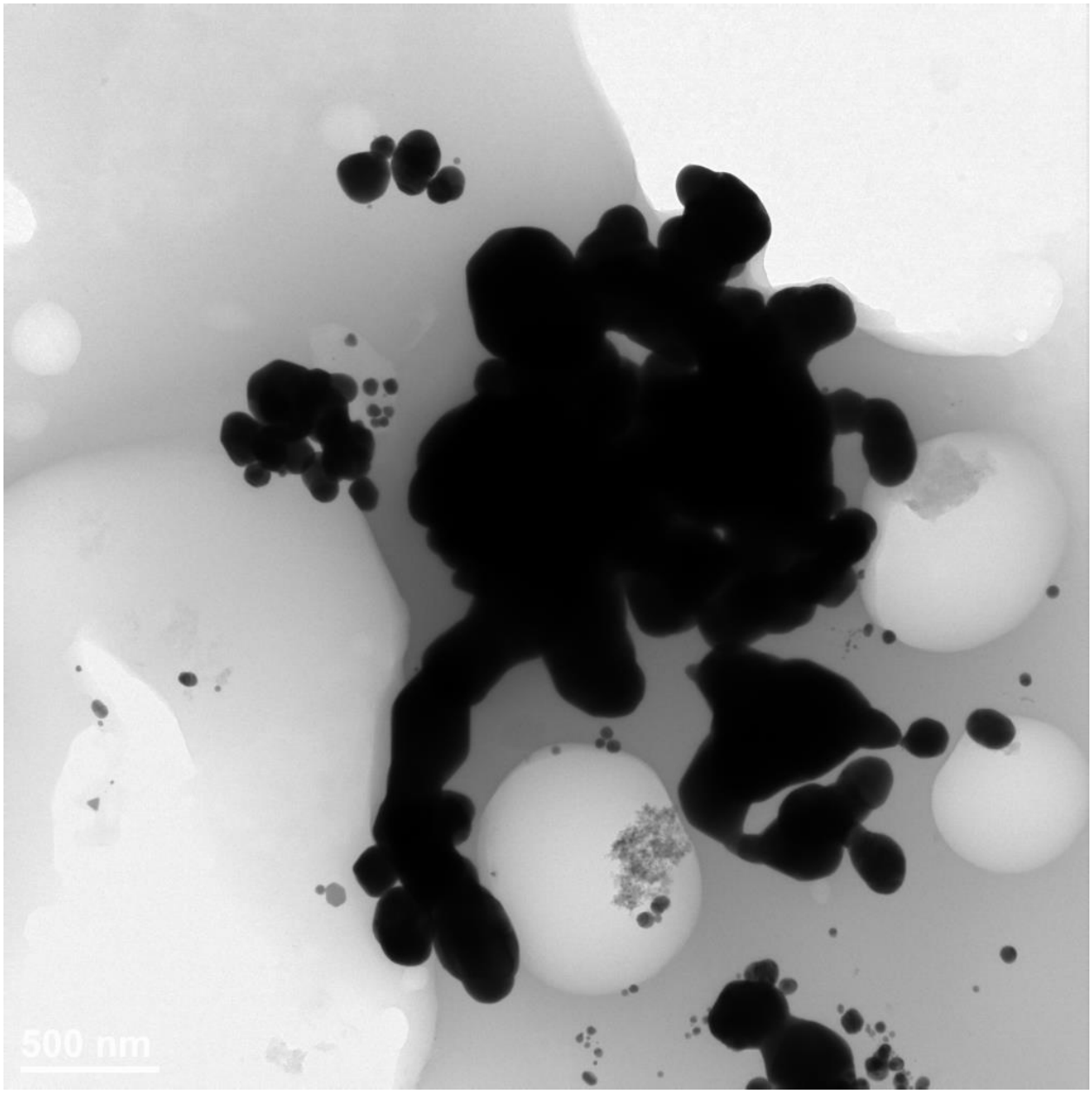

Figure 12. TEM image of $AgNO_3$ and CMC after a hydrogenation reaction.

The oxidation of aldehydes was also tried using the same catalyst. Directly using our system for the reaction afforded excellent yields under mild conditions for benzaldehyde and 4-hydroxybenzaldehyde (Scheme 216, Table 6).

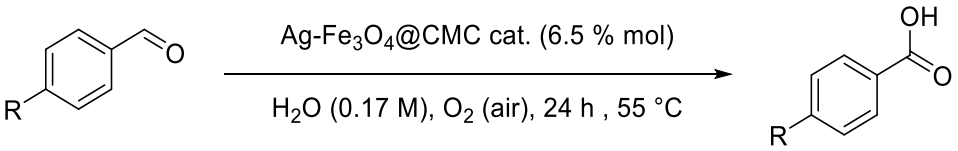

Scheme 216. Ag-Fe_3O_4@CMC-catalyzed aldehyde oxidation in water.

Entry	Reagent	Product	Crude NMR yield (%) (yield without the catalyst in parentheses)
1	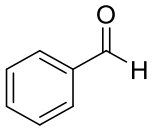	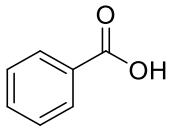	>99 % (80%)
2	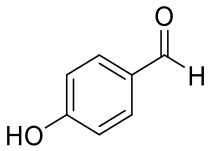	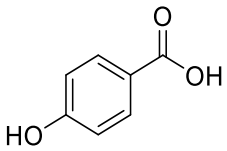	>99 % (0%)

Reaction conditions: 0.33 mmol benzaldehyde, 6.5 mol% Ag-Fe_3O_4@CMC catalyst, 2 mL H_2O, 40 bar H_2, 55 °C, 24 h

Table 6. Ag-Fe_3O_4@CMC-catalyzed aldehyde oxidation in water.

3.6 Conclusion

This work explored the microwave-assisted synthesis of magnetic Ag NPs supported on to CMCs for the catalytic hydrogenation and oxidation of carbonyl compounds in water. A very fast and efficient method for synthesizing the nanocatalyst, Ag-Fe_3O_4@CMC, using microwave is proposed, which should give new possibilities for synthesizing magnetically recoverable catalysts. Notably, CMC provided a cheap and benign capping agent for the nanoparticle synthesis and microwave heating ensures a quick and efficient grafting. The catalyst was as active as its homogeneous counterpart for hydrogenation and could be easily separated and recycled up to 5 times. This is the first example for this application according to our literature survey. Excellent yields were reported for benzaldehyde derivatives, though hydrophobic substrates and sterically hindered ketones had shown poor reactivity.

3.7 Experimental

The catalyst characterization was conducted using TEM, energy dispersive X-ray spectroscopy (EDS), X-ray photoelectron spectroscopy (XPS), thermogravimetric analysis (TGA), XRD, inductively coupled plasma optical emission spectrometry (ICP-OES) and high-

angle annular dark field-TEM (HAADF-TEM). All reactants were purchased from Sigma Aldrich and used as received. When relevant, aldehydes were purified from their oxidation contamination product by distillation. The transmission electron microscopy (TEM) samples were deposited on 400 mesh carbon coated copper grids supplied by Electron Microscopy Sciences. The analyses were performed on the Tecnai 12 microscope (FEI electron optics) equipped with a Lab6 filament at 120kV, equipped with Gatan 792 Bioscan 1k x 1k Wide Angle Multiscan CCD Camera (Gatan Inc.); and FEI G2 F20 Cryo-S/TEM microscope (FEI, Inc) at 200kV, equipped with Gatan Ultrascan 4k x 4k Digital (CCD) Camera System at different magnifications corresponding to different pixel size (defocus level ranging from − 2.5 to − 4.5 μm). ICP measurements were taken using a Thermo ICP-OES to measure Ag content at the elemental wavelength of 328.068nm and Fe content at the elemental wavelength of 238.204 nm. XPS was performed on a VG ESCALAB 3 MKII spectrometer (VG, Thermo Electron Corporation, UK) equipped with an Mg Kα source. XRD was performed using the Bruker D2 Phaser diffractometer using as CuKα source. The catalyst was prepared with a Biotage® Initiator Classic microwave reactor. All hydrogenation reactions were carried out in a Parr Instruments 5000 Series Multiple Reactor System. All reactions were carried out in an oxygen-free glovebox, except where noted, and all solvents were de-gassed for 20 minutes prior to use.

Preparation of Ag@FeSCmP. Commercial FeCSmPs (mesh 326, 350 mg) were suspended in H_2O (35 mL), followed by the slow addition of a freshly made aqueous solution of $AgNO_3$ (213 mg, 20 mol% Ag/Fe, 30mL H_2O) under sonication and inert atmosphere. The resulting mixture was sonicated for 30 minutes. Then the magnetic NPs were thoroughly rinsed with H_2O and EtOH three times, using an external magnet. Ag@FeSCmP was then dried overnight under vacuum.

Preparation of a $Ag(NH_3)_2^+$ solution (60 mM in water). Under air, NH_4OH (80 mg, 28 % NH_3 in water, c.a. 1.3 mmol) was added to an aqueous solution of $AgNO_3$ (30 mg, 0.18 mmol in 3 mL). The solution turned yellow upon ammonia addition, and quickly turned back to a translucent solution upon stirring. It was left to stir at r.t. for 30 minutes under the dark. The resulting translucent solution was degassed with Ar for 5 minutes before being transferred to the glovebox.

Preparation of a Ag@CMC suspension (300 mg/mmol m_{CMC}/n_{Ag} ratio). In a 5 mL microwave vial, the $Ag(NH_3)_2^+$ solution (2 mL, 60 mM) was added to a carboxymethyl cellulose sodium salt solution (3.6 mL, 10 g/L in water). The vial was capped and the solution was irradiated under microwave irradiation at 100 °C for 5 min. The heating time is defined when the desired temperature is reached. A pressure/temperature/time profile of a typical microwave reaction is shown below (Figure 13), showing a slight pressure build-up (up to 2 bar) during the reaction.

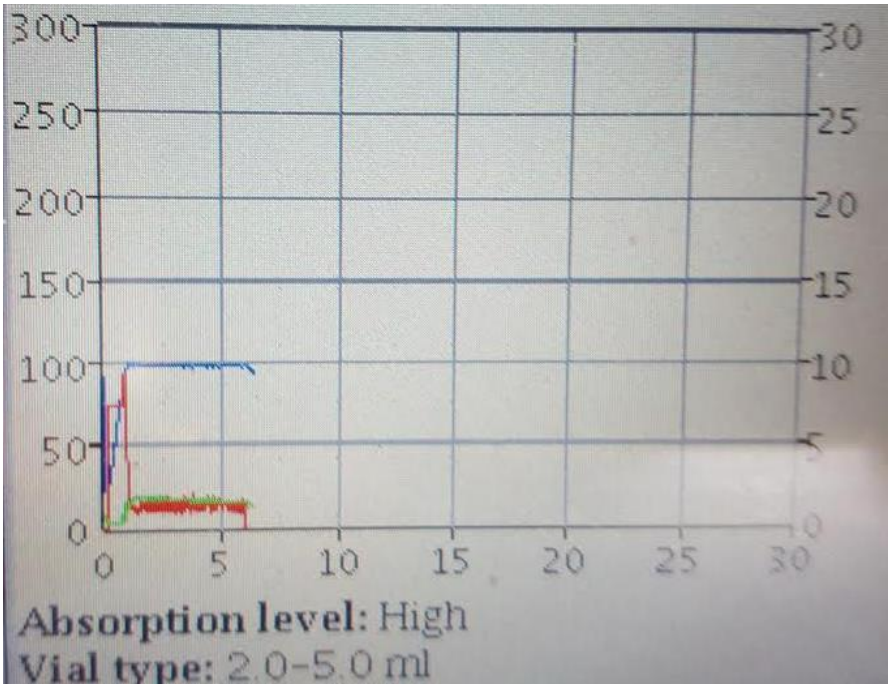

Figure 13. A typical microwave temperature/pressure/time profile (power = red, temperature = blue, pressure = green (axis on the right))

Grafting of Fe_3O_4 on Ag@CMC (39 mg/mmol m_{CMC}/n_{Fe} ratio, Ag/Fe_3O_4 theoretical molar ratio: 1/8). In a 5 mL microwave vial, the iron salts were loaded: $FeSO_4 \cdot 7H_2O$ (53 mg, 0.20 mmol), $FeCl_3 \cdot 6H_2O$ (102 mg, 0.40 mmol) and H_2O (0.9 mL). The solution was stirred a few seconds until it turns into a homogeneous orange translucent solution. Then Ag@CMC (1.2 mL) suspension was added under heavy stirring and NaOH (1.88 mL, 1.25 M) was added drop by drop to the solution, at which point black NPs formed quickly. It was stirred for an additional 5 min under room temperature before being capped and put to microwave at 100 °C

for 5 min. These NPs were then washed three times with water while held to a permanent magnet before being used directly for catalytic tests. Alternatively, they can be washed with ethanol and dried overnight in a vacuum oven for characterization.

Aldehyde hydrogenation. A typical reaction consisted of the re-suspension of the NPs in 9 mL H_2O in a glass vial followed by the addition of the substrate (0.33 mmol). The vial was loaded in a stainless steel autoclave reactor. The solution was purged three times with hydrogen. Under 40 bars of H_2, the reaction mixture was stirred for 24 h at 100 °C. Then the reaction was allowed to cool to room temperature. After carefully releasing the hydrogen, the catalyst was retrieved with a permanent magnet. The aqueous phase was saturated with sodium chloride and extracted with ethyl acetate (3 × 10 mL). The combined organic phase was dried with $MgSO_4$ and concentrated *in vacuo* and the crude oil was analyzed by ^{1}H NMR. For recycling experiments, the catalyst was separated from the liquid phase using an external permanent magnet and washed three times with ethyl acetate and water under air before immediate re-use.

Product isolation. In order to ascertain the nature of the hydrogenation product of the model reaction (using benzaldehyde as a substrate), it was isolated and characterized by ^{1}H NMR. Analytical thin-layer chromatography (TLC) was performed using E. Merck silica gel 60 F254 precoated plates (0.25 mm). Flash chromatography was performed with Biotage Isolera One Flash Purification System, using Biotage SNAP Ultra 25g prepared column. Pure benzyl alcohol was obtained as a colorless oil in 93% isolated yield (33 mg). ^{1}H NMR (Figure 14, 500 MHz, $CDCl_3$, 20 °C): δ 7.37 (m, 4H), δ 7.30 (m, 1H), δ 4.69 (s, 4H).

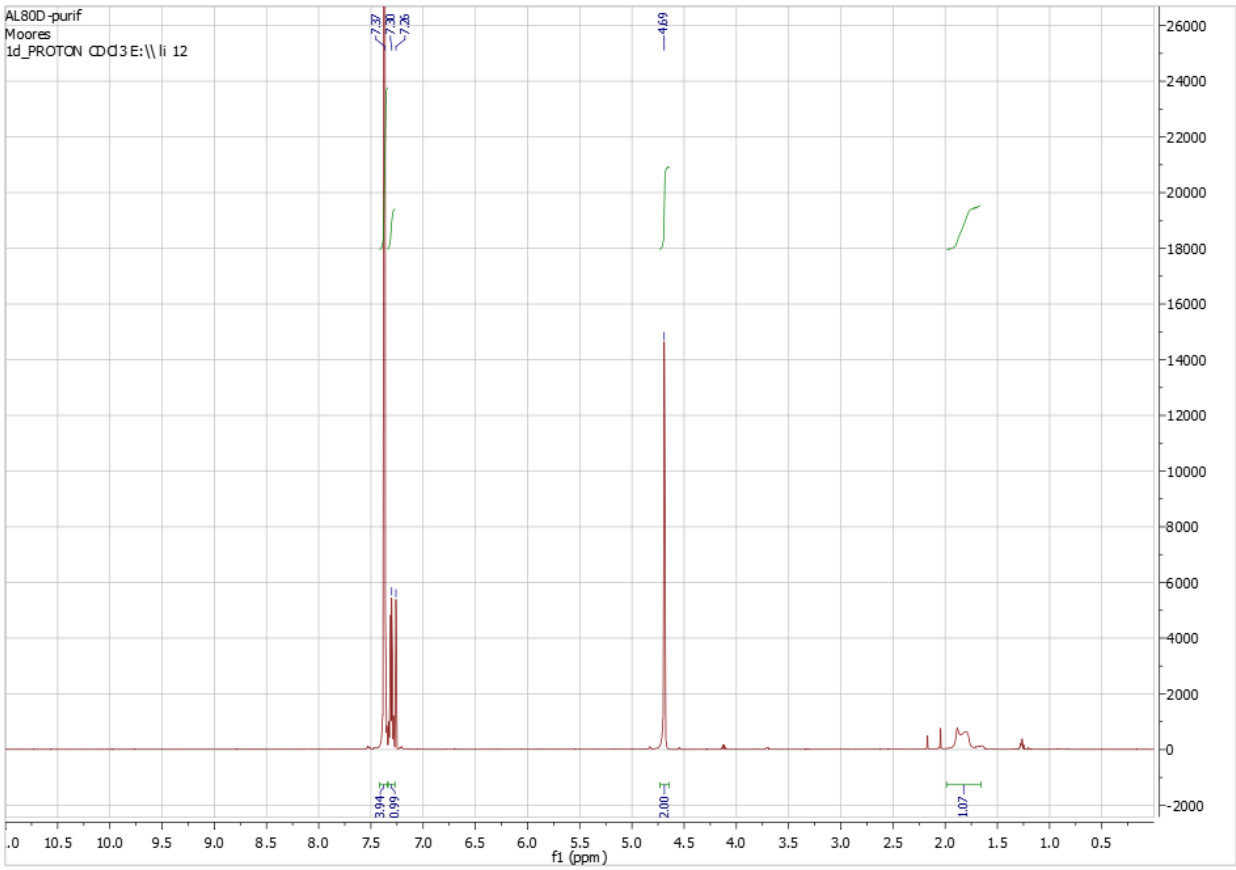

Figure 14. ^{1}H NMR of isolated benzyl alcohol.

Aldehyde oxidation. A typical reaction consisted of the re-suspension of the NPs in 2 mL H_2O in a 5 mL microwave vial followed by the addition of the substrate (0.33 mmol). The vials was capped under air, then the reaction mixture was stirred for 24 h at 55 °C in an oil bath. Then the reaction was allowed to cool to room temperature. After opening the vial, the catalyst was retrieved with a permanent magnet. The aqueous phase was saturated with sodium chloride, acidified with HCl and extracted with ethyl acetate (3 × 10 mL). The combined organic phase was dried with $MgSO_4$ and concentrated *in vacuo* and the crude oil was analyzed by ^{1}H NMR.

3.8 References

1. Astruc, D.; Lu, F.; Aranzaes, J. R., Nanoparticles as recyclable catalysts: the frontier between homogeneous and heterogeneous catalysis. *Angew. Chem. Int. Ed.* **2005,** *44* (48), 7852-7872.

2. Claus, P.; Hofmeister, H., Electron microscopy and catalytic study of Silver catalysts: Structure sensitivity of the hydrogenation of crotonaldehyde. *J. Phys. Chem. B* **1999,** *103* (14), 2766-2775.
3. Shi, L.; Liu, Y.; Liu, Q.; Wei, B.; Zhang, G., Selective reduction of aldehydes and ketones to alcohols with ammonia borane in neat water. *Green Chem.* **2012,** *14* (5), 1372-1375.
4. Claus, P., Selective hydrogenation of α,β-unsaturated aldehydes and other C=O and C=C bonds containing compounds. *Top. Catal.* **1998,** *5* (1), 51-62.
5. Claus, P.; Bron, M.; Tschener, D.; Knop-Gericke, A.; Jentoft, F. C.; Kröhnert, J.; Hohmeyer, J.; Volckmar, C.; Steinhauer, B.; Schlögl, R., Silver as acrolein hydrogenation catalyst: intricate effects of catalyst nature and reactant partial pressures. *Phys. Chem. Chem. Phys* **2007,** *9*, 3559-3569.
6. Claus, P.; Bron, M.; Teschner, D.; Wild, U.; Steinhauer, B.; Knop-Gericke, A.; Volckmar, C.; Wootsch, A.; Schlögl, R., Oxygen-induced activation of silica supported Silver in acrolein hydrogenation. *Appl. Catal., A* **2008,** *341*, 127.
7. Claus, P.; Hohmeyer, J.; Kondratenko, E. V.; Bron, M.; Kröhnert, J.; Jentoft, F. C.; Schlögl, R., Activation of dihydrogen on supported and unsupported Silver catalysts. *J. Catal.* **2009,** *269*, 5-14.
8. Lang, H.; Claus, P.; Steffan, M.; Jakob, A., Silica supported Silver nanoparticles from a Silver(I) carboxylate: Highly active catalyst for regioselective hydrogenation. *Catal. Commun.* **2009,** (10), 437–441.
9. Yadav, G. D.; Mewada, R. K., Selective hydrogenation of acetophenone to 1-phenyl ethanol over nanofibrous Ag-OMS-2 catalysts. *Catal. Today* **2012,** *198* (1), 330-337.
10. De Vos, D. E.; Mertens, P. G. N.; Cuypers, F.; Vandezande, P.; Ye, X.; Verpoort, F.; Vankelecom, I. F. J., Ag^0 and Co^0 nanocolloids as recyclable quasihomogeneous metal catalysts for the hydrogenation of α,β-unsaturated aldehydes to allylic alcohol fragrances. *Appl. Catal., A* **2007,** *325* (1), 130-139.
11. Feng, Y.; Xue, W.; Yin, H.; Meng, M.; Wang, A.; Liu, S., Selective oxidation of 1,2-propanediol to lactic acid catalyzed by hydroxyapatite-supported Pd and Pd-Ag nanoparticles. *RSC Adv.* **2015,** *5* (129), 106918-106929.
12. Lu, A.-H.; Salabas, E. L.; Schüth, F., Magnetic nanoparticles: Synthesis, protection, functionalization, and application. *Angew. Chem. Int. Ed.* **2007,** *46* (8), 1222-1244.
13. Gawande, M. B.; Monga, Y.; Zboril, R.; Sharma, R. K., Silica-decorated magnetic nanocomposites for catalytic applications. *Coord. Chem. Rev.* **2015,** *288*, 118-143.
14. Mrowczynski, R.; Nan, A.; Liebscher, J., Magnetic nanoparticle-supported organocatalysts - an efficient way of recycling and reuse. *RSC Adv.* **2014,** *4* (12), 5927-5952.
15. Govan, J.; Gun'ko, Y., Recent advances in the application of magnetic nanoparticles as a support for homogeneous catalysts. *Nanomaterials* **2014,** *4* (2), 222-241.
16. Wang, D.; Astruc, D., Fast-growing field of magnetically recyclable nanocatalysts. *Chem. Rev.* **2014**, 6949–6985.
17. Rossi, L. M.; Costa, N. J. S.; Silva, F. P.; Wojcieszak, R., Magnetic nanomaterials in catalysis: advanced catalysts for magnetic separation and beyond. *Green Chem.* **2014,** *16* (6), 2906-2933.
18. Varma, R. S., Nano-catalysts with magnetic core: sustainable options for greener synthesis. *Sustainable Chem. Processes* **2014,** *2* (11).
19. Cheng, T.; Zhang, D.; Li, H.; Liu, G., Magnetically recoverable nanoparticles as efficient catalysts for organic transformations in aqueous medium. *Green Chem.* **2014,** *16* (7), 3401-3427.

20. Nasir Baig, R. B.; Varma, R. S., Magnetic Carbon-supported Palladium nanoparticles: An efficient and sustainable catalyst for hydrogenation reactions. *ACS Sustainable Chem. Eng.* **2014,** *2* (9), 2155-2158.
21. Hudson, R.; Feng, Y.; Varma, R. S.; Moores, A., Bare magnetic nanoparticles: sustainable synthesis and applications in catalytic organic transformations. *Green Chem.* **2014,** *16* (10), 4493-4505.
22. Gawande, M. B.; Luque, R.; Zboril, R., The rise of magnetically recyclable nanocatalysts. *ChemCatChem* **2014,** *6* (12), 3312-3313.
23. Polshettiwar, V.; Luque, R.; Fihri, A.; Zhu, H.; Bouhrara, M.; Basset, J.-M., Magnetically recoverable nanocatalysts. *Chem. Rev.* **2011,** *111* (5), 3036-3075.
24. Daou, T. J.; Pourroy, G.; Bégin-Colin, S.; Grenèche, J. M.; Ulhaq-Bouillet, C.; Legaré, P.; Bernhardt, P.; Leuvrey, C.; Rogez, G., Hydrothermal synthesis of monodisperse magnetite nanoparticles. *Chem. Mater.* **2006,** *18* (18), 4399-4404.
25. Hudson, R.; Chazelle, V.; Bateman, M.; Roy, R.; Li, C.-J.; Moores, A., Sustainable Synthesis of Magnetic Ruthenium-Coated Iron Nanoparticles and Application in the Catalytic Transfer Hydrogenation of Ketones. *ACS Sustainable Chem. Eng.* **2015,** *3* (5), 814-820.
26. Hudson, R.; Li, C.-J.; Moores, A., Magnetic Copper-Iron nanoparticles as simple heterogeneous catalysts for the azide-alkyne click reaction in water. *Green Chem.* **2012,** *14* (3), 622-624.
27. Zhou, S.; Johnson, M.; Veinot, J. G. C., Iron/Iron oxide nanoparticles: a versatile support for catalytic metals and their application in Suzuki-Miyaura cross-coupling reactions. *Chem. Commun.* **2010,** *46* (14), 2411-2413.
28. Shafranovsky, E. A.; Petrov, Y. I., Aerosol Fe Nanoparticles with the Passivating Oxide Shell. *J. Nanopart. Res.* **2004,** *6* (1), 71-90.
29. Masnadi, M.; Yao, N.; Braidy, N.; Moores, A., Cu(II) galvanic reduction and deposition onto Iron nano- and microparticles: Resulting morphologies and growth mechanisms. *Langmuir* **2015,** *31* (2), 789-798.
30. Filippo, E.; Serra, A.; Manno, D., Self-assembly and branching of sucrose stabilized Silver nanoparticles by microwave assisted synthesis: From nanoparticles to branched nanowires structures. *Colloids Surf., A* **2009,** *348* (1–3), 205-211.
31. Raveendran, P.; Fu, J.; Wallen, S. L., A simple and "green" method for the synthesis of Au, Ag, and Au-Ag alloy nanoparticles. *Green Chem.* **2006,** *8* (1), 34-38.
32. Liu, F.-K.; Huang, P.-W.; Chu, T.-C.; Ko, F.-H., Gold seed-assisted synthesis of Silver nanomaterials under microwave heating. *Mater. Lett.* **2005,** *59* (8–9), 940-944.
33. Zhao, X.; Xia, Y.; Li, Q.; Ma, X.; Quan, F.; Geng, C.; Han, Z., Microwave-assisted synthesis of Silver nanoparticles using Sodium alginate and their antibacterial activity. *Colloids Surf., A* **2014,** *444* (0), 180-188.
34. Kahrilas, G. A.; Wally, L. M.; Fredrick, S. J.; Hiskey, M.; Prieto, A. L.; Owens, J. E., Microwave-assisted green synthesis of Silver nanoparticles using orange peel extract. *ACS Sustainable Chem. Eng.* **2014,** *2* (3), 367-376.
35. Cinelli, M.; Coles, S. R.; Nadagouda, M. N.; Blaszczynski, J.; Slowinski, R.; Varma, R. S.; Kirwan, K., A green chemistry-based classification model for the synthesis of Silver nanoparticles. *Green Chem.* **2015,** *17* (5), 2825-2839.
36. Nadagouda, M. N.; Speth, T. F.; Varma, R. S., Microwave-assisted green synthesis of silver nanostructures. *Acc. Chem. Res.* **2011,** *44* (7), 469-478.
37. Gawande, M. B.; Shelke, S. N.; Zboril, R.; Varma, R. S., Microwave-Assisted Chemistry: Synthetic Applications for Rapid Assembly of Nanomaterials and Organics. *Acc. Chem. Res.* **2014,** *47* (4), 1338-1348.

38. Raveendran, P.; Fu, J.; Wallen, S. L., Completely "Green" Synthesis and Stabilization of Metal Nanoparticles. *J. Am. Chem. Soc.* **2003,** *125* (46), 13940-13941.
39. Kumar, S. V.; Bafana, A. P.; Pawar, P.; Rahman, A.; Dahoumane, S. A.; Jeffryes, C. S., High conversion synthesis of <10 nm starch-stabilized silver nanoparticles using microwave technology. *Scientific Reports* **2018,** *8* (1), 5106.
40. Nadagouda, M. N.; Varma, R. S., Synthesis of thermally stable carboxymethyl cellulose/metal biodegradable nanocomposites for potential biological applications. *Biomacromolecules* **2007,** *8* (9), 2762-2767.
41. Bo, L.; Xiaoyun, L.; Canfeng, Z.; Xiaoying, W.; Runcang, S., Facile and green synthesis of Silver nanoparticles in quaternized carboxymethyl chitosan solution. *Nanotechnology* **2013,** *24* (23), 235601.
42. Horikoshi, S.; Abe, H.; Torigoe, K.; Abe, M.; Serpone, N., Access to small size distributions of nanoparticles by microwave-assisted synthesis. Formation of Ag nanoparticles in aqueous carboxymethylcellulose solutions in batch and continuous-flow reactors. *Nanoscale* **2010,** *2* (8), 1441-1447.
43. Yin, Y.; Li, Z.-Y.; Zhong, Z.; Gates, B.; Xia, Y.; Venkateswaran, S., Synthesis and characterization of stable aqueous dispersions of silver nanoparticles through the Tollens process. *J. Mater. Chem.* **2002,** *12* (3), 522-527.
44. Meléndrez, M. F.; Medina, C.; Solis-Pomar, F.; Flores, P.; Paulraj, M.; Pérez-Tijerina, E., Quality and high yield synthesis of Ag nanowires by microwave-assisted hydrothermal method. *Nanoscale Research Letters* **2015,** *10* (1), 48.
45. Jia, Z.; Zhou, F.; Liu, M.; Li, X.; Chan, A. S. C.; Li, C.-J., Silver-catalyzed hydrogenation of aldehydes in water. *Angew. Chem. Int. Ed.* **2013,** *52* (45), 11871-11874.
46. Tian, L.; Yang, Q.; Jiang, Z.; Zhu, Y.; Pei, Y.; Qiao, M.; Fan, K., Highly chemoselective hydrogenation of crotonaldehyde over Ag-In/SBA-15 fabricated by a modified "two solvents" strategy. *Chem. Commun.* **2011,** *47* (21), 6168-6170.
47. Chiou, J.-R.; Lai, B.-H.; Hsu, K.-C.; Chen, D.-H., One-pot green synthesis of silver/iron oxide composite nanoparticles for 4-nitrophenol reduction. *J. Hazard. Mater.* **2013,** *248-249*, 394-400.
48. Duan, B.; Liu, F.; He, M.; Zhang, L., Ag-Fe_3O_4 nanocomposites@chitin microspheres constructed by in situ one-pot synthesis for rapid hydrogenation catalysis. *Green Chem.* **2014,** *16* (5), 2835-2845.
49. Han, X. X.; Schmidt, A. M.; Marten, G.; Fischer, A.; Weidinger, I. M.; Hildebrandt, P., Magnetic silver hybrid nanoparticles for surface-enhanced resonance raman spectroscopic detection and decontamination of small toxic molecules. *ACS Nano* **2013,** *7* (4), 3212-3220.
50. Massart, R., Preparation of aqueous magnetic liquids in alkaline and acidic media. *IEEE Trans. Magn.* **1981,** *17* (2), 1247-1248.
51. Cirtiu, C. M.; Raychoudhury, T.; Ghoshal, S.; Moores, A., Systematic comparison of the size, surface characteristics and colloidal stability of zero valent Iron nanoparticles pre- and post-grafted with common polymers. *Colloids Surf., A* **2011,** *390* (1–3), 95-104.
52. Eltouny, N. A.; Ariya, P. A., Fe_3O_4 nanoparticles and carboxymethyl cellulose: A green option for the removal of atmospheric benzene, toluene, ethylbenzene, and *o*-xylene (BTEX). *Ind. Eng. Chem. Res.* **2012,** *51* (39), 12787-12795.
53. Komarneni, S.; Hu, W.; Noh, Y. D.; Van Orden, A.; Feng, S.; Wei, C.; Pang, H.; Gao, F.; Lu, Q.; Katsuki, H., Magnetite syntheses from room temperature to 150°C with and without microwaves. *Ceram. Int.* **2012,** *38* (3), 2563-2568.
54. Prieto, P.; Nistor, V.; Nouneh, K.; Oyama, M.; Abd-Lefdil, M.; Díaz, R., XPS study of silver, nickel and bimetallic silver–nickel nanoparticles prepared by seed-mediated growth. *Appl. Surf. Sci.* **2012,** *258* (22), 8807-8813.

55. Mohammad, A. B.; Yudanov, I. V.; Lim, K. H.; Neyman, K. M.; Rösch, N., Hydrogen Activation on Silver: A Computational Study on Surface and Subsurface Oxygen Species. *J Phys. Chem. C* **2008,** *112* (5), 1628-1635.
56. Lim, K. H.; Mohammad, A. B.; Yudanov, I. V.; Neyman, K. M.; Bron, M.; Claus, P.; Rösch, N., Mechanism of Selective Hydrogenation of α,β-Unsaturated Aldehydes on Silver Catalysts: A Density Functional Study. *Journal of Physical Chemistry C* **2009,** *113* (30), 13231-13240.
57. Grosvenor, A. P.; Kobe, B. A.; Biesinger, M. C.; McIntyre, N. S., Investigation of multiplet splitting of Fe 2p XPS spectra and bonding in iron compounds. *Surf. Interface Anal.* **2004,** *36* (12), 1564-1574.
58. Zhang, W.-M.; Wu, X.-L.; Hu, J.-S.; Guo, Y.-G.; Wan, L.-J., Carbon Coated Fe3O4 Nanospindles as a Superior Anode Material for Lithium-Ion Batteries. *Adv. Funct. Mater.* **2008,** *18* (24), 3941-3946.
59. Stolle, A.; Gallert, T.; Schmöger, C.; Ondruschka, B., Hydrogenation of citral: a wide-spread model reaction for selective reduction of α,β-unsaturated aldehydes. *RSC Adv.* **2013,** *3* (7), 2112-2153.

It's on America's tortured brow that Mickey Mouse has grown up a cow
Now the workers have struck for fame because Lennon's on sale again
See the mice in their million hordes from Ibiza to the Norfolk Broads
Rule Britannia is out of bounds
To my mother, my dog, and clowns

Jones, D.R.; Ronson, M.; Bolder, T.; Woodmansey, M.; Wakeman R. Life on Mars?, *Hunky Dory*, **1971**, *4*, 9:43-13:38.

The Ag-Fe_3O_4@CMC system presented in chapter 3 was advantageous in terms of green chemistry with the synthesis of a water-soluble catalyst using microwave irradiation. The use of water was attractive in terms of toxicity and flammability, however it caused product extraction issues in the case of substrates such as 5-HMF. To overcome solubility issues, we then turned to ball-milling, a less researched method in reduction chemistry. In chapter 4 I will present the metal-free and mechanochemical reduction of carbonyls.

4 Mechanochemical metal-free transfer hydrogenation of carbonyls using polymethylhydrosiloxane as hydrogen source

This chapter is based upon one published article. The American Chemical Society granted permission to reprint the published article, as did all co-authors.

Alain Li, Andréanne Segalla, Chao-Jun Li, Audrey Moores, 'Mechanochemical Metal-Free Transfer Hydrogenation of Carbonyls Using Polymethylhydrosiloxane as the Hydrogen Source', *ACS Sustainable Chem. Eng.*, **2017**, *5*, 11752–11760.

4.1 Abstract

We report herein a new methodology for the rapid and selective reduction of carbonyls in the solid phase. By exploiting mechanical energy and using a cheap and air-stable silane, polymethylhydrosiloxane (PMHS), we can reduce a variety of carbonyl compounds, with catalytic amounts of fluorides. A scope of 19 substrates was explored to probe the generality of the method. In addition, an important biomass-based platform chemical, 5-hydroxymethylfurfural (5-HMF) and an insoluble polymer, polyketone, could be reduced with this methodology. A mechanistic study is also presented, suggesting the active role of volatile silane species. This method is particularly appealing to overcome substrate solubility issues and reduce solvent reliance in organic synthesis.

4.2 Introduction

The reduction of carbonyls to alcohols is a key reaction in the chemical industry, spanning from the production of commodity chemicals to pharmaceutical compounds.[1] On the lab scale, this is often done using stoichiometric amounts of hydrides, such as $NaBH_4$ or $LiAlH_4$.[2] Catalytic methods relying on transition metals allowed to unravel the potential of molecular hydrogen gas for this reaction, *via* the development of highly active and chemo-, regio- and enantioselective systems, with high atom-economy.[3] Alternatively, catalytic transfer hydrogenation reactions have been developed, whereby cheap and available hydrogen sources are selected, for instance alcohols, with the advantage of alleviating the need for high pressure.[4] Alternative reducing agents such as sodium formate,[5] Hantzch ester,[6] various isopropoxides,[7] or silanes[8] have been successfully reported. They also pave the way for hydrogen borrowing strategies, as green cascade methodology to build molecular complexity in one-pot.[9]

Polymethylhydrosiloxane (Me_3Si-$(OSiMeH)_nOSiMe_3$, abbreviated as PMHS) was first reported by Nitzsche and Wick in 1957 for the reductive silylation of carbonyls with organotin compounds. As a waste of the silicon industry, PMHS is an inexpensive and abundant chemical with reducing abilities.[10] Contrary to other silanes, it benefits as well from its non-toxicity, moisture stability, and ability for its Si-H bonds to be easily activated under mild conditions.

Since then, it has been explored in solution phase with different activators such as Ti[11] Cu,[12] Fe,[13] Zn,[14] TFA,[15] fluorides,[16] or bases. Typically, Kobayashi *et al.* used stoichiometric amounts of *tert*-butyl ammonium fluoride (TBAF) or KF, at -70 or 0 °C, to perform both the hydrosilylation and the subsequent Si-O bond cleavage (Scheme 217A).[17] Notably, this scheme based on silicon and fluoride chemistry is completely transition metal-free, and parts from the

use of hazardous traditional hydrides. Further developments involved the use of *t*BuOK and KOH to activate PMHS as shown by the Nikonov group.[18] Their mechanistic studies show a base-induced rearrangement of the polymer into shorter volatile hypervalent silicon species, highly active for carbonyl reduction. PMHS is also a suitable reagent for the chiral reduction of carbonyls.[19]

Beyond carbonyl reduction, silane chemistry has recently been highlighted as a powerful reagent to develop metal-free and non-toxic organic pathways. Cantat *et al.* reported the conversion of CO_2 to afford amine formylation products[20] or formamidine derivatives, using PMHS.[21] They also used Si-H bond as part of a frustrated Lewis Pair (FLP) scheme to reduce CO_2.[22] The Beller group showed as well the convenient conversion of amides into amines with PHMS.[23]

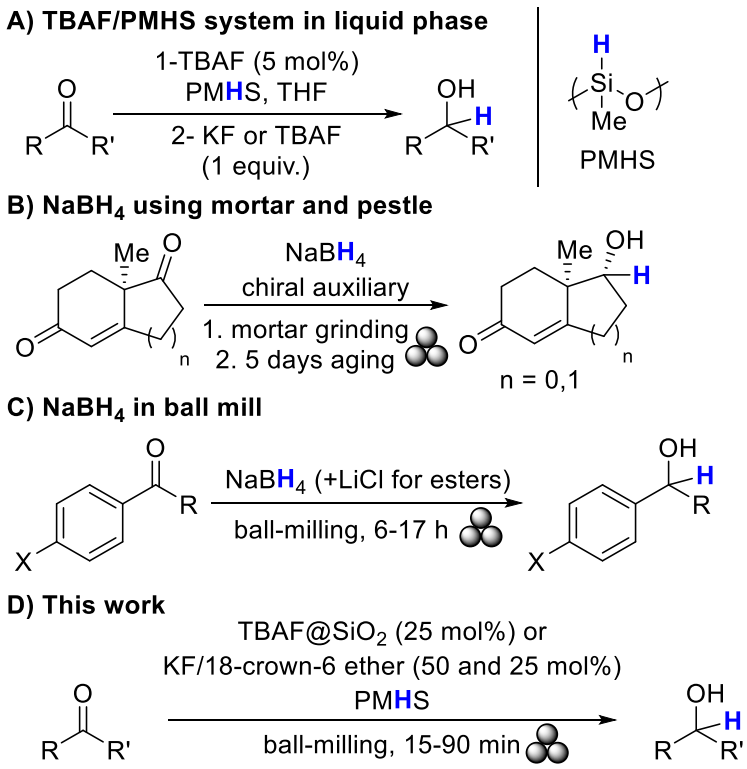

Scheme 217. Selected liquid phase and mechanochemical strategies for carbonyl reduction.

All these methods however call for the use of solvents, either to ensure good gas miscibility, since gas-liquid mixing is often rate-determining,[24] or as the "hydrogen" provider itself.[25] Yet, solvents contribute significantly to waste generation in the chemical enterprise. For instance, an estimation published by Glaxo-Smith-Kline revealed that solvents represented 85% of the total mass of chemicals used in pharmaceutical manufacture.[26] Recently, mechanochemistry, a

method enabling reactions in solid phase, with limited amounts or no solvents, and using mechanical energy emerged as an interesting alternative to liquid-phase methodologies.[27] It also offers new solutions for addressing issues related to recalcitrant or insoluble substrates.[28]

Despite the rising popularity of ball-milling, it has been seldom investigated for carbonyl reduction methodology (see section 1.3.2). Toda *et al.* reported the reduction of ketones using $NaBH_4$ by mortar grinding and aging in a dry atmosphere for 5 days.[29] They could synthesize a range of chiral hydroxyketones of synthetic interest with 100% *ee* using (+)-taddol as a chiral auxiliary Scheme 217B). Mack and co-authors reported the use of $NaBH_4$ in ball milling to reduce a wide range of aromatic carbonyls.[30] By adding LiCl, they could generate $LiBH_4$ *in situ* and reduce esters, although after several hours of milling (Scheme 217C). This system was further studied by Naimi-Jamal *et al.*,[31] who analyzed the sodium tetraalkoxyborate intermediates as well as the selectivity of the reaction. Alternatively, Wang *et al.* performed the reductive amination of aromatic aldehydes, using Hantzch ester as a reductant and zinc chloride as a catalyst.[32] These examples are, to the best of our knowledge, the only examples of solid-state reduction of carbonyls and imines.[33] Although $NaBH_4$ and the Hantzch ester are highly popular, they suffer from safety issues for the former,[34] and toxicity issues for the latter, including the generation of pyridine derivative as byproducts.[35]

In our continued efforts to develop greener chemical reductions, we herein present the reduction of carbonyls using ball milling. We first tested a few biomass-derived molecules (cellulose, lignin, sorbitol and glucose), as well as paraformaldehyde as hydrogen donors, activated by KOH or NaOH. Then, we turned to PMHS, as an industrial waste material, stable and non-toxic hydrogen source activated using catalytic amounts of solid fluorides (TBAF@SiO_2). In the Müller-Rochow process for the synthesis of Me_2SiCl_2, the main feedstock for the silicone industry, $MeHSiCl_2$ is obtained as a byproduct (up to 4 wt% amounts).[36] Upon hydrolysis, this species can be polymerized easily into PMHS. This method afforded moderate to excellent yields on a range of substrates, in short reaction times. Importantly, it opened avenues to address separation issues in the context of 5-hydroxymethylfurfural (5-HMF) hydrogenation and solubility issues for a polyketone reduction.

4.3 MOH-based system

4.3.1 Introduction

Biomass polymers have been reported by former members of the Moores group to be able to reduce metals salts into NPs, then act as capping agents. For instance, Kaushik et *al.* extensively developed crystalline nanocellulose (CNC) to make Ag, Pd, Ru NPs in aqueous solution.[37-39] This strategy has also been explored with CMC in the previous chapter. Rak et *al.* had opted for lignin to prepare Ag, Pd, Re, Ru, and Au NPs in ball-milling conditions.[40-42] Inspired by these works, we first wondered if we could use a CNC or a lignin-based bio-based reductant for the reduction of carbonyls in ball-mill. Indeed, the previous chapter raised a few issues, stemming from the use of H_2O a solvent. As much as H_2O proved to be a safe and affordable reaction medium, using a solvent came with drawbacks during the substrate scope. In the case of 5-HMF and its reduction product, their high solubility in H_2O made their isolation extremely difficult. On the contrary, highly hydrophobic substrates (such as 4-(trifluoromethyl)benzaldehyde) prevented a proper mixing with the catalyst. Thus, we will try to prevent these issues by switching to mechanochemically-induced reactions. Due to the incompatibility of H_2 with ball-milling, we also looked for easy-to-handle reducing agents, preferably based on biomass or industrial waste. We had initially conducted the optimization phase using stainless steel jars and a stainless ball for milling. Eventually, we moved to the current apparatus due to their lower price and similar performance. Furthermore, we had concerns that stainless steel could react with the mixture, as had been reported previously by our group.[40] We used ZrO balls as they were more durable on the long run and harder than Teflon balls.

4.3.2 Results and discussion

We first turned to alkali base-catalyzed transfer hydrogenation. Indeed, MOH (M = Cs, Na, K) can induce a MPV-style hydride transfer between carbonyls and alcohol donors (Scheme 81, see chapter 1 – section 1.6.1).

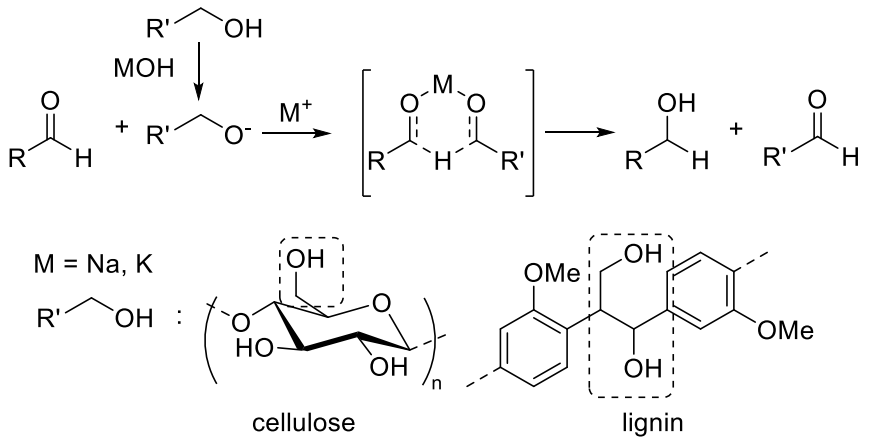

Scheme 218. Primary alcohol found in biopolymers as reductants.

Thus, we first tested the reduction of 4-anisaldehyde in ball-milling conditions, using bio-derived compounds as hydrogen donors, and KOH as a base. CNC or Kraft lignin gave no conversion (Table 7) whereas using sugar monomers such as sorbitol or glucose gave respectively 32% and 50% alcohol yield. However, we observed a concomitant generation of the same amount of carboxylic acid (36 and 41% respectively). This shows that a Cannizzaro-style pathway is occurring, with a dismutation of two equivalents of aldehyde into an alcohol and a carboxylic acid.

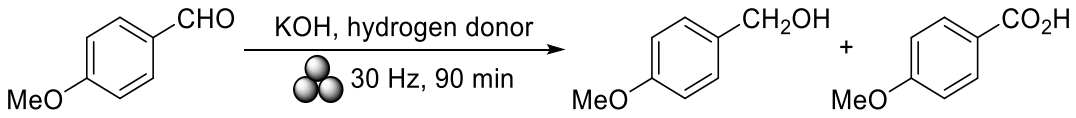

Entry	Hydrogen donor	Result
1	CNC	NR
2	Kraft lignin	NR
3	sorbitol	32% alcohol, 36% acid
4	glucose	50% alcohol, 41% acid

Reaction conditions: 4-anisaldehyde (30 mg, 0.22 mmol), KOH (90 mg, 1.6 mmol), hydrogen donor (80 mg). Ball milling (Teflon jar, 1 ZrO_2 ball) 29.5 Hz, 90 min, 200 mg total material weight. Mesitylene was used as an external standard for NMR analysis.

Table 7. Use of biomass-derived molecules for reduction of 4-anisaldehyde in ball-milling.

We observed the slight excess of alcohol compared to the acid formed in presence of glucose (1.25/1 ratio), whereas sorbitol did not give such an excess (0.9/1). Thus, we thought that the aldehyde function observed on glucose could still act as a reducing function (contributing to 20% of the overall alcohol formation) whereas sorbitol did not possess such an ability.

Therefore, we thought that adding an excess of a sacrificial aldehyde to inhibit the oxidation of the aldehyde substrate. We opted for paraformaldehyde as a solid and inexpensive sacrificial aldehyde. We also switched the base to CaO due to its easier handling and lower hygroscopicity (Table 8). Employing either a 2-fold or 4-fold excess of paraformaldehyde, we raised the alcohol/acid ratio to 2/1 and 3/1 respectively.

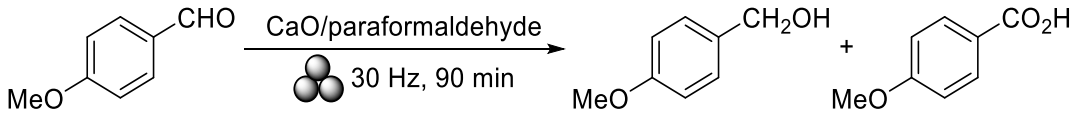

Entry	CaO/paraformaldehyde amounts	Results

1	6.5 equiv. CaO, 2 equiv. paraformaldehyde	67% alcohol, 33% acid
2	5.7 equiv. CaO, 4 equiv. paraformaldehyde	74% alcohol, 26% acid
Reaction conditions: 4-anisaldehyde (48 mg, 0.35 mmol), CaO and paraformaldehyde. Ball milling (Teflon jar, 1 ZrO_2 ball) 29.5 Hz, 90 min, 200 mg total material weight. Mesitylene was used as an external standard for NMR analysis.		

Table 8. Use of formaldehyde for the reduction of 4-anisaldehyde in ball-milling.

Nonetheless, despite the high excesses of paraformaldehyde employed, we still observed a non-negligible formation of carboxylic acid. Under the conditions described above, we could not avoid dismutation of 4-anisaldehyde. Consequently, we looked for alternative reducing agents that are compatible with ball-milling conditions, namely PMHS that has been introduced in the preamble of this chapter.

4.4 TBAF-based system

4.4.1 Optimization and substrate scope

To develop the methodology, we first focused on 4-formylbenzonitrile as a model substrate. Indeed, as a solid electron-poor aromatic aldehyde, it is expected to be more reactive than 4-anisaldehyde under reduction conditions. Several fluoride salts, including KF, LiF and TBAF@SiO_2, were examined. We found that TBAF@SiO_2, a silica-supported fluoride source, was the most successful to activate PMHS with the model substrate. It is a less hygroscopic fluoride source than its liquid counterparts, which we reasoned could prevent any potential water-quenching of the activated silane. As reaction conditions were optimized, we realized that 25 mol% of TBAF@SiO_2 was sufficient in activating PHMS, which is an improvement compared to the Kobayashi's solution methodology relying on stoichiometric amounts of fluoride.[17] After optimizing quantity of reagents and milling time, the corresponding alcohol, 4-(hydroxymethyl)benzonitrile, was obtained in 82% yield within 15 minutes of milling, using 25% TBAF@SiO_2 and 1.7 equivalents of PMHS (Table 9, entry 1).

In an effort to improve the reaction rates, addition of stoichiometric amounts of solvent was tested (typically 0.5 µL per mg of substrate). This method, also known as liquid-assisted grinding (LAG),[43] has been successful, for instance in the synthesis of metal organic frameworks,[44] co-crystallizations,[45] or selective fluorination.[46] Adding EtOAc increased the yield to 94% (Table 9, entry 2). Addition of toluene afforded a moderate yield improvement to 87%, while with THF and notably water, the reaction performance was unchanged (Table 9,

entries 3 to 5). As we will discuss below, the effect of the choice of LAG solvent greatly varied depending on the substrate. Control experiments were conducted to ascertain the role of each component in the system. Replacing TBAF@SiO_2 with KF or LiF (Table 9, entries 6 and 7) or removing either the fluoride source or the PMHS (Table 9, entries 8 and 9) totally disabled the reaction.

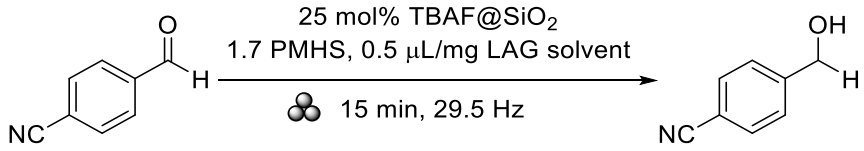

Entry	Modification	Alcohol yield (%)
1	-	82
2	LAG solvent: EtOAc	94
3	LAG solvent: Toluene	87
4	LAG solvent: THF	83
5	LAG solvent: H_2O	82
6	KF as a fluoride source	NR
7	LiF as a fluoride source	NR
8	No TBAF@SiO_2	NR
9	No PMHS	NR

Reaction conditions: 4-formylbenzonitrile, 1.7 PMHS, 25 mol% TBAF@SiO_2, LAG solvent (0.5 µL/mg substrate). Ball milling (Teflon jar, 1 ZrO_2 ball) 29.5 Hz, 200 mg total chemical products weight.

Table 9. Control experiments.

Next were investigated benzaldehyde derivatives. Milling time, fluoride source, and choice of LAG solvent were optimized for each substrate. The detailed results for each substrate and conditions tested are given in Table 17 in the Appendix (section 4.7). Here in the main text we will show only the optimized results. Electron-poor benzaldehydes such as 4-formylbenzonitrile, 4-nitrobenzaldehyde, 4-(trifluoromethyl)benzaldehyde and 3-bromobenzaldehyde (Table 10, entries 1 to 4) gave high yields between 78% to quantitative. EtOAc was the best LAG solvent there, except for 4-nitrobenzaldehyde, which worked better

in absence of such an additive. Notably 4-(trifluoromethyl)benzaldehyde worked well under milling conditions despite being a liquid at room temperature. Chloride-substituted benzaldehydes proved to give different optimal results depending on the position of the substituent, ranging from 56% for 2-chlorobenzaldehyde to 73% for 4-chlorobenzaldehyde and 96% for 3-chlorobenzaldehyde, with the optimal LAG solvent being none, toluene and EtOAc respectively (Table 10, entries 5 to 7). 4-Ethynylbenzaldehyde and 9-anthracenecarboxaldehyde, as electron-rich substrates, were successfully reduced at yields of 84% and 72%, respectively, with no LAG solvent and ethyl acetate respectively (Table 10, entries 8 and 9). 1,2-conjugated unsaturated carbonyls, such as citral, were successfully reduced in moderate yields of 65% with toluene as LAG solvent, despite its lower reactivity due to the absence of a benzylic position (Table 10, entry 10). No trace of the C=C reduction product was detected, showing excellent selectivity (see section 1.2.3). For 4-nitrocinnamaldehyde, initial results gave 28% yield after 15 minutes of milling (Table 10, entry 11). Extending reaction time did not significantly alter the reaction progress. We reasoned that the active species was likely degrading under the milling conditions. Inspired by the approach of the Friščić group,[47] we fractioned the addition of PMHS into three portions of 1 equivalent each, followed by 10 minutes of milling and successfully increased the yield from 28% to 63% (Table 10, entry 12, with 50 mol% TBAF@SiO_2 added once at the beginning of the reaction). Protic aldehydes and imines showed no reactivity to the reaction (Table 10, entries 13 to 15). Most examples in the literature seem to indicate that imine hydrosilylation does not seem to proceed under fluoride activation unless a Lewis acid or a transition metal catalyst is added. We attempted to use $Zn(OTf)_2$ as a Lewis acid to activate the imine, unfortunately to no avail (Table 10, entry 14). With our system, the reaction proceeded very fast, with 15 minutes being the optimal reaction time. Prolonging the reaction for longer than 15 minutes usually does not improve the yield, pointing towards the fast degradation of the active species. In comparison, the reaction times in the carbonyl reduction with $NaBH_4$ was longer, with milling between 6 and 17 hours,[30] while reduction by the Hantzch ester proceeded within 90 minutes of milling.[32]

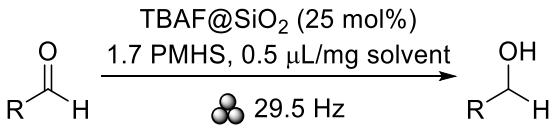

Entry	Substrate	Product	LAG solvent	Time (min)	Yield (%)

1	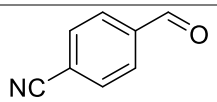	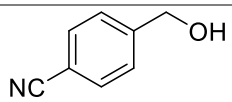	EtOAc	15	94
2	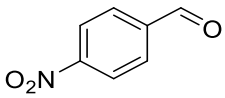	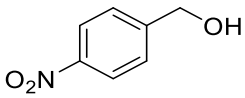	-	15	86
3	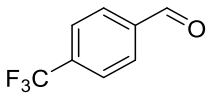	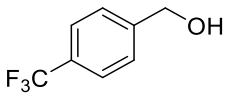	EtOAc	15	78
4	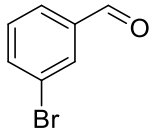	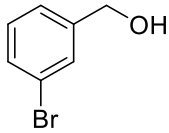	EtOAc	15	quantitative
5	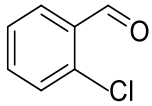	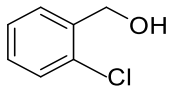	-	15	56
6	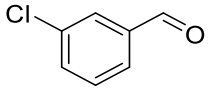	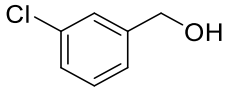	EtOAc	15	96
7	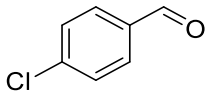	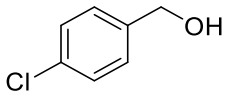	Toluene	15	73
8	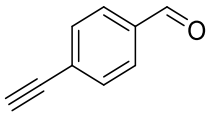	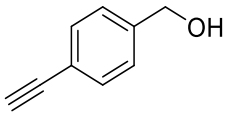	-	15	85
9	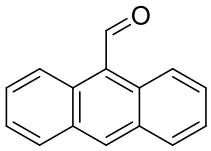	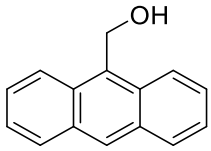	EtOAc	30	72
10	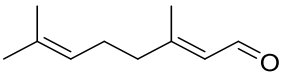	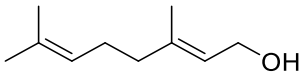	Toluene	15	65[b]
11	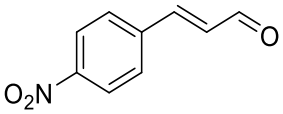	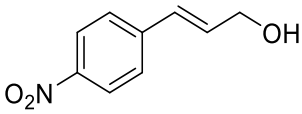	-	15	29
12				3*10	63[a,b]
13	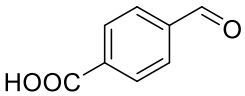	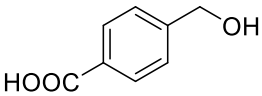	-	90	NR
14	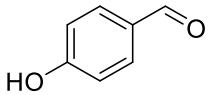	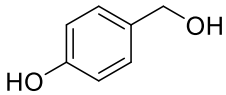	-	90	NR
15	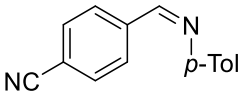	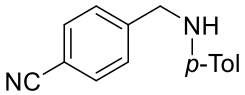	-	90	NR

16	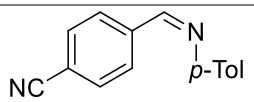	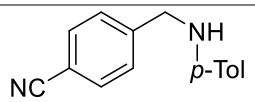	-	90[c]	NR

Reaction conditions: Substrate, 1.7 PMHS, 25 mol% TBAF@SiO_2, LAG solvent (0.5 µL/mg substrate). Ball milling (Teflon jar, 1 ZrO_2 ball) 29.5 Hz, 200 mg total material weight. [a]PMHS was added in three portions consisting of 10 minutes of milling, one equivalent each. 100% selectivity to the C=O reduction product. [b]50 mol% TBAF@SiO_2 was used. [c]25 mol% $Zn(OTf)_2$ was added to the mixture.

Table 10. Scope of aldehydes and imines.

Ketones were then investigated. Electron-poor acetophenones such as 4'-nitroacetophenone, 4'-bromoacetophenone, and 4'-iodoacetophenone (Table 11, entries 1 to 3) gave high yields,[48] following a similar trend to previously reported. With 4'-nitroacetophenone, using 25 mol% TBAF@SiO_2 gave a 71% yield after 90 minutes of milling. In an effort to improve this reaction, we screened other fluorides. While KF gave no reaction, the addition of 25% 18-crown-6 ether in conjunction with 50 mol% KF increased the yield to 81% after only 15 minutes of milling (Table 11, entry 1). The crown ether is known to coordinate with the K^+ cation to enhance the reactivity of the F^- anion, as previously applied by Goldberg et *al.* in solution phase.[49] Similarly to aldehydes, electron-rich or sterically hindered ketones such as 2',6'-dimethoxyacetophenone, 4'-methoxyacetophenone, 4-methylbenzophenone and 4-bromobenzophenone proved to be more challenging, giving no reaction to low yields (Table 11, entries 4 to 7). In the case of 4-methylbenzophenone, increasing the milling time from 30 minutes to 90 minutes decreased the yield from 59% to 44% (Table 11, entry 6), hinting at a possible degradation of the product. 2-bromo-4'-nitroacetophenone was reduced in moderate yield (46 %) with 25 mol% TBAF@SiO_2, while preserving the reactive bromine functionality (Table 11, entry 8). Our system proved completely inactive on aliphatic ketones such as cyclopentanone and camphor (Table 11, entries 9 to 10).

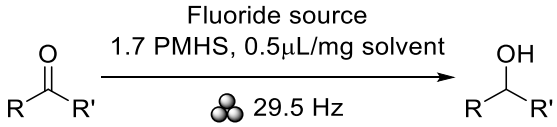

Entry	Substrate	Product	Fluoride	LAG solvent	Time (min)	Yield (%)
1	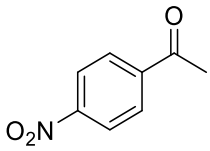	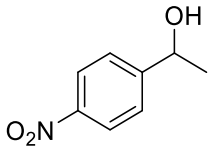	KF/18-crown-6 ether	Toluene	15(90)	86(71[a])

2	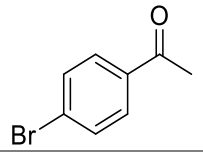	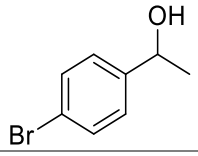	TBAF@SiO_2	Toluene	15	82
3	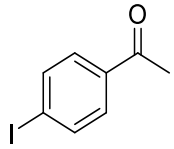	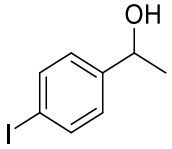	TBAF@SiO_2	-	15	quantitative
4	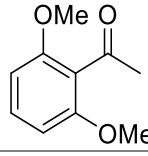	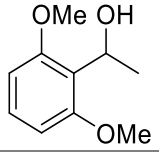	TBAF@SiO_2	-	90	NR
5	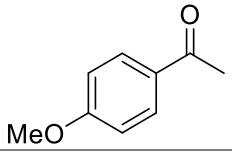	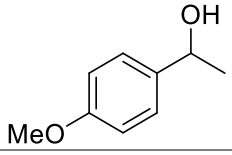	TBAF@SiO_2	EtOAc	15	47
6	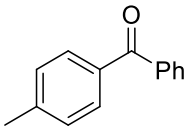	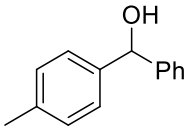	TBAF@SiO_2	-	30(90)	59(44)[b]
7	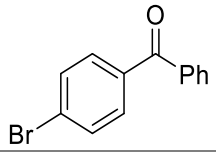	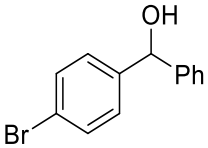	KF/18-crown-6 ether	Toluene	15	40
8	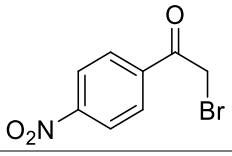	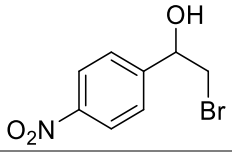	TBAF@SiO_2	EtOAc	15	46
9	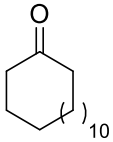	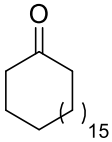	TBAF@SiO_2	-	90	NR
10	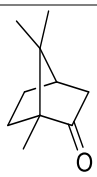	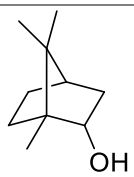	TBAF@SiO_2	-	90	NR

Reaction conditions: Ketone, 1.7 PMHS, 25 mol% TBAF@SiO_2 or 50 mol% KF/25 mol% 18-crown-6 ether, LAG solvent (0.5 µL/mg substrate). Ball milling (Teflon jar, 1 ZrO_2 ball) 29.5 Hz, 200 mg total material weight. [a]Yield in parentheses: TBAF@SiO_2 25 mol%, 90 minutes of milling. [b]Yield in parentheses: TBAF@SiO_2 25 mol%, 90 minutes of milling.

Table 11. Scope of ketones.

To test the feasibility of the process on the gram scale, the reaction was tested in a planetary mill (Scheme 219). After 30 mins of milling at 500 rotations per minute, an isolated yield of 78% was afforded.

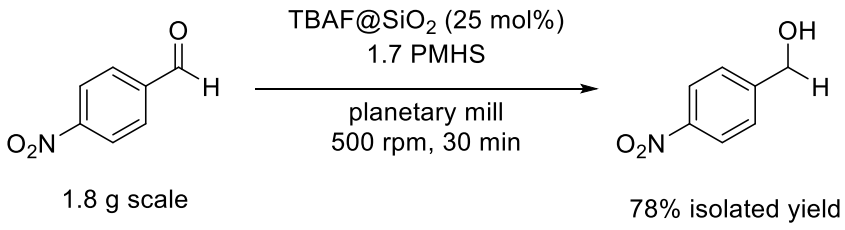

Scheme 219. Gram scale reduction of 4-nitrobenzaldehyde.

4.4.2 5-Hydroxymethylfurfural reduction

To showcase the intrinsic advantages of our system, we investigated specific substrates where the liquid phase reaction shows limitations. 5-HMF is a platform biomass-based chemical that can be produced from the triple dehydration of hexoses.[50] It can be used as a starting material to access a wide range of furan-type compounds. For instance, the aldehyde function can be reduced to obtain 2,5-dihydroxymethylfurfural (DHMF, see section 1.2.2). However, both HMF and DHMF are difficult to extract from water due to their low partition coefficient.[51] Liu et *al.* reported 2-butanol/THF 1:4 ratio as an efficient mixture for HMF extraction.[52] Continuous extraction in biphasic systems such as water/methyl isobutyl ketone (MIBK) mixtures was also reported.[53] All these methods are intricate and require complicated solvent mixtures. Under our standard conditions, with 25 mol% TBAF@SiO_2, 1.7 equivalents of PMHS, and milling for 15 min at 29.5 Hz, only 36% of the product was obtained (Table 12, entry 1). Adding toluene as a LAG solvent only afforded a minor yield increase to 41% (Table 12, entry 2) and increasing the milling time did not change the yield (Table 12, entry 3). Varying milling times between 15 and 90 minutes with or without a LAG solvent afforded at the best a 50% yield. Again, by fractioning the addition of PMHS to the reaction mixture into three equal portions of one equivalent each with 10 minutes of milling upon each addition, the yield could be increased to 69% (Table 12, entry 4). Interestingly, after reaction, both the product and the starting material were easily extracted with ethyl acetate, and a simple filtration. As no water was introduced during either the reaction or the work-up, this procedure solved very simply the challenge of separating HMF and its products from reaction mixtures.

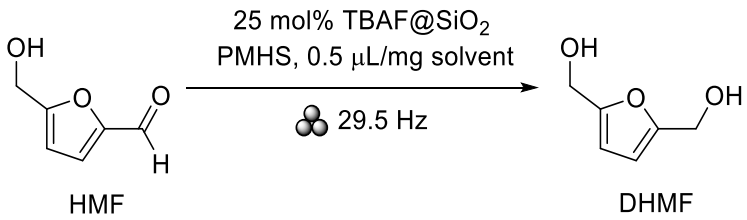

Entry	PMHS (equiv.)	LAG solvent	Time (min)	Yield (%)
1	1.7	-	15	36
2	1.7	Toluene	15	41
3[a]	1.7	-	90	27
4	3 in 3 equal portions	-	10, 3 times	69

Reaction conditions: HMF, PMHS, 25 mol% TBAF@SiO_2, LAG solvent (0.5 µL/mg substrate). Ball milling (Teflon jar, 1 ZrO_2 ball) 29.5 Hz, 200 mg total material weight.
[a]PMHS was added in three portions followed by 10 minutes of milling each.

Table 12. HMF reduction.

Various milling times (15, 30, 60 and 90 minutes) with or without Toluene as a LAG solvent were tested for the reduction of HMF to DHMF. The yield was measured as well as the mass balance (Table 13). As mentioned previously, the yield was at 36% for 15 mins of milling (Table 13, entry 1). By increasing the milling time, it peaked at around 50% for 30 and 60 minutes (Table 13 entries 2 and 3), then dropped back to 36% at 90 minutes (Table 13, entry 4). An average of two experiments was taken for 15 mins and 90 mins of milling (Table 13, entries 1 and 4), showing a sizeable discrepancy of results (up to 18% difference). Adding toluene as a LAG solvent helped boosting the yield, though it seemed to be capped at 50% regardless of the milling time (Table 13, entries 5 to 8). The carbon mass balance (defined as the detectable organic material at the end of the reaction) was at 93% at 15 mins of milling (Table 13, entry 1). It decreased by around 10% for additional milling times (Table 13, entries 2 to 4). Adding a solvent such as Toluene helped bringing the mass balance to almost 100% (Table 13, entries 5, 7 and 8), except for 30 mins of milling (Table 13, entry 6).

Entry	Milling time	Yield (%)	Mass balance (%)
		No LAG	
1	15 mins	36%[1]	93%
2	30 mins	52%	86%
3	60 mins	48%	84%
4	90 mins	36%[2]	88%
Entry	**Milling time**	**LAG (Toluene, 0.5 µL/mg)**	
5	15 mins	41%	99%
6	30 mins	49%	78%
7	60 mins	50%	100%

8	90 mins	50%	100%

[1](average of 30% and 42%) [2](average of 27% and 45%)

Table 13. HMF reduction optimization-yields and mass balance

Hu et *al.* summarized most examples of HMF reduction to DMHF from the literature in a single table.[54] A few selected examples are provided below (Table 14) and the reader is invited to refer to Hu's article for a more exhaustive list. Few metal-free examples have been reported, with the exception of Kim's system conducted in ILs[55] and Afonso's report in THF or water,[56] where they both conducted a Cannizzaro reaction. Under basic conditions, HMF dismutates into DHMF and the corresponding carboxylic acid: by construction, the yield cannot be higher than 50%. Afonso provided an easy and scalable isolation protocol by performing a specific crystallization. Enzymatic processes have been reported, at the cost of a high dilution inherent to such processes.[57] Other examples involve the use of precious metals (Ir, Pd, Au, Pt, Ru, Ag, Cu, Ni) as hydrogenation catalysts, and some of them are listed in the table below.[58-60] Based on Hu's and our own literature survey, our report is the first one of its kind for HMF reduction to DMHF in ball-milling.

Catalyst	Reaction conditions	Results	Reference
TBAF@SiO_2 as an activator	3x1 equiv. PMHS, milling 29.5 Hz, 3x10 min	70% conversion, 100% selectivity	This work
$CuCrO_2$	350 bar H_2, EtOH, 150 °C, 12 h	100% conversion, 90-100% selectivity	58
Ru/support (CeO_x, Mg-Zr,γ-Al_2O_3	28 bar H_2, *t*BuOH-H_2O, 130 °C, 2 h	87-99% yield, 81-94% selectivity	59
[Cannizzaro reaction]	NaOH, Ionic liquid ([EMIm]TFSI) or water/THF	50% yield (dismutation reaction)	55-56
Co/SiO_2 in flow	35 bar H_2, 70 °C, H_2O, 2 h	>80% conversion, >90% selectivity	60
enteric bacterial strains	37 °C, 10 mM substrate in a buffered aqueous solution, 8 h	95% conversion	57

Table 14. HMF reduction to DHMF in the literature.

4.4.3 Polyketone reduction

Finally, we explored the opposite side of the solubility issue. Polyketones are a class of thermoplastic polymers developed by Shell Chemicals (under the name of Carilon) and

produced now by Hyosung. Among other interesting properties, they possess a significantly higher melting point than their polyethylene counterparts, and a low solubility in most solvents. They are produced from CO/olefin copolymerization.[61] Polyketones have a very poor solubility in most solvents. The hydrogenation of their carbonyl functionality has been investigated as a means to improve their ability to dissolve in protic media. In this scheme, even partial reduction can be beneficial. The reduction of polyketones has been reported by Milani and co-workers with the transfer hydrogenation of atactic CO/4-Me-styrene polyketones in liquid phase.[62] Using a 2-propanol/dioxane 5:3 mixture and [Ir(cod)(Me_2bipy)Cl] as a catalyst, they obtained a 70% conversion of the polymer into the corresponding polyalcohol. To the best of our knowledge, this is the sole example of polyketone reduction in the literature. We were interested in exploring this reaction by mechanochemistry, as this methodology has been shown in recent examples to afford sustainable solutions for polymer functionalization and deconstruction challenges.[28, 63] We also saw an opportunity to perform this reaction without relying on any metal. For this reaction, we synthesized polyketone, using Pd catalyzed styrene and carbon monoxide copolymerization with a procedure adapted from Guo et *al* (Scheme 220).[64]

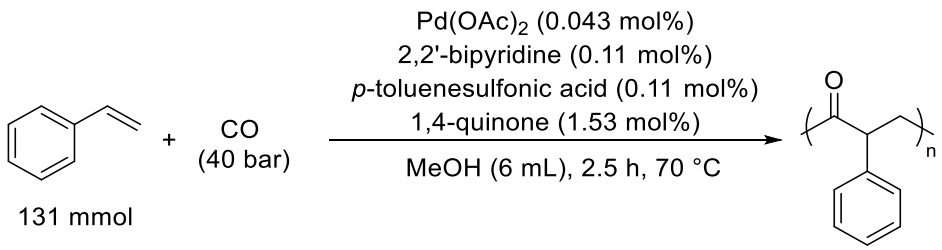

Scheme 220. Polyketone synthesis.

In this fashion, we obtained a polyketone sample featuring a number average molecular weight of 2200 g/mol and weight average molecular weight of 2400 g/mol, as determined by matrix-assisted laser desorption/ionization – time of flight (MALDI-TOF, Figure 15).

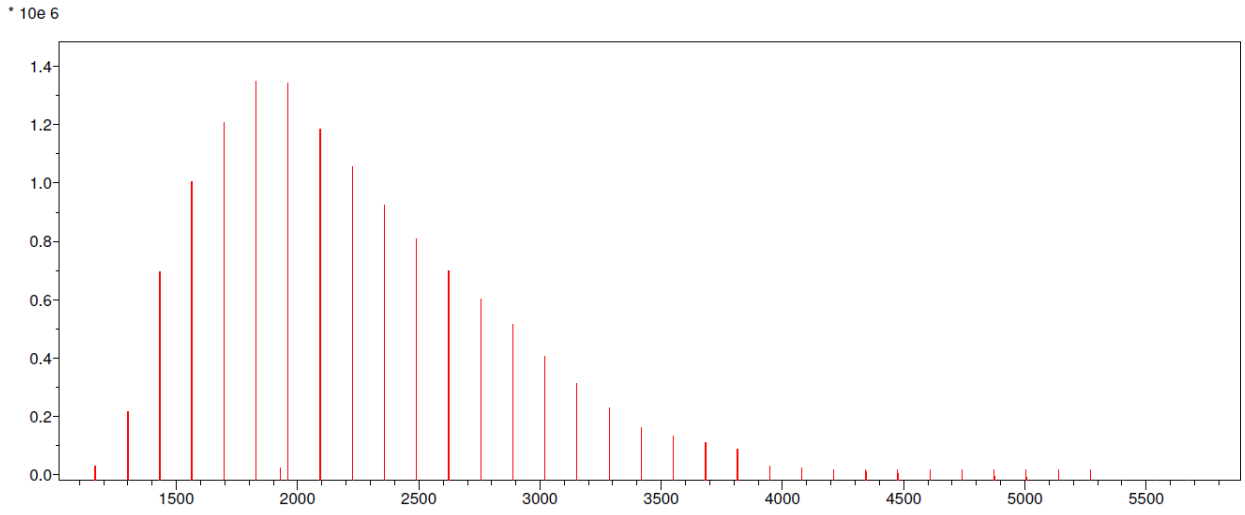

n	ser.	rep.unit	resid.	end1	end2	cation	Mn	Mw	pd	DP	% I.	cnt
1	1	C9H8O	33.1998	105.157	105.157	H	2245.65	2423.13	1.07903	16.9920	99.6	32

Figure 15. MALDI-TOF analysis of the polyketone.

The structure was further confirmed by ^{13}C-MAS NMR (Figure 16).

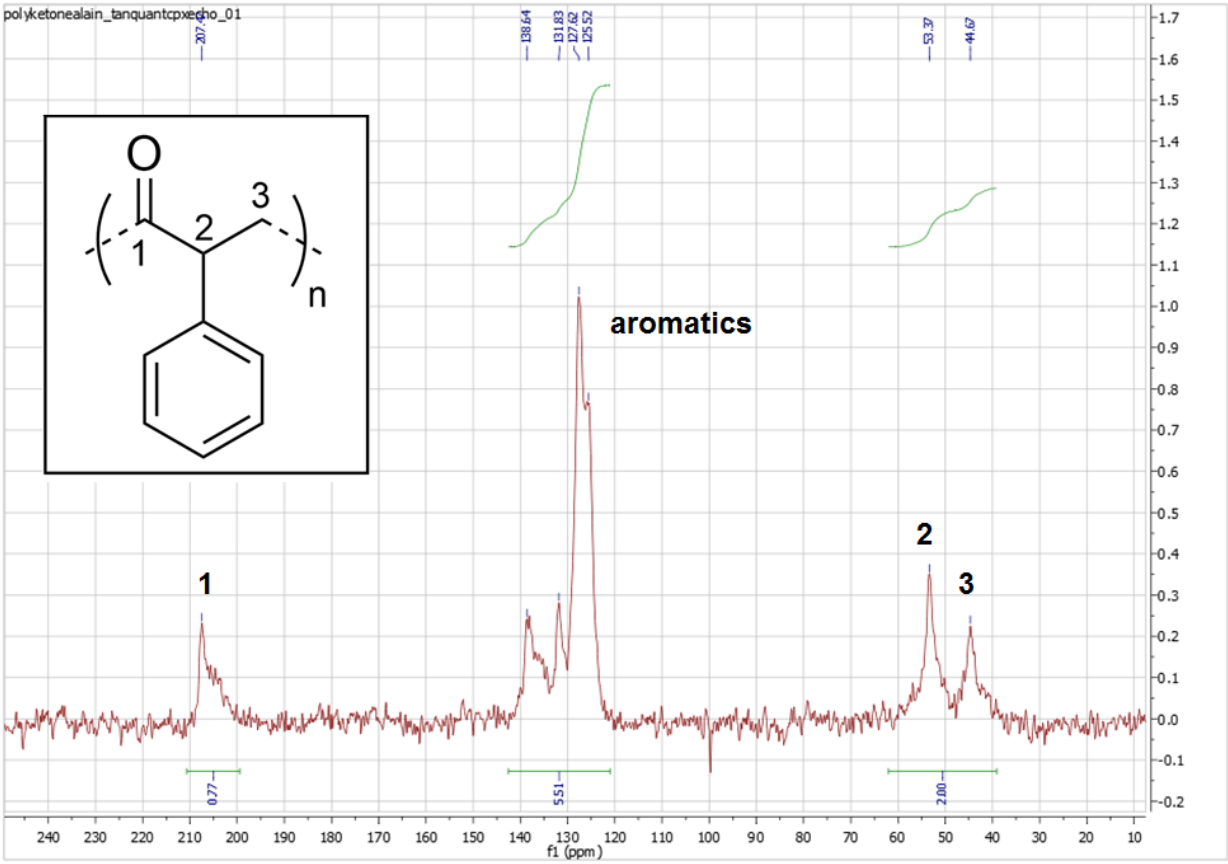

Figure 16. ^{13}C-MAS NMR spectrum of the polyketone.

Identification of the different oxygen peaks by XPS was based on López's report[65] that listed several C=O and C-O containing organic polymers. Sample was contaminated with poly(dimethyl siloxane) (PDMS),[66] which is the adhesive used to hold the sample and overlaps with the signals in the oxygen 1s region (Figure 17) XPS also confirmed the absence of palladium in the samples (Figure 18).

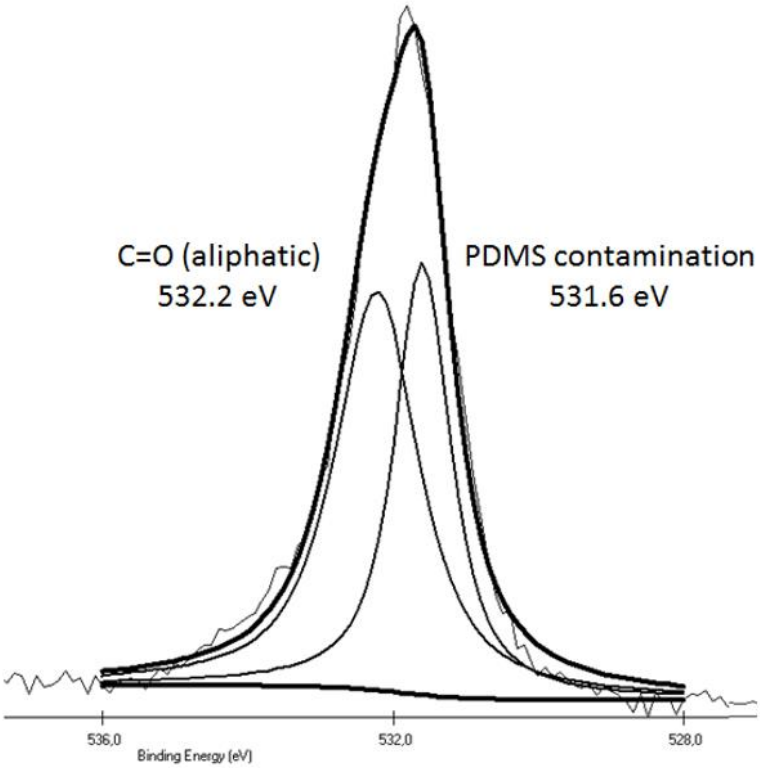

Figure 17. XPS analysis of polyketone – O1s region.

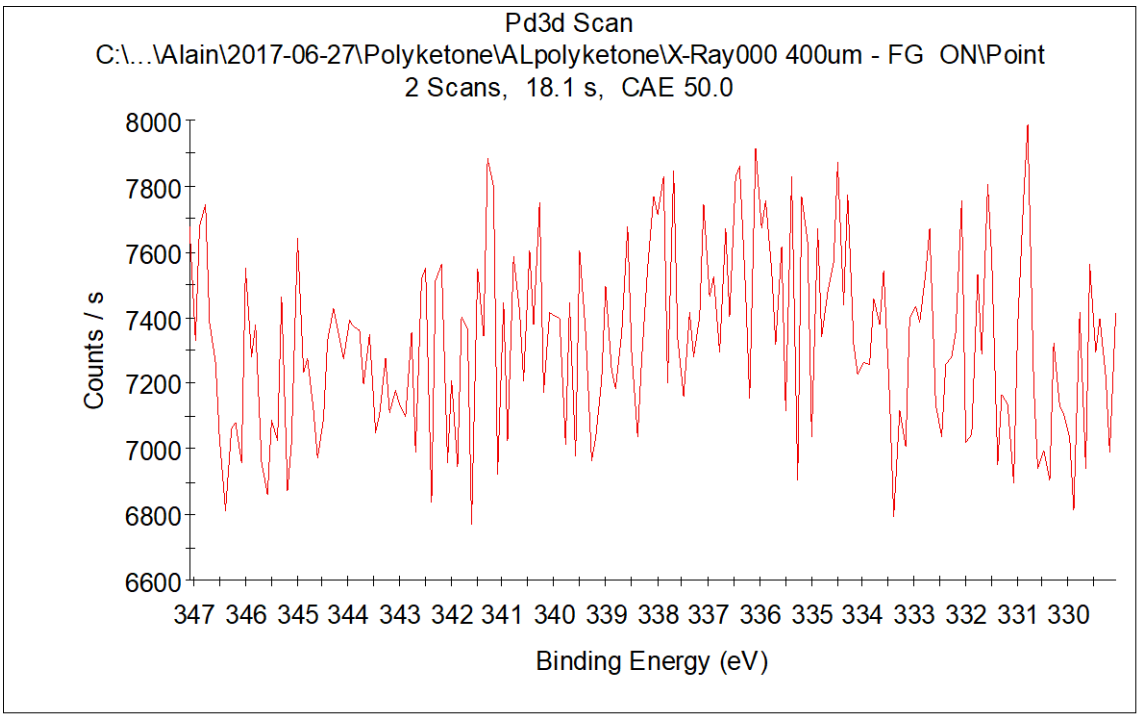

Figure 18. XPS scan of the Pd3d region.

We then loaded this sample in a stainless-steel jar with 2 balls to increase the impact energy, compared to the small molecule substrates. After 90 mins of milling and 2 days of aging 54% of the C=O bonds were converted to C-O bonds (Scheme 221), as shown by XPS (Figure 19).

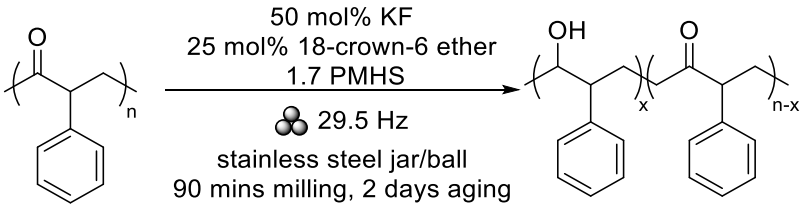

Scheme 221. Polyketone reduction.

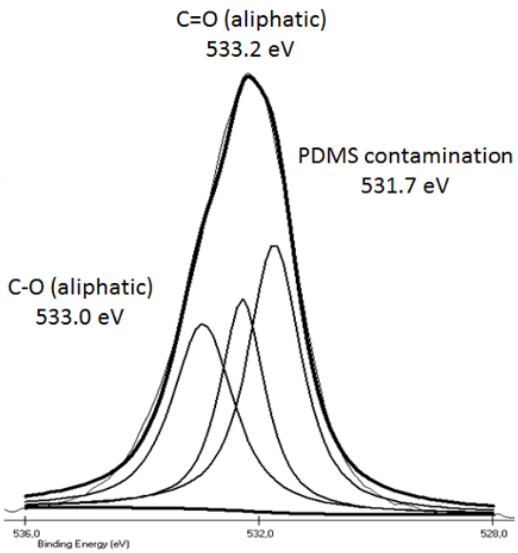

Figure 19. XPS analysis of polyketone after reduction – O1s region.

4.4.4 Mechanism elucidation

The reduction of carbonyls in the solution phase by PMHS has been studied by other researchers. Lawrence originally proposed a 'zipper' mechanism where the fluoride migrates from one monomer to another, activating several Si-H bonds in the process (Scheme 222a).[10] Although this pathway would account for the use of only catalytic amounts of F^- rather than one equivalent per carbonyl, the extremely high bond strength of Si-F (582 kJ/mol) makes it unlikely.

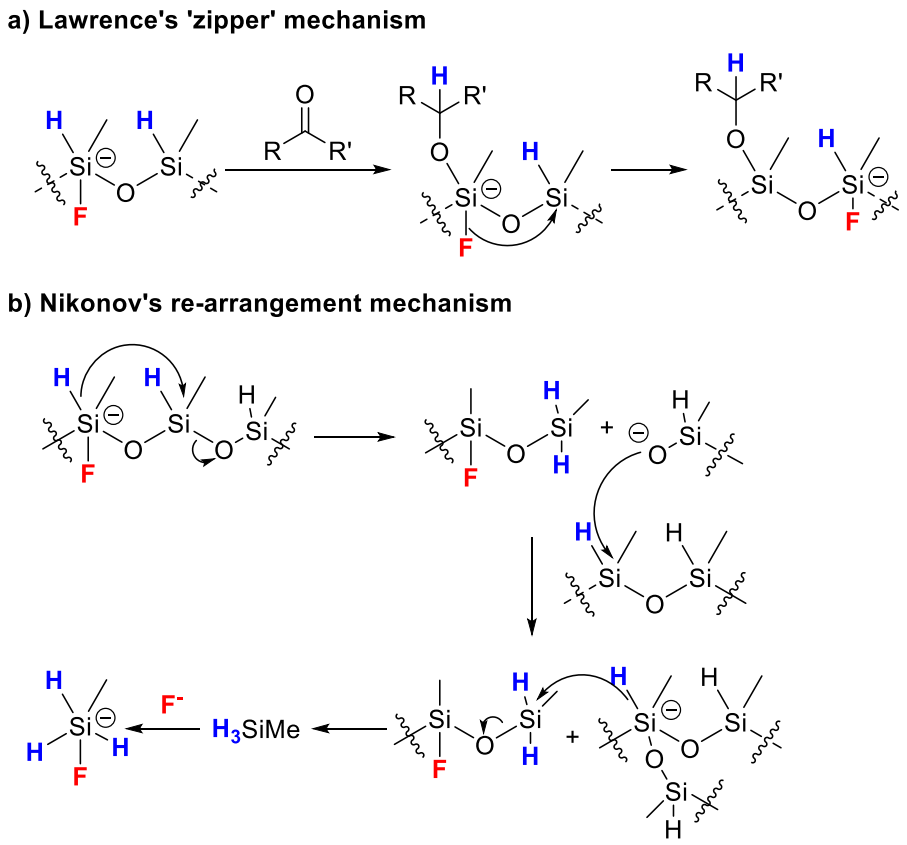

Scheme 222. Proposed mechanisms for the activation of PMHS with fluoride. For clarity, fluoride and active hydrides are highlighted in red and blue, respectively.

Nikonov and coworker revised the mechanism considering that the hydride may migrate along the PMHS chain, before the insertion of the carbonyl occurs.[18] This leads to the rearrangement of the PMHS chain into oligomers and eventually monomeric, volatile H_3SiMe (Scheme 222). H_3SiMe can further react with fluoride to form $[H_3SiFMe]^-$, an hypercoordinate species. Nikonov was able to rationalize their observation that reactivity would drop in an open vessel in solution. In our case, such a mechanism can explain that we observed gas pressure build-up in the jars when they were opened after the milling.

To verify if the mechanochemical reduction reaction relied on the generation of reaction silicon volatiles, we performed a test experiment. Replicating the optimal conditions for the reduction of 4-formylnitrile (Table 10, entry 2), we first milled the PMHS and the TBAF@SiO_2 for 15 minutes alone, carefully opened the jar under the fumehood, and then added the aldehyde to be milled again for 15 minutes (Scheme 223). Only traces amount of product was formed, which is compatible with the active species being gaseous and escaping the reaction vessel upon its opening.

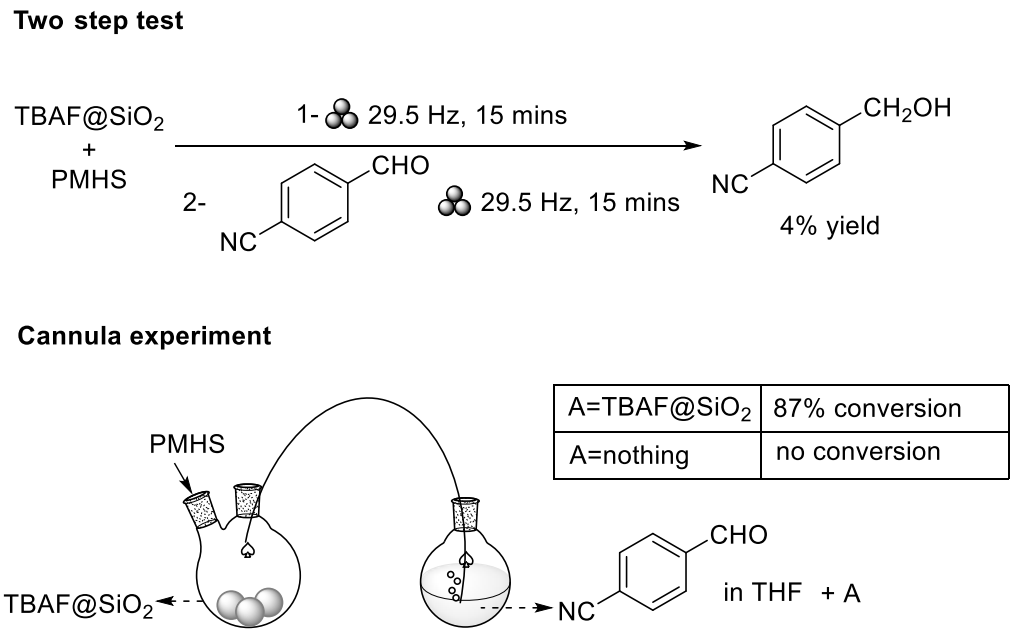

Scheme 223. Two-steps milling and cannula experiments.

To further explore the possibility of a volatile active species, another experiment was designed. A 250 mL round-bottom flask containing TBAF@SiO_2 was sealed with 3 ZrO_2 balls to replicate ball milling conditions under stirring. It was connected to another sealed flask through a cannula immersed into a solution of 4-formylnitrile in THF (Scheme 223). Upon injecting PMHS in the first flask, we observed bubbling in the solution of the second flask and interpreted this as formation of H_3SiMe. The set-up was left for 2 h under vigorous stirring for both flasks, resulting in no conversion of the aldehyde. In a second experiment, TBAF@SiO_2 was added also to the second flask. This time, after 2 hours, 87% of the alcohol product was measured. This result is consistent with the reaction of gaseous H_3SiMe formed in flask 1, with the fluoride source in flask 2 to afford $[H_3SiFMe]^-$ *in situ* and reduce the carbonyl.

When only one equivalent of PMHS per equivalent of starting material was introduced, only 4% of the starting material was converted to the product. However, considering the set-up used, one cannot exclude the instability of the active gas travelling through the cannula, as well as some of the gas being unable to travel to the second flask due to pressure equilibrium.

Influence of water. Finally, the role of water in the mechanism was explored. As pointed out in Table 9, entries 1 and 5, the presence of water at 0.5 µL/mg substrate did not seem to affect the reduction of 4-formylbenzonitrile. However, adding 0.5 µL/mg of water totally shut down the reduction of 4-nitrobenzaldehyde. Therefore, the effect of H_2O may differ from one

substrate to another: we chose to explore greater amounts of water for 4-formylbenzonitrile (Table 15), and lesser amounts of water for 4-nitrobenzaldehyde (Table 16).

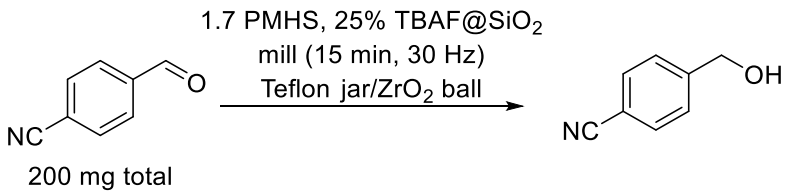

Entry	Modification	Alcohol yield (%)
1	No H_2O	82
2	0.5 µL/mg H_2O	82
3	1 µL/mg H_2O	76
4	2 µL/mg H_2O	51

Reaction conditions: Substrate, 1.7 PMHS, 25 mol% TBAF@SiO_2, LAG solvent (0.5 µL/mg substrate). Ball milling (Teflon jar, 1 ZrO_2 ball) 29.5 Hz, 200 mg total material weight.

Table 15. Influence of water on 4-formylnitrile reduction.

As more water was introduced, the yield for 4-formylnitrile gradually decreased past 0.5 µL/mg. It started at 82% yield (Table 15, entries 1 and 2) and dropped to 76% yield at 1 µL/mg (Table 15, entry 3), then 51% yield at 2 µL/mg (Table 15, entry 4).

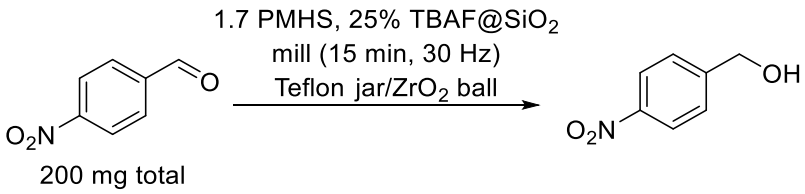

Entry	Modification	Alcohol yield (%)
1	no H_2O	86
2	0.12 µL/mg H_2O	87
3	0.25 µL/mg H_2O	84
4	0.5 µL/mg H_2O	NR

Reaction conditions: Substrate, 1.7 PMHS, 25 mol% TBAF@SiO_2, LAG solvent (0.5 µL/mg substrate). Ball milling (Teflon jar, 1 ZrO_2 ball) 29.5 Hz, 200 mg total material weight.

Table 16. Influence of water on 4-nitrobenzaldehyde reduction.

Concerning 4-nitrobenzaldehyde, the yield decrease was sharper, with a drop from 84% yield to no reaction between 0.25 µL/mg and 0.5 µL/mg (Table 16, Entries 3 and 4).

For both substrates the yield decreased with the amount of water added but differently depending on the substrate. We initially thought that water could quench the hypervalent pentavalent active species, forming H_2 gas and wasting the hydride. This is inconsistent though with the observation that the reaction can tolerate small amounts water. As shown in the tables above, the reaction proceeded with large amounts of water in the case of 4-formylbenzonitrile. At 2 µL/mg of H_2O (Table 15, entry 4), there is a 9-fold excess of H_2O per mole of PMHS (based on the hydride amount), yet the yield still reached 51%.

Another possible rationalization of the role of water (and other solvents in general) can be linked to LAG. In his tutorial review, Friščić[43] showed that at low ratios of solvent volume to weight of compounds (coined as the η parameter), the solubility of the precursors did not affect significantly the co-crystallization rate. The LAG solvent's major contribution to the reaction pertains to molecular diffusion, or as stated by the author, constitutes an "environment in which all participating substances are permanently saturated, therefore eliminating effects of their relative solubilities". At higher η values, where the mixture becomes slurry-like, the solubility becomes preeminent again and significantly affects co-crystallization rate. Applying this reasoning to organic reactions rather than co-crystallizations should be reasonable in that respect. Here, the slightly higher solubility of 4-nitrobenzaldehyde in H_2O (2.34 mg/mL at 25 °C) than that of 4-formylbenzonitrile (0.60 mg/mL at 25 °C) may account for this reasoning.

4.5 Conclusion

We have developed here a ball-milling approach for the selective reduction of a wide range of carbonyl compounds in the absence of any metal catalyst and using an inexpensive and easy-to-handle silane, PMHS. Ball-milling not only enabled a higher reaction rate than solution-based reactions, with typical reaction times of 15 minutes, but it also allowed insoluble substrates to be reduced. We also confirmed that the reaction mechanism proceeded through the *in situ* formation of volatile silicon species, consistent with past accounts.

4.6 Experimental

All chemicals and solvents were purchased from commercial sources and used without purification unless noted. TBAF@SiO_2 (1.5 mmol/g) was purchased from Sigma and was freeze-dried before use and stored in a desiccator. Alternatively, it can be made from TBAF in THF solution (the procedure is provided below). The molecular weight of PMHS was taken to be 65 g/mol for calculations of stoichiometry. A Retsch MixerMill MM 400 was used to perform milling experiments. NMR spectra were recorded on a Bruker AV500 spectrometer operating at 500 MHz for ^{1}H acquisitions and on a Varian VNMRS operating at 400 MHz for the solid state ^{13}C acquisition. Chemical shifts are reported in ppm with a solvent resonance as an internal standard (^{1}H NMR; chloroform as internal standards, indicating 7.26 ppm). Mesitylene was used as an internal NMR standard. Yields were an average of a minimum of two different experiments. XPS was performed on a VG ESCALAB 3 MKII spectrometer (VG, Thermo Electron Corporation, UK) equipped with an Mg Kα source. Polyketone copolymerization with carbon monoxide were carried out in a Parr Instruments 5000 Series Multiple Reactor System. MALDI-TOF measurement was taken on a MALDI Autoflex III-TOF-(BRUKER).

Typical procedure. In a typical reaction, one zirconium oxide ball (10 mm, 3.24 g weight) was added in a 10 mL Teflon milling jar. It was then filled with a total of 200 mg of solid reagent material on one side, and liquids on the other. The jar was carefully closed, wrapped with parafilm and loaded onto the Retsch MM-400 mixer mill. The reactions were conducted over 15 minutes, milling at a frequency of 29.5 Hz. At the end of the reaction, the jar was opened under a fumehood, 5 mL of EtOAc were added to the jar and was manually shaken with the balls for 20 seconds to scrape off the solid content. This operation was done three times to ensure a full product recovery. The three fractions were combined, sonicated for 10 seconds, filtered and then concentrated *in vacuo*. To remove the PMHS byproducts and the activator, the mixture can be recrystallized or dissolved in an EtOAc/hexanes mixture and filtered through a silica plug. The imines were prepared by milling the corresponding aldehydes and amines in presence of Na_2SO_4 for 15 mins at 29.5 Hz.

Preparation of TBAF supported in silica. TBAF in THF solution (1.0 M, 10 mL, 10 mmol) was added to silica powder (230-400 mesh, 6.67 g) in a round-bottom flask. The resulting mixture was dispersed in acetone (20 mL), swirled and sonicated for 30 seconds before being

concentrated under vacuo. The operation was repeated twice to ensure a good dispersion of the TBAF. The sample was freeze-dried and stored under vacuum before use.

Closed flask experiment. A 250 mL round-bottom flask containing TBAF@SiO_2 (300 mg, 0.45 mmol) was sealed with 3 ZrO_2 balls and a magnetic stir bar to replicate ball milling conditions. It was connected through a cannula to another sealed flask containing 4-formylnitrile (50 mg, 0.38 mmol) in THF (15 mL) (Figure 20). For the second experiment, TBAF@SiO_2 (300 mg, 0.45 mmol) was added as well in the second flask. The overall system was flushed with argon for 10 minutes. Upon injecting PMHS (500 mg, 7.7 mmol, 20 equiv.) in the first flask, a gas build-up was observed and the solution in the second flask started bubbling immediately. The set-up was left for 24 h under vigorous stirring (1000 rpm). The content of the second flask was then filtered and concentrated under vacuo before analysis.

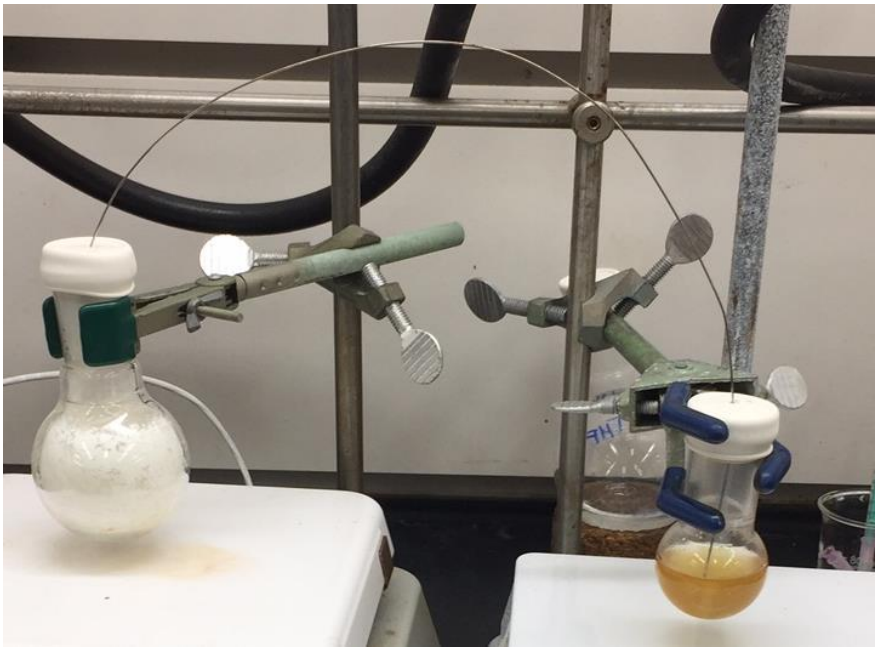

Figure 20. Set-up for the volatile species experiment (after more than 4 h of reaction).

Polyketone. Polyketone was made through copolymerization of styrene and CO based on a protocol of Guo et *al*.[64] $Pd(OAc)_2$ was used instead of Pd/C to allow an easier metal separation from polyketone. Styrene (15 mL, 131 mmol), $Pd(OAc)_2$ (12.8 mg, 57 µmol), 2,2'-bipyridine (23.4 mg, 150 µmol), *para*-toluenesulfonic acid (28.5 mg, 150 µmol), 1,4-quinone (218 mg, 2 mmol), MeOH (6 mL) were loaded in a Teflon liner inside a stainless steel autoclave reactor. Carbon monoxide (40 bar) was flushed into the reactor, then it was heated for 2.5 hours at 70

°C (Scheme 220). It was allowed to cool down, precipitated with an excess of cold methanol, filtered and washed with cold hexanes.

Planetary mill experiment. In a typical reaction, five zirconium oxide balls (10 mm, 3.24 g weight) were added in a Retsch 50 ml zirconia grinding jar. It was then loaded with para-nitrobenzaldehyde (1.78 g, 11.8 mol) and TBAF@SiO_2 (1.95 g, 25 mol%). PMHS (1.30 g, 1.7 equiv.) was added just before sealing the jar with parafilm and loaded onto a Retsch S100 centrifugal ball mill. The reaction was conducted over 30 minutes, milling at 500 rotations per minute. At the end of the reaction, the jar was opened under a fumehood, and the resulting mixture was dispersed in EtOAc, filtered and concentrated under vacuo. A mixture of 1/1 water/ethanol was used to recrystallize the pure product.

4.7 Appendix

Detailed scope. For most of the substrates, both fluoride sources were tested. When they were done, results with the addition of LAG solvent are displayed.

Entry	Substrate	TBAF@SiO_2			KF/18-crown-6		
		No LAG	EtOAc	Toluene	No LAG	EtOAc	Toluene
1	4-cyanobenzaldehyde	82	**94**	87	72	-	-
2	4-(Trifluoromethyl)benzaldehyde	49	**78**	43	20	-	-
3	3-bromobenzaldehyde	**100**	62	37	57	-	-
4	2-chlorobenzaldehyde	**56**	25	35	5	-	-
5	3-chlorobenzaldehyde	65	96	**96**	49	-	-
6	4-chlorobenzaldehyde	71	-	**73**	68	-	-
7	4-ethynylbenzaldehyde	**85**	73	**85**	80	-	-
8	9-anthraldehyde	48	**72** (30 mins)	39 (30 mins)	9	-	-
9	Citral	27	32	43 (**65** for 3*10 mins)	NR	-	-
11	4-nitrocinnamaldehyde	28	26	**29**	1	-	-
12	4’-nitroacetophenone	64 (90 mins	-	-	61	-	**86**
13	4’-bromoacetophenone	73	56	**82**	11	-	-
14	4’-iodoacetophenone	**100**	-	-	**100**	-	-
15	4’-methoxyacetophenone	23	**47**	34	4	15	10
16	4’-methylbenzophenone	16 (**59** at 30 mins)	45	34	12	-	-
17	4-bromobenzophenone	10	-	-	30	13	**40**
18	2-bromo-4’-nitroacetophenone	32	**46**	45	-	-	-

Reaction conditions: Substrate, 1.7 PMHS, 25 mol% TBAF@SiO_2 or 50 mol% KF/25 mol% 18-crown-6 ether, LAG solvent (0.5 µL/mg substrate). Ball milling (Teflon jar, 1 ZrO_2 ball) 29.5 Hz, 15 min, 200 mg total material weight. Best results of the series are indicated in bold.

Table 17. Detailed scope and optimization.

4.8 References

1. Clarke, M. L.; Roff, G. J., Homogeneous Hydrogenation of Aldehydes, Ketones, Imines and Carboxylic Acid Derivatives: Chemoselectivity and Catalytic Activity. In *The Handbook of Homogeneous Hydrogenation*, Wiley-VCH Verlag GmbH: 2008; pp 413-454.
2. Brown, H. C.; Krishnamurthy, S., Forty years of hydride reductions. *Tetrahedron* **1979,** *35* (5), 567-607.
3. Noyori, R., Pursuing practical elegance in chemical synthesis. *Chem. Commun.* **2005,** (14), 1807-1811.
4. Wang, D.; Astruc, D., The Golden Age of Transfer Hydrogenation. *Chem. Rev.* **2015,** *115* (13), 6621-6686.
5. Soni, R.; Hall, T. H.; Mitchell, B. P.; Owen, M. R.; Wills, M., Asymmetric Reduction of Electron-Rich Ketones with Tethered Ru(II)/TsDPEN Catalysts Using Formic Acid/Triethylamine or Aqueous Sodium Formate. *J. Org. Chem.* **2015,** *80* (13), 6784-6793.
6. Yang, J. W.; List, B., Catalytic Asymmetric Transfer Hydrogenation of α-Ketoesters with Hantzsch Esters. *Org. Lett.* **2006,** *8* (24), 5653-5655.
7. de Graauw, C. F.; Peters, J. A.; van Bekkum, H.; Huskens, J., Meerwein-Ponndorf-Verley Reductions and Oppenauer Oxidations: An Integrated Approach. *Synthesis* **1994,** *1994* (10), 1007-1017.
8. Rendler, S.; Oestreich, M., Diverse Modes of Silane Activation for the Hydrosilylation of Carbonyl Compounds. In *Modern Reduction Methods*, Wiley-VCH Verlag GmbH & Co. KGaA: 2008; pp 183-207.
9. Dobereiner, G. E.; Crabtree, R. H., Dehydrogenation as a substrate-activating strategy in homogeneous transition-metal catalysis. *Chem. Rev.* **2009,** *110* (2), 681-703.
10. J. Lawrence, N.; D. Drew, M.; M. Bushell, S., Polymethylhydrosiloxane: a versatile reducing agent for organic synthesis. *J. Chem. Soc., Perkin Trans. 1,* **1999,** (23), 3381-3391.
11. Verdaguer, X.; Berk, S. C.; Buchwald, S. L., Catalytic Method for the Reduction of Lactones to Lactols. *J. Am. Chem. Soc.* **1995,** *117* (50), 12641-12642.
12. Lipshutz, B. H.; Noson, K.; Chrisman, W., Ligand-Accelerated, Copper-Catalyzed Asymmetric Hydrosilylations of Aryl Ketones. *J. Am. Chem. Soc.* **2001,** *123* (51), 12917-12918.
13. Dal Zotto, C.; Virieux, D.; Campagne, J.-M., FeCl3-Catalyzed Reduction of Ketones and Aldehydes to Alkane Compounds. *Synlett* **2009,** *2009* (02), 276-278.
14. Bette, V.; Mortreux, A.; Savoia, D.; Carpentier, J.-F., New developments in zinc-catalyzed asymmetric hydrosilylation of ketones with PMHS. *Tetrahedron* **2004,** *60* (12), 2837-2842.
15. Patel, J. P.; Li, A.-H.; Dong, H.; Korlipara, V. L.; Mulvihill, M. J., Polymethylhydrosiloxane (PMHS)/trifluoroacetic acid (TFA): a novel system for reductive amination reactions. *Tetrahedron Lett.* **2009,** *50* (44), 5975-5977.
16. Drew, M. D.; Lawrence, N. J.; Fontaine, D.; Sehkri, L.; Bowles, S. A.; Watson, W., A Convenient Procedure for the Reduction of Esters, Carboxylic Acids, Ketones and Aldehydes using Tetrabutylammonium Fluoride (or Triton® B) and Polymethylhydrosiloxane. *Synlett* **1997,** *1997* (08), 989-991.

17. Kobayashi, Y.; Takahisa, E.; Nakano, M.; Watatani, K., Reduction of carbonyl compounds by using polymethylhydro-siloxane: reactivity and selectivity. *Tetrahedron* **1997,** *53* (5), 1627-1634.
18. Revunova, K.; Nikonov, G. I., Base-Catalyzed Hydrosilylation of Ketones and Esters and Insight into the Mechanism. *Chem. Eur. J.* **2014,** *20* (3), 839-845.
19. Mimoun, H.; de Saint Laumer, J. Y.; Giannini, L.; Scopelliti, R.; Floriani, C., Enantioselective Reduction of Ketones by Polymethylhydrosiloxane in the Presence of Chiral Zinc Catalysts. *J. Am. Chem. Soc.* **1999,** *121* (26), 6158-6166.
20. Jacquet, O.; Das Neves Gomes, C.; Ephritikhine, M.; Cantat, T., Recycling of Carbon and Silicon Wastes: Room Temperature Formylation of N–H Bonds Using Carbon Dioxide and Polymethylhydrosiloxane. *J. Am. Chem. Soc.* **2012,** *134* (6), 2934-2937.
21. Jacquet, O.; Das Neves Gomes, C.; Ephritikhine, M.; Cantat, T., Complete Catalytic Deoxygenation of CO2 into Formamidine Derivatives. *ChemCatChem* **2013,** *5* (1), 117-120.
22. von Wolff, N.; Lefèvre, G.; Berthet, J. C.; Thuéry, P.; Cantat, T., Implications of CO2 Activation by Frustrated Lewis Pairs in the Catalytic Hydroboration of CO2: A View Using N/Si+ Frustrated Lewis Pairs. *ACS Catal.* **2016,** *6* (7), 4526-4535.
23. Zhou, S.; Junge, K.; Addis, D.; Das, S.; Beller, M., A Convenient and General Iron-Catalyzed Reduction of Amides to Amines. *Angew. Chem.* **2009,** *121* (50), 9671-9674.
24. Rathke, J. W.; Klingler, R. J.; Krause, T. R., Propylene hydroformylation in supercritical carbon dioxide. *Organometallics* **1991,** *10* (5), 1350-1355.
25. Samec, J. S. M.; Backvall, J.-E.; Andersson, P. G.; Brandt, P., Mechanistic aspects of transition metal-catalyzed hydrogen transfer reactions. *Chem. Soc. Rev.* **2006,** *35* (3), 237-248.
26. Sheldon, R. A., Green solvents for sustainable organic synthesis: state of the art. *Green Chem.* **2005,** *7* (5), 267-278.
27. James, S. L.; Adams, C. J.; Bolm, C.; Braga, D.; Collier, P.; Friscic, T.; Grepioni, F.; Harris, K. D. M.; Hyett, G.; Jones, W.; Krebs, A.; Mack, J.; Maini, L.; Orpen, A. G.; Parkin, I. P.; Shearouse, W. C.; Steed, J. W.; Waddell, D. C., Mechanochemistry: opportunities for new and cleaner synthesis. *Chem. Soc. Rev.* **2012,** *41* (1), 413-447.
28. Chen, X.; Yang, H.; Zhong, Z.; Yan, N., Base-catalysed, one-step mechanochemical conversion of chitin and shrimp shells into low molecular weight chitosan. *Green Chem.* **2017,** *19* (12), 2783-2792.
29. Toda, F.; Kiyoshige, K.; Yagi, M., NaBH4 reduction of ketones in the solid state. *Angew. Chem. Int. Ed.* **1989,** *28* (3), 320-321.
30. Mack, J.; Fulmer, D.; Stofel, S.; Santos, N., The first solvent-free method for the reduction of esters. *Green Chem.* **2007,** *9* (10), 1041-1043.
31. Naimi-Jamal, M. R.; Mokhtari, J.; Dekamin, M. G.; Kaupp, G., Sodium Tetraalkoxyborates: Intermediates for the Quantitative Reduction of Aldehydes and Ketones to Alcohols through Ball Milling with NaBH4. *Eur. J. Org. Chem.* **2009,** *2009* (21), 3567-3572.
32. Zhang, Z.; Gao, J.; Xia, J.-J.; Wang, G.-W., Solvent-free mechanochemical and one-pot reductive benzylizations of malononitrile and 4-methylaniline using Hantzsch 1,4-dihydropyridine as the reductant. *Org. Biomol. Chem.* **2005,** *3* (9), 1617-1619.
33. Cravotto, G.; Gaudino, E. C., CHAPTER 3 Oxidation and Reduction by Solid Oxidants and Reducing Agents using Ball-Milling. In *Ball Milling Towards Green Synthesis: Applications, Projects, Challenges*, The Royal Society of Chemistry: 2015; pp 58-80.
34. Hua, D.; Hanxi, Y.; Xinping, A.; Chuansin, C., Hydrogen production from catalytic hydrolysis of sodium borohydride solution using nickel boride catalyst. *Int. J. Hydrogen Energy* **2003,** *28* (10), 1095-1100.

35. Zheng, C.; You, S.-L., Transfer hydrogenation with Hantzsch esters and related organic hydride donors. *Chem. Soc. Rev.* **2012,** *41* (6), 2498-2518.
36. Pachaly, B.; Weis, J., The Direct Process to Methylchlorosilanes: Reflections on Chemistry and Process Technology. In *Organosilicon Chemistry Set*, KGaA, W. V. V. G. C., Ed. 2008.
37. Kaushik, M.; Li, A. Y.; Hudson, R.; Masnadi, M.; Li, C.-J.; Moores, A., Reversing aggregation: direct synthesis of nanocatalysts from bulk metal. Cellulose nanocrystals as active support to access efficient hydrogenation silver nanocatalysts. *Green Chem.* **2016,** *18* (1), 129-133.
38. Kaushik, M.; Friedman, H. M.; Bateman, M.; Moores, A., Cellulose nanocrystals as non-innocent supports for the synthesis of ruthenium nanoparticles and their application to arene hydrogenation. *RSC Adv.* **2015,** *5* (66), 53207-53210.
39. Kaushik, M.; Basu, K.; Benoit, C.; Cirtiu, C. M.; Vali, H.; Moores, A., Cellulose Nanocrystals as Chiral Inducers: Enantioselective Catalysis and Transmission Electron Microscopy 3D Characterization. *J. Am. Chem. Soc.* **2015,** *137* (19), 6124-6127.
40. Rak, M. J.; Saade, N. K.; Friscic, T.; Moores, A., Mechanosynthesis of ultra-small monodisperse amine-stabilized gold nanoparticles with controllable size. *Green Chem.* **2014,** *16* (1), 86-89.
41. Rak, M. J.; Friščić, T.; Moores, A., One-step, solvent-free mechanosynthesis of silver nanoparticle-infused lignin composites for use as highly active multidrug resistant antibacterial filters. *RSC Adv.* **2016,** *6* (63), 58365-58370.
42. Rak, M. J.; Friščić, T.; Moores, A., Mechanochemical synthesis of Au, Pd, Ru and Re nanoparticles with lignin as a bio-based reducing agent and stabilizing matrix. *Faraday Discuss.* **2014,** *170* (0), 155-167.
43. Friscic, T., Supramolecular concepts and new techniques in mechanochemistry: cocrystals, cages, rotaxanes, open metal-organic frameworks. *Chem. Soc. Rev.* **2012,** *41* (9), 3493-3510.
44. Friščić, T.; Reid, D. G.; Halasz, I.; Stein, R. S.; Dinnebier, R. E.; Duer, M. J., Ion- and Liquid-Assisted Grinding: Improved Mechanochemical Synthesis of Metal–Organic Frameworks Reveals Salt Inclusion and Anion Templating. *Angew. Chem. Int. Ed.* **2010,** *49* (4), 712-715.
45. Friscic, T.; Childs, S. L.; Rizvi, S. A. A.; Jones, W., The role of solvent in mechanochemical and sonochemical cocrystal formation: a solubility-based approach for predicting cocrystallisation outcome. *CrystEngComm* **2009,** *11* (3), 418-426.
46. Howard, J. L.; Sagatov, Y.; Repusseau, L.; Schotten, C.; Browne, D. L., Controlling reactivity through liquid assisted grinding: the curious case of mechanochemical fluorination. *Green Chem.* **2017,** *19* (12), 2798-2802.
47. Do, J.-L.; Mottillo, C.; Tan, D.; Štrukil, V.; Friščić, T., Mechanochemical Ruthenium-Catalyzed Olefin Metathesis. *J. Am. Chem. Soc.* **2015,** *137* (7), 2476-2479.
48. Grey, R. A.; Pez, G. P.; Wallo, A., Anionic metal hydride catalysts. 2. Application to the hydrogenation of ketones, aldehydes, carboxylic acid esters, and nitriles. *J. Am. Chem. Soc.* **1981,** *103* (25), 7536-7542.
49. Goldberg, Y.; Ābele, E.; Shymanska, M.; Lukevics, E., Hydrosilylation of carbonyl compounds catalysed by alkali metal fluorides in the presence of crown ethers. *J. Organomet. Chem.* **1991,** *410* (2), 127-133.
50. van Putten, R.-J.; van der Waal, J. C.; de Jong, E.; Rasrendra, C. B.; Heeres, H. J.; de Vries, J. G., Hydroxymethylfurfural, A Versatile Platform Chemical Made from Renewable Resources. *Chem. Rev.* **2013,** *113* (3), 1499-1597.

51. Cukalovic, A.; Stevens, C. V., Production of biobased HMF derivatives by reductive amination. *Green Chem.* **2010,** *12* (7), 1201-1206.
52. Liu, F.; Sivoththaman, S.; Tan, Z., Solvent extraction of 5-HMF from simulated hydrothermal conversion product. *Sustain. Environ. Res.* **2014,** *24* (2), 149-157.
53. Saha, B.; Abu-Omar, M. M., Advances in 5-hydroxymethylfurfural production from biomass in biphasic solvents. *Green Chem.* **2014,** *16* (1), 24-38.
54. Hu, L.; Lin, L.; Wu, Z.; Zhou, S.; Liu, S., Recent advances in catalytic transformation of biomass-derived 5-hydroxymethylfurfural into the innovative fuels and chemicals. *Renew. Sust. Ener. Rev.* **2017,** *74* (Supplement C), 230-257.
55. Kang, E.-S.; Chae, D. W.; Kim, B.; Kim, Y. G., Efficient preparation of DHMF and HMFA from biomass-derived HMF via a Cannizzaro reaction in ionic liquids. *Ind. Eng. Chem. Res.* **2012,** *18* (1), 174-177.
56. Subbiah, S.; Simeonov, S. P.; Esperanca, J. M. S. S.; Rebelo, L. P. N.; Afonso, C. A. M., Direct transformation of 5-hydroxymethylfurfural to the building blocks 2,5-dihydroxymethylfurfural (DHMF) and 5-hydroxymethyl furanoic acid (HMFA) via Cannizzaro reaction. *Green Chem.* **2013,** *15* (10), 2849-2853.
57. Boopathy, R.; Bokang, H.; Daniels, L., Biotransformation of furfural and 5-hydroxymethyl furfural by enteric bacteria. *J. Ind. Microbiol.* **1993,** *11* (3), 147-150.
58. Garber, J. D.; Jones, R. E.; Torleif, U., Hydrogenation of 5-hydroxy-methyl furfural. Google Patents: 1963.
59. Alamillo, R.; Tucker, M.; Chia, M.; Pagan-Torres, Y.; Dumesic, J., The selective hydrogenation of biomass-derived 5-hydroxymethylfurfural using heterogeneous catalysts. *Green Chem.* **2012,** *14* (5), 1413-1419.
60. Lilga, M.; Hallen, R.; Werpy, T.; White, J.; Holladay, J.; Frye, J.; Zacher, A., Hydroxymethylfurfural Reduction Methods and Methods of Producing Furandimethanol. Google Patents: 2007.
61. Drent, E.; Budzelaar, P. H. M., Palladium-Catalyzed Alternating Copolymerization of Alkenes and Carbon Monoxide. *Chem. Rev.* **1996,** *96* (2), 663-682.
62. Milani, B.; Crotti, C.; Farnetti, E., Hydrogen transfer reduction of polyketones catalyzed by iridium complexes: a novel route towards more biocompatible materials. *Dalton Trans.* **2008,** (34), 4659-4663.
63. Wu, H.; Zhao, W.; Hu, H.; Chen, G., One-step in situball milling synthesis of polymer-functionalized graphene nanocomposites. *J. Mater. Chem.* **2011,** *21* (24), 8626-8632.
64. Guo, J.; Wang, B.; Zhu, C., Copolymerization of carbon monoxide and styrene catalyzed by resin-supported palladium polymer. *Express Polym. Lett.* **2007,** *1* (2), 69–76.
65. López, G. P.; Castner, D. G.; Ratner, B. D., XPS O 1s binding energies for polymers containing hydroxyl, ether, ketone and ester groups. *Surf. Interface Anal.* **1991,** *17* (5), 267-272.
66. Louette, P.; Bodino, F.; Pireaux, J.-J., Poly(dimethyl siloxane) (PDMS) XPS Reference Core Level and Energy Loss Spectra. *Surf. Sci. Spectra* **2005,** *12* (1), 38-43.

You contemplate the setting sun, unaware of your disorientation.

Dis-Orient: turned away from the east.

Williams, S.; Black, M.; More, J.; Mr. Nichols, *Sound Mirrors*, **2006**, *5*, 17:16-23:01.

In the previous chapters, we have explored the reduction of carbonyls through various alternative energy inputs to form various useful alcohol products. In this last part, the opposite reaction will be tackled, using a $(Ni_{0.5}Cu_{0.5})Fe_2O_4$ catalyst made by plasma induction. Seen from this perspective, alcohol oxidation is a means to activate otherwise unreactive electrophiles, that can be *in situ* coupled with amines.

5 Plasma-made $(Ni_{0.5}Cu_{0.5})Fe_2O_4$ nanoparticles for alcohol amination under microwave

Alain Li and Nicolas Dumaresq, Andréanne Segalla, Nadi Braidy, Audrey Moores, 'Plasma-made $(Ni_{0.5}Cu_{0.5})Fe_2O_4$ nanoparticles for alcohol amination under microwave, *manuscript in preparation*.

5.1 Abstract

Amine *N*-alkylation is a crucial process in the production of a wide range of chemicals, from bulk and fine chemicals and in particular pharmaceutical compounds. Using an alcohol as the alkylating agent is particularly attractive as most classic alkylating agents feature serious toxicity issues. Up to date, most catalysts are based on homogeneous, noble metal complexes (Ru, Ir). Thus, more efforts should be driven towards recyclable base metal-based catalysts for such industrially promising processes. Here we describe the synthesis of well defined $(Ni_{0.5}Cu_{0.5})Fe_2O_4$ magnetic nanoparticles by plasma induction, and their successful application to alcohol amination. Plasma induction allows precise morphology and size control over nanoparticle synthesis, while allowing the one-pot production of gram quantities of catalyst. By coupling high-end characterization techniques with catalytic optimization, a deep understanding of the role of Ni, Cu and Fe is deciphered for this process. A good scope of amines and alcohols have been coupled in high turnovers.

5.2 Introduction

Amines are essential synthetic building blocks for the chemical industry and for numerous biological processes.[1] Synthetic amines are widely employed in pesticides, pharmaceuticals, dyes, detergents, polymers, lubricants and various other functional materials.[2] For their synthesis, a wide variety of processes is available, such as using halides or tosylates as alkylating agents through the Buchwald-Hartwig coupling.[3-4] However, these coupling partners are toxic, and generate stoichiometric amounts of salts as byproduct. Alternatively, alcohols can be used as safer alkylating agents, generating only H_2O as a byproduct (Scheme 224).[5] They can be activated for C-N coupling *via* their *in situ* dehydrogenation towards the corresponding carbonyl, which enables offsetting their lower electrophilic reactivity. They can then condense with the amine, forming an imine and water as the sole byproduct. The hydrogens "borrowed" from the alcohol can then be re-used to reduce the C=N bond, therefore affording the amine. Overall, the process is redox-neutral, and is called 'borrowing hydrogen'

(BH). Since the early works of Watanabe[6] and Grigg[7] with Ru and Ir complexes as catalysts, and through the seminal works of Fujita[8] and Williams,[9] homogeneous BH has tremendously evolved from expensive metals and ligands, to base metals.[10-11] Although most reports are still based on Ru[12] and Ir,[13-14] recent efforts have focused on base metals such as Fe,[15-17] Mn[18] and Co.[19-20]

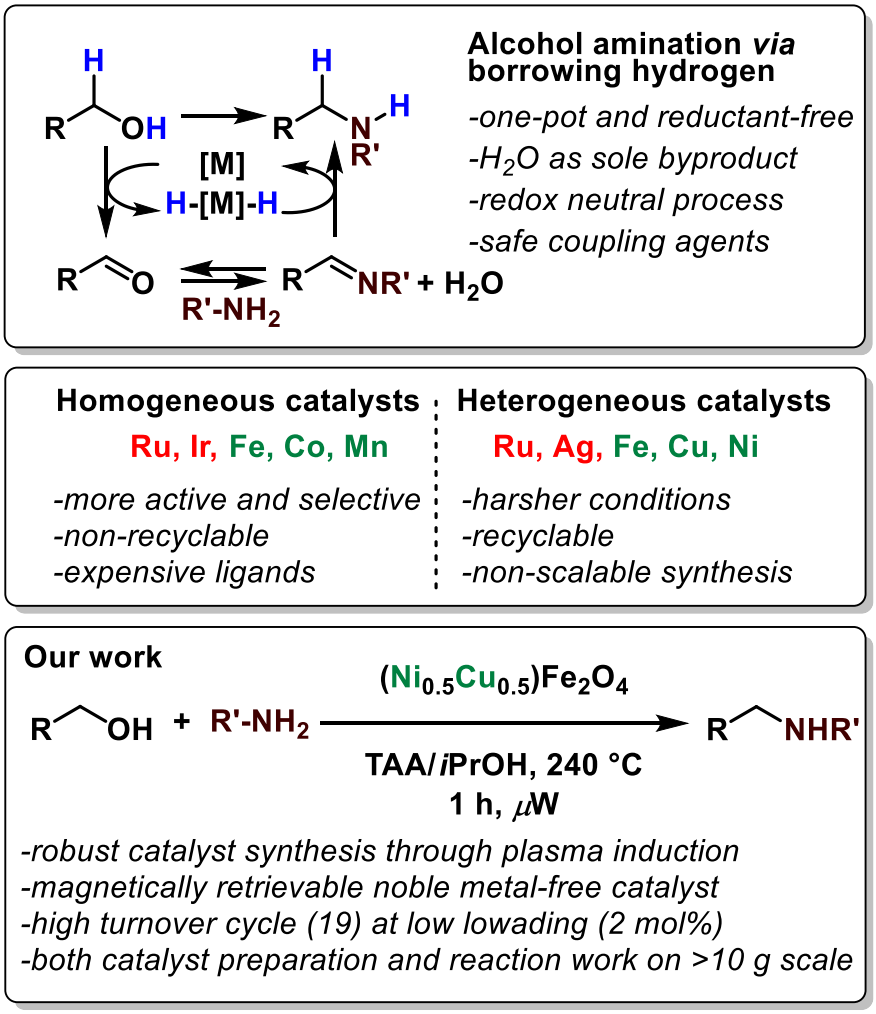

Scheme 224. Overview of this chapter.

In an effort to enable the recycling and the separation of these expensive metal complexes, there has been much development on heterogeneous catalysts.[21] Ru NPs can be supported on Fe_3O_4[22] and Ag NPs has shown a strong potential as well.[23-24] From our perspective though, abundant metals should be used to exploit the full potential of heterogeneous catalysis towards eco-friendlier processes. Fe_3O_4 NPs,[25-26] Cu NPs,[27-28] zeolites,[29] and even metal-free graphene oxide sheets[30] have been reported as catalysts for alcohol amination.

Notably, heterogeneous Ni has been widely explored since its first report in 1932 by Winans et *al*, requiring though 100 bar H_2 at 200°C for the alkylation of cyclohexylamine with EtOH.[31]

Ni has also been shown to be competent for BH when supported on Al_2O_3,[32-34] and can even perform ammonia alkylation in flow synthesis.[35-36] In most examples though, a base (KOH, K_2CO_3) is required to promote the proton removal in the alcohol oxidation step. Yet, the presence of a base is undesirable during the reaction as it may also favor side reactions typical for alcohols and transient carbonyls (Cannizzaro condensation, alcohol dehydration, and aldol condensation). In order to circumvent this issue, other authors have adopted bimetallic catalysts (Au-Pd,[37] Ag-Cu,[38] Pt-Sn,[39] Cu-Al[40]). The most notable example is the Ni/Cu pair for alcohol amination: Cu acts as a dehydrogenation catalyst for the starting alcohol, while Ni performs the hydrogenation of the imine.[41] Cu and Ni stearates with various stabilizers such as Ba stearate have been reported the production of long alkyl chains *N*,*N*-dimethylamines.[42-43] The Shi group reported a $NiCuFeO_x$ catalyst (3.6/1.1/1 weight ratio) through the calcination of metal carbonates then reduction under a H_2 flow.[44] Their alcohol amination scope was extensive, with 113 examples (up to 98% yield, Scheme 225).

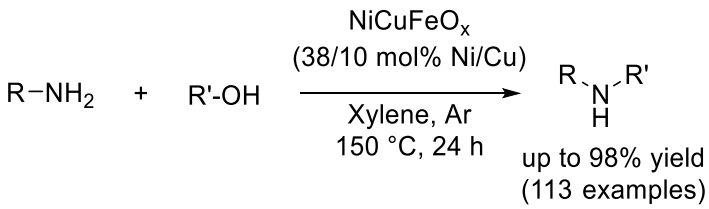

Scheme 225. Former example of Ni/Cu for alcohol amination.

In all these examples, NP synthesis required many time-consuming steps that added up to 12 h in the most optimal cases. For instance, NP annealing is an energy- and time-consuming treatment that is required to increase the crystallinity of the particles. Catalyst reduction using H_2 gas is another common post-synthesis treatment, and both will result in NP sintering and catalytic activity loss. Although sintering can be mitigated using capping agents, they would cause an even greater waste generation, that is all the more undesirable on the big scale.[45] Additionally, in past reports, extensive catalyst characterization was lacking, thus preventing a clear understanding of the active phase, as well as the exact role of each metal. Thus, developing waste-efficient synthesis of well-defined NPs on a big scale is imperative for far-reaching catalytic applications. Furthermore, despite their attractiveness, heterogeneous base metal catalysts (Cu, Ni, Mn, Fe) still require high loadings to offset their lower activity. For instance, up to 38% Ni loading were required in Shi's report. A careful nanostructure design could minimize the metal amounts. To obtain crystalline and well-defined NPs, high temperatures are required to decompose NP precursor and allow ordered growth. In liquid phase though, ligand-free NP agglomeration is difficult to avoid, driving the search for solid-

state[46-48] or gas phase processes.[49] Taking these considerations into account, we turned to induction plasma as a technique for the synthesis of Ni/Cu-containing NPs. Temperatures as high as ~6.000 K and ~10.000 K can be reached in plasma reaction chambers, allowing *in situ* annealing and precise phase control.[50] Through a strict control of precursor residence time and growth quenching, plasma induction allows the single-step production of monodisperse and crystalline NPs at high quantities (up to 30 g/h).[51] Radio-frequency (RF) plasma induction has already been used for the synthesis of ferric oxide nanoparticles from their corresponding metal nitrate salts, such as $ZnFe_2O_4$[52] and $NiFe_2O_4$.[53-54] To the best of our knowledge, no mixed ferrite synthesis from a RF plasma reactor has been reported so far. Herein we report the first example of nanocatalysts for alcohol amination, using $(Ni_{0.5}Cu_{0.5})Fe_2O_4$ NPs made by plasma induction. The catalyst was easily recyclable by magnetic separation and it was able to catalyze the reaction at low metal loadings comparable to that of homogeneous catalysts (<2 mol% of metal).

5.3 Results and discussion

5.3.1 NP synthesis by RF plasma induction

First, $(Ni_{0.5}Cu_{0.5})Fe_2O_4$ NPs were synthesized in an induction thermal plasma reaction chamber, following a procedure already reported previously by us (Braidy group) for the synthesis of $NiFeO_2$ NPs[53-54] and using a plasma setup described elsewhere (Figure 21).[55] The synthesis consisted in the coaxial injection aqueous solution of metal precursors (Fe, Ni and Cu nitrates in a 4/1/1 molar ratio) with a carrier gas (Ar) into an inductively coupled thermal plasma torch. A sheath gas of Ar/O_2 was used to control the trajectory of the NPs and provide them with oxygen atoms. The tip of the atomization probe coincides with the center of an induction thermal plasma torch connected to a 3 MHz RF power supply. As shown in Figure 21, the plasma torch connects into the top of a water-cooled cylindrical chamber (Main reactor).

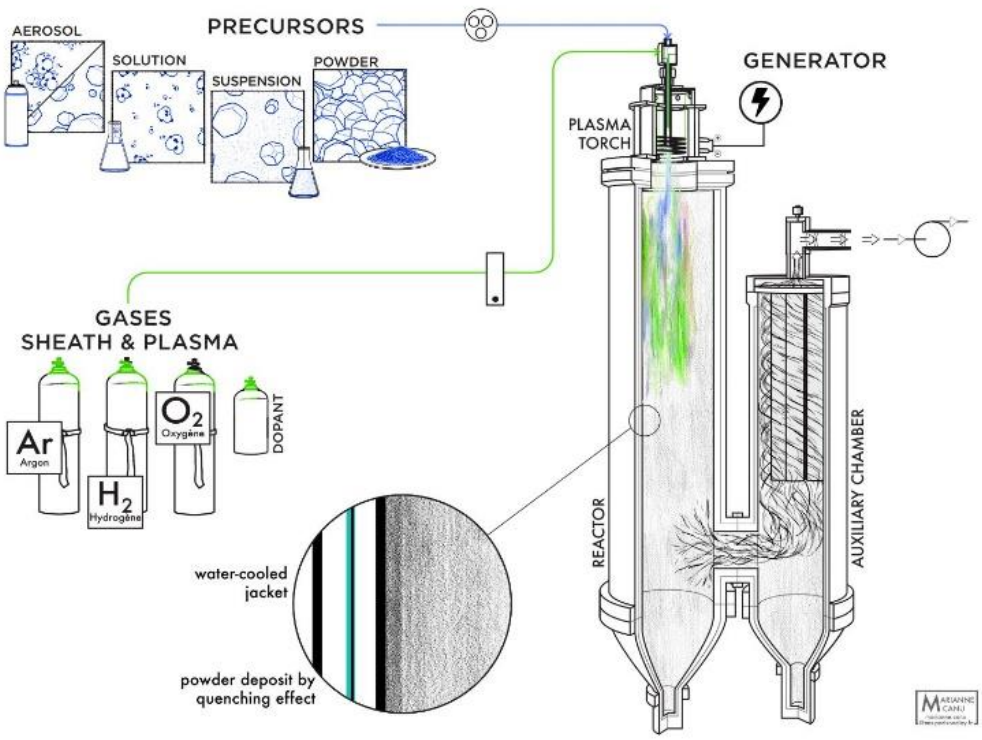

Figure 21. Schematic of inductively coupled radio-frequency plasma reaction chamber.

At its bottom, the main reactor is connected to another water-cooled cylindrical chamber (Auxiliary chamber) which contains 4 microporous filters connected to a vacuum pump. Upon evaporation of H_2O as the carrier solvent of the precursors in the main chamber, homogeneous nucleation of nanoparticles occurs by precursor supersaturation in the plasma phase. The main reactor is designed to recirculate the NPs several times into the high temperature region (Figure 1, blue/green region). During this recirculation, the NPs undergo several melting, quenching and annealing cycles, favoring crystalline particle growth. The entrance of the auxiliary chamber is designed to generate a cyclone, through which only particles with a sufficient hydrodynamic size can pass through and condense on the walls of the auxiliary chamber. With this apparatus, we investigated the synthesis of mixed Ni/Cu ferrite nanoparticles, using a 4/1/1 molar ratio of Fe/Cu/Ni in the precursor solution. We collected separately the resulting NPs from the main and the auxiliary chambers and called the resulting samples $(Ni_{0.5}Cu_{0.5})Fe_2O_4^{MAIN}$ and $(Ni_{0.5}Cu_{0.5})Fe_2O_4^{AUX}$ respectively. $(Ni_{0.5}Cu_{0.5})Fe_2O_4^{AUX}$ constituted about 33% wt of the total powder collected. They were subsequently tested for their catalytic activity.

5.3.2 Characterization

TEM images of $(Ni_{0.5}Cu_{0.5})Fe_2O_4^{MAIN}$ NPs were taken (Figure 22a). Two populations of NPs could be distinguished: small (<10 nm) crystalline aggregates (Figure 22b) as well as large

crystalline hexagonal shaped NPs (<20 nm) (Figure 22c). Additional images are provided in the appendix (Figure 28 to Figure 30). In contrast, only the bigger hexagonal NPs were observed by TEM in $(Ni_{0.5}Cu_{0.5})Fe_2O_4^{AUX}$ (Figure 22d). These well-facetted hexagonal NPs observed in the TEM micrograph are the projection of a truncated octahedron exposing their (111) facets (see Figure 27 in Appendix). This is consistent with the equilibrium Wulff shape of crystals that predicts a truncated octahedron for a FCC structure such as the spinel. As for the smaller NPs in $(Ni_{0.5}Cu_{0.5})Fe_2O_4^{MAIN}$, it can be explained by the fluid dynamics inside of the reactor. As explained before, the cyclone in the auxiliary chamber only lets through well-defined NPs with a sufficient hydrodynamic size, that went through multiple recirculation steps. Insufficiently grown NPs get stuck and quenched onto the main reactor walls creating those small agglomerate as seen in Figure 22 (a and b). The larger, full grown particles were found both in the main chamber where they are formed and in the auxiliary chamber, where they are transferred.

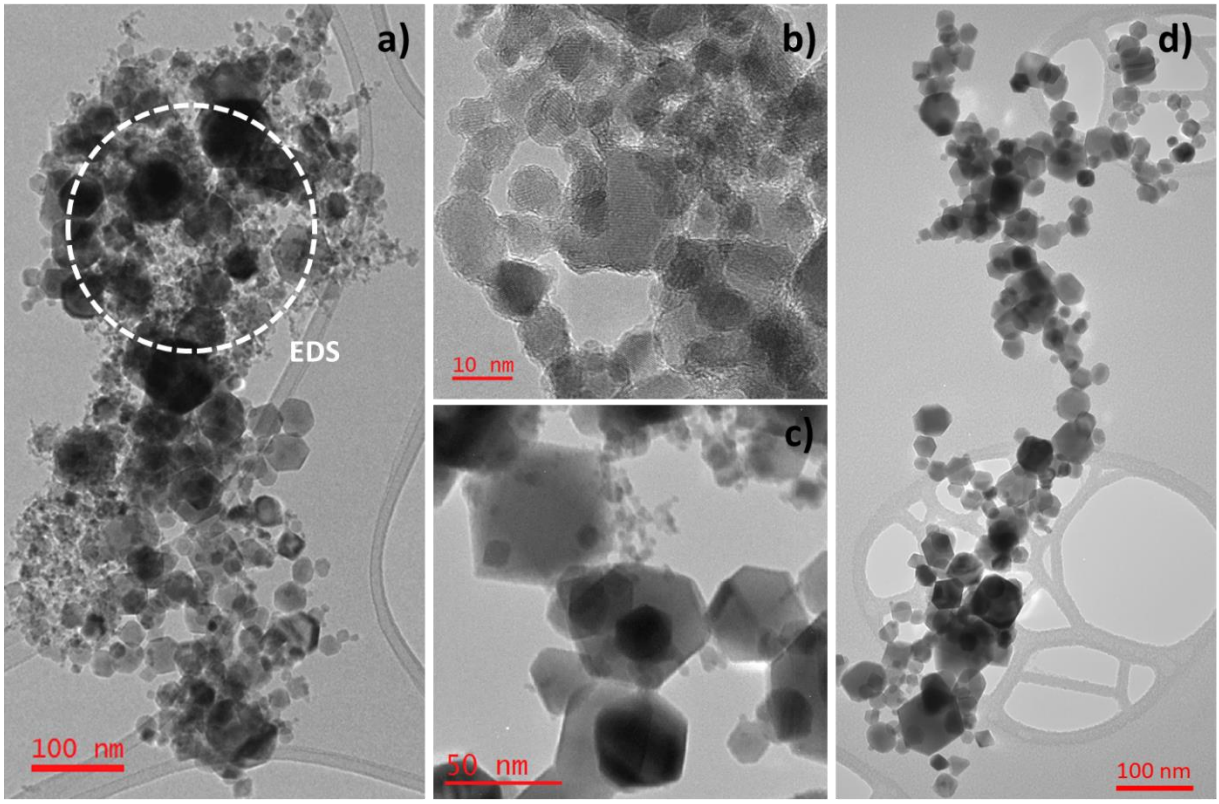

Figure 22. (a) TEM picture of $(Ni_{0.5}Cu_{0.5})Fe_2O_4^{MAIN}$ (White dashed circle indicates the EDS study zone), (b) Closer view of the small crystalline NPs in $(Ni_{0.5}Cu_{0.5})Fe_2O_4^{MAIN}$ (c) Well-defined truncated octahedron NPs in $(Ni_{0.5}Cu_{0.5})Fe_2O_4^{MAIN}$. (d) TEM picture of $(Ni_{0.5}Cu_{0.5})Fe_2O_4^{AUX}$.

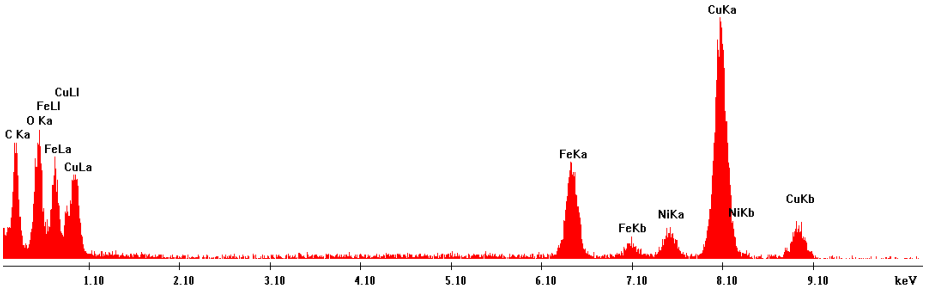

Figure 23. EDS spectrum of $(Ni_{0.5}Cu_{0.5})Fe_2O_4^{MAIN}$ (circle indicated in Figure 22).

The samples were then analyzed by X-ray Fluorescence (XRF) to confirm their bulk composition (Table 18 and Chart 12). The metal ratios observed were close to the expected values, 4/1/1, similarly to our previous studies on the RF plasma synthesis of $NiFe_2O_4$,.[53-54] In $(Ni_{0.5}Cu_{0.5})Fe_2O_4^{MAIN}$ a slightly higher amount of Cu (18.5%) compared to the expected value (16.7%) was observed, whereas a smaller amount of Cu was observed in $(Ni_{0.5}Cu_{0.5})Fe_2O_4^{AUX}$ (15.1%). The Ni amounts were consistently close to the expected value (16.7%): 16.1% and 16.2% for $(Ni_{0.5}Cu_{0.5})Fe_2O_4^{MAIN}$ and $(Ni_{0.5}Cu_{0.5})Fe_2O_4^{AUX}$ respectively. Finally, the trend for Fe amounts was the opposite to that of the Cu amounts: 65.4% and 68.8% for $(Ni_{0.5}Cu_{0.5})Fe_2O_4^{MAIN}$ and $(Ni_{0.5}Cu_{0.5})Fe_2O_4^{AUX}$ respectively (66.7% expected). These discrepancies from the expected values could be explained by the vapor pressure of Cu (2540 K at 20 KPa, a pressure close to the one in the plasma reactor) that is lower than Fe and Ni (2720 K and 2860 K at 20 KPa), causing Cu to stay longer into gas phase and get ejected from the recirculation flow. They get quenched onto the main reactor walls more favorably than Fe and Ni, precipitating out as an oxide.

Sample	**Cu**	**Ni**	**Fe**
$(Ni_{0.5}Cu_{0.5})Fe_2O_4^{MAIN}$	18.5%	16.1%	65.4%
$(Ni_{0.5}Cu_{0.5})Fe_2O_4^{AUX}$	15.1%	16.2%	68.8%
Expected amounts	16.7%	16.7%	66.7%

Table 18. XRF bulk analysis of $(Ni_{0.5}Cu_{0.5})Fe_2O_4$ NPs: molar ratios of Ni, Cu and Fe.

Chart 12. XRF bulk analysis of $(Ni_{0.5}Cu_{0.5})Fe_2O_4$ NPs: molar ratios of Ni, Cu and Fe.

XPS analysis of the samples was performed, to shed light into the surface composition of the samples (Table 19 and Chart 13). The Cu amounts were consistently higher than the expected amounts (16.7%): 42.2% and 24.8% for $(Ni_{0.5}Cu_{0.5})Fe_2O_4^{MAIN}$ and $(Ni_{0.5}Cu_{0.5})Fe_2O_4^{AUX}$ respectively, with a sharp decrease of the Ni amounts: 6.2% and 7.9% for $(Ni_{0.5}Cu_{0.5})Fe_2O_4^{MAIN}$ and $(Ni_{0.5}Cu_{0.5})Fe_2O_4^{AUX}$ respectively. 51.6% of Fe was found at the surface of $(Ni_{0.5}Cu_{0.5})Fe_2O_4^{MAIN}$, whereas a value closer to the expected amounts was found for $(Ni_{0.5}Cu_{0.5})Fe_2O_4^{AUX}$ (67.2% versus 66.7% in theory).

Sample	Cu	Ni	Fe
$(Ni_{0.5}Cu_{0.5})Fe_2O_4^{MAIN}$	42.2%	6.2%	51.6%
$(Ni_{0.5}Cu_{0.5})Fe_2O_4^{AUX}$	24.8%	7.9%	67.2%
Expected amounts	16.7%	16.7%	66.7%

Table 19. XPS analysis of $(Ni_{0.5}Cu_{0.5})Fe_2O_4$ NPs: molar ratios of Ni, Cu and Fe.

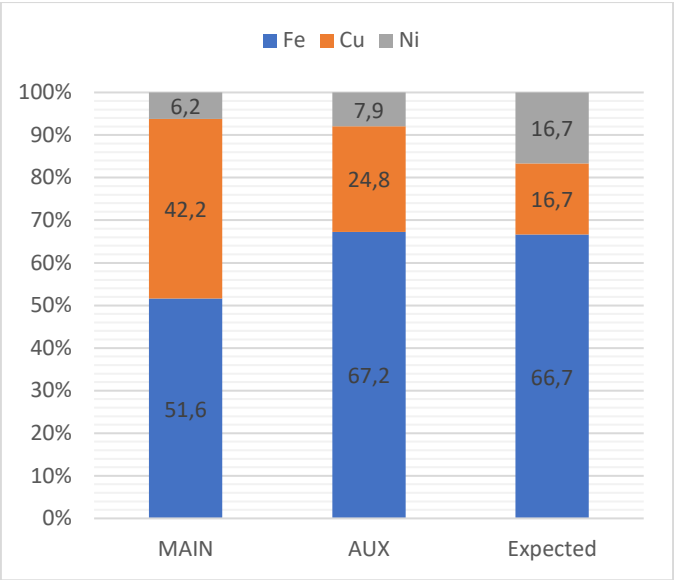

Chart 13. XPS analysis of $(Ni_{0.5}Cu_{0.5})Fe_2O_4$ NPs: molar ratios of Ni, Cu and Fe.

The difference between the metal amounts detected by XRF and XPS indicates that, regardless of the samples, Cu species were predominant on the surface whereas Ni species were prevalent inside the NPs.

Deconvolution of the $Cu2p_{3/2}$ region showed the coexistence of two Cu species on $(Ni_{0.5}Cu_{0.5})Fe_2O_4^{MAIN}$ (Table 20 and Figure 24). The first peak at 931.6 eV can be attributed to $CuFe_2O_4$.[56] It was the only phase detected on $(Ni_{0.5}Cu_{0.5})Fe_2O_4^{AUX}$ and was found present at 57% in $(Ni_{0.5}Cu_{0.5})Fe_2O_4^{MAIN}$. The second peak found in $(Ni_{0.5}Cu_{0.5})Fe_2O_4^{MAIN}$ at 933.6 eV was attributed to CuO (43%).[57]

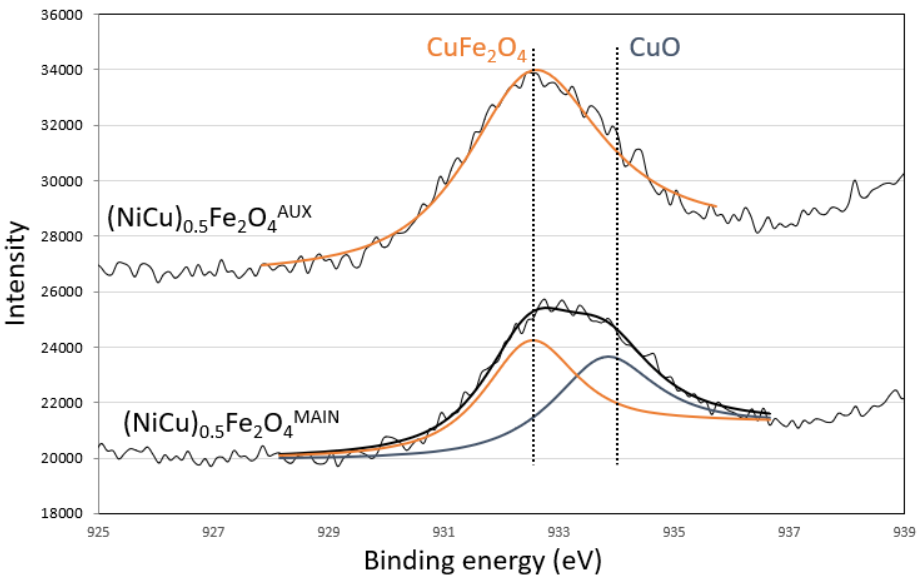

Figure 24. XPS of $(Ni_{0.5}Cu_{0.5})Fe_2O_4^{AUX}$ and $(Ni_{0.5}Cu_{0.5})Fe_2O_4^{MAIN}$ – Cu $2p_{3/2}$ region

Sample	$CuFe_2O_4$ (931.6 eV)	CuO (933.6 eV)
$(Ni_{0.5}Cu_{0.5})Fe_2O_4^{AUX}$	100%	0%
$(Ni_{0.5}Cu_{0.5})Fe_2O_4^{MAIN}$	57%	43%

Table 20. XPS of $(Ni_{0.5}Cu_{0.5})Fe_2O_4^{AUX}$ and $(Ni_{0.5}Cu_{0.5})Fe_2O_4^{MAIN}$ – Cu $2p_{3/2}$ region

The Ni $2p_{3/2}$ region gave a single peak associated with the presence of $NiFe_2O_4$ (854.5 eV), consistently over both $(Ni_{0.5}Cu_{0.5})Fe_2O_4^{AUX}$ and $(Ni_{0.5}Cu_{0.5})Fe_2O_4^{MAIN}$ (Figure 25).[58]

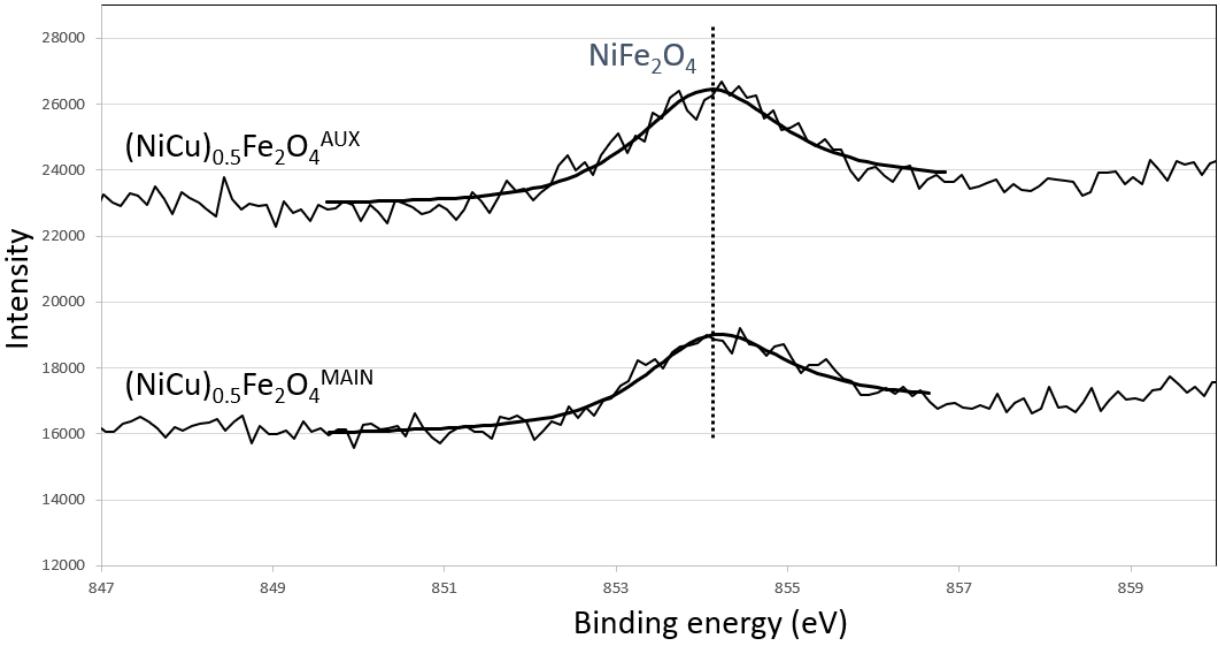

Figure 25. XPS of $(Ni_{0.5}Cu_{0.5})Fe_2O_4^{AUX}$ and $(Ni_{0.5}Cu_{0.5})Fe_2O_4^{MAIN}$ – Ni $2p_{3/2}$ region

The crystallinity of $(Ni_{0.5}Cu_{0.5})Fe_2O_4^{MAIN}$ and $(Ni_{0.5}Cu_{0.5})Fe_2O_4^{AUX}$ has been studied with powder X-ray diffraction (Chart 14). A Rietveld refinement has been performed to determine the relative concentration of each crystalline phase as well as their unit cell parameter (shown in Table 33 in the appendix). Since both $CuFe_2O_4$ and $NiFe_2O_4$ follow an inverse spinel pattern, we considered from the peak fit that every tetrahedral site was occupied with Fe, and that every octahedral site was occupied with Fe, Cu and Ni.[59-60] The R_{wp} and R_{exp} values for both $(Ni_{0.5}Cu_{0.5})Fe_2O_4^{MAIN}$ (2.09 and 1.64 respectively) and $(Ni_{0.5}Cu_{0.5})Fe_2O_4^{AUX}$ (2.58 and 1.65 respectively), as well as the difference plot between our experimental XRD pattern (Chart 14) and our calculated pattern indicate the presence of only one crystalline $(Ni_xCu_y)Fe_{3-x-y}O_4$ spinel phase. Since the CuO observed by XPS was not detected by XRD, we can either conclude that the CuO NPs are amorphous or too small to be detected.

No improvement in the goodness of fit (GOF) was observed when the atomic occupancy of the octahedral sites of the spinel was changed. That can be explained by the X-ray scattering strength of these elements being too close to each other for the method used to make a difference. Since there was no significant change in the refinement when the atomic distribution was changed, the fitting pattern was fixed to be $(Ni_{0.5}Cu_{0.5})Fe_2O_4^{AUX}$. A significant improvement of the fit has been observed when oxygen displacement was allowed, which is characterized by the u parameter in Chart 14.

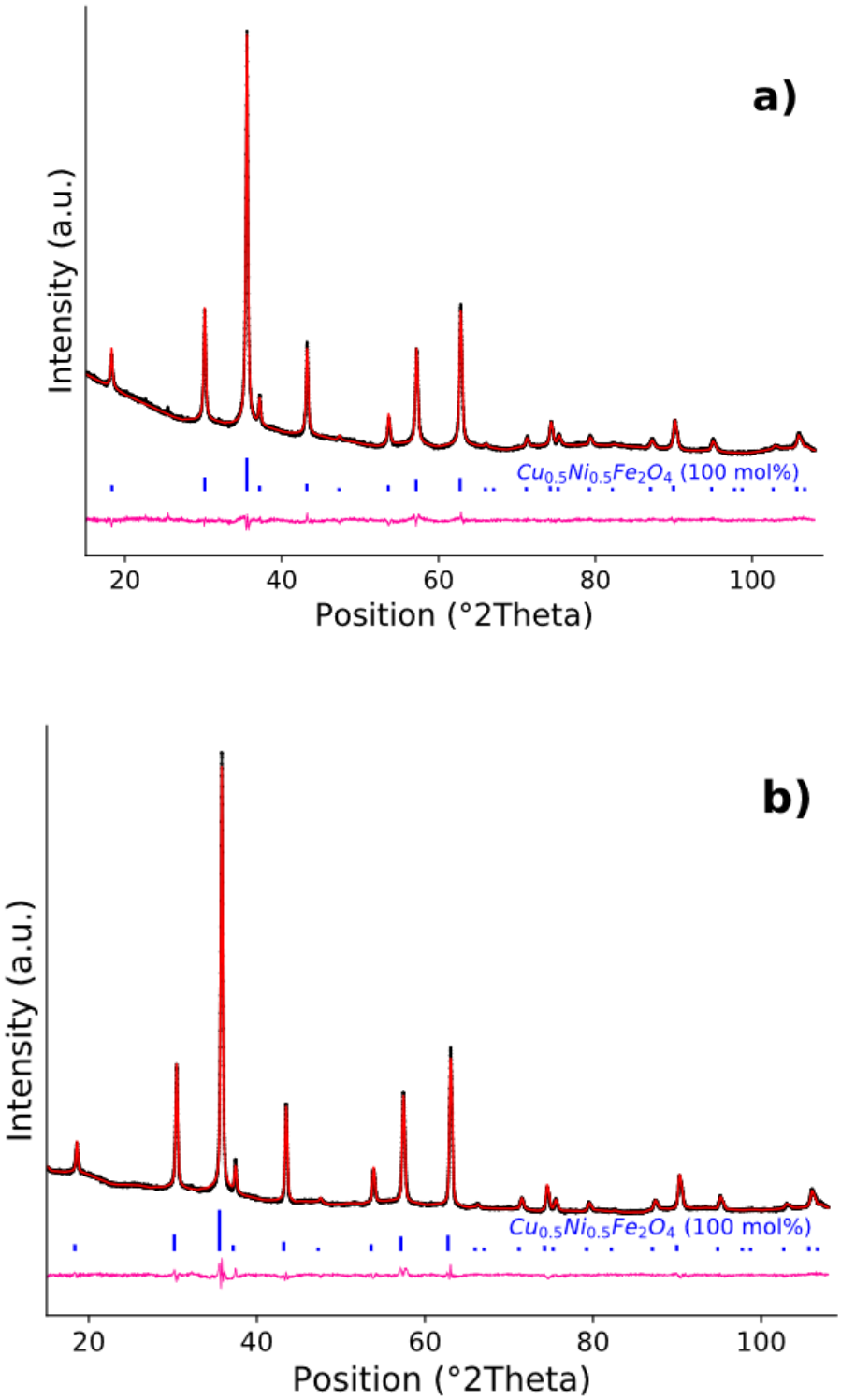

Chart 14. XRD of (a) $(Ni_{0.5}Cu_{0.5})Fe_2O_4^{MAIN}$ (b) $(Ni_{0.5}Cu_{0.5})Fe_2O_4^{AUX}$. Experimental pattern (black line), calculated pattern by Rietveld refinement (red line) and the difference plot (purple line). The stick pattern represents the reference pattern used for the Rietveld calculated pattern.

5.4 Catalytic results

We first tested $(Ni_{0.5}Cu_{0.5})Fe_2O_4^{MAIN}$ for the base-free condensation of aniline with benzyl alcohol. In order to ensure a higher reaction reproducibility and pressure control, we opted for microwave heating (Table 21). Thus, we chose *tert*-amyl alcohol (TAA) as a solvent due to its compatibility with microwave heating and its inability to get dehydrogenated by our catalyst due to its absence of protons in its α position. Under the conditions described below, reaction pressure reached up to 26 bar. A typical temperature and pressure profile is provided in the appendix (Chart 18 and Chart 19). Using one equivalent of benzyl alcohol with the aniline and 10 mol% of the catalyst, we initially obtained 15% of the desired amine along with 64% of the imine after 45 minutes of microwave heating at 240 °C (Table 21, entry 1). We reasoned that addition of an excess of reducer, which in this case is the substrate benzyl alcohol, could push the desired hydrogenation of imine. This indeed increased the yield to 51 and 56%, for respectively 1.5 and 2 equivalents of alcohol (Table 21, entries 2 and 3). Thus, we kept the alcohol excess to 1.5 for the rest of Table 21 experiments. Diminishing the catalyst amount from 50 mg to 40 mg decreased the yield from 51% amine and 36% imine to 29% amine and 60% imine (Table 21, entry 4), but increasing the catalyst amount to 60 mg decreased the yield as well to 27% amine and 50% imine (Table 21, entry 5). The imine product formation was above 26% in entries 1-5, hinting at the difficulty of the catalyst to perform C=N reduction. As we did not want to push beyond adding 1.5 excess of benzyl alcohol, we turned to adding 10 vol% of *i*PrOH, a classic sacrificial hydrogen donor, to our solvent system, increasing the yield to 78% (Table 21, entry 6).

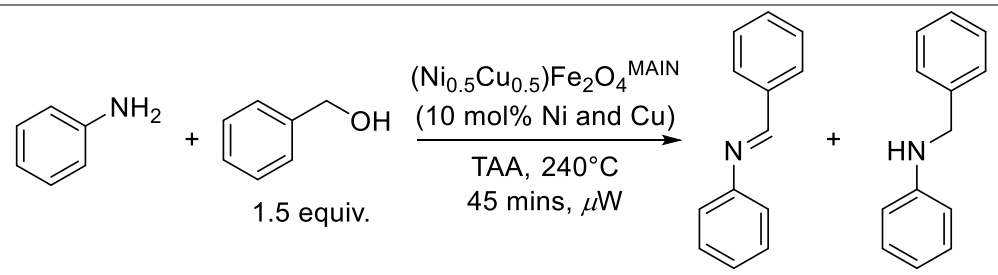

Entry	Modification		Yield (%)	
			Imine	Amine
1	Benzyl alcohol excess	1	64	15
2		1.5	36	51
3		2	26	56
4	Catalyst quantity	40 mg[b]	60	29
5		60 mg[c]	50	27

6	*i*PrOH additive (10 vol%)	2	78

[a]Standard reaction conditions: aniline (1 mmol), benzyl alcohol (1.5 mmol), $(Ni_{0.5}Cu_{0.5})Fe_2O_4^{MAIN}$ (50 mg, 10 mol% of Ni and 10 mol% Cu), *tert*-amyl alcohol (2 mL), Ar, microwave, 240 °C, 45 min. [b] 8 mol% of Ni and Cu [c] 12 mol% of Ni and Cu

Table 21. Reaction of aniline with benzyl alcohol in the presence of $(Ni_{0.5}Cu_{0.5})Fe_2O_4^{MAIN}$ under various conditions[a]

Since the addition of 10 vol% *i*PrOH proved fruitful to assist C=N reduction, we could lower the excess of benzyl alcohol to 1.2 equivalents and pushed the yield to above 70% while minimizing the imine amount to <2% (Table 22). Such an alcohol excess is commonly encountered for catalytic systems in this field, even in homogeneous catalysis.[61-62] With this system we studied the reaction kinetics to better understand the catalytic system and optimize the reaction time, which was fixed to 45 min in all runs described so far. As the reaction proceeds, benzyl alcohol is first consumed rapidly, and is almost completely gone after 30 minutes of reaction (Table 22, entry 4). As could be expected, the imine rapidly builds up as the alcohol gets dehydrogenated and reaches a maximum at 10 min, before slowly dropping, as the amine is steadily produced. Past 55 min of reaction, a plateau of 72-77% yield was reached for the amine with virtually no imine left (<2%) (Table 22, entries 5-8). Between 75 and 90 min, the amine gets re-oxidized back into the imine (41 and 32% respectively) (Table 22, entry 9). With these results in hand, we settled at 1 h for the optimum reaction time.

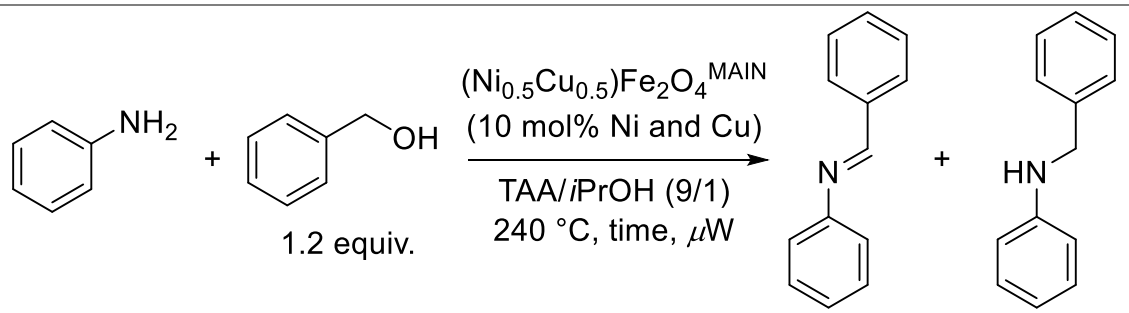

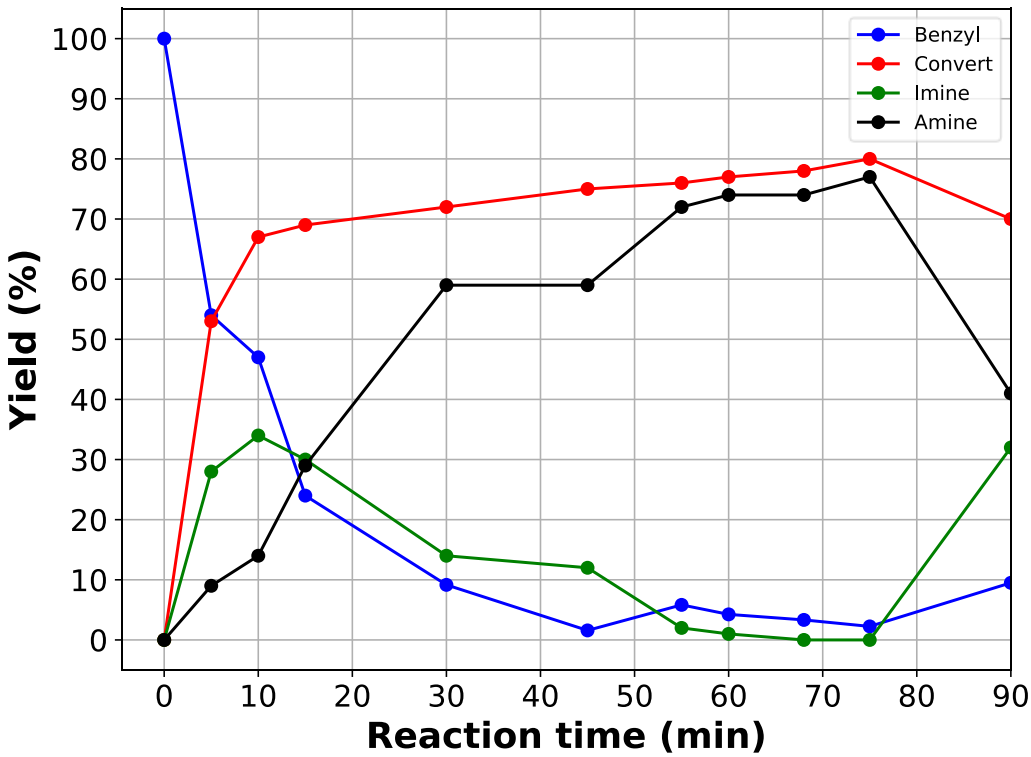

[a]Standard reaction conditions: aniline (1 mmol), benzyl alcohol (1.2 mmol), $(Ni_{0.5}Cu_{0.5})Fe_2O_4^{MAIN}$ (50 mg, 10 mol% of Ni and 10 mol% Cu), *tert*-amyl alcohol/isopropanol (1.8 mL and 0.2 mL), Ar, microwave, 240 °C.

Table 22. Time optimization of the model reaction using *i*PrOH as an additive[a]

5.4.1 Mechanistic studies

We tested different ferrite-based catalysts using our plasma induction method, to probe the role of each metal. Using metal ferrites from the main reactor composed of only one of the two catalytic metals tested, namely $CuFe_2O_4^{MAIN}$ or $NiFe_2O_4^{MAIN}$, drastically decreased the yield to 5% and 1% in amine respectively, with an imine yield of 10% and 4% respectively (Table 23, entries 2 and 3). Mixing in the same batch independently prepared $CuFe_2O_4^{MAIN}$ and $NiFe_2O_4^{MAIN}$ NPs yielded 37% of amine and 36% of imine, confirming that both Cu and Ni are required for the reaction (Table 23, entry 4). Importantly having Cu and Ni within the same particle seems to help with imine reduction to amine, as the comparable run with $(Ni_{0.5}Cu_{0.5})Fe_2O_4^{MAIN}$ provided 74% in amine and 1% in imine (Table 23, entry 1). Using $Fe_3O_4^{MAIN}$ NPs gave no product (Table 23, entry 5). Also, up to now we had focused on studying $(Ni_{0.5}Cu_{0.5})Fe_2O_4^{MAIN}$ from the main reactor. We thus wanted to test $(Ni_{0.5}Cu_{0.5})Fe_2O_4^{AUX}$ collected on the filter of the auxiliary reactors, giving a lower yield as well (8% amine yield with 18% imine, entry 6). Finally, using either $CuFe_2O_4^{AUX}$ or $NiFe_2O_4^{AUX}$ from the filter gave similar trends than with $CuFe_2O_4^{MAIN}$ and $NiFe_2O_4^{MAIN}$ (8 and

1% yield with 6 % and 2% imine, entries 7 and 8). It is worth noting that in almost every case involving only Ni or Cu (Table 23, entries 2, 3, 7 and 8), the mass balance for N-containing products dropped below 75%, whereas it remained higher than 90% when both metals were present (Table 23, entries 1, 4 and 6).

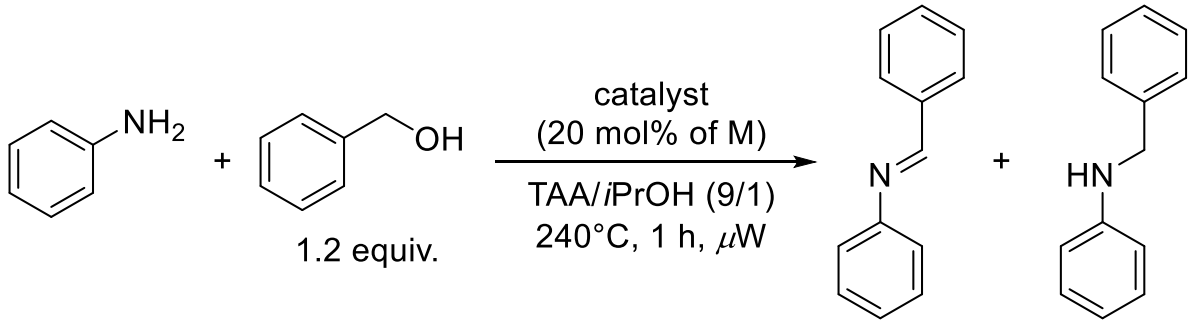

Entry	Modification		Conversion	Yield (%)	
				Imine	Amine
1	$Catalyst^{MAIN}$	$(Ni_{0.5}Cu_{0.5})Fe_2O_4^{MAIN}$	77	1	74
2[b]		$CuFe_2O_4^{MAIN}$	33	10	5
3[c]		$NiFe_2O_4^{MAIN}$	30	4	1
4[d]		$CuFe_2O_4^{MAIN}$ and $NiFe_2O_4^{MAIN}$	79	36	37
5		$Fe_3O_4^{MAIN}$	22	3	0
6[d]	$Catalyst^{AUX}$	$(Ni_{0.5}Cu_{0.5})Fe_2O_4^{AUX}$	34	18	8
7[b]		$CuFe_2O_4^{AUX}$	52	6	8
8[c]		$NiFe_2O_4^{AUX}$	40	2	1

[a]Standard reaction conditions: aniline (1 mmol), benzyl alcohol (1.2 mmol), catalyst (50 mg), *tert*-amyl alcohol/isopropanol (1.8/0.2 mL), Ar, microwave, 240 °C, 1 h
[b]20 mol% Cu
[c]20 mol% Ni
[d]10 mol% Ni and 10 mol% Cu

Table 23. Control experiments[a]

Finally, we looked at the role of each metal in the mechanistic pathway. To better probe the alcohol dehydrogenation step, we heated benzyl alcohol alone under microwave conditions in the presence of various catalysts under inert conditions (240 °C, 1 h). With $(Ni_{0.5}Cu_{0.5})Fe_2O_4^{MAIN}$, 97% of the benzyl alcohol got consumed into various oxidations products: benzaldehyde, benzoic acid, and benzyl benzoate (Table 24, entry 1). Under inert atmosphere, the presence of benzaldehyde can only be explained through a dehydrogenation pathway. Subsequently, benzaldehyde can undergo Cannizzaro dismutation at elevated

temperature to form benzoic acid.[63] Finally, the last product can condense with benzyl alcohol to form benzyl benzoate. Upon using $CuFe_2O_4^{MAIN}$, a similar conversion of 84% was observed (Table 24, entry 2). However, $NiFe_2O_4^{MAIN}$ alone gave a 25% conversion (Table 24, entry 3).

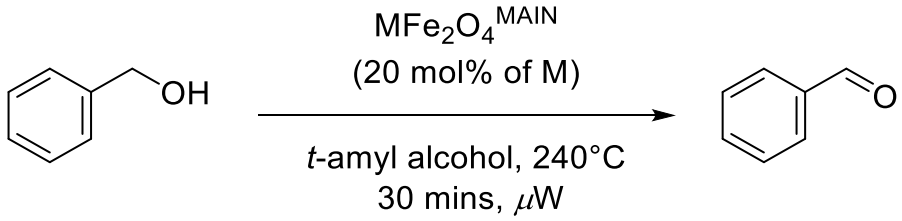

Entry	Catalyst	Conversion (%)
1	$(Ni_{0.5}Cu_{0.5})Fe_2O_4^{MAIN}$	97
2[b]	$CuFe_2O_4^{MAIN}$	84
3[c]	$NiFe_2O_4^{MAIN}$	25

[a]Standard reaction conditions: benzyl alcohol (1 mmol), $(Ni_{0.5}Cu_{0.5})Fe_2O_4^{MAIN}$ (50 mg, 10 mol% of Ni and 10 mol% Cu), *t*-amyl alcohol (2 mL), Ar, microwave, 240 °C, 30 min.
[b]20 mol% Cu
[c]20 mol% Ni

Table 24. Mechanistic investigation on $(Ni_{0.5}Cu_{0.5})Fe_2O_4^{MAIN}$-catalyzed alcohol oxidation[a]

We then investigated the last step of the mechanism, imine reduction. We first made an imine model substrate by ball-milling the corresponding aldehyde and amine in presence of a drying agent (Na_2SO_4) for 15 minutes. Then, we then subjected the imine to hydrogenation conditions (150 °C, 20 bar H_2) in presence of $MFe_2O_4^{MAIN}$ (M = Cu, Ni, $Ni_{0.5}Cu_{0.5}$) for 24 h. With $(Ni_{0.5}Cu_{0.5})Fe_2O_4^{MAIN}$, 30% of the imine was reduced into the corresponding amine (Table 25**Erreur ! Source du renvoi introuvable.**, entry 1). In contrast, switching to $CuFe_2O_4^{MAIN}$ or $NiFe_2O_4^{MAIN}$ gave lower to no yield (0 and 5% respectively, Table 25**Erreur ! Source du renvoi introuvable.**, entries 2 and 3). Such contrast in the catalytic results show that a Ni-Cu synergy is required for the hydrogenation of C=N bonds.

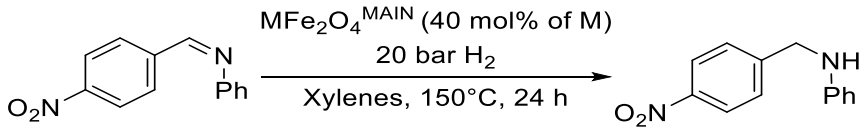

Entry	Catalyst	Conversion (%)
1	$(Ni_{0.5}Cu_{0.5})Fe_2O_4^{MAIN}$	30
2[b]	$CuFe_2O_4^{MAIN}$	0
3[c]	$NiFe_2O_4^{MAIN}$	5

[a]Standard reaction conditions: imine (0.5 mmol), $(Ni_{0.5}Cu_{0.5})Fe_2O_4^{MAIN}$ (50 mg, 20 mol% of Ni and 20 mol% Cu), Xylenes (15 mL), H_2 (20 bar), 150 °C, 24 h. [b] 40 mol% Cu [c] 40 mol% Ni.

Table 25. Mechanistic investigation on $(Ni_{0.5}Cu_{0.5})Fe_2O_4^{MAIN}$-catalyzed imine reduction[a]

Overall, our best catalyst is $(Ni_{0.5}Cu_{0.5})Fe_2O_4^{MAIN}$ (1% imine, 74% amine). Switching to catalyst to separate $CuFe_2O_4^{MAIN}$ and $NiFe_2O_4^{MAIN}$ NPs led to a decrease of the amine yield but did not affect overall conversion (36% imine, 37% amine). However, using $(Ni_{0.5}Cu_{0.5})Fe_2O_4^{AUX}$ gave a drastic conversion drop (18% imine, 8% amine). Along with the XPS results mentioned earlier and the results from Table 24, we can conclude that the presence of the amorphous CuO found in both $(Ni_{0.5}Cu_{0.5})Fe_2O_4^{MAIN}$ and $CuFe_2O_4^{MAIN}$/$NiFe_2O_4^{MAIN}$, and absent in $(Ni_{0.5}Cu_{0.5})Fe_2O_4^{AUX}$ is correlated with high conversions due their capacity to oxidize the alcohol. The second step of the mechanism consists in the condensation of the resulting carbonyl with the amine to form an imine after the loss of a water molecule. Although the elevated temperature in our reaction favors H_2O elimination, we cannot exclude Cu(II) acting as Lewis acid to help imine condensation.[64] Due to $CuFe_2O_4^{AUX}$ and $CuFe_2O_4^{MAIN}$ being both unable to perform the full process despite being able to oxidize alcohol, we can then deduce that a Ni species (identified by XPS to be Ni integrated to the ferrite lattice) assists the C=N reduction step. Furthermore, the presence of both Cu and Ni in the same lattice is required to further push imine reduction to completion, probably facilitating hydrogen transfer between the two metals. Overall, such role assignment for Cu and Ni in alcohol amination is consistent with previous literature studies (Scheme 226).[41]

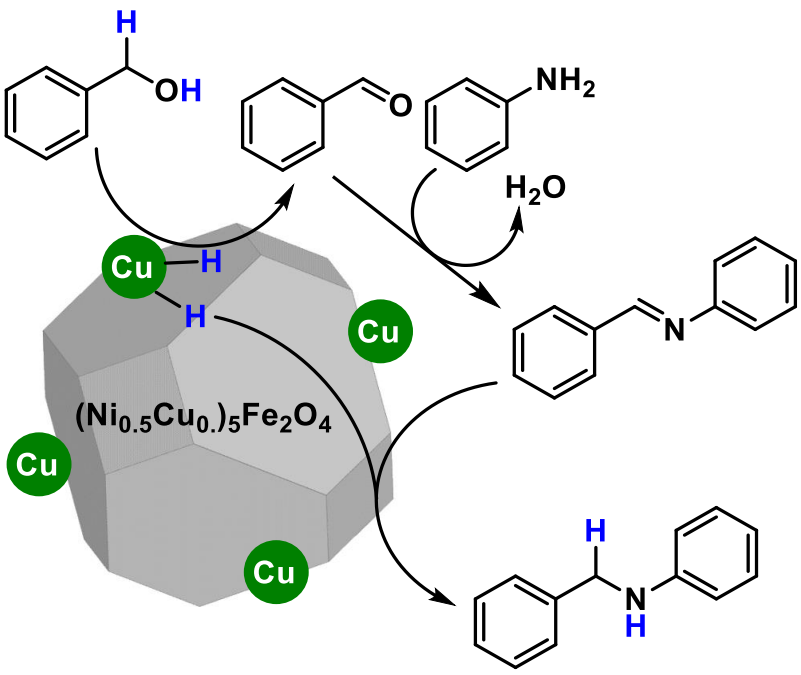

Scheme 226. Proposed mechanistic pathway for $(Ni_{0.5}Cu_{0.5})Fe_2O_4^{MAIN}$-catalyzed alcohol amination.

We then investigated the effect of microwave on the catalyst. All tests described until now were performed in standard glass vials, which are transparent to microwaves. Heating occurs then through the interaction of microwaves with matter inside the vials. Conversely, silicon carbide (SiC) vials are able to fully absorb microwave irradiations themselves, so that they can heat and shelter the material inside the vial from any radiation.[65-66] Using SiC vials, we could then test our catalysis under the same conditions of temperature and pressure, while providing purely thermal heating to the solution. Upon using a SiC vial, the yield in amine decreased from 74% to 30% (Table 26, entries 1 and 2). We also wanted to compare with a pure thermal setup, yet we had to slightly modify the conditions as we could not reproduce our optimal setting thermally. Since the model reaction reached up to 26 bar under microwave at 240 °C, we ran it at lower temperature (130°C, 48h) to run it at oil bath conditions (Table 26, entries 3 and 4). Under these settings, a 11% yield was obtained under microwave heating whereas 5% of yield was obtained when the reaction was conducted in the oil bath. This combination of results clearly indicates that microwave conditions are highly beneficial in our $(Ni_{0.5}Cu_{0.5})Fe_2O_4^{MAIN}$-catalyzed reaction, with a 2/2.5-fold yield increase compared to convective heating conditions. Such activity boost under microwave has been observed previously on other magnetically retrievable catalysts, such as CrO_2 for arene oxidation.[67-68] This could be attributed to local superheating phenomenon around the catalyst,[69] consistently with previous studies on the behavior of $NiFe_2O_4$ under microwave.[70]

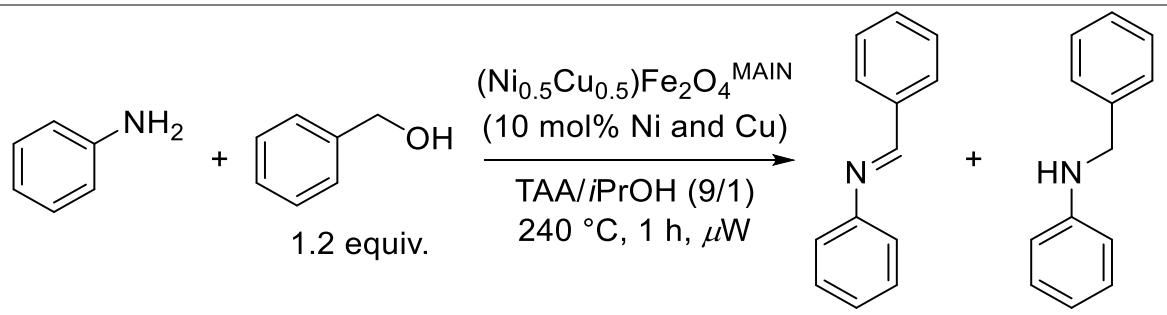

Entry	Setup	Yield (%)	
		Imine	Yield
1	Glass vial	1	74
2	SiC vial	4	30
3	Glass vial[b]	2	11
4	Glass vial, oil bath[b]	1	5

[a]Standard reaction conditions: aniline (1 mmol), benzyl alcohol (1.2 mmol), $(Ni_{0.5}Cu_{0.5})Fe_2O_4^{MAIN}$ (50 mg), *tert*-amyl alcohol/isopropanol (1.8/0.2 mL), Ar, microwave, 240 °C, 1 h.
[b]Same conditions at 130°C, 48h.

Table 26. Microwave control experiments on $(Ni_{0.5}Cu_{0.5})Fe_2O_4^{MAIN}$ for alcohol amination[a]

5.4.2 Substrate scope

In order to understand the scope of the developed process, we tested the catalyst over a range of aniline derivatives (Table 27). 4-methylaniline and 4-nitroaniline reacted in high yields with benzyl alcohol and gave respectively 71% and 67% yield (Table 27, entries 1 and 2). In the case of benzamide only 15% yield was attained in the standard conditions, whereas 65% yield was afforded when isopropanol was removed (Table 27, entry 3). *i*PrOH, besides providing additional hydrogens to reduce the imine, is also a competitor for the alcohol dehydrogenation step. Thus, in this entry imine reduction occurs probably faster than in the model reaction, making the use of *i*PrOH detrimental to the reaction rate. However, 4-chloroaniline and benzenesulfonamide gave only 21% and 27% yield (Table 27, entries 4 and 5).

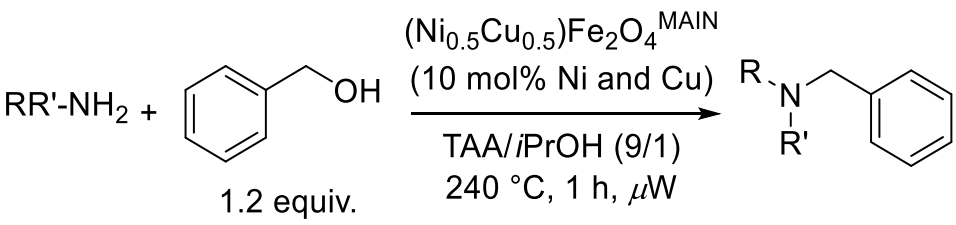

Entry	RR'NH2	Product	Yield (%)

1	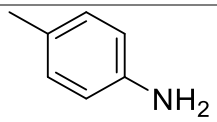	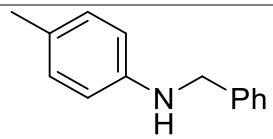	71
2	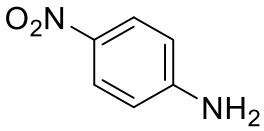	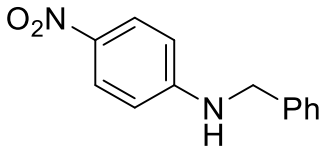	67
3	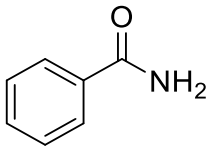	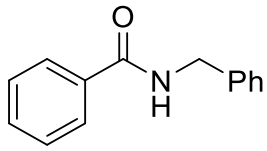	15(65[b])
4	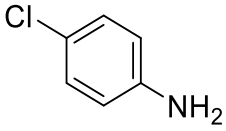	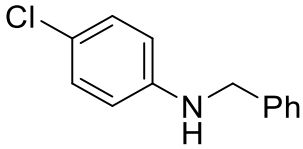	21
5	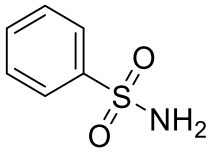	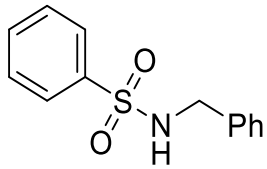	27

[a]Standard reaction conditions: aniline (1 mmol), benzyl alcohol (1.2 mmol), $(Ni_{0.5}Cu_{0.5})Fe_2O_4^{MAIN}$ (50 mg, 10 mol% Cu and 10 mol% Ni), *tert*-amyl alcohol/isopropanol (1.8/0.2 mL), Ar, microwave, 240 °C, 1 h.
[b]no isopropanol was used.

Table 27. Reaction of $(Ni_{0.5}Cu_{0.5})Fe_2O_4^{MAIN}$-catalyzed benzyl alcohol condensation with a range of aniline derivatives[a

Despite their high nucleophilicity, 1-hexylamine and piperidine gave no product, with a 0% starting amine recovery (Scheme 227). As for the sterically hindered diphenylamine, we have fully recovered the starting material with no conversion (Scheme 227).

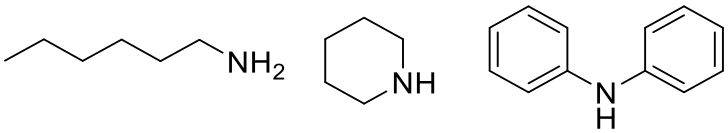

Scheme 227. Unsuccessful substrates.

We then turned to aliphatic short chain alcohols, used as both solvents and alkylating agents (Table 28). MeOH and EtOH remained inactive in our conditions (Table 28, entries 1 and 2). As for *n*-propanol, a 30/52 mixture of the mono- and di-alkylated amine was observed (Table 28, entry 3). Finally, for longer chains *n*-butanol and *n*-hexanol, 80 and 89% respectively of

dialkylated product was observed, stemming from a higher stability of the aldehyde intermediates (Table 28, entries 4 and 5).

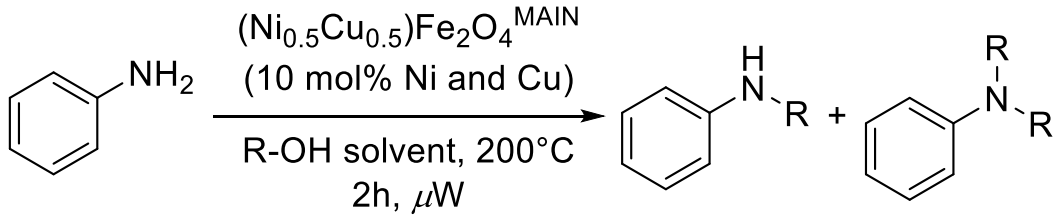

Entry	Alcohol	Yield (%)	
		Mono-alkyl	Bi-alkyl
1	MeOH[b]	0	0
2	EtOH[b]	0	0
3	*n*-propanol	30	52
4	*n*-butanol	16	80
5	*n*-hexanol	11	89

[a]Standard reaction conditions: aniline (1 mmol), alcohol (2 mL), $(Ni_{0.5}Cu_{0.5})Fe_2O_4^{MAIN}$ (50 mg, 10 mol% of Ni and 10 mol% Cu), Ar, microwave, 200°C, 2h. [b] reactions were conducted at 165°C due to pressure constraints.

Table 28. Reaction of aniline with a range of aliphatic alcohols in the presence of $(Ni_{0.5}Cu_{0.5})Fe_2O_4^{MAINa}$

Empowered with a dialkylating catalyst, we decided to test a cyclizing reaction. Using 1,5-pentanediol as an electrophile, we successfully made in one-pot 1-phenylpiperidine through a double alkylation process (Scheme 228).

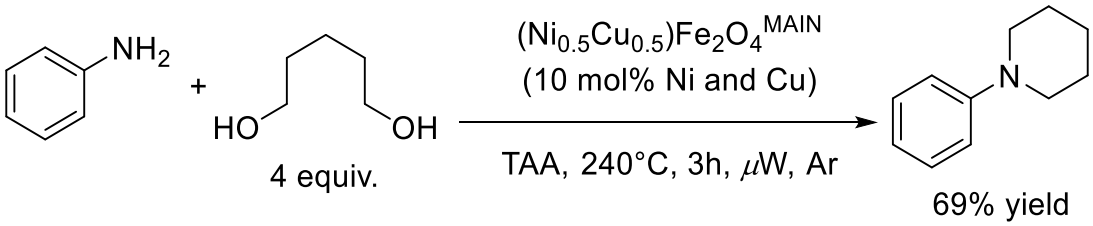

Scheme 228. Cyclization of 1,5-pentanediol with aniline catalyzed by $(Ni_{0.5}Cu_{0.5})Fe_2O_4^{MAIN}$.

We also tested $(Ni_{0.5}Cu_{0.5})Fe_2O_4^{MAIN}$ for the dehydrogenation of 1,2,3,4-tetrahydroquinoline under argon, as a test for the reverse of imine hydrogenation (Scheme 5). After 90 mins at 230°C, we observed the formation of 63% quinoline product. This indicates the ability of our catalyst to de-hydrogenate reactive C-N bonds, as well as C-C bonds in benzylic positions.

Furthermore, this explains the yield decrease under prolonged conditions in our C-N coupling examples (see Table 5, entry 7).

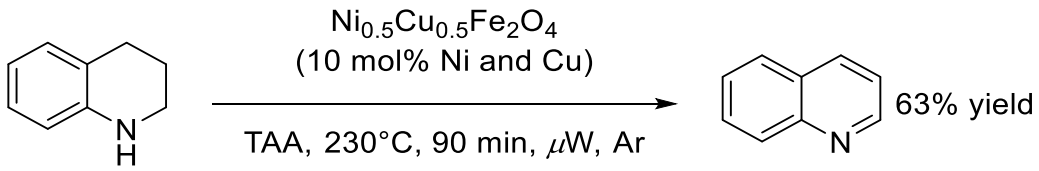

Scheme 5. Dehydrogenation of 1,2,3,4-tetrahydroquinoline.

5.4.3 Recyclability

Exploiting the magneticity of our ferrite-based catalyst, we could easily separate it from the reaction mixture using an external super-magnet. Upon washing it with acetone and drying in vacuum oven, we successfully re-used our catalyst 6 times with a 2-6% yield drop between each cycle (Table 29).

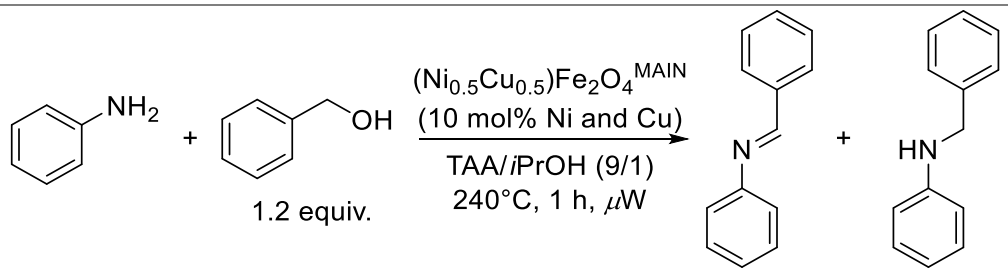

Cycle	Imine (%)	Yield (%)
1	1	74
2	2	68
3	5	64
4	7	62
5	8	58
6	10	56

[a]Standard reaction conditions: aniline (1 mmol), benzyl alcohol (1.2 mmol), $(Ni_{0.5}Cu_{0.5})Fe_2O_4^{MAIN}$ (50 mg), *tert*-amyl alcohol/isopropanol (1.8/0.2 mL), Ar, microwave, 240 °C, 1 h.

Table 29. Recycling experiments for $(Ni_{0.5}Cu_{0.5})Fe_2O_4^{MAIN}$-catalyzed condensation of aniline with benzyl alcohol[a]

To test the applicability of $(Ni_{0.5}Cu_{0.5})Fe_2O_4^{MAIN}$, we scaled up the reaction to 8 mmol of aniline, obtaining a 66% yield (Table 30, entry 1). In these experiments we used a drastically

reduced catalyst loading (1.9 mol% of Ni and Cu) and no TAA.[44] Subsequently, we scaled the model reaction further up to 32 mmol, with a similar yield of 62% (Table 30, entry 2).

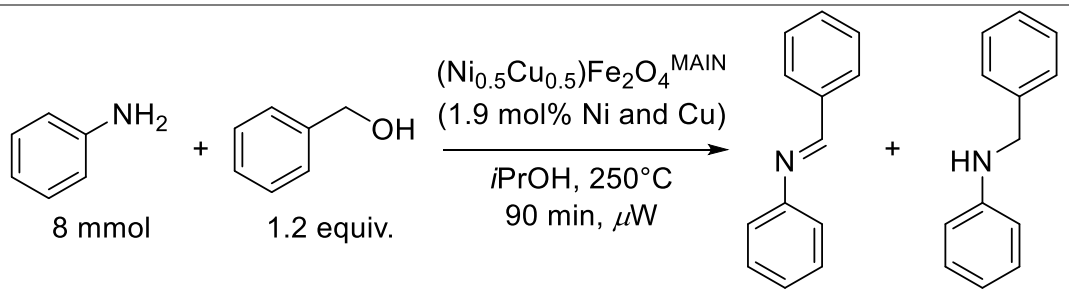

Entry	Modification	Yield (%)	
		Imine	Amine
1	-	9	66
2	32 mmol scale[b]	2	62

[a]Reaction conditions: aniline (8 mmol), benzyl alcohol (10 mmol), $(Ni_{0.5}Cu_{0.5})Fe_2O_4^{MAIN}$ (75 mg, 1.9 mol% of Ni and Cu), *i*PrOH(0.8 mL) Ar, microwave, 250°C, 90 min.
[b]Previous amounts scaled up to 32 mmol of aniline.

Table 30. Reaction of aniline with benzyl alcohol in the presence of $(Ni_{0.5}Cu_{0.5})Fe_2O_4^{MAIN}$ on the gram scale[a]

Based on both Cu and Ni amounts, our turnover number was 18 for Table 12, entry 1, and our cumulated turnover number was 19 after the 6 recycling cycles in Table 11. This value surpasses that of Shi's $NiCuFeO_x$ system reported earlier (11 TON, at 5.8 mol% Ni and 1.7 mol% Cu loadings).[44] Furthermore, it is worth noting that our catalyst proved to be active at low Cu/Ni loadings than theirs (1.9 mol% for each), comparable to that that of homogenous catalysts and without an additional base.

5.4.4 Post-reaction analysis

TEM imaging of the catalyst after reaction after 18 turnover cycles showed the disappearance of the smaller CuO NPs, and an edge smoothening for the bigger ones (Figure 26). Additional images are provided in the appendix (Figure 31 to Figure 33). This indicates either a leaching of the CuO NPs, and/or their aggregation to the bigger ones, following an Ostwald ripening model.

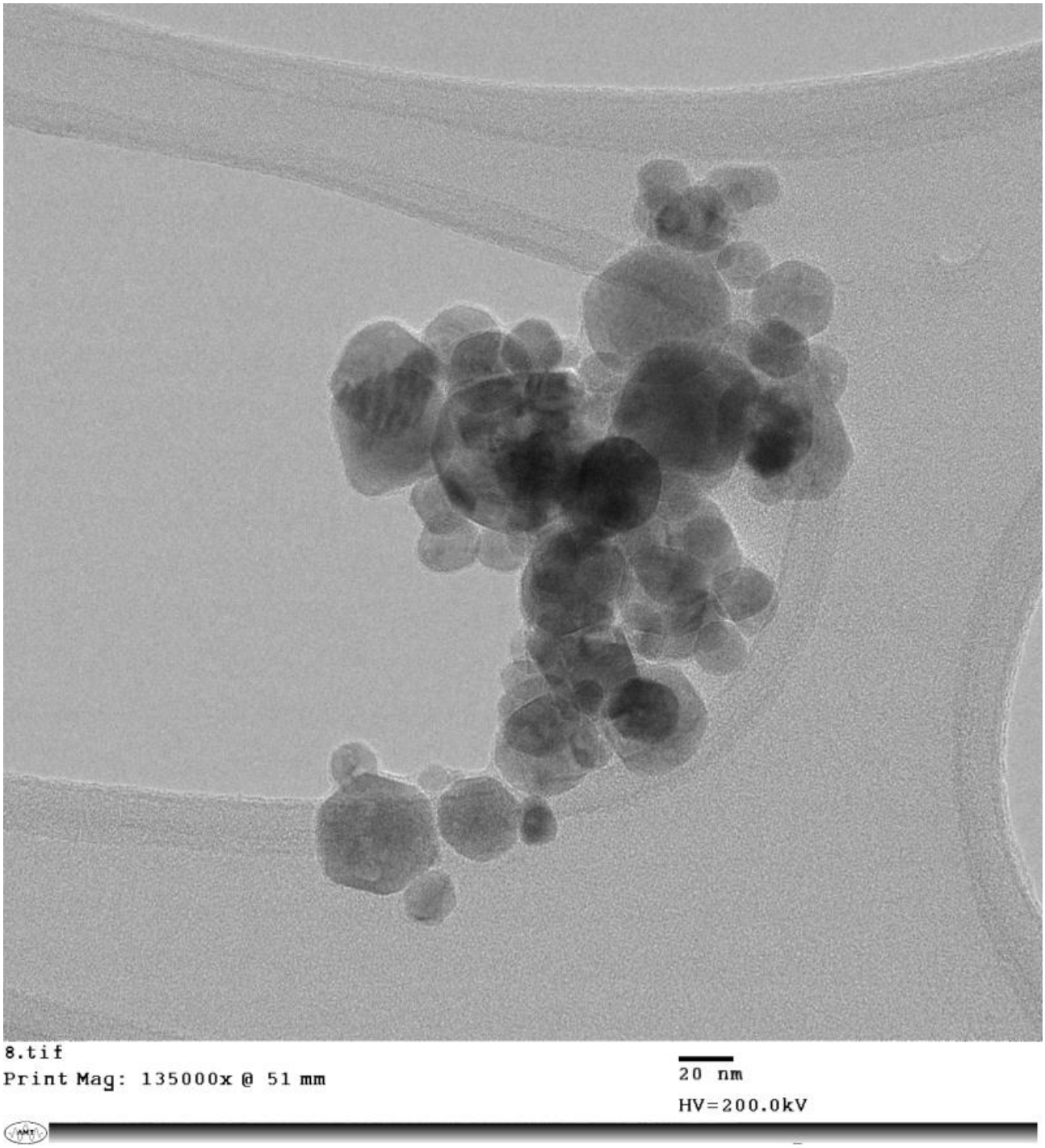

Figure 26. TEM picture of $Ni_{0.5}Cu_{0.5}Fe_2O_4^{MAIN}$ catalyst after reaction.

We performed XPS on the catalyst after reaction after reaction as well, to see the changes that occurred at the NP surface. While the Cu surface coverage decreased from 42.2% to 11.8%, the Ni coverage increased from 6.2% to 10.5% (Table 31 and Chart 15). Deconvolution of the Cu $2p_{3/2}$ region showed a decrease of the CuO peak (from 43% to 33%) (Table 32 and Chart 16), while the Ni $2p_{3/2}$ region did not show any major change (Chart 17). Coupled with our

TEM observations, we believe that a gradual leaching of the CuO NPs occured during the reaction, that is responsible for the activity drop throughout the re-use cycles.

Sample	Cu	Ni	Fe
$Ni_{0.5}Cu_{0.5}Fe_2O_4^{MAIN}$	42.2%	6.2%	51.6%
$Ni_{0.5}Cu_{0.5}Fe_2O_4^{MAIN}$ (After reaction)	11,8%	10,5%	77,7%

Table 31. XPS analysis of $(Ni_{0.5}Cu_{0.5})Fe_2O_4^{MAIN}$ NPs before and after reaction: molar ratios of Ni, Cu and Fe.

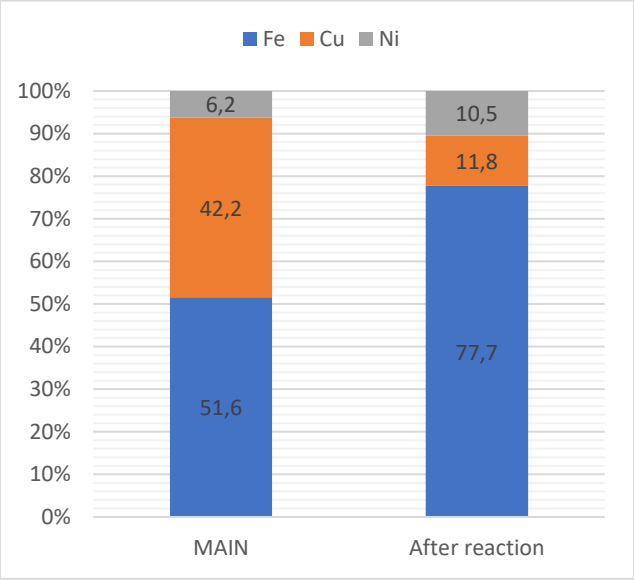

Chart 15. XPS analysis of $(Ni_{0.5}Cu_{0.5})Fe_2O_4^{MAIN}$ NPs before and after reaction: molar ratios of Ni, Cu and Fe.

Sample	$CuFe_2O_4$ (931.6 eV)	CuO (933.6 eV)
$Ni_{0.5}Cu_{0.5}Fe_2O_4^{MAIN}$	57%	43%
$Ni_{0.5}Cu_{0.5}Fe_2O_4^{MAIN}$ (After reaction)	67%	33%

Table 32. XPS of $Ni_{0.5}Cu_{0.5}Fe_2O_4^{MAIN}$ before and after reaction – Cu $2p_{3/2}$ region

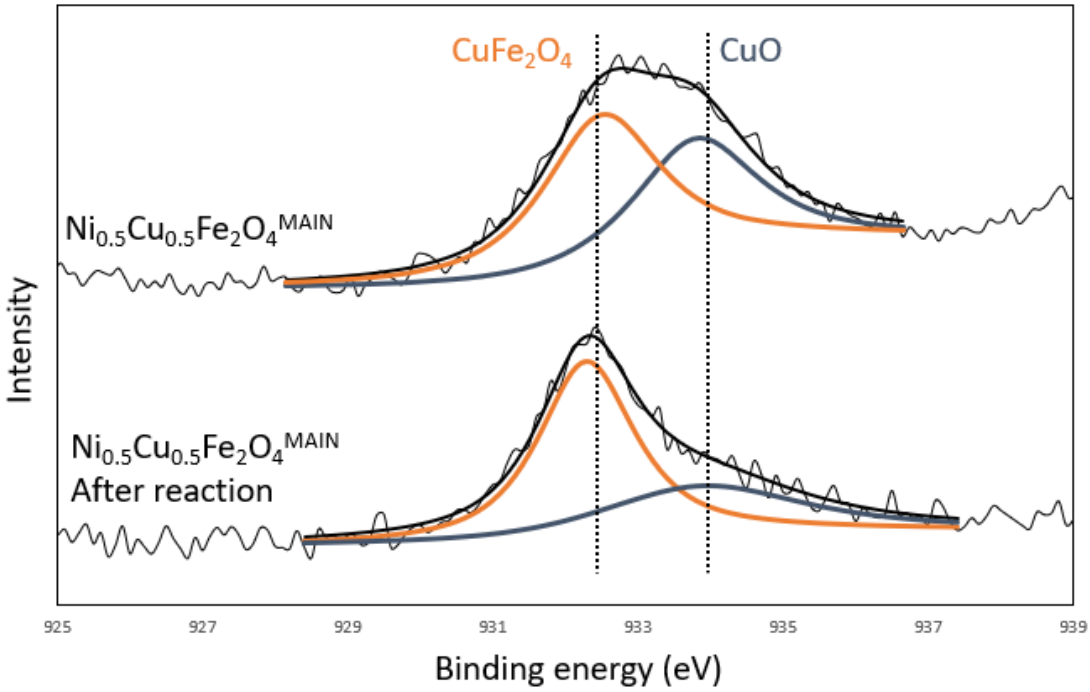

Chart 16. XPS of $Ni_{0.5}Cu_{0.5}Fe_2O_4^{MAIN}$ before and after reaction – Cu $2p_{3/2}$ region

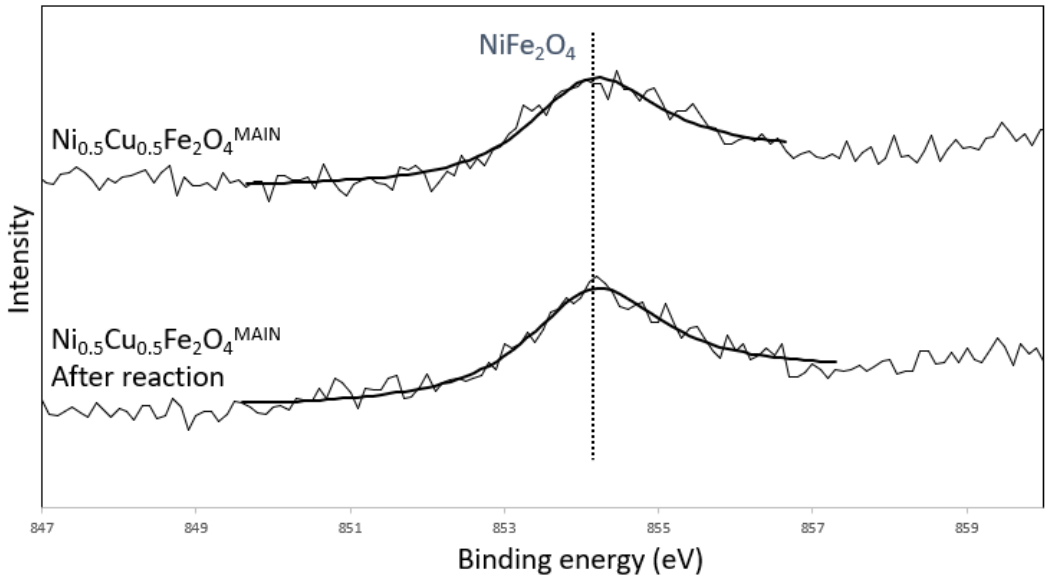

Chart 17. XPS of $Ni_{0.5}Cu_{0.5}Fe_2O_4^{MAIN}$ before and after reaction – Ni $2p_{3/2}$ region

5.5 Conclusion

A magnetically recyclable, heterogeneous and noble metal-free $(Ni_{0.5}Cu_{0.5})Fe_2O_4^{MAIN}$ catalyst was prepared by RF plasma induction. This technique allowed us to produce well-defined nanoparticles at a large scale (c.a. 15 g per synthesis batch), that were successfully characterized by TEM, XPS, XRF and XRD. We also showed their catalytic potency for the

base-free amination of alcohols. In our case, microwave heating allowed up to a 2.5-fold yield increase compared to oil bath heating, as well as a precise temperature/pressure control. The catalyst was shown to be highly active and recyclable up to 6 times. The reaction was easily transposed to the 10 gram-scale, at loadings comparable to that of homogeneous catalyst (up to 2 mol%). Our best turnover (19) surpasses that of heterogeneous Ni/Cu catalysts reported previously. Overall, we showed that plasma induction is a potent tool for nanopowder synthesis, with superior catalytic performances in industrially relevant reactions.

5.6 Experimental

The catalyst characterization was conducted using transmission electron microscopy (TEM), energy dispersive X-ray spectroscopy (EDS), X-ray photoelectron spectroscopy (XPS), and X-ray fluorescence (XRF). The transmission electron microscopy (TEM) samples were deposited on 400 mesh carbon-coated (Lacey) copper grids supplied by Electron Microscopy Sciences. The TEM analyses were performed on the Philips CM200 200 kV TEM, equipped with a AMT XR40B CCD Camera and EDAX Genesis EDS Analysis System. XPS was performed on a VG ESCALAB 3 MKII spectrometer (VG, Thermo Electron Corporation, UK) equipped with an Mg Kα source. All reactants were purchased from Sigma Aldrich and used as received. When relevant, anilines were purified from their oxidation contamination product by vacuum distillation. Unless noted, all catalytic tests were conducted in a Monowave 400 microwave reactor (Anton-Paar), with the glassware (glass or silicon carbide vials) supplied by the vendor. The plasma synthesis was conducted using a PL50 model (Tekna Plasma System Inc., 36 kW), connected to RF power supply (3 MHz, Lepel).

General procedure for catalyst preparation.

The synthesis consisted in the coaxial injection aqueous solution (0.65 mol/L) of $Fe(NO_3)_3 \cdot 9H_2O$, $Cu(NO_3)_2 \cdot 3H_2O$ and $Ni(NO_3)_2 \cdot 6H_2O$ in a 4/1/1 molar ratio with a carrier gas into an inductively coupled thermal plasma torch. Prior injection, reactor pressure was set to 180 torr. The precursor solution was pumped into a water-cooled gas atomization probe using a peristaltic pump at 5 ml/min. Gas were injected at a controlled rate of 62 slpm of O_2 and 5.5 slpm for Ar for the sheath gas, and 62 slpm of Ar for the carrier gas. As NPs accumulated on the filters, the pressure reached up to 330 torr inside the reactor. After 3 hours of reaction, the powder was collected separately in the main chamber and the filter chambers.

General procedure for alcohol amination.

In a typical experiment, the amine (1 mmol), alcohol (1.2 mmol), $(Ni_{0.5}Cu_{0.5})Fe_2O_4^{MAIN}$ (50 mg, 10 mol% Cu and 10 mol% Ni) and the solvent (*tert*-amyl alcohol (1.8mL) and isopropanol (0.2 mL)) were added to a 5 mL microwave vial equipped with a magnetic stirrer. The vial was purged with Ar, sealed with a cap and reacted under microwave at 240 °C for 60 min, then cooled to RT. Acetone (5 mL) was added to disperse the reaction mixture, which was separated from the catalyst using a strong external magnet. The operation was repeated 3 times, then the mixture was filtered through a pad of Celite. The crude reaction mixture was concentrated in vacuo, and analyzed by NMR, using diphenylmethane as an internal standard.

5.7 Appendix

Truncated octahedron

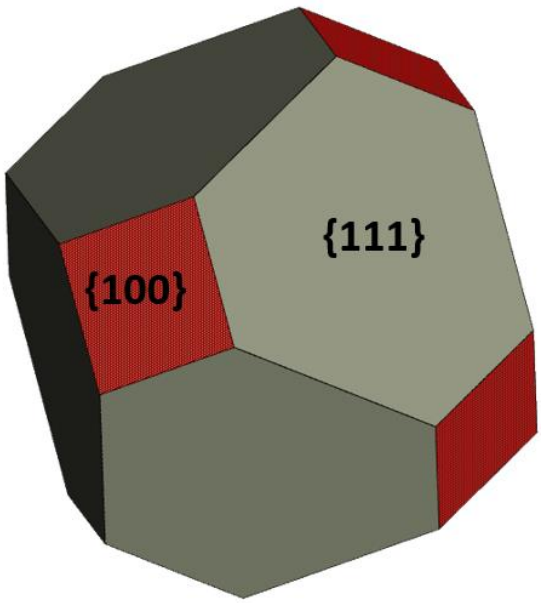

Figure 27. Truncated octahedron facets. The hexagons observed by TEM are the projection of a truncated octahedron exposing their (111) facets

Additional TEM images of the fresh catalyst.

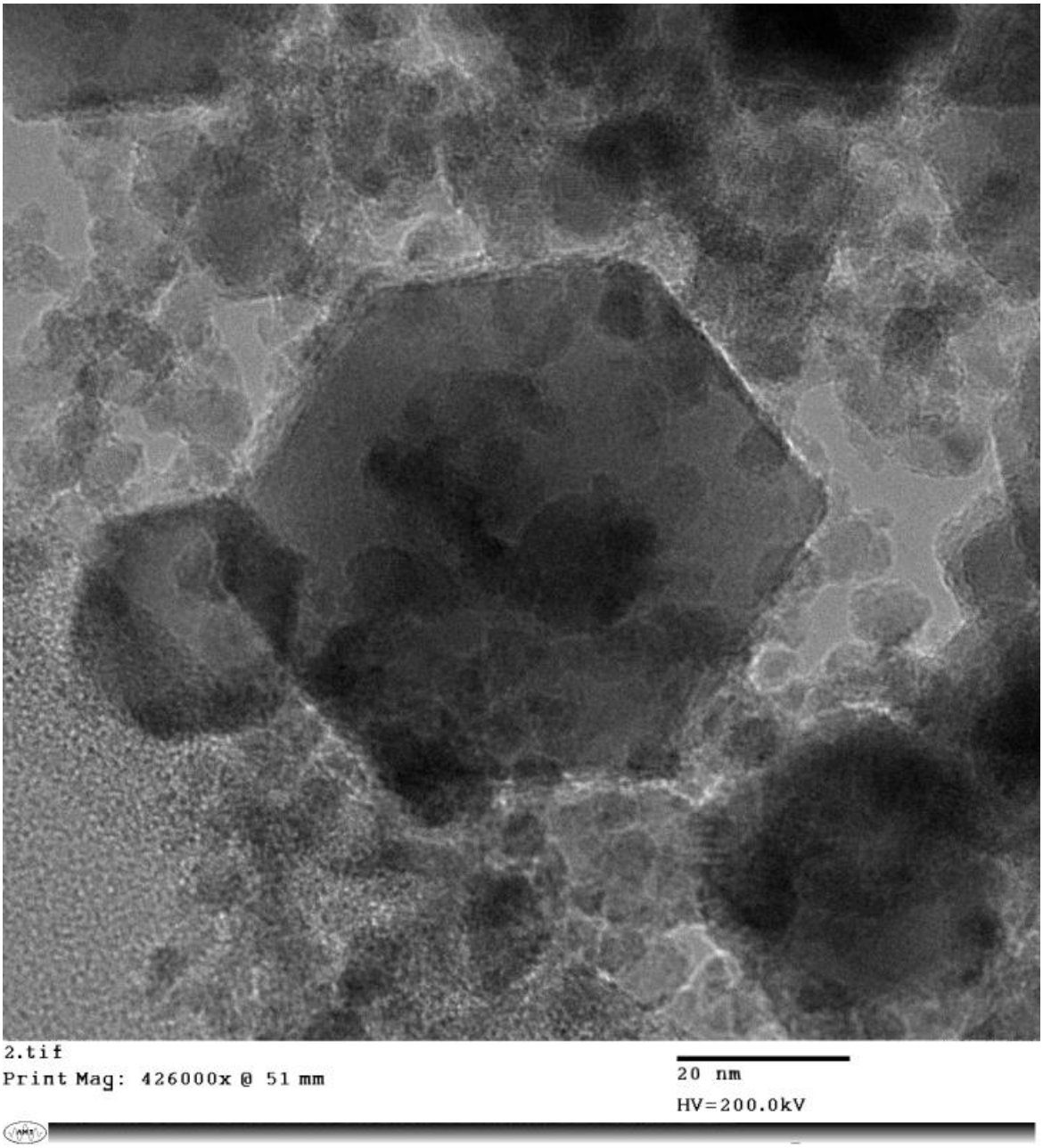
2.tif
Print Mag: 426000x @ 51 mm
20 nm
HV=200.0kV

Figure 28. TEM picture of $(Ni_{0.5}Cu_{0.5})Fe_2O_4^{MAIN}$

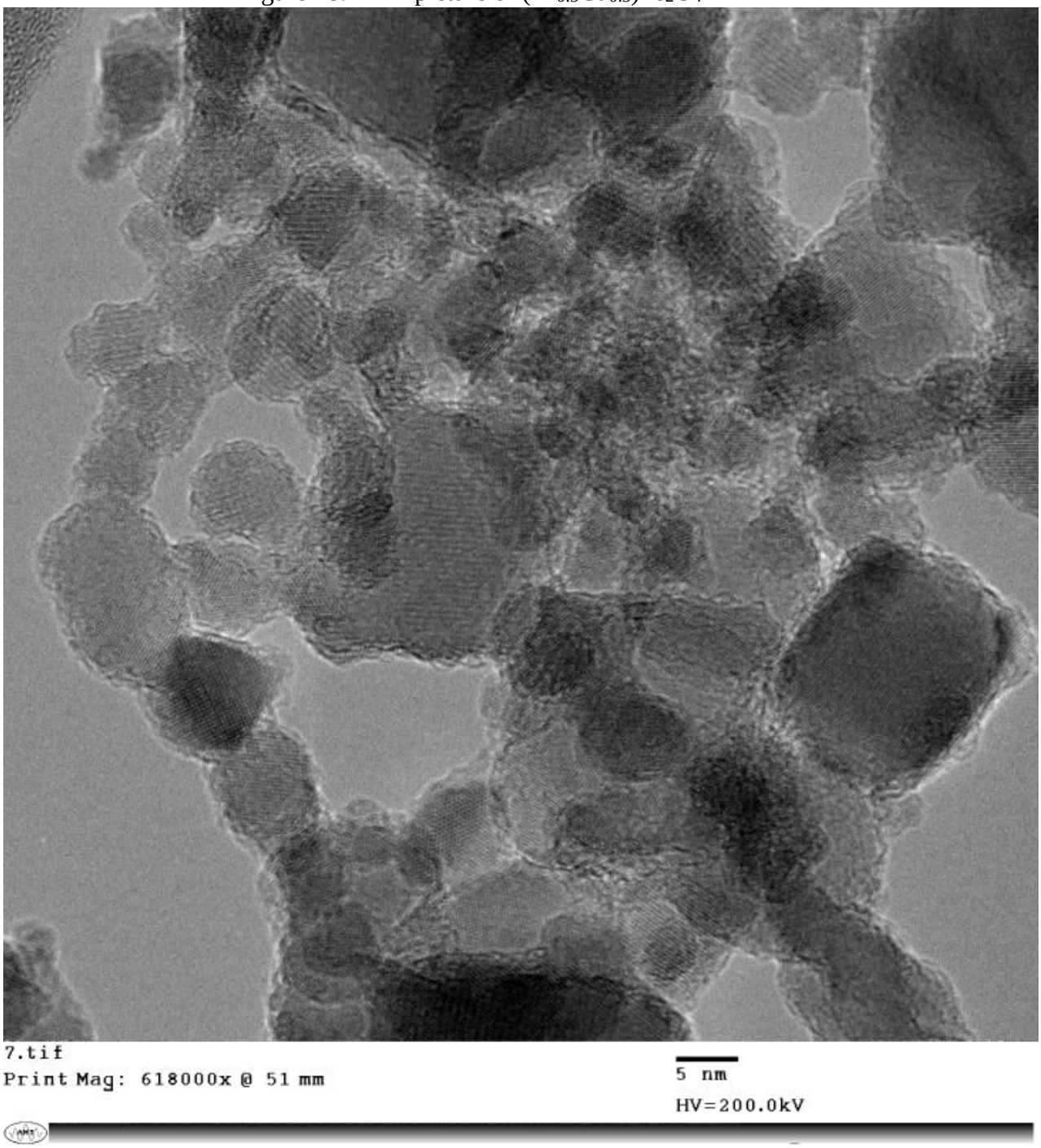

Figure 29. TEM picture of $(Ni_{0.5}Cu_{0.5})Fe_2O_4^{MAIN}$

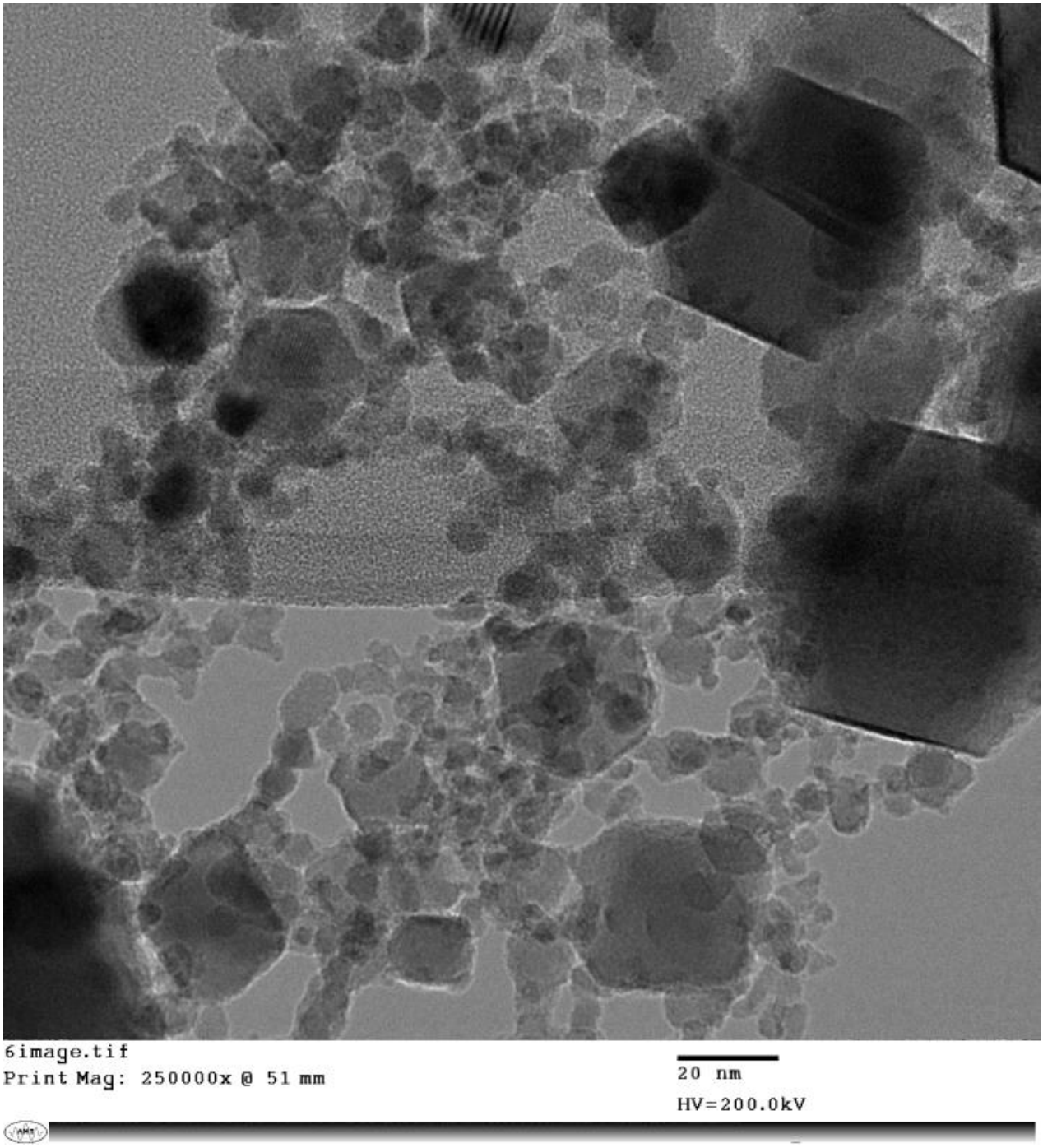

Figure 30. TEM picture of $(Ni_{0.5}Cu_{0.5})Fe_2O_4^{MAIN}$

Additional TEM images of the catalyst after 18 turnover cycles.

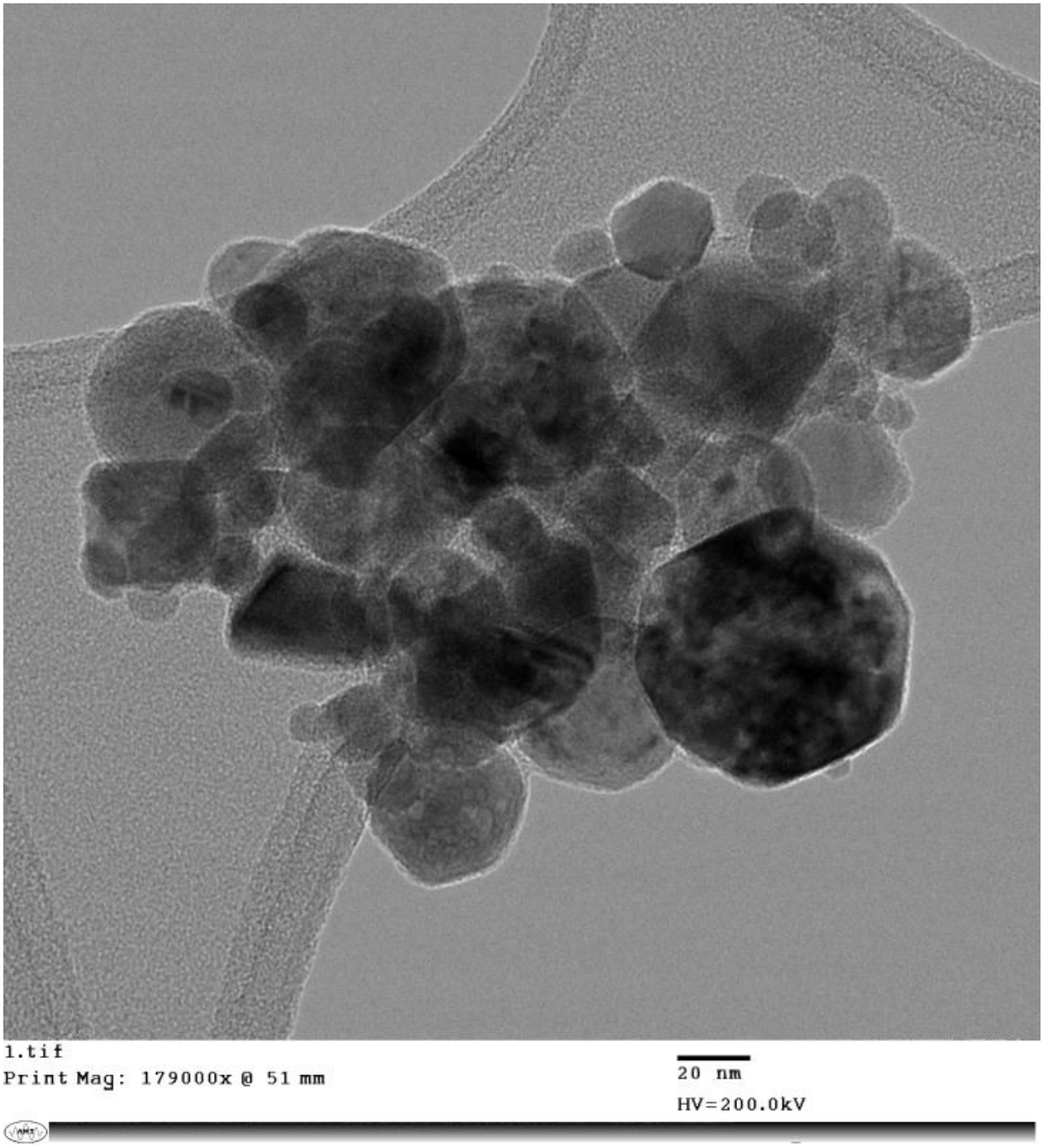

Figure 31. TEM picture of $(Ni_{0.5}Cu_{0.5})Fe_2O_4^{MAIN}$ after reaction

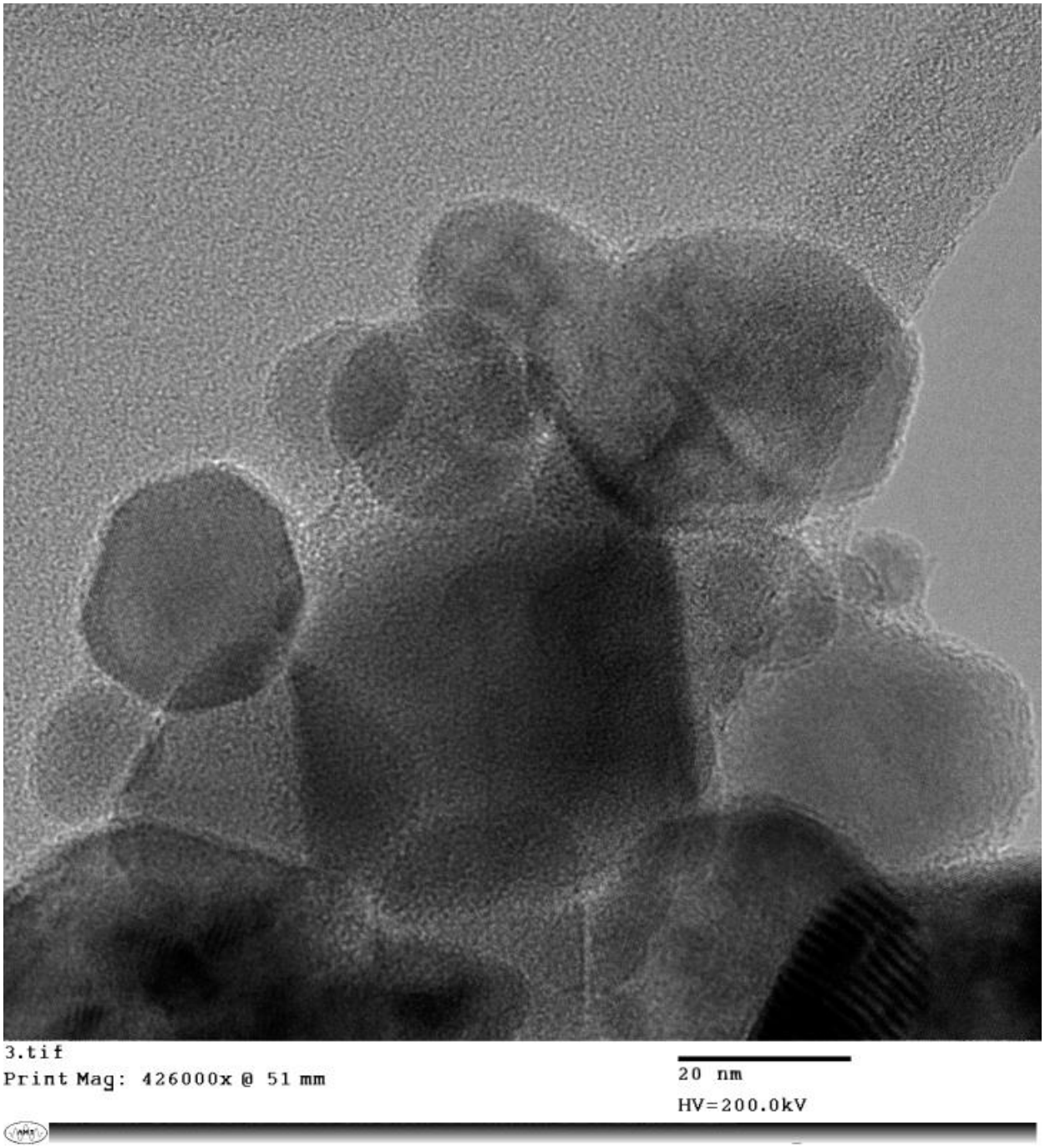

Figure 32. TEM picture of $(Ni_{0.5}Cu_{0.5})Fe_2O_4^{MAIN}$ after reaction

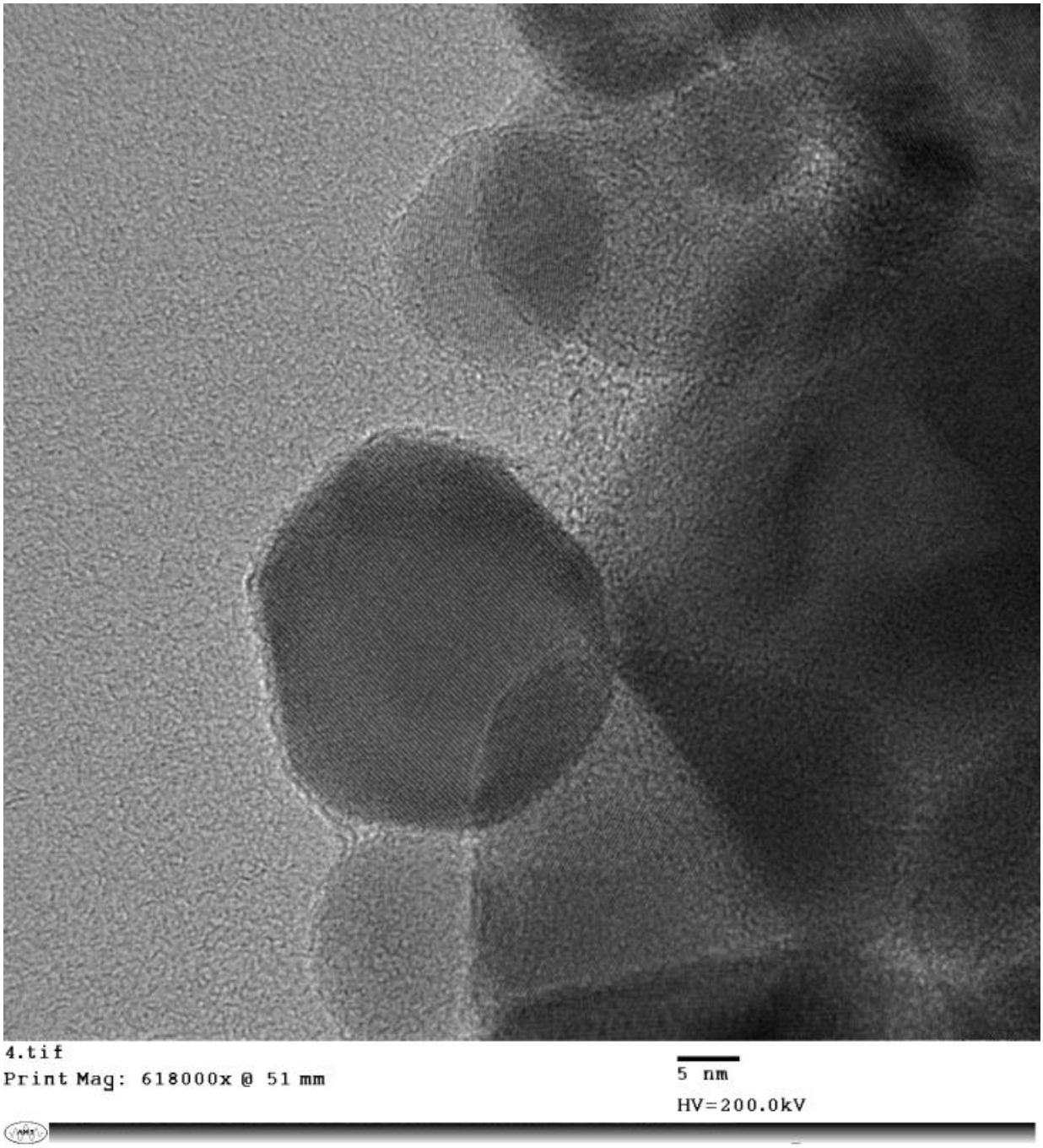

Figure 33. TEM picture of $(Ni_{0.5}Cu_{0.5})Fe_2O_4^{MAIN}$ after reaction

XRD parameters.

Sample	**$(Ni_{0.5}Cu_{0.5})Fe_2O_4^{MAIN}$**	**$(Ni_{0.5}Cu_{0.5})Fe_2O_4^{AUX}$**
R_{wp}	2.09	2.58
R_{exp}	1.64	1.65
GOF	1.63	2.42
Phase (s)	$Ni_{0.5}Cu_{0.5}Fe_2O_4$	$Ni_{0.5}Cu_{0.5}Fe_2O_4$

%Phase (at %)	100	100
Scale factor ($x10^{-4}$)	6.08	6.09
a_0 (Å)	8.3524(7)	8.3629(5)
U	0.0892(8)	0.0718(1)
W	0.0615(1)	0.0606(9)
u	0.2478(9)	0.2483(4)
Average Crystallite size (Å)	388.9	392.0

Table 33. Crystallographic parameters calculated by Rietveld refinement for $(Ni_{0.5}Cu_{0.5})Fe_2O_4^{MAIN}$ and $(Ni_{0.5}Cu_{0.5})Fe_2O_4^{AUX}$

Details on the kinetic profiles.

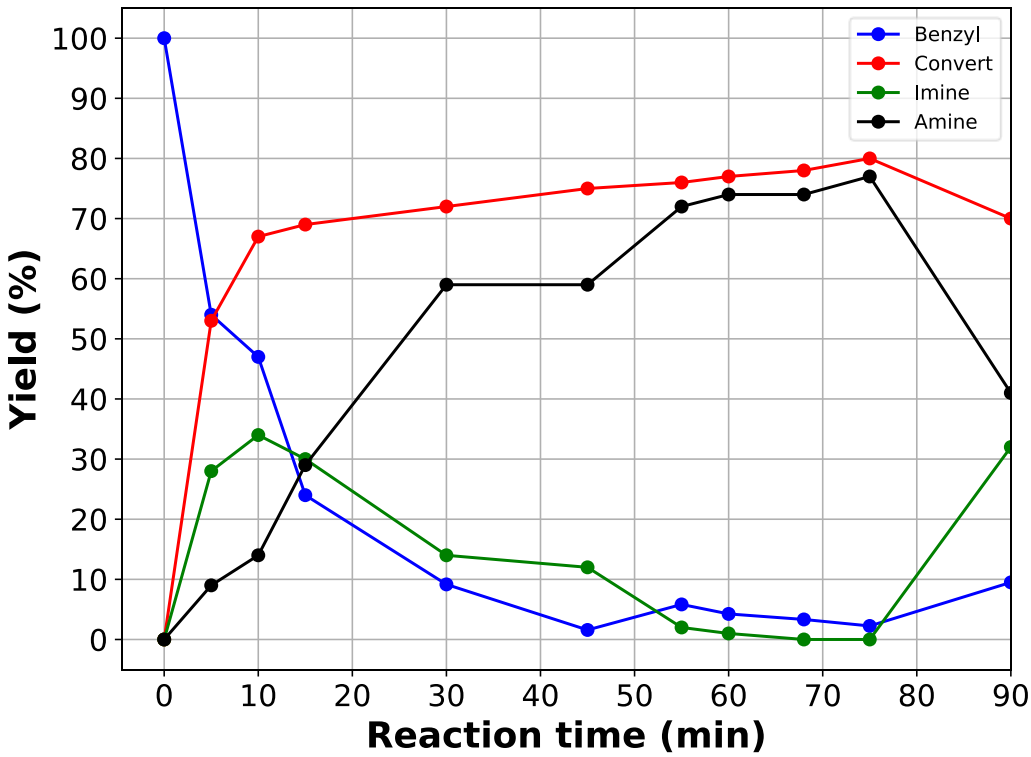

Entry	Reaction time	Yield (%)	
		Imine	Amine
1	5	28	9
2	15	30	29
3	30	14	59
4	45	12	59
5	55	2	72
6	60	1	74

7	68	<1	74
8	75	<1	77
9	90	32	41

[a]Standard reaction conditions: aniline (1 mmol), benzyl alcohol (1.2 mmol), $(Ni_{0.5}Cu_{0.5})Fe_2O_4^{MAIN}$ (50 mg, 10 mol% of Ni and 10 mol% Cu), *tert*-amyl alcohol/isopropanol (1.8 mL and 0.2 mL), Ar, microwave, 240 °C.

Table 34. Time optimization of the model reaction using *i*PrOH as an additive[a]

Microwave heating. The temperature and pressure versus time profiles were taken for the model reaction (Scheme 229). The reaction beginning time (at the 2:36 mark) is defined as when the temperature of the mixture reaches 240 °C (Chart 18). Pressure reached 20.5 bar at the beginning of the reaction, then increased over 1 h to 26 bar (Chart 19). The pressure build-up over the reaction comes from the H_2O generated by imine condensation (see Scheme 224).

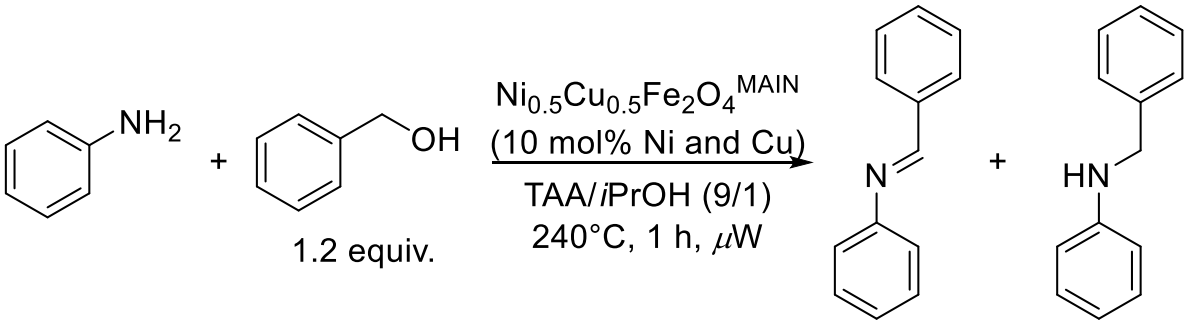

Scheme 229. Model reaction.

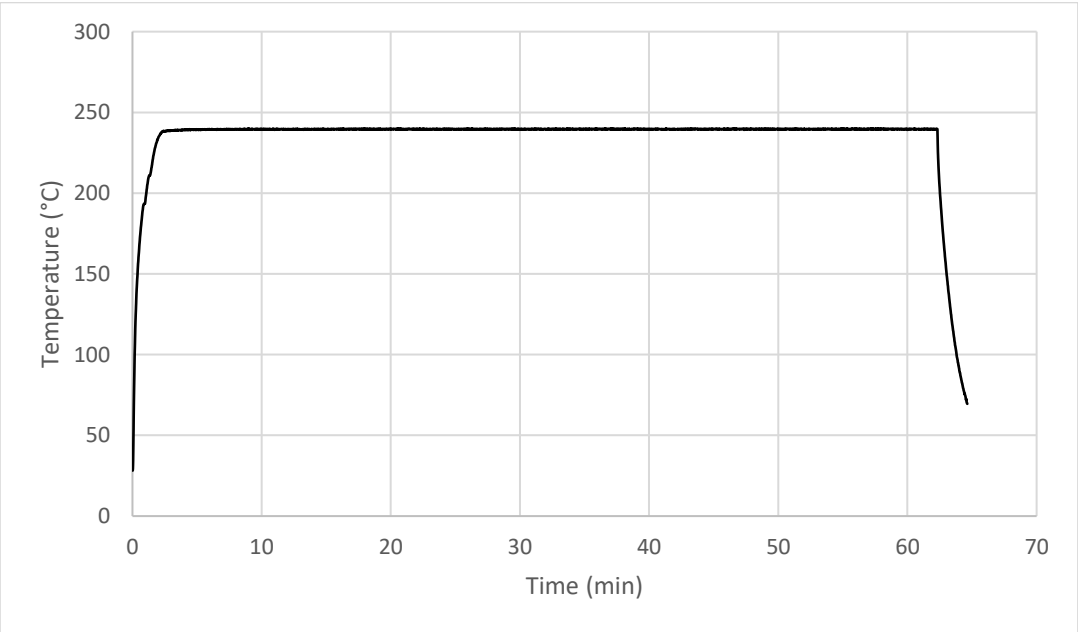

Chart 18. Temperature versus time profile for the model reaction under microwave.

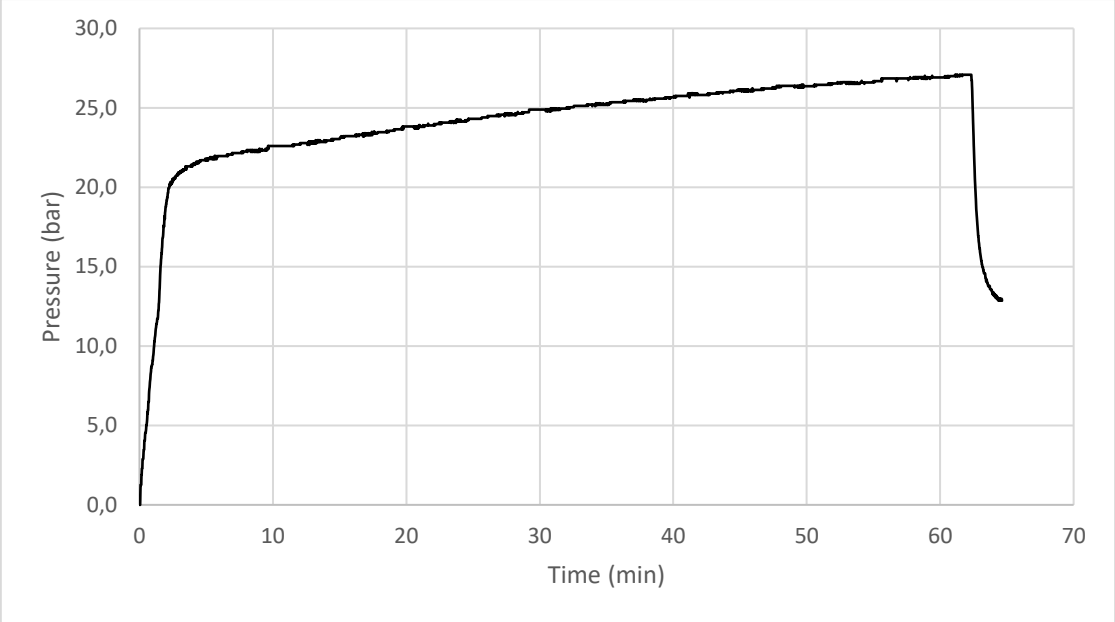

Chart 19. Pressure versus time profile for the model reaction under microwave.

5.8 References

1. Bähn, S.; Imm, S.; Neubert, L.; Zhang, M.; Neumann, H.; Beller, M., The catalytic amination of alcohols. *ChemCatChem* **2011,** *3* (12), 1853-1864.
2. Pera-Titus, M.; Shi, F., Catalytic Amination of Biomass-Based Alcohols. *ChemSusChem* **2014,** *7* (3), 720-722.
3. Hartwig, J. F., Evolution of a Fourth Generation Catalyst for the Amination and Thioetherification of Aryl Halides. *Acc. Chem. Res.* **2008,** *41* (11), 1534-1544.
4. Surry, D. S.; Buchwald, S. L., Biaryl Phosphane Ligands in Palladium-Catalyzed Amination. *Angew. Chem. Int. Ed.* **2008,** *47* (34), 6338-6361.
5. Pelckmans, M.; Renders, T.; Van de Vyver, S.; Sels, B. F., Bio-based amines through sustainable heterogeneous catalysis. *Green Chem.* **2017,** *19* (22), 5303-5331.
6. Watanabe, Y.; Tsuji, Y.; Ohsugi, Y., The ruthenium catalyzed N-alkylation and N-heterocyclization of aniline using alcohols and aldehydes. *Tetrahedron Lett.* **1981,** *22* (28), 2667-2670.
7. Grigg, R.; Mitchell, T. R. B.; Sutthivaiyakit, S.; Tongpenyai, N., Transition metal-catalysed N-alkylation of amines by alcohols. *J. Chem. Soc., Chem. Commun* **1981,** (12), 611-612.
8. Fujita, K.-i.; Li, Z.; Ozeki, N.; Yamaguchi, R., N-Alkylation of amines with alcohols catalyzed by a Cp*Ir complex. *Tetrahedron Lett.* **2003,** *44* (13), 2687-2690.
9. Saidi, O.; Blacker, A. J.; Lamb, G. W.; Marsden, S. P.; Taylor, J. E.; Williams, J. M. J., Borrowing Hydrogen in Water and Ionic Liquids: Iridium-Catalyzed Alkylation of Amines with Alcohols. *Org. Proc. Res. Dev.* **2010,** *14* (4), 1046-1049.
10. Corma, A.; Navas, J.; Sabater, M. J., Advances in One-Pot Synthesis through Borrowing Hydrogen Catalysis. *Chem. Rev.* **2018,** *118* (4), 1410-1459.
11. Irrgang, T.; Kempe, R., 3d-Metal Catalyzed N- and C-Alkylation Reactions via Borrowing Hydrogen or Hydrogen Autotransfer. *Chem. Rev.* **2018**.
12. Gunanathan, C.; Milstein, D., Selective Synthesis of Primary Amines Directly from Alcohols and Ammonia. *Angew. Chem. Int. Ed.* **2008,** *47* (45), 8661-8664.

13. Yamaguchi, R.; Kawagoe, S.; Asai, C.; Fujita, K.-i., Selective Synthesis of Secondary and Tertiary Amines by Cp*Iridium-Catalyzed Multialkylation of Ammonium Salts with Alcohols. *Org. Lett.* **2008,** *10* (2), 181-184.
14. Fujita, K.-i.; Yamaguchi, R., Cp*Ir Complex-Catalyzed Hydrogen Transfer Reactions Directed toward Environmentally Benign Organic Synthesis. *Synlett* **2005,** *2005* (04), 560-571.
15. Yan, T.; Feringa, B. L.; Barta, K., Benzylamines via Iron-Catalyzed Direct Amination of Benzyl Alcohols. *ACS Catal.* **2016,** *6* (1), 381-388.
16. Yan, T.; Feringa, B. L.; Barta, K., Iron catalysed direct alkylation of amines with alcohols. *Nat. Commun.* **2014,** *5*, 5602.
17. Rawlings, A. J.; Diorazio, L. J.; Wills, M., C–N Bond Formation between Alcohols and Amines Using an Iron Cyclopentadienone Catalyst. *Org. Lett.* **2015,** *17* (5), 1086-1089.
18. Elangovan, S.; Neumann, J.; Sortais, J.-B.; Junge, K.; Darcel, C.; Beller, M., Efficient and selective N-alkylation of amines with alcohols catalysed by manganese pincer complexes. *Nat. Commun.* **2016,** *7*, 12641.
19. Rösler, S.; Ertl, M.; Irrgang, T.; Kempe, R., Cobalt-Catalyzed Alkylation of Aromatic Amines by Alcohols. *Angew. Chem. Int. Ed.* **2015,** *54* (50), 15046-15050.
20. Zhang, G.; Yin, Z.; Zheng, S., Cobalt-Catalyzed N-Alkylation of Amines with Alcohols. *Org. Lett.* **2016,** *18* (2), 300-303.
21. Shimizu, K.-i., Heterogeneous catalysis for the direct synthesis of chemicals by borrowing hydrogen methodology. *Catal. Sci. Technol.* **2015,** *5* (3), 1412-1427.
22. Cano, R.; Ramón, D. J.; Yus, M., Impregnated Ruthenium on Magnetite as a Recyclable Catalyst for the N-Alkylation of Amines, Sulfonamides, Sulfinamides, and Nitroarenes Using Alcohols as Electrophiles by a Hydrogen Autotransfer Process. *J. Org. Chem.* **2011,** *76* (14), 5547-5557.
23. Liu, H.; Chuah, G.-K.; Jaenicke, S., N-alkylation of amines with alcohols over alumina-entrapped Ag catalysts using the “borrowing hydrogen” methodology. *J. Catal.* **2012,** *292*, 130-137.
24. Shimizu, K.; Nishimura, M.; Satsuma, A., γ-Alumina-Supported Silver Cluster for N-Benzylation of Anilines with Alcohols. *ChemCatChem* **2009,** *1* (4), 497-503.
25. Martinez, R.; Ramon, D. J.; Yus, M., Selective N-monoalkylation of aromatic amines with benzylic alcohols by a hydrogen autotransfer process catalyzed by unmodified magnetite. *Org. Biomol. Chem.* **2009,** *7* (10), 2176-2181.
26. Gonzalez-Arellano, C.; Yoshida, K.; Luque, R.; Gai, P. L., Highly active and selective supported iron oxide nanoparticles in microwave-assisted N-alkylations of amines with alcohols. *Green Chem.* **2010,** *12* (7), 1281-1287.
27. Jinling, H.; Kazuya, Y.; Noritaka, M., Selective Synthesis of Secondary Amines via N-Alkylation of Primary Amines and Ammonia with Alcohols by Supported Copper Hydroxide Catalysts. *Chem. Lett.* **2010,** *39* (11), 1182-1183.
28. Wu, Y.; Huang, Y.; Dai, X.; Shi, F., Alcohol amination catalyzed by copper powder as a self-supported catalyst. *ChemSusChem 0* (ja).
29. Reddy, M. M.; Kumar, M. A.; Swamy, P.; Naresh, M.; Srujana, K.; Satyanarayana, L.; Venugopal, A.; Narender, N., N-Alkylation of amines with alcohols over nanosized zeolite beta. *Green Chem.* **2013,** *15* (12), 3474-3483.
30. Yang, H.; Cui, X.; Dai, X.; Deng, Y.; Shi, F., Carbon-catalysed reductive hydrogen atom transfer reactions. *Nat. Commun.* **2015,** *6*, 6478.
31. Winans, C. F.; Adkins, H., The alkylation of amines as catalyzed by nickel. *J. Am. Chem. Soc.* **1932,** *54* (1), 306-312.
32. Tomer, A.; Wyrwalski, F.; Przybylski, C.; Paul, J.-F.; Monflier, E.; Pera-Titus, M.; Ponchel, A., Facile preparation of Ni/Al2O3 catalytic formulations with the aid of cyclodextrin

complexes: Towards highly active and robust catalysts for the direct amination of alcohols. *J. Catal.* **2017,** *356*, 111-124.
33. Shimizu, K.-i.; Imaiida, N.; Kon, K.; Hakim Siddiki, S. M. A.; Satsuma, A., Heterogeneous Ni Catalysts for N-Alkylation of Amines with Alcohols. *ACS Catal.* **2013,** *3* (5), 998-1005.
34. Shimizu, K.-i.; Kon, K.; Onodera, W.; Yamazaki, H.; Kondo, J. N., Heterogeneous Ni Catalyst for Direct Synthesis of Primary Amines from Alcohols and Ammonia. *ACS Catal.* **2013,** *3* (1), 112-117.
35. Qi, Y.; Yu, H.; Cao, Q.; Dong, B.; Mu, X.; Mao, A., Nickel Catalyzed Conversion of Cyclohexanol into Cyclohexylamine in Water and Low Boiling Point Solvents. *Catalysts* **2016,** *6* (5), 63.
36. Leung, A. Y. K.; Hellgardt, K.; Hii, K. K. M., Catalysis in Flow: Nickel-Catalyzed Synthesis of Primary Amines from Alcohols and NH3. *ACS Sustainable Chem. Eng.* **2018,** *6* (4), 5479-5484.
37. Taniguchi, K.; Jin, X.; Yamaguchi, K.; Mizuno, N., Facile access to N-substituted anilines via dehydrogenative aromatization catalysis over supported gold-palladium bimetallic nanoparticles. *Catal. Sci. Technol.* **2016,** *6* (11), 3929-3937.
38. Shimizu, K.-i.; Shimura, K.; Nishimura, M.; Satsuma, A., Silver cluster-promoted heterogeneous copper catalyst for N-alkylation of amines with alcohols. *RSC Adv.* **2011,** *1* (7), 1310-1317.
39. He, W.; Wang, L.; Sun, C.; Wu, K.; He, S.; Chen, J.; Wu, P.; Yu, Z., Pt–Sn/γ-Al2O3-Catalyzed Highly Efficient Direct Synthesis of Secondary and Tertiary Amines and Imines. *Chem. Eur. J.* **2011,** *17* (47), 13308-13317.
40. Likhar, P. R.; Arundhathi, R.; Kantam, M. L.; Prathima, P. S., Amination of Alcohols Catalyzed by Copper-Aluminium Hydrotalcite: A Green Synthesis of Amines. *Eur. J. Org. Chem.* **2009,** *2009* (31), 5383-5389.
41. Imabeppu, M.; Kiyoga, K.; Okamura, S.; Shoho, H.; Kimura, H., One-step amination of α,ω-alkylenediols over Cu/Ni-based catalysts. *Catal. Commun.* **2009,** *10* (6), 753-757.
42. Abe, H.; Yokota, Y.; Okabe, K., Amination catalysts for the production of N, N-dimethyldodecylamine from dodecyl alcohol and dimethylamine. *Appl. Catal.* **1989,** *52* (3), 171-179.
43. Kimura, H.; Matsutani, K.; Tsutsumi, S.-i.; Nomura, S.; Ishikawa, K.; Hattori, Y.; Itahashi, M.; Hoshino, H., Basic function of Cu/Ni-based catalyst in a colloidal state for one-pot amination alcohols to N,N-dimethyl tertiary amines. *Catal. Lett.* **2005,** *99* (3), 119-131.
44. Cui, X.; Dai, X.; Deng, Y.; Shi, F., Development of a General Non-Noble Metal Catalyst for the Benign Amination of Alcohols with Amines and Ammonia. *Chem. Eur. J.* **2013,** *19* (11), 3665-3675.
45. Stark, W. J.; Stoessel, P. R.; Wohlleben, W.; Hafner, A., Industrial applications of nanoparticles. *Chem. Soc. Rev.* **2015,** *44* (16), 5793-5805.
46. Malca, M. Y.; Bao, H.; Bastaille, T.; Saadé, N. K.; Kinsella, J. M.; Friščić, T.; Moores, A., Mechanically Activated Solvent-Free Assembly of Ultrasmall Bi2S3 Nanoparticles: A Novel, Simple, and Sustainable Means To Access Chalcogenide Nanoparticles. *Chem. Mater.* **2017,** *29* (18), 7766-7773.
47. Rak, M. J.; Saadé, N. K.; Friščić, T.; Moores, A., Mechanosynthesis of ultra-small monodisperse amine-stabilized gold nanoparticles with controllable size. *Green Chem.* **2014,** *16* (1), 86-89.
48. Rak, M. J.; Friščić, T.; Moores, A., One-step, solvent-free mechanosynthesis of silver nanoparticle-infused lignin composites for use as highly active multidrug resistant antibacterial filters. *RSC Adv.* **2016,** *6* (63), 58365-58370.

49. Kortshagen, U. R.; Sankaran, R. M.; Pereira, R. N.; Girshick, S. L.; Wu, J. J.; Aydil, E. S., Nonthermal Plasma Synthesis of Nanocrystals: Fundamental Principles, Materials, and Applications. *Chem. Rev.* **2016,** *116* (18), 11061-11127.
50. Shunko, E. V.; Stevenson, D. E.; Belkin, V. S., Inductively Coupling Plasma Reactor With Plasma Electron Energy Controllable in the Range From 6 to 100 eV. *IEEE T. Plasma Sci.* **2014,** *42* (3), 774-785.
51. Vollath, D., Plasma Synthesis of Nanoparticles. *KONA Powder Part. J.* **2007,** *25*, 39-55.
52. Mohai, I.; Gál, L.; Szépvölgyi, J.; Gubicza, J.; Farkas, Z., Synthesis of nanosized zinc ferrites from liquid precursors in RF thermal plasma reactor. *J. Eur. Ceram. Soc.* **2007,** *27* (2), 941-945.
53. Bastien, S.; Braidy, N., Controlled synthesis of nickel ferrite nanocrystals with tunable properties using a novel induction thermal plasma method. *J. Appl. Phys.* **2013,** *114* (21), 214304.
54. Bastien, S.; Ricolleau, C.; Braidy, N., Nano-Architecture of Facetted NiFe2O4/(Ni,Fe)O Particles Produced by Induction Plasma. *Plasma Chem. Plasma Process.* **2016,** *36* (5), 1349-1362.
55. Jia, L.; Gitzhofer, F., Nano-Particle Sizing in a Thermal Plasma Synthesis Reactor. *Plasma Chem. Plasma Process.* **2009,** *29* (6), 497.
56. Albuquerque, A. S.; Tolentino, M. V. C.; Ardisson, J. D.; Moura, F. C. C.; de Mendonça, R.; Macedo, W. A. A., Nanostructured ferrites: Structural analysis and catalytic activity. *Ceram. Int.* **2012,** *38* (3), 2225-2231.
57. Deroubaix, G.; Marcus, P., X-ray photoelectron spectroscopy analysis of copper and zinc oxides and sulphides. *Surf. Interface Anal.* **1992,** *18* (1), 39-46.
58. Nawale, A. B.; Kanhe, N. S.; Patil, K. R.; Bhoraskar, S. V.; Mathe, V. L.; Das, A. K., Magnetic properties of thermal plasma synthesized nanocrystalline nickel ferrite (NiFe2O4). *J. Alloys Compd.* **2011,** *509* (12), 4404-4413.
59. Balagurov, A. M.; Bobrikov, I. A.; Maschenko, M. S.; Sangaa, D.; Simkin, V. G., Structural phase transition in CuFe2O4 spinel. *Crystallogr. Rep.* **2013,** *58* (5), 710-717.
60. Bastien, S.; Braidy, N., Reduction and Oxidation Behavior of NixFe3–xO4−δ Spinels Probed by Reactive in Situ XRD. *J Phys. Chem. C* **2018,** *122* (20), 11038-11050.
61. Kaloglu, N.; Özdemir, I.; Gürbüz, N.; Achard, M.; Bruneau, C., Benzimidazolium sulfonate ligand precursors and application in ruthenium-catalyzed aromatic amine alkylation with alcohols. *Catal. Commun.* **2016,** *74*, 33-38.
62. Xie, X.; Huynh, H. V., Tunable Dehydrogenative Amidation versus Amination Using a Single Ruthenium-NHC Catalyst. *ACS Catal.* **2015,** *5* (7), 4143-4151.
63. Geissman, T. A., The Cannizzaro Reaction. In *Organic Reactions*, Sons, J. W., Ed. 2011.
64. Patil, R. D.; Adimurthy, S., Catalytic Methods for Imine Synthesis. *Asian Journal of Organic Chemistry* **2013,** *2* (9), 726-744.
65. Obermayer, D.; Gutmann, B.; Kappe, C. O., Microwave Chemistry in Silicon Carbide Reaction Vials: Separating Thermal from Nonthermal Effects. *Angew. Chem. Int. Ed.* **2009,** *48* (44), 8321-8324.
66. Kremsner, J. M.; Kappe, C. O., Silicon Carbide Passive Heating Elements in Microwave-Assisted Organic Synthesis. *J. Org. Chem.* **2006,** *71* (12), 4651-4658.
67. Lukasiewicz, M.; Bogdal, D.; Pielichowski, J., Microwave-Assisted Oxidation of Side Chain Arenes by MagtrieveTM. *Adv. Synth. Catal.* **2003,** *345* (12), 1269-1272.
68. Bogdal, D.; Lukasiewicz, M.; Pielichowski, J.; Miciak, A.; Bednarz, S., Microwave-assisted oxidation of alcohols using Magtrieve™. *Tetrahedron* **2003,** *59* (5), 649-653.

69. de la Hoz, A.; Díaz-Ortiz, Á.; Moreno, A., Microwaves in organic synthesis. Thermal and non-thermal microwave effects. *Chem. Soc. Rev.* **2005,** *34* (2), 164-178.
70. Polaert, I.; Bastien, S.; Legras, B.; Estel, L.; Braidy, N., Dielectric and magnetic properties of NiFe2O4 at 2.45GHz and heating capacity for potential uses under microwaves. *J. Magn. Magn. Mater.* **2015,** *374*, 731-739.

6 Conclusion and future work

6.1 Conclusion

In this thesis we have tackled several aspects of green chemistry, centered around the reduction of C=O bonds and alcohol activation. Within the themes discussed in chapter 1, we turned in particular to alternative energy inputs to make novel nanostructures or conduct organic reactions that would be challenging to run otherwise. Indeed, only microwave heating enabled to obtain small Ag NPs (2-3 nm) in the synthesis the Ag-Fe_3O_4@CMC NPs (chapter 3), while for the (NiCu)Fe_2O_4-catalyzed alcohol amination (chapter 5) it allowed to surpass previously reported turnover numbers. Bypassing solvent use through mechanochemistry (chapter 4) enabled the reduction of water-soluble substrates (5-HMF) or insoluble products (polyketone), facilitating their work-up. Finally, plasma induction allowed the production of well-defined $(Ni_{0.5}Cu_{0.5})Fe_2O_4$ NPs, on a scale (10g) that would be difficult to attain under conventional methods.

We also paid careful attention to solvent choice by trying to use them in minute amounts or stick to the ones recommended by Sneddon et *al*. in their 2016 update of the GSK solvent selection guide (water, *tert*-amyl alcohol, *i*PrOH).[1] Solvent-free or neat conditions in mechanochemistry enabled very short reaction times (<15 min, see chapter 4). Furthermore, we have used an industrial waste, PMHS, as a reducing agent to reduce the environmental impact of our process.

The catalytic aspect of chapter 3 and 5 revolved around the recyclability theme. Although Ag is a critically endangered element, it exhibits amazing catalytic properties covered in chapter 2, such as C=O selectivity in hydrogenation. To address the former issue while keeping the latter advantage, we have successfully designed in chapter 3 an Ag/Fe/cellulose composite that was magnetic and inherently compatible with water. In chapter 5, we have built a Ni/Cu/Fe trimetallic ensemble where each element had a distinct role: Fe ensures catalyst magneticity, Cu performs alcohol oxidation and catalyzes imine reduction in synergy with Ni.

Thus, we have explored different methods to apply the fundamental principles of green chemistry to fundamental chemical reactions. In particular here, we have adopted a combined approach, to solve various chemical issues (substrate solubility, C=O selectivity, precious metal recycling) while striving for safety.

6.2 Future work

In efforts to expand the concept of magnetically recoverable Ag catalysts prepared by microwave irradiation in water (Chapter 3), other metals could be grafted on cellulose derivatives. For instance, Cu^{2+} salts mixed with either sodium-potassium tartrate (Fehling's reagent[2-3]) or sodium citrate (Benedict's reagent[4]) can react with reducing sugars as well to make Cu_2O NPs. Thus, we could extend our synthetic system to Cu, and test it for water-compatible organic reactions such as oxidative cross-dehydrogenative coupling,[5] A^3 coupling[6] or click condensation.[7]

Future studies on the mechanochemical reduction of carbonyls (Chapter 4) should focus on removing solvents from the work-up as well, with solvent-free extraction methods such as supercritical carbon dioxide (sCO_2).[8-9] For scaling-up purposes, several groups have reported the use of single or twin-screw extrusion for the continuous synthesis of metal-organic frameworks[10-11] or active pharmaceutical ingredient co-crystals.[12] Furthermore the presence of metallic extrusion barrels allows heat control (up to 250 °C), opening prospects for a better control overall on the reaction kinetics.

As for nanoparticle synthesis by plasma induction (Chapter 5), the synthesis could be extended to other spinels such as chromite (MCr_2O_4) or aluminate (MAl_2O_4) NPs. For instance, $CuAl_2O_4$ has been shown to be able to oxidize benzyl alcohol.[13-14] It has further been shown by Leckie et *al*. to be less prone to Cu leaching (using HCl) than CuO and Cu_2O, which could help solve activity drop issues encountered in our works.[15] Lastly, MeOH has proved to be an unreactive alcohol in our substrate scope, while it is an attractive C1 source in amine *N*-methylation.[16] $CuCr_2O_4$ has been shown by Crosswhite et *al*. to be able to oxidize MeOH under microwave conditions, opening new prospects as well in this area.[17]

6.3 References

1. Alder, C. M.; Hayler, J. D.; Henderson, R. K.; Redman, A. M.; Shukla, L.; Shuster, L. E.; Sneddon, H. F., Updating and further expanding GSK's solvent sustainability guide. *Green Chem.* **2016,** *18* (13), 3879-3890.
2. Tao, H.; Wei, L.; Liang, A.; Li, J.; Jiang, Z.; Jiang, H., Highly Sensitive Resonance Scattering Detection of DNA Hybridization Using Aptamer-Modified Gold Nanopaticle as Catalyst. *Plasmonics* **2010,** *5* (2), 189-198.
3. Jiang, Z.; Huang, Y.; Liang, A.; Pan, H.; Liu, Q., Resonance scattering detection of trace microalbumin using immunonanogold probe as the catalyst of Fehling reagent–glucose reaction. *Biosens. Bioelectron.* **2009,** *24* (6), 1674-1678.
4. Wang, D.; Mo, M.; Yu, D.; Xu, L.; Li, F.; Qian, Y., Large-Scale Growth and Shape Evolution of Cu2O Cubes. *Crystal Growth & Design* **2003,** *3* (5), 717-720.
5. Hudson, R.; Ishikawa, S.; Li, C.-J.; Moores, A., Magnetically Recoverable CuFe2O4 Nanoparticles as Highly Active Catalysts for Csp3–Csp and Csp3–Csp3 Oxidative Cross-Dehydrogenative Coupling. *Synlett* **2013,** *24* (13), 1637-1642.

6. Islam, M. M.; Roy, A. S.; Islam, S. M., Functionalized Polystyrene Supported Copper(I) Complex as an Effective and Reusable Catalyst for Propargylamines Synthesis in Aqueous Medium. *Catal. Lett.* **2016,** *146* (6), 1128-1138.
7. Hudson, R.; Li, C.-J.; Moores, A., Magnetic Copper-Iron nanoparticles as simple heterogeneous catalysts for the azide-alkyne click reaction in water. *Green Chem.* **2012,** *14* (3), 622-624.
8. Goto, M.; Sato, M.; Hirose, T., Extraction of peppermint oil by supercritical carbon dioxide. *J. Chem. Eng. Jpn.* **1993,** *26* (4), 401-407.
9. Nguyen, K.; Barton, P.; Spencer, J. S., Supercritical carbon dioxide extraction of vanilla. *J. of Supercritical Fluids* **1991,** *4* (1), 40-46.
10. Crawford, D. E.; Miskimmin, C. K. G.; Albadarin, A. B.; Walker, G.; James, S. L., Organic synthesis by Twin Screw Extrusion (TSE): continuous, scalable and solvent-free. *Green Chem.* **2017,** *19* (6), 1507-1518.
11. Crawford, D.; Casaban, J.; Haydon, R.; Giri, N.; McNally, T.; James, S. L., Synthesis by extrusion: continuous, large-scale preparation of MOFs using little or no solvent. *Chem. Sci.* **2015,** *6* (3), 1645-1649.
12. Morrison, H.; Fung, P.; Tran, T.; Horstman, E.; Carra, E.; Touba, S., Use of Twin Screw Extruders as a Process Chemistry Tool: Application of Mechanochemistry To Support Early Development Programs. *Org. Proc. Res. Dev.* **2018,** *22* (10), 1432-1440.
13. Ragupathi, C.; Vijaya, J. J.; Kennedy, L. J.; Bououdina, M., Nanostructured copper aluminate spinels: Synthesis, structural, optical, magnetic, and catalytic properties. *Mater. Sci. Semicond. Process.* **2014,** *24*, 146-156.
14. Tang, Q.; Gong, X.; Zhao, P.; Chen, Y.; Yang, Y., Copper–manganese oxide catalysts supported on alumina: Physicochemical features and catalytic performances in the aerobic oxidation of benzyl alcohol. *Appl. Catal., A* **2010,** *389* (1), 101-107.
15. Hu, C.-Y.; Shih, K.; Leckie, J. O., Formation of copper aluminate spinel and cuprous aluminate delafossite to thermally stabilize simulated copper-laden sludge. *J. Hazard. Mater.* **2010,** *181* (1), 399-404.
16. Yan, G.; Borah, A. J.; Wang, L.; Yang, M., Recent Advances in Transition Metal-Catalyzed Methylation Reactions. *Adv. Synth. Catal.* **2015,** *357* (7), 1333-1350.
17. Crosswhite, M.; Hunt, J.; Southworth, T.; Serniak, K.; Ferrari, A.; Stiegman, A. E., Development of Magnetic Nanoparticles as Microwave-Specific Catalysts for the Rapid, Low-Temperature Synthesis of Formalin Solutions. *ACS Catal.* **2013,** *3* (6), 1318-1323.